Order Number 1339287

A detailed structural analysis across a regional unconformity, forks of the Canning River, Franklin Mountains, northeastern Brooks Range, Alaska

Ziegler, Jennifer Ann, M.S.

University of Alaska Fairbanks, 1989

U·M·I
300 N. Zeeb Rd.
Ann Arbor, MI 48106

A DETAILED STRUCTURAL ANALYSIS ACROSS A REGIONAL UNCONFORMITY, FORKS OF THE CANNING RIVER, FRANKLIN MOUNTAINS, NORTHEASTERN BROOKS RANGE, ALASKA

A

THESIS

Presented to the Faculty of the University of Alaska

in Partial Fulfillment of the Requirements

for the Degree of

MASTER OF SCIENCE

By

Jennifer Ann Ziegler, A.B.

Fairbanks, Alaska

December 1989

A DETAILED STRUCTURAL ANALYSIS ACROSS A REGIONAL UNCONFORMITY,

FORKS OF THE CANNING RIVER, FRANKLIN MOUNTAINS,

NORTHEASTERN BROOKS RANGE, ALASKA

By

Jennifer Ann Ziegler

RECOMMENDED:

Advisory Committee Chair

Department Head

APPROVED:

Dean, College of Natural Sciences

Dean of the Graduate School

9/26/89

Date

ABSTRACT

Structural analysis on the northern flank of the 'Franklin Mountains anticlinorium,' northeastern Brooks Range, Alaska, addressed the geometry and sequence of structures, and the deformational mechanics of the Franklinian and Ellesmerian sequences, which are separated by a sub-Mississippian unconformity. The anticlinorium is comprised of two horses of Franklinian sequence rocks in a Cenozoic north-vergent duplex thrust system. South-dipping pre-Mississippian slaty cleavage may have been a plane of preferred failure during ramp formation. Above the unconformity, the Kekiktuk Conglomerate remained attached to pre-Mississippian rocks, deforming with them beneath a roof thrust in the Mississippian Kayak Shale. Increased shear stress and overburden pressure beneath overthrust Franklinian sequence rocks may have led to local detachment near the unconformity surface. Above the Kayak Shale, progressive detachment folding and thrust faulting occurred in the Lisburne and Sadlerochit Groups as a result of emplacement of the two underlying horses.

TABLE OF CONTENTS

Page No.

LIST OF FIGURES....14

LIST OF TABLES....20

LIST OF PLATES....23

ACKNOWLEDGMENTS....24

1. INTRODUCTION....25

1.A. LOCATION AND SCOPE OF STUDY....25

1.B. OVERVIEW OF FRANKLIN MOUNTAINS STRUCTURAL ANALYSIS....28

1.B.1. Background Material (Sections 2-4)....28

1.B.2. Description of Structural Geometry....30

1.B.2.a. Field description of structural geometry (Section 5)....30

1.B.2.b. Structural geometry modeled in balanced cross-sections (Section 6)....31

1.B.3. Description of Structural Sequence....31

1.B.3.a. Integration of strain data with balanced cross-section (Section 7)....32

1.B.3.b. Incremental and finite strain determinations (Appendices F-G)....32

1.B.4. Description of Structural Mechanics....32

1.B.4.a. Mechanical factors influencing structural geometry (Sections 8-9)....33

1.B.4.b. Physical properties and conditions (Appendix H)....33

2. REGIONAL FRAMEWORK.....34

2.A. REGIONAL GEOTECTONIC SETTING.....34

2.A.1. Ancestral Brooks Range.....34

2.A.2. Northeastern Brooks Range.....36

2.B. REGIONAL DEPOSITIONAL HISTORY.....37

3. STRUCTURAL STRATIGRAPHY.....41

3.A. STRUCTURAL-STRATIGRAPHIC UNITS OF THE FRANKLINIAN SEQUENCE.....41

3.A.1. Franklinian Sequence Rocks of the Northeastern Brooks Range.....41

3.A.2. Franklinian Sequence Rocks of the Franklin Mountains Anticlinorium.....41

3.B. STRUCTURAL-STRATIGRAPHIC UNITS OF THE ELLESMERIAN SEQUENCE.....45

3.B.1. Ellesmerian Sequence Rocks of the Northeastern Brooks Range.....45

3.B.2.. Ellesmerian Sequence Rocks in the Study Area.....45

4. STRUCTURAL STYLE OF THE NORTHEASTERN BROOKS RANGE AND MODELS APPLIED TO FRANKLIN MOUNTAINS STRUCTURAL ANALYSIS.....50

4.A. REGIONAL STRUCTURES.....50

4.B. PRE-MISSISSIPPIAN STRUCTURAL STYLE.....51

4.C. MODELS FOR CENOZOIC STRUCTURE BASED ON RECENT STUDIES...54

4.C.1. The Duplex Model.....54

4.C.2. Applications of the Duplex Model to the Franklinian Sequence and the Kekiktuk Conglomerate.....57

4.C.3. The Heterogeneous Strain Model.....59

4.C.4. Application of the Heterogeneous Strain Model to the Franklinian Sequence and the Kekiktuk Conglomerate.....59

4.C.5. A Comparison of Duplex and Heterogenerous Strain Models.....59

4.D. CENOZOIC STRUCTURAL STYLE OF THE ELLESMERIAN SEQUENCE...60

4.D.1. Structural Style of the Kekiktuk Conglomerate.....62

4.D.1.a. Observations of other researchers.....62

4.D.1.b. Application of structural models to this study.....62

4.D.2. Structural Style Above the Kekiktuk Conglomerate.....63

5. THE RESPONSE OF STRUCTURAL-STRATIGRAPHIC UNITS TO DEFORMATION.....64

5.A. STRUCTURAL GEOMETRY IN THE FRANKLINIAN SEQUENCE.....64

5.B. STRUCTURAL GEOMETRY IN THE ELLESMERIAN SEQUENCE.....75

5.B.1. Structural Geometry Observed Beneath the Kayak Shale.....75

5.B.2. Structural Geometry of the Kayak Shale.....80

5.B.3. Structual Geometry Observed Above the Kayak Shale..... ..82

5.C. RELATIVE CHRONOLOGY OF DEFORMATION.....85

5.C.1. Pre-Mississippian Deformation (D1).....86

5.C.2. Cenozoic Deformation (D2) of Franklinian Sequence.....88

5.C.3. Cenozoic Deformation (D2) of Ellesmerian Sequence.....88

5.C.4. Cenozoic Deformation (D3).....91

5.D. DEFORMATION MECHANISMS.....91

5.D.1. Deformation Mechanisms in the Franklinian Sequence.....93

5.D.2. Deformation Mechanisms in the Ellesmerian Sequence.....95

5.D.2.a. Deformation mechanisms in the Kekiktuk Conglomerate....95

5.D.2.b. Deformation mechanisms in the Kayak Shale....96

5.D.2.c. Deformation mechanisms in the Lisburne Group....97

5.D.2.d. Deformation mechanisms in the Sadlerochit Group....97

5.E. BASIC STRUCTURAL STYLE BASED ON FIELD OBSERVATIONS....98

6. A MODEL: THE STRUCTURAL GEOMETRY AND EVOLUTION OF THE FRANKLIN MOUNTAINS ANTICLINORIUM....100

6.A. CONSTRUCTION OF FRANKLIN MOUNTAINS ANTICLINORIUM BALANCED CROSS-SECTIONS....102

6.A.1. Location of Cross-Sections....102

6.A.2. Assumptions Made in Cross-Section Construction....102

6.B. CONTENT OF BALANCED CROSS-SECTIONS....104

6.B.1. Franklinian Sequence and Kekiktuk Conglomerate....104

6.B.2. Kayak Shale....111

6.B.3. Lisburne and Sadlerochit Groups....114

6.C. STRUCTURAL SEQUENCE....114

6.C.1. Pre-Cenozoic Evolution....114

6.C.2. Cenozoic Evolution of Franklin Mountains Anticlinorium-- First Stage....115

6.C.3. Cenozoic Evolution of Franklin Mountains Anticlinorium-- Second Stage....116

6.C.4. Cenozoic Evolution of Ellesmerian Sequence Above Kayak Shale....117

6.D. MODEL LIMITATIONS....118

6.E. MODEL IMPLICATIONS....120

6.F. MODEL VALUE....121

7. STRAIN DETERMINATIONS AND KINEMATIC ANALYSES....122

7.A. INTRODUCTION....122

7.A.1. Preparation of Samples....123

7.A.2. Summary of Strain Markers and Presentation of Data....123

7.B. INCREMENTAL STRAIN ANALYSIS....125

7.B.1. Background....125

7.B.2. Franklinian Sequence Sample....129

7.B.2.a. Age of pressure shadows....129

7.B.2.b. Structural position of sample....130

7.B.3. Ellesmerian Sequence Sample....130

7.B.3.a. Age of pressure shadows....131

7.B.3.b. Structural position of sample....131

7.B.4. Summary of Results and Interpretations....131

7.C. FINITE STRAIN ANALYSIS USING QUARTZ GRAINS....132

7.C.1. Methods....132

7.C.2. Samples....132

7.C.2.a. Kekiktuk Conglomerate....133

7.C.2.b. Ivishak Formation....133

7.C.3. Summary of Results and Interpretations....134

7.D. FINITE STRAIN ANALYSIS USING LISBURNE GROUP CORALS....134

7.E. SIGNIFICANCE OF QUANTITATIVE KINEMATIC ANALYSES....136

8. THE INFLUENCE OF MATERIAL PROPERTIES AND PHYSICAL CONDITONS ON THE STRUCTURAL STYLE OF THE FRANKLINIAN SEQUENCE....139

8.A. THE RELATION OF MATERIAL PROPERTIES TO FOOTWALL RAMP ANGLES....139

8.B. A MECHANICAL MODEL FOR THRUST SHEET FORMATION AND DISPLACEMENT....140

8.B.1. The Role of Fluid Pressure in Formation and Displacement of Coherent Thrust Sheets....140

8.B.2. Pre-Mississippian Structural Fabric and the Lithologic Heterogeneity of the Franklinian Sequence....142

8.C. RAMP LOCATION AND DETACHMENT DEPTH FOR SECOND HORSE..145

9. A MECHANICAL CONSIDERATION OF THE STRUCTURAL STYLE OF THE ELLESMERIAN SEQUENCE....148

9.A. STRUCTURAL STYLE BENEATH THE ROOF THRUST....148

9.A.1. The Influence of Structurally Overlying Franklinian Sequence Rocks..149

9.A.1.a. Tectonic load....149

9.A.1.b. Displacement of the first horse and interactions at its leading edge....150

9.A.2. The Influence of Interbedded Shale in the Kekiktuk Conglomerate....150

9.A.3. Tectonic Significance of the Unconformity Surface....154

9.A.4. The Influence of Volume-Fluid Pressure Conditions....155

9.A.4.a. Chocolate-tablet structure....156

9.A.4.b. Extension fractures....156

9.B. STRUCTURAL STYLE IN THE DETACHMENT ZONE.....159

9.B.1. Tectonic Flow of Kayak Shale.....160

9.B.2. Shear Accommodated by Roof Thrust.....160

9.B.2.a. Roof thrust of the Franklin Mountains anticlinorium.....162

9.B.2.b. Roof thrust in western part of northeastern Brooks Range.166

9.C. STRUCTURAL STYLE ABOVE THE ROOF THRUST.....166

9.C.1. Fold Geometry.....166

9.C.1.a. Description of multilayer package.....167

9.C.1.b. Thickness, compositon, and competency of Lisburne Group.....167

9.C.1.c. Thickness, composition, and competency of Sadlerochit Group.....169

9.C.2. Fault Geometry.....169

9.D. INFLUENCES OF DUPLEX THRUST SYSTEM ON ROOF SEQUENCE.....171

9.D.1. Effect of Forming Other Anticlinoria.....171

9.D.2. Relating Folding and Faulting to Horse Emplacement.....173

9.D.3. Effect of Increasing Structural Relief.....175

10. SUMMARY AND CONCLUSIONS OF STUDY.....177

10.A. SUMMARY OF FINDINGS.....177

10.A.1. A Structural Model.....177

10.A.2. Style and Evolution of Cenozoic Structures in the Franklinian Sequence.....179

10.A.3. Structural Style of Ellesmerian Sequence Beneath Kayak Shale.....180

10.A.4. Structural Style of Ellesmerian Sequence in and Above Kayak Shale...181

10.B. SIGNIFICANCE OF STUDY....182

10.B.1. Regional Significance....182

10.B.2. Significance for Field of Structural Geology....183

10.C. SUGGESTIONS FOR FURTHER STUDY....184

APPENDIX A. TERMINOLOGY RELATING TO DUPLEXES AND FAULT-BEND FOLDS....185

APPENDIX B. DESCRIPTION OF MAP UNITS....190

B.1. ELLESMERIAN SEQUENCE....190

B.1.a. Sadlerochit Group....190

B.1.b. Lisburne Group....191

B.1.c. Endicott Group....192

B.2. FRANKLINIAN SEQUENCE....193

B.2.a. Pre-Mississippian Upper Structural-Stratigraphic Package....193

B.2.b. Pre-Mississippian Middle Structural-Stratigraphic Package....193

B.2.c. Pre-Mississippian Lower Structural-Stratigraphic Package....195

APPENDIX C. SUPPLEMENTAL STRUCTURAL DATA....196

APPENDIX D. ASSUMPTIONS MADE IN CONSTRUCTION OF BALANCED CROSS-SECTIONS....199

D.1. ORIENTATION OF DIP PANELS....199

D.2. FAULT-BEND FOLD GEOMETRY....201

D.3. LOCATION OF PIN LINES....202

D.4. BALANCING METHODS USED FOR THE FRANKLINIAN SEQUENCE....205

D.5. SUB-MISSISSIPPIAN ANGULAR UNCONFORMITY....206

D.6. DEPTHS TO DETACHMENT HORIZONS....207

APPENDIX E. ORIENTATIONS OF STRAIN MARKERS.....210

APPENDIX F. INCREMENTAL STRAIN ANALYSIS.....220

F.1. EQUATIONS USED IN CALCULATIONS.....220

F.1.a. Rigid Fiber Model.....220

F.1.b. Deformable Fiber Model.....220

F.2. RESULTS OF INCREMENTAL STRAIN ANALYSIS.....220

F.2.a. Franklinian Sequence Sample.....220

F.2.b. Ellesmerian Sequence Sample.....235

F.3. ANALYSIS OF ANALYTICAL ERROR.....235

F.4. INTERPRETATIONS AND SPECULATIONS.....241

F.4.a. Franklinian Sequence: Pressure Shadow in North-Northwest-Striking Plane.....241

F.4.b. Franklinian Sequence: Pressure Shadows in East-Northeast-Striking Plane.....243

F.4.c. Ellesmerian Sequence Sample.....244

APPENDIX G. FINITE STRAIN ANALYSIS.....248

G.1. EXPLANATION OF ANALYTICAL METHODS.....248

G.1.a. Fry Method.....248

G.1.b. Normalized Fry Method.....249

G.1.c. Phi-R_f Technique.....251

G.2. ANALYTICAL PROCEDURE.....252

G.3. RESULTS.....254

G.3.a. Fry Method.....254

G.3.b. Phi-R_f Technique.....274

G.3.b.1. Strain ellipse....274

G.3.b.2. Initial marker ellipse....277

G.3.b.3. Final marker ellipse....277

G.4. ERROR ANALYSIS....280

G.4.a. Sample Preparation....280

G.4.b. Sample Suitability for Normalized Fry Method....280

G.4.c. Sample Suitablility for Phi-R_f Technique....282

G.4.d. Error Associated With INSTRAIN 2.2 Normalized Fry Method....282

G.4.e. Error Associated With INSTRAIN 2.2 Phi-R_f Technique....282

G.5. INTERPRETATIONS AND SPECULATIONS....286

G.5.a. Significance of Tectonic Strain Ellipse....286

G.5.b. Initial Marker Orientations and Ellipticities....287

G.5.c. Compatibility of Results....289

APPENDIX H. PHYSICAL PROPERTIES AND CONDITIONS....291

H.1. BULK DENSITIES OF UNITS....291

H.2. MAGNITUDE OF LOAD ABOVE KEKITKUK CONGLOMERATE....291

REFERENCES CITED....293

LIST OF FIGURES

Page No.

FIGURE 1. Location of study area in the Franklin Mountains of the northeastern Brooks Range (modified from United States Department of the Interior, 1986).....26

FIGURE 2. Location and physiography of study area between forks of Canning River.....27

FIGURE 3. Regional geologic map of northeastern Brooks Range (modified from Wallace and Hanks, in press).....29

FIGURE 4. Major geotectonic subdivisions of the Brooks Range (Wallace and Hanks, in press).....35

FIGURE 5. Generalized geologic evolution of northern Alaska (Craig et al., 1985).....38

FIGURE 6. Pre-Mississippian rocks exposed in the northeastern Brooks Range (modified from Dutro et al., 1972).....42

FIGURE 7. Structural-stratigraphic packages of Franklinian sequence rocks and lithostratigraphic units mapped in the study area.....43

FIGURE 8. Schematic lithostratigraphic column of units exposed in the study area.....46

FIGURE 9. Deformational history in Lake Peters area prior to Cenozoic orogenesis (modified from Reed, 1968).....52

FIGURE 10. End-member models for Cenozoic structural style of Franklinian sequence.....55

FIGURE 11. Duplex thrust system model of Namson and Wallace (1986), modified from Wallace and Hanks (in press).....56

FIGURE 12. Models for shortening by imbrication or development of penetrative strain in the Kekiktuk Conglomerate.....58

FIGURE 13. Contrasts in structural geometry of the Franklinian and Ellesmerian sequences.....61

FIGURE 14. Equal-area stereographic projections of poles to planes for mesoscopic structures in the Franklinian and Ellesmerian sequences.....67

FIGURE 15. Geologic map of study area with cross-section lines.....69

FIGURE 16. Macroscopic structure of Franklinian sequence rocks exposed in the study area.....70

FIGURE 17. Upper antiform cored by the Franklinian sequence and capped by the Kekiktuk Conglomerate....71

FIGURE 18. Lower antiform cored by the Franklinian sequence and capped by the Kekiktuk Conglomerate....73

FIGURE 19. Pre-Mississippian fold geometry suggested by the relationship between bedding and slaty cleavage (from Ramsay and Huber, 1987)....74

FIGURE 20. Sub-Mississippian angular unconformity defining the interface between the Franklinian sequence and the Kekiktuk Conglomerate....76

FIGURE 21. Exposures of undeformed and deformed Kekiktuk Conglomerate....77

FIGURE 22. Schematic structural geometry of folds, faults, extension fractures, and spaced cleavage in the Kekiktuk Conglomerate....78

FIGURE 23. Geologic map of study area with locations A - P referred to in text....79

FIGURE 24. Imbricates of Kekiktuk Conglomerate observed at location "C" in Figure 23....81

FIGURE 25. Detachment folds and thrust faults developed in the Lisburne Group above the Kayak Shale....84

FIGURE 26. Equal-area stereographic projection of poles to compositional layering (S_0) and slaty cleavage (S_1) in the Franklinian sequence....87

FIGURE 27. Equal-area stereographic projection of poles to bedding in Ellesmerian sequence....90

FIGURE 28. Elements of section-balancing procedure used in this study (modified from DePaor, 1988)....101

FIGURE 29. Locations of balanced cross-sections....103

FIGURE 30. Balanced cross-section across the Franklin Mountains anticlinorium....105

FIGURE 31. Balanced cross-section across the Franklin Mountains anticlinorium (Figure 30), reconstructed to pre-Cenozoic time....106

FIGURE 32. First stage in evolution of the Franklin Mountains anticlinorium....107

FIGURE 33. Balanced cross-section (D-E-H-I in Figure 15) west of primary section (Figure 30)....108

FIGURE 34. Balanced cross-section (F-G-H-I in Figure 15) east of primary section (Figure 30) and Figure 33....109

FIGURE 35. Structural evolution of the Franklin Mountains anticlinorium....110

FIGURE 36. Orientation of Cenozoic tectonic strain ellipsoid in relation to oriented thin-section planes....124

FIGURE 37. Summary of orientations of strain markers in the Franklinian and Ellesmerian sequences....126

FIGURE 38. Geometric constrasts of the rigid fiber model (A) and deformable fiber model (B) in non-coaxial deformation (from Ramsay and Huber, 1983)....128

FIGURE 39. Dependence of differential stress at failure in triaxial compression on the inclination of the cleavage plane to the compression axis (Paterson, 1978)....141

FIGURE 40. Schematic cross-section of the Franklinian sequence and Kekiktuk Conglomerate....144

FIGURE 41. Effect of loading by overthrust faulting on the depth of future detachments and location of ramps (Gretener, 1972)....146

FIGURE 42. Accommodation of displacement above Kekiktuk Conglomerate by overlying Ellesmerian sequence....152

FIGURE 43. Schematic diagrams illustrating possible factors that influenced the behavior of the Kekiktuk Conglomerate during deformation....153

FIGURE 44. Possible explanation for orientations of quartz-filled extension fractures in the Kekiktuk Conglomerate....158

FIGURE 45. Model for the flow of incompetent material into the core of a detachment anticline (from Wiltschko and Chapple, 1977)....161

FIGURE 46. Possible senses of shear accommodated by a roof thrust horizon....163

FIGURE 47. Detachment anticline in the Lisburne Group overturned to the north in the direction of tectonic transport....165

FIGURE 48. Schematic representation of possible interrelationships of buckle folds developed in competent layers (black) and incompetent host materials (unshaded) (Ramsay and Huber, 1987)....170

FIGURE 49. Progressive evolution of foreland sloping duplex thrust system consisting of three thrust sheets, A, B, and C (modified from Mitra, 1986)....186

FIGURE 50. Variations in duplex geometry produced by differences in the degree of overlap between adjacent horses (Mitra, 1986)....187

FIGURE 51. Evolution of a fault-bend fold (after Suppe, 1983).....188

FIGURE 52. Equal-area stereographic projections of poles to compositional layering (S_0) and pre-Mississippian slaty cleavage (S_1) in the upper and lower antiforms.....197

FIGURE 53. Equal-area stereographic projections of poles to bedding planes in the Ellesmerian sequence.....198

FIGURE 54. Effect of the placement of pin lines on location of bedding-plane slip associated with folding (from Woodward et al., 1985).....204

FIGURE 55. Orientation of strain markers in thin-section planes that are subparallel to compositional layering or bedding.....217

FIGURE 56. Orientation of strain markers in thin-section planes that are subvertical and strike east-northeast.....218

FIGURE 57. Orientation of strain markers in thin-section planes that are subvertical and strike north-northwest.....219

FIGURE 58. Parameters measured for calculation of incremental strain from pressure shadows under non-coaxial deformation (Ramsay and Huber, 1983).....222

FIGURE 59. Small marcasite nodule (hatched)and pressure shadow developed in the sub-vertical east-northeast-striking plane of Franklinian sequence sample 87JZ16.....223

FIGURE 60. Large marcasite nodule (hatched) and pressure shadow developed in the sub-vertical east-northeast-striking plane of Franklinian sequence sample 87JZ16.....225

FIGURE 61. Marcasite nodule (hatched) and pressure shadow developed in the subvertical north-northwest-striking plane of Franklinian sequence sample 87JZ16.....227

FIGURE 62. Incremental strain paths for the large and small pressure shadows in the sub-vertical east-northeast-striking plane of sample 87JZ16.....229

FIGURE 63. Incremental strain path for the pressure shadow in the subvertical north-northwest-striking plane of sample 87JZ16.....232

FIGURE 64. Orientation of pressure shadow fibers in the subvertical north-northwest-striking plane of Echooka Formation sample 87JZ45.....236

FIGURE 65. Histogram of fiber angles with respect to bedding for Echooka Formation sample 87JZ45.....238

FIGURE 66. Pressure shadow fiber types identified by Ramsay and Huber (1983).....240

FIGURE 67. Models modified from Sanderson (1982) for the pattern of strain developed in a thrust sheet above a footwall ramp....242

FIGURE 68. Schematic model adapted from Butler (1982) for inducing subvertical extension in the hangingwall during emplacement of underlying thrust sheets....245

FIGURE 69. Possible explanation for the orientation of fibers in sample 87JZ45....246

FIGURE 70. Plots derived from finite strain analyses....250

FIGURE 71. Effect of progressive deformation (A-C) on a series of elliptical objects with an initial orientation Ø and ellipticity R_i (Ramsay and Huber, 1983)....253

FIGURE 72. Interpreted finite strain plots for the bedding-parallel plane of Kekiktuk Conglomerate sample 87JZ25....255

FIGURE 73. Interpreted finite strain plots for Kekiktuk Conglomerate sample 87JZ25....256

FIGURE 74. Interpreted finite strain plots for the north-striking plane of Kekiktuk Conglomerate sample 87JZ25....257

FIGURE 75. Interpreted finite strain plots for bedding-parallel plane of Kekiktuk Conglomerate sample 87JZ31....258

FIGURE 76. Interpreted finite strain plots for east-northeast-striking plane of Kekiktuk Conglomerate sample 87JZ31....259

FIGURE 77. Interpreted finite strain plots for the north-northwest-striking plane of Kekitkuk Conglomerate sample 87JZ31....260

FIGURE 78. Interpreted finite strain plots for the bedding-parallel plane of Kekiktuk Conglomerate sample 87JZ36....261

FIGURE 79. Interpreted finite strain plots for east-striking plane of Kekiktuk Conglomerate sample 87JZ36....262

FIGURE 80. Interpreted finite strain plots for north-striking plane of Kekiktuk Conglomerate sample 87JZ36....263

FIGURE 81. Interpreted finite strain plots for the subhorizontal plane of Ivishak Formation sample 87JZ40....264

FIGURE 82. Interpreted finite strain plots for east-striking plane of Ivishak Formation sample 87JZ40....265

FIGURE 83. Interpreted finite strain plots for north-striking plane of Ivishak Formation sample 87JZ40.....266

FIGURE 84. Normalized Fry method strain ellipses in the subhorizontal plane.....269

FIGURE 85. Normalized Fry method strain ellipses in the subvertical east-northeast-striking plane.....270

FIGURE 86. Normalized Fry method strain ellipses in the subvertical north-northwest-striking plane.....271

FIGURE 87. Tukey sum-difference plot comparing strain ellipses obtained from finite strain analyses by the normalized Fry method and phi-R_f technique.....278

FIGURE 88. Initial marker ellipses determined by the phi-R_f technique, plotted on partially restored cross-section.....288

LIST OF TABLES

Page No.

TABLE 1. Stratigraphic thicknesses (in feet) of lithostratigraphic units in the Ellesmerian sequence....48

TABLE 2. Summary of meso- and macroscopic structures observed in structural-stratigraphic packages of Franklinian and Ellesmerian sequence rocks in the study area....65

TABLE 3. Deformational history of the Franklinian sequence....66

TABLE 4. Deformational features and inferred deformation mechanisms in the Franklinian and Ellesmerian sequences....68

TABLE 5. Total shortening for the Franklinian and Ellesmerian sequences....112

TABLE 6. Comparison of the physical properties of the first and second horses of the Franklin Mountains anticlinorium....113

TABLE 7. Displacement on thrust faults developed in the Ellesmerian sequence....119

TABLE 8. Average finite strain ratios determined by the normalized Fry method and Ø-R_f technique....135

TABLE 9. Summary of basic assumptions made during cross-section construction....200

TABLE 10. Summary of orientations of stylolites in oriented samples from the Franklinian and Ellesmerian sequences....212

TABLE 11. Summary of orientations of extension fractures in oriented samples from the Franklinian and Ellesmerian sequences....213

TABLE 12. Summary of orientations of pressure shadows in oriented samples from the Franklinian and Ellesmerian sequences....214

TABLE 13. Summary of orientations of quartz grains, micaceous minerals, and deformed corals in oriented samples from the Franklinian and Ellesmerian sequences....215

TABLE 14. Summary of orientations of kinematic indicators in oriented samples from the Franklinian and Ellesmerian sequences....216

TABLE 15. Summary of incremental strain determinations, fiber orientations and mineralogy for the small pressure shadow in the subvertical east-northeast-striking plane of pre-Mississippian sample 87JZ16 (Figure 59)....224

TABLE 16. Summary of incremental strain determinations, fiber orientations and mineralogy for the large pressure shadow in the subvertical east-northeast-striking plane of pre-Mississippian sample 87JZ16 (Figure 60).....226

TABLE 17. Summary of incremental strain determinations, fiber orientations and mineralogy for the pressure shadow in the subvertical north-northwest-striking plane of pre-Mississippian sample 87JZ16 (Figure 61).....228

TABLE 18. Comparison of incremental strains calculated by rigid and deformable models of Ramsay and Huber (1983) for the small pressure shadow in the subvertical east-northeast-striking plane of pre-Mississippian sample 87JZ16 (Figure 59).....230

TABLE 19. Comparison of incremental strains calculated by rigid and deformable models of Ramsay and Huber (1983) for the large pressure shadow in the subvertical east-northeast-striking plane of pre-Mississippian sample 87JZ16 (Figure 60).....231

TABLE 20. Comparison of incremental strains calculated by rigid and deformable models of Ramsay and Huber (1983) for the north side of the pressure shadow in the subvertical north-northwest-striking plane of pre-Mississippian sample 87JZ16 (Figure 61).....233

TABLE 21. Comparison of incremental strains calculated by rigid and deformable models of Ramsay and Huber (1983) for the south side of the pressure shadow in the subvertical north-northwest-striking plane of pre-Mississippian sample 87JZ16 (Figure 61).....234

TABLE 22. Orientations of fibers relative to bedding and total strain values determined for eleven pressure shadows in subvertical north-northwest-striking plane of sample 87JZ45 from the Echooka Formation (Figure 64).....237

TABLE 23. Comparison of finite strain ratios determined by the conventional and normalized Fry methods using INSTRAIN 2.2.....267

TABLE 24. Summary of data for strain ellipse shape and orientation determined by the normalized Fry method options of INSTRAIN 2.2.....268

TABLE 25. Normalized Fry method data from INSTRAIN 2.2, ranked in order of decreasing ellipticity of the strain ellipse (R).....273

TABLE 26. Summary of finite strain data derived by the Ø-R_f technique using INSTRAIN 2.2, including the initial and final marker ellipticities (R_i and R_f), the shape of the tectonic strain ellipse (R_S), and the fluctuation in Ø' (F).....275

TABLE 27. Ranked ellipticities for the strain ellipse, Rs, determined by the Ø-R_f technique option of INSTRAIN 2.2.....276

TABLE 28. Samples ranked by the ellipticities of both initial (R_i) and final (R_f) markers.....279

TABLE 29. Finite strain data determined by the normalized Fry method option of INSTRAIN 2.2, sorted by the percent error associated with the determination of the shape and orientation of the strain ellipse by INSTRAIN 2.2 283

TABLE 30. Orientation of strain ellipse axis, Ø, determined by Ø-R_f technique and normalized Fry method options of INSTRAIN 2.2.....285

TABLE 31. Initial (R_i) and final (R_f) marker ellipticities averaged for three samples from the Kekiktuk Conglomerate and compared with those determined for the sample from the Ivishak Formation 290

LIST OF PLATES

PLATE 1. Geologic map of study area between forks of Canning River.

PLATE 2. Primary balanced cross-section constructed across the Franklin Mountains anticlinorium.

PLATE 3. Primary balanced cross-section across the Franklin Mountains anticlinorium, reconstructed to pre-Cenozoic time.

PLATE 4. Primary balanced cross-section, reconstructed to Cenozoic time following the emplacement of the first horse of the anticlinorium.

PLATE 5. Balanced cross-sections constructed across the northern limb of the Franklin Mountains anticlinorium to the west and east of the primary section.

ACKNOWLEDGMENTS

To my thesis committee, Wesley K. Wallace, Lewis H. Shapiro, and Keith F. Watts, I extend heartfelt thanks for the time and interest they invested in my behalf over the past three years, from the initial planning stages to the final editing of this text. I offer special thanks to Wesley K. Wallace, my thesis advisor, for sparking my interest in structural studies in the northeastern Brooks Range, and for his assistance in defining the nature and scope of the study, his guidance and encouragement, and his willingness to grant me the latitude to pursue creative work. The valuable editorial assistance, insight, and ideas of Lewis H. Shapiro and Keith F. Watts are much appreciated and improved this text.

Generous contributions of funds from Chevron U.S.A., Inc., Conoco Inc., Exxon Company, U.S.A., Marathon Oil Company, BP Exploration (Alaska), and Texaco U.S.A. covered helicopter costs necessary for access to and support of fieldwork in the Franklin Mountains. Field research was supported by grants from the American Association of Petroleum Geologists and Amoco Production Company. The Alaska Division of Geological and Geophysical Surveys is thanked for general assistance and logistical support during the fieldwork. Peter B. Skidmore's assistance in the field helped make the summer between the forks of the Canning River a safe, productive, and enjoyable experience. Finally, this study was completed with much appreciated funding from the northeastern Brooks Range Geological Research Program of the Tectonics and Sedimentation Research Group at the University of Alaska Fairbanks.

1. INTRODUCTION

The objective of modern detailed structural analysis is to gain a comprehensive understanding of the geologic structure of a region. Integrating all available data, observations and interpretations, the structural geologist aims to describe the structural evolution of the given region, employing three basic analytical "strategies" (Davis, 1984): (1) descriptive analysis aimed at characterizing the geometry of geologic structures and deciphering the deformational history of the area; (2) kinematic analysis aimed at interpreting the sequence and direction of deformational movements which may have produced the observed structures; and (3) dynamic analysis aimed at modeling the system of forces which may have produced the structural geometry observed and the interpreted sequence of deformational movements. Thus, each strategy addresses distinct aspects of a region's structural evolution.

1.A. LOCATION AND SCOPE OF STUDY

This detailed structural analysis addresses the structural geometry, structural sequence and kinematics, and deformational mechanics of structures in a region of the western Franklin Mountains, between the forks of the Canning River, northeastern Brooks Range, Alaska (longitude 145° 50' W, latitude 69° 05' N). The study area lies within the western Arctic National Wildlife Refuge (ANWR), approximately 100 miles (161 kilometers) south-southeast of Prudhoe Bay, 26 miles (42 kilometers) west-southwest of Mt. Chamberlain, the second highest peak of the Brooks Range at 9,020 feet above sea level, and 124 miles (200 kilometers) west of the United States-Canada border (Figure 1). The roughly 30 mi^2 (77 km^2) study area is bounded to the east by the main fork of the Canning River and to the west by the Marsh Fork (Figure 2). Northern and southern boundaries of the study area lie 4.4 miles (7.1 kilometers) and 12 miles (19.4 kilometers) south of the forks of the Canning, respectively. The north-south extent of the study area was determined by time constraints and the limitations imposed by accessibility and weather conditions. The terrain is mountainous, with nearly 5,000 feet of vertical relief. Roughly 60-70% of the study area is exposed as accessible outcrops, inaccessible cliffs, scree, or slopes

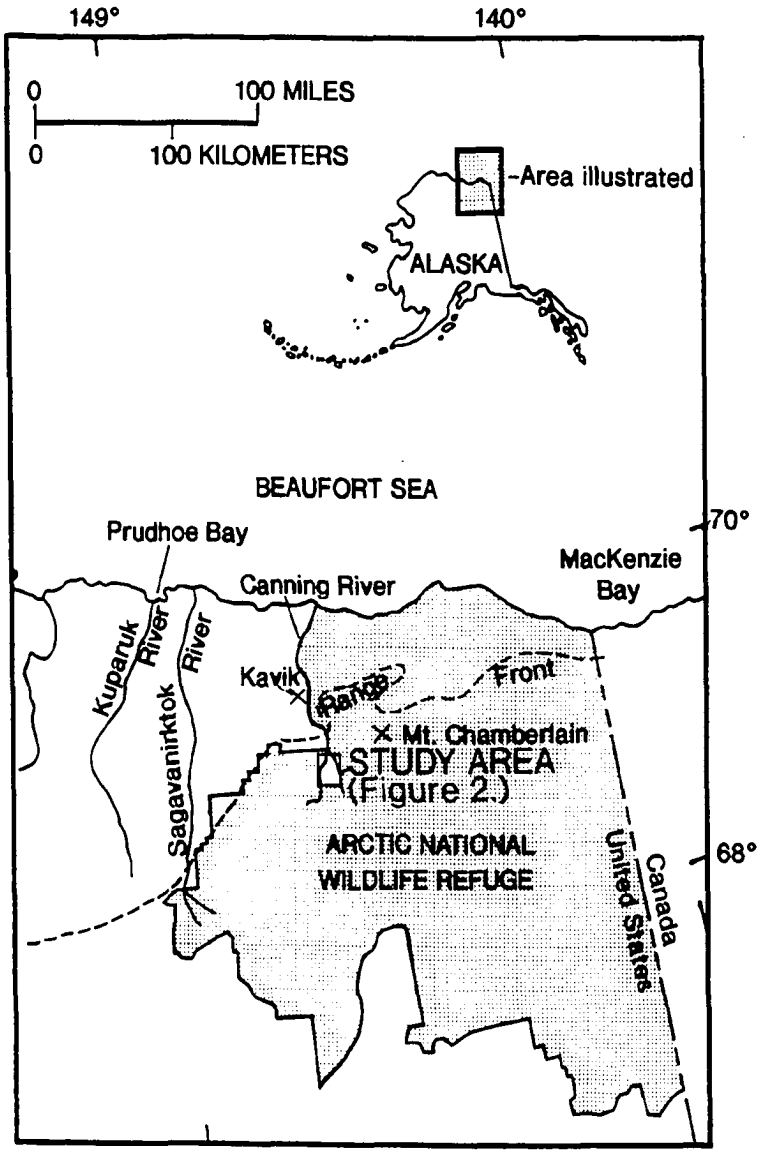

FIGURE 1. Location of study area in the Franklin Mountains of the northeastern Brooks Range, pertinent geographic points, and boundaries of the Arctic National Wildlife Refuge (ANWR) (modified from United States Department of the Interior, 1986).

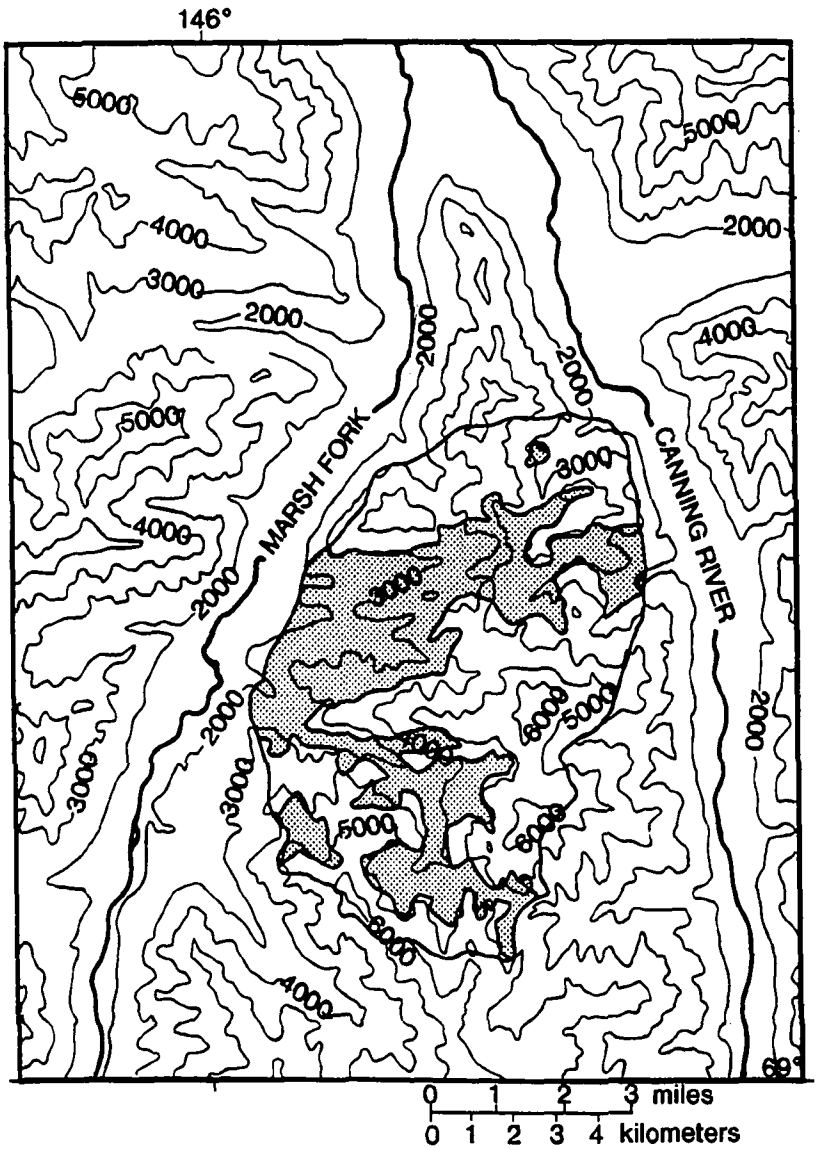

FIGURE 2. Location and physiography of study area between forks of Canning River. Shaded areas are poorly-exposed, tundra-covered river valleys. Topography compiled from Mt. Michelson (A-4) and (A-3) quadrangles.

with thin tundra-cover. Tundra and low thicket cover the remaining 30-40%. The study area was reached and camps were placed and supplied by helicopter from Kavik airstrip (Figure 1). Fieldwork was completed by traverses from several remote spike camps during a seven-week period of June-July, 1987. The study area was mapped at a scale of 1:25,000; structural data and both oriented and unoriented samples were collected.

1.B. OVERVIEW OF FRANKLIN MOUNTAINS STRUCTURAL ANALYSIS

The study area is located in the southwestern portion of the northeastern Brooks Range fold-and-thrust belt, on the north flank of the southern of two anticlinoria which comprise the Franklin Mountains, referred to herein as the "Franklin Mountains anticlinorium" (Figure 3). This study describes and interprets the evolution of structures documented in pre-Mississippian rocks of the Franklinian sequence which lie below a prominent sub-Mississippian angular unconformity, and in the overlying Mississippian to Lower Triassic rocks of the Ellesmerian sequence. The following subsections address the methods employed in each of the analytical strategies of Davis (1984) and how these methodologies are incorporated in this study, and outline the basic organization and content of the thesis.

1.B.1. Background Material (Sections 2-4)

Section 2 reviews the regional geologic framework, including the geotectonic settings of the Brooks Range in general and of the northeastern Brooks Range in particular, and the depositional history of the northeastern Brooks Range. Section 3 outlines the regional structural stratigraphy of the Franklinian and Ellesmerian sequences and describes the structural-stratigraphic units exposed in the study area. Section 4 summarizes current understanding of the structural style expressed by the Franklinian and Ellesmerian sequences. End-member structural models, based upon the interpretations of other researchers, are presented in Section 4. These models provide a framework for discussions of the structural evolution of the Franklin Mountains anticlinorium in Sections 6-9. Appendix A contains pertinent information regarding one of the end-member models. Section 4 discusses some of the

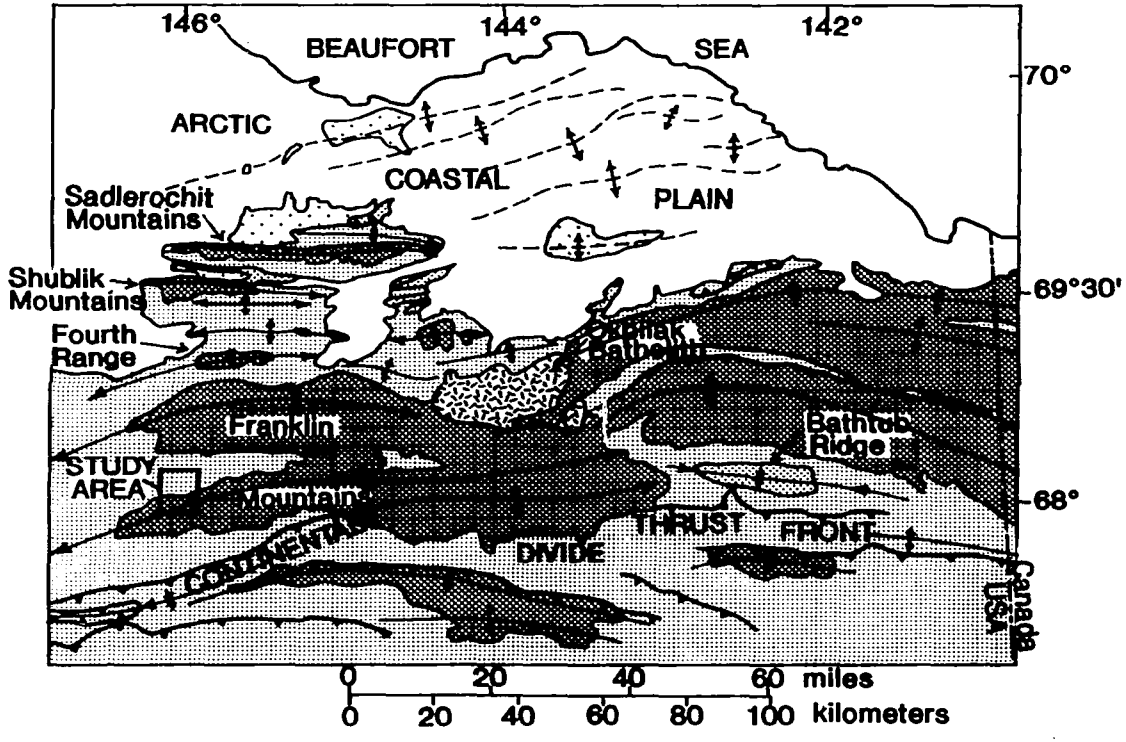

Upper Cretaceous to Tertiary deposits (Brookian sequence)

Lower Cretaceous units (uppermost Ellesmerian and lowermost Brookian sequences)

Mississippian to Lower Cretaceous deposits (Ellesmerian sequence)

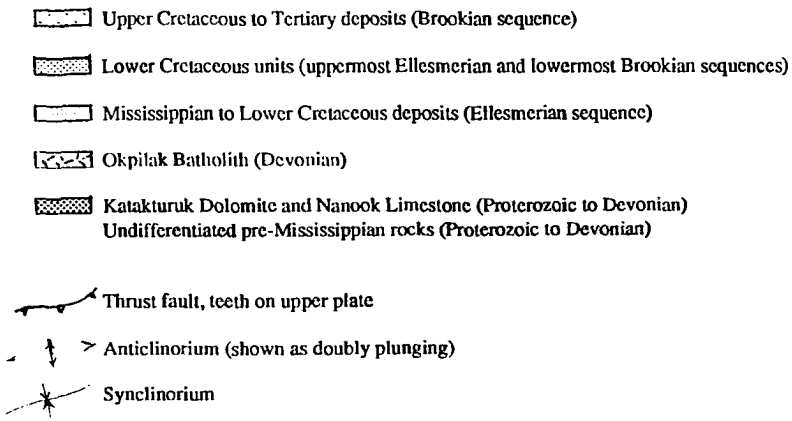

FIGURE 3. Regional geologic map of northeastern Brooks Range (modified from Wallace and Hanks, in press).

implications of these end-member models, in terms of the possible deformational behavior of both the Franklinian sequence rocks that comprise thrust sheets exposed in the region, and of the Ellesmerian sequence rocks that overlie them. Finally, Section 4 also identifies specific problems that are addressed by this study.

1.B.2. Description of Structural Geometry

The fundamental strategy of detailed structural analysis, which Davis (1984) calls descriptive analysis, focuses on recognizing and understanding the geometry, orientation, and relative chronology of geologic structures in a study area. Descriptive analysis incorporates careful, detailed and insightful field observations and systematically collected, representative data regarding the absolute and relative orientations of rock units and structures. These structures are observed and described at mesoscopic, macroscopic, and microscopic scales.

In recent decades, the construction of balanced geologic cross-sections has become a powerful method of modeling the geometry of geologic structures. The concept that bed-length or cross-sectional area is conserved during deformation, allowing construction of a "balanced" or "retrodeformable" cross-section, was first discussed by Dahlstrom (1969). According to the concept, a cross-sectional interpretation of the geometry of deformed rock units must restore to produce a "palinspastic reconstruction," or a coherent picture of the predeformational geometry (Ramsay and Huber, 1987). The construction of a balanced geologic cross-section establishes a framework for relating mesoscopic structures to their position with respect to macroscopic structures. The utility of this modeling method may derive from the apparent fact that there are a limited number of fundamental geometries of thrust fault systems and thrust-related folds that occur in nature and can thus be incorporated into balanced cross-sections constructed across foreland fold-and-thrust belts.

1.B.2.a. Field description of structural geometry (Section 5)

Section 5 addresses the response of the Franklinian and Ellesmerian sequences to deformation,

including the structural geometry developed below and above the sub-Mississippian unconformity, the mechanisms which produced the observed structures, and their relative chronology. Specific goals are (1) to describe structures in the Franklinian sequence and distinguish between those which formed during pre-Mississippian and those which formed during Cenozoic deformation; and (2) to characterize the deformational geometries developed in each structural-stratigraphic unit of the Ellesmerian sequence. The ultimate objective of this section is to establish the basic structural style which characterizes the Franklinian sequence and each structural-stratigraphic unit of the Ellesmerian sequence. Lithologic descriptions of rock units mapped in the Franklinian and Ellesmerian sequences are provided in Appendix B. Structural data included in Appendix C supplement those data in Section 5.

1.B.2.b. Structural geometry modeled in balanced cross-sections (Section 6)

Section 6 presents a balanced cross-section model which is based on the structural geometry described in the preceding section, and on the interpreted basic structural style (i.e. duplexing of Franklinian sequence, detachment folding within Ellesmerian sequence). The objective of this section is to model the evolution of the Franklin Mountains anticlinorium in terms of the displacement and deformational histories of the thrust sheets of Franklinian sequence rocks which core the anticlinorium. Thus, Section 6 proposes a kinematic model for the evolution of the structural geometry observed in the study area. Appendix D describes the assumptions made during the construction of balanced cross-sections across the Franklin Mountains anticlinorium (Plates 2-5).

1.B.3. Description of Structural Sequence

Kinematic analysis, the second strategy of detailed structural analysis, models a sequence of deformational movements which might have produced the observed structural geometry. Two basic methodologies are useful in determining the structural sequence in a study area. First, the construction of time-sequential balanced cross-sections can model macroscopic movements as deformation progresses. A second approach considers how a mesoscopic or microscopic passive marker, such as a quartz vein or

fossil, appears to have been modified during the host rock's deformational history. Quantitative strain determination techniques are valuable in the study of fold-and-thrust belt tectonics. Strain determinations can substantiate the structural sequence modeled in a balanced cross-section. Similarly, construction of balanced cross-sections establishes a framework for viewing strain data in terms of the position of structures being analyzed, and in the context of the sequence of deformational movements modeled at a macroscopic scale.

1.B.3.a. Integration of strain data with balanced cross-section (Section 7)

Building upon the preceding section, Section 7 applies techniques of strain determination and kinematic analysis to the task of understanding and describing the structural sequence. Several oriented thin-sections of rocks of the Franklinian sequence, the Mississippian Kekiktuk Conglomerate, and the Permian-Lower Triassic Sadlerochit Group contain strain indicators from which incremental or finite strains could be determined. Quantitative strain analysis, at a microscopic scale, was aimed at discerning the shape and orientation of the bulk strain ellipse which describes penetrative deformation in a given plane. As a result of this analysis, it may be possible to relate penetrative strain of a sample to its position with respect to the structures modeled in Section 6, thus constraining the geometric and kinematic model with quantitative strain or kinematic data. Strain markers used to infer the orientation of the bulk strain ellipsoid are further described in Appendix E.

1.B.3.b. Incremental and finite strain determinations (Appendices F-G)

Incremental and finite strain determinations are briefly summarized in Section 7. More complete presentations of the results and possible interpretations of incremental and finite strain analyses are addressed in detail in Appendices F and G, respectively.

1.B.4. Description of Structural Mechanics

Dynamic analysis, the third strategy of detailed structural analysis, attempts to model a system of forces which could have created the interpreted geometry and sequence of geologic structures. In a

fold-and-thrust belt geologic setting, dynamic analysis is directed at understanding the mechanics of the thrust system and fault-related folds which may have evolved during deformation. Through the mid-1900s, structural geologists were hard-pressed to propose a mechanism whereby serveral-kilometer-thick coherent packages of rocks could be transported many tens-of-kilometers while remaining intact. A possible partial explanation of this "paradox of overthrusting" was provided by Hubbert and Rubey's (1959) classic paper, which discussed the role of fluid pressure in the mechanics of overthrust faulting. A number of subsequent researchers have challenged and built upon Hubbert and Rubey's theory and mechanical interpretations, and balanced cross-sections have been found to provide valuable information that can constrain such analyses.

1.B.4.a. Mechanical factors influencing structural geometry (Sections 8-9)

Sections 8 and 9 utilize the balanced cross-section models, field observations, strain determinations, and kinematic data in discussions of the physical factors which may have affected the structural styles displayed by the Franklinian and Ellesmerian sequences. The objective of these two sections is to provide possible mechanical explanations for the interpreted response of these rocks to Cenozoic deformation. For the Franklinian sequence, the goal is to identify reasonable mechanical models for the mode of emplacement of the thrust sheets that comprise the anticlinorium, and possible implications of the observed deformational geometry. For the Ellesmerian sequence, the aim is to investigate how structural geometry might have been influenced by the mechanical stratigraphy and by Cenozoic deformation of the underlying Franklinian sequence.

1.B.4.b. Physical properties and conditions (Appendix H)

Appendix H includes calculations of the densities of rock units and the overburden pressures that may have existed at the time of Cenozoic deformation, and investigates the nature of the stresses required and the variables that may have influenced the formation of the anticlinorium. The attempt to quantify physical properties and conditions provides information that is emphasized qualitatively in Sections 8-9.

2. REGIONAL FRAMEWORK

2.A. REGIONAL GEOTECTONIC SETTING

The North American Cordillera formed during Mesozoic-Cenozoic time as a result of convergence along the western margin of the North American plate, probably punctuated by collisions of exotic terranes. Alaska's east-trending Brooks Range constitutes the northernmost portion of this mountain belt, which elsewhere trends north-south, parallel to the western margin of the conterminous United States and Canada. The northeastern Brooks Range forms a salient which protrudes northward from the rest of the Brooks Range, between the Sagavanirktok and Mackenzie Rivers (Figures 1 and 3). The geotectonic evolution of northern Alaska during late Mesozoic-Cenozoic time reflects a plate-tectonic interplay between formation of the Arctic Ocean basin to the north and the accretion and dextral strike-slip motion of tectonostratigraphic terranes to the south, along the northeastern margin of the Pacific Ocean basin (Dutro, 1981; Hubbard et al., 1987; Smith, 1987).

2.A.1. Ancestral Brooks Range

The Mississippian to Jurassic rocks of the Brooks Range apparently formed on a south-facing continental margin and were deformed to create the ancestral Brooks Range during Middle Jurassic to Early Cretaceous time (Dutro, 1981; Craig et al., 1985; Mull, 1985; Hubbard et al., 1987). Associated with convergent collapse of the passive margin, a northward-moving island arc terrane is interpreted to have collided with the continental margin of northern Alaska, resulting in obduction of oceanic crust and island arc material onto the margin of northern Alaska in Middle to Late Jurassic time (Dutro, 1981; Box, 1985; Mull, 1985; Hubbard et al., 1987). In this compressional tectonic setting, the allochthonous thrust slices which comprise the northern, eastern, and southern portions of the Brooks Range (Figure 4) were transported to the north, accommodating up to several hundred kilometers of crustal shortening (Mull, 1982; 1985). To the north of the ancestral Brooks Range, rifting which led to the formation of the Canada basin began during Late Jurassic-Early Cretaceous time, probably slightly later than collapse

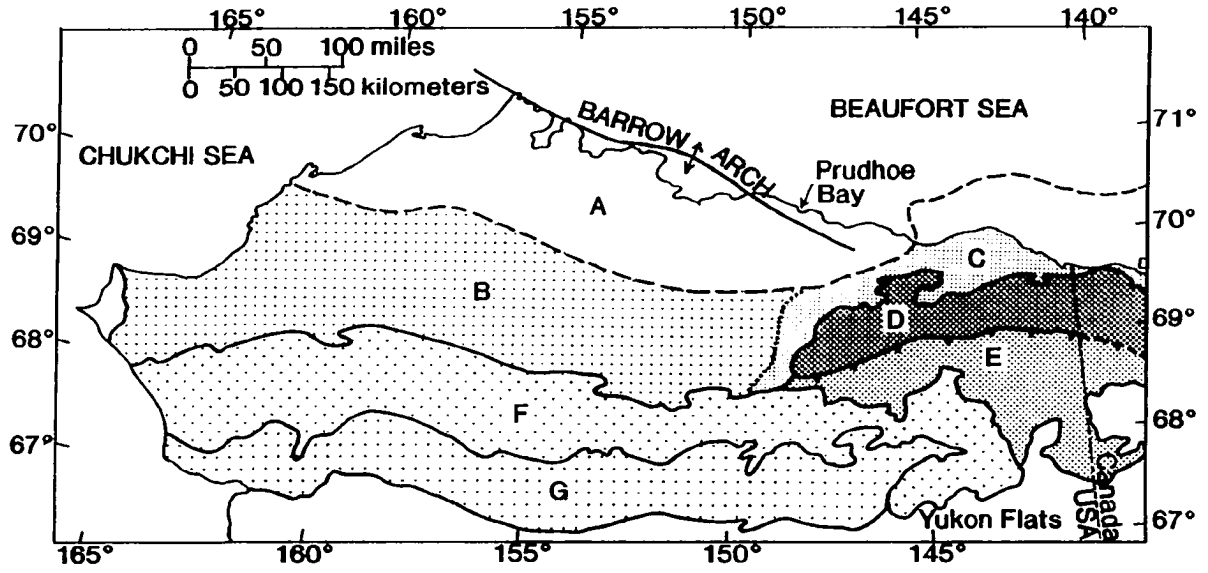

FIGURE 4. Major geotectonic subdivisions of the Brooks Range. (A) Arctic coastal plain and shelf (undeformed foredeep and passive margin deposits); (B) Western and central foothills (deformed foredeep deposits); (C) Eastern foothills, coastal plain and shelf (deformed foredeep deposits); (D) Northeastern Brooks Range (parautochthonous); (E) Eastern Brooks Range (parautochthonous to allochthonous); (F) Northern Brooks Range (allochthonous); (G) Southern Brooks Range (parautochthonous to allochthonous) (Wallace and Hanks, in press).

of the continental margin to the south (Grantz and May, 1983; Crane, 1987; Hubbard et al., 1987; Smith, 1987). Late Jurassic failed rifting was followed by the onset of successful rifting during Hauterivian (Neocomian) time, creating the Arctic continental margin (Hubbard et al., 1987).

2.A.2. Northeastern Brooks Range

The northeastern Brooks Range differs tectonically and structurally from the rest of the Brooks Range in several important ways. First, late Mesozoic-Cenozoic deformation in the northeastern Brooks Range did not involve tectonic transport of allochthonous thrust sheets hundreds of kilometers to the north as occurred in the northern, southern, and eastern portions of the Brooks Range (Figure 4) (Mull, 1982; Wallace and Hanks, in press). Deformed rocks in the northeastern Brooks Range are considered to be parautochthonous, with the magnitude of crustal shortening only on the order of tens of kilometers (Namson and Wallace, 1986; Leiggi, 1987; Wallace and Hanks, in press). Second, as shown in Figure 3, the "continental divide thrust front" represents the southern boundary of the northeastern Brooks Range fold-and-thrust belt, defining the northernmost extent of Mississippian and younger rocks which display north-vergent thrust faults and folds similar to those developed in the Brooks Range to the south and southwest (Wallace and Hanks, in press). In the eastern part of the Brooks Range, thrust sheets indicative of major crustal shortening lie south of the continental divide thrust front, 75 kilometers or more to the south of the range front of the northeastern Brooks Range (Figures 3 and 4). In contrast, in the western part of the Brooks Range such thrust sheets extend to the range front region, which lies at a lower latitude than in the east (Figure 4) (Mull, 1985). Finally, pre-Devonian rocks are extensively exposed in the northeastern Brooks Range (Figure 3) as a consequence of formation of structural highs during the evolution of the fold-and-thrust belt (Figure 3). Elsewhere, rocks of this age are exposed only near the core of the orogenic belt to the south (Wallace and Hanks, in press).

Assuming that the orogenic front migrated from south to north during late Mesozoic-Cenozoic time, the more northerly position of the northeastern Brooks Range with respect to the rest of the Brooks

Range would suggest that this fold-and-thrust belt formed later than the ancestral Brooks Range to the south and west (Wallace and Hanks, in press). This interpretation is supported by U-Pb and K-Ar dates obtained from the Okpilak batholith (Figure 3) in the central portion of the northeastern Brooks Range that indicate that a metamorphic and subsequent cooling event occurred at 61-59 Ma (Dillon, 1987; Dillon et al., 1987; Wallace and Hanks, in press). In addition, a recent apatite fission-track study by O'Sullivan (1988) documents progressively younger ages of rapid cooling (uplift) to the north from Bathtub Ridge (62 Ma), to the Arctic Creek region (37 Ma), with final uplift at the Canning River near the Sadlerochit and Shublik Mountains post-dating uplift at Arctic Creek (Figure 3). This age progression suggests that the orogenic front migrated from south to north during episodic Cenozoic deformation in the northeastern Brooks Range. Cenozoic deformation in the northeastern Brooks Range is also suggested by the presence of deformed Tertiary and Upper Cretaceous rocks in the vicinity of the Sadlerochit and Shublik Mountains (Figure 3), indicating that this northwestern portion of the northeastern Brooks Range probably was not involved in fold-and-thrust belt deformation until the Tertiary (Mull, 1985).

2.B. REGIONAL DEPOSITIONAL HISTORY

The stratigraphy of the northeastern Brooks Range is subdivided into the Franklinian, Ellesmerian, and Brookian sequences, each of which represents a distinct phase in the geotectonic evolution of the region (Figure 5) (Lerand, 1973). These depositional sequences record major cycles of sediment deposition and are bounded by unconformities which reflect important regional changes in basin geometry (Hubbard et al., 1987).

The **Franklinian sequence** is comprised of heterogeneous rocks of pre-Mississippian age (>360 Ma). Moore et al. (1987) suggest that the Franklinian sequence is an amalgamation of tectonostratigraphic terranes, assembled along an active continental margin in the Arctic region prior to Middle Devonian time. Pre-Mississippian rocks in the northeastern Brooks Range are lithologically and

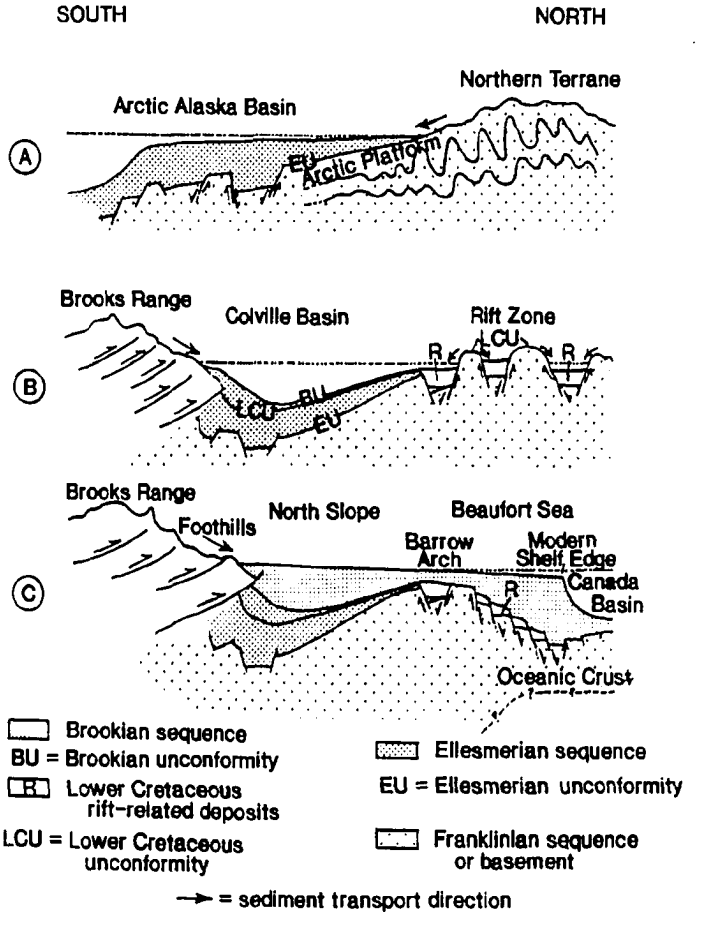

FIGURE 5. Generalized geologic evolution of northern Alaska (Craig et al., 1985). The Middle Devonian-Early Cretaceous geologic setting is shown in (A); Early Cretaceous and Early Cretaceous-Tertiary settings are shown in (B) and (C), respectively.

structurally similar to those observed in the Canadian Arctic Islands, suggesting that northern Alaska may have been adjacent to the Canadian Arctic, northeast of its present location, prior to late Mesozoic-Cenozoic time (Dutro, 1981; Hubbard et al., 1987; Smith, 1987).

A prominent angular unconformity separates pre-Mississippian units of the Franklinian sequence from the **Ellesmerian sequence**, which is comprised of siliciclastic and carbonate rocks interpreted to have been deposited on a south-facing passive continental margin from Mississippian to Early Cretaceous (Neocomian) time (Dutro, 1981). The northern provenance of these sediments is indicated by paleocurrent indicators and by stratigraphic units that have coarse fluvial-deltaic sediments along Alaska's northern margin and pass southward into finer-grained, deeper-water sediments (Keller et al., 1961; Brosgé et al., 1962; Sable, 1977; Dutro, 1981). Mississippian terrigenous clastic rocks are interpreted to have been deposited on the sub-Mississippian unconformity surface by fluvial and deltaic systems, which eventually were flooded during northward transgression (Reed, 1968; Nilsen, 1981; LePain and Crowder, 1989). Extensive shallow-marine carbonate platform deposition characteristic of Mississippian and Pennsylvanian time was terminated by a significant pre-Permian unconformity. Permian calcareous shales and glauconitic sands typically disconformably overlie the Carboniferous limestones (Sable, 1977; Hubbard et al., 1987). Progradation of coarse siliciclastic sands during the Lower Triassic caused clastic sedimentation to commence in a shallow marine environment (Hubbard et al., 1987). By the Late Triassic, phosphatic shales indicate that marine transgression placed the basin in a deep-water setting, with shale and minor sands characterizing Jurassic to Neocomian shelf deposits (Sable, 1977; Dutro, 1981). A Lower Cretaceous unconformity separates the Mississippian-Lower Cretaceous portion of the Ellesmerian sequence from overlying siliciclastic rocks deposited following the onset of Late Jurassic-Early Cretaceous rifting, which led to the formation of an Arctic continental margin and the Canada basin (Crane, 1987; Hubbard et al., 1987; Smith, 1987).

Pre- or syn-rift orogenesis led to uplift of the ancestral Brooks Range, creating a new sediment

source which reversed basin polarity (Mull, 1985; Hubbard et al., 1987). Detritus of the Lower Cretaceous to Recent **Brookian sequence** was shed from the ancestral Brooks Range northward into a foredeep known as the Colville trough (or Colville basin) (Dutro, 1981; Mull, 1985). Flysch grades upward into shallower-water shales of Aptian and Albian age, overlain by Albian and Cenomanian molasse (Mull, 1985). During Neocomian and Aptian time, the axis of the foredeep apparently trended roughly east-west, parallel to the orogenic front of the ancestral Brooks Range (Mull, 1985). However, by Cenomanian time, foredeep deposition was restricted to the eastern region of the Brooks Range, with sediments prograding to the northeast or east (Mull, 1985). Pre-Brookian rocks between the Canada basin to the north and the Colville basin to the south formed a relative structural high which influenced Brookian sedimentation (Hubbard et al., 1987). This east-trending high, called the Barrow arch (Brosgé and Tailleur, 1970), developed as a consequence of uplift and rifting of the Arctic continental margin and was bounded by zones of subsidence to the north and south as Brookian sediments accumulated in the Colville trough (Mull, 1985; Hubbard et al., 1987). Bird and Bader (1987) infer that the Ellesmerian sequence immediately north of the mountain front prior to formation of the northeastern Brooks Range was overlain by nine kilometers of Brookian sediment. Later uplift of the northeastern Brooks Range led to erosion of the Brookian sequence. Lower Cretaceous and younger rocks are not exposed in the Franklin Mountains; the nearest exposures lie roughly 15 miles (24 kilometers) to the north.

3. STRUCTURAL STRATIGRAPHY

Detailed structural analysis in the northeastern Brooks Range must consider the influence of stratigraphy on the structural evolution of the region. The lithostratigraphic units exposed in the region responded to deformation by developing characteristic structural geometries depending upon their material properties, such as mechanical competency, the thickness of beds and viscosity contrasts between interbedded rocks of different lithologies. Contiguous lithostratigraphic units which exhibit similar structural geometric responses to deformation constitute a single "structural-stratigraphic" unit or package.

3.A. STRUCTURAL-STRATIGRAPHIC UNITS OF THE FRANKLINIAN SEQUENCE

3.A.1. Franklinian Sequence Rocks of the Northeastern Brooks Range

The Franklinian sequence exposed in the northeastern Brooks Range includes a heterogeneous pre-Mississippian assemblage of slate, phyllite, quartzite, metachert, carbonate, and metavolcanic rocks. These pre-Mississippian rocks were divided into four informal units by Brosgé et al. (1962), as shown in Figure 6. According to Dutro et al. (1972), these heterogeneous pre-Mississippian units are sufficiently laterally persistent to be mapped as individual formations. However, due to complex folding and faulting, stratigraphic relationships within the pre-Mississippian assemblage have not been determined.

3.A.2. Franklinian Sequence Rocks of the Franklin Mountains Anticlinorium

The pre-Mississippian rocks studied in this structural analysis are referred to collectively as the Franklinian sequence. Franklinian sequence rocks mapped in the study area were grouped into three fault-bounded structural-stratigraphic packages. Designation of lower, middle, and upper packages is based on the relative structural positions of rock packages produced by a combination of pre-Mississippian folding and faulting and Cenozoic thrust faulting (Figure 7). The lithostratigraphic units comprising each structural-stratigraphic package (Figure 7) are summarized below. (For more

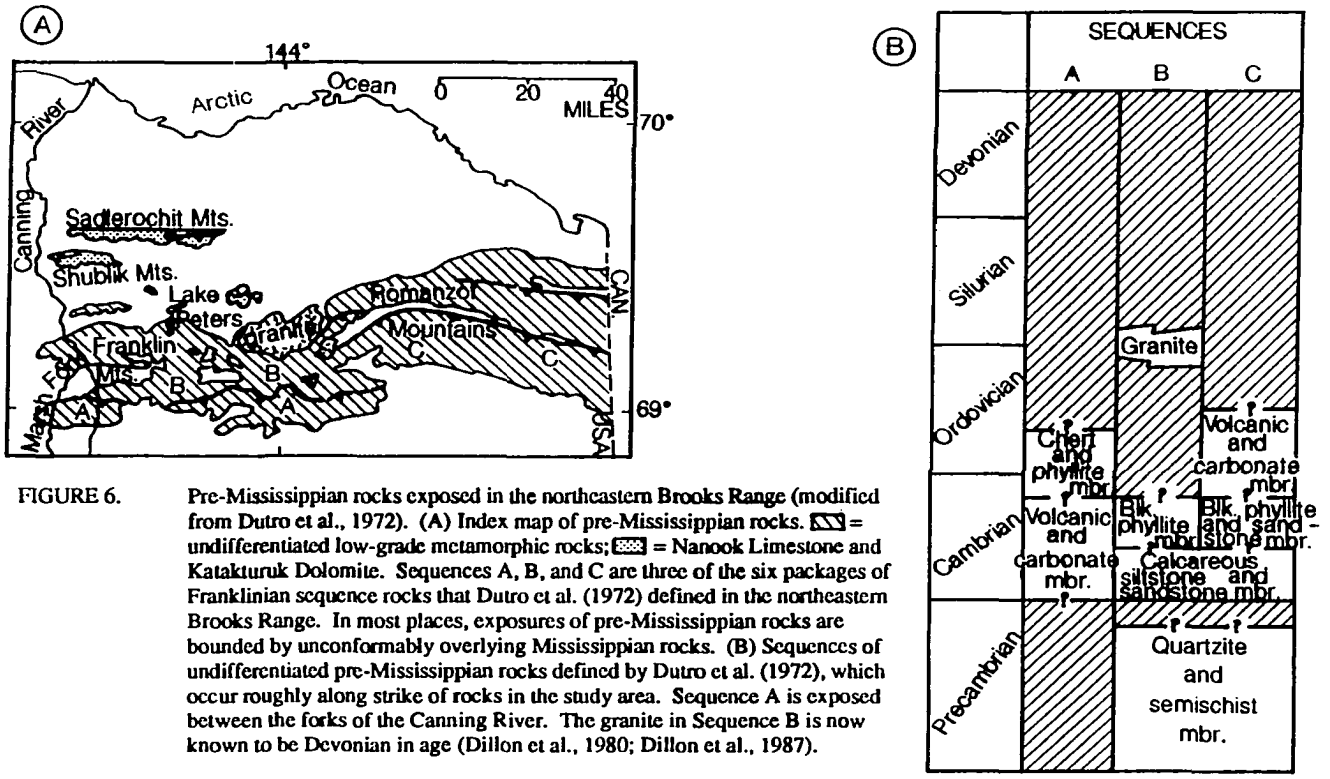

FIGURE 6. Pre-Mississippian rocks exposed in the northeastern Brooks Range (modified from Dutro et al., 1972). (A) Index map of pre-Mississippian rocks. ▨ = undifferentiated low-grade metamorphic rocks; ▩ = Nanook Limestone and Katakturuk Dolomite. Sequences A, B, and C are three of the six packages of Franklinian sequence rocks that Dutro et al. (1972) defined in the northeastern Brooks Range. In most places, exposures of pre-Mississippian rocks are bounded by unconformably overlying Mississippian rocks. (B) Sequences of undifferentiated pre-Mississippian rocks defined by Dutro et al. (1972), which occur roughly along strike of rocks in the study area. Sequence A is exposed between the forks of the Canning River. The granite in Sequence B is now known to be Devonian in age (Dillon et al., 1980; Dillon et al., 1987).

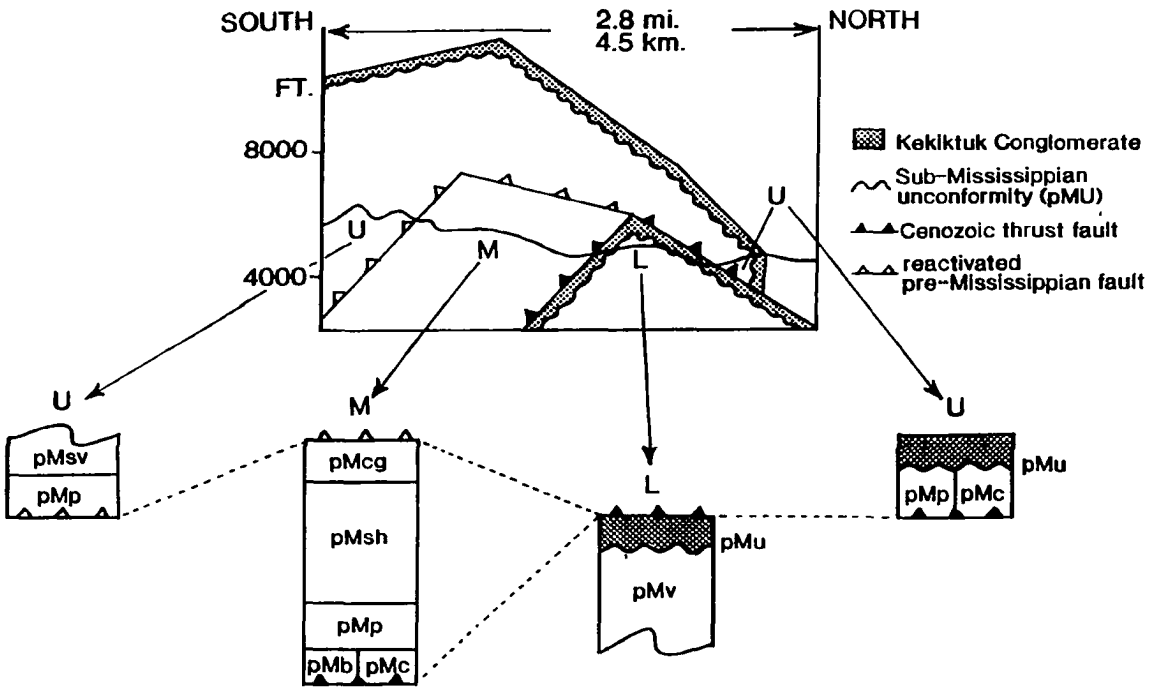

FIGURE 7. Structural-stratigraphic packages of Franklinian sequence rocks and lithostratigraphic units mapped in the study area. U, M, and L = upper, middle, and lower structural-stratigraphic packages, respectively. pMsv = slate-volcanic unit; pMp = phyllite unit; pMc = chloritic phyllite unit; pMb = brecciated unit; pMsh = shale unit; pMcg = chert-greenstone unit; pMv = volcanic unit.

detailed descriptions, refer to Appendix B.)

The **lower structural-stratigraphic package** (pMv) is comprised of a shale and phyllite unit with interbedded limestone, dolostone, and greywacke, which stratigraphically overlies shale with interbedded pillow basalt, volcanic breccia, and greenstone (Figure 7). Early Cambrian trilobites of North American affinity have been collected by Dutro et al. (1972) from a redeposited limestone, interbedded with a greywacke, which outcrops at the Marsh Fork. Since this fossil locale is along strike with the pMv unit in the study area (Plate 1), the lower structural-stratigraphic package may include rocks of Early Cambrian age.

The **middle structural-stratigraphic package** consists of tectonically brecciated phyllite and chert (pMb); purple and green phyllite (pMp); shale and phyllite with interbedded dolostone, sandstone, greenstone, and chert (pMsh); and chert and greenstone with intercalated shale (pMcg) (Figure 7). Along the Marsh Fork to the west of the study area, Moore and Churkin (1984) observed tectonic fragments of Marsh Fork volcanic rocks (pMv?) in a radiolarian chert-argillite unit which contains graptolites of Middle Ordovician age. This Middle Ordovician unit may correlate with units mapped in the middle structural-stratigraphic package.

The **upper structural-stratigraphic package** is exposed in two different parts of the study area. At the southern boundary of the study area, it consists of slate with interbedded chert and intermediate volcanic rocks (pMsv) and purple phyllite (pMp) (Figure 7). Where it structurally overlies the lower structural-stratigraphic package to the north, the upper structural-stratigraphic package consists of purple phyllite (pMp) or chloritic phyllite with interbedded recrystallized quartzite (pMc) (Figure 7). The age of the upper structural-stratigraphic packages cannot be constrained, but is likely Cambro-Ordovician.

As shown in Figure 6, Dutro et al. (1972) group the pre-Mississippian rocks exposed between the forks of the Canning River into "sequence A," which is comprised of the informal chert-phyllite and

volcanic-carbonate members of Brosgé et al. (1962). The lower structural-stratigraphic package may correlate with the volcanic-carbonate member; the middle structural-stratigraphic package, and possibly the upper one, may correlate with the chert-phyllite member. Moore (1987) analyzed samples of Lower Cambrian pillow basalts collected along the Marsh Fork and the Canning River at locations which appear to lie along strike with exposures of volcanic rocks in the study area (pMv). Moore (1987) found these rocks to be tholeiitic to mildly alkaline in composition, and the geochemical data suggest a tectonic affinity with oceanic-island basalts, continental basalts, or enriched midocean-ridge basalts. Moore (1987) cites the pillowed form and adjacent assemblage of greywacke turbidites and thin-bedded argillite with radiolarian chert as evidence supporting a noncontinental environment for the eruption of these volcanic rocks, likely on an oceanic-island or seamount. Thus, some of the Franklinian sequence rocks exposed in the vicinity of the study area may have been deposited in a Cambro-Ordovician ocean basin which was closed prior to Mississippian time.

3.B. STRUCTURAL-STRATIGRAPHIC UNITS OF THE ELLESMERIAN SEQUENCE

3.B.1. Ellesmerian Sequence Rocks of the Northeastern Brooks Range

The lithostratigraphic units which comprise the Ellesmerian sequence vary in terms of lithofacies and stratigraphic thickness across the northeastern Brooks Range. As a result, the structural geometry developed in each of these structural-stratigraphic units, and in the Ellesmerian sequence as a whole, varies somewhat across the region. Lithofacies and stratigraphic thicknesses do not appear to vary significantly within the study area.

3.B.2. Ellesmerian Sequence Rocks in the Study Area

As shown in Figure 8, the three lithostratigraphic elements of the Ellesmerian sequence exposed in the study area are (1) the Mississippian Endicott Group, (2) the Mississippian-Pennsylvanian Lisburne Group, and (3) the Permian-Lower Triassic Sadlerochit Group. As shown in Figure 8 and Plate 1,

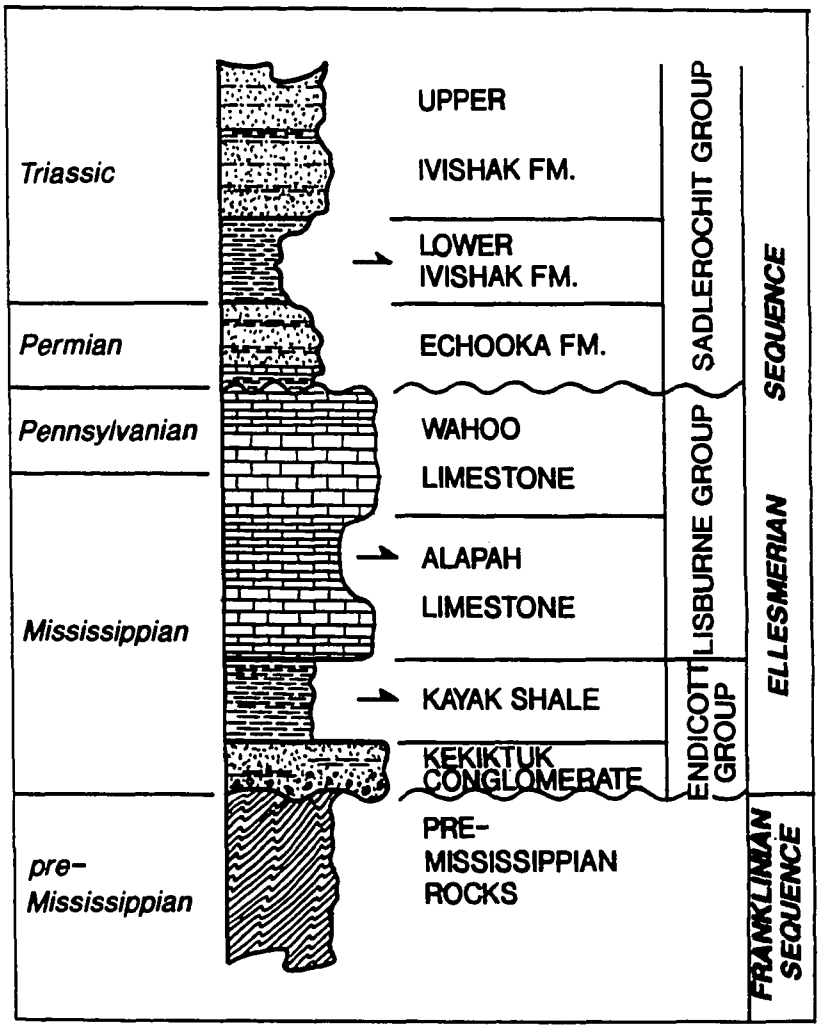

FIGURE 8. Schematic lithostratigraphic column of units exposed in the study area. Stratigraphic thicknesses of units are not to scale. Arrows identify units which are mechanically incompetent compared to adjacent rocks. The Kayak Shale facilitates structural detachment of the Lisburne Group from the Kekiktuk Conglomerate, and contrasting structural geometries are separated by this detachment horizon. Incompetent units contribute to disharmonic and polyharmonic folding within the Lisburne and Sadlerochit Groups.

lithostratigraphic units were mapped within each of these groups (refer to Appendix B for more detailed descriptions). Stratigraphic thicknesses used in balanced cross-sections constructed across the study area (Table 1, Section 6) were estimated from the location of contacts and average attitudes of bedding in the study area. These thicknesses tend to differ from those measured by Mamet and Armstrong (1972) in the Franklin Mountains and by Reed (1968) at Lake Peters (Figure 6, Table 1). In the study area, lithostratigraphic units within the Lisburne and Sadlerochit Groups are likely structurally thickened by internal shortening.

The Mississippian Endicott Group (Tailleur et al., 1967) is comprised of the Kekiktuk Conglomerate and the Kayak Shale. The Kekiktuk Conglomerate unconformably overlies the Franklinian sequence. In the study area, it is a roughly 90-meter-thick sheet of interbedded chert- and quartz-pebble- to cobble-conglomerate and quartzite, with local interbeds of carbonaceous black shale. The contact between the Kekiktuk Conglomerate and the overlying Kayak Shale commonly is gradational, with shale interbeds increasing in abundance upward toward the Kayak Shale. The Kayak Shale is a poorly-exposed, several-hundred-meter-thick unit of fissile, carbonaceous black shale with thin (1-5 cm) limestone interbeds near the contact with overlying carbonates of the Lisburne Group (Table 1).

The Mississippian-Pennsylvanian Lisburne Group (Brosgé et al., 1962) is a thick succession of platform carbonates, conformably overlying the Mississippian Kayak Shale. Three lithostratigraphic units were mapped in the study area: (1) the Mississippian lower Alapah Limestone, a thin- to massive-bedded, cliff-forming unit of lime mudstone and bryozoan-peloidal wackestone and packstone; (2) the Mississippian(?) upper Alapah Limestone, a thin- to medium-bedded unit comprised of lime mudstone and wackestone which forms distinctive talus slopes; and (3) the Pennsylvanian Wahoo Limestone, a thin- to massive-bedded, cliff-forming unit of pelmatozoan-bryozoan wackestone, packstone, and minor grainstone, with interbedded black chert lenses and nodules.

The Permian-Lower Triassic Sadlerochit Group (Leffingwell, 1919; Detterman et al., 1975) is an

TABLE 1. Stratigraphic thicknesses (in feet) of lithostratigraphic units in the Ellesmerian sequence. Published values are arranged from west to east across the northeastern Brooks Range (roughly 100 mi / 161 km). The study area lies to the west of the region studied by Reed (1968), in the Franklin Mountains region studied by Mamet and Armstrong (1972). Thickness values used in balanced cross-sections constructed in this study (Section 6), given in both feet and meters, are based upon field mapping rather than measured stratigraphic sections.

	west	THICKNESSES IN FEET			east	
UNIT	Keller et al. (1961)	Mamet & Armstrong (1972)	Reed (1968)	Sable (1977)	Brosgé et al. (1962)	BALANCED SECTIONS
upper Ivishak	1,000-2,000		>600-700	400	>1,000	over 1,413 (> 431 m)
lower Ivishak			400-500	200-650		997-1,147 (305-350 m)
Echooka	300-600		190-240	175-240		914 (279 m)
Wahoo		600-900	1,300-1,600	40-200	0-1,367	2,036 (622 m)
Alapah		600-750		200-560	600-1,947	790 (241 m)
Kayak		50-1,450	85-400	0-400	960	1,380 (422 m)
Kekik-tuk		at least 200	0-350 usually <150		0-400+ usually <300	approx. 300 (92 m)
					TOTAL THICKNESS	7,830-7980 (2,392-2,437 m)

assemblage of clastic sedimentary rocks that disconformably overlies the Mississippian-Pennsylvanian Lisburne Group. The upper contact of the Sadlerochit Group with the Triassic Shublik Formation is not exposed in the study area. Three lithostratigraphic units of the Sadlerochit Group were mapped in the study area: (1) the Permian Echooka Formation (Keller et al., 1961), comprised of interbedded calcareous shale, calcarenite, and cherty quartz arenite, with minor chert-pebble conglomerate; (2) a lower unit of the Lower Triassic Ivishak Formation (Leffingwell, 1919; Keller et al., 1961; Detterman et al., 1975), a poorly-exposed unit comprised of flaky shale and silty shale; and (3) an upper unit of the Lower Triassic Ivishak Formation, comprised of interbedded quartz sandstone, siltstone, and shale.

Mississippian-Lower Triassic strata in the study area can be subdivided into four structural-stratigraphic units which correspond with distinct lithostratigraphic units of the Ellesmerian sequence: (1) the Kekiktuk Conglomerate, (2) the Kayak Shale, (3) the Lisburne Group, and (4) the Sadlerochit Group. As discussed in Sections 5 and 9, each structural-stratigraphic unit responded to Cenozoic deformation differently, developing unique structural geometries.

4. STRUCTURAL STYLE OF THE NORTHEASTERN BROOKS RANGE AND MODELS APPLIED TO FRANKLIN MOUNTAINS STRUCTURAL ANALYSIS

A number of recent studies address the structural style of the northeastern Brooks Range, considering the geometry of structures in the region and their mode of formation (Rattey, 1985; Kelley and Molenaar, 1985; Leiggi and Russell, 1985; Namson and Wallace, 1986; Oldow et al., 1986, 1987; Kelley and Foland, 1987; Avé Lallemant et al., 1987; and Leiggi, 1987). While their structural models and interpretations differ, these researchers have addressed four basic topics: (1) the structural style of the Franklinian sequence due to pre-Mississippian deformation; (2) the structural style of the Franklinian sequence due to Cenozoic deformation; (3) the structural style of the Ellesmerian sequence; and (4) the mode of Cenozoic uplift of the Franklinian sequence and its influence on the structure of the Ellesmerian sequence.

Early interpretations of the structural style of the northeastern Brooks Range were based upon regional mapping by Reiser et al. (1971) and observations from local studies such as those of Keller et al. (1961), Reed (1968) and Sable (1977). Concurrent with an intensification of interest in petroleum exploration beneath ANWR's coastal plain, a new phase of geologic work in the northeastern Brooks Range began in the early 1980s. Recent studies have incorporated elements largely absent from earlier work, including balanced cross-section models of the structural geometry of this foreland fold-and-thrust belt (Rattey, 1985; Namson and Wallace, 1986; Kelley and Foland, 1987; Leiggi, 1987), and analysis of kinematic data (Oldow et al., 1987).

4.A. REGIONAL STRUCTURES

The northeastern Brooks Range fold-and-thrust belt evolved during Cenozoic time as a consequence of interpreted north-northwest-directed tectonic transport which involved rocks both of the Franklinian and Ellesmerian sequences (Mull, 1985; Wallace and Hanks, 1988a, b, in press). As shown

in Figure 3, the regional structure of the northeastern Brooks Range is characterized by a number of east-trending, doubly-plunging anticlinoria which are cored by Franklinian sequence rocks. These regional anticlinoria are regularly spaced from south to north across the folti-and-thrust belt and define the major mountain ranges which comprise the northeastern Brooks Range (Figures 3 and 6). Pre-Mississippian rocks exposed in the cores of ranges of western ANWR, including the Franklin, Sadlerochit and Shublik Mountains (Figures 3 and 6), form peaks that reach elevations of 4,000 to 7,000 feet (1.2 - 2.1 kilometers) above sea level. In contrast, pre-Mississippian rocks to the north of these ranges lie in the subsurface of the Arctic coastal plain, overlain by the Ellesmerian sequence and up to 26,000 feet (7.9 kilometers) of Cretaceous and Tertiary Brookian foredeep deposits (United States Department of the Interior, 1986). Thus, the Franklinian sequence rocks which core anticlinoria in the northeastern Brooks Range have been uplifted an estimated 9-10 kilometers above the undeformed elevation of the sub-Mississippian unconformity beneath the Arctic coastal plain to the north. These regional anticlinoria are interpreted by Rattey (1985), Namson and Wallace (1986), Kelley and Foland (1987), Leiggi (1987), Oldow et al. (1987), and Wallace and Hanks (1988a, b, in press) to have formed during the Cenozoic evolution of the fold-and-thrust belt, accompanied by complex folding and faulting of Ellesmerian sequence rocks.

4.B. PRE-MISSISSIPPIAN STRUCTURAL STYLE

Because the Franklinian sequence was deformed during both pre-Mississippian and Cenozoic orogenic episodes, the time of formation of individual structures must be determined. Reed's (1968) structural study in the Lake Peters area represents perhaps the first comprehensive effort to identify and describe structures which existed in the Franklinian sequence prior to deposition of the Ellesmerian sequence, and to interpret the deformational history of both sequences. As shown in Figure 9, Reed (1968) identified two episodes of folding and one episode of faulting which he interpreted to have occurred prior to deposition of the Ellesmerian sequence. The first folding event formed broad, open folds with

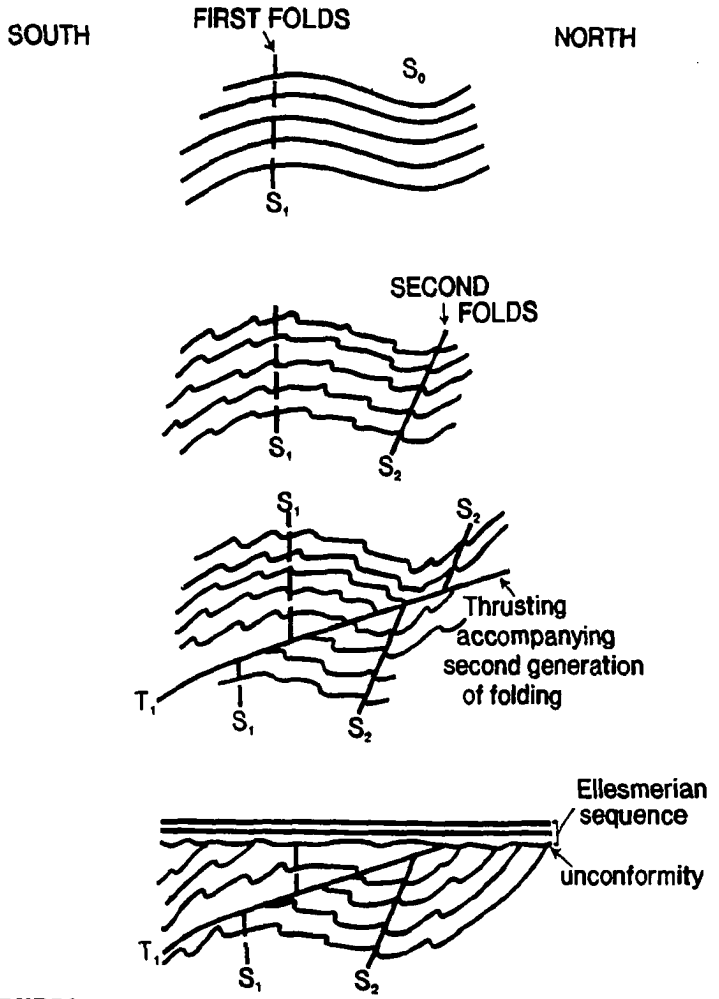

FIGURE 9. Deformational history in Lake Peters area prior to Cenozoic orogenesis (modified from Reed, 1968). Two generations of folds, with S_1 and S_2 axial surfaces, and thrust faults (T_1) were developed prior to deposition of the Ellesmerian sequence upon the sub-Mississippian unconformity surface. The geometry and orientation of folds with S_2 axial surfaces and T_1 faults suggest that these structures formed during north-vergent deformation in pre-Mississippian time.

subvertical axial surfaces (S_1 of Figure 9). Alignment of platy minerals parallel to bedding defined a first generation schistosity. Second generation folds are generally asymmetric with long south limbs and shorter north limbs. The south-dipping axial surfaces of the second folds, and a slaty cleavage interpreted to be coeval with them, are referred to as "S_2" in Figure 9. The geometry of the second folds suggests that these structures formed as a consequence of north-vergent tectonic transport. Second folds were refolded during a third deformation event which folded the sub-Mississippian unconformity. Thrust faults (T_1 of Figure 9) dip gently to the south and cross-cut the axial surfaces of both generations of folds. Such pre-Mississippian faults are truncated by the Kekiktuk Conglomerate and can be distinguished from later faults (T_2) which truncate the Kekiktuk Conglomerate (Reed, 1968). Although Reed (1968) states that the relative ages of folding and thrusting could not be ascertained, he interpreted that the thrust faults formed in pre-Mississippian time, likely in association with the second folding event.

In a recent structural analysis in the Franklin Mountains region, Oldow et al. (1986, 1987) identified strongly overturned to recumbent isoclinal folds with penetrative, bedding parallel, axial planar cleavage and minor sheath folds, as first-generation structures in the Franklinian sequence. The slaty cleavage strikes east to east-northeast and dips either moderately south or gently north. Like Reed (1968), Oldow et al. (1987) considered this prominent slaty cleavage (S_2 of Figure 9) to be a manifestation of pre-Mississippian folding of the Franklinian sequence. Reed's (1968) observations and seismic data from northeastern ANWR cited by Smith (1987) both suggest a north vergence of pre-Mississippian structures. However, Oldow et al. (1987) cite kinematic indicators (asymmetric isoclines and pressure shadows) which suggest a south vergence of pre-Mississippian structures in the Franklin Mountains region. Oldow et al. (1987) may have identified south-vergent pre-Mississippian structures in the Franklinian sequence, but they did not establish that the pressure shadows, in particular, are of unequivocal pre-Mississippian age. It is possible that these pressure shadows are products of either multiple

pre-Mississippian events or of Cenozoic deformation, explaining the discrepancy between their observations and those of Reed (1968), Sable (1977), and Smith (1987). In describing the vergence of structures in the Franklinian sequence, it is essential to know the orientation of those structures with respect to the unconformity surface and local Cenozoic structures, which Oldow et al. (1987) do not do.

4.C. MODELS FOR CENOZOIC STRUCTURE BASED UPON RECENT STUDIES

As shown in Figure 10, two end-member models can be proposed to describe the behavior of the Franklinian sequence during Cenozoic deformation. In the first model (Figure 10A), coherent thrust sheets of Franklinian sequence rocks were displaced and uplifted as horses in a duplex thrust system, forming the regional anticlinoria (Rattey, 1985; Namson and Wallace, 1986; Kelley and Foland, 1987; Leiggi, 1987). In the second model (Figure 10B), Cenozoic shortening was accommodated by internal strain distributed heterogeneously within the Franklinian sequence, forming the regional anticlinoria without requiring the displacement of coherent thrust sheets along discrete thrust surfaces. In the duplex model (Figure 10A), the sub-Mississippian unconformity is shortened by thrust duplication, while in the heterogeneous strain model (Figure 10B) it is shortened by internal strain.

4.C.1. The Duplex Model

Rattey (1985) first suggested that stratigraphic units beneath the Kayak Shale were deformed via a duplex thrust system and similar models were also suggested by Namson and Wallace (1986), Kelley and Foland (1987), Leiggi (1987), and Avé Lallemant et al. (1987). Duplex geometries were employed in northeastern Brooks Range balanced cross-sections by Namson and Wallace (1986) and Leiggi (1987). As shown in Figure 11, Namson and Wallace (1986) and Wallace and Hanks (1988a, b, in press) interpret the regional anticlinoria to be fault-bend folds developed within horses of a northward-propagating duplex thrust system. (Duplex thrust systems and fault-bend folds are reviewed briefly in Appendix A.) Wallace and Hanks (1988a, b, in press) further suggest that the anticlinoria west of the Okpilak batholith (Figure

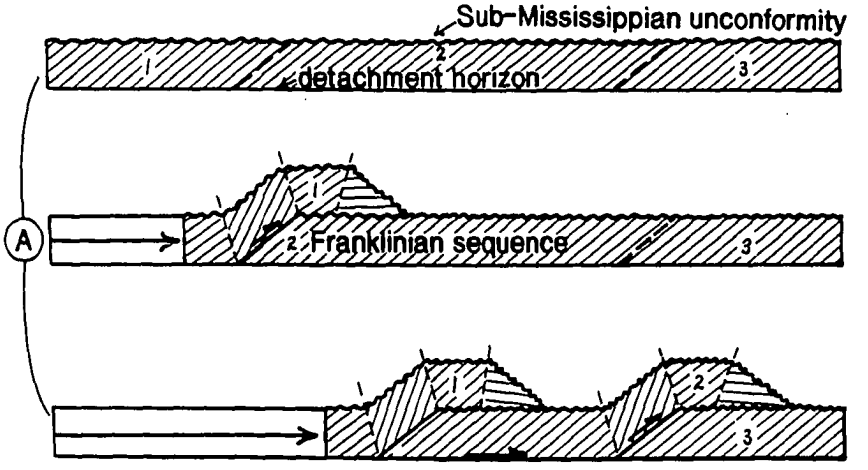

A. In this end-member model, a northward-propagating duplex thrust system deformed the Franklinian sequence, producing culminations which correspond to the regional anticlinoria. South-dipping hatched lines represent the fabric produced during pre-Mississippian deformation of these rocks. In order for such a duplex thrust system to accommodate Cenozoic regional shortening, two detachment horizons must exist, one at depth within the Franklinian sequence and the other in rocks just above the sub-Mississippian unconformity.

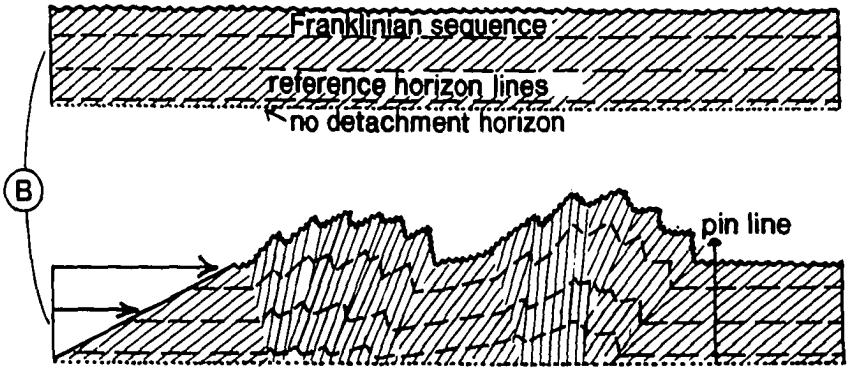

B. Shortening of the unconformity is accommodated by internal strain, as opposed to by thrust duplication as shown in (A). Cenozoic strain is accommodated heterogeneously by Franklinian sequence rocks. Vertical inhomogeneities in shortening associated with north-directed shear might cause positive structural relief of the Franklinian sequence above the sub-Mississippian unconformity surface. Lateral inhomogeneities in shortening might produce multiple anticlinoria and intervening synclinoria across the region.

FIGURE 10. End-member models for Cenozoic structural style of Franklinian sequence.

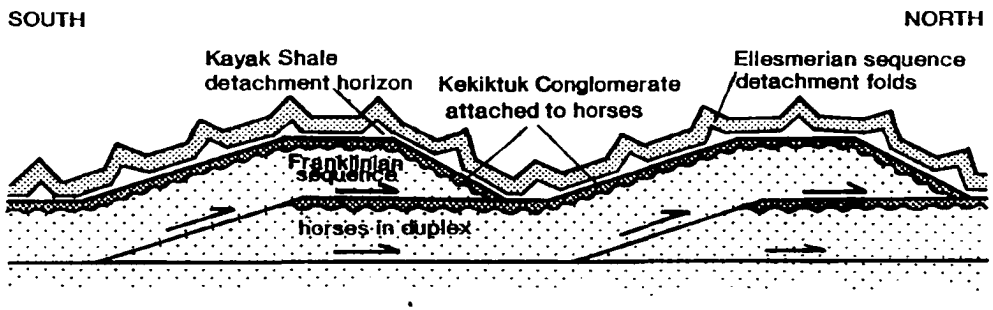

FIGURE 11. Duplex thrust system model of Namson and Wallace (1986), modified from Wallace and Hanks (in press). The floor thrust of the duplex lies at depth in the Franklinian sequence; the roof thrust lies in the Kayak Shale. The Kekiktuk Conglomerate remains structurally attached to pre-Mississippian rocks. The Lisburne and Sadlerochit Groups deformed by detachment folding.

3) are essentially comprised of single horses, while those east of the Okpilak batholith are comprised of multiple horses (refer to Appendix A). O'Sullivan's (1988) apatite fission-track dates from his study across 100 kilometers of the northeastern Brooks Range suggest progressively younger Cenozoic ages of rapid cooling (uplift) toward the north, compatible with a northward-propagating duplex thrust system model.

4.C.2. Applications of the Duplex Model to the Franklinian Sequence and the Kekiktuk Conglomerate

A duplex thrust system could explain the observed Cenozoic structural style of the Franklinian sequence if it is possible to identify (1) floor and roof thrust horizons, (2) antiforms (fault-bend folds) produced as horses were emplaced, and (3) structural duplication of stratigraphy developed as each horse was emplaced over its footwall. Recent regional studies incorporate variations on the duplex theme. Models differ in the interpretation of the position of floor and roof thrust detachment horizons, the tectonic significance of the sub-Mississippian unconformity, and the behavior of the Kekiktuk Conglomerate during deformation (Figures 10 and 12). Rattey (1985) implies that a floor thrust exists at depth within the Franklinian sequence and specifies that the roof thrust of the duplex system lies in the Mississippian Kayak Shale, but commonly steps down to the base of the Mississippian Kekiktuk Conglomerate. Namson and Wallace (1986) confine the roof thrust to the Kayak Shale (Figure 11). Leiggi (1987) suggests that the roof thrust may lie in the Kayak Shale, at the sub-Mississippian unconformity, or in structurally-uppermost Franklinian sequence rocks. However, his cross-sections place the roof thrust entirely within the Franklinian sequence. Avé Lallemant et al. (1987) and Oldow et al. (1987) suggest that the Mississippian Kekiktuk Conglomerate is bounded above and below by detachment horizons, corresponding to the Kayak Shale and unconformity surface, respectively (Figure 12D). In essence, these two detachments constitute a roof thrust "zone" which would permit duplexing of the Kekiktuk Conglomerate as a mechanism for the accommodation of shortening within underlying

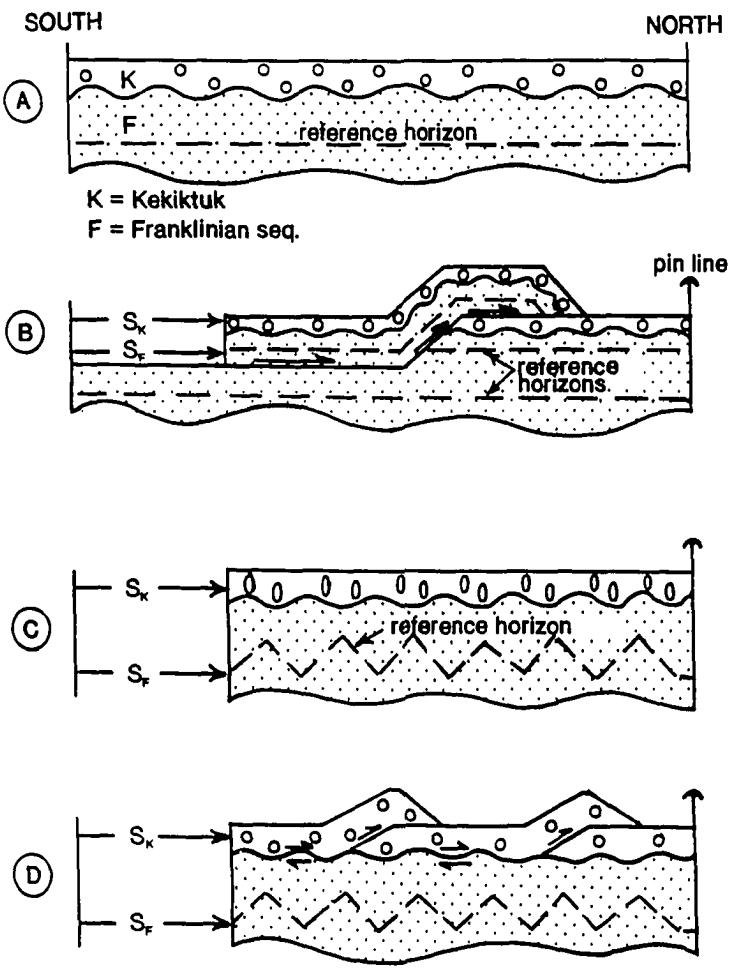

FIGURE 12. Models for shortening by imbrication or development of penetrative strain in the Kekiktuk Conglomerate. (A) Prior to Cenozoic deformation. (B) Shortening of Kekiktuk Conglomerate (S_K) and shortening of Franklinian sequence (S_F) accommodated by imbrication with no internal strain in either; compatible with Figure 10A. (C) S_K and S_F both accommodated entirely by internal strain; compatible with Figure 10B. (D) S_K accommodated by imbrication; S_F accommodated by internal strain; detachment at unconformity surface; intermediate between Figures 10A and 10B.

packages of Franklinian sequence rocks during Cenozoic deformation (Figure 12D).

4.C.3. The Heterogeneous Strain Model

The floor thrust at depth within the Franklinian sequence, required for a duplex thrust system, is not exposed. Thus, it is possible that the regional anticlinoria were formed as a consequence of heterogeneous strain during Cenozoic north-south compression, without the displacement of coherent thrust sheets along discrete thrust surfaces. Without a basal detachment, the magnitude of Cenozoic internal shortening would likely decrease with depth and shortening would be distributed inhomogeneously by a combination of penetrative strain, and mesoscopic and macroscopic folding at wavelengths shorter than those of the regional anticlinoria. This model suggests that the magnitude of Cenozoic internal shortening of the Franklinian sequence should decrease from hinterland to foreland, and that a greater magnitude of shortening should be accommodated by pre-Mississippian rocks which core the anticlinoria than by those which form the intervening synclinoria (Figure 10B).

4.C.4. Application of the Heterogeneous Strain Model to the Franklinian Sequence and the Kekiktuk Conglomerate

Both Oldow et al. (1987) and Avé Lallemant et al. (1987) believe that (1) pre-Mississippian rocks exhibit significant amounts of internal shortening that can be attributed to Cenozoic deformation, and that (2) the Kekiktuk Conglomerate has accommodated this shortening by a combination of internal mesoscopic deformation, penetrative strain, and imbrication, detached at least in part from the Franklinian sequence (Figure 12C-D). Thus, the heterogeneous strain model (Figure 10B) may describe the structural style of the Franklinian sequence to some extent. However, if this model is employed, the existence of regularly spaced anticlinoria and the role of south-dipping thrust faults involving pre-Mississippian rocks, mapped by Reiser at al. (1971) to the east and northeast of the study area, must be reconciled.

4.C.5. A Comparison of Duplex and Heterogeneous Strain Models

The duplex and heterogeneous strain models differ fundamentally in terms of how Cenozoic

shortening is accommodated in both the Franklinian sequence and the Kekiktuk Conglomerate. Consider an undeformed sheet of Kekiktuk Conglomerate which remains structurally attached to underlying pre-Mississippian rocks during Cenozoic deformation. Duplex shortening of the Franklinian sequence beneath a roof thrust in the Kayak Shale would shorten the sheet of Kekiktuk Conglomerate by thrust duplication in an amount equivalent to that accommodated by thrust duplication of the underlying horses of pre-Mississippian rocks (Figure 12B). However, if significant heterogeneous internal shortening of the Franklinian sequence occurred (Figure 10B), the thin sheet of Kekiktuk Conglomerate could respond to such deformation in several ways. First, it could accommodate the shortening internally, incurring substantial penetrative strain and remaining structurally attached to the Franklinian sequence (Figure 12C). Alternatively, the Kekiktuk Conglomerate could detach from the pre-Mississippian rocks at or near the unconformity surface and deform independently of the Franklinian sequence by thrust duplication (Figure 12D), while the underlying pre-Mississippian rocks deform internally to accommodate shortening. Finally, note that the shortening mechanisms shown in Figure 12 are not necessarily mutually exclusive. Where shortening is accommodated by multiple mechanisms, the relative importance of each one must be assessed.

4.D. CENOZOIC STRUCTURAL STYLE OF THE ELLESMERIAN SEQUENCE

All structural studies in the northeastern Brooks Range distinguish between the structural styles exhibited by the Franklinian and Ellesmerian sequences. Recent researchers also recognize that distinctive structural geometries were developed within different structural-stratigraphic units of the Ellesmerian sequence during Cenozoic deformation. The structural style of the Ellesmerian sequence described by Rattey (1985), Namson and Wallace (1986), Oldow et al. (1986, 1987), and Avé Lallemant et al. (1987) is shown schematically in Figure 13. The Kayak Shale detachment horizon subdivides the Ellesmerian sequence into two packages of rocks which exhibit different structural styles developed as a conseqence of

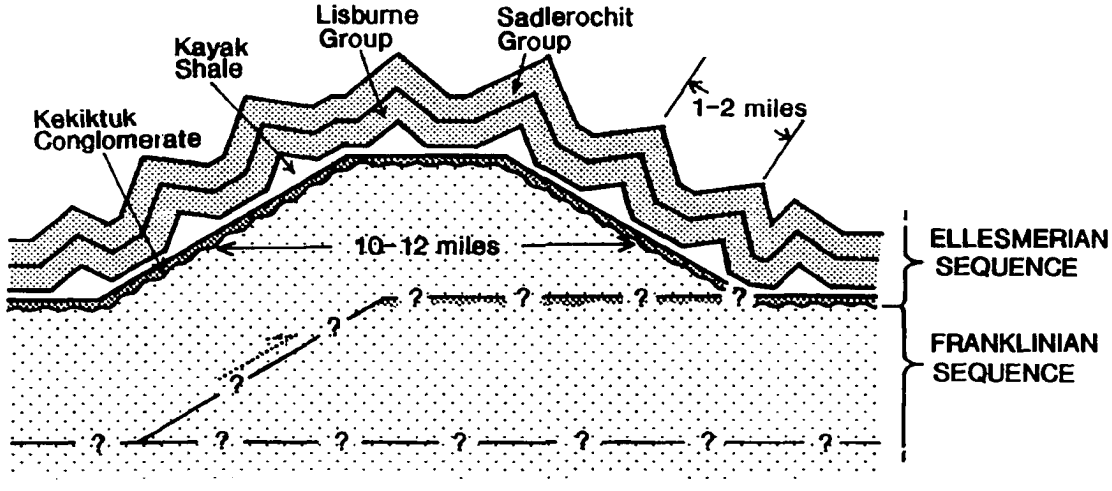

FIGURE 13. Contrasts in structural geometry of the Franklinian and Ellesmerian sequences. Substantially different macroscopic fold wavelengths were developed above and below the Mississippian Kayak Shale. Question marks and discontinuity of the Kekiktuk Conglomerate denote uncertainty regarding the mode of formation of the regional anticlinoria.

deformation: (1) the Kekiktuk Conglomerate and (2) the Lisburne Group and overlying rocks.

4.D.1. Structural Style of the Kekiktuk Conglomerate

Efforts to characterize the structural style of the Kekiktuk Conglomerate must consider how the structural style of the immediately underlying Franklinian sequence might have influenced its deformation, contributing to the formation of the characteristic broad folds that reflect the wavelength of the regional anticlinoria.

4.D.1.a. Observations of other researchers

The Kekiktuk Conglomerate appears to be relatively unstrained (Oldow et al., 1987; Avé Lallemant et al., 1987; Wallace and Hanks, in press). While in many locations the unit is in indisputable depositional contact with underlying pre-Mississippian rocks, in other places the basal Kekiktuk Conglomerate is sheared or structurally imbricated (Oldow et al., 1987). Namson and Wallace (1986) believe that the Kekiktuk Conglomerate remained essentially glued to the Franklinian sequence during the deformational episode which formed the regional anticlinoria (Figures 11 and 13). In contrast, Oldow et al. (1987) state that the Kekiktuk Conglomerate is separated from over- and underlying rocks by detachment surfaces at or near the lower and upper contacts or locally within the immediately adjacent Franklinian sequence or Kayak Shale. Such decoupling is also suggested by Avé Lallemant et al. (1987), who observe that Cenozoic internal shortening of the Franklinian sequence appears to be greater than the shortening accommodated by the Kekiktuk Conglomerate form surface. Imbrication and/or penetrative strain of the Kekiktuk Conglomerate could account for some of this apparent difference in shortening.

4.D.1.b. Application of structural models to this study

In view of the discussion in Section 4.C.5., if the magnitude of Cenozoic internal shortening in the Franklinian sequence is considered to be approximately the same as that observed in the Kekiktuk Conglomerate, then it can be argued that the Kekiktuk Conglomerate remained structurally attached to the Franklinian sequence during Cenozoic deformation (Figure 12B or C). However, if Cenozoic penetrative

strain in the Franklinian sequence is considered to be of a significantly larger magnitude than that observed in the Kekitkuk Conglomerate, then it is appropriate to conclude that the Kekitkuk Conglomerate was structurally detached from the Franklinian sequence during Cenozoic deformation (Figure 12D).

Where the sub-Mississippian unconformity and overlying Kekiktuk Conglomerate were well-exposed, it was possible to study relationships between structures and the style of deformation of the Franklinian sequence, the unconformity, and the Kekiktuk Conglomerate. A major goal of this investigation was to discern whether the Kekiktuk Conglomerate remained structurally attached to pre-Mississippian rocks during Cenozoic deformation, and to investigate how Cenozoic strain was accommodated by the Kekiktuk Conglomerate. Oriented samples were collected for the purpose of describing and quantifying penetrative strain within the Kekiktuk Conglomerate. Values were compared with strains measured in under- and overlying rocks.

4.D.2. Structural Style Above the Kekiktuk Conglomerate

The Kekiktuk Conglomerate is separated from chevron folds and thrust faults in the Lisburne and Sadlerochit Groups by a detachment horizon in the Kayak Shale (Figures 11 and 13) (Namson and Wallace, 1986). The existence of the Kayak Shale detachment is demonstrated by the fact that fold wavelengths above the Kayak Shale are significantly shorter than those defined by the Kekiktuk Conglomerate (Figure 13), indicating that the Lisburne Group and overlying rocks were decoupled from the Kekiktuk Conglomerate during deformation (Namson and Wallace, 1986; Avé Lallemant et al., 1987; Oldow et al., 1987). Exposure of the Kayak Shale within the study area was sufficient in order to address whether or not this unit functioned as a detachment horizon (Sections 5.B.2., 5.D.2.b., 5.E., and 9.B.). Excellent exposure of structures developed above the Kayak Shale, in the Lisburne and Sadlerochit Groups, permitted fold and fault geometries to be characterized in the synclinorium immediately north of the Franklin Mountains anticlinorium (Sections 5.B.3., 5.E. and 9.C.).

5. THE RESPONSE OF STRUCTURAL-STRATIGRAPHIC UNITS TO DEFORMATION

Description of the geometry of mesoscopic structures, measurement of their absolute and relative orientations, and interpretation of the deformational history of Franklinian and Ellesmerian sequence rocks in the study area form the cornerstone of this detailed structural analysis and provide an understanding of the basic structural style of the study area. In this section, the geometry of folds, faults and other geologic structures in the Franklinian and Ellesmerian sequences are characterized and the relative chronology of deformation is interpreted. Types and orientations of structures, basic structural geometry, and contact relations are summarized in Table 2, facilitating comparison of structures observed in the Franklinian and Ellesmerian sequences. The relative chronology of structures in the Franklinian sequence is outlined in Table 3, with structures grouped according to the structural-stratigraphic package in which they occur. Stereographic projections compiled in Figure 14 show the orientations of the several generations of structures observed in the Franklinian and Ellesmerian sequences, assembled to permit comparisons to be made between both the different generations of structures and the two sequences. The inferred deformation mechanisms which contributed to the formation of these structures are also described. Table 4 lists deformation features observed in Franklinian and Ellesmerian sequence rocks and the probable mechanisms which produced these features, grouped according to interpreted chronology.

5.A. STRUCTURAL GEOMETRY IN THE FRANKLINIAN SEQUENCE

Franklinian sequence rocks are exposed in two antiformal, fault-bounded structural packages, each capped by a thin sheet of the Mississippian Kekiktuk Conglomerate (Figures 15 and 16). The antiforms are defined by broad folding of subparallel bedding and slaty cleavage in the pre-Mississippian rocks, and by flexure of the overlying Kekiktuk Conglomerate. As illustrated in a cross-sectional view (Figure 16), the structurally higher antiform is referred to as the upper antiform. The upper antiform (Figure 17) is a broad asymmetric fold with a long limb which dips gently to moderately south and a shorter limb which

TABLE 2. Summary of meso- and macroscopic structures observed in structural-stratigraphic packages of Franklinian and Ellesmerian sequence rocks in the study area.

		LITHOLOGY	CONTACT REL.
ELLESMERIAN SEQUENCE	SADLEROCHIT GROUP	Interbedded calcareous shale, fossiliferous calcarenite, chert-pebble conglomerate, cherty quartzarenite (Pe); flaky shale, silty shale; interbedded quartzarenite, siltstone, shale (lTri).	In disconformable depositional c Pw; local thrust contacts of Pe c Pw over lTri; no apparent struct between beds.
	Disconformity		
	LISBURNE GROUP	Lime mudstone and bryozoan-peloidal wackestone and packstone (Ma); pelmatozoan-bryozoan wackestone, packstone, minor grainstone with interbedded chert lenses and nodules (Pw).	Depositional contact with Mky; disconformable depositional con local thrust contacts with Pw ov Mky over Ma; no apparent struct between beds.
	KAYAK SHALE	Carbonaceous shale with thinly-interbedded limestone near contact with Lisburne Group (Mky).	Apparent gradational contacts w Ma; Mky occurs in hangingwall involving Ellesmerian sequence.
	KEKIKTUK CONGLOMERATE	Quartzite with interbedded chert- and quartz-pebble to cobble conglomerate and minor shale (Mkt).	Basal conglomerate in apparent c contact with Franklinian sequen lower antiform overthrust by roc antiform; Mkt of upper antiform Mky.
	Unconformity		
FRANKLINIAN SEQUENCE	UPPER ANTIFORM (Upper & Middle Structural-Stratigraphic Packages)	Slate-volcanic unit (pMsv); purple-green phyllite (pMp); chloritic phyllite (pMc); brecciated unit (pMb); shale unit (pMsh); chert-greenstone unit (pMcg).	Upper package unconformably o thrust contact between upper and packages (pMcg truncated by pM base of entire package, otherwis structural disruption between unit bedding, cross-bedding and soft-s deformation in sandstone (pMsh) right-side-up.
	LOWER ANTIFORM (Lower Structural-Stratigraphic Package)	Volcanic unit consisting of shale with interbedded limestone, dolostone, greywacke, volcanic breccia, greenstone and pillow basalt (pMv).	Unconformably overlain by Mkt exposed; contacts between beds/l appear to be structurally disrupte at base of greywacke beds indicat right-side-up with sediment trans S with respect to present positio

stratigraphic

area.

	CONTACT RELATIONS	STRUCTURES & ORIENTATION	GEOMETRY OF STRU
ous silty ne,	In disconformable depositional contact with Pw; local thrust contacts of Pe over lTri, and Pw over lTri; no apparent structural disruption between beds.	Folds with ENE-trending axes; moderately well developed E- to ENE-striking spaced cleavage, axial planar to folds; quartz- and calcite-filled extension fractures, ENE-striking, moderately N-dipping; N- to NNW-striking, subvertical cleavage spaced at 0.5-1 m intervals.	1-2 km wavelength folds; loc folds at wavelengths of tens t of meters; axial planar cleava across lithologic contacts.
w).	Depositional contact with Mky; disconformable depositional contact with Pe; local thrust contacts with Pw over lTri and Mky over Ma; no apparent structural disruption between beds.	Folds with ENE-trending axes; solution cleavage axial planar to folds, observed near fold hinges.	1-2 km wavelength folds; loc folds at wavelengths of hundr meters; Class 1B or 1C paral (Ramsay, 1967), C3-C4 and (Hudleston, 1973), local Cla folds on north limb of anticli E4-E5 type (Hudleston, 197
h	Apparent gradational contacts with Mkt and Ma; Mky occurs in hangingwall of thrust faults involving Ellesmerian sequence.	Folding of bedding-parallel slaty cleavage, ENE-trending axes, variable vergence; parasitic folding of limestone interbeds; local secondary cleavage axial planar to N-vergent folds; ENE-striking, N-vergent thrust faults.	C-F shapes, 3-4 amplitudes (1973); wavelengths of 20 cm varying tightness, but interli angles usually <90°; both arc angular hinges; slaty cleavag hangingwall of thrust faults parallel to thrust surfaces.
and	Basal conglomerate in apparent depositional contact with Franklinian sequence; Mkt of lower antiform overthrust by rocks of upper antiform; Mkt of upper antiform overlain by Mky.	Broad folds; fold axis of Mkt capping lower antiform trends ENE, plunging moderately WSW; minor, ENE-striking, S-dipping normal fault; local imbricates (2-4 m-thick), uncertain transport direction; quartz-filled extension fractures (1-3 cm), bedding parallel and normal to bedding, strike both ENE and NNW.	D1-D2 types (Hudleston, 19 fold form similar to that of unconformity surface; some striking extension fractures a and open, other sets are mut perpendicular, local chocolate structure.
een lc); lsh);	Upper package unconformably overlain by Mkt; thrust contact between upper and middle packages (pMcg truncated by pMsv) and at base of entire package, otherwise no obvious structural disruption between units; graded bedding, cross-bedding and soft-sediment deformation in sandstone (pMsh) indicate beds right-side-up.	E-trending, moderately S-dipping slaty cleavage; crenulated slaty cleavage (pMp), axes trending ENE; folded slaty cleavage (pMsh, pMp), some axes trend SSW; minor fault-bend folds in chert, W displacement; minor kink-folds in chert; same extension fractures and spaced cleavage described below.	Crenulation occurs in vicinit fault that emplaced upper ant lower antiform, wavelength folding of slaty cleavage with <0.5 m, amplitude <0.2 m, I types; inconsistent symmetry of minor kink folds suggest
th one	Unconformably overlain by Mkt; base not exposed; contacts between beds/lithologies do not appear to be structurally disrupted; flute casts at base of greywacke beds indicate beds are right-side-up with sediment transport to the S with respect to present position.	E-trending, moderately S- or gently N-dipping slaty cleavage; slaty cleavage and bedding not folded mesoscopically; NE- to ENE- or NNW-striking quartz- and calcite-filled extension fractures, sub-normal to slaty cleavage or bedding, cleavage spaced at 0.5-1 m interval.	Applicable to both antiforms cleavage subparallel to comp layering, indicating tight to folding; extension fractures a cleavage cross-cut slaty cleav compositional layering.

IONS	STRUCTURES & ORIENTATION	GEOMETRY OF STRUCTURES
tact with lTri, and disruption	Folds with ENE-trending axes; moderately well developed E- to ENE-striking spaced cleavage, axial planar to folds; quartz- and calcite-filled extension fractures, ENE-striking, moderately N-dipping; N- to NNW-striking, subvertical cleavage spaced at 0.5-1 m intervals.	1-2 km wavelength folds; local parasitic folds at wavelengths of tens to hundreds of meters; axial planar cleavage refracts across lithologic contacts.
t with Pc; Tri and al disruption	Folds with ENE-trending axes; solution cleavage axial planar to folds, observed near fold hinges.	1-2 km wavelength folds; local parasitic folds at wavelengths of hundreds of meters; Class 1B or 1C parallel folds (Ramsay, 1967), C3-C4 and D3-D4 type (Hudleston, 1973), local Class 2 similar folds on north limb of anticlinorium, E4-E5 type (Hudleston, 1973).
Mkt and thrust faults	Folding of bedding-parallel slaty cleavage, ENE-trending axes, variable vergence; parasitic folding of limestone interbeds; local secondary cleavage axial planar to N-vergent folds; ENE-striking, N-vergent thrust faults.	C-F shapes, 3-4 amplitudes (Hudleston, 1973); wavelengths of 20 cm- 50 m; varying tightness, but interlimb angles usually <90°; both arcuate and angular hinges; slaty cleavage of Mky in hangingwall of thrust faults is sub-parallel to thrust surfaces.
positional Mkt of of upper erlain by	Broad folds; fold axis of Mkt capping lower antiform trends ENE, plunging moderately WSW; minor, ENE-striking, S-dipping normal fault; local imbricates (2-4 m-thick), uncertain transport direction; quartz-filled extension fractures (1-3 cm), bedding parallel and normal to bedding, strike both ENE and NNW.	D1-D2 types (Hudleston, 1973); fold form similar to that of unconformity surface; some NNW-striking extension fractures are en echelon and open, other sets are mutually perpendicular, local chocolate-tablet structure.
rlain by Mkt; iddle) and at o obvious graded iment dicate beds	E-trending, moderately S-dipping slaty cleavage; crenulated slaty cleavage (pMp), axes trending ENE; folded slaty cleavage (pMsh, pMp), some axes trend SSW; minor fault-bend folds in chert, W displacement; minor kink-folds in chert; same extension fractures and spaced cleavage described below.	Crenulation occurs in vicinity of thrust fault that emplaced upper antiform over lower antiform, wavelength <1cm; folding of slaty cleavage with wavelength <0.5 m, amplitude <0.2 m, E4-E5 fold types; inconsistent symmetry; asymmetry of minor kink folds suggest N-vergence.
base not hologies do not flute casts beds are ort to the	E-trending, moderately S- or gently N-dipping slaty cleavage; slaty cleavage and bedding not folded mesoscopically; NE- to ENE- or NNW-striking quartz- and calcite-filled extension fractures, sub-normal to slaty cleavage or bedding, cleavage spaced at 0.5-1 m intervals.	Applicable to both antiforms: slaty cleavage subparallel to compositional layering, indicating tight to isoclinal folding; extension fractures and spaced cleavage cross-cut slaty cleavage or compositional layering.

TABLE 3. Deformational history of the Franklinian sequence. Mesoscopic structures (in ovals) and their orientations (in rectangles) are grouped both in terms of their relative ages and the structural-stratigraphic package in which they were documented. The vertical arrangement of structures within each package is arbitrary, except that brecciation and mylonitization were observed proximal to the D2 thrust fault as shown. Map units which comprise each structural-stratigraphic package are listed (defined in Table 2 and Figure 7). Heavy barbed lines denote thrust contacts.

CENOZOIC MACROSCOPIC STRUCTURE	STRUCTURAL-STRATIGRAPHIC PACKAGE	PRE-MISSISSIPPIAN STRUCTURES	CENOZOIC STRUCTURES	
		1ST GENERATION (D1)	2ND GENERATION (D2)	3RD GENERATION (D3)
STRUCTURALLY HIGHER ANTIFORM	Upper Structural-stratigraphic Package (pMp, pMsv, pMc)	Slaty Cleavage (S1) E-striking mod. S-dipping	None Observed	Spaced Cleavage (S3) NNW- to N-striking subvertical
		Thrust Fault (T1) E-striking mod. S-dipping	Reactivated Thrust (T1) Parasitic, Kink(?) Folds; Fault-bend Folds(?); Crenulation (F2)	Spaced Cleavage (S3)
	Middle Structural-stratigraphic Package (pMb, pMp, pMsh, pMcg)	Slaty Cleavage (S1) E-striking mod. S-dipping	Quartz- and Calcite-Filled Extension Fractures (S2) ENE- / NNW-striking Tectonic Brecciation	Quartz- and Calcite-Filled Extension Fractures (S3) NNW- to N-striking subvertical
STRUCTURALLY LOWER ANTIFORM	Lower Structural-stratigraphic Package (pMv)	Slaty Cleavage (S1) E-striking mod. S-dipping	Thrust Faults (T2) N-vergent mod. N, S-dipping Local Mylonitization (S2) (observed microscopically) Mesoscopic Folds Absent	Spaced Cleavage (S3) N-striking subvertical

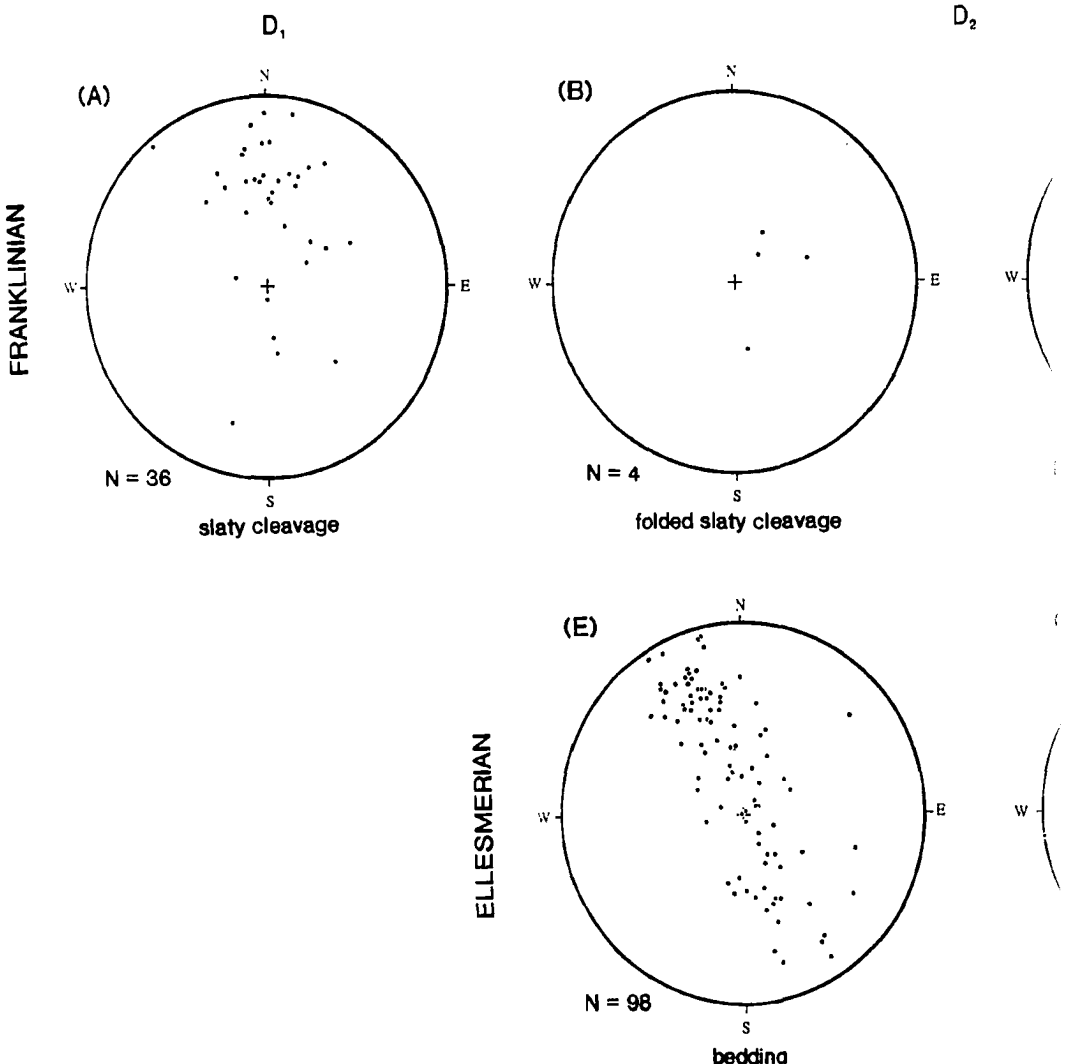

FIGURE 14. Equal-area stereographic projections of poles to planes for mesoscopic structures in the Franklinian sequence (A-D) and the Ellesmerian sequence (E-G) for D_1 (pre-Mississippian), D_2 and D_3 (Cenozoic) events. (A) Slaty cleavage (S_1) in both antiforms; (B) Folded slaty cleavage in upper antiform; (C) Quartz- and calcite-filled extension fractures (S_2) in Franklinian; (D) Spaced cleavage (S_3) in Franklinian; (E) Bedding planes in Ellesmerian; (F) Quartz-filled extension fractures (S_2) in Ellesmerian; (G) Spaced cleavage (S_3) in Ellesmerian.

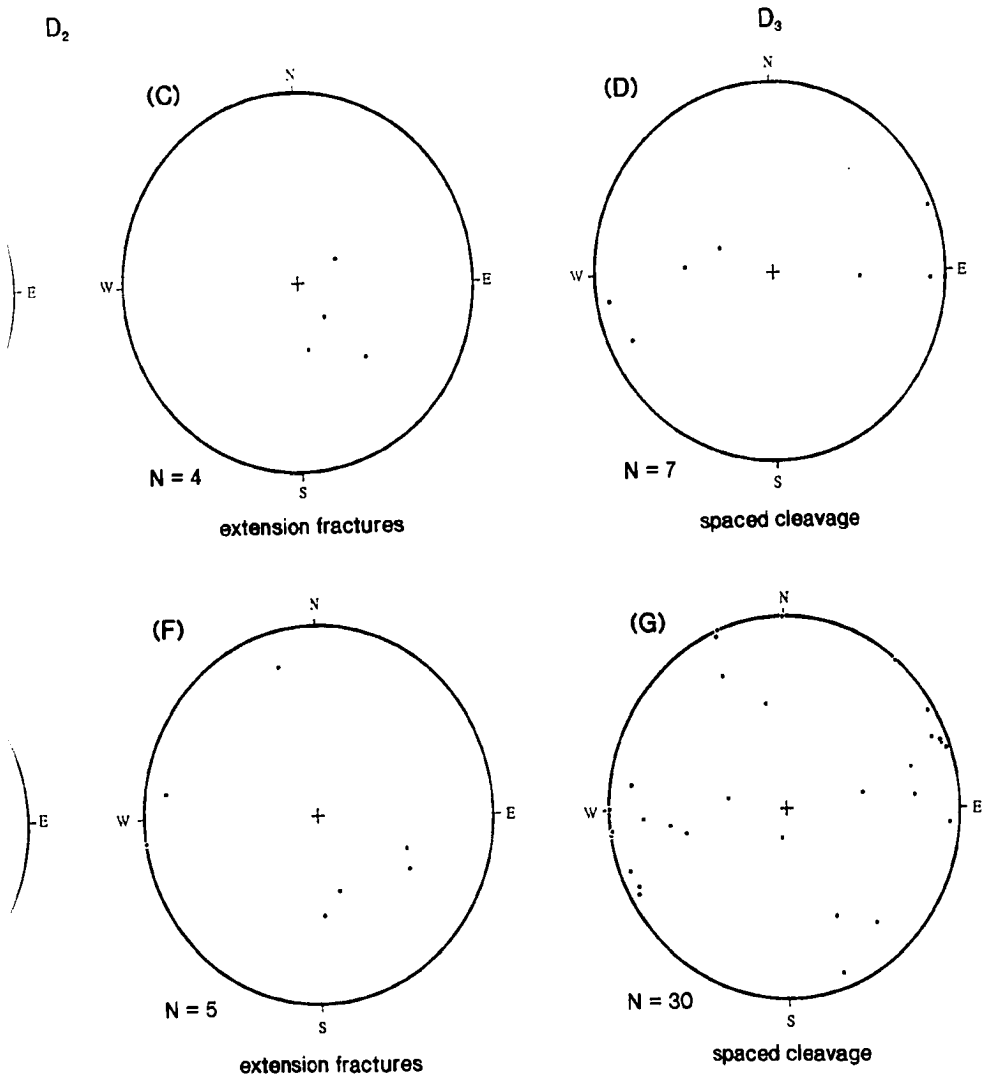

TABLE 4. Deformation features and inferred deformation mechanisms in the Franklinian and Ellesmerian sequences, grouped according to the deformational event with which they are associated. The vertical order of features is arbitrary. Question marks denote uncertainty regarding the relative age of a feature. Mkt = Kekiktuk Conglomerate, Mky = Kayak Shale, PMl = Lisburne Group, TrPs = Sadlerochit Group.

	FRANKLINIAN SEQUENCE		ELLESMERIAN SEQUENCE	
	FEATURE	MECHANISM	FEATURE	MECHANISM
D1	Slaty Cleavage (S1) (assoc. w/ isoclinal folding)	Pressure Solution		
	Undulose ? Extinction ?	Crystal Plasticity	Undulose Extinction in quartz clasts(Mkt)	Crystal Plasticity
D2	Stylolites	Pressure Solution	Stylolites (Mkt, PMl)	Pressure Solution
	Crenulation of S1		Solution Seams (TrPs)	
	Offset / Buckling of Extension Fractures	Pressure Solution w/ Slip (?)	Solution Cleavage	
	Mylonitic Petrofabric	Pressure Solution Crystal Plasticity Cataclasis	Slaty Cleavage (Mky, TrPs)	
			Fissility (Mky, TrPs)	
			Quartz Overgrowths (Mkt)	
			Twinning of Calcite (PMl, TrPs)	Crystal Plasticity
			Bending of Twin Lamellae (PMl)	
			Deformation of Corals (PMl)	
			Undulose Extinction (Mkt)	
			Preferred Orientation of Framework Grains (Mkt, TrPs)	Grain Rotation & Pressure Solution
D3	Spaced Cleavage	Pressure Solution	Spaced Cleavage	Pressure Solution
	? Offset / Buckling of Extension Fractures ?			

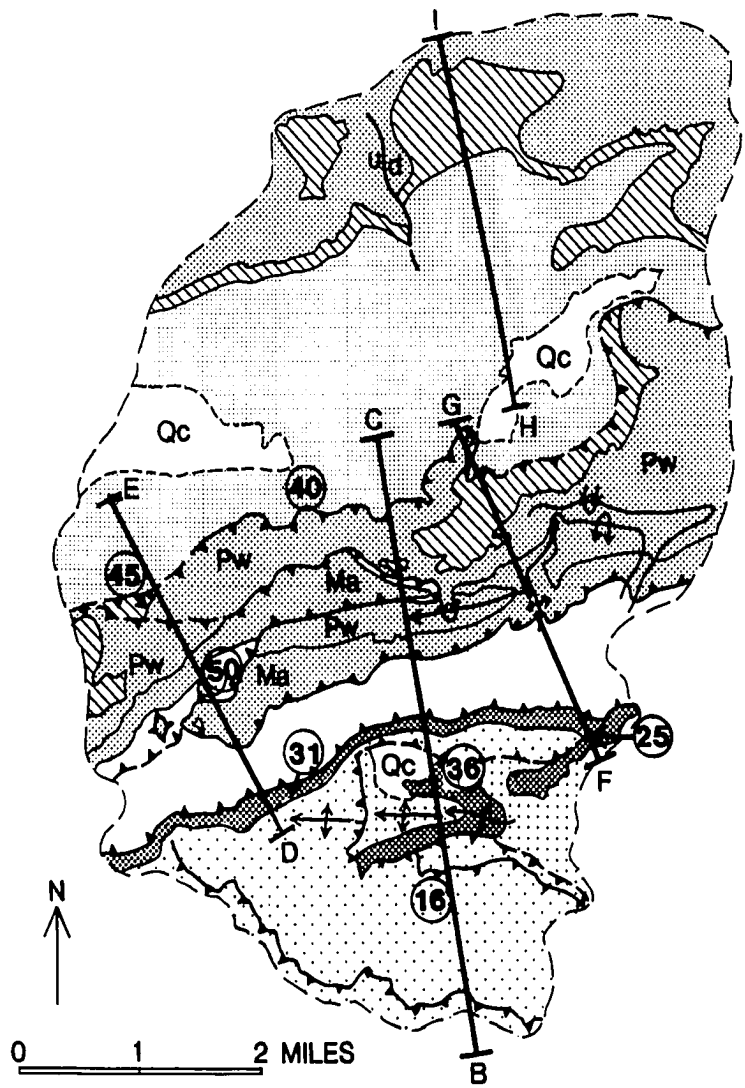

FIGURE 15. Geologic map of study area with cross-section lines, referred to in Section 6. Circled numbers correspond to the locations of oriented samples, discussed in Section 7.

This figure establishes the shading convention used in subsequent figures:

Qc Tundra cover

Lower Triassic Ivishak Formation

Permian Echooka Formation

Mississippian-Pennsylvanian Lisburne Group

Pw = Wahoo Limestone

Ma = Alapah Limestone

Mississippian Kayak Shale

Mississippian Kekiktuk Conglomerate

Franklinian sequence of upper antiform

Franklinian sequence of lower antiform

Thrust fault with teeth on the upper (overthrust) plate

u/d Up/down movement of fault blocks

Identification of oriented sample numbers:

(16) Sample 87JZ16: texturally and compositionally immature pre-Mississippian sandstone, occurring as a lens within the shale unit (pMsh). Contains marcasite nodules with pressure shadows surrounding them.

(25) Sample 87JZ25: fine-medium grained, weakly foliated quartzite of the Kekiktuk Conglomerate, outcropping as several-meter-thick imbricates bounded by shale.

(31) Sample 87JZ31: conglomerate occurring at the base of the Kekiktuk Conglomerate of the upper antiform. Thin-sections primarily consist of quartz matrix of the sample.

(36) Sample 87JZ36: fine-medium grained, weakly foliated quartzite of the Kekiktuk Conglomerate, outcropping as several-meter-thick imbricates bounded by shale.

(40) Sample 87JZ40: medium-grained quartzarenite of the upper portion of the Lower Triassic Ivishak Formation, occurring in the footwall proximal to an east-northeast-trending thrust fault in the Ellesmerian sequence.

(45) Sample 87JZ45: calcareous shale of the Echooka Formation in apparent depositional contact with the Wahoo Limestone. Contains euhedral pyrite crystals with pressure shadows surrounding them.

(50) Sample 87JZ50: colony of lithostrotionoid corals, occurring within an interval of lime mudstone and dominantly bryozoan wackestone of the lower Alapah Limestone.

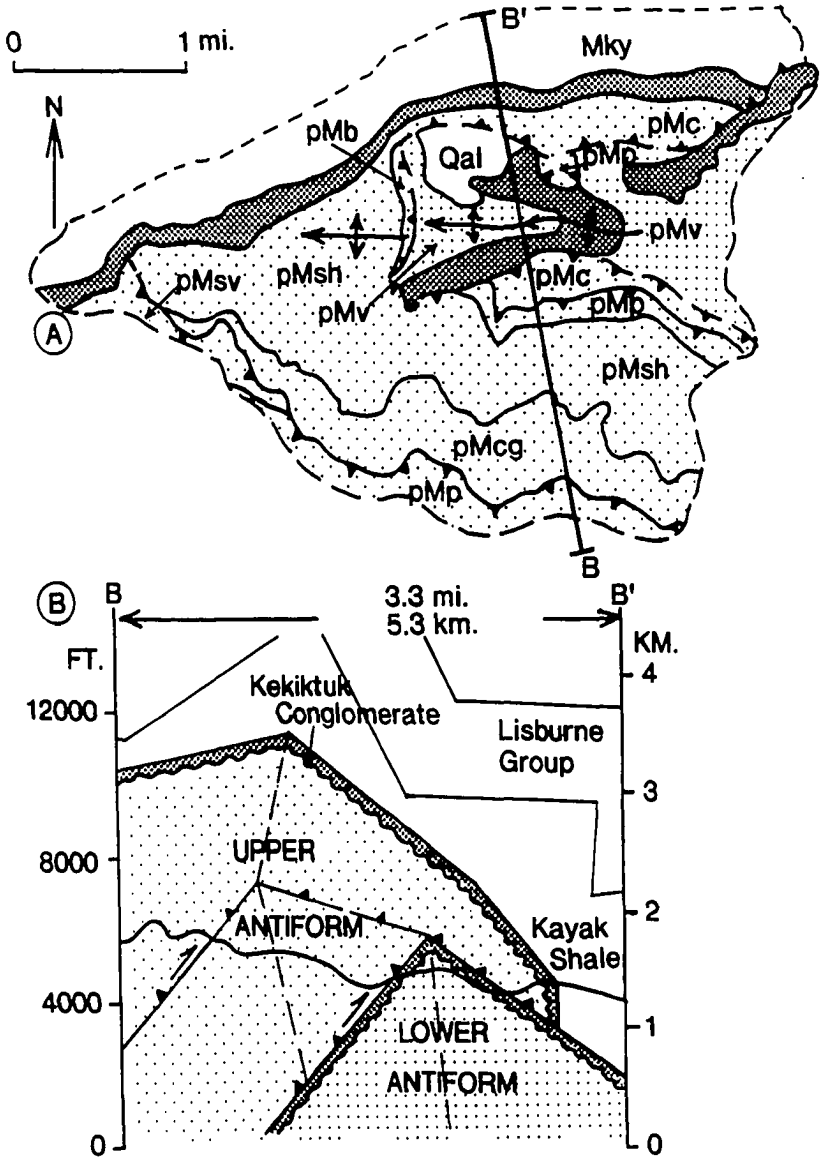

FIGURE 16. Macroscopic structure of Franklinian sequence rocks exposed in the study area. (A) Geologic map of units mapped within the Franklinian sequence. pMsv = slate-volcanic unit; pMp = phyllite unit; pMcg = chert-greenstone unit; pMsh = shale unit; pMb = brecciated unit; pMc = chloritic phyllite unit; pMv = volcanic unit; = Kekiktuk Conglomerate; Mky = Kayak Shale; Qal = tundra cover. (B) Two Cenozoic antiforms (upper and lower) cored by Franklinian sequence and capped by the Kekiktuk Conglomerate.

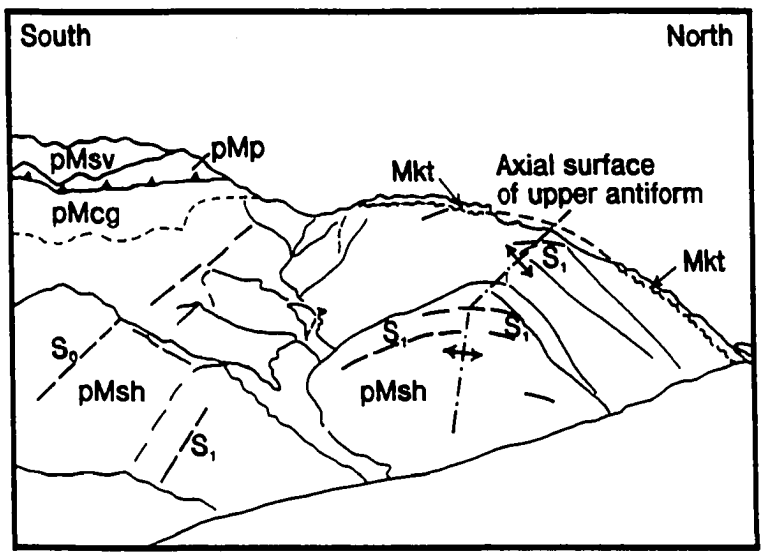

FIGURE 17. Upper antiform cored by the Franklinian sequence and capped by the Kekiktuk Conglomerate. View is to the west from near the crest of the lower antiform. A pre-Mississippian thrust fault truncates the phyllite unit (pMp) toward the left edge of the photo. pMsv = slate-volcanic unit of upper structural-stratigraphic package; pMcg = chert-greenstone unit, and pMsh = shale unit of middle structural-stratigraphic package.

dips moderately north (Plate 2). Pre-Mississippian rocks of the upper antiform structurally overlie the Mississippian Kekiktuk Conglomerate of the lower antiform on both its south and north limbs, emplaced along thrust surfaces which are subparallel to folded bedding in the Kekiktuk Conglomerate (Figures 16 and 18). These thrust faults are interpreted to be parts of a single folded thrust surface that is continuous across the crest of the lower antiform (Figures 16 and 18). Pre-Mississippian rocks coring the lower antiform outcrop over a smaller area than do the pre-Mississippian rocks of the upper antiform (Figure 15). In the upper antiform, Franklinian sequence rocks are exposed over a 5-mile (8.1-kilometer) distance between the capping Kekiktuk Conglomerate in the north and south fold limbs (Plate 2). Since most of the Franklinian sequence rocks exposed in the study area comprise the upper antiform (Figures 15 and 16), a majority of the documented mesoscopic and microscopic structures were observed in rocks located either near the core of this fold or on its north limb.

Pre-Mississippian rocks of the two antiforms display similar structures with similar absolute orientations. The most prominent structure is an east-trending, nearly bed-parallel slaty cleavage (refer to Figure 14, Table 2, and Appendix C). Within the shale unit (pMsh) of the upper antiform (Figures 7 and 16, Plate 1), compositional layering dips more steeply south than slaty cleavage. This relationship, coupled with the facing direction, indicates a structural position on the upper limb of a synformal anticline which has a south-dipping axial surface (Figure 19A). Farther to the north, slaty cleavage dips more steeply to the south than compositional layering; the facing direction is unknown at this location. The relationship between cleavage and compositional layering is compatible with an interpreted structural position either on the upper limb of an overturned anticline (Figure 19B) or on the lower limb of a synformal anticline (Figure 19A). Such field observations suggest that a complex isoclinal fold geometry was developed in the Franklinian sequence during a single progressive pre-Mississippian event or multiple pre-Mississippian deformation events. The moderately south-dipping slaty cleavage documented within the study area indicates that the axial surfaces of first-generation isoclinal folds dip

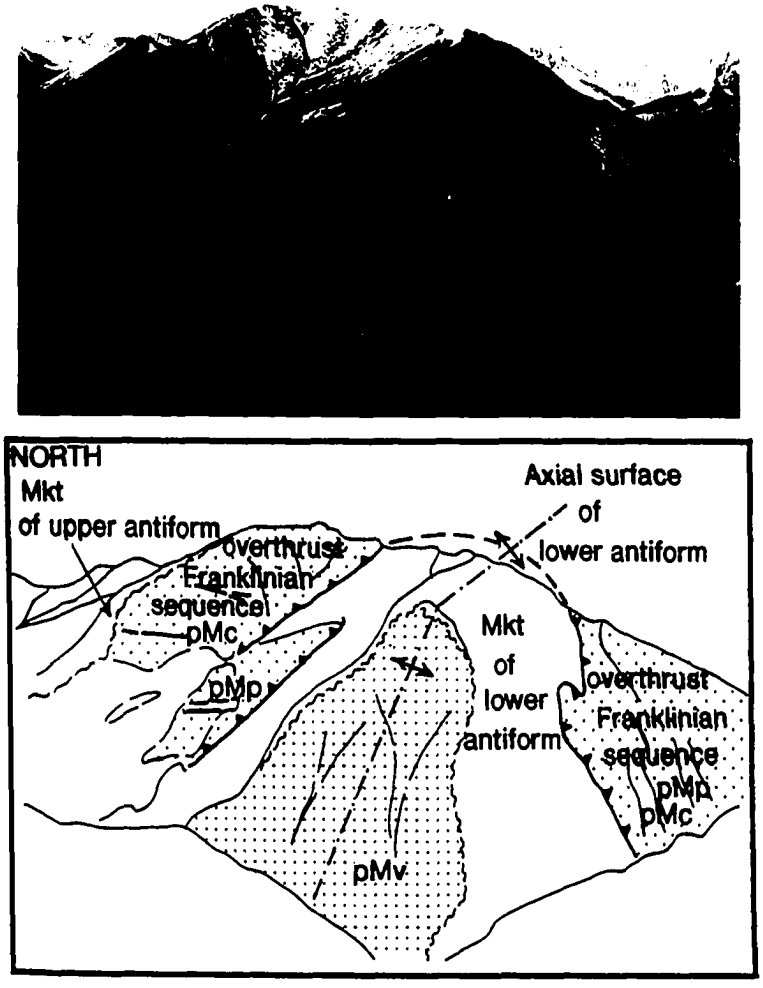

FIGURE 18. Lower antiform cored by the Franklinian sequence and capped by the Kekiktuk Conglomerate. Franklinian sequence rocks of the upper antiform are in thrust contact with the Kekiktuk Conglomerate of the lower antiform. View is to the east-northeast from near the axial surface of the upper antiform in Figure 17. pMv = volcanic unit of lower structural-stratigraphic package; pMc = chloritic phyllite unit, and pMp = phyllite unit of upper structural-stratigraphic package.

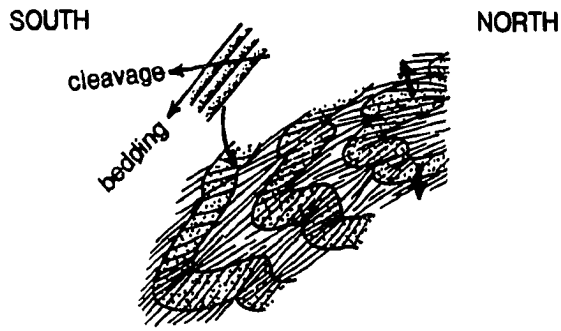

A. Overturned synformal anticline. On upper limb, beds are right-side-up (arrows) with bedding dipping to the south more steeply than cleavage.

B. Overturned anticline. On upper limb, beds are right-side-up (arrows) with cleavage dipping to the south more steeply than bedding.

FIGURE 19. Pre-Mississippian fold geometry suggested by the relationship between bedding and slaty cleavage (from Ramsay and Huber, 1987).

moderately south. The lack of traceable stratigraphic marker horizons made it impossible to define fold limbs and hinges.

5.B. STRUCTURAL GEOMETRY IN THE ELLESMERIAN SEQUENCE

The geometry and orientation of structures in the Ellesmerian sequence differ markedly from those of the Franklinian sequence. Furthermore, structures in the Kekiktuk Conglomerate differ from those in the rest of the Ellesmerian sequence.

5.B.1. Structural Geometry Observed Beneath the Kayak Shale

As shown in Figure 20, a prominent sub-Mississippian angular unconformity separates pre-Mississippian rocks from the Mississippian Kekiktuk Conglomerate. The east-northeast strike and gentle to moderate dip of bedding of the Kekiktuk Conglomerate contrast with the more easterly strike and steeper dip of slaty cleavage and compositional layering in the Franklinian sequence (Table 2). At most exposures in the study area, the sub-Mississippian unconformity appears to represent a depositional contact between the Kekiktuk Conglomerate and the Franklinian sequence. This interpretation is supported by the apparent lack of deformation in the basal Kekiktuk Conglomerate. The basal Kekiktuk Conglomerate typically observed is a quartz- and chert- pebble to cobble conglomerate (Figure 21A). Pebbles and cobbles exhibit variable shapes and random orientations, suggesting that this portion of the unit is relatively undeformed and has not accommodated much strain internally. In most locations, the Franklinian sequence rocks immediately beneath the unconformity do not appear to have been sheared, faulted or otherwise structurally disrupted by motion along or adjacent to the unconformity surface during Cenozoic deformation. (The implications of these observations are considered in Sections 6 and 9).

The Kekiktuk Conglomerate of the lower antiform occurs immediately below the folded surface of the thrust fault which separates the Kekiktuk Conglomerate from structurally overlying pre-Mississippian rocks of the upper antiform (Figures 16 and 22, Plate 2). At location "A" in Figure 23, this east-striking fault dips moderately south, subparallel to the dips of both the south limb of the Kekiktuk

FIGURE 20. Sub-Mississippian angular unconformity defining the interface between the Franklinian sequence and the Kekiktuk Conglomerate. View to the south, with the Kekiktuk Conglomerate dipping to the west (right) at an angle of 34 degrees and slaty cleavage in the underlying Franklinian sequence dipping to the south (into the page) at an angle of 64 degrees.

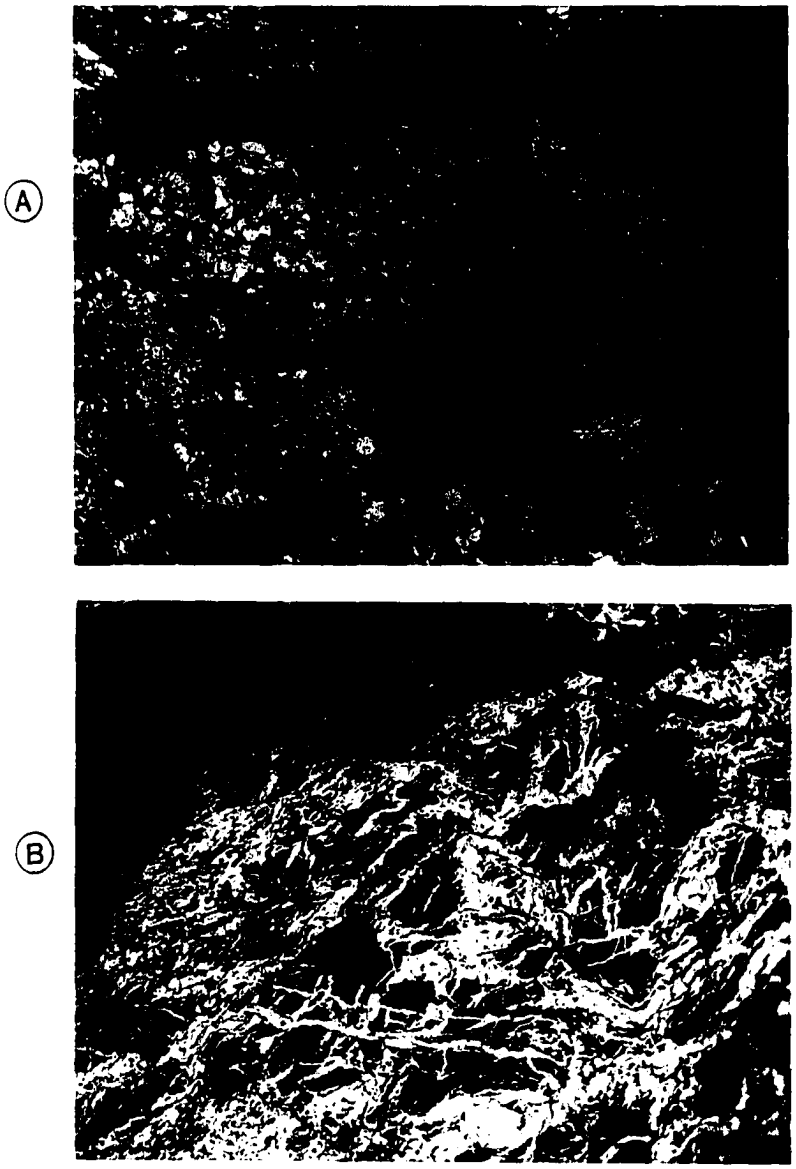

FIGURE 21. Exposures of undeformed and deformed Kekiktuk Conglomerate. (A) Apparently undeformed chert- and quartz-pebble to cobble conglomerate typically observed near the base of the Kekiktuk Conglomerate. (B) Chocolate tablet structure observed in tectonically-brecciated Kekiktuk Conglomerate.

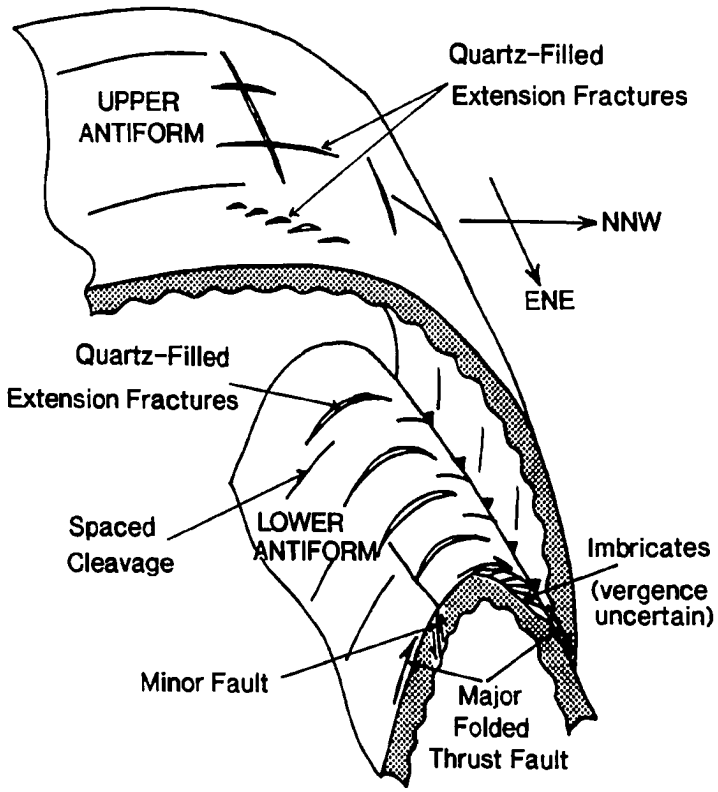

FIGURE 22. Schematic structural geometry of folds, faults, extension fractures, and spaced cleavage in the Kekiktuk Conglomerate.

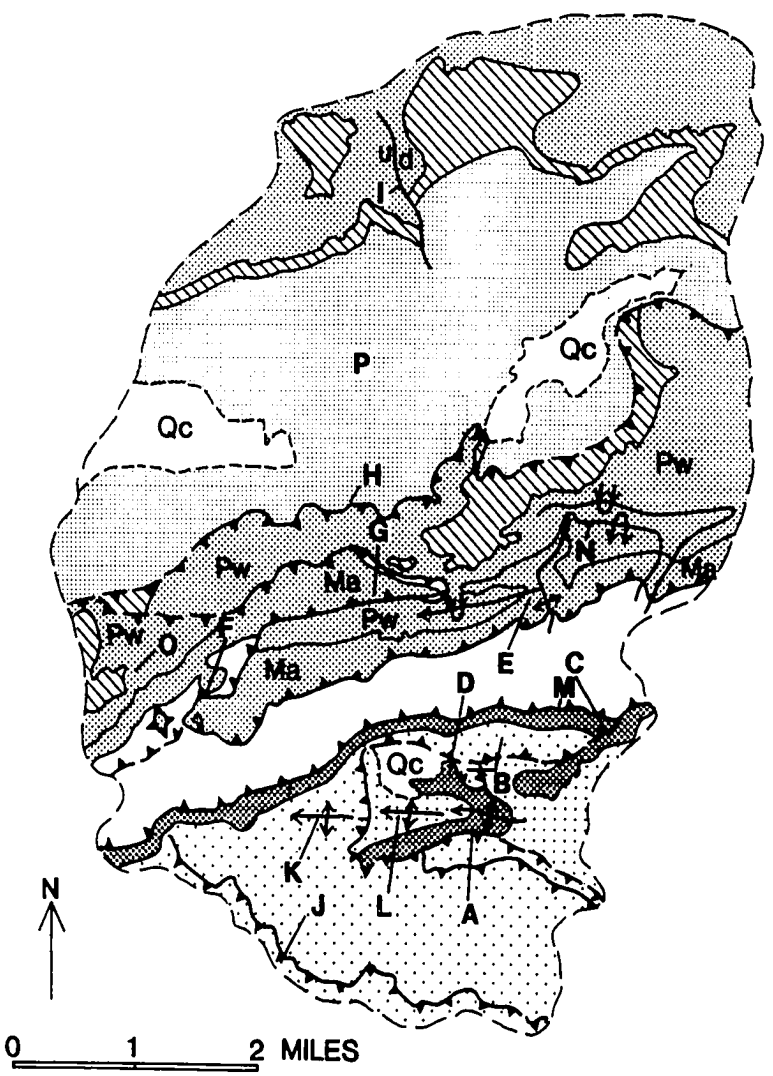

FIGURE 23. Geologic map of study area with locations A - P referred to in text. Explanation of shading scheme is provided in Figure 15.

Identification of locations referred to in the text:

A Moderately south-dipping Cenozoic thrust fault which emplaces Franklinian sequence rocks of the upper antiform over the Kekiktuk Conglomerate of the lower antiform.

B Franklinian sequence rocks of the upper antiform which structurally overlie the north limb of the lower antiform.

C Imbrication of the Kekiktuk Conglomerate along the north limb of the lower antiform. The Kekiktuk of the upper antiform is truncated against the north limb of the Kekiktuk Conglomerate of the lower antiform in this area.

D Imbricates of quartzite of the Kekiktuk Conglomerate, bounded by shale. Near this location, the Kekiktuk Conglomerate is overthrust by purple phyllite (pMp).

E Disharmonic folding of the Alapah Limestone in the cores of map-scale detachment folds developed in the Wahoo Limestone above the Kayak Shale.

F North-vergent mesoscopic folds in the Kayak Shale. A closely spaced cleavage is axial planar to these folds. Thin interbeds of limestone exhibit 26% shortening.

G Overturned syncline in the Wahoo Limestone truncated by thrust fault which emplaces the Kayak Shale and Alapah Limestone over the Wahoo Limestone.

H Prominent east-northeast-trending, moderately south-dipping thrust fault emplaces the Wahoo Limestone (and Echooka Formation to the east of this location) over the Ivishak Formation.

I North-northwest-trending fault truncates folded rocks of the Wahoo Limestone and Echooka Formation. Interpreted to be a west-dipping reverse fault formed during D_3.

J Pre-Mississippian thrust fault within the Franklinian sequence of the upper antiform. Interpreted to have been reactivated during Cenozoic deformation.

K Axial surface of upper antiform developed in the Franklinian sequence.

L Axial surface of lower antiform developed in the Franklinian sequence.

M Quartz veinlets developed in the Kayak Shale in proximity to a gradational contact with the Kekiktuk Conglomerate.

N Axial surface of recumbent anticline developed within the Lisburne Group, the most prominent and impressive map-scale detachment fold observed in the study area.

O Disharmonic folding of the Wahoo Limestone developed in a relatively tight syncline.

P Polyharmonic folding of interbedded sandstone, siltstone, and shale of the Ivishak Formation in the core of a broad sycline.

Conglomerate and slaty cleavage within the upper antiform (Figures 16 and 22, Plate 2). At location "B" in Figure 23, this folded fault dips gently to moderately north, subparallel to the dip of the Kekiktuk Conglomerate which forms the north limb of the lower antiform (Figures 16 and 22, Plate 2).

On the north limb of the lower antiform the Kekiktuk Conglomerate is structurally disrupted by smaller-scale faults, likely genetically related to the presence of overthrust pre-Mississippian rocks (discussed in Section 8). At locations "C" and "D" in Figure 23, where pre-Mississippian rocks have been thrust over the Kekiktuk Conglomerate of the lower antiform, the Kekiktuk Conglomerate of the lower antiform has been imbricated. As shown in Figure 24, at location "C" several-meter-thick imbricates of foliated quartzite of the Kekiktuk Conglomerate are structurally bounded by shale. Since the precise trajectory of the faults which produced the observed structural duplication at locations "C" and "D" is not well-exposed, it was not possible to ascertain the tectonic transport direction of these imbricates based on the stacking of imbricate slices (Figure 22). Mesoscopic faults locally involve the Kekiktuk Conglomerate of the lower antiform. On the south limb of the antiform near the fold axis, a steeply south-dipping fault plane strikes east-northeast, subparallel to the trend of the axis of the lower antiform (Figure 22). Pebbles and cobbles have been sheared ductilely near the fault plane, indicating minor (0.5 meter), downward-to-the-south displacement of the hangingwall (southern) block (Figure 22). No significant mesoscopic faults were recognized in the Kekiktuk Conglomerate capping the upper antiform.

5.B.2. Structural Geometry of the Kayak Shale

Contrasts in the geometry, wavelength and amplitude of folds developed in units above and below the Mississippian Kayak Shale indicate that Lisburne and Sadlerochit Group rocks are decoupled from the Kekiktuk Conglomerate. A roughly 1,000-1,150-meter-thick interval of poorly exposed Kayak Shale separates broad folds with wavelengths of several kilometers developed in the Kekiktuk Conglomerate (Figures 17 and 18) from folds with wavelengths of hundreds-of-meters developed in the Alapah

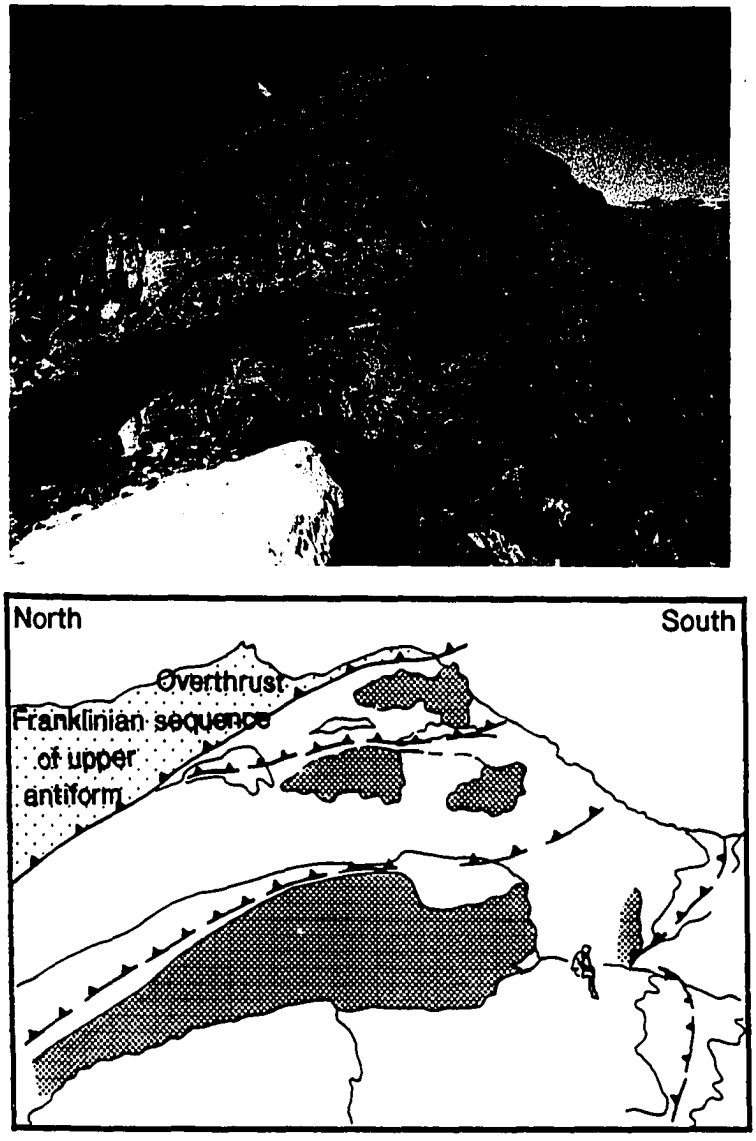

FIGURE 24. Imbricates of Kekiktuk Conglomerate observed at location "C" in Figure 23. View is to the northeast, along strike of the Kekiktuk Conglomerate of the lower antiform. Shaded portions of the line drawing correspond to quartzite imbricates; imbricates are separated by black shale intervals.

Limestone of the Lisburne Group (e.g. location "E" in Figure 23).

The mesoscopic structural geometry of the Kayak Shale is best exposed in drainages immediately west of location "F" in Figure 23. The Kayak Shale contains a well-developed slaty cleavage that is oriented subparallel to compositional layering. This slaty cleavage was folded during Cenozoic deformation. Folds within the Kayak Shale vary in shape, wavelength, and amplitude, and are disharmonic with respect to folds developed in the underlying Kekiktuk Conglomerate and the overlying Alapah Limestone. The shortest wavelength folds occur in 1-2 cm-thick limestone interbeds near the contact with the Alapah Limestone. The amplitude of these parasitic folds is generally less than 10 cm. Minimum shortening averages 26% and no consistent vergence of folds was observed. Longer-wavelength folds (tens-of-meters) typically have amplitudes of less than 10 meters. Such folds have variable directions of vergence due to an irregular geometric form characterized by multiple, variably oriented axial surfaces. North-vergent folds with wavelengths of several meters and amplitudes of roughly a meter were observed near location "F" in Figure 23. In this vicinity, a gently south-dipping secondary cleavage (possibly a solution cleavage) strikes east to east-northeast, axial planar to the north-vergent folds.

Near location "F" (Figure 23) and at isolated exposures elsewhere in the study area, the Kayak Shale is not folded at a mesoscopic scale. For example, slaty cleavage in the Kayak Shale in the hangingwall of thrust faults near locations "F" and "G" in Figure 23 appears to be subparallel to the fault surfaces. This would suggest rotation due to slip along slaty cleavage surfaces. Thus, thrust faults and geometrically irregular and complex folds in the Kayak Shale accommodate shortening and suggest that substantial tectonic flow occurred within this mechanically incompetent structural-stratigraphic unit. The role of the Kayak Shale as a detachment horizon is discussed in Sections 6 and 9.

5.B.3. Structural Geometry Observed Above the Kayak Shale

The average wavelength of map-scale folds developed in the Lisburne and Sadlerochit Groups to

the north of the anticlinorium is on the order of 1-2 kilometers (Figure 23, Plates 1, 2, and 5). Folds on the north limb of the Franklin Mountains anticlinorium are overturned to the north and become progressively more upright toward the core of the synclinorium north of the anticlinorium (Plates 1 and 5). Based on field mapping and general observation of well-exposed folds in the Lisburne Group, the thicknesses of fold limbs and hinges appears to remain relatively constant. Some thinning of fold limbs is likely in tight folds that are strongly overturned.

Several thrust faults truncate Ellesmerian sequence rocks in the study area. These local faults likely formed subsequent to the major episode of folding in the study area. (Possible temporal and geometric relationships between folds and faults are discussed in Section 9.) Fault cut-offs have been eroded from hangingwalls; therefore, the magnitude of displacement on these faults could not be determined directly from field data. Displacement values and the interpreted evolution of these faults are considered in Sections 6 and 9, respectively, based on the geometry of balanced cross-sections. The geometry of four faults is described below:

(1) Structural duplication of the Kayak Shale and Alapah Limestone occurs near location "F" in Figure 23, with the Kayak Shale interpreted to have functioned as a detachment zone. The Kayak Shale at this location dips moderately north, suggesting the orientation of the fault surface. The hangingwall sequence of Kayak Shale and Alapah Limestone is folded, and the fault truncates folds developed in the Alapah and Wahoo Limestones in the footwall. Asymmetry of folds in the Kayak Shale suggests northward displacement of the hangingwall sequence with respect to the footwall sequence. Thus, this fault is interpreted to be a north-dipping thrust fault which has accommodated northward displacement of the hangingwall sequence (Plate 5).

(2) At location "G" in Figures 23 and 25, the Alapah Limestone truncates underlying folds in the younger Wahoo Limestone. Exposure of the fault indicates that it dips to the southwest near location "G" (Figure 23). If this fault is linked with the north-dipping fault at location "F" (mentioned above),

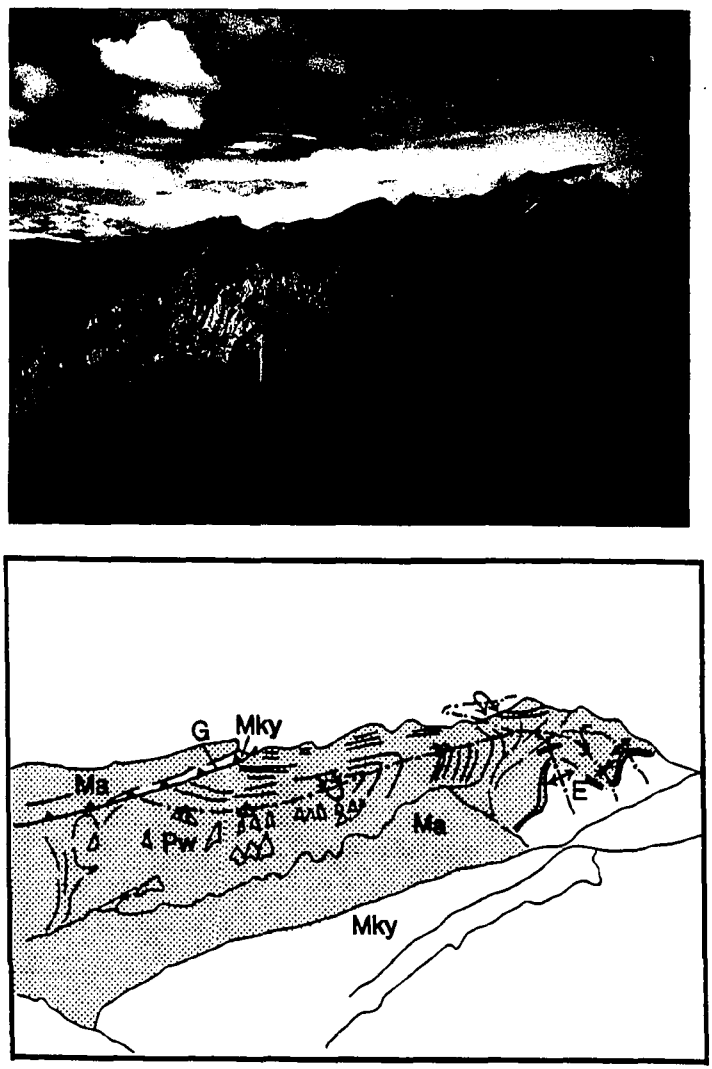

FIGURE 25. Detachment folds and thrust faults developed in the Lisburne Group (shaded) above the Kayak Shale. View is to the northeast, oblique to the strike of the main exposure of Kayak Shale in the middle of the study area. Locations "E" and "G" in the line drawing are shown in Figure 23.

this implies that the fault surface was folded synchronous with or subsequent to faulting (Plate 2). Kayak Shale occurs beneath the Alapah and above the Wahoo Limestone, suggesting that this thrust fault soles in the Kayak Shale (Figure 25).

(3) The Pennsylvanian(?) Wahoo Limestone overlies and truncates the upper part of the Lower Triassic Ivishak Formation at location "H" in Figure 23, indicating the presence of a thrust fault. This fault likely dips more steeply south than the moderately south-dipping bedding in both the Wahoo and Ivishak. Toward the east, along strike of the fault, the hangingwall unit changes from the Wahoo Limestone to the Echooka Formation and then back to the Wahoo (Figure 23). Since thrust faults are generally regarded to be essentially planar surfaces which cut upward through a stratigraphic section in the direction of transport, the fact that this fault intersects the same contact twice along strike suggests that bedding was folded prior to faulting (See geometry in Plate 5).

(4) The three faults described above trend east-northeast, parallel to the strike of most Cenozoic structures. An exception to this pattern is a north-trending fault observed at location "I" in Figure 23. Mapped contacts of folded Lisburne and Sadlerochit Groups on both sides of the fault suggest that the western block has been upthrown with respect to the eastern block. While the actual fault surface was not observed, map relations indicate that the fault likely dips moderately to the west. Given such an orientation and sense of displacement, this structure is considered to be a reverse fault associated with an episode of easterly tectonic transport which occurred subsequent to folding of the Ellesmerian sequence, possibly D_3 (discussed in Section 5.C.4.).

5.C. RELATIVE CHRONOLOGY OF DEFORMATION

Structures observed in the Ellesmerian sequence were formed during Cenozoic deformation, which can be subdivided into a major progressive event, D_2, which is interpreted to have resulted in formation of the Franklin Mountains anticlinorium, and a subsequent, poorly-understood and relatively minor(?) event,

D_3. It is difficult to distinguish between pre-Mississippian (D_1) and Cenozoic (D_2) structures in the Franklinian sequence since both generations of structures are similar in orientation (Table 3).

The orientation of Cenozoic structures in Franklinian sequence rocks is likely influenced by the type and orientation of the pre-Mississippian structures present in these rocks. Wallace and Hanks (in press) suggest that east-trending pre-Mississippian structures established a structural grain in the Franklinian sequence. Cenozoic deformation may have reactivated pre-Mississippian structures, and Cenozoic structures in the Franklinian sequence may have preferentially formed along the pre-Mississippian structural grain (Wallace and Hanks, in press). Finally, the types of structures developed in the Franklinian sequence vary locally, likely dependent on the material properties of the heterogeneous suite of pre-Mississippian rocks. For example, pre-Mississippian slaty cleavage or Cenozoic folding of this cleavage is developed in shale, slate, and phyllite but is not developed in the more massive greenstone, chert, or sandstone intervals within the Franklinian sequence.

5.C.1. Pre-Mississippian Deformation (D_1)

The pervasive, east-trending, nearly bed-parallel slaty cleavage (S_1) observed in rocks of the Franklinian sequence is interpreted to represent an axial planar cleavage associated with tight to isoclinal pre-Mississippian folding (F_1) (Section 5.A., Table 2). As shown on an equal-area stereographic projection (Figure 26), the best fit girdles to plotted poles to compositional layering (S_0) and cleavage surfaces (S_1) have similar orentations, suggesting that S_0 and S_1 are nearly coplanar in the Franklinian sequence. Bedding and slaty cleavage dip moderately to the south except on the north limbs of the two Kekiktuk-capped antiforms, where bedding and slaty cleavage have been folded so that they dip to the north. The east strike of cleavage planes in Figure 14A contrasts with the generally east-northeast strike of bedding planes in the Ellesmerian sequence (Figure 14E). East-trending structures are not observed in

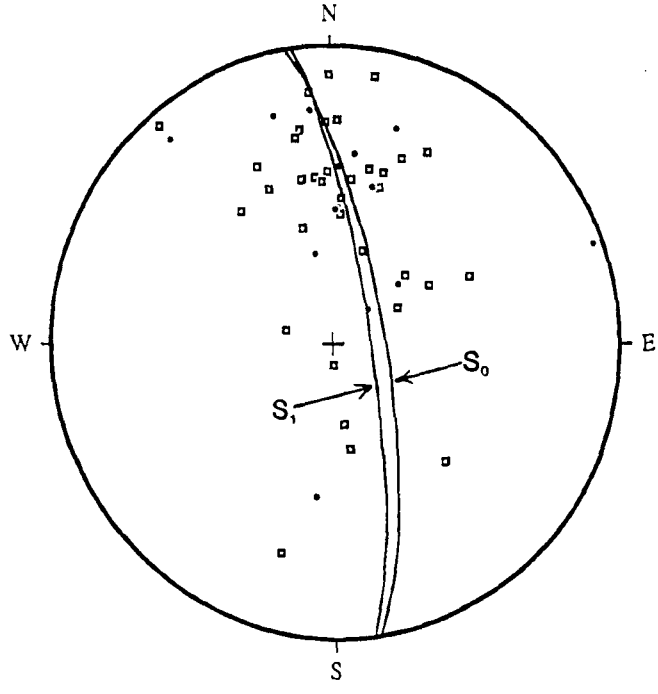

FIGURE 26. Equal-area stereographic projection of poles to planes of compositional layering (S_0) and slaty cleavage (S_1) in the Franklinian sequence. • = S_0 (N = 13); ▫ = S_1 (N = 36). Similar orientations of best-fit girdles indicates that S_0 and S_1 are nearly coplanar. Best-fit girdle of S_0 = 351 / 75 NE; best-fit girdle of S_1 = 352 / 79 NE.

the Ellesmerian sequence; thus, slaty cleavage developed in the Franklinian sequence is inferred to be the result of pre-Mississippian deformation.

An east-trending, moderately south-dipping fault at the southern boundary of the study area truncates the middle structural-stratigraphic unit of the Franklinian sequence but offsets neither the sub-Mississippian unconformity surface nor the overlying Mississippian Kekiktuk Conglomerate (location "J" in Figure 23). This structure (described in Section 5.A.) is interpreted to be a thrust fault (T_1, similar to that shown in Figure 9) formed during pre-Mississippian deformation, prior to erosion of the sub-Mississippian unconformity, and deposition of the Kekiktuk Conglomerate. Slaty cleavage in the hangingwall of this fault zone dips less steeply than that in the footwall. Such separate cleavage domains would be expected if faulting accompanied or post-dated cleavage formation.

5.C.2. Cenozoic Deformation (D_2) of Franklinian Sequence

Cenozoic structures of major importance include the two pre-Mississippian-cored antiforms (F_2) defined by the folding of both slaty cleavage (S_1) and the overlying Kekiktuk Conglomerate (locations "K" and "L" in Figure 23). North-vergent thrust faults (T_2) emplaced the Franklinian sequence over the Mississippian Kekiktuk Conglomerate at the north edge of the Franklin Mountains anticlinorium (Figure 17, locations "A" and "C" in Figure 23). Other D_2 structures include (1) local small-scale folds and mesoscopic crenulation (F_2) of pre-Mississippian slaty cleavage (Figure 14B) with F_2 axes trending east to east-southeast (Table 2), and (2) quartz- and calcite-filled extension fractures which cross-cut pre-Mississippian slaty cleavage and generally strike east-northeast or northwest (Section 5.A., Tables 2 and 3, Figure 14C).

5.C.3. Cenozoic Deformation (D_2) of Ellesmerian Sequence

Thrust faults and the axes of major folds in the northeastern Brooks Range generally trend east or

east-northeast where pre-Mississippian rocks are involved, and trend east-northeast in Mississippian and younger units (Figure 3) (Wallace and Hanks, in press). Since both pre-Mississippian and Mississippian and younger rocks were deformed the same northward-migrating Cenozoic event(s), the east-northeast structural trend exhibited by the Mississippian and younger units suggests a north-northwest direction of tectonic transport during Cenozoic deformation of the northeastern Brooks Range.

A stereographic plot of poles to bedding in Ellesmerian sequence rocks (Figure 27) forms a north-northwest-trending girdle of points. The axes of Cenozoic folds in the Ellesmerian sequence can be inferred to trend normal to the girdle of bedding poles, or east-northeast (Figures 15 and 27). Assuming that fold axes trend normal to the direction of shortening, Figure 27 suggests that Cenozoic shortening occurred in a north-northwest/south-southeast direction. Since Cenozoic deformation in the northeastern Brooks Range is interpreted to have progressed from south to north (Section 2.A.2.), the girdle in Figure 27 can be cited as evidence supporting a north-northwest direction of tectonic transport during D_2, the major Cenozoic deformational event.

Thrust faults (T_2) involving Ellesmerian sequence rocks are folded, and folds in the Lisburne and Sadlerochit Groups are truncated by faults (Section 5.B.3.), suggesting that Cenozoic deformation (D_2) of the Ellesmerian sequence involved multiple generations of folding and thrust faulting. There is no evidence which indicates that these D_2 structures formed during a series of separate and distinct folding and faulting episodes, collectively referred to as D_2. Rather, D_2 was likely a progressive deformational event, with the apparent generations of folds and faults associated with major stages in the evolution of local structures in the study area. Temporal and structural relationships between deformation of the Ellesmerian sequence and formation of the Franklin Mountains anticlinorium are addressed in Section 9.

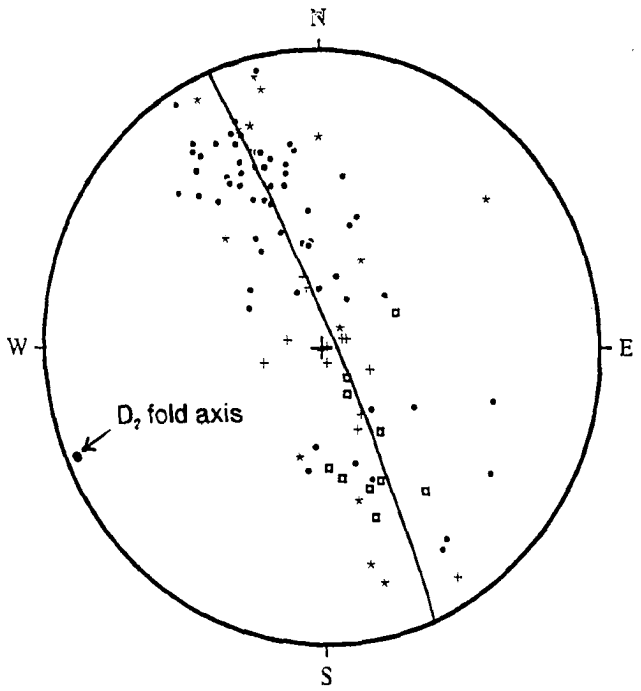

FIGURE 27. Equal-area stereographic projection of poles to bedding in Ellesmerian sequence (N = 98). □ = Kekiktuk Conglomerate (N = 10); + = Kayak Shale (N = 13); ⋆ = Lisburne Group (N = 14); • = Sadlerochit Group (N = 61). Best-fit girdle of bedding planes is shown, striking 337 degrees and dipping 86 degrees to the northeast. Inferred from this plot, the Cenozoic fold axis trends 247 degrees and plunges 4 degrees to the southwest.

5.C.4. Cenozoic Deformation (D_3)

The mode and time of formation of the north-northwest- to north-striking, subvertical spaced cleavage, observed in both Franklinian and Ellesmerian sequence rocks (Figures 14D and 14G), are difficult to establish. This cleavage could be a solution cleavage formed as a result of roughly east-west shortening during an event referred to as D_3, which followed the main period of north-northwest-directed Cenozoic folding and thrust faulting. North-northwest-trending stylolites crosscut the planes of slaty cleavage or compositional layering in Franklinian and Ellesmerian sequence rocks (Appendix E), establishing that roughly east-west Cenozoic shortening affected these rocks at least locally. Spaced cleavage surfaces tend to be stained by a calcite precipitate, possibly a residue generated by pressure solution. However, it is also possible that these surfaces represent tensional fractures formed in association with relative east-west extension, possibly coincident with roughly north-south shortening during D_2. Analogous structures would be the north-northwest-trending, subvertical quartz- and calcite-filled extension fractures developed in Franklinian and Ellesmerian sequence rocks, interpreted to be D_2 structures (Tables 2 and 3). The north-northwest-striking reverse fault within the Ellesmerian sequence (location "I" in Figure 23, described in Section 5.B.3.b.) might be either a D_3 contractional structure or an accommodation fault formed during D_2.

5.D. DEFORMATION MECHANISMS

Deformation mechanisms which operate at a particular scale are dependent on physical parameters which include temperature, confining pressure, fluid pressure, deviatoric stress, strain rate, and material properties of the rock units involved (Mitra, 1987). Pelitic rocks of the Franklinian sequence contain a mineralogic assemblage of quartz-chlorite-sericite-calcite, with minor rutile, pyrite, iron oxide, and clay minerals. Such an assemblage suggests that these pre-Mississippian rocks have experienced, at the most,

lower greenschist facies metamorphism. Deformational features observed in Ellesmerian sequence rocks can be attributed, probably in large part, to penetrative strain and fluid-mineral interactions, without requiring that temperatures reached metamorphic levels. Quartz overgrowths locally surround quartz grains. Quartz subgrains, intergranular fine-grained white mica, and quartz-filled extension fractures occur in the Kekiktuk Conglomerate. Such features are considered to be the products of pressure solution, limited recrystallization, and fluid flux through the Kekiktuk Conglomerate. Other deformational overprints include the formation of a slaty cleavage in the Kayak Shale, extensive twinning of calcite and the development of an axial planar pressure solution cleavage and stylolites in the Lisburne Group, and the development of axial planar cleavage in the Sadlerochit Group.

Low-temperature deformation mechanisms likely produced the features indicative of penetrative strain observed in the Franklinian and Ellesmerian sequences. Groshong (1988) suggests that the upper boundary of the low-temperature deformation field occurs at roughly one-third the melting temperature of the framework minerals. For quartzose and calcareous rocks, this boundary is marked by the formation of subgrains by recrystallization, or more than 15% strain accommodated by crystal-plastic features such as twin lamellae, deformation bands, and undulatory extinction (Groshong, 1988). Since quartz subgrains were developed in the Kekiktuk Conglomerate and a significant amount of plastic deformation of calcite was observed locally in the Lisburne Group (strain quantified in Section 7), conditions might have come close to the upper boundary of low-temperature deformation at some locations in the study area. Conodont alteration indices (CAI's) obtained from Lisburne Group samples from the Shublik Mountains and the Fourth Range to the north of the study area have an average value of 4, ranging between values of 3 and 6 (P.D. Gruzlovic, 1989; pers. commun.), with the higher values obtained from the Fourth Range and the region to its south (K.F. Watts, 1989; pers. commun.). Such CAI values suggest that, north of the study area, the Lisburne Group reached temperatures of at least 200°C and as high as 300°C during Cenozoic deformation. An overburden pressure of roughly 2 kbars would have been produced by some 9

kilometers of Brookian sediment which Bird and Bader (1987) suggest overlay the Ellesmerian sequence at the mountain front at the time of Cenozoic deformation.

Table 4 summarizes deformation features observed in the Franklinian and Ellesmerian sequences, grouped according to the deformational event during which they are interpreted to have formed. Note that most of these features were observed microscopically and can be attributed, in most cases, to pressure solution and crystal-plastic deformation mechanisms. Sections 5.D.1. and 5.D.2. discuss (1) the mechanisms which may have formed these deformation features and the structures listed in Table 2, (2) the basis for determining the relative chronology of mechanisms, and (3) their possible significance. The absolute orientations of deformation features observed in the Franklinian and Ellesmerian sequences are presented in Appendix E and the kinematic significance of some of the features described in this section are discussed. The orientations of these deformation features relative to local structures are also shown in Appendix E.

5.D.1. Deformation Mechanisms in the Franklinian Sequence

Most deformational features observed in the Franklinian sequence cross-cut (and, therefore, post-date) the prominent slaty cleavage (S_1), which is believed to be a pre-Mississippian structural fabric which formed in association with isoclinal folding during D_1. The slaty cleavage (S_1) observed in pre-Mississippian shale, slate, and phyllite was likely produced by pressure solution along surfaces normal to the direction of shortening, subparallel to the axial surfaces of F_1 folds. As the following examples show, in some instances it was possible to establish the relative chronology of mechanisms operative during Cenozoic deformation, following the formation of S_1: (1) Slaty cleavage is locally cross-cut by quartz- and calcite-filled extension fractures (S_2), which strike east-northeast and display extension sub-parallel to cleavage (S_1). Locally, such filled fractures are offset along S_1 and are crumpled

lengthwise (Table 4, Appendix E), suggesting that pressure solution occurred during Cenozoic deformation (D_2) in a plane parallel to S_1, possibly with some slip along S_1. Similarly, more massive pre-Mississippian rocks contain quartz- and calcite-filled mesoscopic and microscopic extension fractures which were subsequently buckled by shortening and offset by pressure solution in a plane normal to that of the extension fractures. (2) Pressure shadows, with cumulative fiber lengths on the order of 0.5-1.0 centimeters, were developed in a pre-Mississippian sandstone, surrounding marcasite nodules of about one-centimeter in diameter. Minerals forming these pressure shadows crystallized in the sequence chlorite --> quartz --> calcite. This sequence of pressure shadow minerals may indicate the relative ages of deformation features in similar rocks which involved crystallization of chlorite, quartz, and calcite. (The probable Cenozoic age of these pressure shadows is established in Section 7.) (3) A tectonically brecciated zone with a mylonitic petrofabric occurs in the hangingwall, just above a major, moderately south-dipping Cenozoic thrust fault (T_2) at location "A" in Figure 23. In a subvertical plane roughly parallel to the inferred north-northwest Cenozoic tectonic transport direction, the asymmetry of shear sense indicators (sheared porphryoblasts, S-C protomylonite fabric) records both to-the-north and to-the-south shear along a surface subparallel to the thrust fault (Section 7.A.2., Appendix E).

Pressure solution and crystal-plastic deformation mechanisms of indeterminate age (due to the absence of cross-cutting relationships with established D_1 structures) affected discrete rock surfaces and volumes in the Franklinian sequence. Metacherts contain several sets of stylolites which are interpreted to have formed normal to the direction of shortening, either during pre-Mississippian or Cenozoic deformation. (Refer to Table 10 in Appendix E for orientations.) Insoluble opaque material and some chlorite fibers are concentrated along these dissolution surfaces. In addition, rock volumes were affected by crystal-plastic deformation mechanisms which may have operated during both pre-Mississippian and Cenozoic deformational events. Dislocation glide likely produced undulatory extinction in quartz grains

occurring in pre-Mississippian greywacke. Franklinian sequence carbonates were twinned locally. Some bent twin lamellae were observed, indicating that deformation occurred subsequent to twinning.

5.D.2. Deformation Mechanisms in the Ellesmerian Sequence

It is difficult to establish a relative chronology of deformation mechanisms in Ellesmerian sequence rocks since observed features rarely cross-cut each other. Since different physical conditions and material properties determined the structural geometry above and below the Kayak Shale detachment horizon, the types of deformation mechanisms which affected rocks of the Ellesmerian sequence might be expected to vary accordingly.

5.D.2.a. Deformation mechanisms in the Kekiktuk Conglomerate

Framework grains in samples of Kekiktuk Conglomerate quartzite are estimated to be 90% monocrystalline quartz, 2-5% aggregates of polycrystalline quartz, and 5% microcrystalline quartz (chert). Of the monocrystalline quartz and polycrystalline aggregates, an estimated 3-5% exhibit straight extinction, 93-95% exhibit slightly undulose extinction, and 2% exhibit strongly undulose extinction. The undulose extinction observed in the majority of framework grains in these Kekiktuk Conglomerate samples can probably be attributed to crystal-plastic deformation (Groshong, 1988). Such grain-scale deformation could have occurred during pre-Mississippian and/or Cenozoic deformational events, prior to and/or following deposition of the Kekiktuk Conglomerate.

Since adjacent grains in these samples rarely have similar optic orientations, it does not appear that originally large framework grains were reduced in size by granulation or dynamic recrystallization. Although the optical orientations of grains were not analyzed quantitatively, the apparent absence of a preferred orientation might suggest that grains were strained prior to deposition of the Kekiktuk Conglomerate, during pre-Mississippian deformation.

Rotation of framework grains, crystal-plastic deformation, and pressure solution on surfaces normal to the direction of maximum shortening produced a preferred orientation of subelliptical quartz

grains (described by methods discussed in Section 7 and Appendix G). Varying amounts of intergranular fine-grained white mica (pyrophyllite?; cf. Reed, 1968) are present in the Kekiktuk Conglomerate, causing the fringes of affected quartz grains to appear ragged. Subgrains border some quartz framework grains, suggesting that recrystallization has occurred locally. In addition, transgranular deformation features, including stylolites and fractures, cross-cut framework grains in the Kekiktuk Conglomerate. (For orientations and additional details, refer to Appendix E.) Partially-dissolved grains abut stylolite surfaces; however, the volume of material dissolved by pressure solution is impossible to estimate. Microfractures locally transect grains; no shear displacement is evident along these surfaces. Some grain-boundary sliding appears to have occurred, resulting in minor fracturing and granulation at the margins of involved grains; no systematic directional pattern of movement is apparent.

5.D.2.b. Deformation mechanisms in the Kayak Shale

Pressure solution produced the well-developed slaty cleavage which was then progressively folded during D_2 deformation of the Kayak Shale, accompanied by the local development of a secondary, axial planar, closely spaced solution cleavage. The early, subsequently folded slaty cleavage was likely produced by compactional shortening directed normal to bedding, while the secondary solution cleavage would have formed as a result of shortening normal to fold axes.

Near the contact with the underlying Kekiktuk Conglomerate (location "M" in Figure 23), quartz veinlets cross-cut and follow slaty cleavage. These veinlets exhibit no preferred orientation and both truncate and are folded with slaty cleavage. Such relationships suggest that the veinlets are broadly synchronous with mesoscopic folding of the Kayak Shale at this location, interpreted to have occurred during D_2 (Section 5.B.2.). The presence of these veinlets indicates that, coincident with deformation, a fracture network existed in the Kayak Shale, and dissolved silica was present in the system. As discussed above, pressure solution affected the Kekiktuk Conglomerate during Cenozoic deformation. Since quartz

overgrowths were observed only locally in the Kekiktuk Conglomerate, it is possible that dissolved silica may have been removed from an open system, rather than being reprecipitated locally as overgrowths. Thus, it can be speculated that dissolved silica may have migrated stratigraphically upward from the Kekiktuk Conglomerate, filling fractures in the Kayak Shale.

5.D.2.c. Deformation mechanisms in the Lisburne Group

Deformation of the Lisburne Group carbonates occurred by crystal-plastic and pressure solution mechanisms. In order to assess the extent of crystal-plastic deformation, the number of twin planes in calcite grains (echinoderm fragments) were counted for three mutually-perpendicular thin-sections per sample (Jamison and Spang, 1976). For several samples of the Alapah and Wahoo Limestones, of the roughly 120 calcite grains counted per thin-section, an average of 37% were twinned on one plane, 56% on two planes, and 7% on three planes. Twin planes seemed to show no consistent pattern of orientation in similarly oriented thin-sections, and the number of samples was insufficient to detect any pattern of variation in the extent of twinning at various locations in the study area. Near the thrust fault at location "H" in Figure 23, in the plane of bedding, twin planes within calcite grains are offset by slip (Appendix G), twin lamellae are curved in all thin-sections, and bryozoans and crinoids show maximum elongation in a generally north-south direction. At location "F" in Figure 23, lithostrotionoid corals are deformed such that cross-sections perpendicular to the stems are elliptical, elongated in a northwest-southeast direction. (These corals were used for strain determinations discussed in Section 7.)

Prominent bedding-parallel stylolites were observed in the Wahoo Limestone. Pressure solution likely began during diagenesis and may have recurred in response to local bedding-normal shortening strain associated with Cenozoic deformation. A pressure solution cleavage occurs in some fold hinges and is generally axial planar to folds, suggesting an axis of shortening normal to fold axial surfaces.

5.D.2.d. Deformation mechanisms in the Sadlerochit Group

Deformation of the Permian Echooka Formation occurred by crystal-plastic, pressure solution,

and extension-related mechanisms. Calcareous rocks in the Echooka Formation near the contact with the Lisburne Group contain twinned calcite grains (echinoderm fragments). An average of 41% of the calcite grains were twinned on one plane, 55% on two planes, and 4% on three planes (using the same counting procedure as for the Lisburne Group samples). Bedding-parallel stylolites indicate that pressure solution affected these basal strata, recording local shortening strain normal to bedding. Quartz pressure shadows are developed around euhedral pyrite in calcareous shale near the contact with the underlying Lisburne Group (Section 7 and Appendix F).

Deformation of the Lower Triassic Ivishak Formation occurred by pressure solution, crystal-plastic, grain-rotation, and fracture mechanisms. Pressure solution affected surfaces parallel to bedding, producing the fissility characteristic of shaley intervals. Grain-rotation, and possibly crystal-plastic deformation, produced a preferred orientation of subelliptical framework grains in grain-supported quartz sandstone (Section 7 and Appendix G.) Discontinuous solution seams occur along, but generally do not transect, boundaries of framework grains. Local, subvertical and generally north- to north-northwest-striking quartz-filled extension fractures cross-cut Ivishak Formation sandstone.

5.E. BASIC STRUCTURAL STYLE BASED ON FIELD OBSERVATIONS

The Cenozoic structural style of the Franklinian sequence is regarded to be intermediate between the two end-member models of Figure 10. No floor thrust within the Franklinian sequence is exposed in the study area; however, at least one Cenozoic imbricate thrust fault climbed through the Franklinian sequence, emplacing pre-Mississippian rocks of the upper antiform over the Kekiktuk Conglomerate of the lower antiform. Based on the structural geometry described in Section 5.A., the two antiforms, each with a carapace of the Mississippian Kekiktuk Conglomerate, can be interpreted to be fault-bend folds formed at the leading edges of two horses in a duplex thrust system (discussed in Appendix D.2.). Thus, field observations are compatible with the regional structural style suggested by Rattey (1985), Namson and Wallace (1986), and Leiggi (1987). If Cenozoic tectonic transport was to the north-northwest (as

suggested in Section 5.C.3.), in a foreland-propagating duplex the upper antiform would have formed first and been refolded by subsequent formation of the lower antiform due to emplacement of the second horse (refer to Figure 49 in Appendix A).

Within the study area, the majority of Cenozoic shortening of Franklinian sequence rocks is interpreted to have been accomplished by thrust imbrication, with the resulting structural duplication creating the positive structural relief of the anticlinorium (Figure 16, Plate 2). Smaller-scale Cenozoic internal deformation of Franklinian sequence rocks does not appear to accommodate a substantial amount of shortening. The lack of widespread internal Cenozoic deformation of these thrust sheets may indicate that they behaved as semi-rigid blocks, displaced along discrete fault surfaces. Field observations suggest that much of the Cenozoic deformation of pre-Mississippian structures and strata may be localized immediately above and below the major Cenozoic thrust fault which separates the two antiforms and may have been accommodated, in large part, by internal deformation of mechanically incompetent shales and phyllites.

The contrasts in structural geometry above and below the Mississippian Kayak Shale indicate that this mechanically incompetent structural-stratigraphic unit functioned as a major detachment zone. Thus, the Kayak Shale is interpreted to house the roof thrust of the proposed duplex thrust system. Beneath the Kayak Shale, the Kekiktuk Conglomerate appears to overlie an unmodified depositional contact with pre-Mississippian rocks at most locations in the study area, suggesting that this structural-stratigraphic unit remained attached to the Franklinian sequence during Cenozoic deformation (similar to Figure 12B or C). Above the Kayak Shale, detachment folds and thrust faults were developed in the Lisburne and Sadlerochit Groups during progressive shortening of the underlying Franklinian sequence by folding and faulting.

6. A MODEL: THE STRUCTURAL GEOMETRY AND EVOLUTION OF THE FRANKLIN MOUNTAINS ANTICLINORIUM

In constructing a retrodeformable cross-section across a portion of a fold-and-thrust belt, such as the Franklin Mountains of the northeastern Brooks Range, the geologist incorporates fundamental, objective mesoscopic structural data and field observations with subjective interpretation of the macroscopic structural style (Figure 28). A carefully and systematically constructed cross-section should constitute both an admissible and viable geometric model; that is, one which is consistent with the available data, observed structural geometry, and assumptions or interpretations made prior to and during construction, and can be restored from the deformed state to an unstrained state (Elliott, 1983; Woodward et al., 1985). The structural "truth" of such a geometric model is determined by the extent to which the model is an accurate representation of the actual geometry, both above and below the present erosion surface. In addition to surficial structural data and field observations, any available seismic or well-log data further constrain and improve the accuracy of a balanced cross-section.

The balanced cross-sections constructed across the Franklin Mountains anticlinorium (Plates 2 -5) incorporate all of the field data, but no seismic or well-log data were available to provide additional constraints on these models (Figure 28). Given the field observations and structural data presented in Section 5, these cross-sections represent the best interpretation of the macroscopic structural geometry of the Franklin Mountains anticlinorium and the synclinorium to its north. Without any direct knowledge of the structures which actually occur at depth, the "truth" of these models must be evaluated in terms of the validity of the cross-sections. Since these cross-sections are retrodeformable and kinematically feasible geometric models which incorporate a number of assumptions that can be defended to varying degrees, they are regarded to be both viable and admissible models. However, it must be stressed that each cross-section represents only one of the possible interpretations of the field observations and structural data.

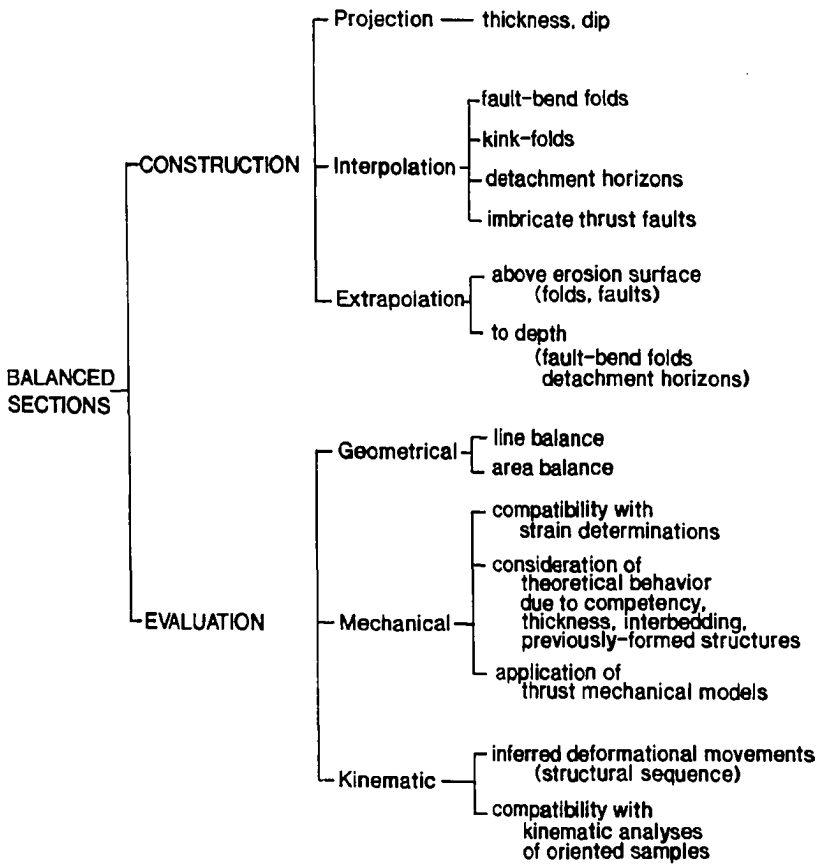

FIGURE 28. Elements of section-balancing procedure used in this study (modified from DePaor, 1988).

6.A. CONSTRUCTION OF FRANKLIN MOUNTAINS ANTICLINORIUM BALANCED CROSS-SECTIONS

6.A.1. Location of Cross-Sections

Field observations and both mesoscopic and macroscopic structural data formed the basis for the construction of the primary balanced geologic cross-section across the Franklin Mountains anticlinorium (Plate 2) and two shorter sections which illustrate the geometry of folds and faults developed in the Ellesmerian sequence on the northern limb of the anticlinorium (Plate 5). Cross-sections were constructed perpendicular to the strikes of map-scale structures. There are several bends and one offset in the 19.7-mile (31.8-kilometer) line of the primary cross-section and in the shorter 5.7-mile (9.2-kilometer) eastern and western sections (Figure 29). A 7.6-mile (12.3-kilometer) portion of the primary cross-section across the anticlinorium (B-C-H-I in Figure 29) and the two shorter cross-sections (D-E-H-I and F-G-H-I in Figure 29) lie within the study area. Structural data for these sections were obtained from field traverses near the lines of section. The 3.4-mile (5.4-kilometer) northern and 8.6-mile (13.9-kilometer) southern segments of the primary cross-section (Plate 2) lie outside the boundary of the study area; data used for construction of these segments were obtained from W.K. Wallace (1988, pers. commun.). Much of the structural data for the northern and southern segments was obtained from the vicinity of the Marsh Fork of the Canning River, and was projected east to east-northeast, along strike and considering plunge, over a distance of up to several miles into the plane of section.

6.A.2. Assumptions Made in Cross-Section Construction

In order to define the validity and limitations of a balanced cross-section, it is important to delineate and justify all assumptions made in cross-section construction. Along with data, these assumptions constrain the structural geometry shown in the cross-section and impose limitations on subsequent kinematic and mechanical modeling based on the cross-section. Assumptions commonly made during the construction of balanced cross-sections include (1) thicknesses of units, (2) tectonic

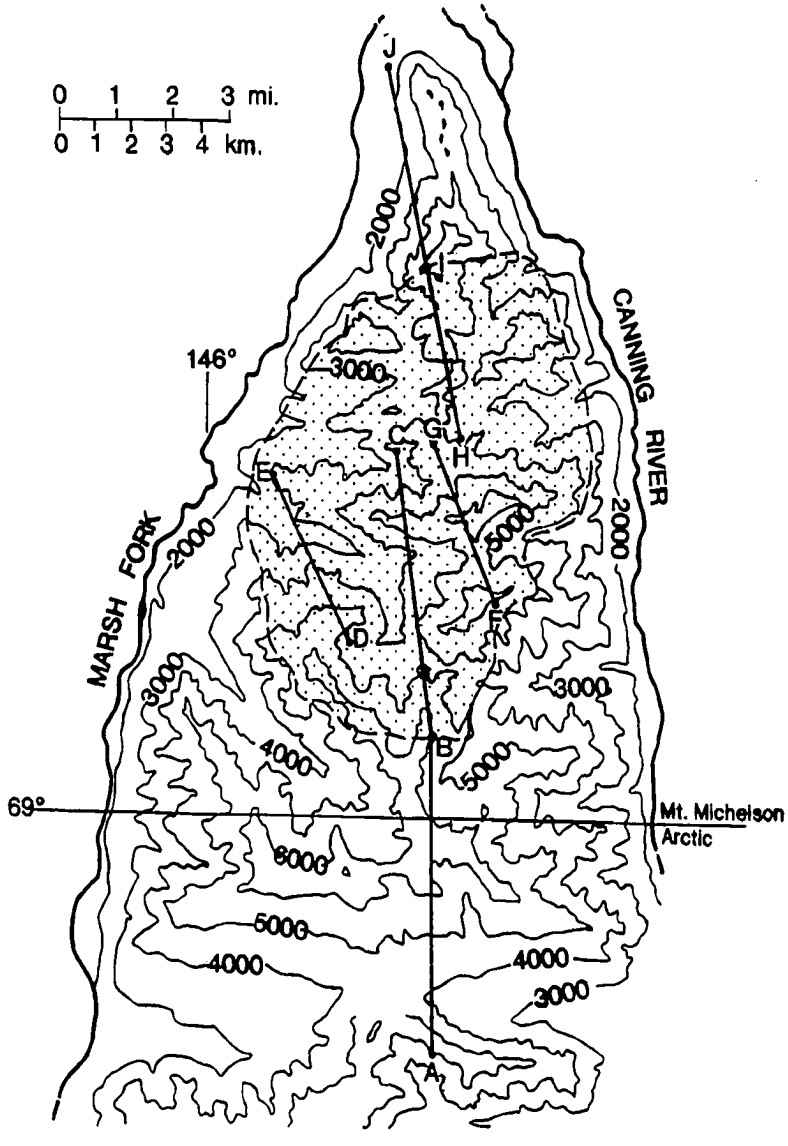

FIGURE 29. Locations of balanced cross-sections. Note that A-B lies to the south of the study area, largely within the Arctic quadrangle; I-J lies to the north of the study area. Stippled region enclosed by dashed lines represents study area.

transport direction, (3) conservation of bed-length and area, (4) kink-folding and parallel folding by flexural-slip, and (5) plane strain. Appendix D addresses how these assumptions were applied to the Franklin Mountains anticlinorium. Appendix D also discusses in detail the assumptions made regarding (1) the orientation of dip panels, (2) fault-bend fold geometry, (3) location of pin lines, (4) balancing methods used for the Franklinian sequence, (5) the sub-Mississippian angular unconformity, and (6) depths to detachment horizons.

6.B. CONTENT OF BALANCED CROSS-SECTIONS

Balanced cross-sections across the Franklin Mountains anticlinorium (Figures 30, 33-34, Plates 2 and 5) reflect three distinct geometric responses of structural-stratigraphic units to Cenozoic deformation: (1) several-kilometer-thick packages of Franklinian sequence rocks and the Kekiktuk Conglomerate were displaced on thrust faults and broadly folded above footwall flat-to-ramp and ramp-to-flat transitions; (2) incompetent Kayak Shale flowed ductilely, effectively detached from overlying Ellesmerian sequence rocks and underlying rocks, developing a complex and chaotic pattern of internal shortening and radical variations in thickness; and (3) prompted by flow of the Kayak Shale and structural separation from underlying rocks, the Lisburne and Sadlerochit Groups formed detachment folds which have wavelengths on the order of 1-2 kilometers in the synclinorium to the north of the anticlinorium.

6.B.1. Franklinian Sequence and Kekiktuk Conglomerate

In this model, the anticlinorium is comprised of a major thrust sheet (the first horse) and a minor thrust sheet (the second horse), detached at depths of 5.4 and 3.1 kilometers below sea level, respectively (Figure 30, Appendix D.6.). The first horse, 4.7 kilometers thick and more than 20 kilometers in length, was displaced to the north, accommodating a total of 11.2 kilometers of shortening (Figures 30-32, 35C). This thrust sheet is comprised of the middle and upper structural-stratigraphic packages of Franklinian sequence rocks mapped in the study area, separated by a pre-Mississipian thrust fault (Section 5.C.1., Figures 30-32) which balancing methods require to have accommodated 2.4 kilometers of

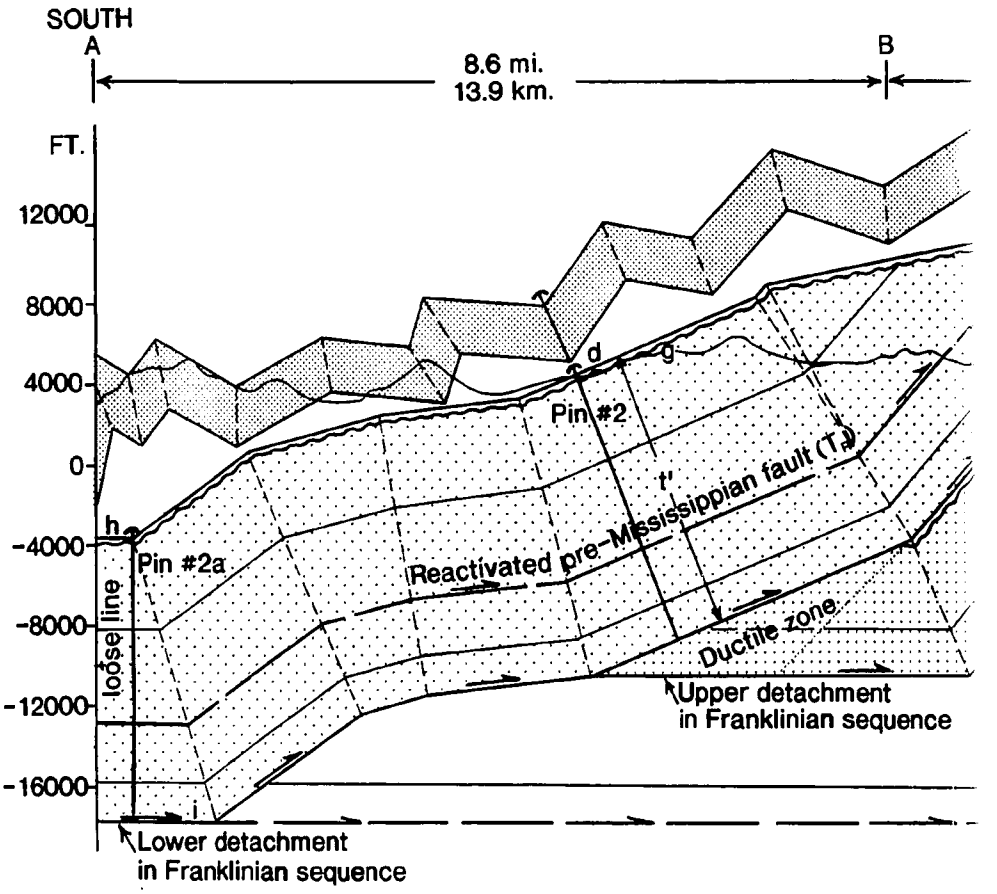

FIGURE 30. Balanced cross-section across the Franklin Mountains anticlinorium. The contact between the upper and lower Ivishak Formation is shown. B-C-H-I lies within the study area. Numbers refer to the location of oriented samples, discussed in Section 7. Thrust faults located at "G" and "H" are referred to in the text and are shown in Figure 23. Lower case letters mark locations referred to in Sections 6.B.1., 6.B.3, and Appendix D.6.

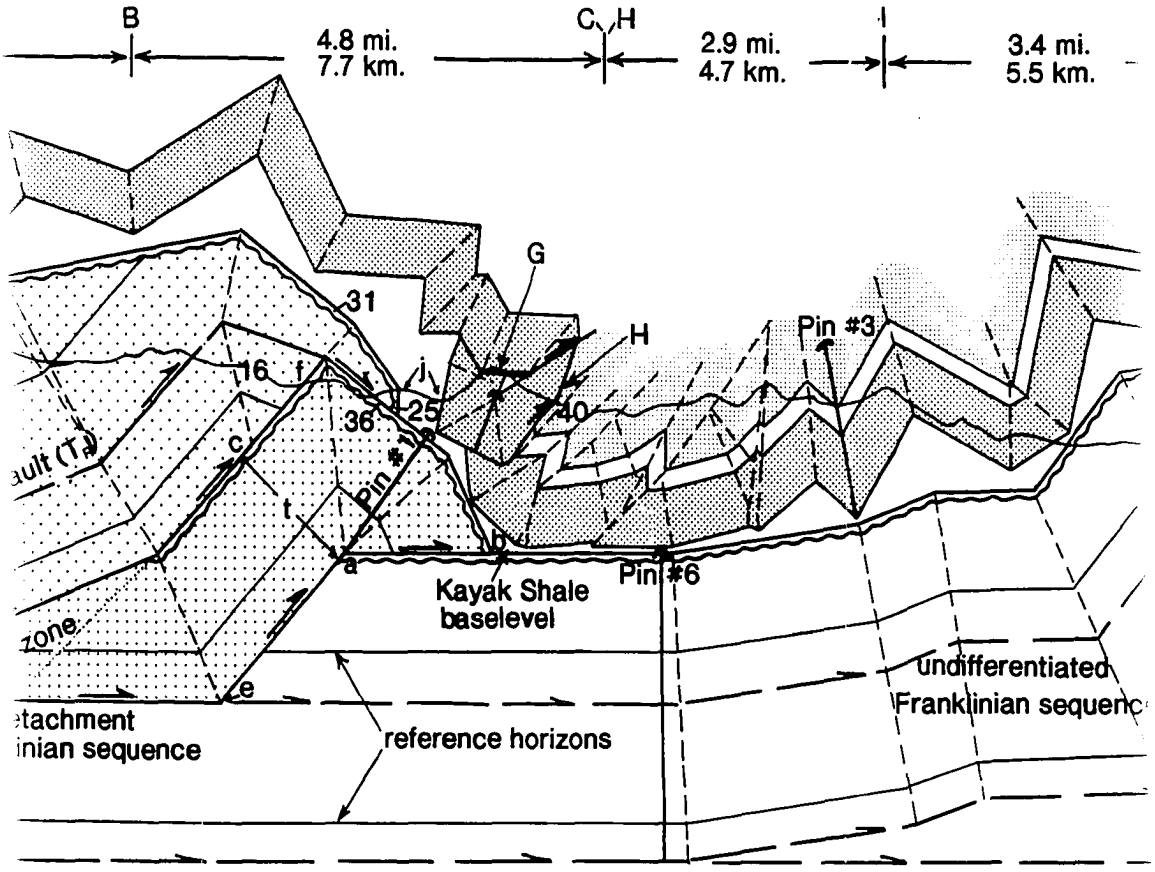

...orium. The
...own. B-C-H-I lies
...ed samples,
...re referred to in
...locations referred

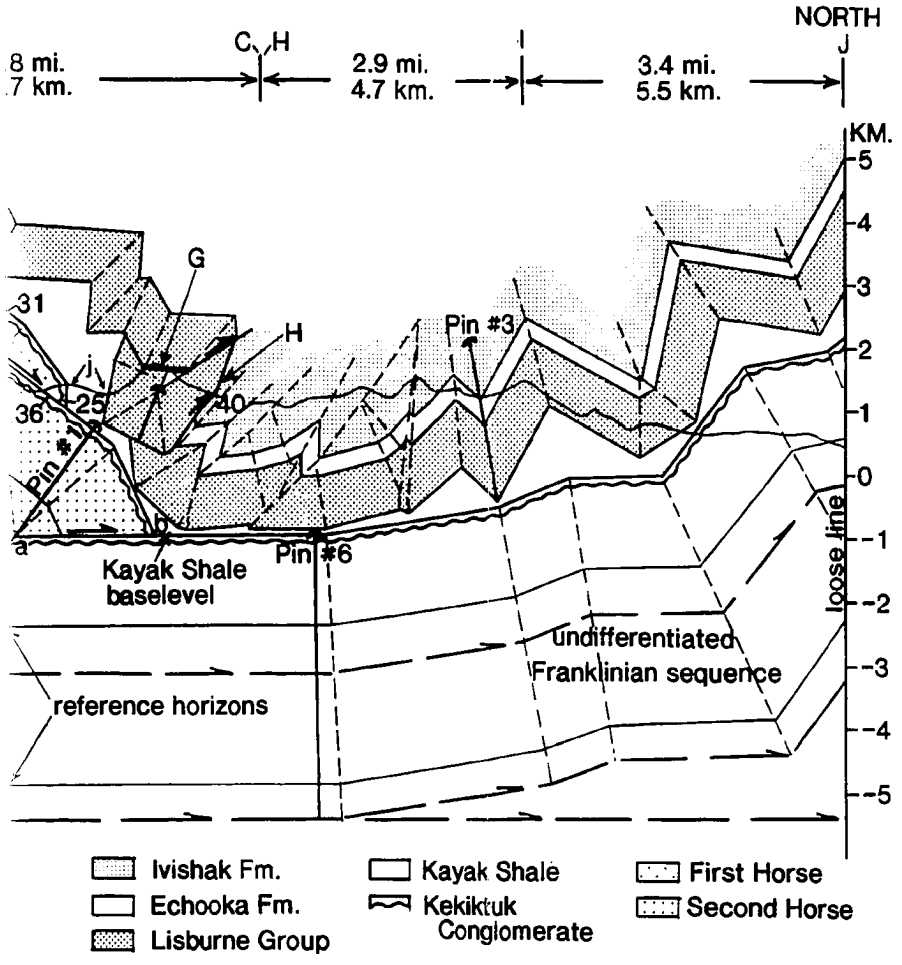

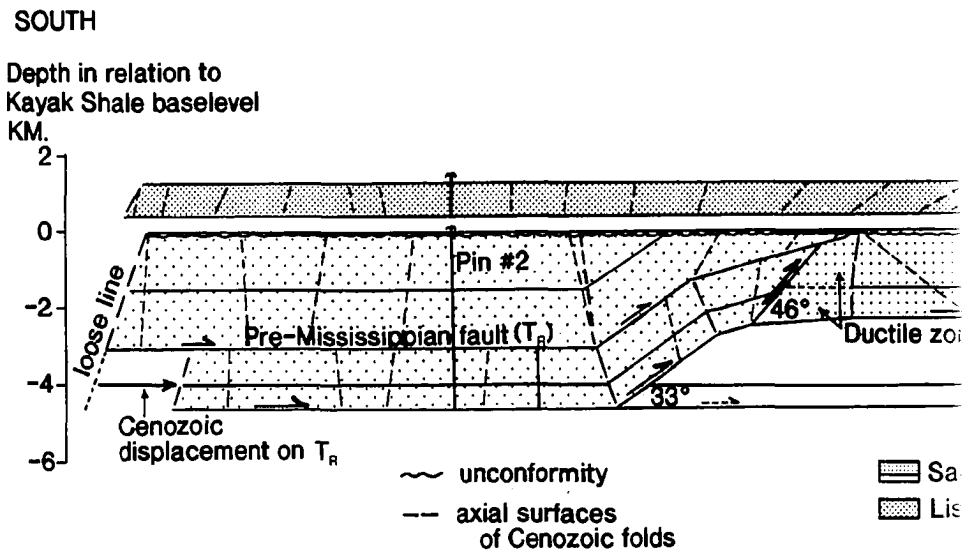

FIGURE 31. Balanced cross-section across the Franklin Mountains anticlinorium (Figure 30), reconstructed to pre-Cenozoic time. Dashed lines represent axial surfaces of Cenozoic folds. The Kayak Shale and the ductile zone at the trailing edge of the second horse were area balanced. Cenozoic shortening of the Franklinian sequence is roughly 11 kilometers, or 44%; shortening of the Lisburne and Sadlerochit Groups is roughly 10.5 kilometers, or 42%.

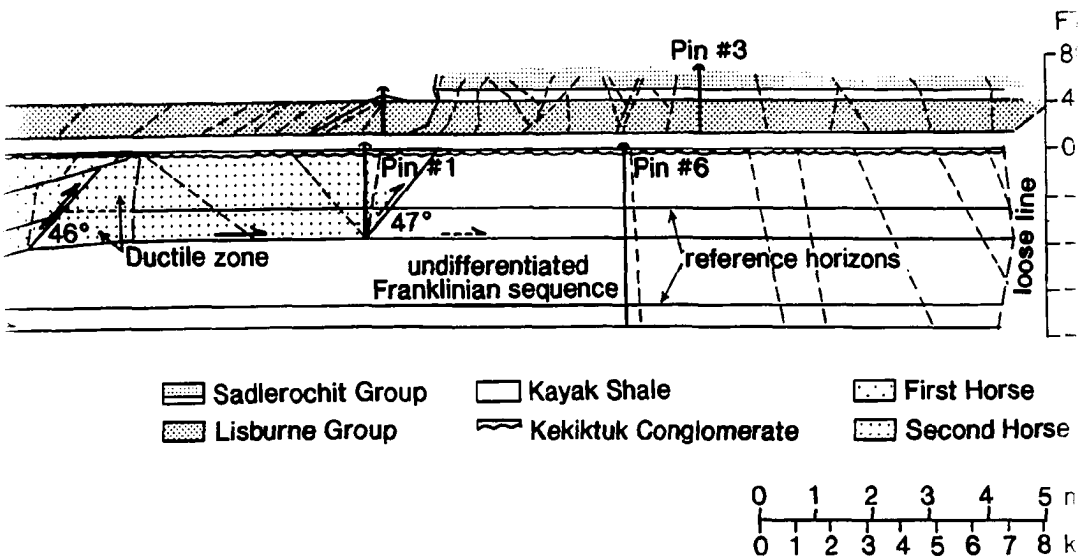

ım (Figure
ıxial surfaces
ıailing edge of
Franklinian
ıburne and

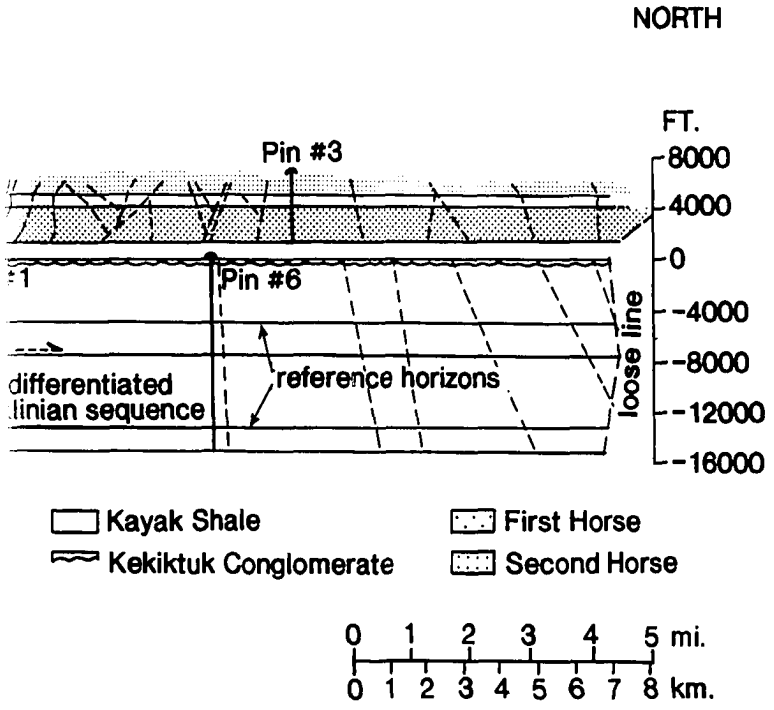

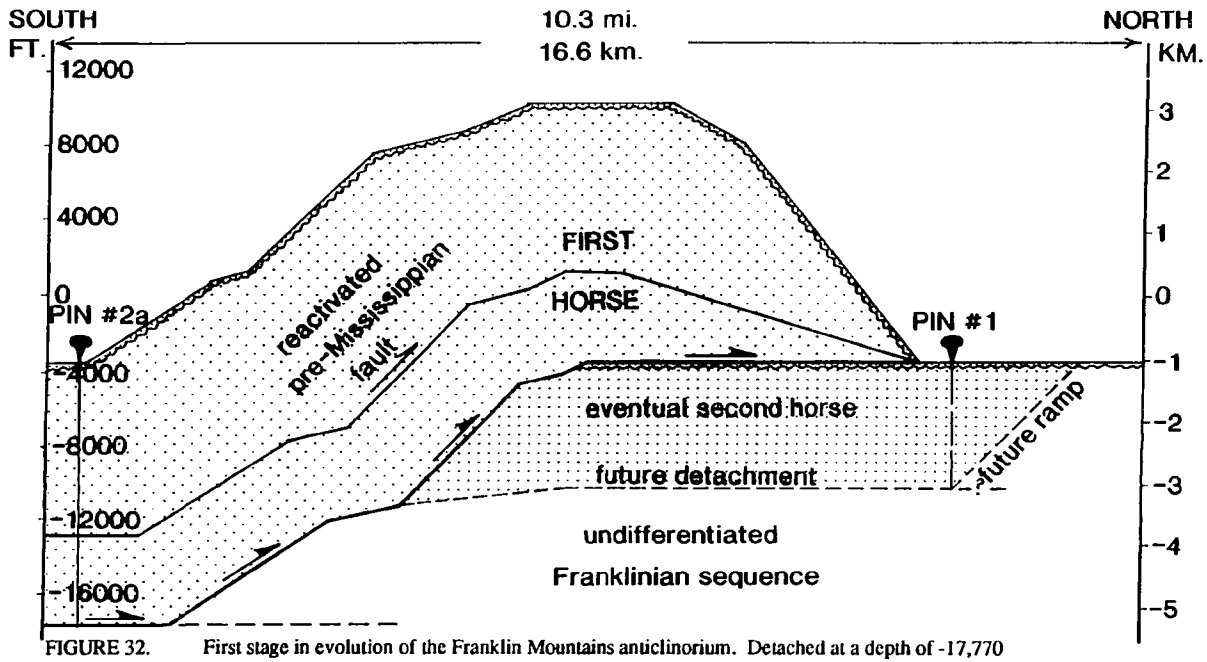

FIGURE 32. First stage in evolution of the Franklin Mountains anticlinorium. Detached at a depth of -17,770 feet (5.4 kilometers), the first horse was displaced northward, accommodating roughly 8 kilometers of shortening and uplifting the Kekiktuk Conglomerate at the crest of the anticlinorium some 4-5 kilometers above the undeformed Kekiktuk Conglomerate to the north. The anticlinorium was produced as a result of fault-bend folding at the leading edge of the thrust sheet. Subsequent to emplacment of the first horse, the basal detachment stepped up to a depth of -10,250 feet (3.1 kilometers) and propagated to a point just north of the leading edge of the first horse. Failure occurred at this point, forming a ramp up which the second horse was then displaced.

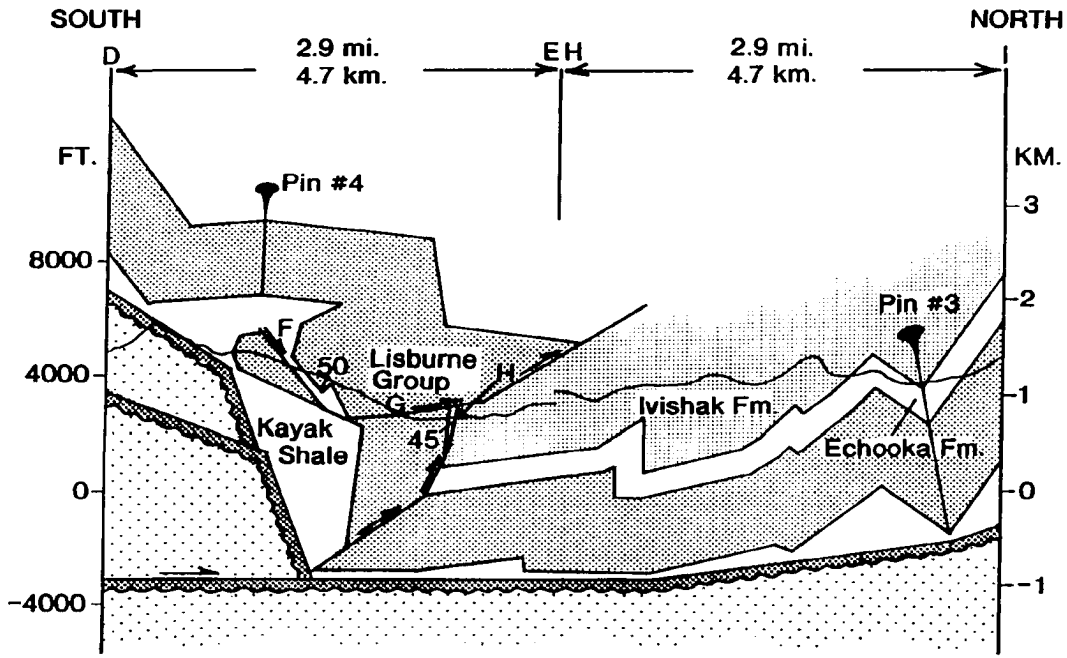

FIGURE 33. Balanced cross-section (D-E-H-I in Figure 15) west of primary section (Figure 30). "45" and "50" correspond to the location of samples discussed in Section 7. Thrust faults "G" and "H" are referred to in the text and shown in Figure 23. "F" corresponds to the location of north-vergent folding of the Kayak Shale, shown in Figure 23 and discussed in Section 9. Shortening of the Lisburne and Sadlerochit Groups is approximately 47 %.

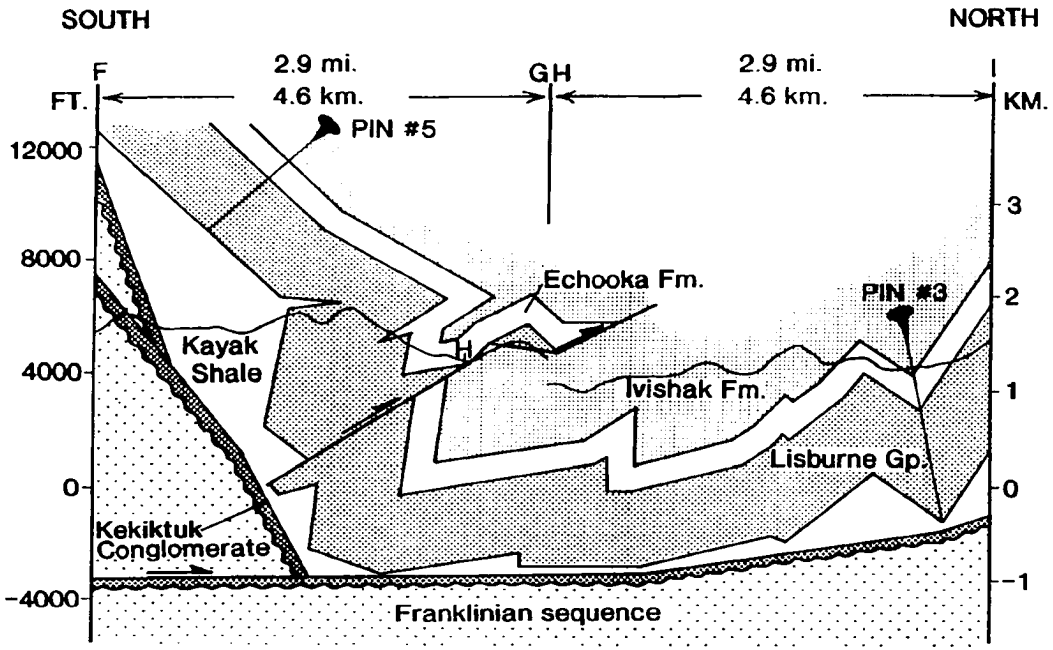

FIGURE 34. Balanced cross-section (F-G-H-I in Figure 15) east of primary section (Figure 30) and Figure 33. Thrust fault "H" is shown in Figure 23 and referred to in the text. Shortening of the Lisburne and Sadlerochit Groups is approximately 40 %.

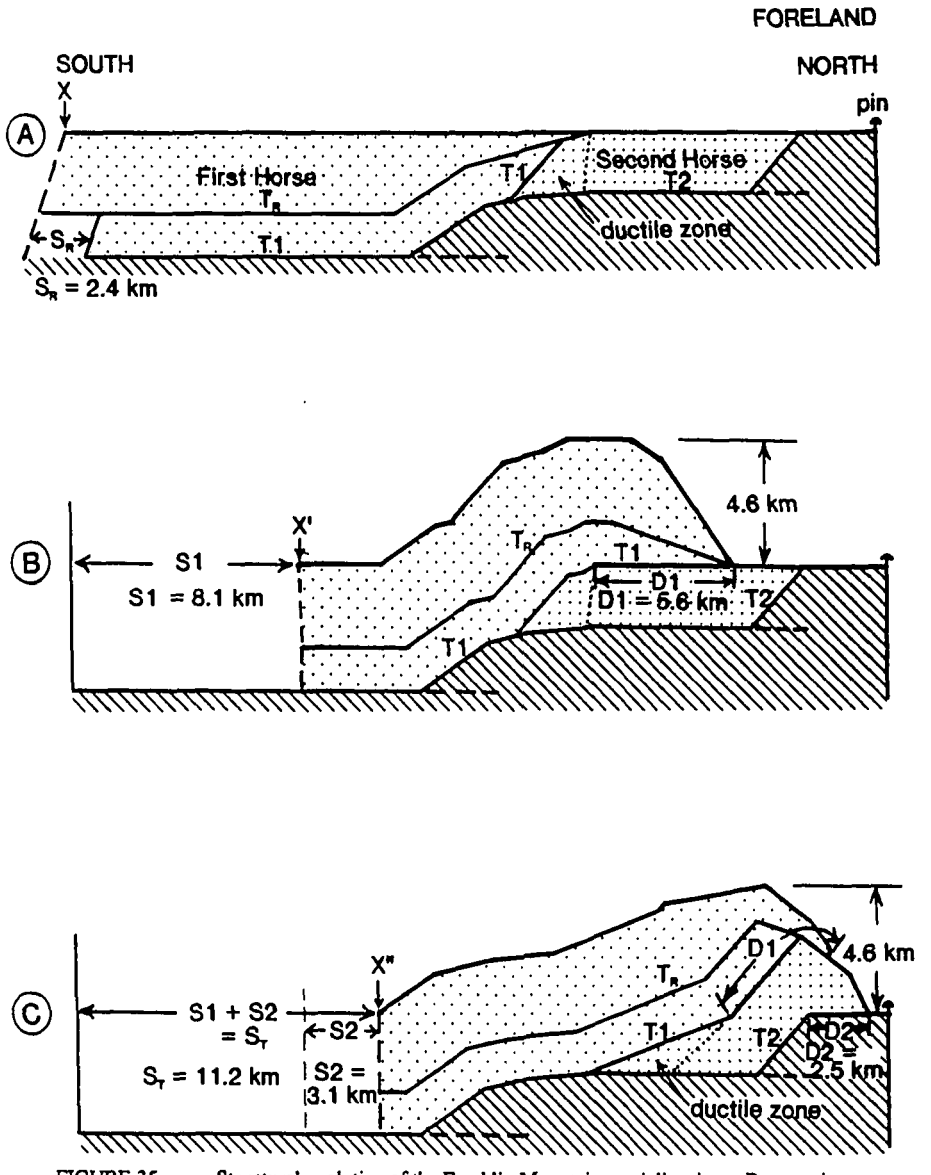

FIGURE 35. Structural evolution of the Franklin Mountains anticlinorium. Progressive Cenozoic shortening of the Franklinian sequence occurred as the first and second horses were emplaced, with displacement (D1 and D2) on thrust faults (T1 and T2). S1 and S2 correspond to the shortening accommodated by the first and second horses, respectively. S_R is the Cenozoic shortening accommodated by reactivation of the pre-Mississippian thrust fault (T_R) in the first horse.

shortening during Cenozoic deformation (Figures 30 and 35). The second horse, 2.3 kilometers thick and 9.3 kilometers long, accommodated 3.1 kilometers of shortening (Figures 30-32, and 35).

Values for the thickness, length, displacement and shortening of these horses (Tables 5 and 6) were measured from the primary balanced cross-section (Figure 30) and the reconstructed versions of that section (Figures 31 and 32). The methods and reasoning which led to the derivation of these values are described further in Section 6.C. As discussed in Appendix D.6., horse thickness and detachment depth were constrained by (1) the depth of the Kekiktuk Conglomerate in the synclinoria to the south and north of the anticlinorium, (2) the orientations of the south-dipping panels of the fault-bend folds, assumed to reflect the dip of underlying footwall ramps, and (3) the elevation of the Kekiktuk Conglomerate at the crest of the anticlinorium, used to determine horse thickness at various locations (i.e. between "f" and "g" in Figure 30).

6.B.2. Kayak Shale

Since bedding continuity and thickness were severely disrupted during Cenozoic deformation, area balance techniques were applied to the Kayak Shale. Given the undeformed bed-lengths of the bounding Kekiktuk Conglomerate and Alapah Limestone, the thickness of the Kayak Shale was estimated to be 1,380 feet (422 meters). This value is comparable to the maximum thickness of 1,450 feet (443 meters) cited by Mamet and Armstrong (1972), and is somewhat greater than the average of 960 feet (293 meters) determined by Brosgé et al. (1962) (Table 1). Both Reed (1968) at Lake Peters and Sable (1977) in the Romanzof Mountains determined the Kayak Shale to be less than 400 feet thick (122 meters) (Table 1). The amplitude of detachment anticlines cored by the Kayak Shale was determined by projecting the dips of fold panels in the Lisburne and Sadlerochit Groups measured at the surface to depth, assuming kink-folding. Estimated maximum fold amplitudes and wavelengths from within the study area were used in extrapolation of eroded Ellesmerian section on the crest of the anticlinorium to the south of the study area.

TABLE 5. Total shortening for the Franklinian and Ellesmerian sequences, determined from the balanced cross-sections shown in Figures 30 and 33-34.

SEQUENCE	LOCATION	UNDEFORMED LENGTH (L)	DEFORMED LENGTH (L')	SHORTENING (L-L')	% SHORTENING
FRANKLINIAN	PRIMARY SECTION PIN #2 -- PIN # 6	25.3 km	14.1 km	11.2 km	44 %
ELLESMERIAN	PRIMARY SECTION PIN #2 -- PIN #3	27.4 km	16 km	11.4 km	42 %
	WESTERN SECTION PIN #4 -- PIN #3	13.8 km	7.3 km	6.5 km	47 %
	EASTERN SECTION PIN #5 -- PIN #3	13.1 km	7.8 km	5.3 km	40 %

TABLE 6. Comparison of the physical properties of the first and second horses of the Franklin Mountains anticlinorium, determined from the primary balanced cross-section (Figure 30).

	Thickness	Length	Ramp Angle (degrees)	Detachment Depth	FIRST STAGE		SECOND STAGE	
					Shortening	Thrust Displacement	Shortening	Thrust Displacement
FIRST HORSE	4.7 km	> 20 km	33, 46	5.4 km	8.1 km (S1) 72% of total	5.6 km (D1)	3.1 km (S2)	— (pinned to second horse)
SECOND HORSE	2.3 km	9.3 km	47	3.1 km			3.1 km (S2) 28% of total	2.5 km (D2)

Total Shortening = S1 + S2
= 11.2 km

6.B.3. Lisburne and Sadlerochit Groups

For the portion of the primary cross-section within the study area (B-C-H-I in Figure 30), the geometry of folds and faults in the Lisburne and Sadlerochit Groups incorporates field observations and bedding attitudes, projected to depth using kink-fold geometry (Appendix D). Thrust faults in the Ellesmerian sequence were projected to depth, soling within the Kayak Shale, a demonstrated detachment horizon in the study area.

To the north and south of the study area, where the Ellesmerian sequence is unmapped or eroded, the average fold wavelength (1-2 kilometers) and average interlimb angles (95-110 degrees) from near the northern boundary of the study area were applied. The amplitude of these folds was determined by maintaining a relatively constant thickness (1,500 meters) of Kayak Shale in the cores of detachment anticlines, noting that at least 1,000 meters of Kayak Shale are exposed in the core of one such detachment fold (location "j" in Figure 30). Consequently, the structural geometry depicted for these areas is a speculative and simplistic approximation.

6.C. STRUCTURAL SEQUENCE

The model for the structural evolution of the Franklin Mountains anticlinorium (shown in Figures 30-32 and 35) considers the geometry of pre-Mississippian structures in the Franklinian sequence and the sequence of structures developed in both Franklinian and Ellesmerian sequences during Cenozoic deformation. The Cenozoic evolution of the thrust sheets in the Franklinian sequence and capping Kekiktuk Conglomerate is subdivided into two stages, related to the emplacement of the first and second horses, respectively. Cenozoic structures developed in the Kayak Shale, Lisburne and Sadlerochit Groups, however, are more difficult to associate with specific deformational events.

6.C.1. Pre-Cenozoic Evolution

The reconstructed cross-section shown in Figure 31 portrays the pre-Cenozoic structural geometry which served as the template upon which Cenozoic deformation was superimposed. In this model of

pre-Cenozoic structure, the Franklinian sequence consists of two deformed packages of rocks, separated by a thrust fault (T_R in Figure 31). Since this fault offsets neither the unconformity surface nor the overlying Ellesmerian sequence, such deformation must have occurred prior to deposition of the Kekiktuk Conglomerate. It is impossible to reconstruct the original stratigraphic succession and/or structural geometry which existed prior to pre-Mississippian deformation, since a substantial volume of Franklinian sequence rocks was eroded prior to Mississippian time and the original stratigraphic relationships between packages of deformed rocks are not known. The lines shown within packages of Franklinian sequence rocks in Figures 30-32 are referred to as "reference horizons." These lines were constructed parallel to the footwall of each thrust package in Figure 30. It is important to note that these reference horizons have no physical significance; they do not represent the actual dips of Franklinian sequence rocks with respect to the sub-Mississippian unconformity surface. In pre-Cenozoic time (Figure 31), the Ellesmerian sequence is shown as an undeformed, flat-lying stratigraphic succession consisting of the Kekiktuk Conglomerate through the Sadlerochit Group, unconformably overlying a horizontal sub-Mississippian erosion surface.

6.C.2. Cenozoic Evolution of Franklin Mountains Anticlinorium--First Stage

During the first stage in the evolution of the anticlinorium (Figures 32 and 35A-B), a basal detachment developed at a depth of 5.4 kilometers below sealevel. A package of previously folded and faulted pre-Mississippian rocks, 4.7 kilometers thick and over 20 kilometers long, was structurally isolated by the basal detachment, a roof thrust in the Kayak Shale, and leading and trailing imbricate thrust faults. This composite first horse was displaced 5.6 kilometers up a footwall ramp comprised of 33- and 46-degree ramp sections and two short 14- to 25-degree flat sections (Figure 35B). The configuration of this ramp is based on the assumption that the orientation of the Kekiktuk Conglomerate capping the upper antiform reflects the orientation of ramps and flats in an underlying thrust surface. Measured from the balanced cross-sections (Figure 35), emplacement of this thrust sheet accomplished

roughly 8 of the 11.2 kilometers of total Cenozoic shortening of the Franklinian sequence. In order to balance the primary cross-section, it is necessary that the pre-Mississippian fault within the first horse (T_R in Figure 35A) was reactivated during emplacement of the horse, accommodating 2.4 kilometers of shortening. Reactivation of this fault cannot be substantiated by field evidence. However, given its moderate south dip at an angle similar to that of the inferred footwall ramp, it is not unlikely that this thrust surface could have been reactivated during Cenozoic deformation. Upon clearing the footwall ramp, the leading edge of this horse flexed, forming a fault-bend fold above the ramp-to-flat transition in the footwall. Flexural-slip, parallel to the reference horizons and bedding in the Kekiktuk Conglomerate, is required by the pin line location chosen on the backlimb of the antiform.

6.C.3. Cenozoic Evolution Franklin Mountains Anticlinorium--Second Stage

The second stage in the evolution of the anticlinorium was accompanied by a northward step-up of the basal detachment from 5.4 to 3.1 kilometers below sealevel (Figure 32). This new detachment propagated 9.3 kilometers to the north before cutting upward, forming a 9.3-kilometer-long second horse and a ramp up which it could be displaced (future detachment and ramp shown in Figure 32). The footwall ramp dipped 47 degrees to the south and intersected the top surface of the Kekiktuk Conglomerate at a point roughly 2.7 kilometers to the north of the leading edge of the first horse (Figure 32). The rear portion of the second horse was area-balanced during cross-section construction, constituting the so-called "ductile zone" shown in Figures 30-32 and 35. This ductile zone was required in order to reconcile the moderately steep south dip of the south limb of the lower antiform with the more gentle south dip of the south limb of the upper antiform, given the interpreted depths of the upper and lower detachments and the locations of Pins #1 and #2. The second horse was displaced 2.5 kilometers over the footwall ramp, accommodating 3.1 kilometers of shortening (Figure 35C). Presumably pinned to the second horse, the first horse was carried northward in a piggy-back style, also accommodating 3.1 kilometers of shortening. Upon clearing the footwall ramp, the leading edge of the second horse formed a

fault-bend fold, defining the lower antiform in the Franklinian sequence and its capping veneer of Kekiktuk Conglomerate (Figure 30). As a consequence of emplacement of the second horse, new fold hinges formed in overlying portions of the first horse, modifying the geometry of the first-formed and structurally higher fault-bend fold (compare Figures 30 and 32, Figures 35B-C).

Comparing Figures 35B and 35C, the average 40-degree south dip of the Kekiktuk Conglomerate along the backlimb of the anticlinorium in Figure 32 was decreased to 22 degrees after the second horse was emplaced. This decrease in dip is a consequence both of area-balancing the so-called ductile zone of the rear portion of the second horse, and of further modifying the trailing footwall cutoff of the second horse by flexural slip associated with its emplacement. The Kekiktuk Conglomerate beds which define the north flank of the anticlinorium maintained a mean dip of 52 degrees in both Figures 30 and 32 (or Figures 35B and C). Comparison of Figures 30 and 32 (or Figures 35B and C) suggests that the initial 4.6 kilometers of positive structural relief, produced when the first horse was emplaced, was not increased by emplacement of the second horse. Instead, the geometric form of the anticlinorium was modified as the leading edge of the first horse was uplifted and the dip of the backlimb decreased. Note that this change in geometry is inferred from a partially reconstructed cross-section (Figure 32). However, models constructed by Mitra (1986) suggest that duplexes consisting of multiple horses display asymmetric geometries (with steeper forelimbs) if subsequent horses in the duplex are shorter and accommodate less shortening than the first horse emplaced (compare Figures 50A and 50C in Appendix A). Thus, since the second horse is both shorter and accommodates less shortening than the first horse (Table 6), it may not be surprising that the geometry of the anticlinorium is asymmetric (like Figure 50C in Appendix A) following emplacment of the second horse in Figure 30.

6.C.4. Cenozoic Evolution of Ellesmerian Sequence Above Kayak Shale

Detachment folds and thrust faults developed in Ellesmerian sequence rocks stratigraphically above the Kekiktuk Conglomerate in response to regional shortening of underlying rocks. The truncated folds

and folded thrust faults on the north flank of the anticlinorium (Figures 30 and 33-34) suggests that some folding occurred prior to faulting in the Ellesmerian sequence, with subsequent folding of thrust faults. (The influence of the emplacement of horses on the formation of structures in the Ellesmerian sequence above the Kayak Shale is discussed in Section 9.) Measured from the balanced cross-sections (Figures 30 and 33-34), displacements on thrust faults traced between the three cross-sections appear to remain relatively constant along strike and appear to decrease toward the north (Table 7).

6.D. MODEL LIMITATIONS

One of the main topics addressed by this study is the mode in which polydeformed, weakly-metamorphosed Franklinian sequence rocks responded to Cenozoic deformation. Determination of detachment depths and construction of the subsurface geometry of Franklinian sequence rocks which core this anticlinorium were based entirely upon the projection of the fault-bend fold geometery of Suppe (1983) to depth (Appendix D.2.). As mentioned in Section 5.E. (and to be discussed in Section 8), it appears that pre-Mississippian rocks in this study area accommodated most Cenozoic shortening by duplexing, with a relatively minor amount of shortening accommodated by small-scale folding and faulting within thrust packages.

Only a limited amount of data were available to construct and constrain the model. Measurements of shortening and kinematic inferences (Sections 7 and 8) drawn from these cross-sections must be viewed with the realization that (1) cross-section construction involved major assumptions regarding both the style of Cenozoic deformation in these rocks and the extrapolation of structural geometry to depth, that (2) cross-sections describe an end-member model (Figure 10A) which likely cannot describe the detailed structural geometry of the anticlinorium adequately, and that (3) cross-sections yield minimum shortening values that do not account for small-scale internal shortening.

Additional structural information is needed for the Franklinian sequence rocks to the south of the study area, especially for those exposed at low elevations, in order to test the validity of the assumptions

TABLE 7. Displacement on thrust faults in the Ellesmerian sequence, and estimated shortening accommodated by faulting and folding in three balanced cross-sections.

		WESTERN SECTION (FIGURE 33)	PRIMARY SECTION (FIGURE 30)	EASTERN SECTION (FIGURE 34)
NORTH	DISPLACEMENT ON FAULT AT "H" IN FIGURE 23	406 m Ø = 45°, S = 287 m	860 m Ø = 45°, S = 608 m	760 m Ø = 30-45°, S = 537-658 m
SOUTH	DISPLACEMENT ON FAULT AT "G" IN FIGURE 23	1400 m Ø = 30°, S = 1212 m	1500 m Ø = 25°, S = 1360m	——
TOTAL SHORTENING BY FAULTING		1499 m (23% of total shortening)	1968 m (17% of total shortening)	537-658 m (10-12% of total shortening)
TOTAL SHORTENING (TABLE 6.)		6.5 km	11.4 km	5.3 km
SHORTENING BY FOLDING (SUB-TRACTING)		5 km (77% of total shortening)	9.4 km (83% of total shortening)	4.6-4.8 km (88-90% of total shortening)

Note: Given the displacement measured on each fault and the dip of the fault surface (Ø) in the balanced cross-sections, the shortening (S) = (displacement)cosØ.

made and the geometry modeled. Few constraints are available to apply to the geometry of detachment folds and thrust faults in the Ellesmerian sequence which either exist at depth or existed prior to erosion from the crest of the Franklin Mountains anticlinorium south of the study area. Thus, the Ellesmerian sequence exposed in the synclinorium to the north of the anticlinorium (Figures 33 and 34) might be expected to record more accurate (but not necessarily more representative) shortening values than those obtained from the entire extent of the primary cross-section, which includes simplistic fold geometries on the crest and backlimb of the anticlinorium.

6.E. MODEL IMPLICATIONS

The cross-sections constructed across the Franklin Mountains anticlinorium employ accepted balancing methodologies. Thus, if assumptions and interpretations of the basic structural style are valid, the duplex model which was used may describe the mode of formation and structural geometry of the anticlinorium and the horses which comprise it. Broad flexure and thrust duplication of the Kekiktuk Conglomerate which caps the thrust sheets in the Franklinian sequence accommodates Cenozoic shortening of roughly 44% (calculated at the base of the Kekiktuk Conglomerate between Pin #2 and Pin #6 in Plate 2, Figures 30 and 31). Since in this model the Kekiktuk Conglomerate remained attached to the Franklinian sequence during Cenozoic deformation, pre-Mississippian rocks which comprise these thrust sheets were also shortened in length by 44%. Calculated between Pin #2 and Pin #3 at the base of the Lisburne Group (Figures 30 and 31, Plates 2 and 3), 42% shortening has been accommodated in Ellesmerian sequence rocks above the Kekiktuk Conglomerate, mainly by detachment folding (Tables 6 and 7). Measured in the synclinorium to the north of the anticlinorium, shortening in the Ellesmerian sequence is 47% between Pin #4 and Pin #3 in the western section (Figure 33, Plate 5) and 40% between Pin #5 and Pin #3 in the eastern section (Table 6, Figure 34, Plate 5). Approximately the same magnitude of Cenozoic shortening is recorded above and below the Kayak Shale detachment horizon. There does not appear to be a significant difference between shortening values in the Ellesmerian sequence

calculated within the synclinorium (47% and 40%) and the shortening of the Ellesmerian sequence across the entire primary cross-section (42%).

6.F. MODEL VALUE

Construction of balanced cross-sections across the Franklin Mountains anticlinorium serves serveral purposes: As already shown, (1) the deformed section enables Cenozoic shortening to be estimated for the Franklin Mountains study area; and, as addressed in subsequent sections, (2) the deformed and partially-restored sections establish an evolutionary framework within which to view microscopic kinematic data (Section 7), and (3) the deformed section furnishes parameters needed in order to model dynamic aspects of the evolution of the Franklin Mountains anticlinorium (Sections 8 and 9).

7. STRAIN DETERMINATIONS AND KINEMATIC ANALYSES

7.A. INTRODUCTION

Microscopic strain determinations and quantitative kinematic analyses expand the scope of this detailed structural analysis to a microscopic scale, enhancing understanding of the mode of deformation and structural sequence for the study area. The objective of strain determinations was to determine the extent to which deformation altered the shapes and orientations of geologic objects or features, referred to as "strain markers," within Franklinian and Ellesmerian sequence rocks. These markers (described in this section and in Appendix E) record the shape and orientation of the strain ellipse and provide information about the sequence of deformational movements that affected the host rock body. The balanced cross-sections shown in Figures 30-34 establish a geometric framework which enables mesoscopic and microscopic kinematic data for a small number of samples to be considered in terms of position of the sample relative to local structures as they evolved. The microscopic kinematic data are generally consistent with the balanced cross-section model of macroscopic structures, supporting the series of deformational movements which the balanced cross-sections model for the evolution of the Franklin Mountains anticlinorium.

The ultimate goals of the strain determinations described in this section are to understand how Cenozoic strain was distributed across the sub-Mississippian unconformity surface, and to determine the deformational behavior of the Kekiktuk Conglomerate in the study area. Specific objectives of such analyses are (1) to measure strain in the Franklinian sequence, (2) to attempt to discriminate between and quantify pre-Mississippian and Cenozoic components of strain in the Franklinian sequence by analyzing strain markers interpreted to be of pre-Mississippian or Cenozoic age (assessed by deciphering the relative chronology of structures and strain markers within the Franklinian sequence, and comparing the types and orientations of markers observed in both sequences), (3) to measure strain in the Kekiktuk Conglomerate, and (4) to compare penetrative strain measurements within the Ellesmerian sequence.

Incremental and finite strain methodology, sample descriptions, and analytical findings are summarized in this section. More complete discussion and interpretation of results are provided in Appendices F and G. Different methods of finite strain analysis were applied to a variety of markers, permitting comparison of strains determined by the various analytical methods. However, the limited number of samples available or suitable for analysis by each of the methods makes interpretation of the results highly speculative and difficult to substantiate. Replicate samples were not analyzed, so the reproducibility of the results of each method was not tested. Efforts to relate kinematic data to the evolution of particular structures in the study area were hampered by the fact that samples were lacking from some important locations, and the various strain markers used were not ubiquitous.

7.A.1. Preparation of Samples

Three mutually-perpendicular thin-sections were prepared where possible for each oriented sample. These thin-sections represent the inferred XY-, YZ-, and XZ-planes (Figure 36) of the Cenozoic tectonic strain ellipsoid, where X is the major axis, Y is the intermediate axis, and Z is the minor axis of the ellipsoid. One plane coincides with the east- to east-northeast-striking plane of slaty cleavage in foliated Franklinian sequence rocks or to bedding in nonfoliated Franklinian and Ellesmerian sequence rocks. A second plane is subvertical and strikes approximately north-northwest, perpendicular to the strike of compositional layering. This plane is subparallel to the inferred Cenozoic tectonic transport direction and roughly coincides with the plane of D_3 spaced cleavage. The third plane strikes east-northeast and is perpendicular to the other two planes. For most samples, either the north-northwest-striking plane or the plane that is parallel to bedding or compositional layering was oriented in the field. Thin-sections were cut such that their edges correspond to two of the three principal axes of the inferred Cenozoic strain ellipsoid.

7.A.2. Summary of Strain Markers and Presentation of Data

Nine oriented samples from the Franklinian sequence and seven oriented samples from the

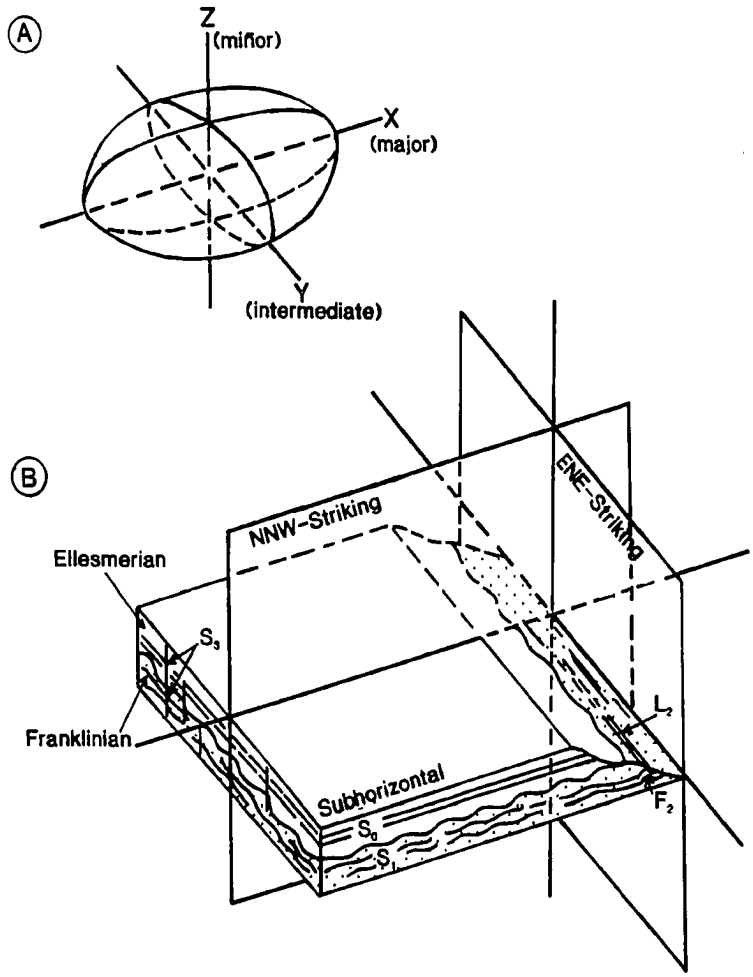

FIGURE 36. Orientation of Cenozoic tectonic strain ellipsoid in relation to oriented thin-section planes. (A) Inferred orientation of Cenozoic tectonic strain ellipsoid. Lengths of X-, Y-, and Z-axes are arbitrary. (B) Orientations of planes of thin-sections prepared from oriented samples of Franklinian and Ellesmerian sequence rocks. This figure is schematic and does not show the actual relationship between bedding in the Ellesmerian sequence (S_0) and slaty cleavage in the Franklinian sequence (S_1). There is an estimated 40-degree discordance between the dips of the subhorizontal planes shown for the Franklinian and Ellesmerian sequences, and, therefore, a similar discordance between the dips of the east-northeast-striking planes.

Ellesmerian sequence record the orientations of strain ellipses in the XY-, YZ-, and XZ-planes, determined by the orientation of stylolites, extension fractures, pressure shadows, crystal-plastic features, and shear fabrics. The orientations of these strain markers (described in detail in Appendix E) were found to reflect different strains depending on the setting from which they came: (1) north- to north-northwest-directed shortening associated with the Cenozoic deformational event that formed the Franklin Mountains anticlinorium, (2) northwest extension subparallel to the Cenozoic tectonic transport direction, (3) the response to increased overburden developed as a consequence of thrust sheet emplacement, (4) shear along the surface separating the two horses, inferred to have occurred during thrust emplacement of the first horse, or (5) a later stage of interpreted east-west Cenozoic shortening. The orientations of strain markers in the three thin-section planes are shown in Figure 37. The trends of strain markers in the plane of bedding or compositional layering were superimposed on a geologic map (Figure 55 in Appendix E and Figure 73 in Appendix G). Orientations (defined by the rake, as described in Appendix F) of strain markers in the east-northeast-striking plane were plotted on an east-west schematic cross-section (Figure 56 in Appendix E and Figure 74 in Appendix G). Orientations of markers in the north-northwest-striking plane were plotted on a north-south balanced cross-section (Figure 57 in Appendix E and Figure 75 in Appendix G).

7.B. INCREMENTAL STRAIN ANALYSIS

7.B.1. Background

Incremental strain analysis techniques were applied to curved quartz, chlorite, and calcite fibers in pressure shadows that surround marcasite nodules or pyrite crystals. These incremental strain analyses assume that (1) the pressure shadows formed during deformation of the host rock body, (2) the orientation of a pressure shadow fiber in a given plane records the orientation of the major-axis of the tectonic strain ellipse at the time the fiber formed, (3) the length of a pressure shadow fiber is a function of the magnitude of extensile strain in that plane, (4) the path of fiber orientations was produced as a

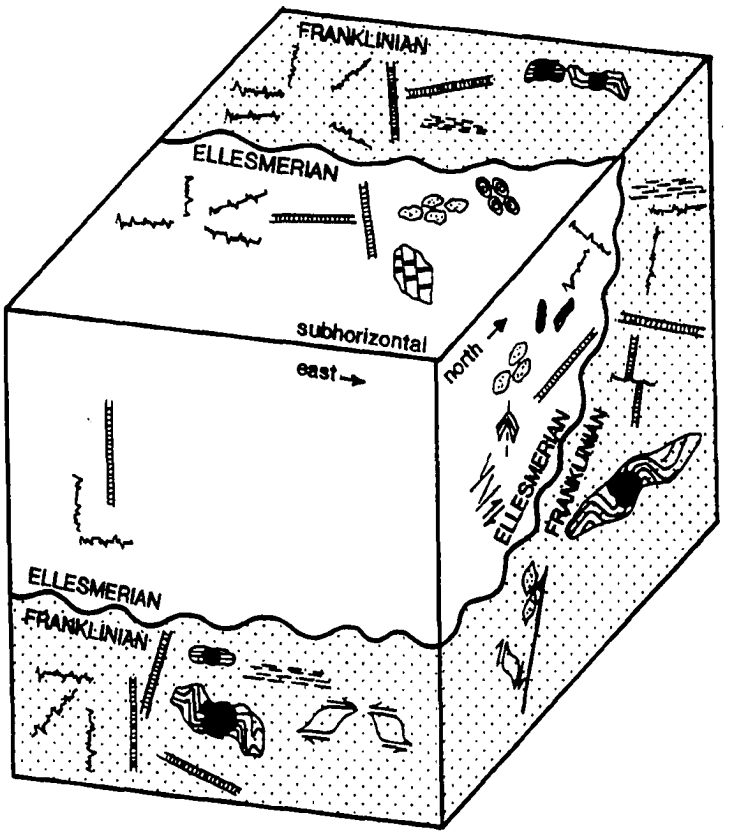

FIGURE 37. Summary of orientations of strain markers in the Franklinian and Ellesmerian sequences. (= stylolites; = extension fractures; = pressure shadows; preferred orientations or crystal plastic features: = subelliptical quartz grains, = subelliptical corals, = kinked micas, = platy minerals; shear fabrics: = sheared calcite grains, = asymmetric porphyroclasts, = S-C protomylonite).

consequence of changes in orientation of the tectonic strain ellipsoid during deformation of the host rock body, and (5) segments which comprise the path of fiber orientations correspond to distinct stages in the evolution of the host rock body's structural geometry. Analyses of pressure shadows in the Franklinian sequence are integrated with other kinematic data, with the thrust sheet geometry modeled in schematic and sequential balanced cross-sections through the Franklin Mountains anticlinorium, and with the kinematic model of Butler (1982) for the emplacement of thrust sheets and the model of Sanderson (1982) for the development of fault-bend folds (Appendix F). Analyses of pressure shadows in the Sadlerochit Group are considered in terms of the structural position of the sample relative to the interpreted geometry and evolution of local folds and thrust faults in the Ellesmerian sequence (Appendix F). It is important to emphasize that analysis of one or two pressure shadows from one sample location cannot determine, or even adequately support, any particular kinematic model for the evolution of the Franklin Mountains anticlinorium.

Ramsay and Huber (1983) present two end-member models for the behavior of pressure shadow fibers during deformation. In the rigid fiber model (Figure 38A), after fibers are formed they are undeformable and act in a rigid way like the central resistant object around which the pressure shadow developed. In the deformable fiber model (Figure 38B), after fibers are created they deform in a manner like that of the rock matrix which surrounds the central rigid object. Ramsay and Huber (1983) suggest that the geometry of quartz fibers generally follows the rigid fiber model, while chlorite and calcite can follow either model, and they outline methods for the calculation of incremental strains associated with each stage of fiber orientation (Appendix F). In order to calculate incremental strain for rigid or deformable fiber models it is necessary to measure (1) fiber orientation, (2) length of fibers within a similar angular range of orientation, and (3) the maximum diameter of the resistant object in the mean direction of each fiber segment (refer to Appendix F). Total strain can be determined by summing the calculated incremental strains.

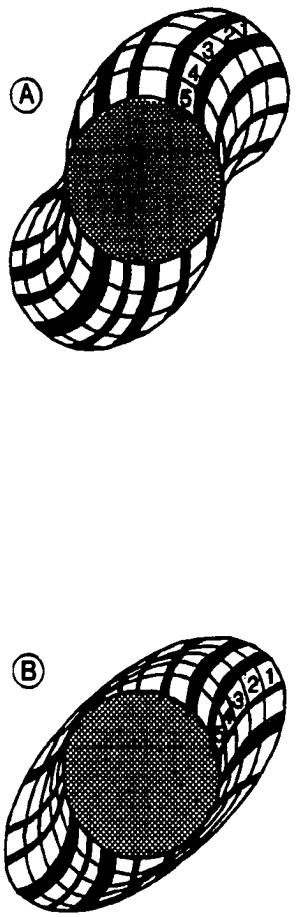

FIGURE 38. Geometric constrasts of the rigid fiber model (A) and deformable fiber model (B) in non-coaxial deformation (from Ramsay and Huber, 1983). Fiber increment 1 formed first; increment 5 formed last. This labelling scheme for denoting the relative ages of fiber increments is used in Appendix F.

7.B.2. Franklinian Sequence Sample

Incremental strain analysis techniques were applied to three pressure shadows in oriented sample 87JZ16 from the Franklinian sequence, two shadows in the east-northeast-striking plane and one in the north-northwest-striking plane. These pressure shadows surround two large (1 cm in diameter) marcasite nodules that were found, fortuitously, during thin-section preparation. (One cut intersected a nodule in the north-northwest-striking plane; another cut intersected a second nearby nodule in the east-northeast-striking plane. No other marcasite nodules were found in this or other samples. It was not possible to analyze a pressure shadow in the plane of compositional layering since both nodules were cross-cut in this plane.) Sample 87JZ16 is a matrix-supported, texturally and compositionally immature sandstone comprised of 0.1-0.2 mm calcite, albite, and subangular quartz framework grains, in a matrix of chlorite, clay, and opaque minerals. This pre-Mississippian sandstone was only observed at the location of sample 87JZ16 (location "16" in Figure 15); thus, it is interpreted to be a discontinuous sand lens within the extensive, dominantly shale unit of the Franklinian sequence (pMsh).

7.B.2.a. Age of pressure shadows

It is necessary to determine the age of the pressure shadows in sample 87JZ16 in order to view incremental strain calculations in terms of the structural evolution of the study area. Chlorite fibers at the periphery of the shadows are interpreted to have formed first, followed by quartz and calcite fibers which are in contact with the central marcasite nodules. The chlorite fibers are subparallel to compositional layering in the sandstone which is, in turn, subparallel to slaty cleavage. This slaty cleavage is interpreted to have formed as a consequence of pre-Mississippian deformation (Section 5.C.1.). Therefore, in order to determine the age of these pressure shadows, it is necessary to establish whether these chlorite fibers formed synchronous with or after the slaty cleavage.

Chlorite fibers, subparallel to slaty cleavage, are associated with quartz and calcite veins which cross-cut slaty cleavage in other thin-sections of nearby rocks. This relationship supports the

interpretation that first-formed chlorite fibers post-date the formation of pre-Mississippian slaty cleavage, and formed in a regime characterized by maximum extension subparallel to slaty cleavage. The next major deformational event known to have affected the Franklinian sequence is the Cenozoic episode which formed the regional anticlinoria, folding and faulting the overlying Ellesmerian sequence cover rocks. Thus, the chlorite fibers are assumed to have formed at some point during this regional event, although it is possible that they formed during an undocumented pre-Mississippian event following cleavage formation. (Refer to Appendix F for speculation regarding specific movements during which chlorite fibers might have formed.) Quartz and calcite fibers which touch the central marcasite nodules likely formed in response to the most recent Cenozoic deformational movements of sample 87JZ16.

7.B.2.b. Structural position of sample

Sample 87JZ16 occurs within the shale unit (pMsh) which comprises much of the middle structural-stratigraphic package of the Franklinian sequence rocks exposed in the study area (Figure 16 or Plate 1), and is located near the base of the first horse which comprises much of the Franklin Mountains anticlinorium (location "16" in Figures 15 and 30). The first horse is interpreted to have been fault-bend folded in the vicinity of this sample location, forming the upper antiform which was documented during mapping. Sample 87JZ16 also lies above the south-dipping backlimb of the lower antiform that is interpreted to be a fault-bend fold in the second horse. Thus, the pressure shadows developed in this sample may reflect deformational movements associated with (1) thrust emplacement of the first horse, (2) fault-bend folding of the first horse, and/or (3) geometric modification of the first horse caused by subsequent emplacement of the second horse. The preferred interpretation is that the pressure shadows formed during (1) and (2) above. Appendix F includes speculations regarding the relation of the strain path obtained from each pressure shadow to these deformational movements. (Strain paths are shown in Figures 62 and 63 in Appendix F.)

7.B.3. Ellesmerian Sequence Sample

Incremental strain analysis was applied to eleven pressure shadows in the north-northwest-striking plane of oriented Sadlerochit Group sample 87JZ45. These pressure shadows are comprised of straight and slightly curved quartz fibers which surround 0.15-0.30 mm euhedral pyrite crystals. Pyrite crystals with associated pressure shadows were only observed in this sample and only in the north-northwest-striking plane. Pressure shadows are developed on north (up-dip) and south (down-dip) sides of five of the eleven pyrite crystals, shadows are developed only on the north side of five crystals, and a shadow is developed only on the south side of one crystal. The orientation of fiber segments and cumulative fiber lengths were measured for each side of these pressure shadows.

7.B.3.a. Age of pressure shadows

Most of the quartz fibers of the eleven pressure shadows are subparallel to compositional layering in the calcareous shale, compatible with shortening normal to this plane. These pressure shadows formed either in association with post-Permian diagenesis, or during Cenozoic deformation. Deformational movements that would be compatible with bedding-normal flattening in this sample are discussed in Appendix F.

7.B.3.b. Structural position of sample

Sample 87JZ45 is located at the base of the Echooka Formation (location "45" in Figure 15), near the contact with the underlying Wahoo Limestone. Bedding of both the Echooka Formation and the Wahoo Limestone dips steeply to the southeast. This sample was obtained from a package of Pennsylvanian Wahoo Limestone and Permian Echooka Formation on the northern flank of the anticlinorium. As shown in Figure 33 (location "45"), this package of Ellesmerian sequence rocks has been thrust northward over the Lower Triassic Ivishak Formation along a fault which is interpreted to dip moderately to the southeast.

7.B.4. Summary of Results and Interpretations

Incremental strain analysis of pressure shadows developed in Franklinian sequence sample 87JZ16

indicate average total major extensile strains of 45% and 39% in the north-northwest-strking and east-northeast-striking planes, respectively. As suggested in Appendix F, it may be possible to correlate fiber orientations with stages in the modeled emplacement of the two horses which comprise the Franklin Mountains anticlinorium. Analysis of pressure shadows developed in Echooka Formation sample 87JZ45 indicate an average total major extensile strain of 112% in the north-northwest-striking plane. It is possible that these shadows were developed by bedding-normal maximum shortening, or by an interbed flexural-slip mechanism during folding (Appendix F). It is important to note that strains calculated for samples of Franklinian and Ellesmerian sequence rocks should not be compared (Appendix F).

7.C. FINITE STRAIN ANALYSIS USING QUARTZ GRAINS

7.C.1. Methods

Finite strain analysis techniques were applied to subelliptical quartz grains in oriented samples of the Mississippian Kekiktuk Conglomerate and Lower Triassic Ivishak Formation. The Fry method (Fry, 1979) was used to determine the orientation and ellipticity of the tectonic strain ellipse in each of the three mutually-perpendicular thin-section planes (Figure 36). The phi-R_f method described by Ramsay and Huber (1983) was used to determine the orientation of the tectonic strain ellipse, as well as the mean orientation and ellipticity of subelliptical grains prior to and following deformation. Since only four oriented samples were analyzed, the sample population is statistically small. No replicate sample planes were analyzed, so the reproducibility of the results is unknown. Sample locations are widely spaced throughout the study area, making it inappropriate to deduce details of the pattern of finite strain in the Ellesmerian sequence. However, the different locations of samples relative to major structures in the study area make it possible to speculate upon relationships between finite strain and the structural position of the sample. In order to substantiate the speculations presented in Appendix G, replicate and additional analyses of rocks from similar and other structural positions would be required.

7.C.2. Samples

Finite strain analysis techniques were applied to thin-sections of the bedding-parallel, north-northwest-striking, and east-northeast-striking planes of three samples of the Kekiktuk Conglomerate and one sample of the Ivishak Formation described below.

7.C.2.a. Kekiktuk Conglomerate

Sample 87JZ31 is a quartz- and chert-pebble conglomerate obtained from the stratigraphic base of the sheet of Kekiktuk Conglomerate which caps the upper antiform (location "31" in Figures 15 and 30). Quartz grains in this sample range in diameter from 0.5 to 4.0 mm. Samples 87JZ25 and 87JZ36 are weakly foliated, fine- to medium-grained quartzites comprised of quartz grains which average 0.2 mm in diameter. Sample 87JZ25 is located at the northern leading edge of the horse that forms that antiform (location "25" in Figures 15 and 30), in the vicinity of the thrust fault which places the first horse in contact with the underlying second horse. Sample 87JZ36 is located near the stratigraphic top of the sheet of Kekiktuk Conglomerate which caps the lower antiform developed in the second horse, structurally beneath sample 87JZ25 (location "36" in Figures 15 and 30).

These samples exhibit a fabric defined by the alignment of the long axes of subelliptical quartz grains, particularly evident in thin-sections of the east-northeast- and north-northwest-striking planes. Grains in sample 87JZ31 are in contact with each other and grain boundaries are curved or sutured. In samples 87JZ25 and 87JZ36, intergranular fine-grained white mica and marginal quartz subgrains cause some grains to be separated; touching grains have straight, curved, and sutured boundaries. Stylolites locally cross-cut grains in all three samples of the Kekiktuk Conglomerate.

7.C.2.b. Ivishak Formation

Sample 87JZ40 is a very fine-grained quartzarenite comprised of 0.05-0.1 mm subrounded quartz framework grains cemented by calcite and quartz. This Sadlerochit Group sandstone is matrix-supported; however, where adjacent grains touch each other boundaries are typically slightly curved. While pressure solution produced a few seams of opaque material visible in thin-sections of the east-northeast- and

north-northwest-striking planes, individual framework grains do not appear to be cross-cut by stylolites. Sample 87JZ40 is located near the prominent east-northeast-trending thrust fault which emplaced the Pennsylvanian Wahoo Limestone northward over the Lower Triassic Ivishak Formation (location "40" in Figures 15 and 30).

7.C.3. Summary of Results and Interpretations

The samples from the Kekiktuk Conglomerate and Ivishak Formation record relatively low finite strains. The average finite strain ratio determined by both the Fry method and the phi-R_f technique has a value of 1.22 for Kekiktuk Conglomerate samples and 1.17 for the Ivishak Formation sample. Average strain ratios measured by the Fry method and phi-Rf technique for the three sample planes are presented in Table 8. Data obtained by both methods are sorted and compared in Tables 23-30 in Appendix G.

It is significant that finite strain analysis documents only minor penetrative strain in the Kekiktuk Conglomerate. In addition, strain ratios determined for the Kekiktuk Conglomerate are comparable to those determined for the Ivishak Formation of the Sadlerochit Group (Table 8). Note, however, that the mechanism for cross-section-scale shortening was thrust duplication for the Kekiktuk Conglomerate and detachment folding for the Sadlerochit Group. Observation of similar finite strains in these two structural-stratigraphic units suggests that equivalent magnitudes of Cenozoic tectonic strain were recorded both above and below the Kayak Shale detachment horizon. As shown in Figure 15, with the exception of sample 87JZ31 from the Kekiktuk Conglomerate, the samples are located adjacent to Cenozoic thrust faults. It is interesting to note that even at these locations, where strain is most likely to be greatest, the strain measured by these methods is low and of the same magnitude as that determined for sample 87JZ31.

7.D. FINITE STRAIN ANALYSIS USING LISBURNE GROUP CORALS

Deformed lithostrotionoid corals in the bedding plane of sample 87JZ50 from the Alapah Limestone (location "50" in Figures 15 and 33) have an average ellipticity of R = 1.43. The long axes

TABLE 8. Average finite strain ratios determined by the normalized Fry method and Ø - R_f technique. Finite strain values are low for both the Kekiktuk Conglomerate and the Ivishak Formation, ranging between R = 1.10 and 1.35, averaging R = 1.20. Strain ratios for samples from the Kekiktuk and the Ivishak are similar in value.

		AVERAGE STRAIN RATIOS		
	PLANE	KEKIKTUK	IVISHAK	Difference (Kek. - Ivis.)
NORM. FRY	BED-11	1.21	1.20	0.01
	ENE	1.21	1.11	0.10
	NNW	1.14	1.16	- 0.02
Ø - Rf	BED-11	1.36	1.15	0.21
	ENE	1.26	1.32	- 0.06
	NNW	1.25	1.10	0.15

of thirty-three of these elliptical markers exhibit an average trend of 137 degrees. Assuming that the corals were originally circular markers in this plane, the shape and orientation of these corals are interpreted to represent the shape and orientation of the tectonic strain ellipse. The ellipticity of these markers records an extensile strain of 43%, and their orientation in the bedding plane indicates maximum elongation subparallel to the north-northwest Cenozoic tectonic transport direction.

7.E. SIGNIFICANCE OF QUANTITATIVE KINEMATIC ANALYSES

Several points should be made regarding the possible significance of incremental and finite strain determinations for the Franklinian and Ellesmerian sequence samples. First, it may be important to note that the orientation of the major axis of the strain ellipse in the bedding plane, determined from the deformed corals in sample 87JZ50, contrasts with the orientation of the major axis suggested by the orientation of strain markers in the Franklinian sequence and Kekiktuk Conglomerate samples (discussed in Appendix E). Most strain markers in the plane of compositional layering in the Franklinian sequence and the plane of bedding in the Kekiktuk Conglomerate record a major axis of the Cenozoic tectonic strain ellipse which trends approximately east-northeast, presumably reflecting north-northwest-directed maximum shortening associated with Cenozoic deformation. The major axis of the Cenozoic tectonic strain ellipse suggested by Lisburne Group sample 87JZ50 trends northwest, subparallel to the direction of inferred Cenozoic tectonic transport.

Differences in strain ellipsoid orientation above and below the Kayak Shale detachment on the north flank of the anticlinorium are likely a function of differences in the inferred mechanisms of folding and faulting and the material properties of the involved rocks. Since the sample from the Alapah Limestone (87JZ50) is an aggregate of calcite grains that tend to deform plastically, strain in this sample might be expected to reflect the direction in which these rocks were tectonically transported. This sample was obtained from the hangingwall in the vicinity of a north-dipping, north-vergent thrust fault that truncates tight detachment folds, soling in the Kayak Shale ("50" in Figure 33). In contrast, the

Kekiktuk Conglomerate and Franklinian sequence rocks record strains associated with fault-bend folding that occurred during the emplacement of the horses comprising the anticlinorium. Therefore, quartz grains in the Kekiktuk Conglomerate might be expected to rotate, plastically deform, and/or undergo pressure solution such that their long axes became oriented normal to the direction of maximum shortening, in an east-northeast direction.

The total extensile strains of 39% and 45% determined for the respective east-northeast-striking and north-northwest-striking planes of sample 87JZ16 from the Franklinian sequence are comparable to the 43% extensile strain determined by the analysis of the deformed corals in sample 87JZ50 from the Alapah Limestone. Finite strain values determined by the Fry method and phi-R_f technique for samples from both the Kekiktuk Conglomerate and Ivishak Formation do not appear to vary appreciably between the three thin-section planes (Table 8).

Finite strains determined by the normalized Fry method and phi-R_f technique for samples from the Kekiktuk Conglomerate and Ivishak Formation are similar in magnitude; however, these values are less than those determined either by incremental strain analysis of Franklinian sequence and Echooka Formation samples or by finite strain analysis of corals in the Lisburne Group. Rigid quartz grains in competent quartzites from the Kekiktuk Conglomerate and quartzarenite from the Ivishak Formation would not be expected to record as much strain as either pressure shadows developed around rigid grains in incompetent phyllites of the Franklinian sequence and shale of the Echooka Formation, or plastically-deforming limestone of the Lisburne Group.

In conclusion, quantitative kinematic analyses support the idea that roughly equivalent and relatively small amounts of Cenozoic shortening have been accommodated by internal strain within the major structural-stratigraphic units, above and below both the Kayak Shale detachment horizon and the sub-Mississippian unconformity. The strain determinations are consistent with the balanced

cross-section and the assumptions upon which it is based. In this model, the Kekiktuk Conglomerate is assumed to remain attached to the Franklinian sequence during Cenozoic deformation. The amount of shortening above the Kayak Shale (average of 42%) is a function of the amount of Cenozoic shortening (44%) resulting from thrust duplication of underlying Franklinian sequence rocks and the capping Kekiktuk Conglomerate. Strain determinations suggest that the less competent, more strain-prone lithostratigraphic units in the Franklinian and Ellesmerian sequences record maximum extensile strains which approximate the magnitude of shortening calculated from the balanced cross-sections, or roughly 40-45%. Although it is difficult to demonstrate convincingly given the limited scope of the strain analyses, it is tempting to conclude that these strain values reflect local penetrative strain associated with the formation of cross-section-scale structures. Strain would vary in magnitude depending on the position of the sample within these structures. In addition, strain values would differ between lithostratigraphic units depending on their material properties and style of deformation.

8. THE INFLUENCE OF MATERIAL PROPERTIES AND PHYSICAL CONDITIONS ON THE STRUCTURAL STYLE OF THE FRANKLINIAN SEQUENCE

Given the physical properties of the thrust sheets (i.e. thickness, length, etc.), the physical conditions which might have influenced the development of the observed structural geometry are discussed in this section. The structural style exhibited by the Franklinian sequence can be better understood based on consideration of the physical factors that might have influenced the character of the response of pre-Mississippian rocks to Cenozoic deformation.

8.A. THE RELATION OF MATERIAL PROPERTIES TO FOOTWALL RAMP ANGLES

In the primary balanced cross-section constructed across the Franklin Mountains anticlinorium (Figures 30-32), the ramps over which the first and second horses were displaced slope at 33-46 degrees and 47 degrees, respectively. Compared to other fold-and-thrust belts, the ramp angles modeled for the anticlinorium are unusually steep. For example, initial step-up angles for ramps in the western Taiwan overthrust belt, determined by Dahlen et al. (1984), cluster around a mean angle of 13.3 +/- 2.4 degrees.

The prominent east-striking, moderately south-dipping pre-Mississippian slaty cleavage observed in Franklinian sequence phyllites, slates, and shales exposed in the study area may have functioned as a structural grain which favored the formation of steep ramps during Cenozoic deformation. Since the dip of this slaty cleavage averages 49 degrees, similar to the 33- to 46- and 47-degree ramp angles, pre-Mississippian slaty cleavage may have functioned as a preferential failure plane for ramp formation. If the ramp angles modeled in the primary balanced cross-section (Figure 30, Plate 2) are correct, then it would appear that thrust surfaces formed along the moderately- to steeply-dipping cleavage planes.

Paterson (1978) suggests how it might have been mechanically feasible for thrust surfaces to form along slaty cleavage. For a variety of foliated rocks, Paterson (1978) investigated the relationship

between the magnitude of differential stress required for failure under triaxial compression and the inclination of the cleavage plane relative to the compression axis. Figure 39 shows that, over a range of confining pressures, the lowest differential stresses at failure were observed when the compression axis was oriented at a 45 degree angle to cleavage for phyllite, and at a 30 degree angle for slate and shale. While it might seem that a large differential stress would be required to create a 45-degree ramp angle, Paterson's (1978) experimental work suggests that this is not necessarily the case. Since pre-Mississippian slaty cleavage is oriented at an angle of roughly 45 degrees with respect to an inferred subhorizontal Cenozoic regional orogenic compressive stress, a lower magnitude of differential stress would be required to cause failure along these steeply-oriented planes than would be required to form a failure plane at any other orientation (Figure 39).

8.B. A MECHANICAL MODEL FOR THRUST SHEET FORMATION AND DISPLACEMENT

Applying the ideas of Paterson (1978) to the thrust sheets that comprise the Franklin Mountains anticlinorium poses several important questions: If pre-Mississippian slaty cleavage in the Franklinian sequence was at an orientation with respect to the regional axis of compression that was favorable for failure, how could coherent thrust sheets have formed? And, how could these packages of previously deformed, weakly metamorphosed rocks have been displaced as semi-rigid thrust sheets, exhibiting relatively little apparent internal deformation?

8.B.1. The Role of Fluid Pressure in Formation and Displacement of Coherent Thrust Sheets

Field observations suggest that the two horses were not penetratively deformed during Cenozoic emplacement. For example, pre-Mississippian slaty cleavage in shales, phyllites, and slates is only locally crenulated or folded. The thrust faults, which emplaced the horses and resulted in formation of the two broad antiforms, are the major Cenozoic structures which involve these rocks. Applying the ideas of

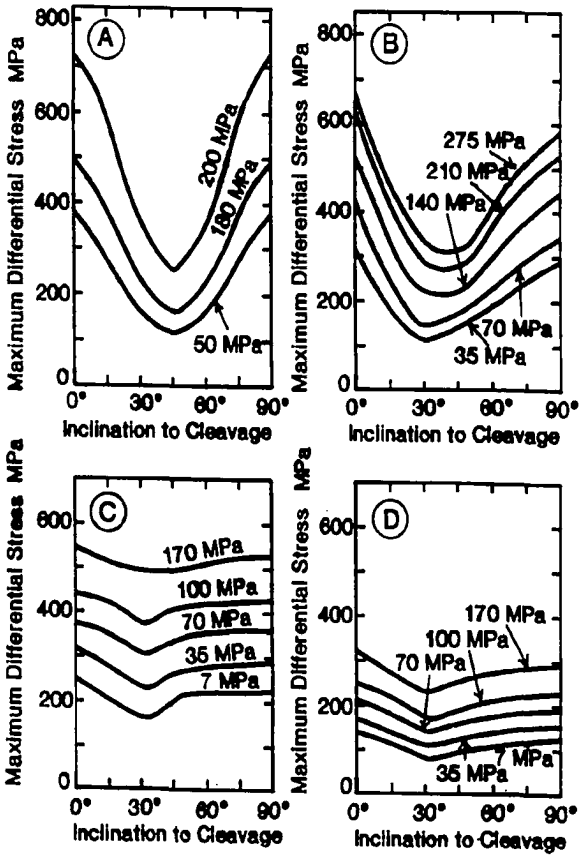

FIGURE 39. Dependence of differential stress at failure in triaxial compression on the inclination of the cleavage plane to the compression axis for foliated rocks at the confining pressures shown. (A) Moretown Phyllite; (B) Slate; (C) Green River Shale 1; (D) Green River Shale 2 (Paterson, 1978).

Davis et al. (1983), the apparent lack of extensive internal Cenozoic deformation suggests that these thrust sheets had either significant internal strength or low basal friction, perhaps developed as a consequence of high fluid pressure conditions. It is likely that the first horse could not have been displaced as a coherent package of rocks unless reasonably high fluid pressure existed within the wedge and along the basal detachment. Without elevated fluid pressures, it would likely be impossible to develop a duplex thrust system consisting of coherent rock packages like that shown in Figure 10A; pervasive internal deformation and tectonic flow of these weakly-metamorphosed rocks would likely occur in a manner similar to that shown in Figure 10B.

Quartz- and calcite-filled extension fractures, interpreted to be of Cenozoic age, cross-cut pre-Mississippian slaty cleavage in the Franklinian sequence. These structures likely formed under conditions of high fluid pressure. In addition, indirect reasoning suggests that high fluid pressure conditions existed in pre-Mississippian rocks during Cenozoic deformation: (1) Map-scale structures suggest, and the balanced cross-sections constructed from field data are compatible with the interpretation, that a duplex thrust system produced regional Cenozoic shortening of the Franklinian sequence. (2) Field observation of the pre-Mississippian rocks comprising the first and second horses in the study area suggests that thrust sheets of Franklinian sequence rocks in the Franklin Mountains region may have behaved as relatively rigid packages of rocks during Cenozoic deformation. (3) The primary balanced cross-section provides estimates of the thicknesses (3-5 km) and lengths (9 and >20 km) of these thrust sheets; regional stratigraphy and seismic interpretation suggest the amount of overburden at the time of Cenozoic deformation (9 km) (Bird and Bader, 1987). In order for (1) and (2) to be true, and given the physical properties/conditions in (3), it is likely that high fluid pressure conditions existed in the Franklinian sequence, at least along the floor thrust horizon, during Cenozoic deformation.

8.B.2. Pre-Mississippian Structural Fabric and the Lithologic Heterogeneity of the Franklinian Sequence

High fluid pressure conditions might have been the dominant factor which enabled the first horse to be displaced, but high fluid pressure cannot explain why these rocks were displaced as coherent packages, behaved rigidly, and developed little internal deformation during Cenozoic deformation. The response of the Franklinian sequence to Cenozoic deformation was likely influenced by factors such as the orientation of pre-Mississippian structures and the lithologic heterogeneity of the asssemblage.

Pre-Mississippian deformation of the Franklinian sequence is interpreted to have involved tight to isoclinal folding and thrust faulting (Section 5.C.1.). Based on the orientation of pre-Mississippian bed-parallel slaty cleavage within the study area, the axial surfaces of these folds dip moderately south. It is likely that the crests and troughs of these folds constitute subhorizontal panels (Figure 40). In theory, coherent thrust sheets could be formed if the Cenozoic tectonic load was transmitted along these subhorizontal horizons, with failure occurring along moderately south-dipping, bed-parallel slaty cleavage in the fold limbs (Figure 40). In addition, north-vergent pre-Mississippian thrust faults (such as T_R in Figures 30-31 and 35) would have reoriented pre-Mississippian bedding and slaty cleavage, producing south-dipping panels that could have functioned as preferential failure planes during Cenozoic deformation (Figure 40). Thus, the pre-Mississippian structures in the Franklinian sequence may have formed a ramp-flat geometry that permitted deformed packages of rocks to be isolated and displaced as rigid and coherent thrust sheets during Cenozoic deformation.

The Franklinian sequence in the study area consists of competent chert, volcanic rocks, sandstone, and minor carbonate rocks, interlayered with incompetent phyllite, shale, and minor slate. Even though the more massive, competent pre-Mississippian rocks generally appear relatively undeformed at a mesoscopic scale, microscopic examination reveals that pressure solution, crystal-plastic deformation, recrystallization, twinning, extension fracturing, and shear occurred during deformation (Section 5.D., Table 4). The slight to moderate degree of internal deformation observed in these competent rocks suggests that the load imposed during Cenozoic deformation did not exceed the relatively high internal

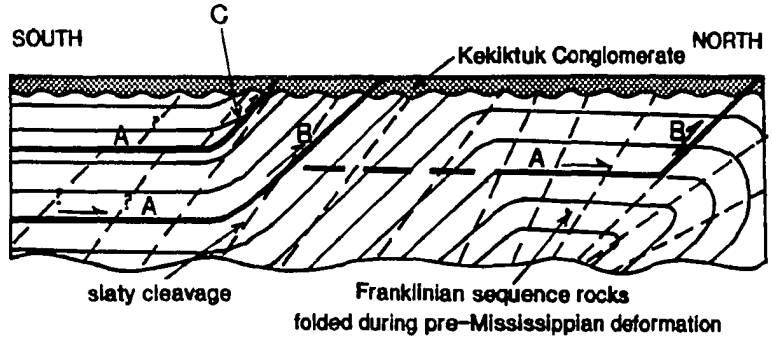

FIGURE 40. Schematic cross-section of the Franklinian sequence and Kekiktuk Conglomerate, showing the possible influence of pre-Mississippian structures on the formation of thrust sheets during Cenozoic deformation. A pre-Mississippian ramp-flat geometry, produced by a combination of folding and faulting, may have favored formation of thrust faults subparallel to tightly or isoclinally folded layers (A and B) and subparallel to slaty cleavage (B). Pre-Mississippian thrust faults (C) may have been reactivated during Cenozoic deformation.

strength of these lithologies. Thus, competent layers may have protected incompetent layers from deformation, accounting in part for the apparent strength of these thrust sheets.

8.C. RAMP LOCATION AND DETACHMENT DEPTH FOR THE SECOND HORSE

Figure 32 depicts the structural geometry of the Franklin Mountains anticlinorium following thrust emplacement of the first horse. Observe that the location of the ramp, over which the second horse will be emplaced during the next evolutionary stage, lies close to the leading edge of the overlying first horse. In addition, note that the basal detachment steps up from a depth of 5.4 kilometers below sealevel to 3.1 kilometers below sealevel beneath the eventual second horse, and that this step-up occurs beneath the first horse. Is there a mechanical explanation for the apparent relationship between the position of the first thrust sheet and both the location of the future ramp and the step-up of the basal detachment?

Gretener's (1972) ideas on how a thrust system propagates from hinterland to foreland may be applied to the Franklin Mountains anticlinorium model shown in Figure 32. It is likely that the first horse ceased to be displaced toward the foreland when it was no longer energetically favorable to push the fault-bend folded leading edge of the thrust sheet above the eventual second horse (Figure 32), perhaps when fluid pressure dropped such that displacement was no longer mechanically feasible. Gretener (1972) suggests that fast loading by thrusting may generate high fluid pressures in impermeable thrust-overridden rocks, reducing the effective overburden pressure and favoring the formation of a new detachment horizon along a zone of high fluid pressure (Figure 41). Thus, emplacement of the first horse may have led to the formation in its footwall of the basal detachment of the eventual second horse (Figure 32). However, it is impossible to cite evidence indicative of high fluid pressure at this structural level because the detachment at the base of the second horse is not exposed, and the lithology and physical properties of the structural-stratigraphic unit in which this detachment lies are unknown.

As fluid pressure increases (Figure 42), Gretener (1972) locates the ramp over which the next

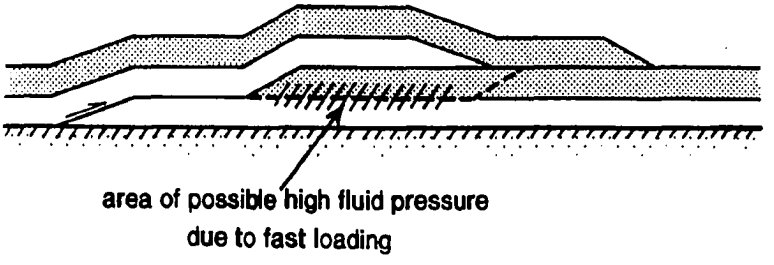

A. Activation of a lower thrust plane.

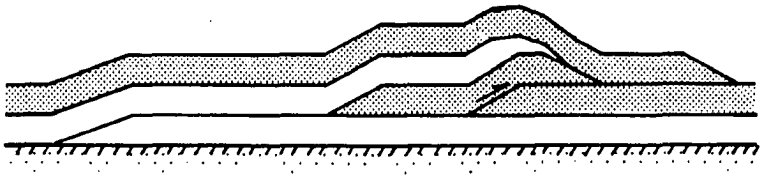

B. Old thrust is carried piggyback and folded over the new step.

FIGURE 41. Effect of loading by overthrust faulting on the depth of future detachments and location of ramps (Gretener, 1972).

thrust sheet will be emplaced in undeformed rocks immediately in front of the already emplaced thrust sheet. Following Gretener's (1972) model, fluid pressures might be expected to be low toward the foreland from the first-emplaced horse compared with those within pre-Mississippian rocks beneath the first horse. The ramp over which the second horse was eventually displaced (Figure 32) might have formed when a sufficient load was transferred to a favorably oriented incompetent layer, with failure occurring along slaty cleavage planes.

9. A MECHANICAL CONSIDERATION OF THE STRUCTURAL STYLE OF THE ELLESMERIAN SEQUENCE

Distinct structural geometries are developed within different parts of the Ellesmerian sequence, as illustrated in the balanced cross-section (Figure 30): those displayed by (1) the Mississippian Kekiktuk Conglomerate, (2) the Mississippian Kayak Shale, and (3) the Mississippian to Lower Triassic Lisburne and Sadlerochit Groups. These geometric distinctions reflect differences in the mechanical competency of constituent lithostratigraphic units and in their structural position with respect to the roof thrust of the modeled duplex thrust system in the Mississippian Kayak Shale. Important material properties and physical conditions which may have influenced the response of the Ellesmerian sequence to deformation are discussed in this section. In particular, the response of the Ellesmerian sequence to Cenozoic deformation was strongly influenced by the structural stratigraphy of the estimated 2,350-meter succession of Mississippian and younger strata presently exposed in the study area.

9.A. STRUCTURAL STYLE BENEATH THE ROOF THRUST

The style and distribution of deformation within the Kekiktuk Conglomerate places potential constraints upon the model used to explain the structural evolution of the Franklin Mountains anticlinorium (Sections 4.C.3. and 4.D.1). The style of deformation of the Kekiktuk Conglomerate varies from place to place within the study area. For example, mesoscopically undeformed conglomerate horizons and dominantly depositional contacts between the Kekiktuk Conglomerate and the Franklinian sequence were observed, as well as local imbrication and tectonic brecciation of the Kekiktuk Conglomerate (Section 5). Finite strain analyses of several samples documented penetrative strain within the Kekiktuk Conglomerate, similar in magnitude to that measured for a sample of the Sadlerochit Group (Section 7). Behavior of the Kekiktuk Conglomerate during deformation may have been influenced by a number of factors, including the presence or absence of structurally overlying pre-Mississippian rocks, the effect of interbedded shale in the unit, and the interplay between volume changes and fluid pressure

conditions within the Kekiktuk Conglomerate.

9.A.1. The Influence of Structurally Overlying Franklinian Sequence Rocks

Within the study area, the Kekiktuk Conglomerate is overlain either (1) depositionally by the Kayak Shale, or (2) by thrust emplaced Franklinian sequence rocks. The Kekiktuk Conglomerate observed in the study area is more highly deformed where it structurally underlies pre-Mississippian rocks. The most highly deformed Kekiktuk Conglomerate observed (local imbrication and tectonic brecciation, prevalent quartz-filled extension fractures) occurs on the northern limb of the lower antiform (Figures 18 and 22). Since the Kekiktuk Conglomerate is structurally overlain by Franklinian sequence rocks of the first horse at this location (Figure 19), it is tempting to speculate that higher strains were developed in these thrust-overridden rocks than in the Kekiktuk Conglomerate where it was overlain by the Kayak Shale in an undisrupted stratigraphic succession.

9.A.1.a. Tectonic load

Since the magnitude of shear stress acting on the stratigraphic top surface of the Kekiktuk Conglomerate is a function of the overburden pressure, thrust emplacement of rocks of the Franklinian sequence over the Kekiktuk Conglomerate should result in higher values of shear stress along this interface than would be expected as a consequence of displacement of only stratigraphically overlying Mississippian and younger rocks along the proposed roof thrust in the Kayak Shale. The relative differences in load at various structural positions are reasonably well constrained if the primary balanced cross-section (the source of thrust sheet thickness values) is an accurate geometric model. Within the study area, the balanced cross-section model suggests that thrust emplaced Franklinian sequence rocks at the leading edge of the first horse contributed to an increase in overburden pressure on the Kekiktuk Conglomerate of the lower antiform of only 6-12% (Appendix H). Where 4.7 kilometers of Franklinian sequence rocks are interpreted to overlie structurally the unexposed Kekiktuk Conglomerate of the second horse to the south of the study area (Figure 32), an increase in overburden pressure of 28% would be

expected (Appendix H). The above calculations suggest that the overburden pressure affecting the Kekiktuk Conglomerate of the lower antiform may not have been significantly greater than that which affected the Kekiktuk Conglomerate of the upper antiform. (The strain analyses discussed in Section 7 and Appendix G failed to identify any significant difference in the magnitude of penetrative strain developed in the Kekiktuk Conglomerate of the two antiforms, results compatible with the only minor difference in values estimated for overburden pressure.) Thus, factors other than the magnitude of the tectonic load most likely contributed to the extensive mesoscopic deformation observed locally in the Kekiktuk Conglomerate of the lower antiform.

9.A.1.b. Displacement of the first horse and interactions at its leading edge

The Kekiktuk Conglomerate appears to be most highly deformed in the footwall of a thrust on the north limb of the lower antiform, at a structural position near or along strike with the point where the Kekiktuk Conglomerate of the first horse is truncated against that of the underlying second horse (location "36" in Figure 30). It is possible that this deformation might reflect conditions unique to a structural position beneath the leading edge of a thrust sheet. Displacement of the first horse likely ceased when postulated high fluid pressure along the detachment dropped such that too much energy was required to continue to push the fault-bend folded leading edge of the thrust sheet above the eventual second horse, and/or it became mechanically unfeasible to continue to displace the thrust sheet above its basal detachment (Section 8.C.). Assuming that the force which drove thrust faulting remained essentially constant during orogenesis, as fluid pressure dropped, displacement would likely have ceased, resulting in "stick," or a locking-up of simple-shear displacement along the thrust surface (Gretener, 1972). If a drop in fluid pressure occurred above the Kekiktuk Conglomerate of the second horse, the Kekiktuk Conglomerate might be expected to be more highly deformed as a consequence of the effective increase in load.

9.A.2. The Influence of Interbedded Shale in the Kekiktuk Conglomerate

Displacement occurred above the Kekiktuk Conglomerate during Cenozoic deformation, either in association with thrust emplacement of Franklinian sequence rocks or with detachment folding in overlying Mississippian and younger rocks above the roof thrust in the Kayak Shale. Such displacement appears to have been distributed over a zone of variable thickness. Whether this zone of displacement included none of, some of, or the entire stratigraphic thickness of the Kekiktuk Conglomerate likely depended on the rocks that were in contact with the top surface of the Kekiktuk Conglomerate. A substantial thickness of Kayak Shale (422 m determined from balanced cross-section) is considered to have depositionally overlain the Kekiktuk Conglomerate prior to deformation (Figure 42). Detachment folding observed above the Kayak Shale indicates that it was thick enough to permit the Lisburne Group and overlying rocks to be totally decoupled from the Kekiktuk Conglomerate (Figure 42). In this case, displacement would have been accommodated entirely within the Kayak Shale; displacement related to shortening above the roof thrust probably did not affect the Kekiktuk Conglomerate (Figure 42). In contrast, where Franklinian sequence rocks have been thrust over the Kekiktuk Conglomerate of the second horse, the Kayak Shale is absent, likely having been bulldozed ahead of the first horse as it was emplaced. The postulated high fluid pressure along the detachment surface would allow the first horse to glide over the Kekiktuk Conglomerate of the eventual second horse. However, instead of displacement being accommodated within a significant thickness of incompetent Kayak Shale, the base of the first horse would be in direct contact with the Kekiktuk Conglomerate in the footwall. Coupling across this fault likely would have led to accommodation of some displacement within the Kekiktuk Conglomerate of the footwall (Figure 43). If the zone of displacement included the Kekiktuk Conglomerate, it is possible that the thickness of this zone was influenced by the stratigraphy of the unit.

For the sake of simplicity, the Kekiktuk Conglomerate was treated earlier (Section 4, Figure 12) as a homogeneously deforming structural-stratigraphic unit. In fact, it is a lithologically heterogeneous structural-stratigraphic unit. The Kekiktuk Conglomerate observed in the study area consists of roughly

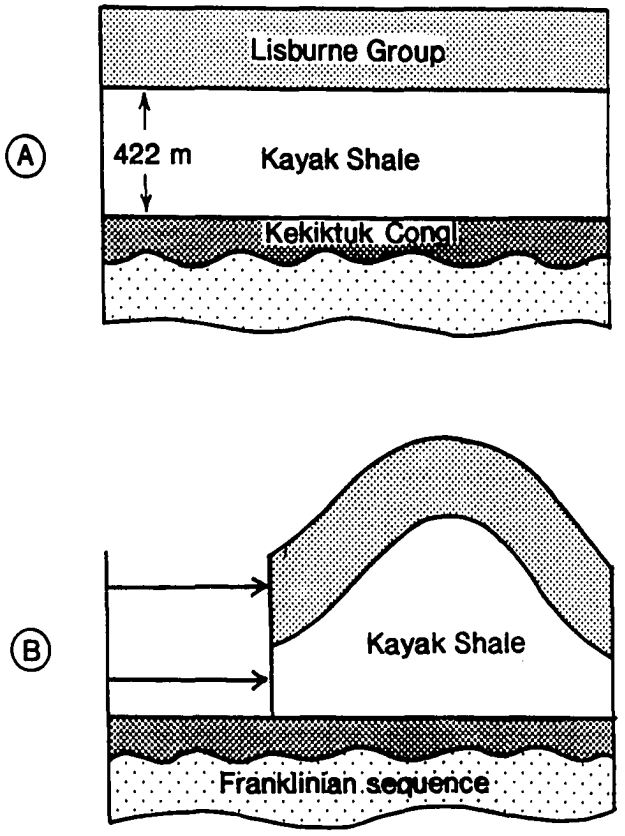

FIGURE 42. Accommodation of displacement above Kekiktuk Conglomerate by overlying Ellesmerian sequence. (A) Prior to deformation. A substantial thickness of Kayak Shale separates the Kekiktuk from the rest of the Ellesmerian sequence. (B) Lisburne Group and overlying rocks deform by detachment folding. Displacement accommodated by the Kayak Shale. No displacement related to shortening above the Kayak Shale roof thrust affects the Kekiktuk Conglomerate. The Kekiktuk Conglomerate is totally detached from overlying rocks.

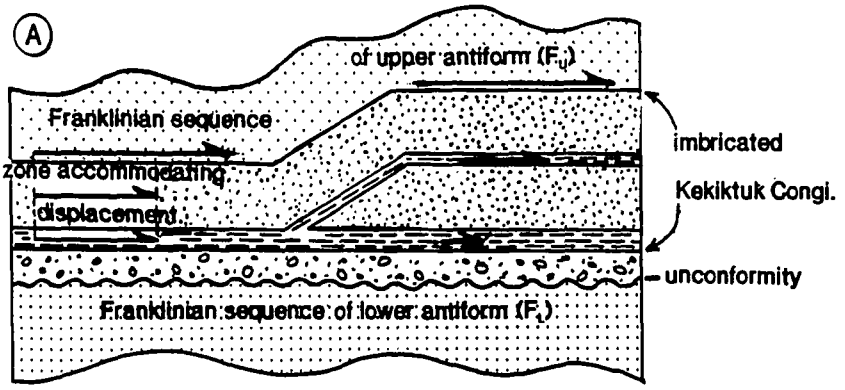

(A) Where structurally overlain by Franklinian sequence rocks with no Kayak Shale present, displacement is transferred to Kekiktuk Conglomerate. Shale interbeds facilitate imbrication and accommodate displacement. The basal Kekiktuk Conglomerate and unconformity do not accommodate displacement.

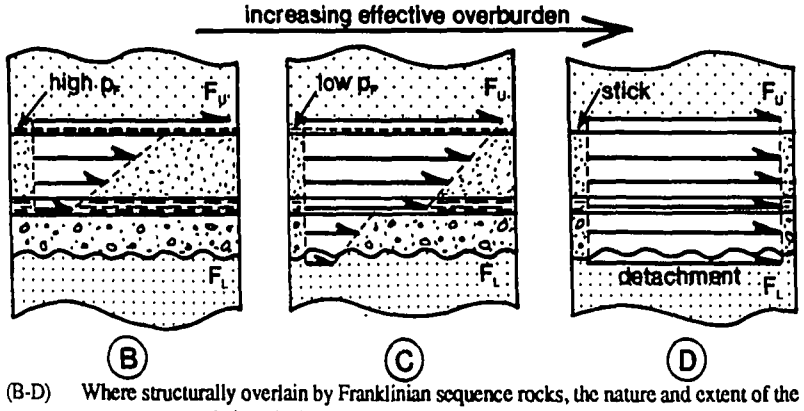

(B-D) Where structurally overlain by Franklinian sequence rocks, the nature and extent of the zone accommodating displacement within the Kekiktuk Conglomerate is likely influenced by factors including fluid pressure conditions along the overlying thrust surface and the magnitude of the tectonic load. Decreasing fluid pressures effectively increase overburden pressure. As effective overburden pressure is increased, the zone of displacement expands to include the basal Kekiktuk Conglomerate and underlying Franklinian sequence rocks (C). Coupling of the structurally overlying Franklinian sequence rocks and Kekiktuk Conglomerate might result in detachment at or near the unconformity surface. Note that the mechanism of displacement (imbrication, penetrative strain, or detachment) is not identified, except across detachments that are specifically shown.

FIGURE 43. Schematic diagrams illustrating possible factors that influenced the behavior of the Kekiktuk Conglomerate during deformation. Unshaded regions represent the zone of displacement accommodated by the Kekiktuk Conglomerate. The lengths of arrows are proportional to the magnitudes of displacement accommodated at various positions within the Kekiktuk Conglomerate.

55% quartzite, 40% quartz- and chert-pebble conglomerate, and 5% shale. Thin (30-40 cm) shale interbeds occur sporadically between quartzite and conglomerate horizons. As shown in Figure 43A, slip might occur within these shale interbeds, causing local imbrication within the Kekiktuk Conglomerate. (Figure 24 documents one of two locations where imbricated quartzite and shale were observed.) Displacement would be accommodated by such imbrication, decreasing the magnitude of displacement that must be accommodated by underlying rocks (Figure 43A). Thus, displacement along shale interbeds may have protected both lower portions of the Kekiktuk Conglomerate and the unconformity surface itself from the effects of displacement of overlying Franklinian sequence rocks (Figure 43B).

As presented in Section 7, finite strains determined from quartz grain shapes in the Kekiktuk Conglomerate do not significantly differ for the 9 sample planes analyzed (3 planes for each of 3 samples). Oriented samples 87JZ25 and 87JZ36 were obtained from the two locations where imbrication was observed; sample 87JZ31 was obtained from the basal Kekiktuk Conglomerate of the upper antiform, which is overlain by the Kayak Shale. Similar low strain values suggest that, even where the Kekiktuk Conglomerate is structurally overlain by the Franklinian sequence, some mechanism existed in order to accommodate displacement without the development of significant amounts of penetrative strain. Imbrication, as described above (Figure 43A), would be an example of such a mechanism. In the study area, imbrication involved only the upper portion of the Kekiktuk Conglomerate (Figure 22) and, where exposed, the unconformity surface appears to be an undisrupted depositional contact in most locations. Note that the style of imbrication shown in Figure 43A differs from that shown in Figure 12D in that the latter involves the entire thickness of the Kekiktuk Conglomerate and necessitates detachment from underlying rocks.

9.A.3. Tectonic Significance of the Unconformity Surface

At most locations in the study area, the sub-Mississippian unconformity appears to be a depositional surface which has not accommodated significant shear displacement. However, near the crest

of the antiform of the second horse, the Franklinian sequence immediately below the Kekiktuk Conglomerate is mylonitic at some locations. This would suggest that slip occurred near the unconformity surface within immediately underlying pre-Mississippian rocks, such as is shown in Figure 43C. Since the Kekiktuk Conglomerate is imbricated and tectonically brecciated on the north-dipping limb of this same antiform, it may be that mylonitization of immediately underlying Franklinian sequence rocks occurs where the Kekiktuk Conglomerate is most highly deformed. The increasing overburden pressure and greater basal shear stress, resulting from increasing the thrust load and frictional resistance along the detachment, may have resulted in transmission of stress through the Kekiktuk Conglomerate and consequent slip along the unconformity (Figure 43C-D). With the slightly lower overburden pressure resulting where the only load is the depositional overburden, the Kayak Shale was likely sufficiently thick to prevent transmission of shear stress to the Kekiktuk Conglomerate and unconformity (Figure 42). If shale interbeds facilitated imbrication of the Kekiktuk Conglomerate where the Franklinian sequence was thrust over it, structural thickening of the Kekiktuk Conglomerate prevented transmission of slip to the unconformity surface (Figure 43A).

9.A.4. The Influence of Volume-Fluid Pressure Conditions

Volume changes and fluid pressure conditions within the Kekiktuk Conglomerate potentially could have enabled the unit to resist deformation. According to Paterson (1978), penetrative strain might not be evident if significant dilation accompanied deformation. Dilation effectively increases the porosity of the rock, decreasing the actual pore pressure (Paterson, 1978). As pore fluid pressure decreases, more stress is required in order to produce a given magnitude of penetrative strain than was required when fluid pressures were higher prior to dilation (Paterson, 1978). Thus, dilation can effectively increase the strength of a rock unit. Based on the observation of chocolate-tablet structure, it is possible that dilation may have produced such a strength increase in the Kekiktuk Conglomerate on the north limb of the lower antiform, perhaps accounting, in part, for the low magnitude of penetrative strain documented. In

contrast, the significance of quartz-filled extension fractures for volume-fluid pressure conditions is more difficult to determine.

9.A.4.a. Chocolate-tablet structure

Tectonic brecciation occurs in the form of a chocolate-tablet structure (Figure 21B) near location "D" in Figure 23, where pre-Mississippian rocks have been thrust over the Kekiktuk Conglomerate of the lower antiform. This would suggest that there was a net volume gain resulting from fluid moving into the Kekiktuk Conglomerate. Sample 87JZ36 is a medium-grained, weakly foliated quartzite obtained from imbricated Kekiktuk Conglomerate in the vicinity of tectonically brecciated exposures. Finite strains measured for this sample are low (ave. R = 1.21), similar in magnitude to values determined for sample 87JZ31 (ave. R = 1.27), which was obtained from the upper antiform where the Kekiktuk Conglomerate is not structurally overlain by Franklinian sequence rocks. The stress transmitted to the Kekiktuk Conglomerate from overlying rocks was likely greater at the location of sample 87JZ36 than at the location of sample 87JZ31 due, in large part, to the absence of the Kayak Shale above sample 87JZ36 (Section 9.A.2.). While the strain recorded by sample 87JZ36 might be anticipated to exceed the strain in sample 87JZ31, such a difference was not distinguished by the strain analyses. Therefore, it is possible that dilation in the vicinity of sample 87JZ36 may have enabled the Kekiktuk Conglomerate to resist penetrative deformation.

9.A.4.b. Extension fractures

As discussed in Section 5 and illustrated in Figure 22, quartz-filled extension fractures commonly cross-cut the Kekiktuk Conglomerate of both antiforms. The fact that extension fractures in both antiforms are quartz-filled indicates that dissolved silica was present in the system, probably at the time of fracture formation. In order to suggest the volume-fluid pressure conditions associated with the formation of these filled fractures, it is necessary to determine the source of the dissolved silica. In addition, in order to view volume-fluid pressure inferences in the context of the structural evolution of the study area, it is

necessary to establish the time of formation of the extension fractures relative to emplacement of the first and second horses, and to consider their orientations relative to these macroscopic structures. However, observations of the quartz-filled extension fractures in the study area are insufficient to constrain fully the volume-fluid pressure conditions which existed in the Kekiktuk Conglomerate during the evolution of the Franklin Mountains anticlinorium.

Pressure solution, known to affected the Kekiktuk Conglomerate (Section 5.D.2.a.), produced dissolved silica which could have migrated within the unit, filling extension fractures. In this case, the net volume of the unit would have remained constant with local fluctuations in effective pore fluid pressure likely. Alternatively, dissolved silica might have migrated into the Kekiktuk Conglomerate, filling extension fractures. In this case, the net volume of the system would have increased, possibly leading to a decrease in effective pore fluid pressure which might have increased the strength of the Kekiktuk Conglomerate. If dissolved silica entered the system, its potential source must be considered. Dehydration of the Kayak Shale could have produced dissolved silica which might fill fractures in the upper antiform. If dissolved silica which filled fractures in the Kekiktuk Conglomerate of the lower antiform was derived from an outside source, it must have come from structurally overlying Franklinian sequence rocks. Dehydration might have occurred along the overlying thrust surface.

The orientations of extension fractures (Figure 22) are consistent with their formation during fault-bend folding which is interpreted to have produced the antiforms (Appendix D.2.). The axes of these folds trend east-northeast, plunging moderately west-southwest (Figure 15, Plate 1). East-northeast-striking, bedding-normal fractures in the upper antiform (Figure 22) likely formed when the Kekiktuk Conglomerate flexed along an east-northeast-trending axis (Figure 44A). North-northwest-striking, subvertical fractures (Figure 22) reflect extension parallel to the fold axes of both antiforms, likely associated with the plunge of these structures (Figure 44B). Based on the interpreted evolution of the Franklin Mountains anticlinorium (Section 6.C.), the upper antiform is

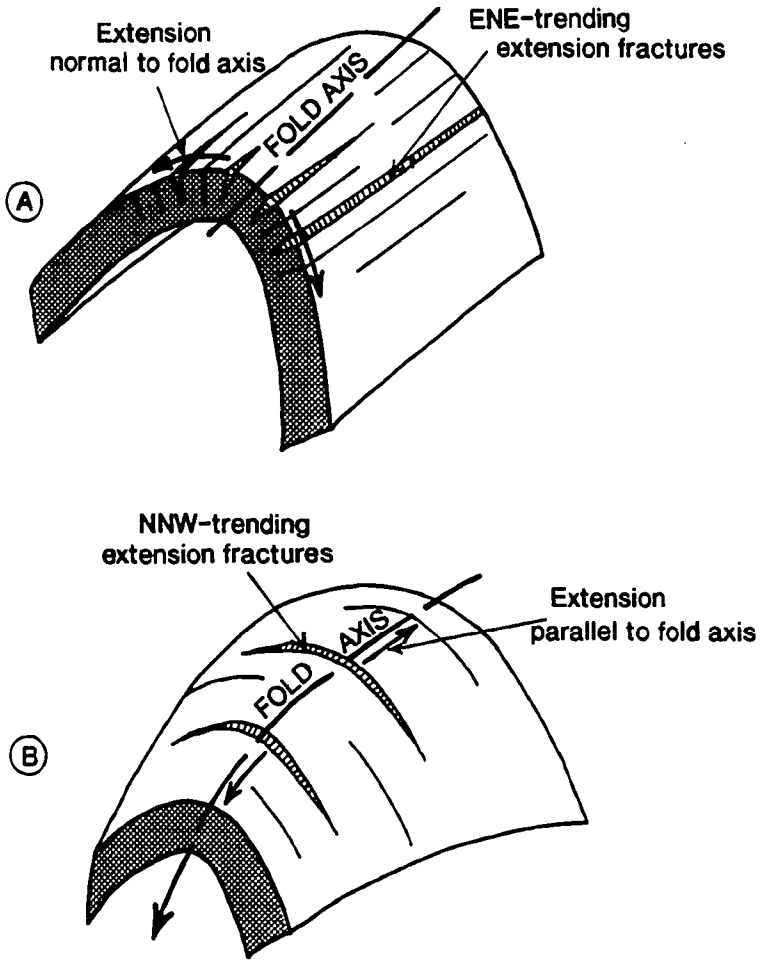

FIGURE 44. Possible explanation for orientations of quartz-filled extension fractures in the Kekiktuk Conglomerate, provided that fractures formed in association with folding which formed the upper and lower antiforms. (A) East-northeast-striking fractures form as a result of extension normal to the fold axis. (B) North-northwest-striking fractures form as a result of extension parallel to fold axis, possibly associated with the moderate west plunge of the upper and lower antiforms.

inferred to have formed when the first horse was emplaced, overprinted by subsequent formation of the lower antiform when the second horse was emplaced (Figures 30 and 32). Thus, if fractures formed during formation of the antiforms, fractures in the upper antiform might have formed either during emplacement of either horse, while those in the lower antiform most likely formed when the second horse was emplaced. In the upper antiform, cross-cutting relationships were not observed to permit determination of the relative ages of fractures. Thus, inferences regarding volume-fluid pressure conditions in the upper antiform may be associated with the emplacement of either horse. Given the field and thin-section observations, it is impossible to demonstrate that the volume of the system increased during deformation. The lack of apparent quartz overgrowths in the Kekiktuk Conglomerate of the upper antiform, in a sample (87JZ31) which contains microstylolites indicative of pressure solution, suggests that dissolved silica from within the unit may have migrated to fill the extension fractures developed in these rocks.

While there does not appear to be a strong relationship between extension fractures and the presence or absence of structurally overlying Franklinian sequence rocks, extension fractures may be somewhat more prevalent in the lower antiform, over which Franklinian sequence rocks have been thrust. The geometry of the antiforms may be a more important factor to consider. The lower antiform is a much tighter fold than the upper antiform (Figure 22). The Kekiktuk Conglomerate is exposed in the crest of the lower antiform, while it is exposed only in the north limb of the upper antiform in the study area. Extension fractures associated with flexural folding likely would be more prevalent near fold hinges and in relatively tight folds. Thus, in the study area, fractures might be anticipated to be more prevalent in the lower antiform due to fold geometry, without requiring a difference in volume-fluid pressure conditions between the upper and lower antiforms.

9.B. STRUCTURAL STYLE IN THE DETACHMENT ZONE

The structural style exhibited within the roof thrust zone is determined by the material properties

of the Kayak Shale, which permitted tectonic flow and internal shortening, and by the sense of shear along the roof thrust.

9.B.1. Tectonic Flow of Kayak Shale

According to Wiltschko and Chappie (1977), it becomes increasingly difficult to move weak material from between two relatively more competent layers as the thickness of the weak material decreases. As shown in Figure 45, detachment folds in overlying, more competent strata evolve as incompetent material is displaced from the synclines into the cores of anticlines, resulting in progressive broadening of the synclines and thinning of the underlying weak material (Wiltschko and Chapple, 1977).

In the balanced cross-section of Figure 30, the Kayak Shale is modeled to have flowed into the cores of map-scale detachment anticlines, and from the synclinorium to the upper flanks of the anticlinorium. As might be expected for a structural-stratigraphic unit that has deformed by flow, the magnitude of internal shortening observed within the Kayak Shale tends to be variable, especially in the cores of anticlines where chaotic folding has occurred. Given that the Kayak Shale in the study area is a substantially thick and mechanically incompetent unit, it would not be mechanically difficult to induce tectonic flow of the unit into the cores of detachment anticlines developed in the Lisburne Group and overlying rocks. Furthermore, in the flat trough of the synclinorium immediately to the north of the Franklin Mountains anticlinorium (Figures 30, 33, and 34), the Kayak Shale is shown to be significantly less than 422 meters thick, the stratigraphic thickness of the unit estimated by area balancing. This would suggest that the unit has flowed out of the synclinorium, possibly displaced either to the south toward the crest of the Franklin Mountains anticlinorium, or northward up the backlimb of the next anticlinorium to the north of the study area.

9.B.2. Shear Accommodated by Roof Thrust

Banks and Warburton (1986) define a passive-roof duplex as one with a roof thrust which has a backthrust sense of displacement (toward the hinterland) relative to the foreland-vergent displacement of

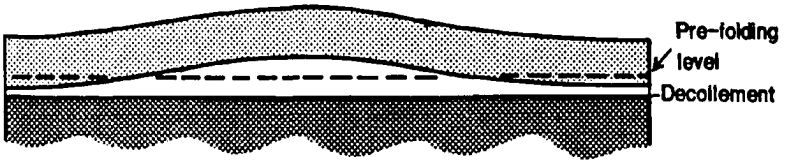

FIGURE 45. Model for the flow of incompetent material into the core of a detachment anticline (from Wiltschko and Chapple, 1977). A detachment anticline develops in the structurally competent (lightly-shaded) unit as a consequence of synclinal thinning in the deformed zone (unshaded) above a décollement. The dashed horizontal line defines the position of the base of the lightly-shaded unit prior to folding. Synclinal thinning occurred where the base of the competent unit now lies below the pre-folding level. At the core of the anticline, the base of the competent unit lies above the pre-folding level; the area of the unshaded unit lying above the pre-folding level represents the amount of rock transported from flanks and synclinal troughs (Wiltschko and Chapple, 1977).

horses within the duplex (Figure 46A). In a passive-roof duplex, shortening due to emplacement of each horse is accommodated in the roof sequence directly overlying that horse, with the roof sequence remaining relatively stationary (Banks and Warburton, 1986). The backthrust sense of displacement along the roof thrust is a natural consequence of the roof sequence remaining relatively stationary with respect to the foreland-vergent displacement of the horses (Figure 46A) (Banks and Warburton, 1986). In a passive-roof duplex, the shortened roof sequence is transported piggy-back fashion toward the foreland as deformation progresses toward the foreland; however, rocks of the roof sequence generally structurally overlie the horse with which their shortening is genetically linked.

If a duplex has an active roof thrust, both horses and the roof sequence are displaced toward the foreland from the outset (Figure 46B) (Banks and Warburton, 1986). In an active-roof duplex (Figure 46B), shortening of a given portion of the roof sequence probably was not due to displacement of the underlying horse. Thus, unlike a passive-roof duplex, displacement of a horse in an active-roof duplex is accommodated by shortening of the roof sequence toward the foreland from that horse.

To what extent, if any, did the Kayak Shale detachment function as a passive roof thrust? This question may be addressed for the Franklin Mountains anticlinorium based on the geometry of mesoscopic and map-scale structures within the study area, and for the duplex in the western portion of the northeastern Brooks Range based on the model of Wallace and Hanks (1988a, b, in press).

9.B.2.a. Roof thrust of the Franklin Mountains anticlinorium

In the primary balanced cross-section (Figure 30), duplexing of the Franklinian sequence accommodates approximately the same magnitude of shortening (44%) as detachment folding and thrust faulting of the Lisburne and Sadlerochit Groups above the Kayak Shale detachment (42%). Within the study area, it is impossible to determine the relative position of the rocks of the roof sequence with respect to the Franklinian sequence prior to Cenozoic deformation. However, the geometry and orientation of mesoscopic and map-scale structures in the study area may indicate the sense of

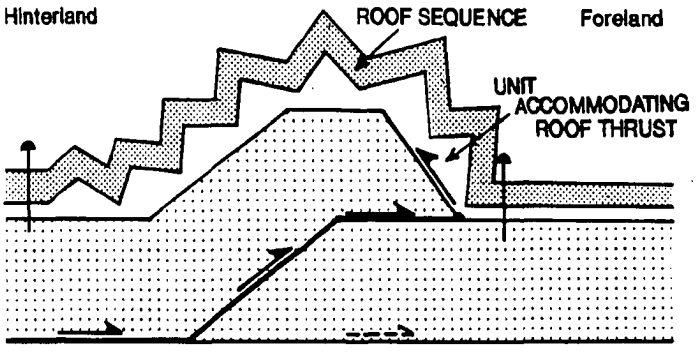

A. Passive roof thrust. During horse emplacment, the roof sequence is shortened above the duplex; no displacement occurs on the horizon of the roof thrust beyond the leading edge of the duplex in direction of foreland. A backthrust (toward hinterland) sense of displacement occurs on the roof thrust. Successive segments of the roof sequence are deformed as emplacement of horses progresses toward the foreland. Thrust faults and folds developed in the roof sequence commonly dip toward the foreland, indicating vergence toward the hinterland.

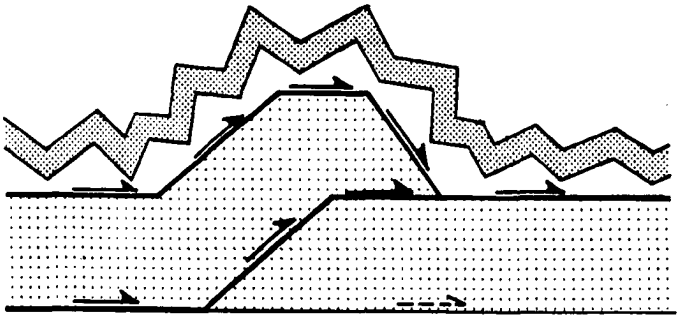

B. Active roof thrust. In this foreland-vergent duplex thrust system, displacement of both the horses and the roof thrust is toward the foreland. Because displacement above the roof thrust is toward the foreland, at any given location, rocks above the roof thrust will be displaced prior to emplacement of the underlying horse. Thrust faults and the axial surfaces of folds developed in the roof sequence commonly dip toward the hinterland.

FIGURE 46. Possible senses of shear accommodated by a roof thrust horizon.

displacement accommodated by the roof thrust, and, therefore, the extent to which the Kayak Shale detachment functioned as a passive roof thrust on the north flank of the anticlinorium.

The balanced cross-sections constructed across the anticlinorium (Figure 30) and on its northern flank (Figures 33 and 34) may suggest that the Kayak Shale functioned as an active roof thrust on the north flank of the anticlinorium. Shortening of the roof sequence in the eastern cross-section shown in Figure 33 averages 47%, compared to 42% determined across the entire cross-section (Figure 30). The marginally greater apparent magnitude of shortening accommodated by the roof sequence in the synclinorium (Figure 33) suggests that the Lisburne Group and overlying rocks may have been transported from the south into the synclinorium. Thus, shortening attributed to emplacement of the two horses which comprise the anticlinorium may have been accommodated by roof sequence rocks toward the foreland from these horses.

Field observations from the north flank of the anticlinorium and the synclinorium to its north documented north-vergent structures in the roof sequence and the Kayak Shale. On the steep northern flank of the anticlinorium and in the synclinorium immediately to the north, detachment folds in the Lisburne and Sadlerochit Groups are strongly- to slightly-overturned to the north, with south-dipping axial surfaces. The asymmetry of these folds is best illustrated by the prominent recumbent anticline developed in the Lisburne on the north flank of the anticlinorium (Figure 47, location "N" in Figure 23). The bottom, stratigraphically-inverted limb is shorter than the top, stratigraphically-upright limb of the fold (Figure 47). While the axial surfaces of folds formed in association with emplacement of the first horse would likely be rotated to the north by subsequent emplacement of the second horse, fold asymmetry indicates that at least local north-vergent displacement of the roof sequence occurred. In addition, a top-to-the-north shear sense is suggested by the asymmetry of folds several meters in wavelength developed in the Kayak Shale near location "F" in Figures 23 and 33. The geometry and orientation of these map-scale and mesoscopic folds suggest that northward transport of the roof sequence

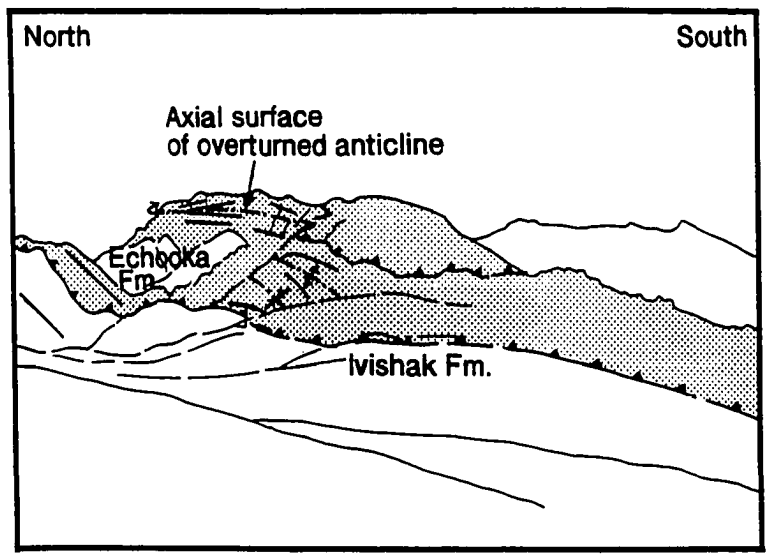

FIGURE 47. Detachment anticline in the Lisburne Group overturned to the north in the direction of tectonic transport. The thrust fault shown in the line drawing corresponds to that of location "H" in Figure 23.

occurred on the north flank of the anticlinorium. Thrust faults developed in the Ellesmerian sequence on the north flank of the anticlinorium at locations "F" and "H" in Figures 23 and 33-34 accommodate northward displacement of hangingwall rocks. No thrust faults exhibiting a backthrust sense of displacement were observed, suggesting that the Kayak Shale did not function as a passive roof thrust on the northern flank of the anticlinorium.

9.B.2.b. Roof thrust in western part of northeastern Brooks Range

The Kayak Shale pinches out stratigraphically at the Sadlerochit Mountains, approximately 35 miles (56 kilometers) north of the study area, effectively pinning the roof sequence to the underlying Franklinian sequence at this location (Wallace and Hanks, 1988a, b, in press). At a regional scale, the roof sequence to the south of this pinning point appears to have been shortened above the horses which comprise the duplex (Wallace and Hanks, 1988a, b, in press), as would be the case in a passive-roof duplex. Thus, although the Kayak Shale appears to function largely as an active roof thrust on the north flank of the Franklin Mountains anticlinorium, the Kayak Shale can be considered to be a passive roof thrust at the scale of the entire duplex.

9.C. STRUCTURAL STYLE ABOVE THE ROOF THRUST

This subsection offers possible explanations for the fold and fault geometries developed in the Lisburne and Sadlerochit Groups, which comprise the roof sequence in the study area. The structural style exhibited by this roof sequence is mainly influenced by the mechanical competency and thicknesses of the mapped lithostratigraphic units and of their constituent strata.

9.C.1. Fold Geometry

The main controls on fold geometry (Ramsay and Huber, 1987) applicable to a discussion of the Lisburne and Sadlerochit Groups include (1) the overall scale of the multilayer package being folded; (2) the thicknesses of the constituent layers, and whether or not these layers are grouped into mechanically significant units (e.g. lithostratigraphic units grouped into structural-stratigraphic units); (3) the

composition and mechanical competency of units in the sequence; (4) the nature of the boundary constraints on the folding rock units; and (5) the mechanical properties of the interfaces between layers.

9.C.1.a. Description of multilayer package

The stratigraphic thickness of the Lisburne and Sadlerochit Groups exposed in the study area is estimated to be 1,900 meters, the thickness used in balanced cross-section construction (Table 1). As shown in Table 1, the Lisburne Group accounts for 863 meters of the 1,900-meter total thickness. The Sadlerochit Group disconformably overlies the Lisburne Group, but the attitude of bedding within the Sadlerochit Group is estimated to be within 5-10 degrees of the strike and dip in the underlying Lisburne Group.

Both the Lisburne and Sadlerochit Groups are comprised of lithologically-distinct formations whose fold geometries are functions of the stratigraphic thicknesses and rheologic properties of the various component lithologies. Within the Lisburne Group, the mechanically competent lower Alapah and Wahoo Limestones are separated by the less competent and thicker upper Alapah Limestone. Compared to the lower Alapah and the Wahoo Limestones, the upper Alapah is more thinly-bedded and micritic (Section 3.B.2.), causing it to be relatively incompetent (Figure 8). Within the Sadlerochit Group, the Echooka and Ivishak Formations are comprised of interbedded relatively thin clastic layers of differing lithology and mechanical competency. Because of the higher proportion of incompetent shales and siltstones relative to competent sandstones and carbonates within these formations, as well as the tendency for individual beds in the Sadlerochit Group to be thinner than in the Lisburne Group, the Sadlerochit Group is considered to be a less competent structural-stratigraphic unit than the Lisburne Group.

9.C.1.b. Thickness, composition, and competency of Lisburne Group

The Lisburne Group constitutes a 863-meter-thick, mechanically competent unit which is sandwiched between the 422-meter-thick, highly incompetent Kayak Shale and the 1,015- to

1,060-meter-thick Sadlerochit Group. Within a multilayered sequence like the Ellesmerian, a thick, mechanically competent unit can function as a tectonic "strut." Folds of a given form, amplitude, and wavelength develop within this strut-member, dependent on its thickness and competency relative to bounding layers, determining the dominant wavelength displayed within the multilayered sequence. Simplistically speaking, the Lisburne Group can be viewed as a strut-member within the Kayak Shale-Lisburne Group-Sadlerochit Group multilayered package. In a general sense, the Lisburne Group determines a dominant map-scale fold wavelength which is reflected by harmonic folds in the overlying Sadlerochit Group.

In detail, however, Lisburne Group fold geometry is more complex. In the study area, disharmonic folds within the Lisburne occur at two locations ("E" and "O" in Figure 23). Such disharmonic folds develop where two competent layers are fairly widely separated from each other. As shown in Figure 48B, these competent layers tend to fold independently of each other, with each one exhibiting a characteristic wavelength dependent upon its thickness and the contrast in competency between the layer and matrix (Ramsay and Huber, 1987). At location "E" in Figure 23, disharmonic folding of the competent lower Alapah Limestone with respect to the competent Wahoo Limestone occurs (also shown in Figure 25). Substantial thicknesses of the highly incompetent Kayak Shale and relatively incompetent upper Alapah Limestone bound the more competent lower Alapah. The lower Alapah Limestone is thin in comparison to the Kayak Shale and the upper Alapah (Plate 1), enabling the lower Alapah to develop its own fold wavelength independent of that developed in the overlying Wahoo Limestone. Disharmonic folds of the Wahoo Limestone with respect to the upper Alapah Limestone and Echooka Formation occur at location "O" in Figure 23. These disharmonic folds are developed in the core of a syncline near the contact with an overlying incompetent calcareous shale of the Echooka Formation. The less competent bounding lithostratigraphic units (upper Alapah and Echooka) likely constituted a matrix of sufficient thickness to permit independent, disharmonic fold development within

the Wahoo Limestone.

9.C.1.c. Thickness, composition, and competency of Sadlerochit Group

In the study area, the Echooka Formation is overlain by flaky shale which constitutes the lower part of the Ivishak Formation. Although shale intervals occur within the Echooka Formation and the upper part of the Ivishak Formation, the shale at the base of the Ivishak Formation is thicker and less silty in comparison. Some tectonic flow likely occurred within this shale and, as a result, folds developed in the more competent upper part of the Ivishak Formation are probably disharmonic with respect to those in the Echooka Formation.

Ramsay and Huber (1987) suggest that harmonic folds tend to develop in a multilayer package if competent layers are of uniform thickness and are spaced uniformly, and if there is little contrast in the ductility of competent and incompetent layers. The Echooka and Ivishak Formations each are comprised of units of differing lithology and, hence, each can be considered a multilayer package. These lithologic layers are all relatively thin and do not vary appreciably in thickness. For the sandstones and siltstones of the upper part of the Ivishak Formation, in particular, the contrasts in ductility are likely small. Harmonic folds (Figure 48C) are generally observed within the Echooka and Ivishak formations.

In the core of the major syncline at location "P" in Figure 23, near a gradational contact between the lower and upper parts of the Ivishak Formation, mesoscopic folds occur in a package comprised of 10-30 cm-thick shale, siltstone, and sandstone interbeds. These folds appear to be polyharmonic, in harmony with the overall fold pattern (Figure 48D). Relative to the overlying part of the Ivishak Formation, shorter-wavelength folds likely developed in this interval since it is more thinly bedded. Development of a shorter fold wavelength might have been possible because the thinly-interbedded interval lies above an incompetent shale.

9.C.2. Fault Geometry

North-vergent thrust faults truncate Ellesmerian sequence rocks on the north-dipping flank of the

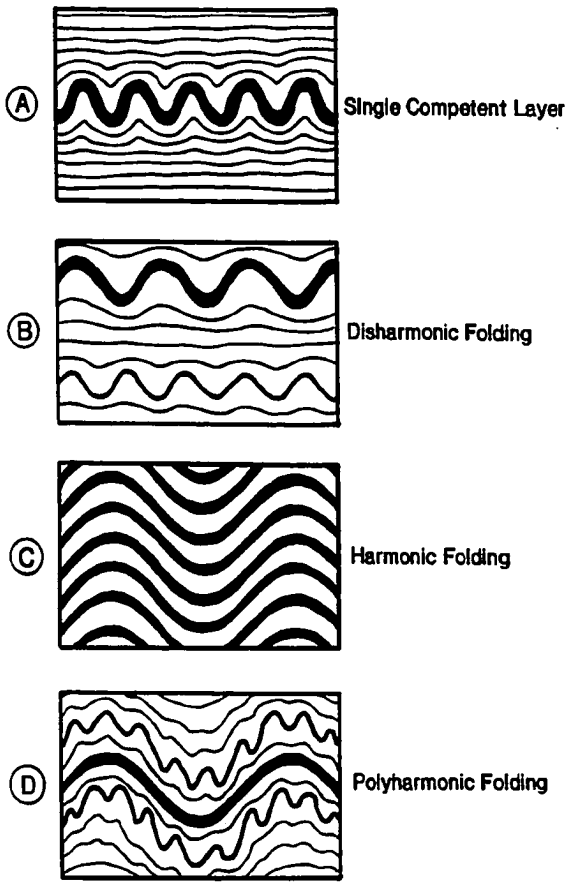

FIGURE 48. Schematic representation of possible interrelationships of buckle folds developed in competent layers (black) and incompetent host materials (unshaded) (Ramsay and Huber, 1987).

Franklin Mountains anticlinorium. In several locations, map patterns and the cross-section interpretation show that early-formed folds have been truncated by faults which commonly appear to have broken through the hinges of overturned anticlines in the Lisburne and Sadlerochit Groups. As shown in the three balanced cross-sections (Figures 30, 33, and 34), Kayak Shale occurs at the base of the hangingwall sequence of faults near locations "F" and "G" in Figure 23, indicating that the faults probably sole within this highly incompetent unit. If the roof sequence were transported to the north with the north limb of the anticlinorium, faults could have formed at fold hinges or along limbs to alleviate space problems as shortening increased.

South-vergent thrust faults were not observed in the study area. While the fault at location "G" in Figure 30 was initially interpreted to be a backthrust, it was difficult to incorporate such an interpretation in the balanced cross-section. In this model, the fault is interpreted to have truncated a pre-existing fold, isolating a wedge of Kayak Shale from the core of the anticline at the base of the hangingwall sequence. The north vergence of thrust faults in the Ellesmerian sequence provides strong evidence that the Kayak Shale functioned as an active roof thrust in the study area, transporting the roof sequence northward with the north limb of the anticlinorium.

9.D. INFLUENCES OF DUPLEX THRUST SYSTEM ON ROOF SEQUENCE

Evolutionary relationships between the structural style of the two horses beneath the roof thrust of the duplex and that observed in the Ellesmerian sequence above the roof thrust are investigated in this subsection. Topics discussed include the effects of forming the regional anticlinoria, emplacing the two horses of the Franklin Mountains anticlinorium, and increasing local structural relief.

9.D.1. Effect of Forming Other Anticlinoria

Shortening observed in the Ellesmerian sequence above the Kayak Shale detachment developed in response to the shortening of underlying rocks by means of a duplex thrust system. However, the attempt to relate specific structures in the roof sequence to specific structures or events in the evolution of

the underlying thrust system poses several questions: Can it be assumed that most of the shortening observed in the overlying roof sequence developed in response to the emplacement of the two thrust sheets which comprise the Franklin Mountains anticlinorium? Did earlier deformation south of the Franklin Mountains anticlinorium affect the roof sequence within the study area? Similarly, did the subsequent formation of the anticlinorium to the north affect the study area?

As shown in Figure 3, prominent east-northeast-trending, north-northwest-vergent thrust faults approximately 12 miles (20 kilometers) to the southwest and southeast of the study area involve both the Franklinian and Ellesmerian sequences. Assuming that Cenozoic deformation proceeded from south to north in this region, these thrust faults are interpreted to have accommodated shortening prior to the formation of the Franklin Mountains anticlinorium, which includes the southernmost horses of the duplex in the western portion of the northeastern Brooks Range. While significant northward transport of the cover sequence to the south of the study area appears to have occurred in the vicinity of these thrust faults (W.K. Wallace, 1989, pers. commun.), it seems unlikely that a significant amount of the shortening associated with that deformation would have been accommodated by the roof sequence in the study area. Detachment folds of significant amplitude likely did not form in the roof sequence in the study area until emplacement of the first horse of the Franklin Mountains anticlinorium occurred, probably the next shortening event to occur as deformation progressed northward.

According to the proposed northward-propagating duplex model, thrust sheets to the north of the study area were emplaced following formation of the Franklin Mountains anticlinorium. If a foreland-propagating deformation front has moved toward the foreland with respect to a given location, then rocks in that area will be transported passively above the orogenic basal detachment toward the foreland, but with much less deformation than occurred during the initial fold-and-thrust deformation at that location. In theory, therefore, shortening associated with the formation of the northern anticlinorium should not involve significant deformation in the roof sequence in the study area, with the likely

exception of rocks at the northern boundary of the study area, which were tilted on the backlimb of that anticlinorium.

9.D.2. Relating Folding and Faulting to Horse Emplacement

Two main processes are involved in the emplacement of a fault-bend folded horse: First, by definition, a fault-bend fold forms above flat-to-ramp and ramp-to-flat transitions in the footwall, requiring that the thrust surface form prior to displacement of the thrust sheet (Boyer and Elliott, 1982). Therefore, before such a thrust sheet can be displaced, it is necessary for mechanical failure to occur along a basal detachment horizon and form a footwall ramp. Internal shortening of the future horse may accompany these events, requiring some shortening to occur in the eventual roof sequence. Second, as the thrust sheet is displaced over the footwall ramp, the leading edge of the thrust sheet is fault-bend folded. Fault displacement and related folding during this process account for the vast majority of shortening beneath the roof thust. Therefore, assuming that the roof sequence in the study area was not shortened significantly during prior shortening events localized to the south (Section 9.D.1), it follows that most deformation in the roof sequence occurred when the first and second horses were displaced over their respective footwall ramps and fault-bend folded at their leading edges. As determined from the balanced cross-section (Section 6.C.), emplacement of the first horse accommodated roughly 8 of the 11 kilometers of total Cenozoic shortening, with emplacement of the second horse accomplishing the remaining 3 kilometers of shortening. Thus, in terms of relative shortening, most folds in the roof sequence probably formed as a result of emplacement of the first horse.

Given a constant compressive force from the hinterland, intuition suggests that as displacement of a horse becomes energetically or mechanically difficult to sustain, the process of formation of another horse would begin. It is possible, maybe even likely, that this second horse would begin to be displaced before displacement of the first horse ceased; however, most of the shortening accommodated by emplacement of the first horse would probably have occurred prior to this time. The majority of

shortening associated with emplacement of the second horse would occur when that horse is displaced over its footwall ramp. Thus, periods of major shortening would likely be interspersed with periods during which internal adjustments occur, leading to the formation of subsequent horses but accommodating relatively little shortening in comparison with that accommodated by the actual thrust emplacement of horses. Thus, it is likely that shortening in the roof sequence above a duplex thrust system would occur in pulses rather than in a single continuous event. Furthermore, in a passive-roof duplex, such shortening would be expected to be spatially and temporally related to the emplacement of underlying horses.

For the Franklin Mountains anticlinorium, a pulse of deformation would have occurred during emplacement of the first horse. Following this event there was probably a relative hiatus, during which the second horse underwent a phase of internal deformation, forming a basal detachment horizon and ramp. Another pulse of deformation would begin as the second horse began to be displaced up this footwall ramp. Tightening and overturning of existing folds probably accompanied emplacement of the second horse. Thrust faulting in the roof sequence appears to have post-dated early folding, but was not necessarily synchronous with fold formation. If most folding occurred during emplacement of the first horse, then thrust faulting occurred either prior to thrust displacement of the second horse or during emplacement of the second horse. These faults accommodate minor displacements (on the order of a kilometer) and are folded, indicating that faulting was followed by additional folding.

In conclusion, "pulses" of deformation are inferred to have occurred based on field observations of fold and fault geometry in the Ellesmerian sequence, and the interpretation that formation of the Franklin Mountains anticlinorium involved the separate emplacement of two horses. In order to support the idea that pulses of deformation occurred in association with duplexing of the Franklinian sequence, it would be necessary to establish absolute temporal links between structures observed above and below the Kayak Shale roof thrust. Such links could not be established in this study, so it remains possible that folding

and faulting in the Ellesmerian sequence occurred during a single progressive deformational event within which the effects of emplacement of the first and second horses are indistinguishable.

9.D.3. Effect of Increasing Structural Relief

The balanced cross-sections shown in Figures 30 and 33 suggest that formation of the Franklin Mountains anticlinorium produced 4.6 kilometers of positive structural relief. Uplifting the roof sequence by 4.6 kilometers would have increased the gravitational potential of these rocks significantly. In fact, Mull (1982) has suggested that cascade folding occurred as a result of gravity sliding induced during late Mesozoic-Cenozoic uplift throughout the southern Brooks Range. While it is now believed that Cenozoic uplift of pre-Mississippian rocks in the northeastern Brooks Range was driven by a duplex thrust system rather than by vertical tectonism (Rattey, 1985; Namson and Wallace, 1986; Avé Lallemant et al., 1987; Kelley and Foland, 1987; and Leiggi, 1987), there is no reason why deformation of the roof sequence could not have been affected by a gravitational component.

It is important to note that the north-vergent features observed on the north limb of the Franklin Mountains anticlinorium also could have formed in association with horse emplacement, without significant influence by gravity. One possible way to determine whether or not a gravitational overprint actually exists might be to document and compare fold and thrust fault geometries in the Ellesmerian sequence on the crests, forelimbs and backlimbs elsewhere on the regional anticlinoria. A gravitational component of deformation, if it exists, ought to be most evident in the form of break-away faults and unroofed zones on the crests of the anticlinoria and north-vergent structures on their steeply dipping forelimbs. However, if north-vergent structures were observed along backlimbs or crests of the anticlinoria, this would suggest that these structures did not form primarily under the influence of gravity, although the effect of gravity would be less pronounced on these gently dipping parts of the anticlinoria. Rather, the sense of displacement of the roof thrust might best account for north-vergent structures on the backlimbs or crests of anticlinoria, without requiring any gravitational influence for their formation.

Documentation of such north-vergent structures would indicate that the Kayak Shale functioned as an active roof thrust at locations other than on the north flank of the Franklin Mountains anticlinorium.

10. SUMMARY AND CONCLUSIONS OF STUDY

10.A. SUMMARY OF FINDINGS

10.A.1. A Structural Model

The balanced cross-sections, and the field observations and data which they incorporate, support the hypothesis that a northward-propagating duplex thrust system formed the Franklin Mountains anticlinorium. Floor, imbricate, and roof thrusts bound the thrust sheets (horses) of the duplex. Emplacement of these horses during Cenozoic deformation resulted in 4-5 kilometers of positive structural relief. Detachment horizons, located at depths of several kilometers within the Franklinian sequence, functioned as floor thrusts of the duplex. Faults branched from these surfaces and propagated upward through the Franklinian sequence, defining footwall ramps over which rock packages were subsequently displaced during thrusting. Imbricate thrust faults merged upward into the mechanically incompetent Kayak Shale, which acted as the roof thrust of the duplex. The primary balanced cross-section depicts the structural geometry developed in the Franklinian and Ellesmerian sequences and reflects 44% shortening of the Franklinian sequence and Kekiktuk Conglomerate, and 42% shortening of the Lisburne Group and overlying rocks. This model is constrained both by structural observations and the models and methodology of Suppe (1983) and Woodward et al. (1985).

It should be stressed that the thrust sheet geometry modeled for the Franklinian sequence is only as valid a structural portrayal as is the assumption that these polydeformed and weakly metamorphosed rocks acted as coherent fault-bounded structural-stratigraphic packages during Cenozoic deformation, deforming in a manner similar to the end-member model shown in Figure 10A. If principles of fault-bend fold geometry as described by Suppe (1983) can reasonably be applied, then there are few other geometric solutions which incorporate the available structural data and yield a balanced cross-section.

Interpretations of structural sequence in the Franklin Mountains study area incorporate kinematic and mechanical methods and models of Ramsay (1967), Gretener (1972), Paterson (1978), Fry (1979),

Butler (1982), Sanderson (1982), Davis et al. (1983), Ramsay and Huber (1983), and Erslev (1988). Strain analyses enhanced understanding of the local structural sequence, expanding the scope of this detailed structural analysis to a microscopic scale and providing insights into the role of penetrative strain in the area. With the balanced cross-section as a framework, strain data for a small number of samples were considered in terms of sample position relative to evolving local structures. Orientations of strain markers such as stylolites, extension fractures, shear fabrics, pressure shadows, and crystal-plastic features were found to be compatible with (1) north- to north-northwest-directed shortening associated with the Cenozoic deformational event which formed the Franklin Mountains anticlinorium, (2) the response to increased overburden resulting from thrust sheet emplacement, (3) shear along the surface separating the two horses, inferred to have occurred during thrust emplacement of the first horse, and (4) an interpreted later stage of Cenozoic east-west shortening.

The penetrative strains measured for samples from the Franklinian and Ellesmerian sequences may have developed as a local consequence of fault-bend folding, thrust faulting, and detachment folding. The magnitude of such internal shortening probably is a reflection of, and not an addition to, the total shortening estimated across the Franklin Mountains anticlinorium. Total extensile strains of 39% and 45% were determined from pressure shadows in the east-northeast- and west-northwest-striking planes, respectively, of a sample from the Franklinian sequence. These strains are comparable to the 43% extensile strain determined from the ellipticity of deformed corals in the bedding plane of a sample from the Lisburne Group. If the total strain determined in the Franklinian sequence sample is indeed a measure of Cenozoic strain, then similar magnitudes of Cenozoic strain appear to have developed above and below both the sub-Mississippian unconformity surface and the Kayak Shale roof thrust horizon. Finite strain analysis of the shape and orientation of quartz grains documents relatively minor penetrative strain in the Kekiktuk Conglomerate, comparable to strain determined for a sample from the Ivishak Formation. This would suggest that approximately the same magnitude of Cenozoic tectonic strain may occur both above

and below the Kayak Shale detachment horizon.

10.A.2. Style and Evolution of Cenozoic Structures in the Franklinian Sequence

Franklinian sequence rocks are interpreted to have been displaced during Cenozoic deformation by a north-northwest-vergent duplex thrust system. This led to the formation of a number of regional anticlinoria in the northeastern Brooks Range, one being the so-called 'Franklin Mountains anticlinorium.' The majority of Cenozoic shortening of the Franklinian sequence in this anticlinorium is interpreted to have been accomplished by the displacement of a major thrust sheet and another minor thrust sheet, creating the positive structural relief of the anticlinorium. The apparent lack of extensive and significant internal Cenozoic deformation in Franklinian sequence rocks would suggest that these thrust sheets had either significant internal strength or low basal friction, the latter perhaps as a consequence of high fluid pressure conditions along the inferred basal detachment.

Two pre-Mississippian-cored antiforms, each one capped by a veneer of the Mississippian Kekiktuk Conglomerate, can be interpreted to be fault-bend folds formed at the leading edges of two horses within the duplex. In a foreland-propagating duplex, the upper antiform would have formed first and been refolded by subsequent emplacement of the lower horse and formation of the lower antiform. According to the structural sequence modeled in the balanced cross-section, the major horse, 4.7 kilometers thick and over 20 kilometers long, was emplaced first. The basal detachment then stepped up to the north from a depth of 5.4 kilometers to 3.1 kilometers below sealevel. It is possible that the basal detachment stepped up to a preferential failure plane in a zone of high fluid pressure that developed beneath the first horse as a result of its emplacement. The second horse, 2.3 kilometers thick and 9 kilometers long, was detached at a depth of 3.1 kilometers below sealevel and displaced roughly 3 kilometers to the north. The location of the ramp for the eventual second horse, toward the foreland from the evolving anticlinorium, may reflect the lesser strength of these rocks as compared to that of rocks strengthened by tectonic loading by the first horse. The initial 4.6 kilometers of positive structural relief

was not increased by emplacement of the second horse.

The first and second horses were emplaced up 33- to 46-degree and 47-degree footwall ramps, respectively. Moderately south-dipping pre-Mississippian slaty cleavage may have been a plane of preferred failure during ramp formation. The experimental work of Paterson (1978) suggests that a lower magnitude of differential stress would be required to cause failure along these planes than would be required for a plane at any other orientation.

10.A.3. Structural Style of Ellesmerian Sequence Beneath Kayak Shale

The nature of the interface between the Kekiktuk Conglomerate and overlying rocks may be the factor which determined whether the unconformity surface remained a depositional contact or was modified into a tectonic contact. At most locations in the study area, the Kekiktuk Conglomerate appears to have remained attached to pre-Mississippian rocks and deformed with them beneath a roof thrust in the Mississippian Kayak Shale. Thin shale interbeds in the Kekiktuk Conglomerate may have facilitated local imbrication, accommodating slip within the Kekiktuk Conglomerate, thereby precluding slip on the unconformity surface itself. With the increased effective overburden pressure and shear stress associated with emplacement of an overlying thrust sheet, shear strain may have affected a greater thickness of rocks, thus causing slip along the unconformity surface itself.

The Kekiktuk Conglomerate is most highly deformed where pre-Mississippian rocks have been thrust over it. Stick along the thrust surface might have been induced by the absence of the Kayak Shale, which would have accommodated shortening above the Kekiktuk Conglomerate if it were present, and a greater effective overburden than that due to the Ellesmerian sequence alone, possibly accentuated by low fluid pressures along the thrust surface. Under such conditions, stress likely would have been transmitted to the Kekiktuk Conglomerate much more effectively and, as a result, significant penetrative strain might have developed in the unit. Where the Kekiktuk Conglomerate is overlain only by the normal stratigraphic sequence of the Kayak Shale and the Lisburne and Sadlerochit Groups, the magnitude of

shear stress applied to the Kekiktuk Conglomerate is likely to have been much less than that due to the tectonic load of structurally overlying Franklinian sequence rocks. It is possible that volume-fluid pressure conditions helped enable the Kekiktuk Conglomerate to resist penetrative deformation locally.

10.A.4. Structural Style of Ellesmerian Sequence in and Above Kayak Shale

The contrasting structural geometries that developed above and below the Kayak Shale indicate that this mechanically incompetent structural-stratigraphic unit functioned as a major detachment zone, the roof thrust horizon of the proposed duplex thrust system. The Kayak Shale is interpreted to have flowed into the cores of map-scale detachment anticlines, as well as from the synclinorium into the northern limb of this anticlinorium and the southern limb of the one to its north. Internal shortening and movement of material into the cores of detachment folds was probably accommodated, in part, by thinning in the synclines.

Above the Kayak Shale, detachment folds and thrust faults were developed in the Lisburne and Sadlerochit Groups during pulses of folding and faulting related to emplacement of the two underlying horses. A parallel-fold geometry was used in constructing the balanced cross-sections and some strain indicators support folding by an interbed flexural-slip mechanism. Where shortening is greatest, local tight, overturned folds are best described as similar folds with probable attenuation of limbs and thickening at hinges, accommodated by penetrative strain of competent lithologies (such as the limestones of the Lisburne Group) and by flow of incompetent interbeds (such as the Kayak Shale or shales of the Sadlerochit Group). At several locations, thrust faults have truncated early folds in Ellesmerian sequence rocks of the roof sequence and were themselves subsequently folded. These faults are interpreted to sole within the Kayak Shale and possibly developed as folds tightened and space problems resulted.

In a general sense, the Lisburne Group acted as a tectonic strut within the Ellesmerian sequence, determining the dominant wavelength of map-scale detachment folds. Relatively thin, competent

intervals bounded by thicker incompetent intervals were able to develop independent fold wavelengths and deform disharmonically with respect to other intervals. For example, disharmonic folding was possible within the Lisburne Group since the competent lower Alapah Limestone is thin in comparison with the Kayak Shale and the upper Alapah. Harmonic folding is observed within the Echooka and Ivishak Formations because beds within the multilayered sequence of both formations are relatively thin and of a constant thickness.

As a consequence of the process of thrust sheet emplacement, deformation of the roof sequence may have occurred in distinct pulses. Most shortening in the roof sequence probably resulted from displacement of the major and minor thrust sheets over their footwall ramps. The two horses probably were emplaced successively, with a relative hiatus in deformation occurring prior to displacement of the second horse. Since 8 of the total of 11 kilometers of thrust shortening were accommodated by emplacement of the first horse, most shortening of the roof sequence likely occurred during its emplacement. Furthermore, it appears that some northward tectonic transport of the roof sequence did occur, perhaps dominating over any backthrust sense of shear that occurred along the Kayak Shale roof thrust. Finally, emplacement of these thrust sheets of Franklinian sequence rocks resulted in 4.6 kilometers of structural relief, raising the possibility that gravity may have influenced northward, down-slope transport of the roof sequence on the moderately to steeply dipping northern limb of the anticlinorium.

10.B. SIGNIFICANCE OF STUDY

10.B.1. Regional Significance

The detailed local mapping and structural analysis conducted in the Franklin Mountains for this study expand upon and update previous, largely reconnaisance-style, mapping and structural studies. In particular, efforts to decipher the deformational history of the Franklinian sequence, distinguishing structures of pre-Mississippian and Cenozoic age, contribute to understanding the regional structural

evolution of these rocks. Local balanced cross-sections characterize the fold and fault geometries characteristic of the southwestern portion of the northeastern Brooks Range fold-and-thrust belt. The cross-sections constructed as part of this study are based upon extensive local field observations, complementing Namson and Wallace's (1986) balanced cross-section of the northeastern Brooks Range, which transects the Franklin Mountains anticlinorium. From these detailed cross-sections it was possible (1) to estimate the magnitude of local Cenozoic shortening of both the Franklinian and Ellesmerian sequences, (2) to interpret the geometry and mode of involvement of Franklinian sequence rocks in Cenozoic deformation, (3) to suggest a sequence of thrust-related movements which could have produced the interpreted structural geometry of the Franklinian sequence, (4) to interpret the factors controlling fold and fault geometry in the Ellesmerian sequence, and (5) to investigate the possible influence of pre-Mississippian rocks on the deformation of the overlying Ellesmerian sequence.

10.B.2. Significance for Field of Structural Geology

This detailed structural analysis demonstrates the utility of both balanced cross-sections and methods of quantitative kinematic analysis in understanding and modeling the structural geometry and sequence, and the mechanics of deformation in a fold-and-thrust belt geologic setting. The study documents in detail the geometry of part of a regional Cenozoic duplex and the geometry of structures which accommodate shortening in the roof of the duplex. Looking at the horses, which are capped by a thin, mechanically competent Mississippian quartzite, the study addressed the influence of a pre-Mississippian structural fabric on the type, orientation, and geometry of Cenozoic structures formed in these rocks. In addition, the study examined the sense of displacement accommodated by the mechanically incompetent Kayak Shale, a prominent detachment zone in this region, and the inferred roof thrust of the Cenozoic duplex thrust system. Finally, the study considered the influence of stratigraphy and shortening beneath the roof thrust on the geometry of detachment folds and thrust faults developed in the structural-stratigraphic units above the roof thrust.

10.C. SUGGESTIONS FOR FURTHER STUDY

Further structural analysis in the vicinity of the Franklin Mountains anticlinorium should focus on 1:25,000 scale mapping and structural observations of Franklinian sequence rocks exposed in the core of the anticlinorium to the south of the study area (both at high elevations and along the Canning River and the Marsh Fork), and to the west of the study area where the anticlinorium plunges beneath the Marsh Fork, exposing the sub-Mississippian unconformity surface and Ellesmerian sequence rocks on the crest of the anticliniorium. Such study should be directed at (1) better characterizing the styles and amount of shortening associated with pre-Mississippian and Cenozoic deformation of the Franklinian sequence, (2) investigating the mode and extent of deformation of the Kekitkuk Conglomerate, and the structural relationships across the sub-Mississippian unconformity surface, and (3) documenting the geometry and vergence of structures in the Kayak Shale. Both (1) and (2) might provide some test of the balanced cross-section model constructed in this study, and (3) would address the driving mechanism of shortening within and above the roof thrust horizon.

The systematic collection of oriented Franklinian sequence samples for incremental and finite strain analyses might test the validity of speculations made in this study regarding the significance of the pattern of Cenozoic strain developed in these thrust sheets. In addition, oriented samples from each structural-stratigraphic unit of the Ellesmerian sequence and from different structural positions would permit additional finite strain estimates to be made. These strain determinations might provide a comprehensive view of the pattern of strain developed in these rocks, both in terms of (1) vertical variations between structural-stratigraphic units within a given map-scale structure, and (2) lateral variations (along strike and in the inferred direction of tectonic transport) within each structural-stratigraphic unit. Such studies might constrain better the mechanism of fold development in Mississippian and younger rocks of the roof sequence and improve shortening estimates made in this structural analysis.

APPENDIX A. TERMINOLOGY RELATING TO DUPLEXES AND FAULT-BEND FOLDS

The mechanical effect of a duplex thrust system, shown in Figure 49, is to transfer slip from a floor thrust to a roof thrust via a series of imbricate thrust faults that link the floor and roof thrusts (Dahlstrom, 1970; Boyer and Elliott, 1982; Mitra, 1986). A stratigraphic horizon which acts as a floor or roof thrust is commonly referred to as a "décollement," or "detachment" by northeastern Brooks Range researchers, including Rattey (1985), Kelley and Molenaar (1985), Namson and Wallace (1986), and Leiggi (1987). A thrust slice (such as A, B, or C in Figure 49), bounded on all sides by imbricate, floor and roof thrusts, is called a "horse" (Boyer and Elliott, 1982). Duplex thrust systems are interpreted to propagate toward the foreland of fold-and-thrust belts, with each new thrust sheet forming beneath and ahead of its predecessor (Figure 49) (Boyer and Elliott, 1982). As each subsequent horse is emplaced, the overlying, previously formed horses are carried passively above the floor thrust toward the foreland; hence, a duplex is commonly referred to as a "piggy-back" thrust system (Boyer and Elliott, 1982; Butler, 1982). Structural relief created by a duplex thrust system commonly produces a doubly-plunging structural high, or a "culmination," in a fold-and-thrust belt (Figure 50) (Dahlstrom, 1970; Boyer and Elliott, 1982; Butler, 1982). As illustrated in Figure 50, duplex geometry and the internal geometry of culminations are influenced by the length, thickness, ramp angle, and displacement of the constituent horses (Boyer and Elliott, 1982; Mitra, 1986).

As a horse in a duplex thrust system is displaced over a footwall ramp ("FWR" in Figure 51), the horse is folded into an antiformal structure called a "fault-bend fold" (Figure 51) (Suppe, 1983). The forelimb of a fault-bend fold develops where the staircase trajectory of a thrust fault results in emplacement of a hangingwall ramp ("HWR" in Figure 51) over a footwall flat ("FWF" in Figure 51) (Butler, 1982). The backlimb of a fault-bend fold develops where a hangingwall flat ("HWF" in Figure 51) is emplaced over a footwall ramp ("FWR" in Figure 51) (Butler, 1982). As shown in Figure 50,

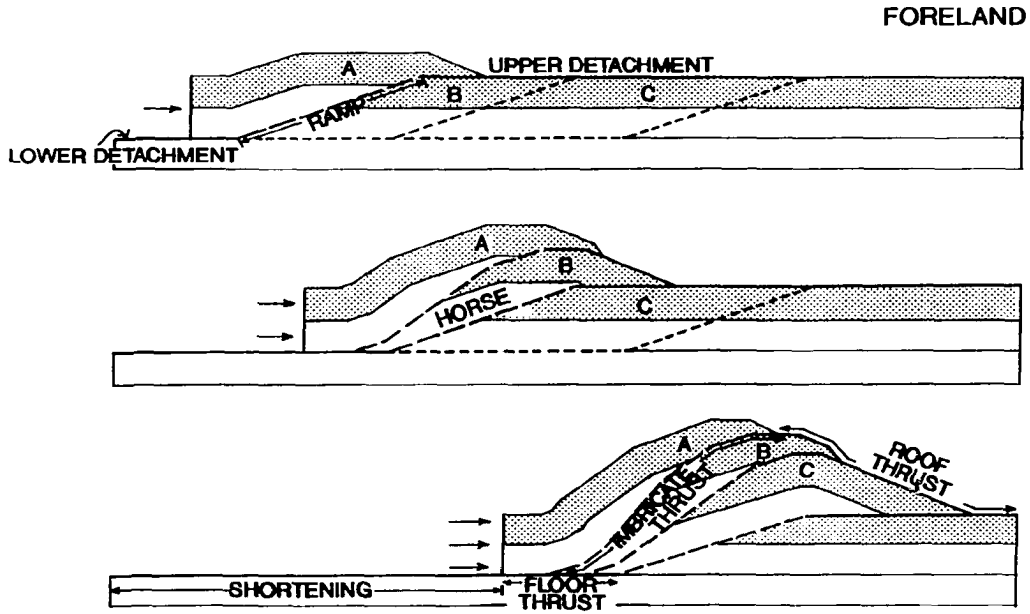

FIGURE 49. Progressive evolution of foreland sloping duplex thrust system consisting of three thrust sheets, A, B, and C (modified from Mitra, 1986). Lower and upper detachments and linking ramps isolate duplex horses A, B, and C. The existence of floor and roof thrust horizons permits displacement of packages of rocks (horses) separated by imbricate thrust faults. Progressive shortening occurs as horses are displaced toward the foreland.

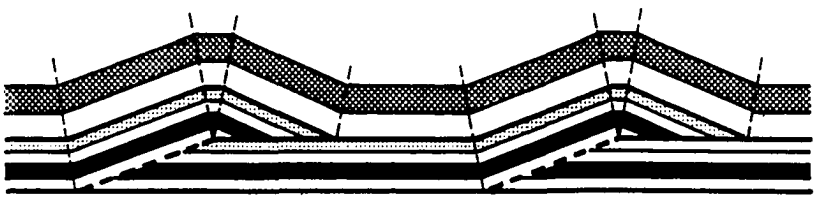

A. Independent ramp anticline. Two independent ramp anticlines, separated by a broad syncline, are produced when the final spacing between the two thrusts is much greater than the relative displacements on the individual thrusts (Mitra, 1986).

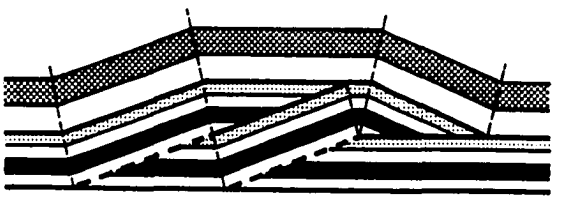

B. True duplex. A "true duplex" is defined as a duplex with parallel floor and roof thrusts at the contact between adjacent horses (Mitra, 1986). This geometry is produced when the final spacing between two thrusts is equal to the relative displacements on the individual thrusts.

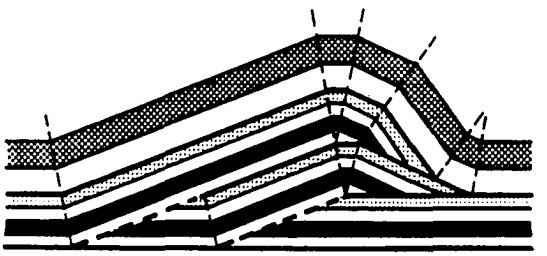

C. Overlapping ramp anticline. Large displacements on the two thrusts results in complete overlap of the crests of the two anticlines, producing a greater duplex height than in (A) or (B) (Mitra, 1986). This type of duplex is referred to as an "anticlinal stack" by Boyer and Elliott (1982).

FIGURE 50. Variations in duplex geometry produced by differences in the degree of overlap between adjacent horses (Mitra, 1986).

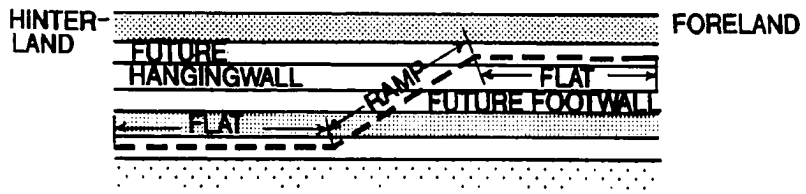

A. Staircase trajectory of thrust surface comprised of ramps and flats. Rocks overlying the thrust surface constitute the hangingwall; those beneath it are referred to as the footwall.

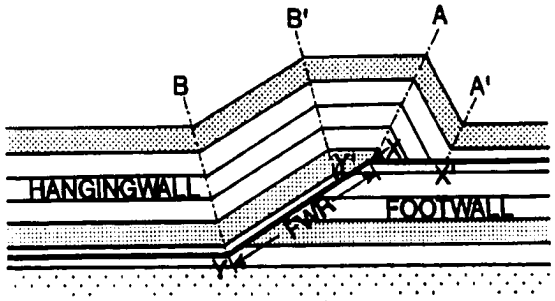

B. As hangingwall rocks are displaced over the footwall ramp (FWR), an antiformal fault-bend fold is developed. Hangingwall points originally located at X and Y have been displaced to X' and Y'. Kink fold axial surfaces A and B form in the hangingwall above respective ramp-to-flat and flat-to-ramp transitions in the footwall. A' and B' mark respective ramp-to-flat and flat-to-ramp transitions in the hangingwall.

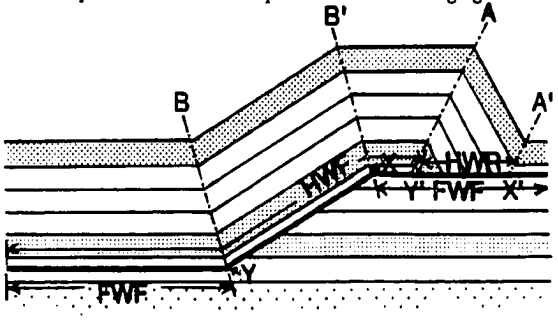

C. With continued displacement of hangingwall rocks toward the foreland, the kink-bands A-A' and B-B' grow in length. B-B' reaches its maximum length when B' is adjacent to X, the FWR to FWF transition. A-A' attains maximum length when Y' clears the FWR to FWF transition. The flat crest of the fault-bend fold, A-B', will lengthen if displacement continues past this stage.

FIGURE 51. Evolution of a fault-bend fold (after Suppe, 1983).

such folds can form in each horse of a duplex thrust system. Note that Suppe's (1983) model (Figure 51) incorporates the assumptions that bed thickness remains constant, bed length is conserved, and layer-parallel slip accommodates bending of strata. The kinematics of fault-bend folding are described by Suppe (1983) as follows (Figure 51): With progressive displacement of the hangingwall block relative to the footwall, kink bands A-A' and B-B' grow in width and the structural relief of the hangingwall increases. Axial surface A is in the hangingwall overlying point X in the footwall, which marks the FWR to FWF transition at the top of the FWR. Axial surface B is in the hangingwall overlying point Y in the footwall, which marks the FWF to FWR transition at the base of the FWR. Axial surfaces A and B maintain fixed positions with respect to the footwall, with the beds in the hangingwall block rolling through these axial surfaces as displacement proceeds. Two other axial surfaces, A' and B', are fixed with respect to the hangingwall and mark the HWR to HWF transition at point X' and the HWF to HWR transition at point Y', respectively. In contrast with A and B, these axial surfaces move as displacement occurs. When Y' reaches point X, the kink bands A-A' and B-B' cease to grow, marking the locations of the HWR and FWR, respectively. With continued displacement, axial surface B' remains fixed with respect to the footwall at point X, and axial surface A moves with the hangingwall above point Y'.

APPENDIX B. DESCRIPTION OF MAP UNITS

B.1. ELLESMERIAN SEQUENCE

B.1.a. Sadlerochit Group

Stratigraphic nomenclature and age determinations for the Sadlerochit Group are based on Keller et al. (1961) and Detterman et al. (1975). Map units of the Ivishak Formation are similar to those of Reed (1968).

lTriu **Lower Triassic upper Ivishak Formation (Sandstone-Siltstone Unit)**

Pyritic quartz sandstone: fine- to medium-grained, moderately well-sorted with subrounded grains, silica- and calcite-cemented, tabular beds 0.5-1.0 m thick, locally convolute-bedded, light to medium dark gray, weathers rusty to olive gray. Fine-grained quartz sandstone and siltstone with thinly interbedded shale: in gradational contact with pyritic quartz sandstone, laminated and cross-bedded in tabular sets 0.5-1.0 m thick, dark gray, weathers gray to olive brown, orange-brown weathering cleavage surfaces are common. This quartz sandstone-siltstone-shale unit constitutes the majority of the upper Ivishak Formation and outcrops as low resistant ridges and forms 10-20 cm rectangular blocks. Quartz sandstone: medium-grained, moderately well-sorted with subrounded grains, beds 0.5-1.5 m thick, silica-cemented, dark gray, weathers brown to dark gray. Thin, discontinuous quartz veins commonly intersect bedding in this quartz sandstone and cream-colored calcite stains on cleavage surfaces are characteristic. Texturally mature quartz sandstone with normally graded interbeds of dark gray siltstone and shale: fine- to medium-grained, silica-cemented with subrounded grains, laminated to 1.0 m thick beds in tabular sets, light brown to medium gray, weathers gray to olive brown.

lTril **Lower Triassic lower Ivishak Formation (Shale Unit)**

Shale and silty shale: fine-grained, flaky, dark gray to black, buff weathering, well-developed

bed-parallel slaty cleavage, poorly exposed.

Pe **Permian Echooka Formation**

Calcarenite: medium-grained, massive-bedded, gray, rusty to cream weathering, cross-cut by thin, discontinuous secondary quartz veins. Cherty quartz arenite: interbedded with dark gray to black, rusty weathering shale that separates it from the calcarenite, medium-grained, beds 0.5-1.5 m thick, dark gray to black, tan to red weathering with limonite stains. Locally, 1.0-2.0 m intervals of coarse-grained, buff to orange weathering fossiliferous calcarenite or calcareous white and dark gray chert pebble conglomerate occur near the base of the sequence. Gray calcarenite, 1.0-2.0 m thick, or calcareous shale disconformably overlies the Wahoo Limestone.

B.1.b. Lisburne Group

Stratigraphic nomenclature and age determinations for the Lisburne Group are based on Brosgé et al. (1962), Armstrong et al. (1970), and Sable (1977).

Pw **Pennsylvanian Wahoo Limestone**

Interbedded lime mudstone, bioclastic wackestone and packstone with minor grainstone: fine- to medium-grained, thin- (30 cm) to massive-bedded, medium to dark gray, weathers buff to light gray. Irregularly shaped nodules and discontinuous lenses of dark gray to black chert are common; abundantly fossiliferous with fauna including crinoids, bryozoans, and brachiopods. Outcrops as a resistant, cliff-forming unit.

Mau **Mississippian upper Alapah Limestone**

Interbedded lime mudstone, bioclastic wackestone and minor packstone: fine-grained, thin- to medium-bedded (20 cm-1.0 m), light to medium gray, weathers buff to light gray, forms distinctive talus aprons beneath the Wahoo Limestone.

Mal **Mississippian lower Alapah Limestone**

Interbedded lime mudstone and bioclastic wackestone: fine- to medium-grained, thin- (20 cm) to massive-bedded, light to medium gray, weathers gray to tan, outcrops as cliff-former below the upper Alapah Limestone.

B.1.c. **Endicott Group**

Stratigraphic nomenclature and age determinations for the Endicott Group are based on Brosgé et al. (1962), Dutro et al. (1972), and Armstrong and Mamet (1975).

Mky **Mississippian Kayak Shale**

Carbonaceous black shale: fissile, laminated to thin-bedded (10 cm), weathers orange, poorly exposed, typically tundra-covered. Interbeds of argillaceous limestone (1 cm-0.5 m thick) occur near the contact with the overlying lower Alapah Limestone. Prevalent quartz veins (0.5-2.0 cm thick) occur parallel to and cross-cut bedding near the contact with the underlying Kekiktuk Conglomerate.

Mkt **Mississippian Kekiktuk Conglomerate**

Quartzite: medium-grained, texturally and compositionally mature, well-sorted subrounded grains, silica-cemented with some secondary calcite cement, light to medium gray, 40 cm-1.0 m thick beds. Near the base of the Kekiktuk Conglomerate, quartzite is interbedded with 0.2-0.4 m thick beds of gray and white chert pebble- and cobble-conglomerate. Intervals of carbonaceous black shale (30 cm-2.0 m thick) occur sporadically between quartzite and conglomerate horizons. Quartz veins locally cross-cut the unit, commonly subnormal to bedding. Where in fault contact with pre-Mississippian rocks, the Kekiktuk Conglomerate commonly forms discontinuous, 0.25-2.5 m thick lens-shaped imbricate slices bound by dark gray to black shale.

B.2. FRANKLINIAN SEQUENCE

Depositional relationships within and between pre-Mississippian map units are unknown due to deformational overprints such as isoclinal folding and thrust faulting. Map units are grouped into three fault-bounded structural-stratigraphic packages.

B.2.a. Pre-Mississippian Upper Structural-Stratigraphic Package

pMsv Pre-Mississippian Slate-Volcanic Unit

Slate, chert, and volcanic rocks: red slate with intercalated intervals (2-4 m thick) of red to white chert that weathers gray. Volcanic rocks, including tan weathering andesite, were observed only as float; therefore, their relationship with the slate and chert is unknown.

pMp Pre-Mississippian Phyllite Unit

Purple, green, and gray phyllite: Fissile, foliation surfaces locally spotted with magnetite grains, minor intercalated intervals (0.5-1.0 m thick) of massive, dark gray chert. Repetition of this unit within the study area is interpreted to be due to faulting.

pMc Pre-Mississippian Chloritic Phyllite Unit

Phyllite: chloritic, tan to greenish-tan, intercalated lenses (10 cm-2 m thick) of dark gray metaquartzite and metaconglomerate with quartz-filled extension fractures normal to foliation. This unit is found structurally overlying the Kekiktuk Conglomerate and locally appears to be mylonitic, with quartz stringers and stretched pebbles in the plane of foliation.

B.2.b. Pre-Mississippian Middle Structural-Stratigraphic Package

pMcg Pre-Mississippian Chert-Greenstone Unit

Chert and greenstone with intercalated shale: discontinuous lenses of dark gray massive chert and tan-orange weathering massive greenstone, with gray-brown to black shale typically separating chert from greenstone. Chert intervals (1-4 m thick) are commonly cross-cut by prominent quartz-filled extension fractures. This is a resistant unit that upholds the higher,

precipitous peaks.

pMsh **Pre-Mississippian Shale Unit**

Gray to black shale and gray phyllite, with intercalated orange weathering dolostone, fine-grained olive-brown weathering sandstone, orange to tan weathering greenstone, and thin- (10 cm thick) to massive-bedded dark gray chert. Interbeds are less than 25 m thick and vary in degree of continuity along strike.

dss Dolostone/Sandstone

gs Greenstone

ch Chert

pMp **Pre-Mississippian Phyllite Unit**

Purple, green, and gray phyllite: Fissile, foliation surfaces locally spotted with magnetite grains, minor intercalated intervals (0.5-1.0 m thick) of massive, dark gray chert. Repetition of this unit within the study area is interpreted to be due to faulting.

pMc **Pre-Mississippian Chloritic Phyllite Unit**

Phyllite: chloritic, tan to greenish-tan, intercalated lenses (10 cm-2 m thick) of dark gray metaquartzite and metaconglomerate with quartz-filled extension fractures normal to foliation. This unit is found structurally overlying the Kekiktuk Conglomerate and locally appears to be mylonitic, with quartz stringers and stretched pebbles in the plane of foliation.

pMb **Pre-Mississippian Brecciated Unit**

Tan to greenish-tan, tectonically brecciated phyllite with intercalated dark gray chert. Both bedded and masssive chert intervals occur, with beds commonly 10 cm thick and locally faulted on a small-scale. Discontinuous lenses (0.5-1.5 m thick) of massive dark gray chert typically are cross-cut by quartz-filled extension fractures. This tectonically brecciated unit is confined to the fault zone where the phyllite or chloritic phyllite units are thrust over the

Kekiktuk Conglomerate.

B.2.c. Pre-Mississippian Lower Structural-Stratigraphic Package

pMv Pre-Mississippian Volcanic Unit

Fissile, carbonaceous black shale interbedded with tectonically(?) brecciated limestone outcropping as tan weathering, resistant towers, orange weathering dolostone, basalt and greywacke (locally with flute casts). An orange weathering, vesicular basalt with pillow structures and mafic volcanic breccia is intercalated with lesser amounts of a similar black shale. Greenish-brown weathering massive volcanic breccia and brown weathering greenstone are also intercalated with shale and appear to underlie stratigraphically the vesicular basalt and volcanic breccia.

APPENDIX C. SUPPLEMENTAL STRUCTURAL DATA

The orientations of pre-Mississippian slaty cleavage (S_1) in the Franklinian sequence are compiled in Figure 14A. In Figure 52, these data are combined with orientations of bedding (S_0) and attitudes measured in the upper and lower antiforms are plotted separately. The equal-area stereographic projections shown in Figures 52A and 52B are similar, suggesting that there is no significant difference in the orientations of S_1 and S_0 within the Franklinian sequence rocks of the upper and lower antiforms. Both Figures 52A and 52B indicate that S_1 and S_0 dip moderately south in the study area.

The orientations of bedding in the structural-stratigraphic and major lithostratigraphic units of the Ellesmerian sequence are shown in Figures 14E and 27. In Figure 53A-E, the orientations of bedding are shown on separate equal-area stereographic projections for the Kekiktuk Conglomerate (Figure 53A), Kayak Shale (Figure 53B), Lisburne Group (Figure 53C), Echooka Formation (Figure 53D), and Ivishak Formation (Figure 53E). In Figures 53A-E, average orientations of bedding planes change from the north-dipping Kekiktuk Conglomerate exposed on the north limb of the anticlinorium, to the dominantly south-dipping Sadlerochit Group (Figures 53D-E) exposed in the synclinorium to the north of the Franklin Mountains anticlinorium. Bedding in the Kekiktuk Conglomerate reflects the orientation of the sub-Mississippian unconformity which was folded when the north limb of the anticlinorium formed. Except for near the northern boundary of the study area, folds in the Lisburne and Sadlerochit Groups are generally overturned to the north, accounting for the south-dipping bedding planes in Figures 54C-E.

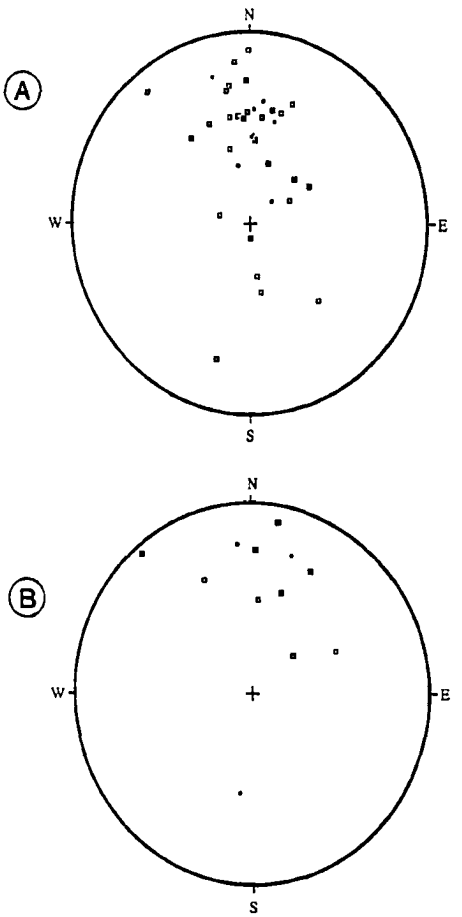

FIGURE 52. Equal-area stereographic projections of poles to compositional layering (S_0) and pre-Mississippian slaty cleavage (S_1) in the upper (A) and lower (B) antiforms. • = S_0; ▪ = S_1. In (A), N = 36; in (B), N = 12.

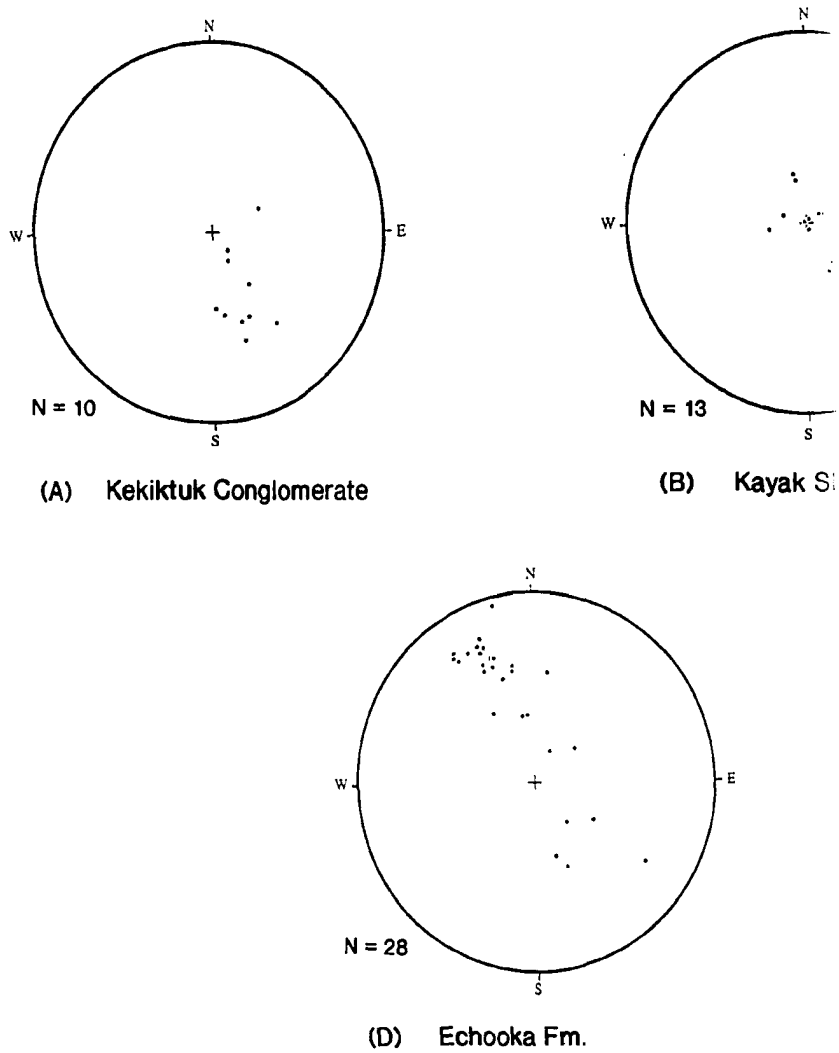

FIGURE 53. Equal-area stereographic projections of poles to bedding planes in the Ellesmerian sequence. (A) Kekiktuk Conglomerate; (B) Kayak Shale; (C) Lisburne Group; (D) Echooka Formation; (E) Ivishak Formation.

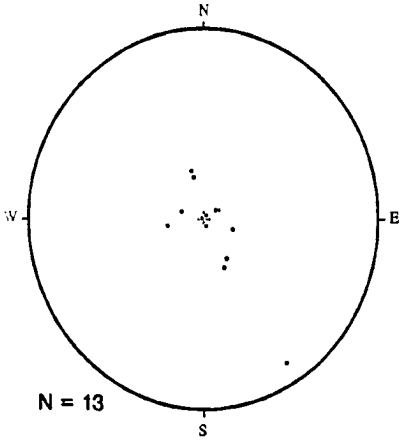

(B) Kayak Shale

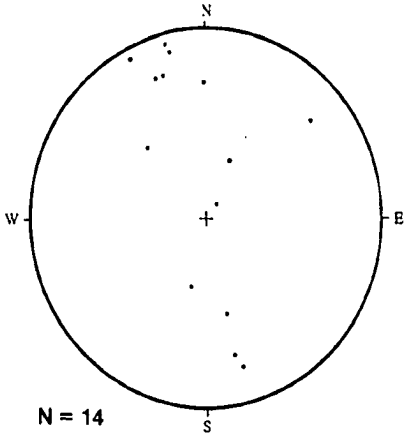

(C) Lisburne Group

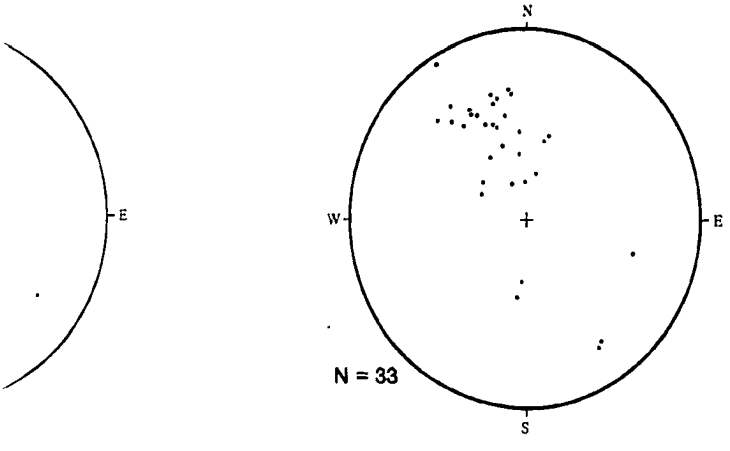

(E) Ivishak Fm.

APPENDIX D. ASSUMPTIONS MADE IN CONSTRUCTION OF BALANCED CROSS-SECTIONS

Although it may be possible to restore a cross-section to the undeformed state, such an apparently viable model may be incorrect if certain assumptions or interpretations prove to be invalid. A number of important assumptions were made in the construction of balanced cross-sections across the Franklin Mountains anticlinorium. These cross-sections are considered to be valid geometric models; however, some important assumptions made in order to construct or balance the cross-sections are more difficult to defend than are others. Several assumptions are commonly made during the construction of balanced cross-sections; Table 9 outlines these assumptions as they apply to this study. Assumptions and interpretations made which are specific to this study are addressed in detail below.

D.1. ORIENTATION OF DIP PANELS

Field measurements of the attitude of bedding and cleavage surfaces were used to define extensive planar panels of constant dip, separated by mappable axial surfaces, which define the major structures of the study area. Dip panels may reasonably characterize the orientation of bedding and slaty cleavage in pre-Mississippian rocks because the attitudes of bedding and slaty cleavage change progressively over a distance of kilometers. Identification of dip panels in the Franklinian sequence rocks of the upper antiform is complicated by the broad curvature of the Kekiktuk Conglomerate which caps these pre-Mississippian rocks, making it difficult to locate axial surfaces precisely. Since the lower antiform is a relatively tight fold with a well-exposed hinge zone (Figure 18), the dip panels which represent the north and south limbs of this antiform are separated by an easily mappable axial surface.

Dip panels in the Ellesmerian sequence are well-defined, coinciding with the dips of straight limbs of relatively tight folds which have distinct axial surfaces. As with the Franklinian sequence, an effort was made to distinguish the orientations of such dip panels from those of mesoscopic structures superimposed upon the larger-scale structures. Folds with wavelengths on the order of meters to

TABLE 9. Summary of basic assumptions made during cross-section construction.

ASSUMPTION	REASON FOR ASSUMPTION	APPLICATION	DESCRIPTION
THICKNESSES OF UNITS	Need to establish thicknesses used. Versions of the same cross-section constructed using different stratigraphic thicknesses may display very different structural geometries.	Ellesmerian sequence (Discussion of Franklinian sequence in Appendix D.5.)	Values derived from 1:25,00 and from stratigraphic section near forks of Canning River and Armstrong (1972) and at by Reed (1968). Thicknesse constant throughout study ar
TECTONIC TRANSPORT DIRECTION	Cross-sections should be constructed parallel to tectonic transport direction.	Cenozoic deformation event affected both sequences; most clearly expressed in Ellesmerian sequence.	NNW-girdle of bedding plan Ellesmerian sequence (Figur represent tectonic transport d explained in Section 5.C.3.
CONSERVATION OF BED-LENGTH AND AREA	Cross-sections are conventionally balanced by maintaining constant values of bed length and area in deformed and undeformed sections.	Franklinian sequence	Constant length of reference lines and area of thrust pack maintained. Reference horiz parallel to footwall.
		Ellesmerian sequence	Constant bed-length and area for Kekiktuk, Lisburne, and Constant area maintained for Shale.
KINK-FOLDING AND PARALLEL FOLDING BY FLEXURAL-SLIP	Kink geometry (Suppe, 1983) describes idealized parallel folds comprised of planar dip panels that intersect at axial surface. Constant thickness of limbs; interlimb angle bisected by axial surface. Folds form by mechanism of interbed flexural-slip.	Franklinian sequence	Used kink geometry (Suppe constructing geometry of fir horses; implies flexural-slip mechanism.
		Ellesmerian sequence	Used kink geometry (Suppe units except Kayak Shale, n bed thickness except in simi north limb of anticlinorium flexural-slip as fold mechan
PLANE STRAIN	To construct a cross-section that is retrodeformable by area-balance methods, need to assume that no material moved into or out of the cross-section plane during deformation.	Franklinian sequence	Assumed for lower, middle, structural-stratigraphic pack Figures 30-32.
		Ellesmerian sequence	Assumed for all structural-st units in Figures 30, 31, and

	ASSESSMENT OF VALIDITY	
DESCRIPTION	SUPPORTING	QUESTIONING
ılues derived from 1:25,000 mapping ıd from stratigraphic sections measured ar forks of Canning River by Mamet ıd Armstrong (1972) and at Lake Peters Reed (1968). Thicknesses assumed ınstant throughout study area (Table 1).	Values based primarily upon field observations; no facies or thickness changes observed. Constant thicknesses expected given small size of study area with respect to regional extent of continental platform deposits of Ellesmerian sequence.	No sections measured in study area; thickness of Kayak Shale determined by area balancing, thus poorly constrained.
NW-girdle of bedding planes in lesmerian sequence (Figure 27) may present tectonic transport direction as plained in Section 5.C.3.	Figure 27 similar to those of Oldow et al. (1986) and Reed (1968). NNW- to N-trending lines of section are perpendicular to strike of most bedding planes, trend of Cenozoic fold axes and thrust faults.	Structures in Franklinian sequence suggest N versus NNW transport (Section 5.C. discusses influence of pre-Mississippian structural grain on trend of Cenozoic structures in these rocks).
ınstant length of reference horizon ies and area of thrust packages aintained. Reference horizons are rallel to footwall.	Need some method to balance pre-Mississippian rocks. Supplemented by strain considerations (Section 7).	May not be valid for cleaved or strained rocks (Woodward et al., 1985). Should incorporate strain data (Cooper and Trayner, 1986; DePaor, 1988; Woodward et al., 1986).
ınstant bed-length and area maintained r Kekiktuk, Lisburne, and Sadlerochit. ınstant area maintained for Kayak ale.	Rocks not significantly strained so can assume lengths and areas not altered by deformation.	Kayak Shale likely responded to deformation in a ductile manner; area may not have remained constant.
ed kink geometry (Suppe, 1983) in nstructing geometry of first and second rses; implies flexural-slip as fold echanism.	Kink geometry permits upper and lower antiforms to be projected to depth, constraining geometry of anticlinorium.	Open folds in upper and lower antiforms defined by change in dip of slaty cleavage over distance of several hundred meters.
ed kink geometry (Suppe, 1983) for all its except Kayak Shale, maintaining d thickness except in similar folds on rth limb of anticlinorium; implies xural-slip as fold mechanism.	Straight-limbed parallel folds observed in Lisburne and Sadlerochit Groups N of anticlinorium; hinges rounded but arc of curvature small compared to wavelength; folds essentially angular.	Broad folds in Kekiktuk defined by smooth curvature rather than by distinct dip panels; complex folding and flow of Kayak Shale precludes imposing constraints of kink geometry.
ssumed for lower, middle, and upper ructural-stratigraphic packages in gures 30-32.	Necessary assumption in order to balance section; metamorphic grade is low; few structures indicative of internal flow out of plane of section.	Upper and lower antiforms plunge moderately W, producing greater thicknesses and lengthened fold limbs in deformed section.
ssumed for all structural-stratigraphic nits in Figures 30, 31, and 33-34.	Total shortening of Lisburne and Sadlerochit Groups constant along strike (Sections 6.C.4. and 6.E.); fold axes sub-horizontal (Figure 27); flow of Kayak Shale within plane of section, coring detachment anticlines (Section 9.B.).	Some mesoscopic structures suggest ENE-WSW extension; units displaced from cores of overturned folds on north limb of anticlinorium (Section 9.D.3.); Kayak Shale may have flowed to ENE-WSW in response to NNW-vergent shortening.

tens-of-meters are characteristic of the Kayak Shale, and are relatively common within the Lisburne and Sadlerochit Groups of the Ellesmerian sequence, increasing the difficulty of separating attitudes of mesoscopic structures from those of larger-scale structures appropriate to the scale of the cross-section. Extensive and chaotic mesoscopic flow-folding within the Kayak Shale suggests that using dip panels to represent the deformational geometry of this unit grossly oversimplifies the structural style and fails to portray the extent of internal shortening within this unit (refer to Table 9). Good exposure of cross-section-scale structures in the Lisburne and Sadlerochit Groups enabled major dip panels to be characterized accurately.

D.2. FAULT-BEND FOLD GEOMETRY

Geometric modeling of the thrust packages of Franklinian sequence rocks and the Kekiktuk Conglomerate which comprise the Franklin Mountains anticlinorium is based on the interpretation of the upper and lower antiforms as fault-bend folds within a northward-propagating duplex thrust system, formed during Cenozoic thrust faulting. Franklinian sequence rocks of the upper antiform overlie the Kekiktuk Conglomerate on the north and south limbs of the lower antiform (Figure 18). Franklinian sequence rocks of the upper antiform have been eroded from the crest of the lower antiform (Figures 16 and 18); therefore, it is not immediately evident that the pre-Mississippian rocks overlying the north and south limbs of the lower antiform are parts of the same thrust package. However, at location "C" in Figure 23, the Kekiktuk Conglomerate of the upper antiform is truncated by the Kekiktuk Conglomerate which forms the north limb of the lower antiform, indicating that the presently north-dipping thrust fault on the northern limb is north-vergent, cutting up-section toward the north (Figure 16B). This relationship suggests that these thrusts are continuous over the lower antiform, constituting a folded north-vergent thrust fault (Figures 16 and 18). Since this thrust cuts up-section from south to north, it defines a hangingwall ramp (Figure 51). The Kekiktuk Conglomerate and Franklinian sequence rocks which constitute the upper antiform are folded above this hangingwall ramp, forming a fault-bend fold by

the definition of Suppe (1983) (Appendix A). Since this thrust fault defines the upper contact of the Kekiktuk Conglomerate which caps the lower antiform, it is interpreted to have been folded during formation of the lower antiform, hence subsequent to formation of the upper antiform. Only the hinge region of the lower antiform is exposed in the study area (Figure 18). Therefore, it is impossible to demonstrate that this structure formed as a fold above a ramp in an underlying thrust surface.

The balanced cross-sections shown in Figures 30 and 32 (Plates 2 and 4) were constructed by projecting fault-bend fold geometry (Suppe, 1983) both above and below the erosion surface. As described in Appendix D.6., the constraints imposed by this geometric modeling method permitted ramp angles, horse thicknesses, and detachment depths to be determined. Thus, the validity of the geometry in these cross-sections depends directly on the validity of applying fault-bend fold geometry (Suppe, 1983) to these thrust sheets. Note that Suppe (1983) models the geometry of fault-bend folds formed by flexure of and slip along initially horizontal layers. The south-dipping pre-Mississippian structural fabric within the Franklinian seqence rocks in the study area might cause fault-bend folds formed in these rocks to differ geometrically and mechanically from those of Suppe (1983).

D.3. LOCATION OF PIN LINES

The process of restoring a balanced cross-section to an undeformed state involves locating pin lines normal to bedding within major folds and thrust sheets and then straightening out beds assuming that no flexural-slip occurs at the pin lines. Folding is modeled to occur by simple shear along unpinned portions of bedding planes as units in an undeformed layercake stratigraphy are displaced along thrust faults. The amount of simple shear imposed is related to the tightness of folding and to the location of pin lines. As discussed below, several major pin lines were used in order to balance the three cross-sections in Figures 30-34: one pin within each thrust sheet in the Franklinian sequence (Pins #1, #2 and #2a in Figures 30-32, Plates 2-4), one or more local pin lines in fault-bounded packages of Ellesmerian sequence rocks on the north limb of the anticlinorium (Pins #4 in Figure 34 and #5 in

Figure 34), and pins within the Ellesmerian sequence near the northern boundary of the study area (Pin #3 in Figures 30-34, Plates 2-5) and to the south of the study area (Pin #2 in Figures 30-31, Plates 2 and 3).

The first step in restoring the primary balanced cross-section (Figure 30, Plate 2) is to unfold the lower antiform and replace the second horse in the structural position it occupied prior to displacement. (In a northward propagating duplex model, the thrust sheet bearing the lower antiform would have been emplaced after the thrust sheet bearing the upper antiform. Therefore, these thrust sheets are referred to as the "first" and "second" horses in terms of their order of emplacement, as discussed in Section 6.C.) The geometry of the lower antiform is well-defined and constrains the location and orientation of the footwall ramp over which the second horse was displaced, assuming that fault-bend fold geometry (Suppe, 1983) can be applied. In order for the cross-section to be retrodeformable, the hangingwall at the leading edge of the second horse must match the underlying footwall ramp upon restoration (compare Figures 30 and 31). Therefore, the pin line within the second horse (Pin #1) was located on the forelimb of the lower antiform such that hangingwall and footwall cut-offs would match when the deformed cross-section was restored (Figures 31-33). These cut-offs do not match if the pin is placed in the flat part of the second horse. The location of Pin #1 results in geometric modification of the trailing edge of the second horse due to flexural-slip when this horse is restored to its position prior to emplacement.

The pin line within the first horse (Pin #2) was located on the gently south-dipping backlimb of the upper antiform, just to the south of the boundary of the study area, maximizing slip along Kekiktuk Conglomerate bedding planes in the forelimb of the upper antiform (Figure 22). The orientation of a strain ellipse obtained from a sample of the Kekiktuk Conglomerate on the forelimb of the upper antiform (Section 7, Appendix H) is compatible with bedding-parallel shear induced by a backlimb pin line (Figure 54). While field observations and strain analyses support the use of a backlimb pin line like Pin #2, this pin line location led to some difficulties in determining shortening for the partially reconstructed cross-section (Figure 32, Plate 3). The extension imposed subparallel to bedding in the

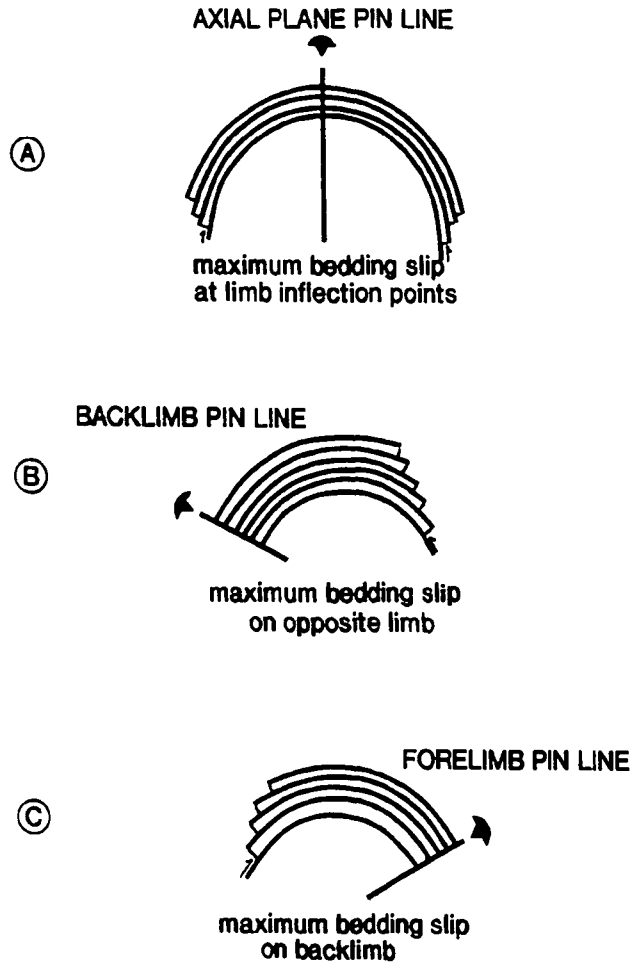

FIGURE 54. Effect of the placement of pin lines on location of bedding-plane slip associated with folding (from Woodward et al., 1985).

Kekiktuk Conglomerate at the leading edge of the first horse in the partially reconstructed model (Figure 32) effectively shifted point X' in Figure 35B toward the foreland, inflating the value of S1 to 9.2 kilometers. Since total shortening, S_T, and S2 are measured from the deformed section (Figure 30) and are unaffected by this extension, S1 can be adjusted, where $S1^* = S_T - S2 = 8.1$ kilometers.

Local pin lines within the Ellesmerian sequence were located at the hinges of major folds. For all three cross-sections, the same pin line (Pin #3) was used to balance the Ellesmerian sequence in the synclinorium to the north of the Franklin Mountains anticlinorium. Woodward et al. (1985) note that a well-developed axial planar cleavage indicates that zero slip occurred at fold hinges and, therefore, is the proper location for a local pin line, maximizing slip at the inflexion points of fold hinges (Figure 54). East-northeast-trending meso- and macroscopic folds in the Lisburne and Sadlerochit Groups display a moderately well developed axial planar cleavage. Pin #3 pierces the well-exposed hinge of a syncline near the northern boundary of the study area (Figures 30, 33 and 34, Plates 2-5). The pin line within the Ellesmerian sequence on the backlimb of the anticlinorium was arbitrarily placed in the core of a syncline above Pin #2 in the Franklinian sequence. There is no evidence to suggest that the Ellesmerian seqence was pinned to the Franklinian sequence at this location.

D.4. BALANCING METHODS USED FOR THE FRANKLINIAN SEQUENCE

Balancing methods conventionally applied to packages of sedimentary rocks were applied to the low-grade metamorphic rocks of the Franklinian sequence. While Woodward et al. (1985) suggest that conventional balancing methods can be used for rocks metamorphosed to greenschist facies or lower grades, treatment of these rocks as competent, fault-bounded sedimentary packages risks simplification or misrepresentation of structural style. When cross-sections contain mechanically incompetent rocks, it is difficult and may be inappropriate to construct and restore cross-sections using basic balancing techniques, since (1) folds may not display a parallel fold geometry, (2) folding may have occurred by a mechanism other than flexural-slip, and (3) non-plane strain may exist.

Within the study area, the Franklinian sequence is predominantly comprised of shales and phyllites, mechanically incompetent lithologies which typically respond to deformation in a somewhat ductile fashion. Franklinian sequence rocks likely behaved ductilely to some extent during pre-Mississippian deformation, with non-plane strain and isoclinal folds of non-parallel fold geometry developed (Section 5.C.1.). However, pre-Mississippian structures in these rocks were overprinted as a consequence of Cenozoic deformation, making it exceedingly difficult to assess how these rocks responded during each deformational event. While it is difficult to determine how pre-Mississippian structures influenced subsequent deformation, it is possible that these rocks might have behaved as semi-rigid packages during Cenozoic deformation. In this case, Cenozoic structures in the Franklinian sequence could be more easily modeled in balanced cross-sections. Since the magnitude of Cenozoic internal shortening within pre-Mississippian rocks and the Kekiktuk Conglomerate appears to have been minor compared to the shortening produced by Cenozoic thrust faulting and macroscopic folding (Section 8), these rocks are inferred to have behaved as relatively coherent, semi-rigid packages during Cenozoic deformation. Therefore, conventional balancing methods were applied, although it is acknowledged that it may not be entirely appropriate to do so.

D.5. SUB-MISSISSIPPIAN ANGULAR UNCONFORMITY

In order to construct a balanced cross-section across the Franklin Mountains anticlinorium, it was necessary to establish a possible geometric relationship between bedding (S_0) or slaty cleavage (S_1) in the Franklinian sequence, and the sub-Mississippian unconformity surface upon which the Ellesmerian sequence was deposited. Since pre-Mississippian rocks are interpreted to have been tightly to isoclinally folded during pre-Mississippian deformation, an angular unconformity surface that was originally relatively planar would be expected to truncate bedding and cleavage in the limbs of pre-Mississippian folds at a relatively constant angle (Figure 40). In constructing the primary cross-section (Plate 2 or Figure 30), a 40- to 50-degree south dip of S_0/S_1 was maintained with respect to the sub-Mississippian

unconformity surface, which was presumed to have been originally horizontal. This south dip is compatible with the observation that, in the study area, S_0 and S_1 in the Franklinian sequence on the south limbs of both upper and lower antiforms dip to the south with respect to the unconformity at an average angle of 49 degrees.

The assumption of an originally horizontal sub-Mississippian unconformity surface might be supported if it could be shown that a thin sheet of Kekiktuk Conglomerate, of regional extent and essentially constant thickness, was deposited on the unconformity surface. In the study area, the Kekiktuk Conglomerate everywhere overlies and at several locations is in unequivocal depositional contact with the unconformity surface (Section 5.B.1.). The average stratigraphic thickness of the Kekiktuk Conglomerate, estimated from field mapping to be 90-100 meters, is comparable with that in sections measured by Mamet and Armstrong (1972) near the forks of the Canning River (at least 61 meters), and by LePain and Crowder (1989) in the Franklin Mountains to the northeast (70 meters). Therefore, local and regional field observations suggest that it may be reasonable to assume that the unconformity surface originally was essentially horizontal.

D.6. DEPTHS TO DETACHMENT HORIZONS

The primary balanced cross-section (Figure 30, Plate 2) contains three structural detachment horizons: one in the Kayak Shale, corresponding to the roof thrust of the duplex, and two detachments in the Franklinian sequence, the lower of which corresponds to the floor thrust of the duplex (Figures 30-34, Appendix A). The detachment horizon in the Mississippian Kayak Shale is interpreted to lie at a sub-scalevel depth of 3,200 to 3,500 feet (roughly one kilometer), at the base of the Kayak Shale beneath the synclinorium to the north of the Franklin Mountains anticlinorium. (Rather than being a discrete horizon, the detachment is probably more accurately a zone that may include of much of, if not the entire, stratigraphic thickness of the Kayak Shale.) The depth of this detachment was determined by projection to depth of contacts and surficial data from the Ellesmerian sequence in the synclinorium, assuming that

units are not structurally duplicated at depth by unexposed thrust faults. Using a duplex model such as that shown in Figure 11, the depth of the Kayak Shale detachment corresponds to a base level to which the top surface of the Kekiktuk Conglomerate that caps the first and second horses must restore when the cross-sections are reconstructed (Figure 35). The structural relief of the Franklin Mountains anticlinorium is measured from this baselevel (Figure 35).

The depth of the upper unexposed detachment horizon in the Frankinian sequence was inferred from the projection of fault-bend fold geometry (Suppe, 1983) to depth. The Kayak Shale baselevel was projected to the south to the point which intersects the axial surface of the lower antiform ("a" in Figure 30). The geometry of the north limb of the fault-bend fold in the second horse can be constructed by projecting the dip panel representing the north limb of the lower antiform to depth, to the point where it intersects the baselevel ("b" in Figure 30). The footwall ramp beneath the lower antiform dips south from point "a" (Figure 30) at the same angle as the south limb of the lower antiform. This construction process defines the backlimb of the fault-bend fold in the second horse and enables the thickness of the second horse to be determined ("t" in Figure 30). Since the top surface of the Kekiktuk Conglomerate on the backlimb of the lower antiform (e.g. "c" in Figure 30) must restore to the baselevel defined by "a" (Figure 30), the upper detachment can be inferred to lie at a depth "t" beneath the Kayak Shale baselevel. Measured from the primary cross-section (Figure 30), the depth of this upper detachment is 3.1 kilometers (10,250 feet) below sealevel.

The depth of the lower unexposed detachment in the Franklinian sequence was inferred from the relatively complex and partially-eroded geometry of the upper antiform, and the location of the upper detachment in the Franklinian sequence. The orientation of the Kekiktuk Conglomerate on the backlimb of the upper antiform (W.K. Wallace, 1988; pers. commun.) was used to define a dip panel ("d" in Figure 30) which, as with the backlimb of the lower antiform, was assumed to reflect the dip of a thrust surface at some unknown depth beneath it. In this case, the underlying thrust surface was inferred to define the

trailing edge of the second horse. The upper detachment was projected to the south from the base of the footwall ramp ("e" in Figure 30) and the second horse was restored to its original position using Pin #1 (Figures 30-32). In order to locate the trailing edge of the second horse it was necessary to determine a length of the second horse that was compatible with various constraining factors, including (1) the extensive exposure of pre-Mississippian rocks between "f" and "g" (Figure 30), and indication of the relative thickness of the first horse, (2) the orientation of dip panel "d" (Figure 30), and (3) the Kayak Shale baselevel to the south of the anticlinorium ("h" in Figure 30). The thickness of the first horse ("t'" in Figure 30) corresponds to the depth of the lower detachment beneath the Kayak Shale base level to the south of the anticlinorium ("h" in Figure 30). This complex construction process determined that the lower detachment lies at a depth of 5.4 kilometers (17,700 feet) below scalevel.

APPENDIX E. ORIENTATIONS OF STRAIN MARKERS

Franklinian and Ellesmerian sequence rocks contain mesoscopic and microscopic strain markers which both define the general orientation of the strain ellipse in a plane, and provide information about the sequence of pre-Mississippian and/or Cenozoic deformational movements that produced the structural geometry observed. The strain markers in the Franklinian sequence which pre-date the formation of the anticlinorium during D_2 display similar orientations relative to the sub-Mississippian unconformity surface. Strain markers which formed during or subsequent to formation of the anticlinorium should be compatible with the position of the sample with respect to Cenozoic structures.

The strain markers observed include stylolites, extension fractures, pressure shadows, subelliptical quartz grains, deformed corals, and asymmetric mylonitic shear fabrics:

Stylolites form as a consequence of dissolution on surfaces that are oriented perpendicular to the direction of maximum compressive stress. Such surfaces typically are defined by a sawtooth trace of insoluble material or partially dissolved grains.

Extension fractures form normal to the direction of maximum elongation. Fibers of minerals which fill extension fractures are oriented subparallel to the direction of maximum elongation.

Pressure shadows can develop around rigid bodies such as garnet porphryoblasts, or pyrite and magnetite crystals. Mineral fibers which comprise a shadow are oriented parallel to the direction of maximum elongation, similar to the orientation of fibers which fill extension fractures. Fiber growth is believed to progress from the periphery of the shadow toward the rigid body. Curved fibers are interpreted to reflect changes in the direction of maximum elongation during deformation. Therefore, the orientation of each fiber segment between points of inflexion represents the orientation of the major-axis of the strain ellipse which characterized that increment of deformation.

Preferred orientations of elongate quartz grains or platy micaceous and clay minerals define a planar fabric normal to the direction of maximum compression and parallel to the direction of maximum

elongation. The planar fabric appears as a linear fabric in intersecting planes.

Plastic deformation of initially circular cross-sections of coral stems indicates the orientation and shape of the strain ellipse in that plane. The long-axis of the elliptical coral stems coincides with the major axis of the strain ellipse, or the direction of maximum elongation in that plane.

Kinematic indicators include asymmetric porphryoclasts in mylonitic samples, S-C mylonite fabric, and offset calcite twin lamellae. Counter-clockwise rotation is considered to be a sinistral (or negative) shear sense; clockwise rotation is considered to be a dextral (or positive) shear. In theory, shear planes are oriented at approximately 30 degrees to the direction of maximum compression.

Orientations and interpretations of these strain markers are shown in Figure 37 and summarized in Tables 10-14 for nine oriented samples from the Franklinian sequence and seven from the Ellesmerian sequence. Figures 55-57 show the trends of strain markers in the three mutually-perpendicular planes defined in Section 7.A.1. Tables 10-14 describe the trend of each type of strain marker in the plane of compositional layering (Franklinian sequence) or bedding (Ellesmerian sequence); orientations in the east-northeast-striking and north-northwest-striking planes are described in terms of rake, or the angle between the marker and a horizontal line in the plane. In this and the following appendices, a positive rake is defined by a clockwise rotation either from east for the east-northeast-striking plane, or from north for the north-northwest-striking plane.

TABLE 10. Summary of orientations of stylolites in oriented samples from the Franklinian and Ellesmerian sequences. Each box under "trend" and "rake" represents an orientation documented for one or multiple strain indicators in thin-sections of the three planes listed. Orientations listed first for each sequence in each plane represent the dominant orientations observed in the thin-sections; the relative importance of indicators of a given orientation decreases toward the bottom of the list for each sequence in a plane. The trends bracketed by parentheses were only observed in one sample and, thus, are considered to be of minor importance.

STYLOLITES					
PLANE	SEQ.	TREND	RAKE	INTERPRETATION	AGE
SUBPARALLEL TO COMPOSITIONAL LAYERING IN FRANKLINIAN SEQUENCE OR BEDDING IN ELLESMERIAN SEQUENCE	F	70		N-NNW compression	D_2
		90-94			
		342-351		WSW-ENE compression	D_3
		(36)		?	?
		(120)		WSW-ENE compression	D_3
	E	63-77		NNW compression	D_2
		(47)		?	D_2/D_3
		(93-104)		N compression	D_2
		(320)		WSW-ENE compression	D_3
SUBVERTICAL ENE-STRIKING	F		subhoriz	thrust-increased overburden	D_2
			subvert	E-W compression	D_3
	E		mod W	mod W plunge of anticlinorium	D_2
			subhoriz	diagenesis/bed-normal compress.	D_2?
			subvert	E-W compression	D_3
SUBVERTICAL NNW-STRIKING	F		gentle N	thrust-increased overburden	D_2
			mod steep S	N compression?	D_2?
	E		mod steep N	N-NNW compression	D_2
			gentle S	?	D_2 ?
			normal S_0	bed-parallel compression	D_2?
			parallel S_0	bed-normal compression	D_2?

TABLE 11. Summary of orientations of extension fractures in oriented samples from the Franklinian and Ellesmerian sequences. Each box under "trend" and "rake" represents an orientation documented for one or multiple strain indicators in thin-sections of the three planes listed. Orientations listed first for each sequence in each plane represent the dominant orientations observed in the thin-sections; the relative importance of indicators of a given orientation decreases toward the bottom of the list for each sequence in a plane.

EXTENSION FRACTURES					
PLANE	SEQ.	TREND	RAKE	INTERPRETATION	AGE
PARALLEL TO COMPOS. LAYERING OR BEDDING	F	60		NNW-SSE extension	?
		328-330		ENE-WSW extension	D_2
	E	73		NNW-SSE extension	?
		300, 327		ENE-WSW extension	D_2
SUBVERT. ENE-STRIKING	F		subvert-W	E-W extension	D_2 ?
			mod E	?	?
	E		subvert	E-W extension	D_2 ?
SUBVERT. NNW-STRIKING	F		mod N	extension parallel to S_1	D_2 ?
			steep S	?	?
	E		subhoriz	extension, subvert axis	D_2

TABLE 12. Summary of orientations of pressure shadows in oriented samples from the Franklinian and Ellesmerian sequences. The orientations of fiber increments which comprise each pressure shadow are listed from the periphery of the shadow to its core (P-->C). The trends or rakes listed in single boxes record the orientations of fibers in pressure shadows comprised of straight fibers of a single orientation. For these straight fibers, the dominant orientations for each sequence in each plane are listed first.

PRESSURE SHADOWS					
PLANE	SEQ.	TREND	RAKE	INTERPRETATION	AGE
PARALLEL TO COMPOSITONAL LAYERING OR BEDDING (1)	F	72		ENE extension	D_2
		P 323		NW extension	?
		P 95		E extension	D_2
		C 68		ENE extension	
		334		NW extension	D_3
	E	19		NNE extension	?
		62		ENE extension	D_2
SUBVERTICAL ENE-STRIKING (2)	F		subhoriz	E-W extension	D_2 ?
			P gentle E	four-stage path related to emplacement of thrust sheets (Appendix F)	D_2
			steep W		
			subvert		
			C E		
SUBVERTICAL NNW-STRIKING (3)	F		P gentle S	five-stage path related to emplacement of thrust sheets (Appendix F)	D_2
			subhoriz		
			steep N		
			gentle N		
			C steep S		

TABLE 13. Summary of orientations of quartz grains, micaceous minerals, and deformed corals in oriented samples from the Franklinian and Ellesmerian sequences. Planes labelled (1), (2), and (3) refer to the planes listed in Table 12. The dominant orientations for each sequence in each plane are listed first. A.S. = axial surface.

PREFERRED ORIENTATIONS					
PLANE	SEQ.	TREND	RAKE	INTERPRETATION	AGE
1	F	86		NNW-SSE compression	D_2?
	E	78		NNW compression (quartz)	D_2
		137		NW extension (corals)	D_2?
2	F		subhoriz	subvert. thrust-rel. compression	D_2
3	F		steep S	subparallel to major thrust fault	D_2
			gentle N	increased overburden pressure	D_2
	E		gentle S	thrust-increased overburden	D_2
			A.S=steep S	N compression	D_2

TABLE 14. Summary of orientations of kinematic indicators in oriented samples from the Franklinian and Ellesmerian sequences. The orientation listed in each box represents the dominant trend or rake observed in multiple thin-sections from each sequence in a given plane. Planes labelled (1), (2), and (3) refer to the planes listed in Table 12.

KINEMATIC INDICATORS					
PLANE	SEQ.	TREND	RAKE	INTERPRETATION	AGE
1	E	328		shear assoc. N-NNW compress.	D_2
2	F		subhoriz	E-W shear, empl. of 2nd horse	D_2
3	F		mod S	dextr. shear rel. to major thrust	D_2
	E		subhoriz	dextr. shear oblique to maj thrust	D_2

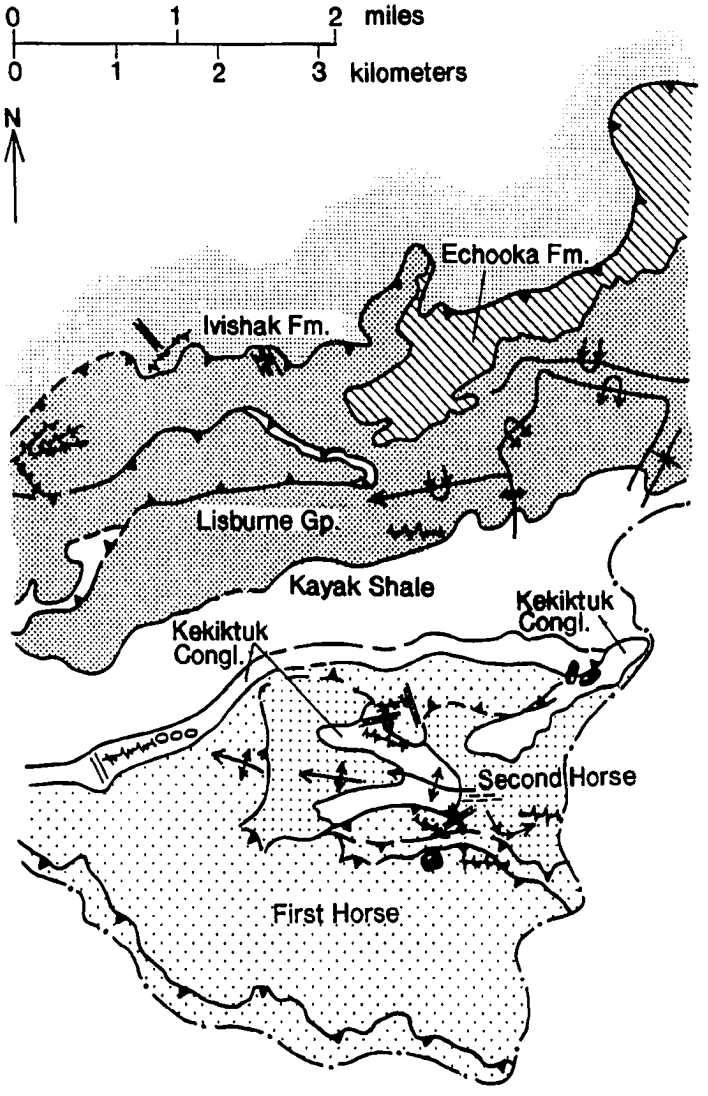

FIGURE 55. Orientations of strain markers in thin-section planes that are subparallel to compositional layering in the Franklinian sequence or bedding in the Ellesmerian sequence. = stylolites; = extension fractures; = fractures; = pressure shadows; preferred orientations and crystal plastic features: = subelliptical quartz grains, = platy minerals; = shear of calcite twin lamellae.

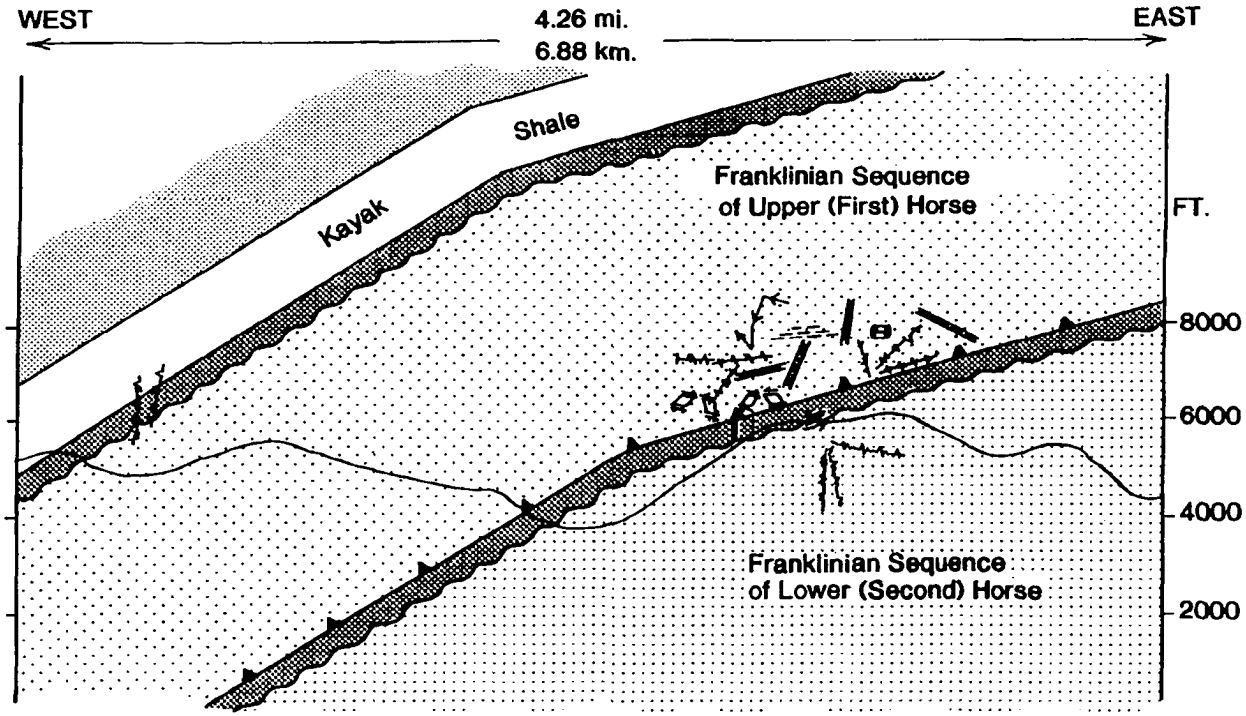

FIGURE 56. Orientations of strain markers in thin-section planes that are subvertical and strike east-northeast. = stylolites; = extension fractures; = pressure shadows; preferred orientations and crystal plastic features: = platy minerals; shear fabrics: = asymmetric porphyroblasts.

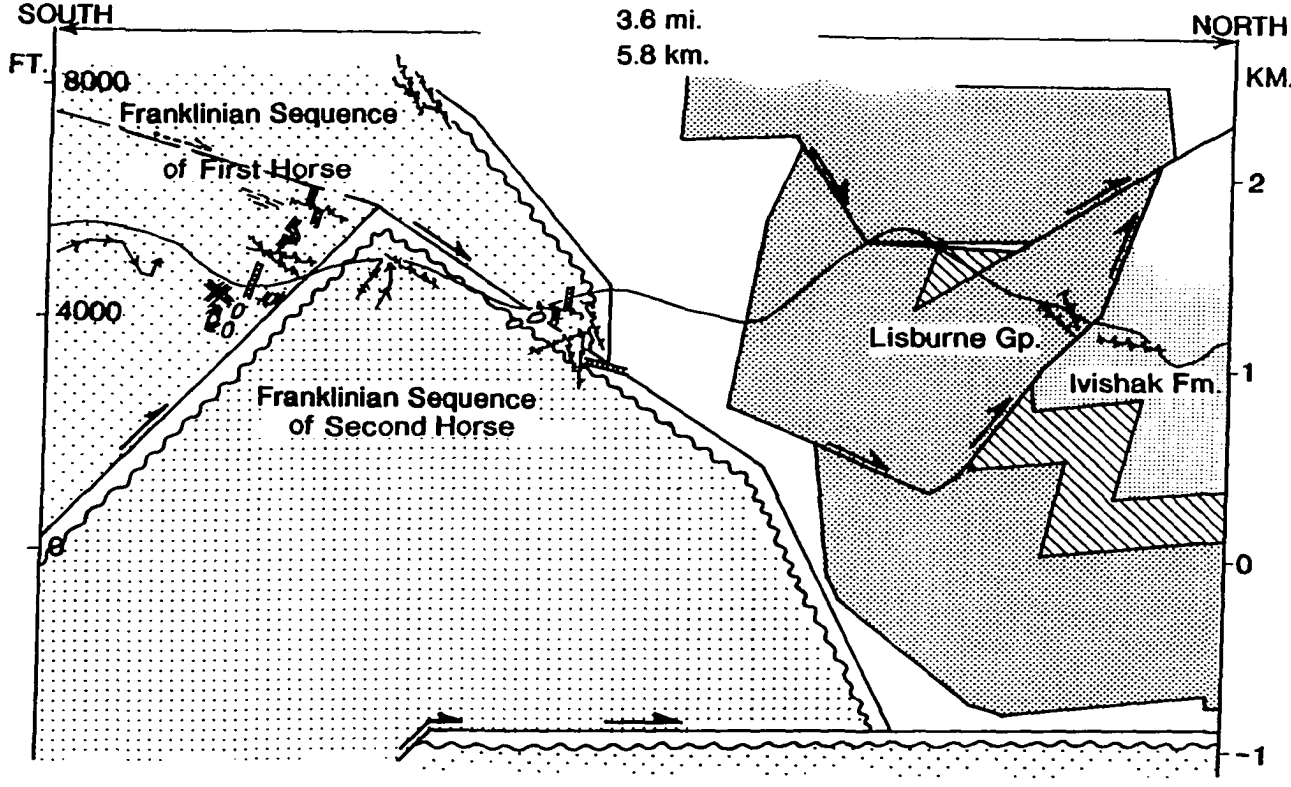

FIGURE 57. Orientations of strain markers in thin-section planes that are subvertical and strike north-northwest.. = stylolites; = extension fractures; = pressure shadows; preferred orientations and crystal plastic features: = subelliptical quartz grains, = platy minerals; shear fabrics: = asymmetric porphyroblasts.

APPENDIX F. INCREMENTAL STRAIN ANALYSIS

F.1. EQUATIONS USED IN CALCULATIONS

F.1.a. Rigid Fiber Model

As stated by Ramsay and Huber (1983), in non-coaxial deformation "the effective rigid body length in the direction of later increments is a function of the difference in angle Ø between an early formed fiber and the direction of the later increment." In the rigid fiber model equation, ∂l_n is the length of fibers in a given increment, L is the radius of the central rigid marcasite nodule, and Ø is the angle between ∂l_n and ∂l_{n-1} (Figure 58). The equation below defines the incremental strain, e_n, associated with each fiber increment within the pressure shadow; summation of these incremental strains yields the total strain. For the n^{th} increment in the pressure shadow,

$e_n = \partial l_n / (L + \sum_{f}^{n-1} \partial l_n \cos Ø_n)$ (Ramsay and Huber, 1983).

F.1.b. Deformable Fiber Model

In the deformable fiber model, an original fiber length ∂l_1 is modified to a length $\partial l_1'$ and orientation Ø' by the next strain increment with a fiber length ∂l_2 and oriented at an angle Ø to the direction of ∂l_1:

$\partial l_1' = \partial l_1 [(1 + \partial l_2/L)^2 \cos^2 Ø + \sin^2 Ø]^{0.5}$

$\tan ø' = \tan ø / (1 + \partial l_2/L)$ (Ramsay and Huber, 1983).

These modified values are then used in the equation listed above for the calculation of incremental strain by the rigid fiber model.

F.2. RESULTS OF INCREMENTAL STRAIN ANALYSIS

F.2.a. Franklinian Sequence Sample

The mineralogy and gross form of the pressure shadows which surround marcasite nodules in the

subvertical east-northeast- and north-northwest-striking planes of sample 87JZ16 (location "16" in Figures 15 and 30) are shown in Figures 59-61. Tables 15-17 summarize fiber rake, relative angle, mineralogy, and rigid fiber incremental strain for the pressure shadow in the north-northwest-striking plane and for the two pressure shadows in the east-northeast-striking plane. Time-progressive paths of fiber orientation for each sample are shown in Figures 62 and 63, scaled to units of incremental strain and oriented in the sample plane.

The three pressure shadows are comprised of combinations of eleven segments, each of which has a characteristic fiber orientation, length, and mineralogy (Tables 15-17). As shown in Figures 59-61, these segments lie between fiber isogons which define fibers of similar orientation. Incremental strains were calculated for each segment and each side of the pressure shadows, using both rigid and deformable fiber models of Ramsay and Huber (1983). Tables 18-21 summarize the incremental strains calculated for each shadow by both models. Summation of incremental strains yields total strains of roughly 0.40 and 0.50 strain units for respective north and south sides of the pressure shadow in the north-northwest-striking plane, and 0.56 and 0.21 for the large and small pressure shadows, respectively, in the east-northeast-striking plane. Strain values determined by rigid and deformable fiber models differ by an average of +/- 0.008 and 0.015 strain units for the pressure shadows in the east-northeast- and north-northwest-striking planes, respectively. The difference in strain between fiber models is 1.4% and 3.8% of the total strain for the small and large shadows in the east-northeast-striking plane, and 3.0-3.8% of the total strain for the shadows in the north-northwest-striking plane. Thus, the difference between incremental strain values calculated by the two methods is insignificant in relation to the total strain determined from incremental values.

Ramsay and Huber (1983) suggest that the rigid fiber model is most appropriate for pressure shadows (1) which are comprised of quartz fibers, (2) for which the shape of the outside edge of the shadow mimics the outline of the rigid body, and (3) which have longest fiber lengths for the last-formed,

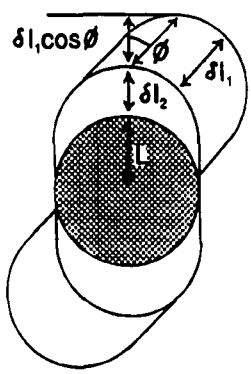

FIGURE 58. Parameters measured for calculation of incremental strain from pressure shadows under non-coaxial deformation (Ramsay and Huber, 1983). ∂l = fiber length; L = radius of marcasite nodule; Ø = orientation of fiber increment with respect to the previously formed increment.

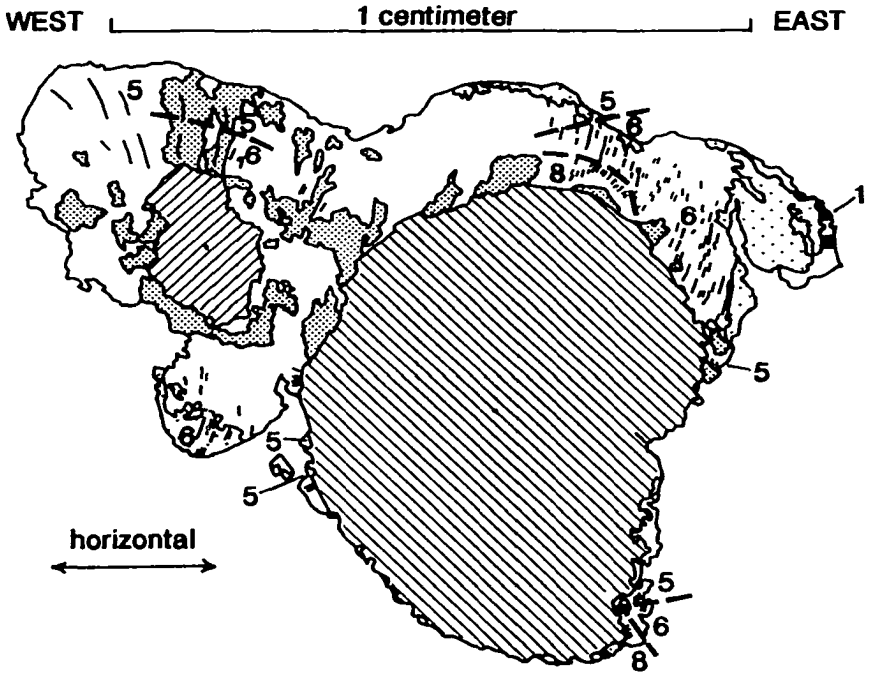

FIGURE 59. Small marcasite nodule (hatched) and pressure shadow developed in the subvertical east-northeast-striking plane of Franklinian sequence sample 87JZ16. Sample plane strikes 81 degrees and dips 46 degrees to the northwest. ▭ = chlorite; ▭ = quartz; ▭ = calcite. Broad dashed lines are isogons which define zones of fibers of similar orientation. Numbers refer to stages of fiber formation. Stage 1 fibers formed first; Stage 8 fibers formed last.

TABLE 15. Summary of incremental strain determinations, fiber orientations and mineralogy for the small pressure shadow in the subvertical east-northeast-striking plane of pre-Mississippian sample 87JZ16 (Figure 59).

STAGE	STRAIN rigid model (strain units)	RAKE angle from E (c-wise rotation is positive)	FIBER TREND/PLUNGE (degrees)	FIBER MINERALOGY
1	0.046	160	274 / 13	chlorite
2				
3				
4				
5	0.084	72	016 / 44	quartz
6	0.354	89	352 / 46	quartz & calcite
7				
8	0.090	132	299 / 33	quartz & calcite
9				
10				
11				

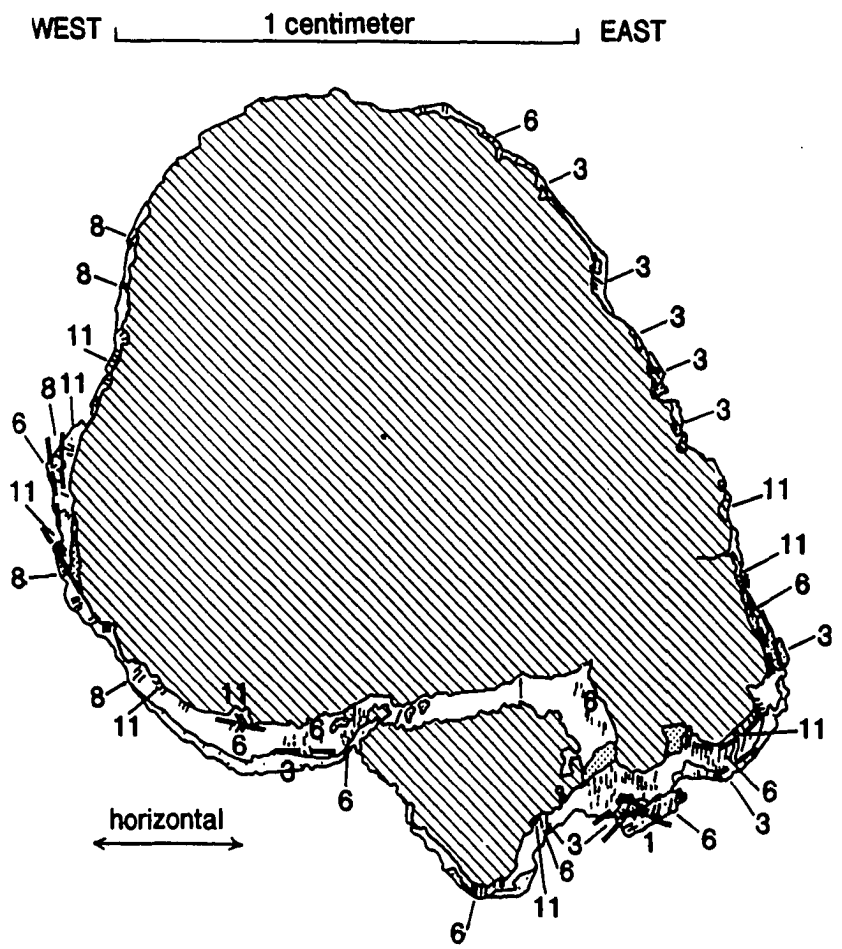

FIGURE 60. Large marcasite nodule (hatched) and pressure shadow developed in the subvertical east-northeast-striking plane of Franklinian sequence sample 87JZ16. Sample plane strikes 81 degrees and dips 46 degrees to the northwest. ▭ = chlorite; ▭ = quartz; ▭ = calcite. Broad dashed lines are isogons which define zones of fibers of similar orientation. Numbers refer to stages of fiber formation. Stage 1 fibers formed first; Stage 11 fibers formed last.

TABLE 16. Summary of incremental strain determinations, fiber orientations and mineralogy for the large pressure shadow in the subvertical east-northeast-striking plane of pre-Mississippian sample 87JZ16 (Figure 60).

STAGE	STRAIN rigid model (strain units)	RAKE angle from E (c-wise rotation is positive)	FIBER TREND/PLUNGE (degrees)	FIBER MINERALOGY
1	0.082	160	274 / 13	quartz & chlorite
2				
3	0.027	44	047 / 30	chlorite & quartz
4				
5				
6	0.042	93	347 / 46	quartz
7				
8	0.031	148	285 / 23	quartz
9				
10				
11	0.024	36	046 / 31	quartz

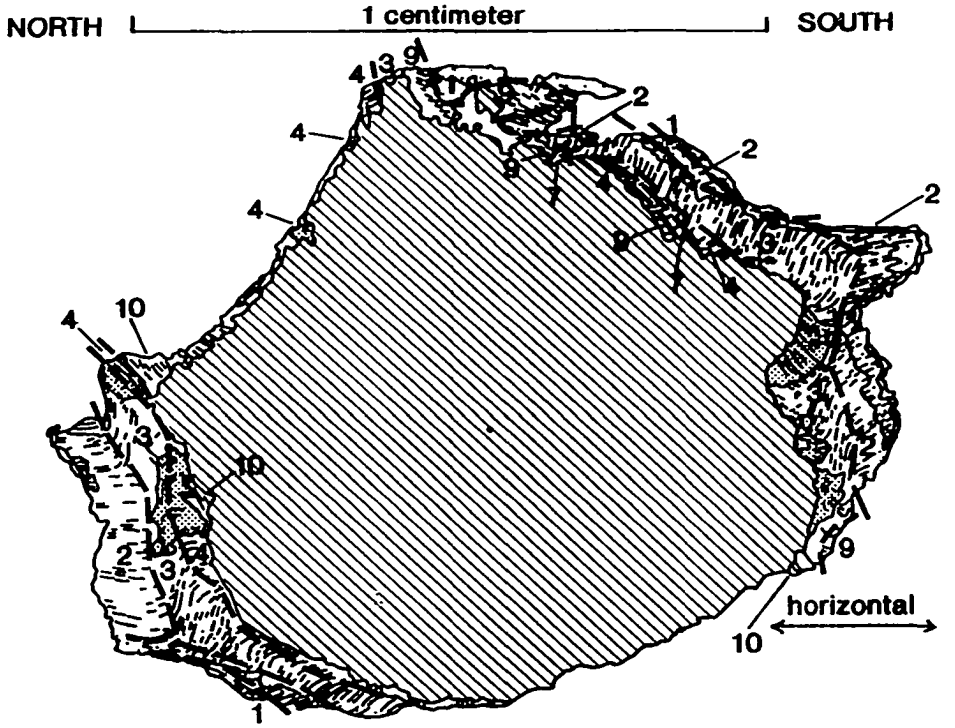

FIGURE 61. Marcasite nodule (hatched) and pressure shadow developed in the subvertical north-northwest-striking plane of Franklinian sequence sample 87JZ16. Sample plane strikes 354 degrees and dips 88 degrees to the southwest. ▭ = chlorite; ▭ = quartz; ▭ = calcite. Broad dashed lines are isogons which define zones of fibers of similar orientation. Numbers refer to stages of fiber formation. Stage 1 fibers formed first; Stage 10 fibers formed last.

TABLE 17. Summary of incremental strain determinations, fiber orientations and mineralogy for the pressure shadow in the subvertical north-northwest-striking plane of pre-Mississippian sample 87JZ16 (Figure 61).

STAGE	STRAIN rigid model (strain units)	RAKE angle from N (c-wise rotation is positive)	FIBER TREND/PLUNGE (degrees)	FIBER MINERALOGY
1	0.080	160	175 / 20	chlorite & quartz
2	0.112	0	174 / 00	quartz & chlorite
	0.052	13	354 / 07	quartz
3	0.130	60	350 / 60	quartz & calcite
4	0.037	16	354 / 19	quartz & calcite
5				
6				
7	0.021	0	174 / 00	calcite & quartz
8				
9	0.047	119	177 / 60	calcite & quartz
10	0.009	127	176 / 53	quartz & calcite
11				

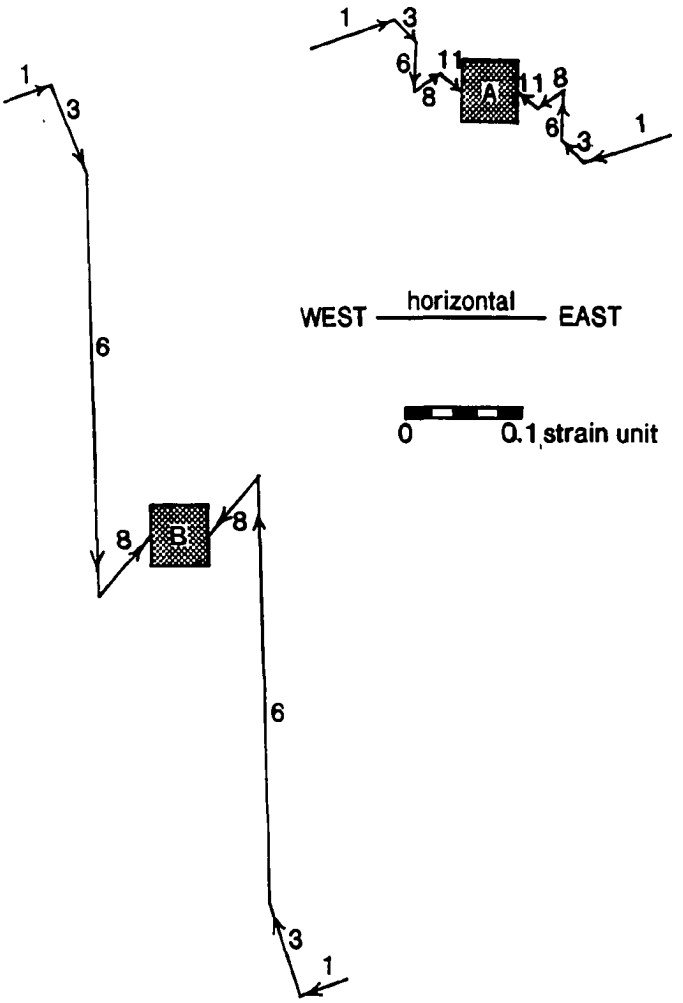

FIGURE 62. Incremental strain paths for the large and small pressure shadows in the subvertical east-northeast-striking plane of sample 87JZ16. (A) Large marcasite nodule of Figure 60. (B) Small marcasite nodule of Figure 59. Numbers refer to stages of fiber formation. The lengths of path segments are scaled to incremental strain values calculated for each segment.

TABLE 18. Comparison of incremental strains calculated by the rigid and deformable fiber models of Ramsay and Huber (1983) for the small pressure shadow in the subvertical east-northeast-striking plane of pre-Mississippian sample 87JZ16 (Figure 59).

FIBER MODEL VALUES FOR SMALL PRESSURE SHADOW			
STAGE	STRAIN UNITS RIGID	STRAIN UNITS DEFORMABLE	DIFFERENCE rigid - deformable
1	0.046	0.033	+ 0.013
2			
3			
4			
5	0.084	0.086	- 0.002
6	0.354	0.340	+ 0.014
7			
8	0.090	0.090	0
9			
10			
11			
TOTAL STRAIN	0.574	0.549	+ 0.025

TABLE 19. Comparison of incremental strains calculated by the rigid and deformable fiber models of Ramsay and Huber (1983) for the large pressure shadow in the subvertical east-northeast-striking plane of pre-Mississippian sample 87JZ16 (Figure 60).

FIBER MODEL VALUES FOR LARGE PRESSURE SHADOW			
STAGE	STRAIN UNITS RIGID	STRAIN UNITS DEFORMABLE	DIFFERENCE rigid - deformable
1	0.082	0.091	- 0.009
2			
3	0.027	0.027	0
4			
5			
6	0.042	0.047	- 0.005
7			
8	0.031	0.028	+ 0.003
9			
10			
11	0.024	0.025	- 0.001
TOTAL STRAIN	0.206	0.218	- 0.012

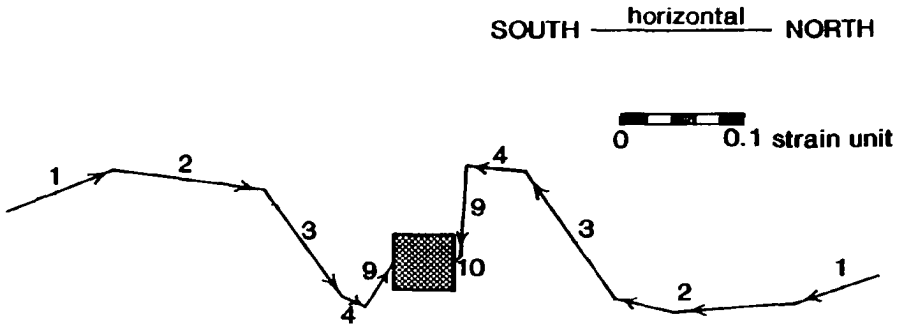

FIGURE 63. Incremental strain path for the pressure shadow in the subvertical north-northwest-striking plane of sample 87JZ16. Numbers refer to stages of fiber formation. The lengths of path segments are scaled to incremental strain values calculated for each segment.

TABLE 20. Comparison of incremental strains calculated by the rigid and deformable fiber models of Ramsay and Huber (1983) for the north side of the pressure shadow in the subvertical north-northwest-striking plane of pre-Mississippian sample 87JZ16 (Figure 61).

FIBER MODEL VALUES FOR NORTH SIDE OF PRESSURE SHADOW			
STAGE	STRAIN UNITS RIGID	STRAIN UNITS DEFORMABLE	DIFFERENCE rigid - deformable
1	0.095	0.068	+ 0.027
2	0.127	0.112	+ 0.015
3	0.119	0.125	- 0.006
4	0.022	0.026	- 0.004
5			
6			
7	0.021	0.026	- 0.005
8			
9	0.047	0.062	- 0.015
10			
11			
TOTAL STRAIN	0.431	0.419	+ 0.012

TABLE 21. Comparison of incremental strains calculated by the rigid and deformable fiber models of Ramsay and Huber (1983) for the south side of the pressure shadow in the subvertical north-northwest-striking plane of pre-Mississippian sample 87JZ16 (Figure 61).

FIBER MODEL VALUES FOR SOUTH SIDE OF PRESSURE SHADOW			
STAGE	STRAIN UNITS RIGID	STRAIN UNITS DEFORMABLE	DIFFERENCE rigid - deformable
1	0.075	0.043	+ 0.032
2	0.102	0.070	+ 0.032
	0.052	0.048	+ 0.004
3	0.140	0.146	- 0.006
4	0.052	0.063	- 0.011
5			
6			
7			
8			
9	0.082	0.109	- 0.027
10	0.009	0.014	- 0.005
11			
TOTAL STRAIN	0.512	0.493	+ 0.019

central fiber segments. The pressure shadows appear to exhibit a dominantly rigid fiber model geometry, given that quartz is the major mineral in each shadow, and that fiber isogons and shape of the pressure shadow peripheries mimic the outline of the central marcasite nodules.

F.2.b. Ellesmerian Sequence Sample

The paths of fiber orientation for eleven pressure shadows in the XZ-plane of Echooka Formation sample 87JZ45 (location "45" in Figures 15 and 33) are compiled in Figure 64, scaled to units of incremental strain and oriented in the plane. These quartz pressure shadows fringe euhedral pyrite crystals and are comprised of one to five fiber increments, with the angle between fibers and bedding in the sample ranging from 0 to 87 degrees. The rakes of fibers with respect to bedding are compiled in Table 22. Plotted in the histogram shown in Figure 65, these values form two populations, one subparallel to bedding and the other with a rake that is 20 to 60 degrees less steep than bedding.

Incremental strains were not calculated for each fiber segment because segments are short (generally less than 0.05 mm) and in places poorly-defined. Cumulative fiber lengths of these shadows range from 0.05 to 0.3 mm, with an average of roughly 0.06 mm. These cumulative lengths were used to calculate an approximate total strain using the rigid fiber model of Ramsay and Huber (1983). Total strains calculated for each pressure shadow range from 0.40 to 4.00 strain units, with an average total strain of 1.12 strain units. As evident from Table 22, total strains seem to be greater for quartz pressure shadows developed on only one side of pyrite crystals. Since the cumulative length of pressure shadow fibers is as long as or longer than the diameter of the pyrite crystals, total strains are of a much greater magnitude than those calculated for the Franklinian sequence shadows for which fiber lengths are much shorter than the diameter of the marcasite nodules (Figure 58, F.1.a. and F.1.b.).

F.3. ANALYSIS OF ANALYTICAL ERROR

The ultimate accuracy of incremental strain determinations is likely affected by some degree of error associated with sample preparation. In order to determine maximum extensile strain values for

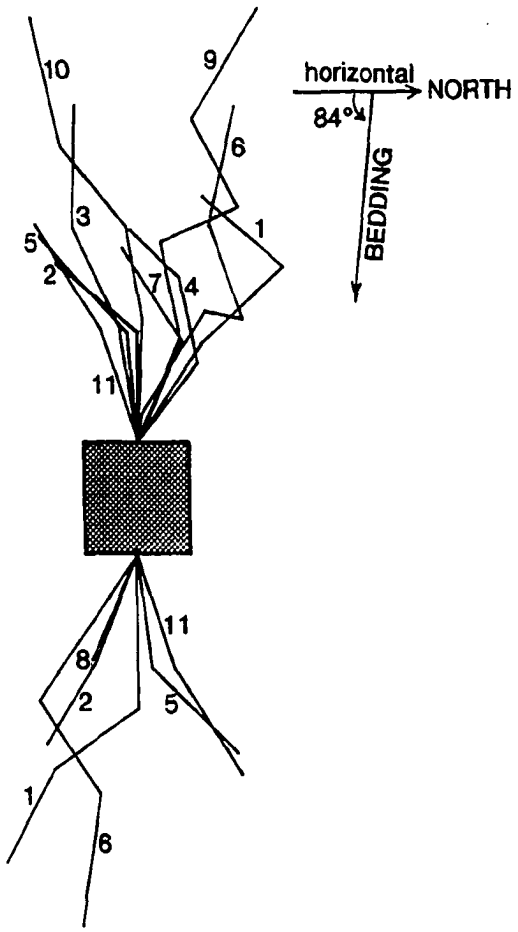

FIGURE 64. Orientation of pressure shadow fibers in the subvertical north-northwest-striking plane of Echooka Formation sample 87JZ45. Sample plane is vertical and strikes 333 degrees. Numbers identify the eleven shadows observed and are also used in Table 22. The length of fibers, totalling roughly 0.4 mm., is depicted schematically.

TABLE 22. Orientations of fibers relative to bedding and total strain values determined for eleven pressure shadows in the subvertical north-northwest-striking plane of sample 87JZ45 from the Echooka Formation (Figure 64).

ORIENTATION OF FIBER INCREMENTS (1 formed first; S0 = rake of bedding = - 82 or +98 degrees; A = S0 - RAKE; neg. A means rake is to N; pos. A means rake is to S at angle less steep than bedding)											
SHADOW	1		2		3		4		5		TOTAL
SIDE	rake	A	rake	A	rake	A	rake	A	rake	A	STRAIN
1 NORTH	38	- 50	- 42	40	- 55	27					0.75
1 SOUTH	- 61	21	- 35	47	90	08					0.44
2 NORTH	37	- 51	- 87	- 05							0.40 - 0.70
2 SOUTH	- 58	24	- 68	14							0.40
3 NORTH	- 88	- 06	52	- 46	70	- 28					1.84
4 NORTH	29	- 69	72	- 26	- 52	30					1.42
5 NORTH	33	- 65	72	- 26							0.75
5 SOUTH	44	- 54	73	- 25							0.85
6 NORTH	77	05	70	- 28	11	- 87	- 58	- 24			0.77 - 1.38
6 SOUTH	- 80	02	53	- 45	- 55	27					0.77 - 1.05
7 NORTH	56	- 42	- 64	18							1.00 - 1.25
8 SOUTH	- 65	17									2.67 - 4.00
9 NORTH	- 58	24	61	- 37	- 22	60	78	- 20	- 67	15	0.40 - 1.60
10 NORTH	77	- 21	48	- 50	80	- 18	- 82	0			2.40
11 NORTH	56	- 42	61	- 37							1.00 - 1.25
11 SOUTH	55	- 43	72	- 26							0.75
									AVERAGE TOTAL STRAIN		1.12

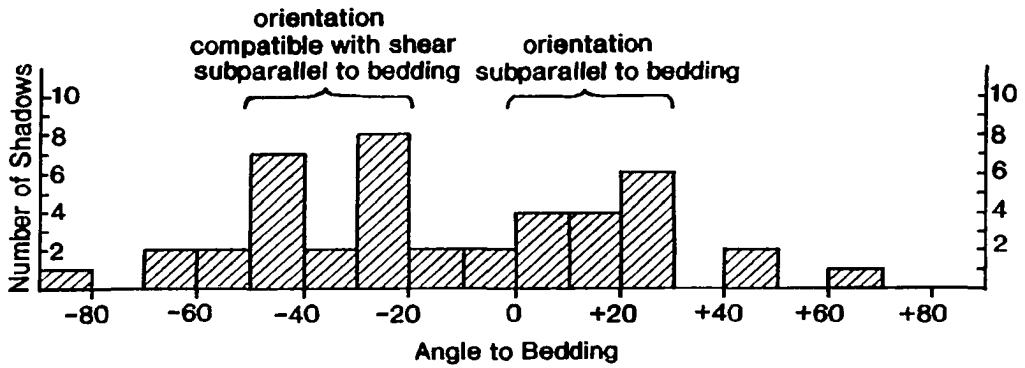

FIGURE 65. Histogram of fiber angles with respect to bedding for Echooka Formation sample 87JZ45. Two subpopulations of fiber orientations were observed in the eleven shadows analyzed: one oriented subparallel to bedding, and the other oriented at an angle of 20-40 degrees to bedding, compatible with shear subparallel to this surface.

pressure shadows formed during Cenozoic deformation, thin-section planes must be oriented so as to correspond to one of the principal planes through the Cenozoic tectonic strain ellipsoid. Assuming that the absolute orientation of one of these planes was measured in the field, some error is associated with estimating the orientations of the other two mutually-perpendicular planes from partial data (such as lineation) using a stereographic solution method. Even if planes are accurately oriented, it can be difficult to cut thin-section chips precisely. For example, if the east-northeast-striking plane of sample 87JZ16 were oriented more accurately or cut more precisely, the pressure shadows shown in Figures 59 and 60 probably would be symmetrically developed on both sides of the marcasite nodule. It is estimated that the strikes and dips of the thin-section planes could deviate from the true orientation of the strain ellipsoid planes by up to 10-15 degrees. Second, establishing accurate orientations (rakes) of pressure shadow fibers in the thin-section plane requires accurate determination of the trend and plunge of the edges of the thin-section. Thin-sections were cut such that their edges corresponded to the X-, Y-, or Z-axis of the Cenozoic tectonic strain ellipsoid defined by the intersection of two of the three mutually-perpendicular principal planes of the strain ellipsoid. Error in the orientation of the thin-section edges would be proportional to the error associated with accurate orientation of the thin-section plane.

Additional analytical error is associated with calculating incremental strain values from pressure shadow data. Imprecise measurement of fiber rake, the relative angle between adjacent fibers, fiber length, or diameter of the central rigid body will cause strain values calculated by either the rigid or deformable fiber models of Ramsay and Huber (1983) to be imprecise, also. In addition, it is possible that fiber orientations do not reflect the orientation of the strain ellipsoid during deformation. As shown in Figure 66, Ramsay and Huber (1983) distinguish between displacement-controlled and face-controlled fiber types. Strain histories cannot be determined from the orientation of face-controlled fibers which develop perpendicular to the margin of the rigid body. Failure to exclude all face-controlled fiber data will lead to erroneous incremental strain calculations.

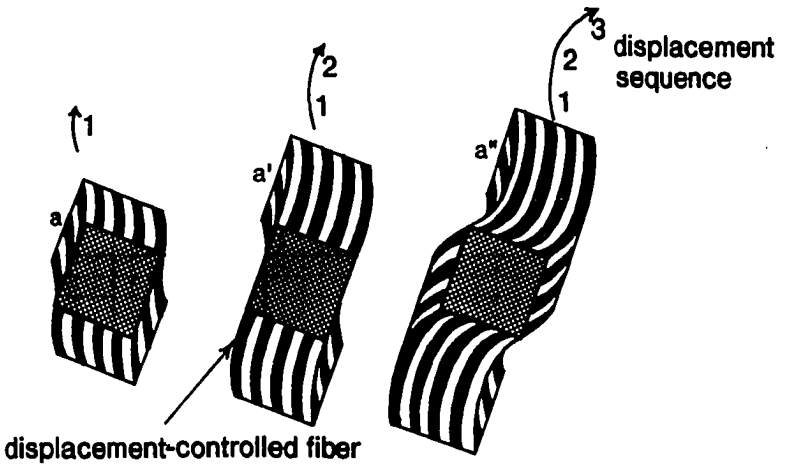

A. Development of a pressure shadow around an euhedral rigid crystal. The fibers are displacement controlled; those originally formed along the wall of the crystal at (a) are slid along the wall to (a') and at the end stages are isolated from the wall on which they formed at (a") (Ramsay and Huber, 1983).

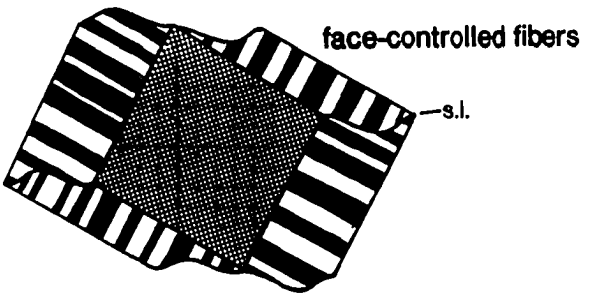

B. Geometric form of face-controlled fibers. The suture line (s.l.) between differently oriented face-controlled fiber groups can be used to determine the displacement history (Ramsay and Huber, 1983).

FIGURE 66. Pressure shadow fiber types identified by Ramsay and Huber (1983).

Finally, it is likely that some error results from applying a rigid fiber model to the mixed-mineralogy fibers of the Franklinian sequence pressure shadows. These pressure shadows satisfy the criteria for the rigid fiber model with the exception that first-formed fibers tend to be longer than last-formed fibers. Since the incremental strains calculated by rigid and deformable fiber models differ by 1.4-3.8% of the total strain in the sample, an error of 1-4% would result if all fibers were deformable rather than rigid. If these pressure shadows are composite, composed of both rigid quartz and deformable chlorite and calcite fibers, incremental strains are likely in error by less than 3.8% of the total strain.

F.4. INTERPRETATIONS AND SPECULATIONS

F.4.a. Franklinian Sequence: Pressure Shadow in North-Northwest-Striking Plane

This pressure shadow is subdivided into five major segments which correspond to strain increments 1, 2, 3, 4, and 9 (Table 17, Figures 61 and 63). Each segment is designated as a stage which bears the number of the corresponding strain increment. As described in Section 7, pressure shadows in sample 87JZ16 are inferred to have formed during Cenozoic deformation, perhaps in association with emplacement of the thrust sheets which comprise the Franklin Mountains anticlinorium.

To provide a possible explanation for the progressive change in fiber orientation for this pressure shadow, it is necessary to consider what sort of strain pattern may have existed at various structural positions and evolutionary stages during the formation of the anticlinorium. As shown in Figure 67, Sanderson (1982) has modeled the strain variation in a thrust sheet as it is emplaced over a footwall ramp and forms a fault-bend fold at its leading edge. The balanced cross-section model for the evolution of the Franklin Mountains anticlinorium incorporates elements of both of Sanderson's (1982) "bending fold" and "flexural-slip" models: Bed thickness is maintained and folds are assumed to have formed by flexural-slip parallel to bedding, in accordance with Sanderson's (1982) flexural-slip model. However, in order to balance the cross-section which models the geometry prior to emplacement of the second horse (Figure

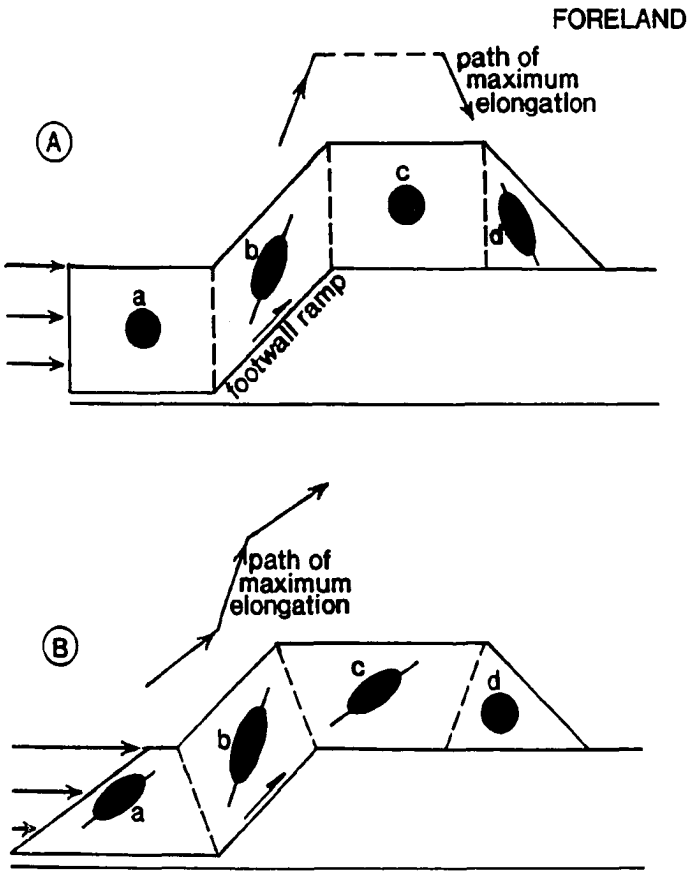

FIGURE 67. Models modified from Sanderson (1982) for the pattern of strain developed in a thrust sheet above a footwall ramp. (A) Bending model. (B) Flexural slip model. The path of maximum elongation represents the strain path that might be recorded by a marker displaced through zones (a) to (d) as a consequence of passively draping a thrust sheet over the footwall in (A), or actively displacing it up a footwall ramp, accompanied by interbed slip (B).

32), it was necessary to impose bed-parallel extension in the leading edge of this first thrust sheet. Thus, an element of Sanderson's (1982) bending model is inferred in the structural geometry modeled in Figure 30.

In view of Sanderson's (1982) models, Stages 1, 2, 3, and 4 could have formed as the first thrust sheet moved up the footwall ramp, across a footwall flat, and was bent, forming a fault-bend fold at its leading edge (Figures 63 and 67). Reflected by pressure shadow incremental strain calculations (Tables 20 and 21), extensile strains associated with movement of the first horse up the ramp (Stage 1), across a flat (Stage 2), and fault-bend folding (Stages 3 and 4) would be 8%, 5-11%, and 13%, respectively.

The final stage in the evolution of the pressure shadow in the north-northwest-striking plane may be related to the last major deformational movement these rocks experienced. Sample 87JZ16 is located toward the hinterland of the fault-bend fold developed in the second horse (Figure 30). Given the structural position of the sample and the geometry modeled, the last major movement of sample 87JZ16 may have occurred when the second horse was displaced up a footwall ramp, carrying the first horse piggyback. The second horse is not interpreted to have moved any appreciable distance along a footwall flat above the Kekiktuk Conglomerate (Figure 30). The orientation of the last-formed, Stage 9 fibers is consistent with the orientation of the direction of principal elongation in a thrust sheet above a footwall ramp in both of Sanderson's (1982) models. The incremental strain calculated from this pressure shadow suggests that 5% extensile strain may be associated with this last recorded movement (Tables 20 and 21).

F.4.b. Franklinian Sequence: Pressure Shadows in East-Northeast-Striking Plane

The small pressure shadow in the east-northeast-striking plane of sample 87JZ16 (location "16" in Figures 15 and 30) is subdivided into four segments which correspond to strain increments 1, 3, 6, and 8 (Table 15, Figures 59 and 62). The large pressure shadow in the same plane is subdivided into five segments which correspond to strain increments 1, 3, 6, 8, and 11 (Table 16, Figures 60 and 62). Each

of these strain increments is designated as a stage which bears the number of the corresponding strain increment. The gentle east rake of Stage 1 may be a consequence of initial uplift of Franklinian sequence rocks of the first horse in which the sample lies. Stages 3 (or 5) and 6 may record subvertical extension developed in the hangingwall above a lateral ramp (Butler, 1982) (Figure 68). Such transport-normal displacements could have occurred in the first horse as it was flexed above the moderately west-plunging lower antiform which is interpreted to have evolved in the second horse during its emplacement (Figure 68).

F.4.c. Ellesmerian Sequence Sample

As shown in Figure 64, quartz fibers near the periphery of the pressure shadows and those in contact with the central pyrite crystals are generally subparallel to compositional layering in the north-northwest-striking plane of Echooka Formation sample 87JZ45 (location "45" in Figures 15 and 33). The orientations of these earliest- and latest-formed fibers are compatible with compression normal to bedding (or extension parallel to bedding). The earliest bedding-parallel fibers could have formed during compaction and diagenesis in Permo-Triassic or later time. It is also possible that elongation subparallel to bedding occurred in association with Cenozoic thrust faulting. A prominent thrust fault in the vicinity of sample 87JZ45 dips moderately to the southeast, and bedding dips steeply in the same direction. As shown in Figure 69, maximum elongation subparallel to bedding would be expected for a gently- to moderately-dipping fault plane which dips approximately 60 degrees less steeply than bedding.

Quartz fibers in the central portion of these pressure shadows have various orientations (Figure 64); however, a number of north-raking fibers are oriented at 30 to 60 degrees (average of 50-55 degrees) to compositional layering (Figures 64 and 65). As shown in Figures 65 and 69, fibers at an approximate orientation of 60 degrees to compositional layering are compatible with bedding-parallel shear. A sheared crinoid stem found in calcareous shale near the location of sample 87JZ45 supports such a microscopic kinematic interpretation. Since slip occurs between bedding planes in association with flexural folding,

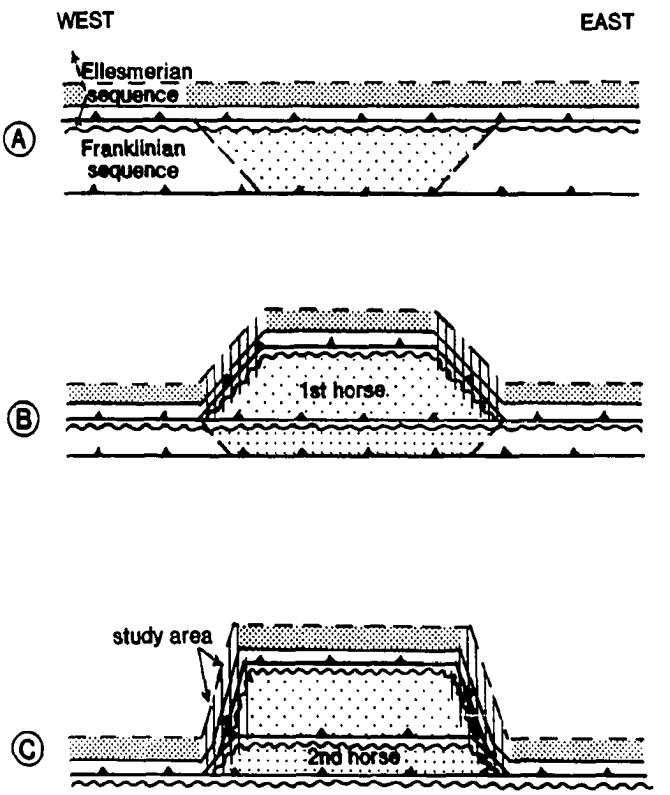

FIGURE 68. Schematic model adapted from Butler (1982) for inducing subvertical extension in the hangingwall during emplacement of underlying thrust sheets. Viewing direction is parallel to the direction of tectonic transport. (A) Geometry prior to emplacement of the first horse. (B) The first horse is emplaced. (C) The second horse is emplaced beneath the first horse. In (B) and (C) subvertical extension occurs above a lateral ramp, in pre-Mississippian and Mississippian and younger rocks which form the east- and west-dipping walls of the evolving culmination.

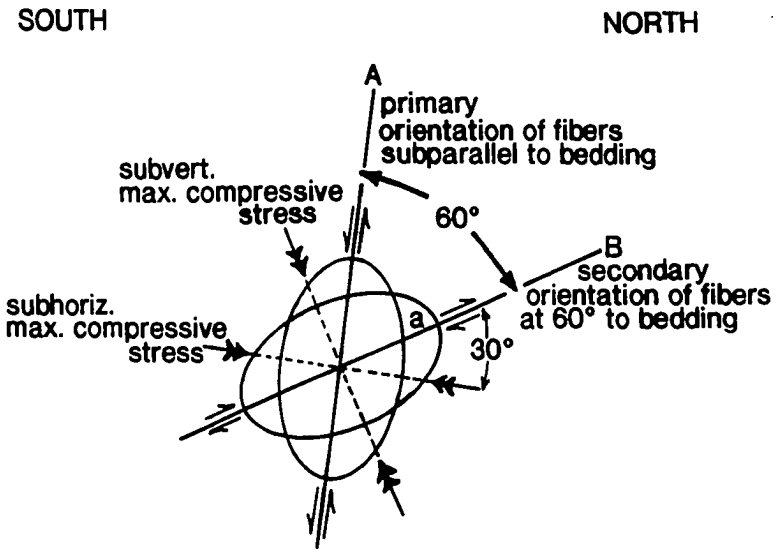

FIGURE 69. Possible explanation for the orientation of fibers in sample 87JZ45. Bedding in this sample dips to the south at 84 degrees. The primary orientation (A) of fibers in the pressure shadows is subparallel to bedding. A subpopulation of fibers (B) dips to the south, at an angle of roughly 60 degrees to (A). The orientation of the strain ellipse associated with the formation of fibers of orientation (B) is compatible with a subvertical maximum compressive stress. One of the theoretical shear planes, (a), corresponds to the orientation of bedding depicted by fibers of orientation (A). Thus, fibers at 60 degrees to bedding may have formed as a consequence of bedding-parallel shear induced by a subvertical, rather than a subhorizontal, maximum compressive stress.

incremental strain analysis may suggest that folds in the vicinity of sample 87JZ45 formed by a flexural-slip mechanism.

APPENDIX G. FINITE STRAIN ANALYSIS

G.1. EXPLANATION OF ANALYTICAL METHODS

Two basic methods of finite strain analysis were applied to thin-sections prepared from the bedding-parallel, east-northeast-striking, and north-northwest-striking planes of three oriented samples from the Kekiktuk Conglomerate and one sample from the Ivishak Formation (Figure 15). A center-to-center strain determination technique, known as the Fry method, was used to determine the strain ellipse shape and orientation from the redistribution of points representing the centers of quartz grains in quartzite and quartz sandstone samples. The phi-R_f technique was applied to the same thin-sections to determine the shape and orientation of the tectonic strain ellipse superimposed upon initially subelliptical grains. Since both methods yielded the same sort of data, it was possible to investigate the similarity of results obtained by two methods of finite strain determination. However, replicate samples were not analyzed and, therefore, the reproducibility of results obtained by either method cannot be demonstrated.

G.1.a. Fry Method

A graphical center-to-center technique developed by Fry (1979) analyzes the geometric pattern of grain centers produced by deformation of a rock body. In addition to the original presentation by Fry (1979) and discussion by Ramsay and Huber (1983), the Fry method has been tested, applied, and evaluated by Ribeiro et al. (1983), Lacassin and van den Driessche (1983), Crespi (1986), Onasch (1986), and Erslev (1988).

The Fry method requires that the surface to be evaluated is comprised of a statistically uniform distribution of grains in which there is a random spatial distribution of grain center-points and a relatively constant distance between points in an undeformed aggregate. Since mineral grains in a rock body usually have a characteristic initial size, a statistically uniform distribution is typically produced due to the fact that center-points of grains cannot be closer together than twice the grain radius. The spatial distribution of grain center-points which neighbor a given center-point is a function of the average

particle size and how closely the grains of the aggregate are packed. Deformation modifies the distance between grain center-points. In principle, when an aggregate of uniformly-distributed grains is deformed, the greatest separation of grain center-points is parallel to the long axis of the strain ellipse, and the minimum distance between center-points is parallel to the short axis of the strain ellipse (Ramsay and Huber, 1983). The distance between two center-points is a reflection of the longitudinal strain in this direction which is, in turn, a function of the strain ellipse orientation and dimensions in that plane (Ramsay and Huber, 1983).

The Fry method can be done by hand or, more efficiently, utilizing a computer program such as that developed by Erslev (1988). The basic procedure is as follows: (1) On a basemap, mark the location of center-points of all grains in the sample plane. (2) Create an overlay with a central reference point. (3) Keeping the azimuth of the overlay constant, place the central reference point over each center-point and mark on the overlay the locations of all other grain center-points (Ramsay and Huber, 1983). As shown in Figure 70, the Fry method produces a graphical plot which is characterized by a vacancy of points developed around the central reference point due to the fact that particles cannot lie closer together than the sum of their radii. A circular vacancy field is developed when center-to-center distances are the same in all directions from the reference point, indicating that the aggregate has not been strained. An elliptical vacancy field indicates that the aggregate has been strained, and its shape and orientation correspond to the shape and orientation of the strain ellipse.

G.1.b. Normalized Fry Method

The concept of a normalized Fry method is proposed by Erslev (1988). Erslev (1988) points out that, in a given thin-section plane, the actual three-dimensional center-points of most grains are not intersected. Apparent center-to-center distances are true center-to-center distances only when the three-dimensional center-points of grains are intersected by the thin-section plane. Erslev (1988) suggests that the Fry method could better determine strain ellipse shape and orientation if center-to-center distances

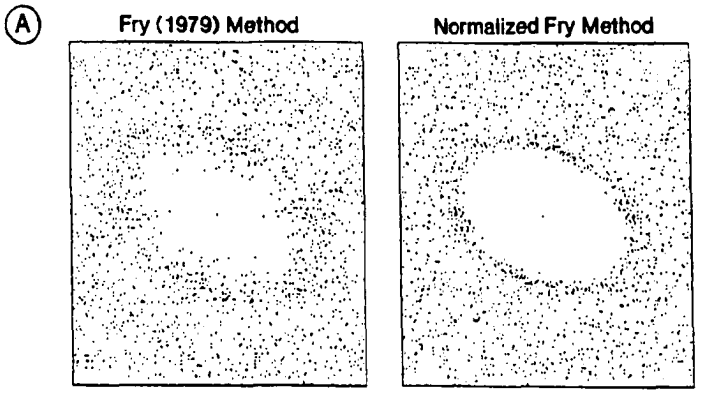

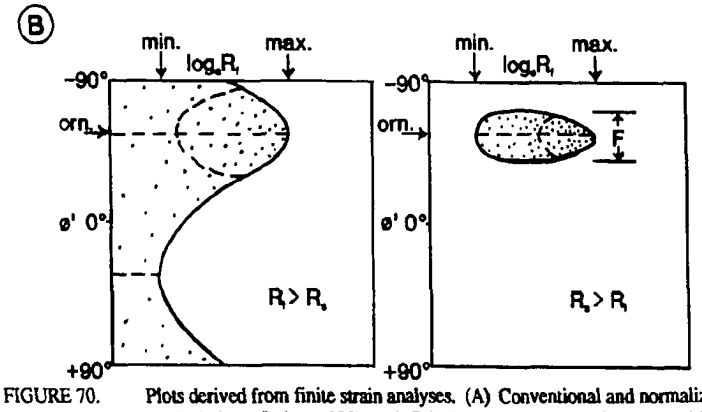

FIGURE 70. Plots derived from finite strain analyses. (A) Conventional and normalized Fry method plots (Erslev, 1988). (B) Principle features of R_f/ϕ' plots used for computing the strain R_S (Ramsay and Huber, 1983). The orientation of the major axis of the strain ellipse in sample plane, ø', is defined by "orn." in the plots. R_S is the ellipticity of the tectonic strain ellipse. R_f and R_i correspond to the ellipticities of markers following and prior to superimposing R_S, respectively. F represents the fluctuation in values of ø' in the sample plane. The minimum and maximum final marker ellipticities are defined by the positions of "min." and "max."

are divided by the sum of grain radii, eliminating the variable of grain size. Such normalized center-to-center distances decrease toward one as grains become closer together; for grains that touch each other the normalized center-to-center distance is equal to one, regardless of grain radii. Comparing the conventional and normalized Fry method plots shown in Figure 70 it is evident that normalization produces a more sharply-defined vacancy field, making interpretation of strain ellipse shape and orientation less subjective than when the conventional Fry method is used. Erslev (1988) does not identify or discuss error introduced by the normalization process.

G.1.c. Phi-R_f Technique

The phi-R_f technique, introduced by Ramsay (1967), can be used to measure finite strain recorded on a surface which contains marker objects of an initially elliptical shape. This technique has been applied by Dunnet (1969) and others, and is outlined by Ramsay and Huber (1983). In theory, the observed elliptical marker shape, R_f, is produced as a result of superimposing a homogeneous tectonic strain on a marker with an initially elliptical shape, R_i. The shape of the final object ellipse (R_f) is a function of the shape and orientation of both the initial object ellipse (R_i) and the strain ellipse (R_s). In addition, ductility contrasts between markers and matrix can influence the final marker shapes; however, a high ratio of grains to matrix reduces this effect. A ductile matrix typically records more deformation than do relatively competent marker grains (Dunnet, 1969). For closely-packed aggregates, ductility contrasts probably do not influence finite strain determinations significantly.

Finite strain determination by the phi-R_f technique involves measuring the ellipticity, R_f, and the orientation, Ø', of the deformed marker objects on a given surface. Data are analyzed graphically by plotting R_f versus Ø', with Ø' having values of 90 to -90 degrees. The maximum initial marker ellipticity, $R_{i\,max}$, and R_s can be calculated from graphical determination of (1) the relationship between

R_i and R_s, (2) maximum and minimum R_f values, and (3) the range of orientation of ellipse long axes, termed the fluctuation, F (Figures 70 and 71). Equations necessary for such calculations are given in section G.4.e.

As shown in Figure 71, the shape of R_f versus Ø' plots is dependent on the relationship between R_s, R_f, and R_i. For an unstrained sample consisting of randomly oriented markers of a constant initial ellipticity, the plot of R_f versus Ø' is linear with F = 180 degrees (Figure 71A). Imposing a homogeneous strain causes the long axes of the marker objects to rotate toward the orientation of the long axis of the strain ellipse, with data points tending to cluster around Ø' of the strain ellipse. In Figure 73B, the ellipticity of the strain ellipse (R_s) is less than that of the initial object (R_i), and F = 180 degrees. In this case, data points define a bell-shaped curve which is centered on a Ø' value which corresponds to the orientation of the major axis of the strain ellipse. In Figure 71C, where the ellipticity of the strain ellipse (R_s) is greater than that of the initial object (R_i), the R_f versus Ø' plot closes and F decreases to less than 90 degrees. As shown in Figure 71 (B and C), markers with long axes initially oriented parallel and perpendicular to the long axis of the strain ellipse have final ellipticities which are greater and less than that of the strain ellipse, respectively. Plotted R_f values range between minimum and maximum values which are defined by initial marker ellipse long axis orientations perpendicular and parallel to the long axis of the strain ellipse, respectively.

G.2. ANALYTICAL PROCEDURE

Fry, normalized Fry, and phi-R_f analyses were completed for the XY-, YZ-, and XZ-planes of four samples using an IBM-compatible integrated fabric analysis program, INSTRAIN 2.2, developed and copyrighted by Eric Erslev of Colorado State University. Each sample plane was prepared for analysis as follows: (1) Grain outlines were traced from representative photomicrographs of each thin-section. (2)

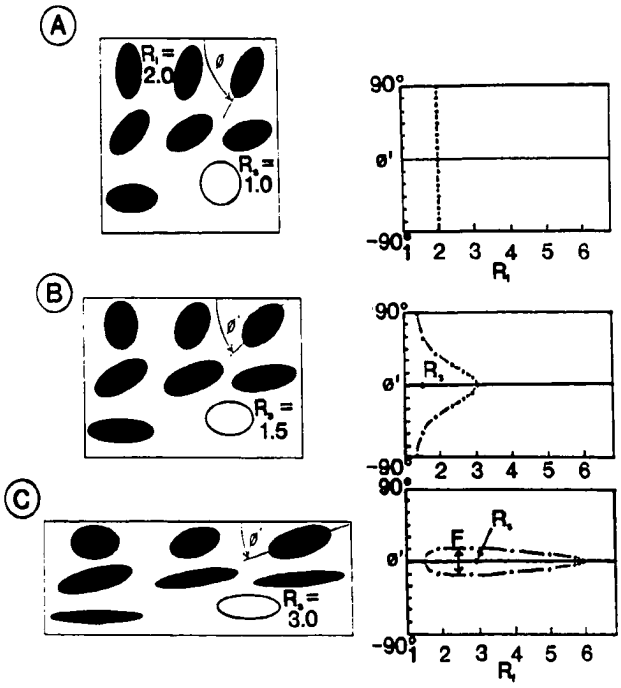

FIGURE 71. Effect of progressive deformation (A-C) on a series of elliptical objects with an initial orientation Ø and ellipticity R_i (Ramsay and Huber, 1983). After deformation, characterized by a strain ellipse of ellipticity R_s, the original marker ellipses change shape (final ellipticity R_f) and orientation (final orientation Ø'). F is the fluctuation.

The approximate center-points for an average of 177 adjacent grains were marked on these bases. (3) In addition to the center-points, the four end-points of the long and short axes of the characteristically subelliptical grains were located. (4) Basemaps were digitized, determining the x- and y- Cartesian coordinates of the center and four axis end-points for each grain. (5) Digitized data were used with the Fry, normalized Fry, and phi-R_f options of INSTRAIN 2.2.

G.3. RESULTS

Figures 72-83 contain INSTRAIN 2.2 plots generated for each sample plane using the Fry method and phi-R_f technique.

G.3.a. Fry Method

Table 23 compares strain ellipse shape and orientation data obtained for each sample by conventional and normalized Fry method options of INSTRAIN 2.2. Average ellipticities determined by the conventional and normalized Fry methods were R = 1.20 and R = 1.18, respectively. In 7 of the 12 cases, the ellipticity determined by the normalized Fry method exceeded that determined by the conventional Fry method. Averages of 23.9% and 14.1% error were associated with the determination of strain ellipse shape and orientation by conventional and normalized Fry methods, respectively. Given its apparently better accuracy, only data obtained from the normalized Fry method were further analyzed.

Table 24 records the number of grains analyzed for each sample, R, Ø (in relation to horizontal with positive values for relative counterclockwise rotation), percent error, and the trend and rake of ellipse long axes (determined stereographically from the known orientation of the sample planes provided in Figures 72-83, and the rake of the axis in each plane). Strain ellipse shape and orientation determined by the normalized Fry method for the plane subparallel to bedding are plotted on a geologic map (Figure 84). Similar data for the east-northeast-striking plane are plotted on an east-west schematic cross-section (Figure 85), and data for the north-northwest-striking plane are plotted on a north-south balanced cross-section (Figure 86).

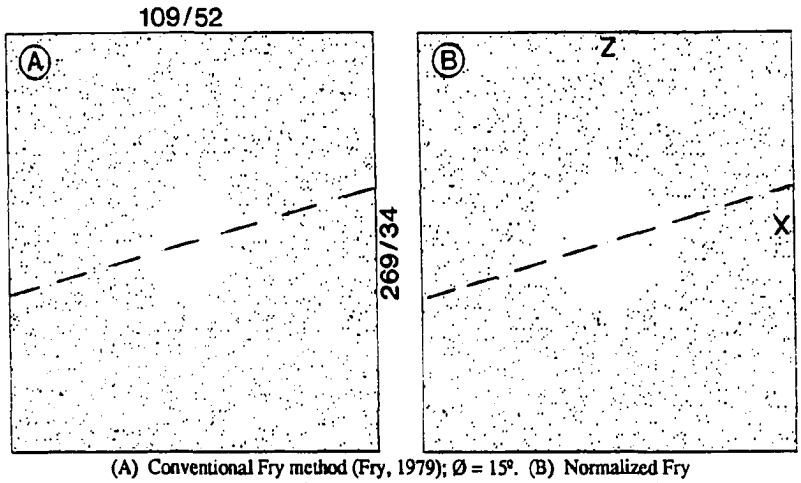

(A) Conventional Fry method (Fry, 1979); Ø = 15°. (B) Normalized Fry method (Erslev, 1988); Ø = 16°. In (A) and (B), dashed lines define Ø, determined by INSTRAIN 2.2; selection factor = 1.00; sample size = 160 grains. Orientations of thin-section edges are given. This is the XZ-plane of the strain ellipsoid determined for the sample.

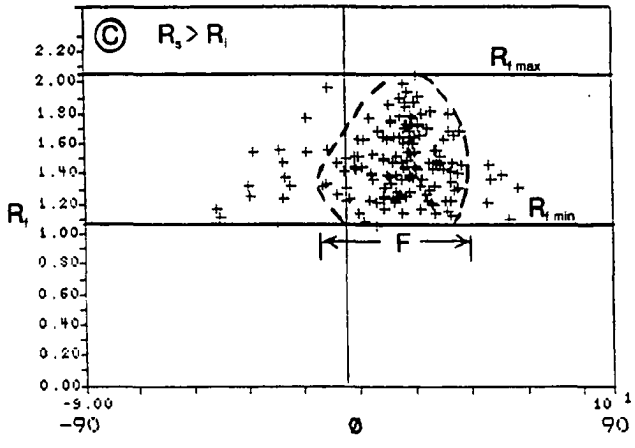

(C) Phi-R_f technique (Ramsay, 1967); Ø = 17°, determined by INSTRAIN 2.2. Plot interpreted by visual inspection.

FIGURE 72. Interpreted finite strain plots for the bedding-parallel plane of Kekiktuk Conglomerate sample 87JZ25. Sample plane strikes 96 degrees and dips 80 degrees to the northwest. Sample location is shown in Figures 15 and 30.

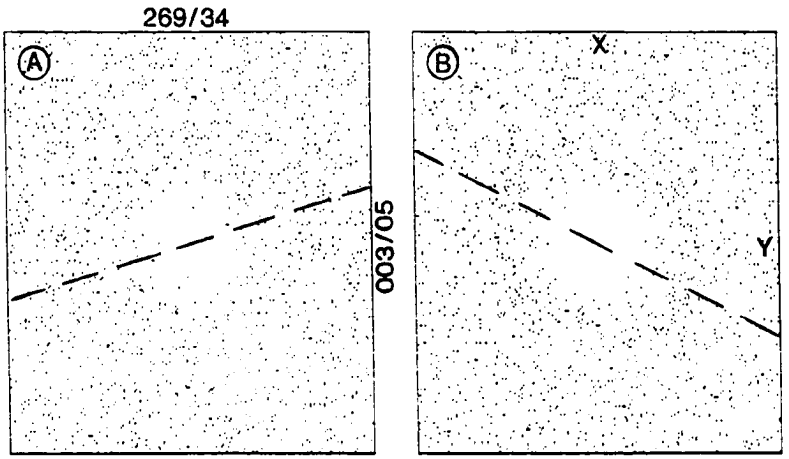

(A) Conventional Fry method (Fry, 1979); Ø = 16°. (B) Normalized Fry method (Erslev, 1988); Ø = -25°. In (A) and (B), dashed lines define Ø, determined by INSTRAIN 2.2; selection factor = 0.95; sample size = 146 grains. Orientations of thin-section edges are given. This is the XY-plane of the strain ellipsoid determined for the sample.

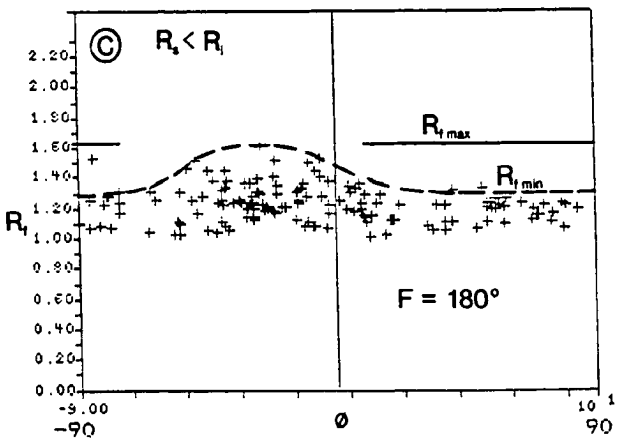

(C) Phi-R_f technique (Ramsay, 1967); Ø = -8°, determined by INSTRAIN 2.2. Plot interpreted by visual inspection.

FIGURE 73. Interpreted finite strain plots for Kekiktuk Conglomerate sample 87JZ25. Sample plane strikes 8 degrees and dips 34 degrees to the northwest. Sample location is shown in Figures 15 and 30.

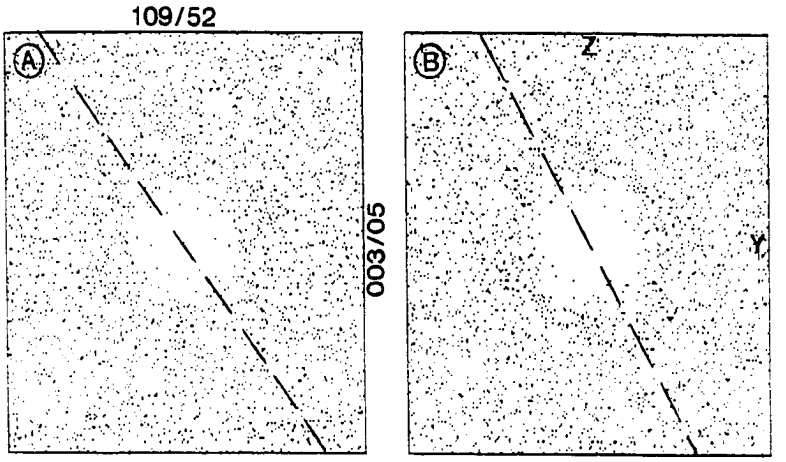

(A) Conventional Fry method (Fry, 1979); Ø = -53°. (B) Normalized Fry method (Erslev, 1988); Ø = -61°. In (A) and (B), dashed lines define Ø, determined by INSTRAIN 2.2; selection factor = 0.95; sample size = 224 grains. Orientations of thin-section edges are given. This is the YZ-plane of the strain ellipsoid determined for the sample.

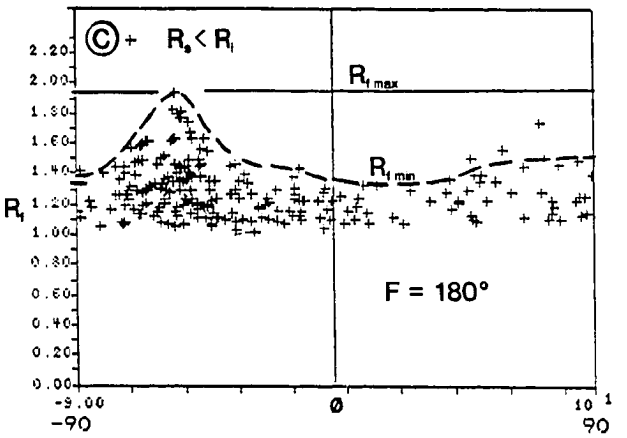

(C) Phi-R_f technique (Ramsay, 1967); Ø = -27°, determined by INSTRAIN 2.2. Plot interpreted by visual inspection.

FIGURE 74. Interpreted finite strain plots for the north-striking plane of Kekiktuk Conglomerate sample 87JZ25. Sample plane strikes north and dips 56 degrees to the east. Sample location is shown in Figures 15 and 30.

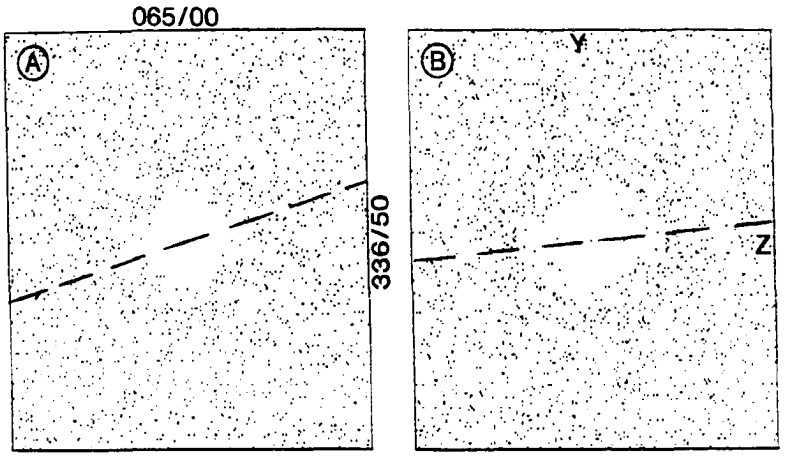

(A) Conventional Fry method (Fry, 1979); Ø = 12°. (B) Normalized Fry method (Erslev, 1988); Ø = 5°. In (A) and (B), dashed lines define Ø, determined by INSTRAIN 2.2; selection factor = 0.95; sample size = 130 grains. Orientations of thin-section edges are given. This is the YZ-plane of the strain ellipsoid determined for the sample.

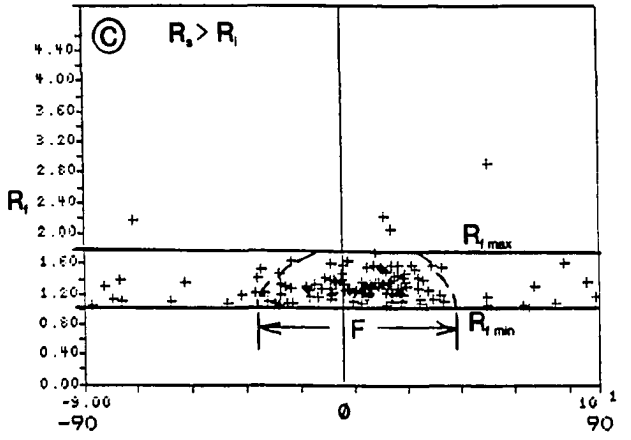

(C) Phi-R_f technique (Ramsay, 1967); Ø = 5°, determined by INSTRAIN 2.2. Plot interpreted by visual inspection.

FIGURE 75. Interpreted finite strain plots for bedding-parallel plane of Kekiktuk Conglomerate sample 87JZ31. Sample plane strikes 65 degrees and dips 50 degrees to the northwest. Sample location is shown in Figures 15 and 30.

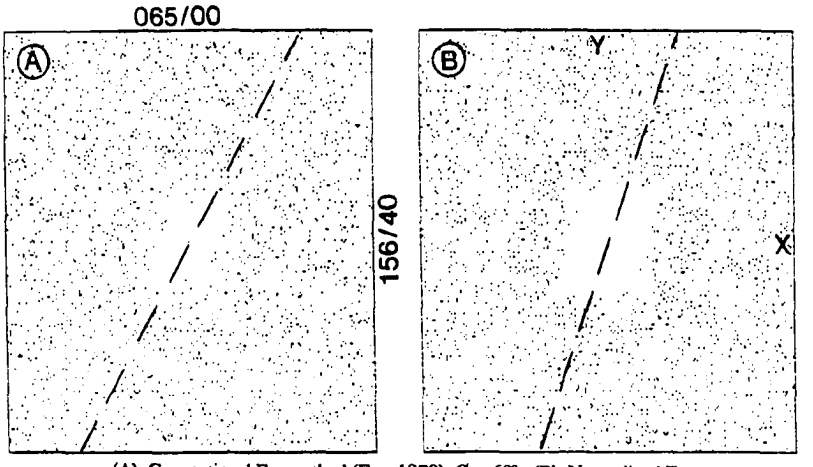

(A) Conventional Fry method (Fry, 1979); Ø = 60°. (B) Normalized Fry method (Erslev, 1988); Ø = 70°. In (A) and (B), dashed lines define Ø, determined by INSTRAIN 2.2; selection factor = 0.95; sample size = 150 grains. Orientations of thin-section edges are given. This is the XY-plane of the strain ellipsoid determined for the sample.

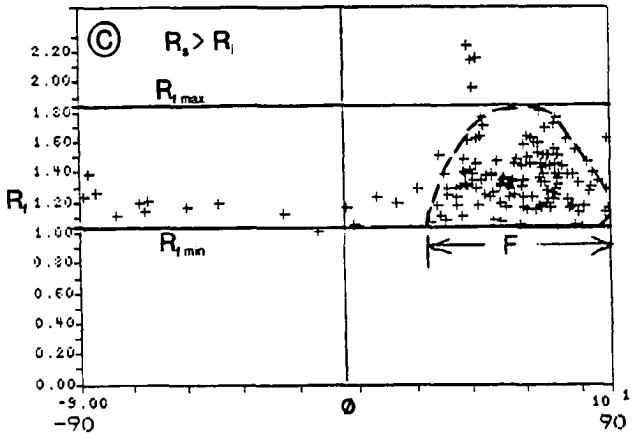

(C) Phi-R_f technique (Ramsay, 1967); Ø = 49°, determined by INSTRAIN 2.2. Plot interpreted by visual inspection.

FIGURE 76. Interpreted finite strain plots for east-northeast-striking plane of Kekiktuk Conglomerate sample 87JZ31. Sample plane strikes 65 degrees and dips 40 degrees to the southeast. Sample location is shown in Figures 15 and 30.

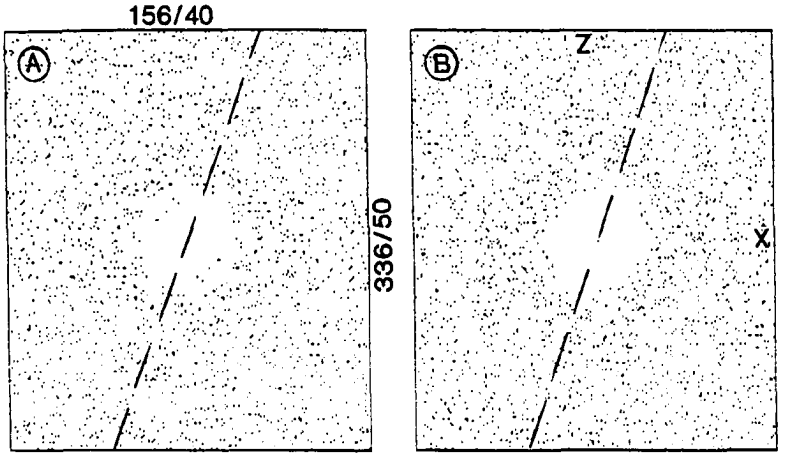

(A) Conventional Fry method (Fry, 1979); Ø = 68°. (B) Normalized Fry method (Erslev, 1988); Ø = 70°. In (A) and (B), dashed lines define Ø, determined by INSTRAIN 2.2; selection factor = 0.95; sample size = 133 grains. Orientations of thin-section edges are given. This is the XZ-plane of the strain ellipsoid determined for the sample.

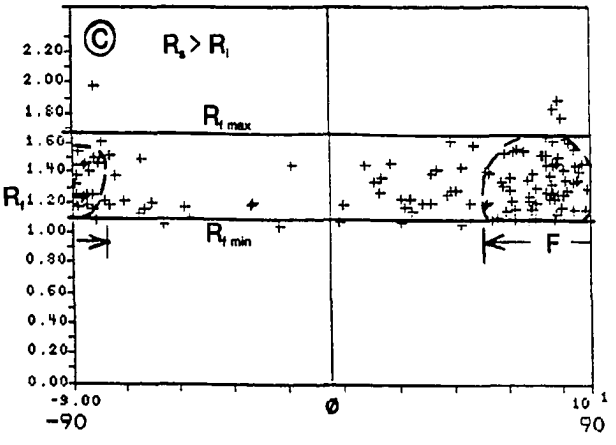

(C) Phi-R_f technique (Ramsay, 1967); Ø = 18°, determined by INSTRAIN 2.2. Plot interpreted by visual inspection.

FIGURE 77. Interpreted finite strain plots for the north-northwest-striking plane of Kekitkuk Conglomerate sample 87JZ31. Sample plane is vertical and strikes 336 degrees. Sample location is shown in Figures 15 and 30.

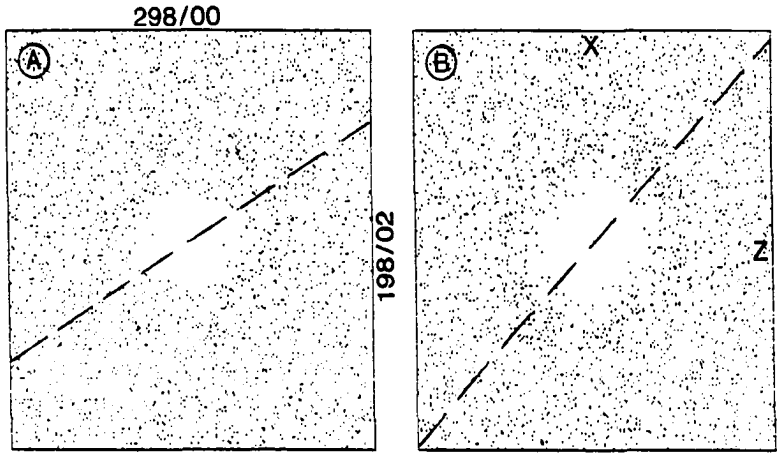

(A) Conventional Fry method (Fry, 1979); Ø = 31°. (B) Normalized Fry method (Erslev, 1988); Ø = 46°. In (A) and (B), dashed lines define Ø, determined by INSTRAIN 2.2; selection factor = 1.00; sample size = 225 grains. Orientations of thin-section edges are given. This is the XZ-plane of the strain ellipsoid determined for the sample.

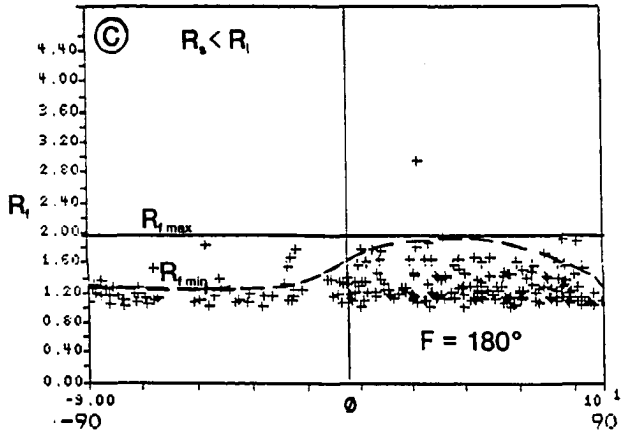

(C) Phi-R_f technique (Ramsay, 1967); Ø = 20°, determined by INSTRAIN 2.2. Plot interpreted by visual inspection.

FIGURE 78. Interpreted finite strain plots for the bedding-parallel plane of Kekiktuk Conglomerate sample 87JZ36. Sample plane strikes 118 degrees and dips 2 degrees to the southwest. Sample location is shown in Figures 15 and 30.

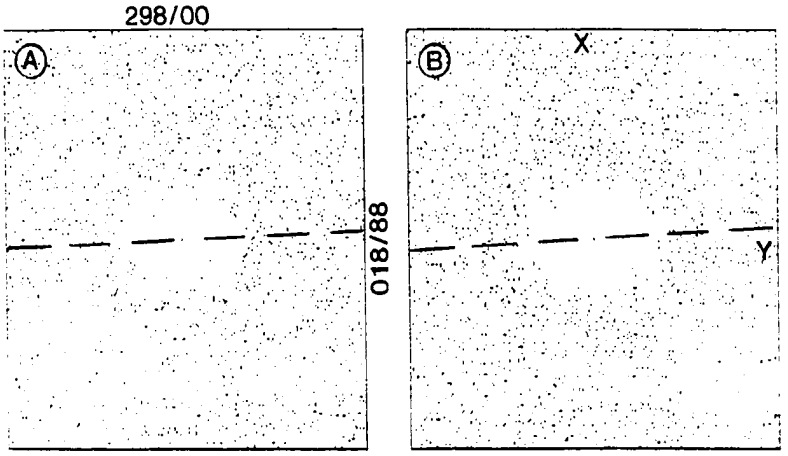

(A) Conventional Fry method (Fry, 1979); Ø = 2°. (B) Normalized Fry method (Erslev, 1988); Ø = 3°. In (A) and (B), dashed lines define Ø, determined by INSTRAIN 2.2; selection factor = 1.00; sample size = 201 grains. Orientations of thin-section edges are given. This is the XY-plane of the strain ellipsoid determined for the sample.

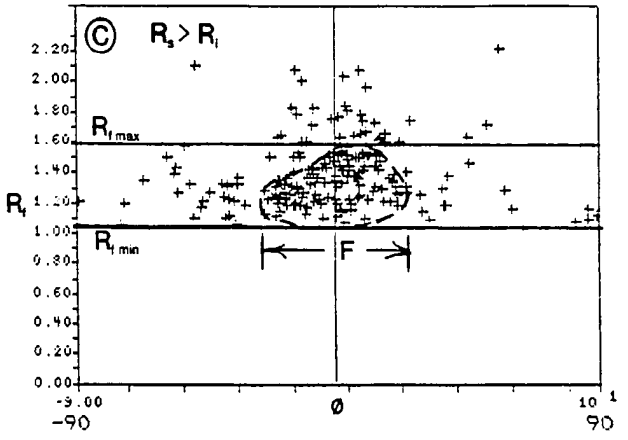

(C) Phi-R_f technique (Ramsay, 1967); Ø = -2°, determined by INSTRAIN 2.2. Plot interpreted by visual inspection.

FIGURE 79. Interpreted finite strain plots for east-striking plane of Kekiktuk Conglomerate sample 87JZ36. Sample plane strikes 118 degrees and dips 88 degrees to the northeast. Sample location is shown in Figures 15 and 30.

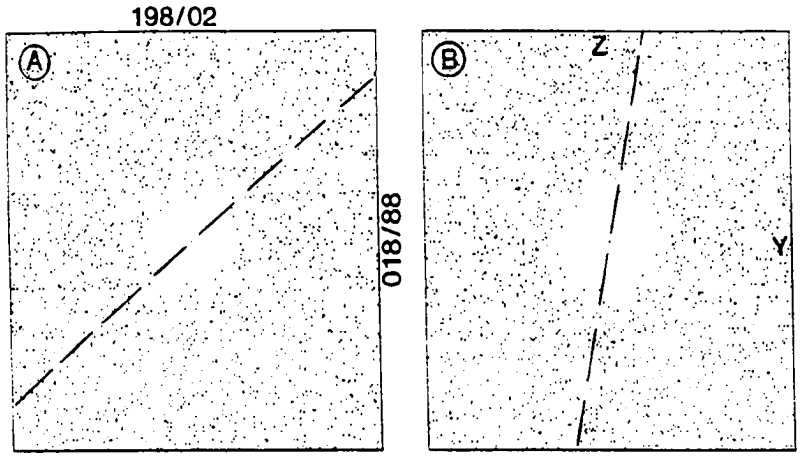

(A) Conventional Fry method (Fry, 1979); Ø = 40°. (B) Normalized Fry method (Erslev, 1988); Ø = 80°. In (A) and (B), dashed lines define Ø, determined by INSTRAIN 2.2; selection factor = 0.95; sample size = 178 grains. Orientations of thin-section edges are given. This is the YZ-plane of the strain ellipsoid determined for the sample.

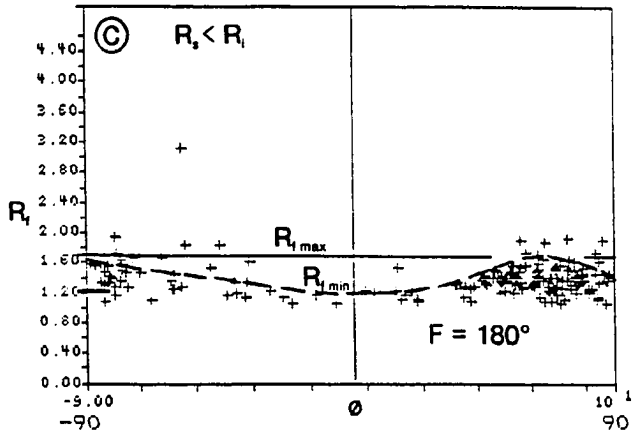

(C) Phi-R_f technique (Ramsay, 1967); Ø = 30°, determined by INSTRAIN 2.2. Plot interpreted by visual inspection.

FIGURE 80. Interpreted finite strain plots for north-striking plane of Kekiktuk Conglomerate sample 87JZ36. Sample plane is vertical and strikes 18 degrees. Sample location is shown in Figures 15 and 30.

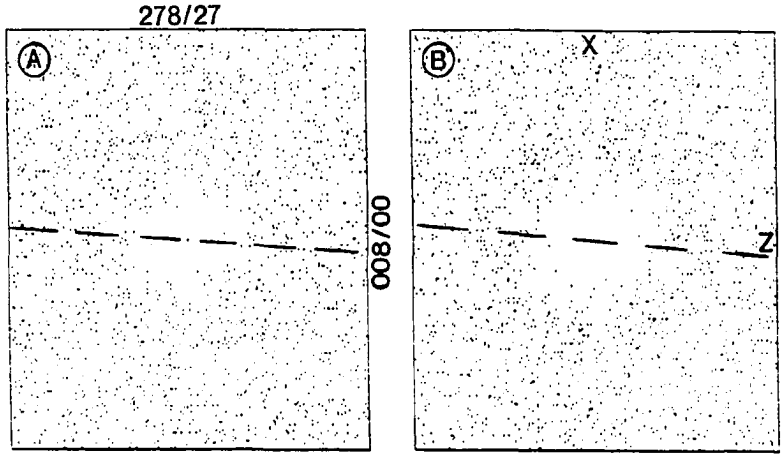

(A) Conventional Fry method (Fry, 1979); Ø = -3°. (B) Normalized Fry method (Erslev, 1988); Ø = -4°. In (A) and (B), dashed lines define Ø, determined by INSTRAIN 2.2; selection factor = 1.15; sample size = 183 grains. Orientations of thin-section edges are given. This is the XZ-plane of the strain ellipsoid determined for the sample.

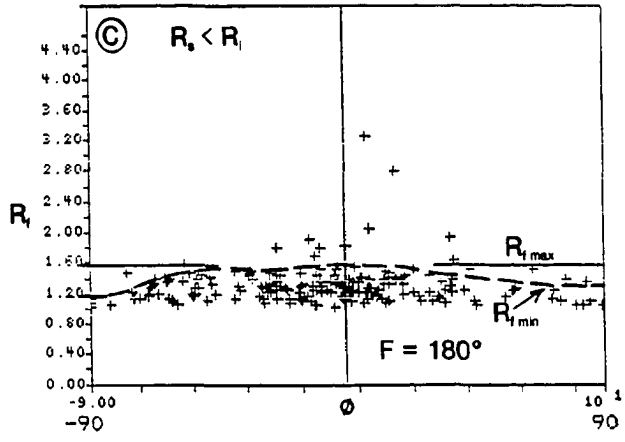

(C) Phi-R_f technique (Ramsay, 1967); Ø = -8°, determined by INSTRAIN 2.2. Plot interpreted by visual inspection.

FIGURE 81. Interpreted finite strain plots for the subhorizontal plane of Ivishak Formation sample 87JZ40. Sample plane strikes 8 degrees and dips 27 degrees to the northwest. Sample location is shown in Figures 15 and 30.

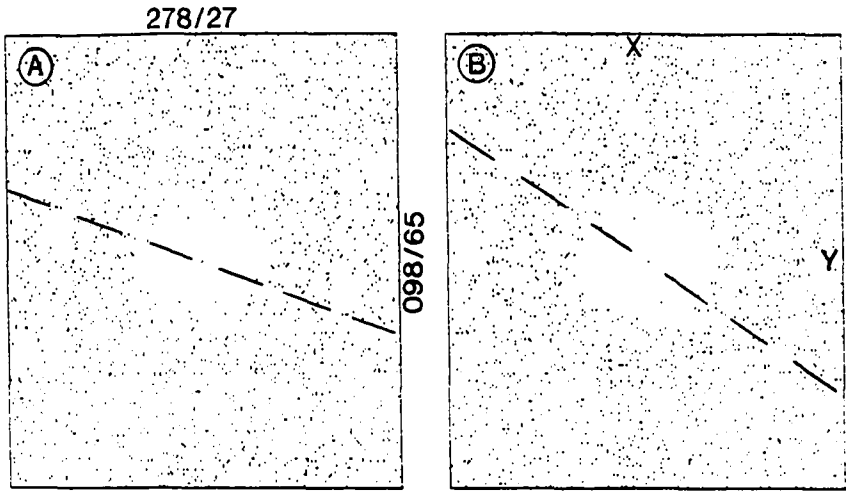

(A) Conventional Fry method (Fry, 1979); Ø = -18°. (B) Normalized Fry method (Erslev, 1988); Ø = -32°. In (A) and (B), dashed lines define Ø, determined by INSTRAIN 2.2; selection factor = 1.00; sample size = 187 grains. Orientations of thin-section edges are given. This is the XY-plane of the strain ellipsoid determined for the sample.

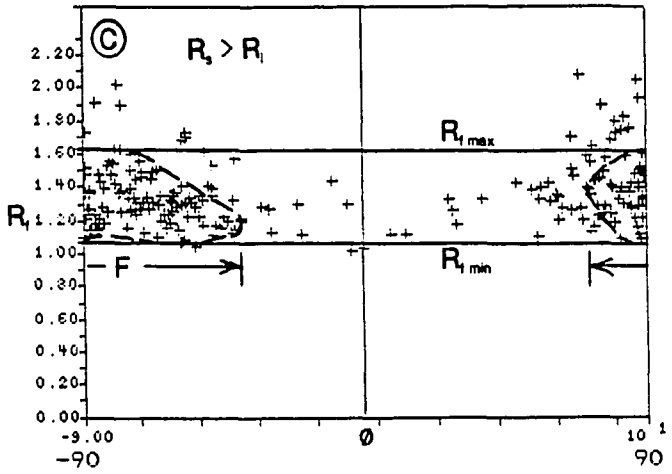

(C) Phi-R_f technique (Ramsay, 1967); Ø = -9°, determined by INSTRAIN 2.2. Plot interpreted by visual inspection.

FIGURE 82. Interpreted finite strain plots for east-striking plane of Ivishak Formation sample 87JZ40. Sample plane is vertical and strikes 98 degrees. Sample location is shown in Figures 15 and 30.

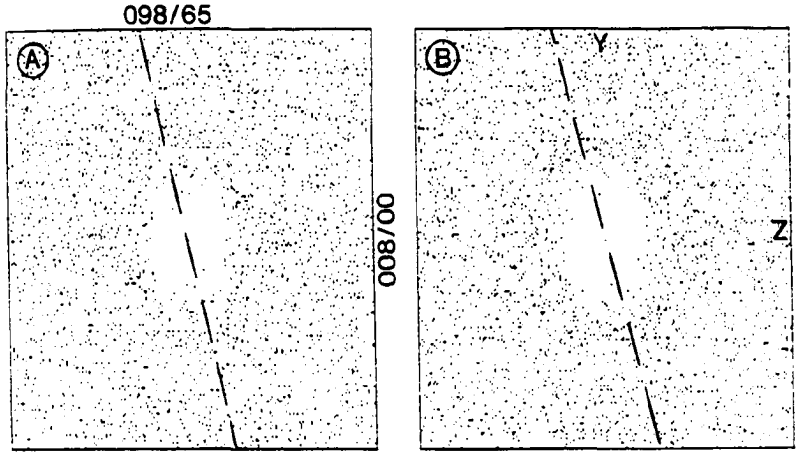

(A) Conventional Fry method (Fry, 1979); Ø = -77°. (B) Normalized Fry method (Erslev, 1988); Ø = -75°. In (A) and (B), dashed lines define Ø, determined by INSTRAIN 2.2; selection factor = 0.95; sample size = 205 grains. Orientations of thin-section edges are given. This is the YZ-plane of the strain ellipsoid determined for the sample.

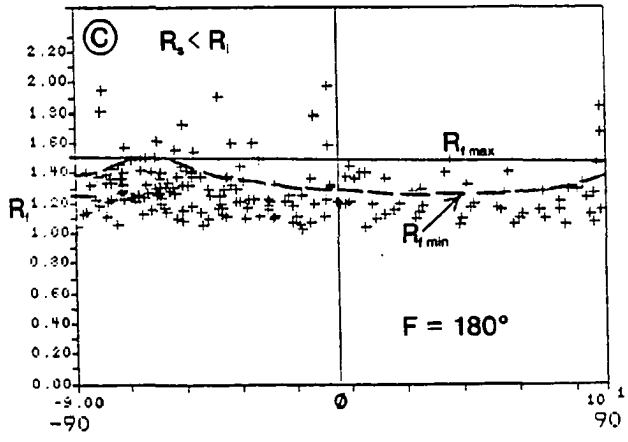

(C) Phi-R_f technique (Ramsay, 1967); Ø = -24°, determined by INSTRAIN 2.2. Plot interpreted by visual inspection.

FIGURE 83. Interpreted finite strain plots for north-striking plane of Ivishak Formation sample 87JZ40. Sample plane strikes 8 degrees and dips 65 degrees to the southeast. Sample location is shown in Figures 15 and 30.

TABLE 23. Comparison of finite strain ratios determined by the conventional and normalized Fry methods using INSTRAIN 2.2. BED = plane roughly parallel to bedding; ENE = subvertical east-northeast-striking plane; NNW = subvertical north-northwest-striking plane. The orientations of sample planes are provided in Figures 72-83. Sample locations are shown in Figure 15.

			CONVENTIONAL FRY METHOD (Fry, 1979)			NORMALIZED FRY METHOD (Erslev, 1988)		
	SAMPLE PLANE		R	Ø +cc-wise	% ERROR	R	Ø +cc-wise	% ERROR
KEKIKTUK CONGL.	25	BED	1.35	+ 15	20.9	1.34	+ 16	12.9
		ENE	1.11	+ 16	24.2	1.14	- 25	12.4
		NNW	1.08	- 53	21.8	1.09	- 61	13.4
	31	BED	1.13	+ 12	24.9	1.15	+ 5	14.6
		ENE	1.30	+ 60	25.9	1.23	+ 70	12.8
		NNW	1.14	+ 68	24.5	1.17	+ 70	13.9
	36	BED	1.30	+ 31	26.9	1.13	+ 46	13.9
		ENE	1.36	+ 2	28.0	1.25	+ 3	14.6
		NNW	1.13	+ 40	22.0	1.15	+ 80	14.4
IVISHAK	40	BED	1.16	- 3	24.8	1.20	- 4	15.5
		ENE	1.05	- 18	20.1	1.11	- 32	15.1
		NNW	1.34	- 77	23.0	1.16	- 75	15.7
	AVERAGE		1.20		23.9	1.18		14.1

TABLE 24. Summary of data for strain ellipse shape and orientation determined by the normalized Fry method options of INSTRAIN 2.2. BED = plane roughly parallel to bedding; ENE = subvertical east-northeast-striking plane; NNW = subvertical north-northwest-striking plane. XY, YZ, and XZ refer to planes of the strain ellipsoid determined for each sample. The orientations of sample planes are provided in Figures 72-83. Sample locations are shown in Figure 15.

				NORMALIZED FRY METHOD (Erslev, 1988)					
	SAMPLE PLANE			NO. GRAINS	R	Ø +cc-wise	MAJOR AXIS TREND	RAKE	% ERROR
KEKIKTUK CONGL.	25	BED	XZ	160	1.34	+ 16	103	36	12.9
		ENE	XY	146	1.14	- 25	303	32	12.4
		NNW	YZ	224	1.09	- 61	339	19	13.4
	31	BED	YZ	130	1.15	+ 5	181	37	14.6
		ENE	XY	150	1.23	+ 70	336	70	12.8
		NNW	XZ	133	1.17	+ 70	248	04	13.9
	36	BED	XZ	225	1.13	+ 46	252	02	13.9
		ENE	XY	201	1.25	+ 3	298	04	14.6
		NNW	YZ	178	1.15	+ 80	198	83	14.4
IVISHAK	40	BED	XZ	183	1.20	- 4	282	27	15.5
		ENE	XY	187	1.11	- 32	098	05	15.1
		NNW	YZ	205	1.16	- 75	182	14	15.7
	AVERAGE			177	1.18				14.1

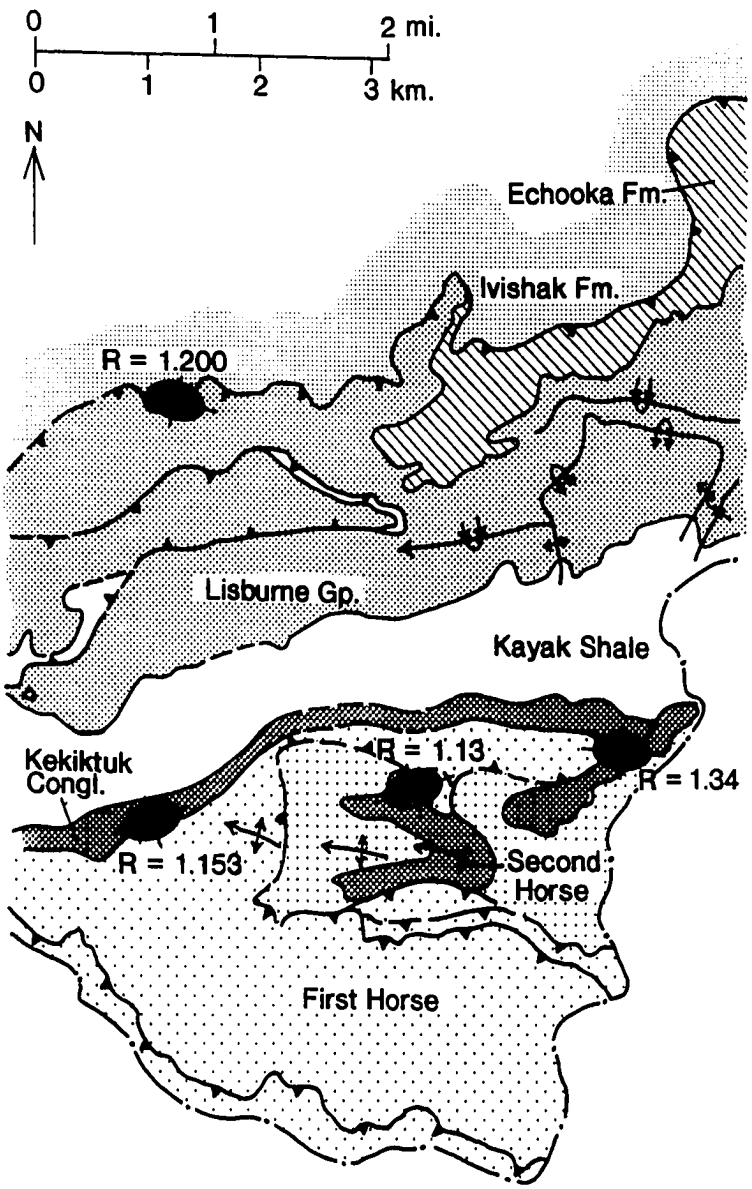

FIGURE 84. Normalized Fry method strain ellipses in the subhorizontal plane. The locations of ellipses correspond to the positions of samples shown in Figure 15. The shape of all ellipses is the same and not to scale. Actual ellipticities are printed beside the ellipses.

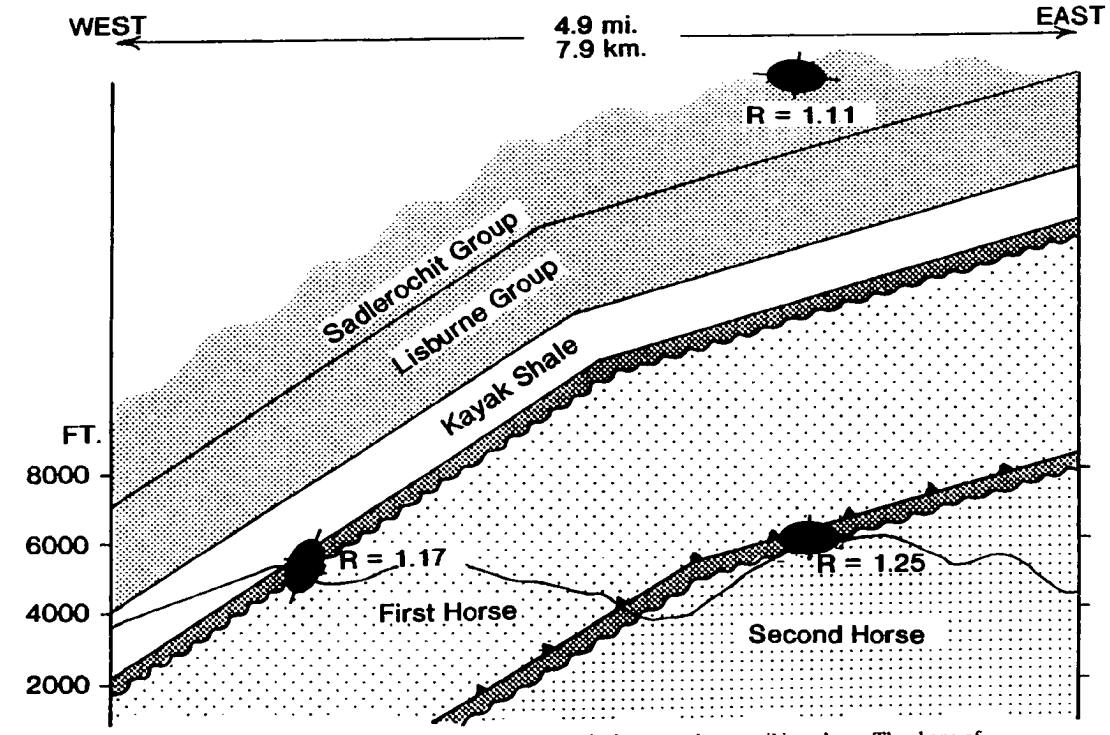

FIGURE 85. Normalized Fry method strain ellipses in the subvertical east-northeast-striking plane. The shape of all ellipses is the same and is not to scale. Actual ellipticities are printed beside the ellipses, as well as the sample numbers shown in Figure 15.

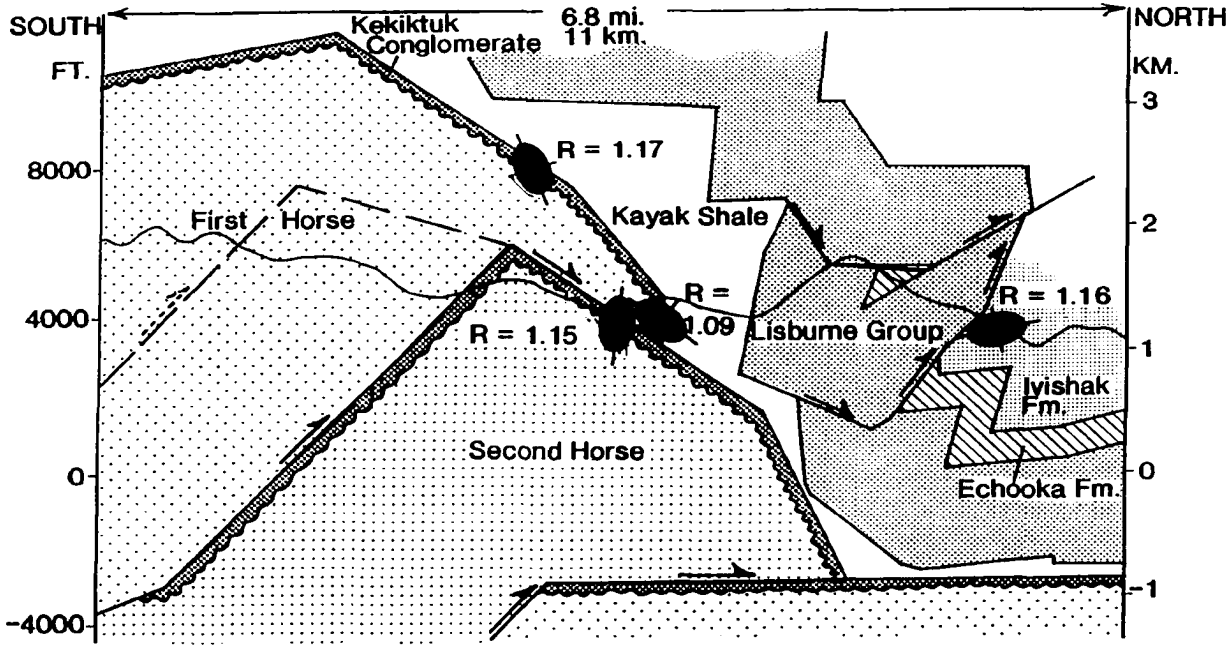

FIGURE 86. Normalized Fry method strain ellipses in the subvertical north-northwest-striking plane. The locations of ellipses correspond to the positions shown in Figure 30. The shape of all ellipses is the same and is not to scale. Actual ellipticities are printed beside the ellipses.

Tables 24 and 25 show that the ellipticity of grains varies from sample to sample and between sample planes. It is important to note that the ellipticities observed in the Kekiktuk Conglomerate samples are comparable in value to those of the Ivishak Formation sample. Strain ratios (ellipticity) range from a maximum of 1.34 for bedding plane of Kekiktuk Conglomerate sample 87JZ25 to a minimum of 1.09 for the north-northwest-striking plane of the same sample, with an average ellipticity of 1.18. Average strain ratios for the bedding-parallel, east-northeast-striking, and north-northwest-striking planes of Kekiktuk Conglomerate samples are 1.21, 1.21, and 1.14, respectively. These values may be compared with respective strain ratios of 1.20, 1.11, and 1.16 for the Ivishak Formation sample. Since the initial shape and orientation of grains is unknown, it is impossible to translate these strain ratios into strain percentages. Qualitatively, the ellipticities obtained by the normalized Fry method indicate low strains in all planes of both Kekiktuk Conglomerate and Ivishak Formation samples. (For example, if markers were initially circular, ellipticities would record strains ranging from 8% to 25%, with an average strain of roughly 15%.)

INSTRAIN 2.2 includes a selection factor parameter in normalized calculations of strain ellipse shape and orientation. The selection factor, which typically has a value of 0.90 to 1.10, reflects the degree of overlap of grains in the sample plane. The numeric value of the selection factor represents the percentage of the center-to-center distance between two given grains which the algorithm will use to include another grain as a nearest neighbor. The selection factor can be input by the analyst, with lower values appropriate where significant grain-to-grain overlap is observed. In this analysis, selection factor values used were those which minimized the percentage error associated with determination of strain ellipse shape and orientation for a given sample plane. Selection factors ranged in value from 0.95 to 1.15, with low values used for the Kekiktuk Conglomerate samples (87JZ25, 87JZ31, and 87JZ36) which are comprised of more closely-packed grains than the Ivishak Formation sample (87JZ40). Average selection factors used for the bedding-parallel, east-northeast-striking, and north-northwest-strking

TABLE 25. Normalized Fry method data from INSTRAIN 2.2, ranked in order of decreasing ellipticity of the strain ellipse (R). BED = plane roughly parallel to bedding; ENE = subvertical east-northeast-striking plane; NNW = subvertical north-northwest-striking plane. The orientations of sample planes are provided in Figures 72-83. Sample locations are shown in Figure 15. (+cc-wise means that Ø is positive in a counter-clockwise direction from east in the bedding-parallel and east-northeast-striking planes, or from north in the north-northwest-striking plane.)

	NORMALIZED FRY METHOD (Erslev, 1988)				
RANK	SAMPLE PLANE	SEL. FACTOR	R	Ø +cc-wise	% ERROR
1	25 BED	1.00	1.34	+ 16	12.9
2	36 ENE	1.00	1.25	+ 3	14.6
3	31 ENE	0.95	1.23	+ 70	12.8
4	40 BED	1.15	1.20	- 4	15.5
5	31 NNW	0.95	1.17	+ 70	13.9
6	40 NNW	0.95	1.16	- 75	15.7
7	36 NNW	0.95	1.15	+ 80	14.4
8	31 BED	0.95	1.15	+ 5	14.6
9	25 ENE	0.95	1.14	- 25	12.4
10	36 BED	1.00	1.13	+ 46	13.9
11	40 ENE	1.00	1.11	- 32	15.1
12	25 NNW	0.95	1.09	- 61	13.4
AVE.		0.98	1.18		14.1

planes of the four samples are 1.03, 0.98, and 0.95, respectively. These average values suggest that grains are most closely-packed in the north-northwest-striking plane and least closely-packed in the bedding-parallel plane of thin-sections, as might be expected for a deformed rock body. Finally, Table 25 fails to show a correlation between either the selection factor and the percentage error or the ellipticity.

G.3.b. Phi-R_f Technique

Table 26 summarizes (1) harmonic mean of R_f and Ø values calculated by INSTRAIN 2.2; (2) maximum and minimum R_f values, and the fluctuation F, derived from INSTRAIN 2.2 phi-R_f plots; and (3) the shape of each tectonic strain ellipse, R_S, calculated from the preceding derived values. Since all R_S values are greater than one, it can be concluded that markers in the sample planes have been strained. For 6 of the 12 sample planes, F = 180 degrees, indicating that R_S is less than R_i (like Figure 71B). For the remaining 6 samples where F = 90 degrees, R_S is greater than R_i (like Figure 71C).

G.3.b.1. Strain ellipse

As shown in Table 26, calculated values for R_S range from 1.10 for the north-northwest-striking plane of Ivishak Formation sample 87JZ40 to 1.47 for the bedding plane of Kekiktuk Conglomerate sample 87JZ25, with an average strain ratio of 1.26. Average strain ratios for the bedding-parallel, east-northeast-striking, and north-northwest-striking planes of Kekiktuk Conglomerate samples are 1.35, 1.26, and 1.25, respectively. These values may be compared to respective strain ratios of 1.15, 1.32, and 1.10 for the Ivishak Formation sample. Table 27 ranks sample planes in order of decreasing R_S and gives an average rank of each sample plane as determined by both normalized Fry and phi-Rf analyses. For highly ranked sample planes (i.e. large ellipticities), the agreement between Fry and phi-R_f ranking is good to excellent; for lower-ranked sample planes (i.e. small ellipticities), the agreement between Fry and phi-R_f ranking is fair to good.

TABLE 26. Summary of finite strain data derived by the Ø - R_f technique using INSTRAIN 2.2, including the initial and final marker ellipticities (R_i and R_f), the shape of the tectonic strain ellipse (R_s), and the fluctuation in Ø' (F). BED = plane roughly parallel to bedding; ENE = subvertical east-northeast-striking plane; NNW = subvertical north-northwest-striking plane. XY, YZ, and XZ identify the planes of the strain ellipsoid determined for each sample. The orientations of sample planes are provided in Figures 72-83. Sample locations are shown in Figure 15.

			Ø - Rf TECHNIQUE (Ramsay, 1967; Ramsay & Huber, 1983)					
SAMPLE	PLANE		Rf harm. mean	Rf Maximum	Rf Minimum	Rs	Ri Maximum	F
25	BED	XZ	1.43	2.05	1.06	1.47	1.39	58
	ENE	XY	1.21	1.62	1.30	1.12	1.45	180
	NNW	YZ	1.27	1.94	1.33	1.21	1.61	180
31	BED	YZ	1.29	1.79	1.01	1.35	1.33	75
	ENE	XY	1.33	1.84	1.03	1.38	1.34	65
	NNW	XZ	1.30	1.68	1.10	1.36	1.24	43
36	BED	XZ	1.26	1.98	1.29	1.24	1.60	180
	ENE	XY	1.35	1.59	1.04	1.29	1.24	35
	NNW	YZ	1.35	1.69	1.22	1.18	1.44	180
40	BED	XZ	1.27	1.57	1.18	1.15	1.36	180
	ENE	XY	1.33	1.63	1.07	1.32	1.23	49
	NNW	YZ	1.27	1.51	1.26	1.10	1.38	180
AVERAGE			1.31	1.74	1.16	1.26	1.38	

TABLE 27. Ranked ellipticities for the strain ellipse, R_S, determined by the Ø - R_f technique option of INSTRAIN 2.2. The average rank for each sample plane represents an average of the ranks determined by the normalized Fry method (Table 25) and the Ø - Rf technique (Table 26). BED = plane roughly parallel to bedding; ENE = subvertical east-northeast-striking plane; NNW = subvertical north-northwest-striking plane. The orientations of sample planes are provided in Figures 72-83. Sample locations are shown in Figure 15.

RANKED Ø - Rf STRAIN RATIOS AVERAGED WITH FRY METHOD RANKS			
Ø - RF RANK	SAMPLE PLANE	Rs	AVE. RANK
1	25 BED	1.47	1
2	31 ENE	1.38	2.5
3	31 NNW	1.37	4
4	31 BED	1.35	6
5	40 ENE	1.32	8
6	36 ENE	1.29	4
7	36 BED	1.29	8.5
8	25 NNW	1.21	10
9	36 NNW	1.18	8
10	40 BED	1.15	7
11	25 ENE	1.12	10
12	40 NNW	1.10	9

Figure 87 is a Tukey sum-difference plot that compares tectonic strain ellipse shapes: R_S determined by the phi-R_f technique and $R_{(Fry)}$ determined by the normalized Fry method. The sum of R_S and $R_{(Fry)}$ increases along the x-axis with data points lying toward the right reflecting the largest ellipticities. The distance of the data point above the datum is a measure of the difference between the ellipticities determined by the two techniques. In Figure 87, samples lying above the datum have R_S values which exceed $R_{(Fry)}$; those lying below the datum have $R_{(Fry)}$ values which exceed R_S. Figure 87 indicates that R_S values typically exceed $R_{(Fry)}$. As suggested by Table 27, the relative magnitude of strain ratios determined by both methods are similar for the sample planes. However, the absolute magnitude of these ratios varies between the two methods, with the phi-R_f technique tending to yield greater strains than the normalized Fry method, with the greatest differences observed for Kekiktuk Conglomerate sample 87JZ31.

G.3.b.2. Initial marker ellipse

Table 28 ranks values for the maximum initial ellipticity of marker grains, R_i. These ellipticities range from 1.23 for the east-northeast-striking plane of Ivishak Formation sample 87JZ40 to 1.61 for the north-northwest-striking plane of Kekiktuk Conglomerate sample 87JZ25, with an average ellipticity of 1.38. Average ellipticities for the bedding-parallel, east-northeast-striking, and north-northwest-striking planes of the Kekiktuk Conglomerate samples are 1.44, 1.34, and 1.43, respectively. These values may be compared to respective ratios of 1.36, 1.23, and 1.38 for the Ivishak Formation sample.

G.3.b.3. Final marker ellipse

Table 28 ranks values calculated for the final ellipticity of marker grains, R_f. Harmonic mean R_f values calculated by INSTRAIN 2.2 range from 1.21 for the east-northeast-striking plane of Kekiktuk

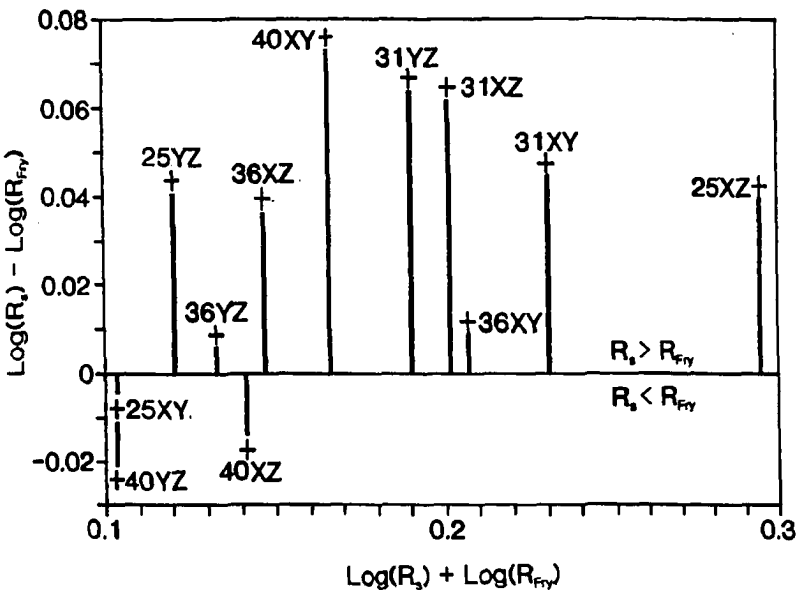

FIGURE 87. Tukey sum-difference plot comparing strain ellipses obtained from finite strain analyses by the normalized Fry method and phi-R_f technique. For 9 of 12 sample planes, the ellipticities determined by the phi-R_f technique exceed those determined by the normalized Fry method. Samples lying toward the right have higher total ellipticities and are more highly strained than those lying toward the left margin of the graph. The distance which separates sample points from the datum is a direct measure of the discrepancy between normalized Fry method and phi-R_f finite strain determinations. A close correlation between ellipticities obtained by these two methods is exhibited by sample points lying close to the datum.

TABLE 28. Samples ranked by the ellipticities of both initial (R_i) and final (R_f) markers. BED = plane roughly parallel to bedding; ENE = subvertical east-northeast-striking plane; NNW = subvertical north-northwest-striking plane. The orientations of sample planes are provided in Figures 72-83. Sample locations are shown in Figure 15.

RANKED STRAIN RATIOS INITIAL MARKERS			RANKED STRAIN RATIOS FINAL MARKERS		
RANK	SAMPLE PLANE	Ri Maximum	RANK	SAMPLE PLANE	Rf har. mean
1	25 NNW	1.61	1	25 BED	1.43
2	36 BED	1.60	2	36 ENE	1.35
3	25 ENE	1.45	3	36 NNW	1.35
4	36 NNW	1.44	4	40 ENE	1.33
5	25 BED	1.39	5	31 ENE	1.33
6	40 NNW	1.38	6	31 NNW	1.30
7	40 BED	1.36	7	31 BED	1.29
8	31 ENE	1.34	8	40 BED	1.27
9	31 BED	1.33	9	25 NNW	1.27
10	31 NNW	1.24	10	40 NNW	1.27
11	36 ENE	1.24	11	36 BED	1.26
12	40 ENE	1.23	12	25 ENE	1.21
	AVE.	1.38		AVE.	1.31

Conglomerate sample 87JZ25 to 1.43 for the bedding plane of the same sample (Table 26), with an average ellipticity of 1.31. Average ellipticities for the bedding-parallel, east-northeast-striking, and north-northwest-striking planes of Kekiktuk Conglomerate samples are 1.33, 1.30, and 1.31, respectively. These values may be compared to respective ratios of 1.27, 1.33, and 1.27 for the Ivishak Formation sample.

G.4. ERROR ANALYSIS

G.4.a. Sample Preparation

Sample preparation errors include those associated with sample orientation (described in Appendix F) and grain basemap preparation. A sample of 150-200 adjacent grains, representative of the size, orientation, and packing observed in the thin-section, was selected for each thin-section. A basemap of grain outlines was prepared for each sample. The next step in basemap preparation involved extrapolating subelliptical grain forms to elliptical shapes, and locating the center-points and the major and minor axis end-points of these extrapolated ellipses. It is important to acknowledge the subjectivity associated with the extrapolation and end-point location processes. If the extrapolated grain ellipses are inaccurate, then finite strain values determined from these basemaps will be erroneous. An effort was made not to bias ellipse extrapolation as a consequence of observing an apparent orientation pattern as the basemap was prepared.

G.4.b. Sample Suitability for Normalized Fry Method

The normalized Fry method effectively identifies tectonic strain ellipse shape and orientation only if the sample meets certain criteria. First, the sample must be an aggregate of markers with a statistically uniform distribution. Marker center-points should be anticlustered; that is, they should be distributed such that the distance between centers is relatively constant. Erslev's (1988) normalization algorithm takes into account the fact that the degree of anticlustering is reduced in going from three- to two-dimensions. Second, if the sample is strained, deformation must have been homogeneous for the

given population of marker grains. Application of the Fry method to samples deformed by a pressure solution mechanism can yield "misleading or uninterpretable results," according to Onasch (1986).

Onasch (1986) presents four models of pressure solution deformation: homogeneous pressure solution both at a constant volume and with a volume loss, and inhomogeneous pressure solution with markers both preserved and destroyed. Onasch (1986) concludes that incorrect strain determinations are likely if pressure solution involves a volume loss or if dissolution surfaces are widely spaced. Pressure solution deformation in Kekiktuk Conglomerate samples falls into the categories which Onasch (1986) suggests may yield incorrect strain determinations. While inhomogeneous pressure solution is observed in Kekiktuk Conglomerate samples 87JZ25 and 87JZ36, grain populations were selected from locations where no stylolite surfaces transected the thin-section. Homogeneous pressure solution with a possible volume loss is observed in Kekiktuk Conglomerate sample 87JZ31. Although the Kekiktuk Conglomerate has quartz-filled extension fractures in the area of this sample, few quartz overgrowths are readily observed in thin-sections. Third, the marker distribution should not exhibit an original pattern of ellipticity or preferred orientation due to clastic behavior (Lacassin and van den Driessche, 1983). Finally, a sufficient number of markers must be included in the analysis in order to define strain ellipse shape and orientation adequately. Crespi (1986) notes that the strength of the girdle of high point density, defining the central vacancy field, is more a function of the degree of anticlustering than of the number of data points. Irrespective of the number of data points, in a poorly anticlustered distribution, the vacancy field cannot be as well-defined as for a strongly anticlustered distribution. By Crespi's (1986) calculation, for a well-sorted quartz sandstone, the minimum number of data points needed to define the central vacancy field is 200-250. An average of 177 grains was used to determine finite strain ellipse shape and orientation in this analysis. Erslev (1988) notes that normalization improves definition of the central vacancy field, perhaps decreasing the minimum number of grains needed. Therefore, the number of grains used in these analyses was likely adequate for finite strain determinations.

G.4.c. Sample Suitability for Phi-R_f Technique

The phi-R_f technique seems to be less sensitive to sample properties than the Fry method. Asymmetry of R_f versus Ø' plots has been suggested to indicate an initial fabric or preferred orientation of markers. Since plots obtained for this analysis show a generally symmetric distribution of data points, it is concluded that an original preferred orientation of grains did not exist.

Dunnet (1969) states that a minumum of 50 conglomerate or grit particles can yield R_s values that are reproducible to within roughly +/- 0.05 strain units. Thus, the average of 177 grains per sample is likely sufficient for finite strain determinations in this analysis.

G.4.d. Error Associated With INSTRAIN 2.2 Normalized Fry Method

As shown in Table 29, the percent error associated with the determination of strain ellipse shape and orientation by INSTRAIN 2.2 varies between samples, independent of the number of grains analyzed, the shape of the strain ellipse in a given plane, or the selection factor used. Average associated errors range from a minimum of 12.9% for Kekiktuk Conglomerate sample 87JZ25 to a maximum of 15.4% for Ivishak Formation sample 87JZ40, with Kekiktuk samples 87JZ31 and 87JZ36 averaging 13.8% and 14.3%, respectively. While it seems reasonable that more error might be associated with determination of strain ellipse shape and orientation for those samples with relatively low ellipticities or fewer data points, this does not appear to be the case. In addition, while the largest average error occurs for the Ivishak Formation sample, which is less closely packed and has a higher average selection factor than the Kekiktuk Conglomerate, percent error for Kekiktuk Conglomerate samples varies between samples and planes within each sample.

G.4.e. Error Associated With INSTRAIN 2.2 Phi-R_f Technique

INSTRAIN 2.2 estimates the average orientation of the axis of the marker ellipse R_f, plus or minus a number of degrees, based on the plot of R_f versus Ø' for a given population of markers. As

TABLE 29. Finite strain data determined by the normalized Fry method option of INSTRAIN 2.2, sorted by the percent error associated with the determination of the shape and orientation of the strain ellipse by INSTRAIN 2.2. BED = plane roughly parallel to bedding; ENE = subvertical east-northeast-striking plane; NNW = subvertical north-northwest-striking plane. The orientations of sample planes are provided in Figures 72-83. Sample locations are shown in Figure 15.

	NORMALIZED FRY METHOD (Erslev, 1988)				
RANK	SAMPLE PLANE	NO. GRAINS	R	SEL. FACTOR	% ERROR
1	40 NNW	205	1.16	0.95	15.7
2	40 BED	183	1.20	1.15	15.5
3	40 ENE	187	1.11	1.00	15.1
4	31 BED	130	1.15	0.95	14.6
5	36 ENE	201	1.25	1.00	14.6
6	36 NNW	178	1.15	0.95	14.4
7	31 NNW	133	1.17	0.95	13.9
8	36 BED	225	1.13	1.00	13.9
9	25 NNW	224	1.09	0.95	13.4
10	25 BED	160	1.34	1.00	12.9
11	31 ENE	150	1.23	0.95	12.8
12	25 ENE	146	1.14	0.95	12.4
AVE.		177	1.18	0.98	14.1

shown in Table 30, there appears to be a significant lack of precision in determination of the R_f major axis orientation by INSTRAIN 2.2. The phi-R_f technique determined Ø' values within a range of 18 to 70 degrees, averaging plus or minus 45 degrees.

Analyst subjectivity can be a source of significant error in the interpretation of R_f versus Ø' plots. Calculated values for R_s and R_i are strongly influenced by decisions regarding plot shape, as well as by the estimation of maximum and minimum R_f values. A number of the R_f versus Ø'plots of Figures 72-83 might be described as borderline bell-shaped curves or closed concentrations of data points. The decision as to whether these plots are bell-shaped or closed determines the relationship between R_s and R_i. In addition, the maximum and minimum R_f values must be estimated from R_f versus Ø' plots in order to calculate R_s and R_i for a given sample plane. Quantitative expressions used to calculate R_s and R_i differ depending on whether $R_s > R_i$ or $R_i > R_s$, with R_f maximum and minimum values as variables:

For $R_s > R_i$,

$$R_s = (R_{f\,max} \cdot R_{f\,min})^{0.5}$$

$$R_{i\,max} = (R_{f\,max} / R_{f\,min})^{0.5}$$

and $F = \tan^{-1} [R_s(R_{i\,max}^2 - 1) / [(R_{i\,max}^2 \cdot R_s^2 - 1)(R_s^2 - R_{i\,max}^2)]^{0.5}]$.

For $R_i > R_s$,

$$R_s = (R_{f\,max} / R_{f\,min})^{0.5}$$

$$R_{i\,max} = (R_{f\,max} \cdot R_{f\,min})^{0.5}$$

and $F = 180$ degrees.

TABLE 30. Orientation of the strain ellipse axis, Ø, determined by the Ø - R_f technique and normalized Fry method options of INSTRAIN 2.2. Note the apparent lack of precision in the determination of Ø by the Ø - R_f technique, and the varying agreement between values determined by the two strain determination techniques. BED = plane roughly parallel to bedding; ENE = subvertical east-northeast-striking plane; NNW = subvertical north-northwest-striking plane. The orientations of sample planes are provided in Figures 72-83. Sample locations are shown in Figure 15.

ORIENTATION OF STRAIN ELLIPSE MAJOR AXIS				
SAMPLE	PLANE	Ø - Rf Ø +/- deg. cc-wise positive	Normalized Fry Ø	Difference (deg.) (Ø - Rf) - (Fry)
25	BED	17 +/- 18	16	1
	ENE	- 8 +/- 44	- 25	- 17
	NNW	- 27 +/- 46	- 61	- 34
31	BED	5 +/- 31	5	0
	ENE	49 +/- 36	70	21
	NNW	18 +/- 67	70	52
36	BED	20 +/- 49	46	26
	ENE	- 2 +/- 28	3	5
	NNW	30 +/- 57	80	50
40	BED	- 8 +/- 39	- 4	4
	ENE	- 9 +/- 70	- 32	- 23
	NNW	- 24 +/- 50	- 75	- 51
			AVE. DIFF.	24

G.5. INTERPRETATIONS AND SPECULATIONS

G.5.a. Significance of Tectonic Strain Ellipse

In order for finite strain determinations to supplement understanding of the structural evolution of the study area, it is necessary to consider what stage in the evolution of the Franklin Mountains anticlinorium is represented by the shape and orientation of the derived tectonic strain ellipses. According to the proposed duplex model , the most recent deformation of these rocks would have occurred as a consequence of the emplacement of the second horse beneath the first horse comprising the Franklin Mountains anticlinorium (Figure 30).

When plotted on the map or cross-sections of Figures 84-86, strain ellipses determined by the normalized Fry method are generally compatible with the inferred stress regime associated with formation of the Franklin Mountains anticlinorium. In the bedding-parallel plane shown in Figure 84, strain ellipse long axes trend east-northeast to east-southeast, an orientation compatible with the roughly north-directed compressive stress that was likely associated with the modeled thrust emplacement of the two horses comprising the anticlinorium. In the east-northeast-striking plane (Figure 85), the strain ellipse long axis for the Kekiktuk Conglomerate capping the first horse is compatible with extension in the hangingwall over a lateral ramp, induced during emplacement of the second horse (as shown in Figure 68). Also in the east-northeast-striking plane, the subhorizontal orientation of the major axis of the strain ellipse for the Kekiktuk Conglomerate capping the second horse may reflect the increased overburden pressure and shear strain developed as a consequence of emplacing this second horse beneath the first one. The orientation of this strain ellipse and that for the Ivishak Formation sample are compatible with movement of material or maximum elongation of markers perpendicular to the transport direction. In the north-northwest-striking plane (Figure 86), the orientations of two of the three Kekiktuk Conglomerate strain ellipses are compatible with the strain patterns shown in Sanderson's (1982) models (Figure 67). The low strain ratio (R = 1.09) determined for the third Kekiktuk Conglomerate sample,

located at the leading edge of the first horse in Figure 86, may corroborate the zero-strain modeled by Sanderson (1982) in his flexural-slip model (Figure 70). For the Ivishak Formation, the strain ellipse orientations in the east-northeast- and north-northwest-striking planes may be reflections of overburden pressure or of marker elongation parallel in the direction of tectonic transport.

G.5.b. Initial Marker Orientations and Ellipticities

Since the average calculated $R_{i\ max}$ values shown in Table 26 are greater than one, grains are interpreted to have been elliptical prior to the recorded deformational event. The average $R_{i\ max}$ value (1.38) exceeds the average R_S value (1.26), suggesting a relationship between R_i and R_S similar to that illustrated in Figure 71B. In theory, the final marker ellipticity, R_f, was produced as a result of superimposing R_S upon R_i. It was suggested previously that R_f may be the product of tectonic strain associated with the emplacement of the second horse beneath the first horse of the Franklin Mountains anticlinorium. Therefore, $R_{i\ max}$ could be the product of deformation associated with thrust emplacement of the first horse which is interpreted to have first formed the anticlinorium. Based on this interpretation, initial marker ellipses in the north-northwest-striking plane are plotted on the balanced cross-section that depicts the structural geometry modeled to exist before thrust emplacement of the second horse (Figure 88). Assuming that the strain ellipsoid orientation and tectonic transport direction for the thrust emplacement of the first and second horses was approximately the same, the orientations of the marker ellipses in Figure 88 were determined by maintaining the same spatial orientation of the strain ellipses (R_S) in both Figures 86 and 88. The orientation of the initial marker ellipse for sample 87JZ31 ("31" in Figure 89) is compatible with the direction of maximum elongation shown in Sanderson's (1982) bending model (Figure 71A). The orientation of markers in sample 87JZ36 ("36" in Figure 88) may be a reflection of shear felt in the eventual second horse as a consequence of emplacement of the first horse. Sample 87JZ25 ("25" in Figure 88) lies at the leading edge of the first horse and the markers in

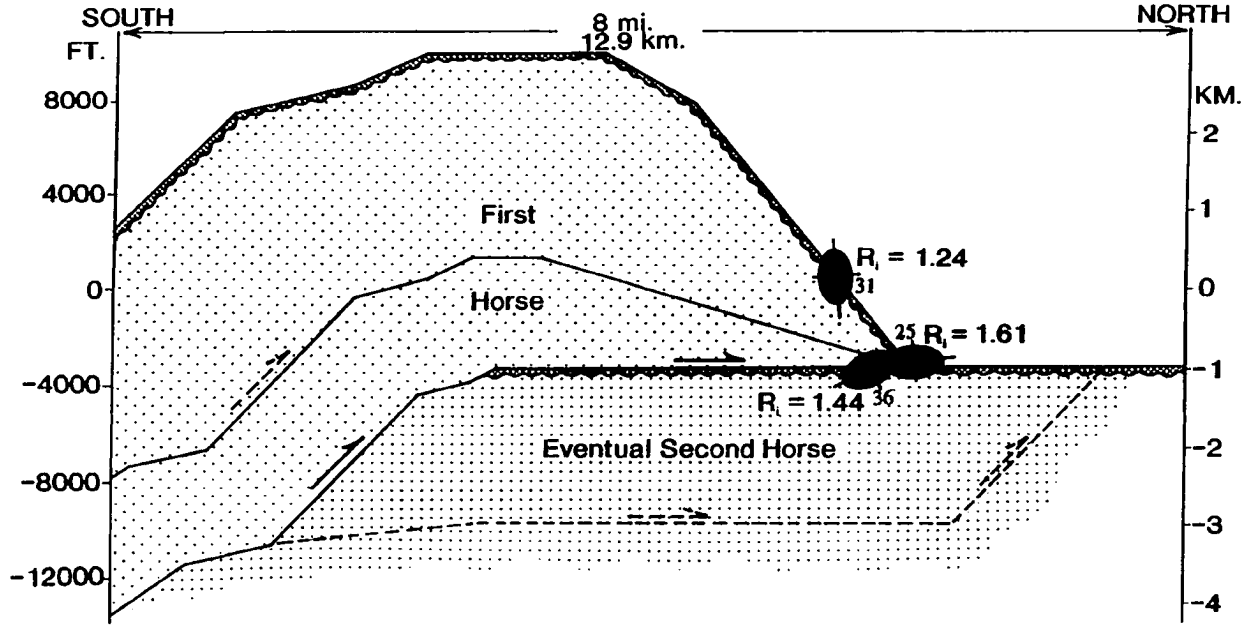

FIGURE 88. Initial marker ellipses determined by the phi-R_f technique, plotted on partially restored cross-section depicting the geometry of the anticlinorium which existed prior to emplacement of the second horse. The locations of ellipses correspond to reconstructed sample locations. The orientation of ellipses was determined in relation to the unconformity surface. The shape of all ellipses is the same and is not to scale. Actual ellipticities are printed beside the ellipses, as well as the sample numbers shown in Figures 15 and 30.

this sample are more elliptical than those in the other two samples, perhaps as a result of greater deformational stress felt at the leading tip of the first horse.

G.5.c. Compatibility of Results

Comparing Kekiktuk Conglomerate and Ivishak Formation values shown in Tables 9 and 31, it appears that the initial marker shape may be somewhat more elliptical for Kekiktuk Conglomerate samples, whereas the final shape of grains is the same. The strain ratio averaged from normalized Fry and phi-R_f results is roughly similar for Kekiktuk Conglomerate and Ivishak Formation samples, suggesting that all samples may have been subjected to Cenozoic deformations of similar magnitude. While it is possible that finite strain determinations do not accurately reflect the shape and/or orientation of the strain or marker ellipsoids, results appear to be compatible with the proposed structural geometry and evolution of the Franklin Mountains anticlinorium. However, not enough data exist to substantiate this conclusion.

TABLE 31. Initial (R_i) and final (R_f) marker ellipticities averaged for three samples from the Kekiktuk Conglomerate and compared with those determined for the sample from the Ivishak Formation. BED = plane roughly parallel to bedding; ENE = subvertical east-northeast-striking plane; NNW = subvertical north-northwest-striking plane.

		AVE. MARKER ELLIPTICITIES		
	PLANE	KEKIKTUK CONGL.	IVISHAK	Difference (Kek. - Ivis.)
Ri (max.)	BED	1.44	1.36	0.08
	ENE	1.34	1.23	0.11
	NNW	1.43	1.38	0.05
Rf (harm.)	BED	1.33	1.27	0.06
	ENE	1.30	1.33	- 0.03
	NNW	1.31	1.27	0.04

APPENDIX H. PHYSICAL PROPERTIES AND CONDITIONS

H.1. BULK DENSITIES OF UNITS

Based on average densities from gamma-gamma density well logs from Beli Unit-1 and other wells to the northwest of the study area (Robbins, 1987).

Pre-Mississippian rocks	= 2.7 E+3 kg/m^3
Endicott Group	= 2.6 E+3 kg/m^3
Lisburne Group	= 2.7 E+3 kg/m^3
Sadlerochit Group	= 2.5 E+3 kg/m^3
Shublik Formation	= 2.6 E+3 kg/m^3
Kingak Shale	= 2.45 E+3 kg/m^3
Brookian sequence rocks	= 2.45 E+3 kg/m^3.

H.2. MAGNITUDE OF LOAD ABOVE KEKIKTUK CONGLOMERATE

(1) Depositional overburden:

Thickness of Ellesmerian sequence = 2.3 km (balanced cross-section)

Thickness of Ellesmerian sequence = 0.6 km (not represented in study area; values from Reed (1968), Sable (1977), Bird and Molenaar (1987)

Thickness of Brookian sequence = 9.0 km (Bird and Bader, 1987)

Total thickness = 11.9 km.

(2) Pressure, σ_z, above Kekiktuk Conglomerate resulting from depositional overburden:

Using $\rho = 2500$ kg/m^3,

$\sigma_z = (2500)(9.8)(11900) = 292$ MPa.

(3) Overburden pressure above the Kekiktuk Conglomerate of the second horse resulting from tectonic loading by thrust emplacement of the first horse:

Measuring thickness of first horse above the second horse (i.e. above the lower antiform in Figure 30), t = 0.7 to t = 1.7 km. Therefore, H = 11.9 km + t, and σ_z = (2500)(9.8)(12600) = 309 MPa to σ_z = (2500)(9.8)(13600) = 333 MPa. Therefore, thust emplacement of the leading edge of the first horse over the eventual second horse would cause overburden pressure on the top surface of the Kekiktuk Conglomerate of the second horse to increase by 6-12% from that attributed to the presence of depositionally overlying rocks.

The maximum overburden pressure due to emplacement of the first horse would theoretically occur to the south of the study area where t = 4.7 km, the thickness of the first horse (Figure 32). Here, H = 11.9 + 4.7 = 16.6 km and σ_z = (2500)(9.8)(16600) = 407 MPa. This tectonic overburden pressure would represent a 28% increase from the load of depositionally overlying rocks.

REFERENCES CITED

Armstrong, A.K., and Mamet, B.L., 1975, Carboniferous biostratigraphy, northeastern Brooks Range, Arctic Alaska: United States Geological Survey Professional Paper 884, 29p.

Armstrong, A.K., Mamet, B.L., and Dutro, J.T., 1970, Foraminiferal zonation and carbonate facies of Carboniferous (Mississippian and Pennsylvanian) Lisburne Group, central and eastern Brooks Range, Arctic Alaska: American Association of Petroleum Geologists Bulletin, v. 54, p. 687-698.

Avé Lallemant, H.G., Oldow, J.S., Handschy, J.W., and Haley, J.C., 1987, Tectonic Implications of Shear Along the Kekiktuk - Neruokpuk Contact, Northeastern Brooks Range, Alaska: EOS, v. 68, no. 44, p. 1457.

Banks, C.J., and Warburton, J., 1986, 'Passive-roof' duplex geometry in the frontal structures of the Kirthar and Sulaiman mountain belts, Pakistan: Journal of Structural Geology, v. 8, n. 3/4, p. 229-237.

Bird, K.J., and Bader, J.W., 1987, Chapter 3: Regional geologic setting and history of petroleum exploration, in Petroleum Geology of the Arctic National Wildlife Refuge, Northeastern Alaska: United States Geological Survey Bulletin 1778, p. 17-25.

Bird, K.J., and Molenaar, C.M., 1987, Chapter 5: Stratigraphy, in Petroleum Geology of the Arctic National Wildlife Refuge, Northeastern Alaska: United States Geological Survey Bulletin 1778, p. 37-59.

Box, S.E., 1985, Early Cretaceous orogenic belt in northwestern Alaska: Internal organization, lateral extent, and tectonic interpretation, in Howell, D.G., ed., Tectonostratigraphic terranes of the Circum-Pacific region: Circum-Pacific Council for Energy and Mineral Resources Earth Science Series 1, p. 137-145.

Boyer, S.E., and Elliott, D., 1982, Thrust systems: American Association of Petroleum Geologists Bulletin, v. 66, n. 9, p. 1196-1230.

Brosgé, W.P., Dutro, J.T. Jr., Mangus, M.D., and Reiser, H.N., 1962, Paleozoic sequence in eastern Brooks Range, Alaska: American Association of Petroleum Geologists Bulletin, v. 46, no. 12, p. 2174-2198.

Brosgé, W.P., and Tailleur, I.L., 1970, Depositional history of northern Alaska, in Adkison, W.L. and Brosgé, M.M., eds., Los Angeles: American Association of Petroleum Geologists, Pacific Section, p. D1-D18.

Butler, R.W.H., 1982, Hangingwall strain: a function of duplex shape and footwall topography: Tectonophysics, v. 88, p. 235-246.

Cooper, M.A, and Trayner, P.M., 1986, Thrust-surface geometry: implications for thrust-belt evolution and section-balancing techniques: Journal of Structural Geology, v. 8, n. 3/4, p. 305-312.

Craig, J.D., Sherwood, K.W., and Johnson, P.P., 1985, Geologic report for the Beaufort Sea planning area, Alaska: United States Department of the Interior Offshore Continental Shelf Report MMS 85-0111, 192p.

Crane, R.C., 1987, Arctic reconstruction from an Alaskan point of view, in Tailleur, I.L., and Weimer, P., eds., Alaska North Slope Geology: Pacific Section SEPM, and Alaska Geological Society, Book 50, p. 769-783.

Crespi, J.M., 1986, Some guidelines for the practical application of Fry's method of strain analysis: Journal of Structural Geology, v. 8, n. 7, p. 799-808.

Dahlen, F.A., Suppe, J., and Davis, P., 1984, Mechanics of fold-and-thrust belts and accretionary wedges: cohesive Coulomb theory: Journal of Geophysical Research, v. 89, p. 10,087-10,101.

Dahlstrom, C.D.A., 1970, Structural geology in the eastern margin of the Canadian Rocky Mountains: Bulletin of Canadian Petroleum Geology, v. 18, p. 332-406.

Dahlstrom, C.D.A., 1969, Balanced cross sections: Canadian Journal of Earth Sciences, v. 6, p. 743-757.

Davis, D., Suppe, J., and Dahlen, F.A., 1983, Mechanics of fold-and-thrust belts and accretionary wedges: Journal of Geophysical Research, v. 88, n. B2, p. 1153-1172.

Davis, G.H., 1984, Structural Geology of Rocks and Regions: John Wiley & Sons, New York, 492p.

De Paor, D.G., 1988, Balanced section in thrust belts Part I: Construction: American Association of Petroleum Geologists Bulletin, v. 72, n. 1, p. 73-90.

Detterman, R.L., Reiser, H.N., Brosgé, W.P., and Dutro, J.T. Jr., 1975, Post-Carboniferous stratigraphy of northeastern Alaska: United States Geological Survey Professional Paper 886, 46p.

Dillon, J.T., 1987, Latest Cretaceous-earliest Tertiary metamorphism in the northeastern Brooks Range, Alaska: Geological Society of America Cordilleran Section Abstracts with Programs, v. 19, no. 6, p. 373.

Dillon, J.T., Tilton, G.R., Decker, J.E., and Kelly, M.J., 1987, Resource implications of magmatic and metamorphic ages for Devonian igneous rocks in the Brooks Range, in Tailleur, I.L., and Weimer, P., eds., Alaska North Slope Geology: Pacific Section, SEPM, and Alaska Geologic Society, Book 50, p. 713-723.

Dunnet, D., 1969, A technique of finite strain analysis using elliptical particles: Tectonophysics, v. 2, p. 117-136.

Dutro, J.T. Jr., 1981, Geology of Alaska bordering the Arctic Ocean, in Nairn, A.E.M., Churkin, M. Jr., and Stehli, F.G., The ocean basins and margins, v. 5, The Arctic Ocean: Plenum Press, New York, p. 21-36.

Dutro, J.T. Jr., Brosgé, W.P., and Reiser, H.N., 1972, Significance of recently discovered Cambrian fossils and reinterpretation of Neruopuk formation, northeastern Alaska: American Association of Petroleum Geologists Bulletin, v. 56, no. 4, p. 808-815.

Elliott, D., 1983, The construction of balanced cross-sections: Journal of Structural Geology, v. 5, p. 101.

Erslev, E.A., 1988, Normalized center-to-center strain analysis of packed aggregates: Journal of Structural Geology, v. 10, n. 2, p. 201-209.

Fry, N., 1979, Random point distributions and strain measurement in rocks: Tectonophysics, v. 60, p. 89-105.

Grantz, A., and May, S.D., 1983, Rifting history and structural development of the continental margin north of Alaska, in Studies in continental margin geology, Watkins, J.S., and Drake, C.L., eds.: American Association of Petroleum Geologists Memoir 34, p. 77-100.

Gretener, P.E., 1972, Thoughts on overthrust faulting in a layered sequence, in North American thrust-faulted terranes, compiled by Perry, W.J., Roeder, D.H., Lageson, D.R.: American Association of Petroleum Geologists Reprint Series No. 27, p. 72-96.

Groshong, R.H., Jr., 1988, Low-temperature deformation mechanisms and their interpretation: Geological Society of America Bulletin, v. 100, p. 1329-1360.

Hubbard, R.J., Edrich, S.P., and Rattey, R.P., 1987, Geologic evolution and hydrocarbon habitat of the 'Arctic Alaska microplate', in Tailleur, I.L., and Weimer, P., eds., Alaska North Slope Geology: Pacific Section, SEPM, and Alaska Geologic Society, Book 50, p. 797-830.

Hubbert, M.K., and Rubey, W.W., 1959, Role of fluid pressure in mechanics of overthrust faulting: Geological Society of America Bulletin, v. 70, p. 115-206.

Hudleston, P.J., 1973, Fold morphology and some geometrical implications of theories of fold development: Tectonophysics, v. 16, p. 1-46.

Jamison, W.R., and Spang, J.H., 1976, Use of calcite twin lamellae to infer differential stress: Geological Society of America Bulletin, v. 87, p. 868-872.

Keller, A.S., Morris, R.H., and Detterman, R.L., 1961, Geology of the Shaviovik and Sagavanirktok Rivers region, Alaska: United States Geological Survey Professional Paper 303-D, p. 169-222.

Kelley, J.S., and Foland, R.L., 1987, Structural Style and Framework Geology of the Coastal Plain and Adjacent Brooks Range: United States Geological Survey Bulletin 1778, p. 255-270.

Kelley, J.S., and Molenaar, C.M., 1985, Detachment tectonics in Sadlerochit and Shublik Mountains and applications for exploration beneath coastal plain, Arctic National Wildlife Range, Alaska: American Association of Petroleum Geologists Bulletin, v. 69, no. 4, p. 667.

Lacassin, R., and van den Driessche, J., 1983, Finite strain determination of gneiss: application of Fry's method to porphyroid in southern Massif Central (France): Journal of Structural Geology, v. 5, n. 3/4, p. 245-253.

Leffingwell, E. de K., 1919, The Canning River region, northern Alaska: United States Geological Survey Professional Paper 109, 251p.

Leiggi, P.A., 1987, Style and age of tectonism of the Sadlerochit Mountains to Franklin Mountains, Arctic National Wildlife Refuge, Alaska, in Tailleur, I.L., and Weimer, P. eds., Alaska North Slope Geology: Pacific Section, SEPM, and Alaska Geologic Society, Book 50, p. 749-756.

Leiggi, P.A., and Russell, B.J., 1985, Style and age of tectonism of Sadlerochit Mountains to Franklin Mountains, Arctic National Wildlife Refuge (ANWR), Alaska: American Association of Petroleum Geologists Bulletin, v. 69, no. 4, p. 668.

LePain, D.L., and Crowder, R.K, 1989, Deposition of the Endicott Group (Mississippian) in the central Franklin Mountains, northeastern Alaska: Geological Society of America Cordilleran/Rocky Mountain Section Abstracts With Programs, in press.

Lerand, M., 1973, Beaufort Sea, in McCrossam, R.G., ed., The future petroleum provinces of Canada -- their geology and potential: Canadian Society of Petroleum Geology Memoir 1, p. 315-386.

Mamet, B.L, and Armstrong, A.K., 1972, Lisburne Group, Franklin and Romanzof Mountains, northeastern Alaska: United States Geological Survey Professional Paper 800-C, p. C127-C144.

Mitra, S., 1987, Regional variations in deformation mechanisms and structural styles in the central Appalachian orogenic belt: Geological Society of America Bulletin, v. 98, p. 569-590.

Mitra, S., 1986, Duplex structures and imbricate thrust systems: geometry, structural position, and hydrocarbon potential: American Association of Petroleum Geologists Bulletin, v. 70, n. 9, p. 1087-1112.

Moore, T.E., 1987, Geochemistry and tectonic setting of some volcanic rocks of the Franklinian assemblage, central and eastern Brooks Range, in Tailleur, I.L., and Weimer, P. eds., Alaska North Slope Geology: Pacific Section, SEPM, and Alaska Geologic Society, Book 50, p. 691-710.

Moore, T.E., Brosgé, W.P., Churkin, M. Jr., and Wallace, W.K., 1987, Pre-Mississippian accreted terranes of northeastern Brooks Range, Alaska, in Tailleur, I.L., and Weimer, P. eds., Alaska North Slope Geology: Pacific Section, SEPM, and Alaska Geologic Society, Book 50, p. 711.

Moore, T.E., and Churkin, M., Jr., 1984, Ordovician and Silurian graptolite discoveries from the Neruokpuk Formation (sensu lato), northeastern and central Brooks Range, Alaska, in Blodgett, R.B., ed., Paleozoic geology of Alaska and northwestern Canada, Newsletter No. 1: Anchorage, Alaska, Alaska Geological Society, p. 21-23.

Mull, C.G., 1985, Cretaceous tectonics, depositional cycles, and the Nanushuk Group, Brooks Range and Arctic Slope, Alaska: United States Geological Survey Bulletin 1614, p. 7-37.

Mull, C.G., 1982, Tectonic evolution and structural style of the Brooks Range, Alaska: An illustrated summary, in Powers, R.B., ed., Geologic studies of the Cordilleran thrust belt: Rocky Mountain Association of Geologists, Denver, Colorado, v. 1, p. 1-45.

Namson, J.S., and Wallace, W.K., 1986, A structural transect across the northeastern Brooks Range: Geological Society of America Abstracts with Programs, v. 18, no. 2, p. 163.

Nilsen, T.H., 1981, Upper Devonian and Lower Mississippian redbeds, Brooks Range, Alaska, in Miall, A.D., ed., Sedimentation and tectonics in alluvial basins: Geological Association of Canada Special Paper 23, p. 187-219.

Oldow, J.S., Avé Lallemant, H.G., Julian, F.E., and Seidensticker, C.M., 1987, Ellesmerian(?) and Brookian deformation in the Franklin Mountains, northeastern Brooks Range, Alaska, and its bearing on the origin of the Canada Basin: Geology, v. 15, p. 37-41.

Oldow, J.S., Avé Lallemant, H.G., Julian, F.E., and Seidensticker, C.M., 1986, Franklin Mountains, NE Brooks Range, Alaska, Part I: Late Mesozoic and Cenozoic Brookian Deformation: Geological Society of America Abstracts with Programs, v. 18, no. 2, p. 167.

Onasch, C.M., 1986, Ability of the Fry method to characterize pressure-solution deformation: Tectonophysics, v. 122, p. 187-193.

O'Sullivan, P.B., 1988, Apatite fission-track study of the thermal history of Permian to Tertiary sedimentary rocks in the Arctic National Wildlife Refuge, northeastern Alaska: Master's thesis, University of Alaska Fairbanks, 184p.

Paterson, M.S., 1978, Experimental Rock Deformation - The Brittle Field: Springer-Verlag, 254 p.

Ramsay, J.G, 1967, Folding and Fracturing of Rocks: McGraw Hill, New York, 568p.

Ramsay, J.G., and Huber, M.I., 1987, The Techniques of Modern Structural Geology Volume 2: Folds and Fractures: Academic Press, Inc., 393p.

Ramsay, J.G., and Huber, M.I., 1983, The Techniques of Modern Structural Geology Volume 1: Strain Analysis: Academic Press, Inc., 307p.

Rattey, R.P., 1985, Northeastern Brooks Range, Alaska: New evidence for complex thin-skinned thrusting: American Association of Petroleum Geologists Bulletin, v. 69, no. 4, p. 676.

Reed, B.L., 1968, Geology of the Lake Peters area, northeastern Brooks Range, Alaska: United States Geological Survey Bulletin 1236, 132 p.

Reiser, H.N., Brosgé, W.P., Dutro, J.T. Jr., and Detterman, R.K., 1971, Preliminary geologic map, Mt. Michelson quadrangle, Alaska: United States Geological Survey Open-File Report 71-237, scale 1:200,000.

Ribeiro, A., Killberg, M.C., and Possolo, A., 1983, Finite strain estimation using 'anti-clustered' distributions of points: Journal of Structural Geology, v. 5, n. 3/4, p. 233-243.

Robbins, S.L., 1987, Chapter 15: Gravity interpretation of the coastal plain, in Petroleum Geology of the Arctic National Wildlife Refuge, Northeastern Alaska: United States Geological Survey Bulletin 1778, p. 219-224.

Sable, E.G., 1977, Geology of the western Romanzof Mountains, Brooks Range, northeastern Alaska: United States Geological Survey Professional Paper 897, 84p.

Sanderson, D.J., 1982, Models of strain variation in nappes and thrust sheets: a review: Tectonophysics, v. 88, p. 201-233.

Smith, D.G., 1987, Late Paleozoic to Cenozoic reconstructions of the Arctic, in Tailleur, I.L., and Weimer, P., eds., Alaska North Slope Geology: Pacific Section SEPM, and Alaska Geological Society, Book 50, p. 785-795.

Suppe, J., 1983, Geometry and kinematics of fault-bend folding: American Journal of Science, v. 283, p. 684-721.

Tailleur, I.L., Brosgé, W.P., and Reiser, H.N., 1967, Palinspastic analysis of Devonian rocks in northwestern Alaska, in International symposium on the Devonian System, v. 2: Alberta Society of Petroleum Geologists, p. 1345-1361.

United States Department of the Interior, 1986, Draft Arctic National Wildlife Refuge, Alaska, coastal plain resource assessment, 172p.

Wallace, W.K., and Hanks, C.L., 1988a, Lateral variations in the range-front structure of the northeastern Brooks Range, Arctic National Wildlife Refuge (ANWR), Alaska: Geological Society of America Abstracts with Programs, v. 20, n. 3, p. 241.

Wallace, W.K., and Hanks, C.L., 1988b, Stratigraphic controls on lateral variations in the structural style of the northeastern Brooks Range, Arctic National Wildlife Refuge (ANWR), Alaska: American Association of Petroleum Geologists Bulletin, v. 72, no. 2, p. 256.

Wallace, W.K., and Hanks, C.L., in press, Systematic vertical and lateral variations in structural geometry in the northeastern Brooks Range, Alaska: submitted to American Association of Petroleum Geologists Bulletin.

Wiltschko, D.V., and Chapple, W.M., 1977, Flow of weak rocks in Appalachian plateau folds: American Association of Petroleum Geologists Bulletin, v. 61, n. 5, p. 653-670.

Woodward, N.B., Gray, D.R., Spears, D.B., 1986, Including strain data in balanced cross-sections: Journal of Structural Geology, v. 8, n. 3/4, p. 313-324.

Woodward, N.B., Boyer, S.E., Suppe, J., 1985, An outline of balanced cross-sections: University of Tennessee Department of Geological Sciences, Studies in Geology 11, 2nd edition, 170 p.

PLATE 1 GEOL

NORT

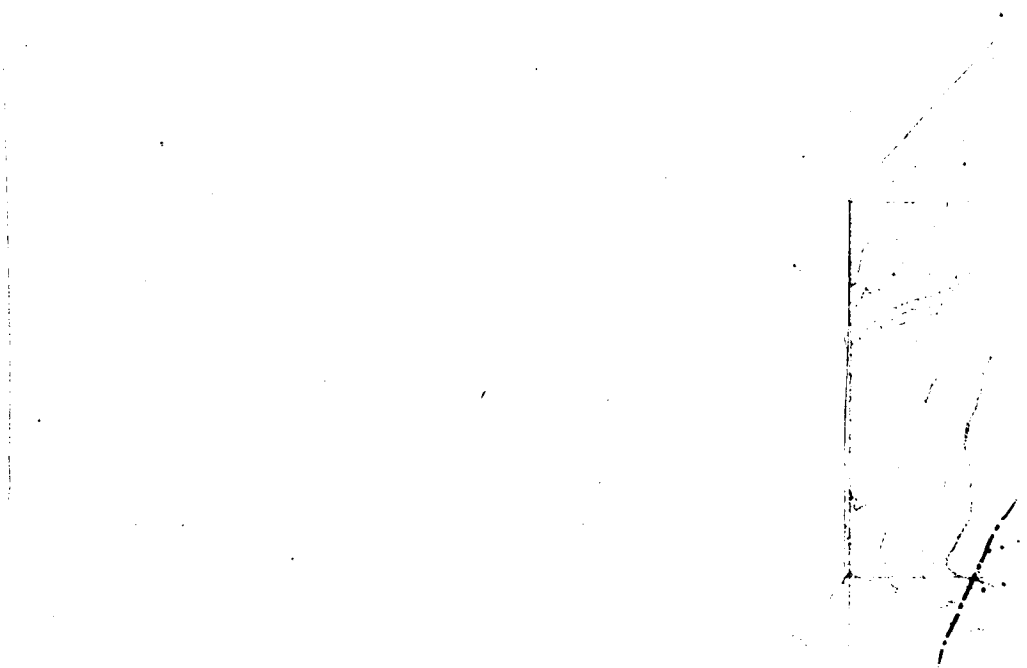

GEOLOGIC MAP OF STUDY AREA BE
NORTHEASTERN BROOKS RANGE, A

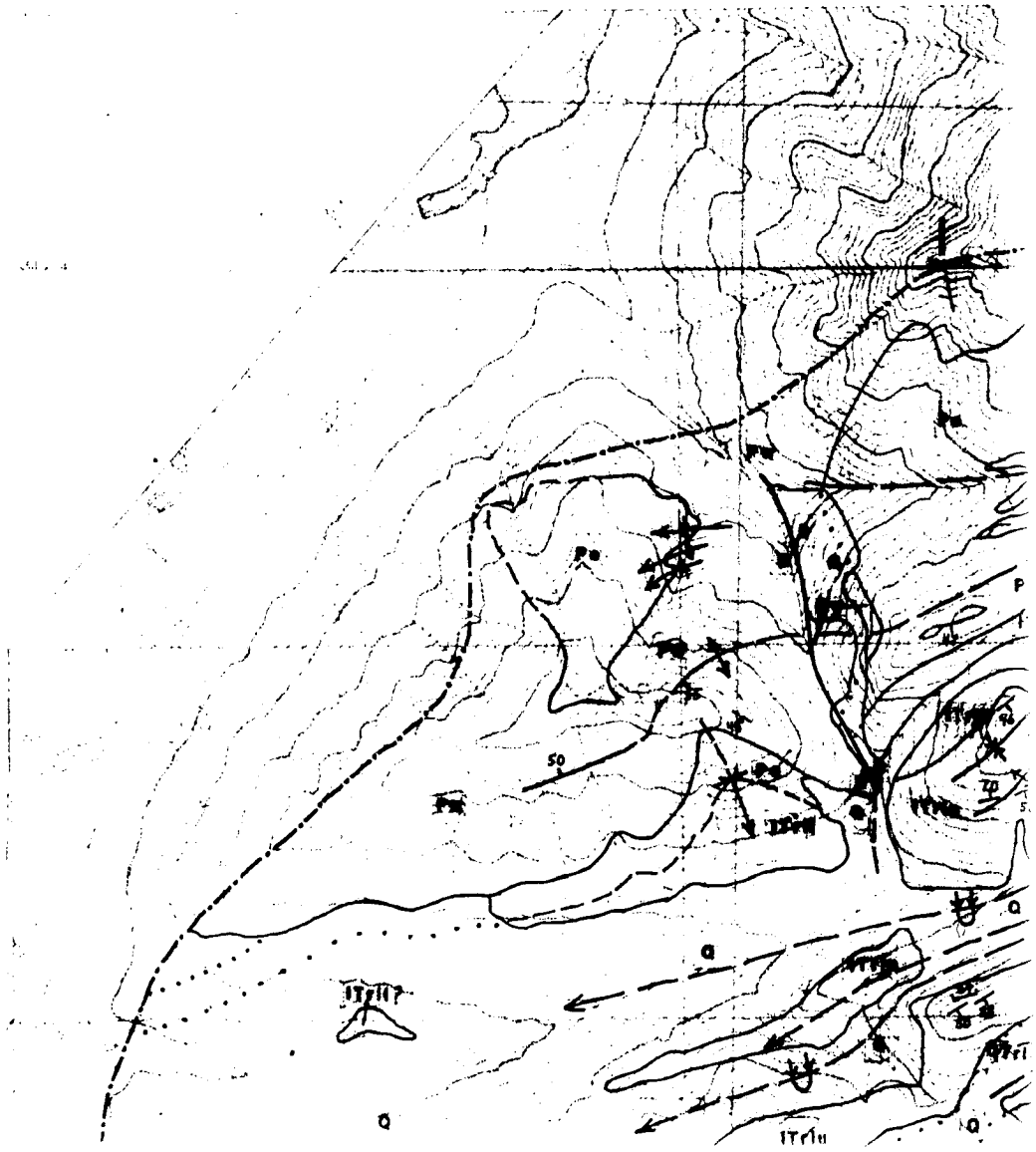

EA BETWEEN FORKS OF CANNING F

NGE, ALASKA

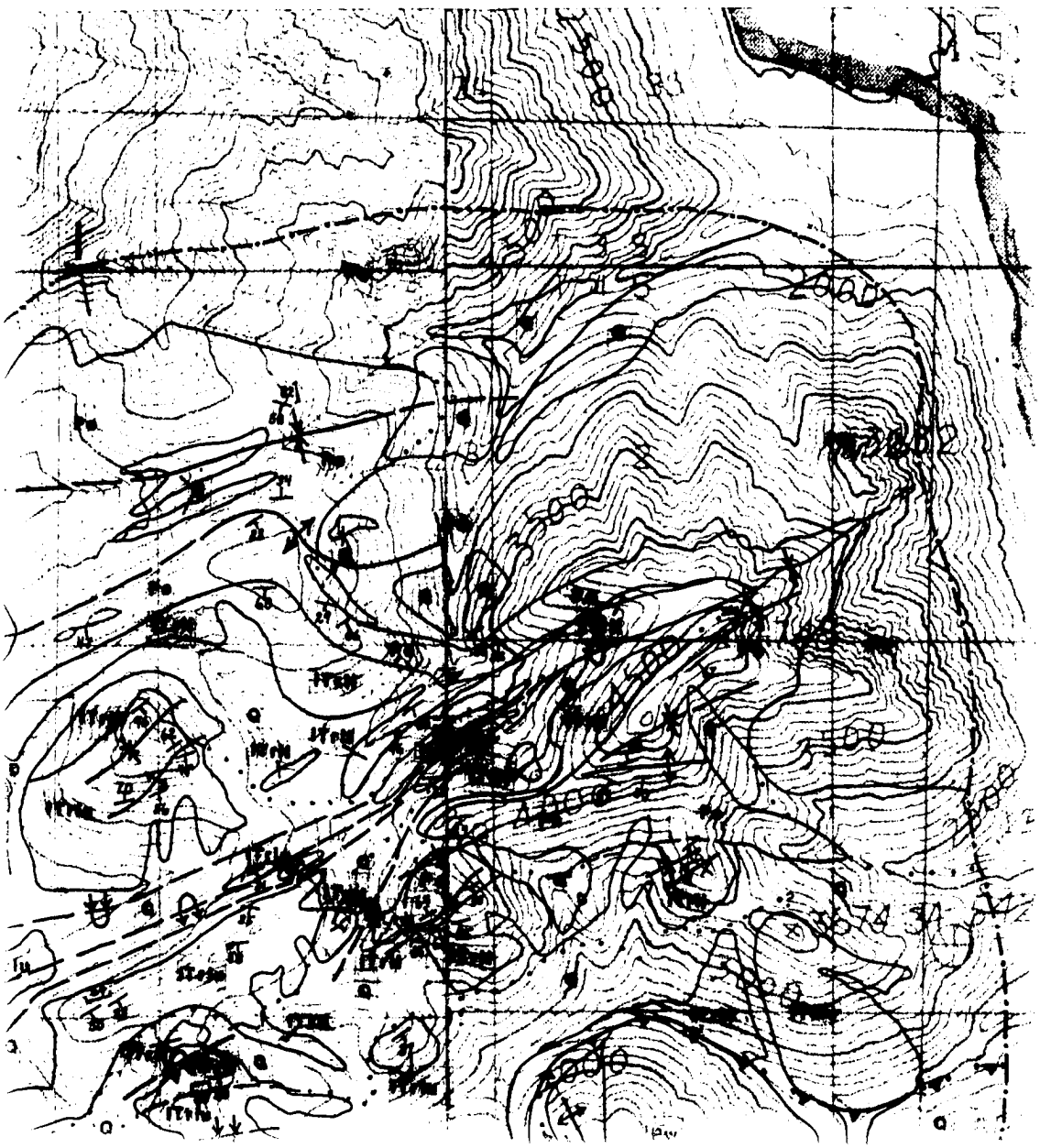

INING RIVER, FRANKLIN MOUNTAINS

EXPLANATI

25 St

50 Str

Str

43 64 Str

IN MOUNTAINS,

EXPLANATION OF MAP SYMBOLS

Strike and dip of beds

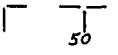

Strike and dip of bedding; uncertain

Strike of vertical bedding

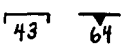

Strike and dip of cleavage; foliation

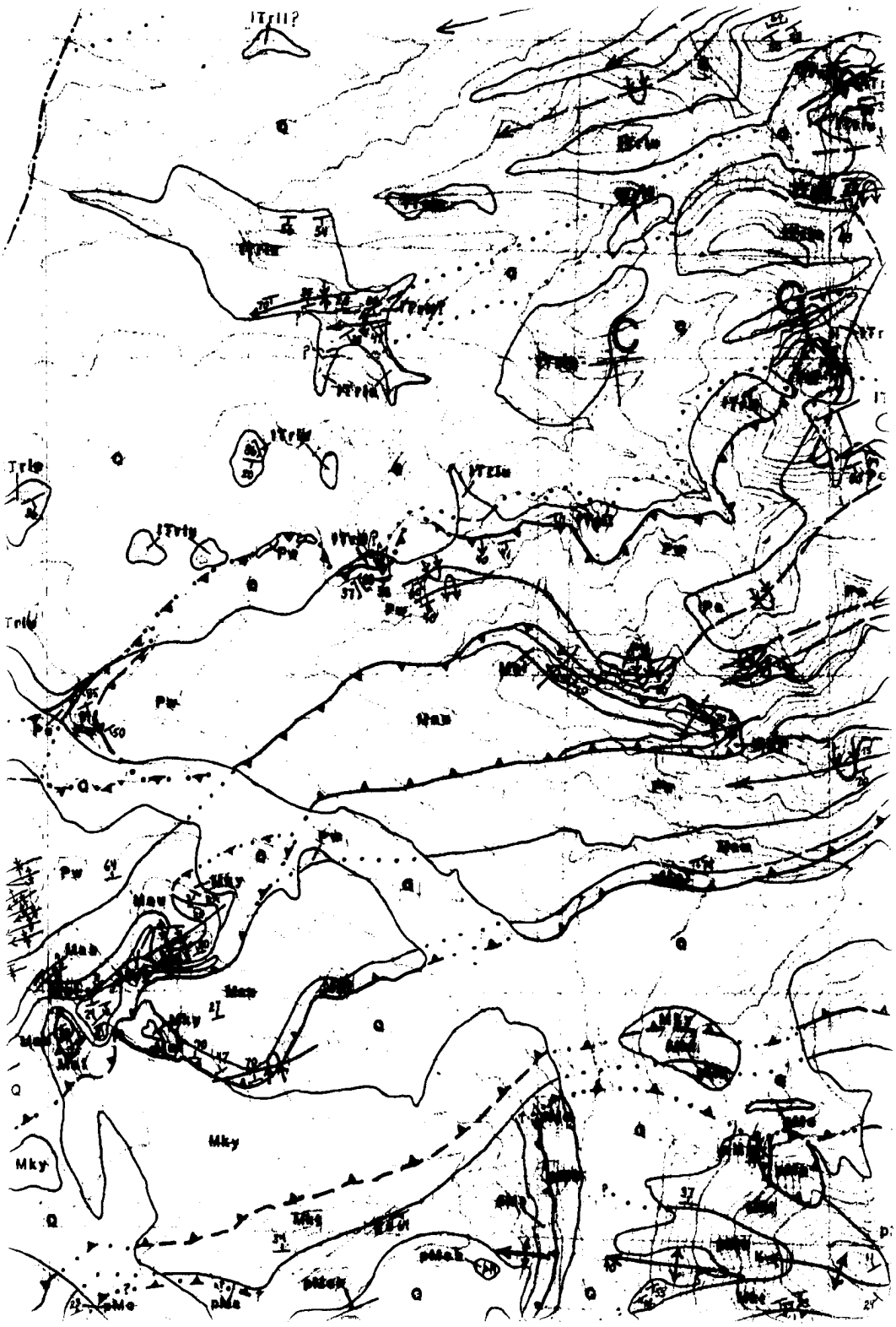

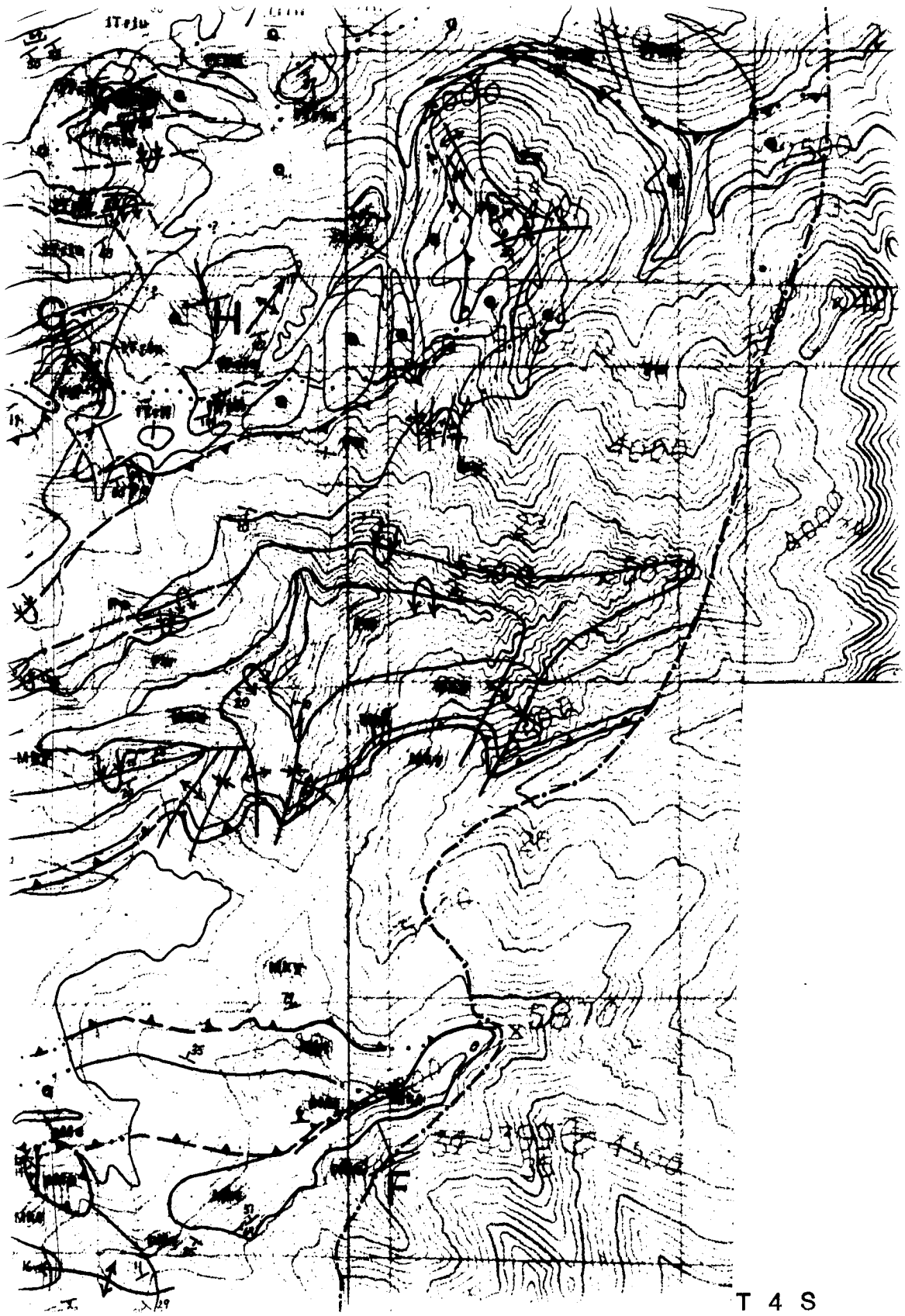

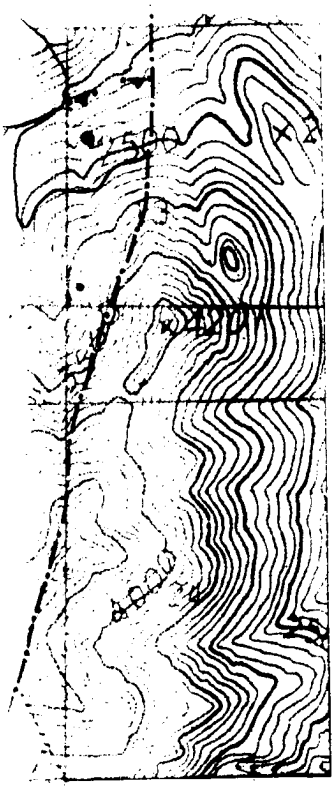

Stri

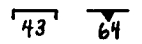

Strik

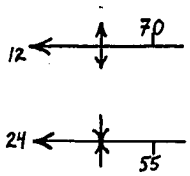

Antic
dip of
dashe

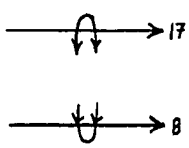

Over
show
dash

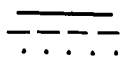

Conta
appr

Thrus
dash
dotte
upper
which

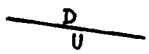

Fault

(Refer to Appen

lTriu	Lower
lTril	Lower
Pe	Permi
Pw	Penns

T 4 S

Strike of vertical bedding

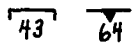

Strike and dip of cleavage; foliation

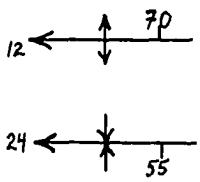

Anticline (top) and syncline, showing trace and dip of axial surface and plunge of axis; dashed where approximately located

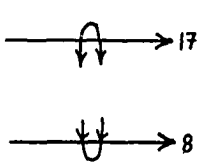

Overturned anticline (top) and overturned syncline, showing trace of axial surface and plunge of axis; dashed where approximately located

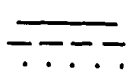

Contact; solid where known, dashed where approximately located, dotted where inferred

Thrust fault; solid where known, dashed where approximately located, dotted where inferred, sawteeth on upper plate (Also used to delineate a map unit which acts as a detachment or is brecciated.)

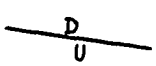

Fault (D,downthrown side; U, upthrown side)

(Refer to Appendix B for description of map units.)

lTriu	Lower Triassic upper Ivishak Formation
lTril	Lower Triassic lower Ivishak Formation
Pe	Permian Echooka Formation
Pw	Pennsylvanian Wahoo Limestone

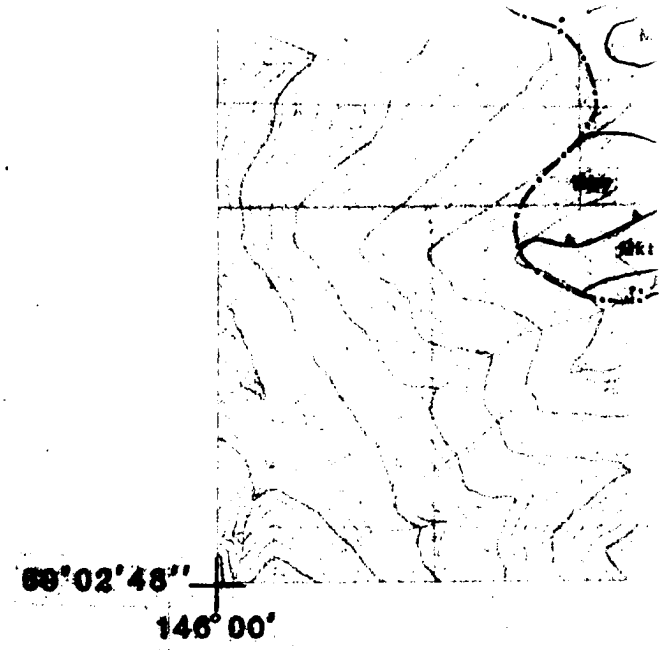

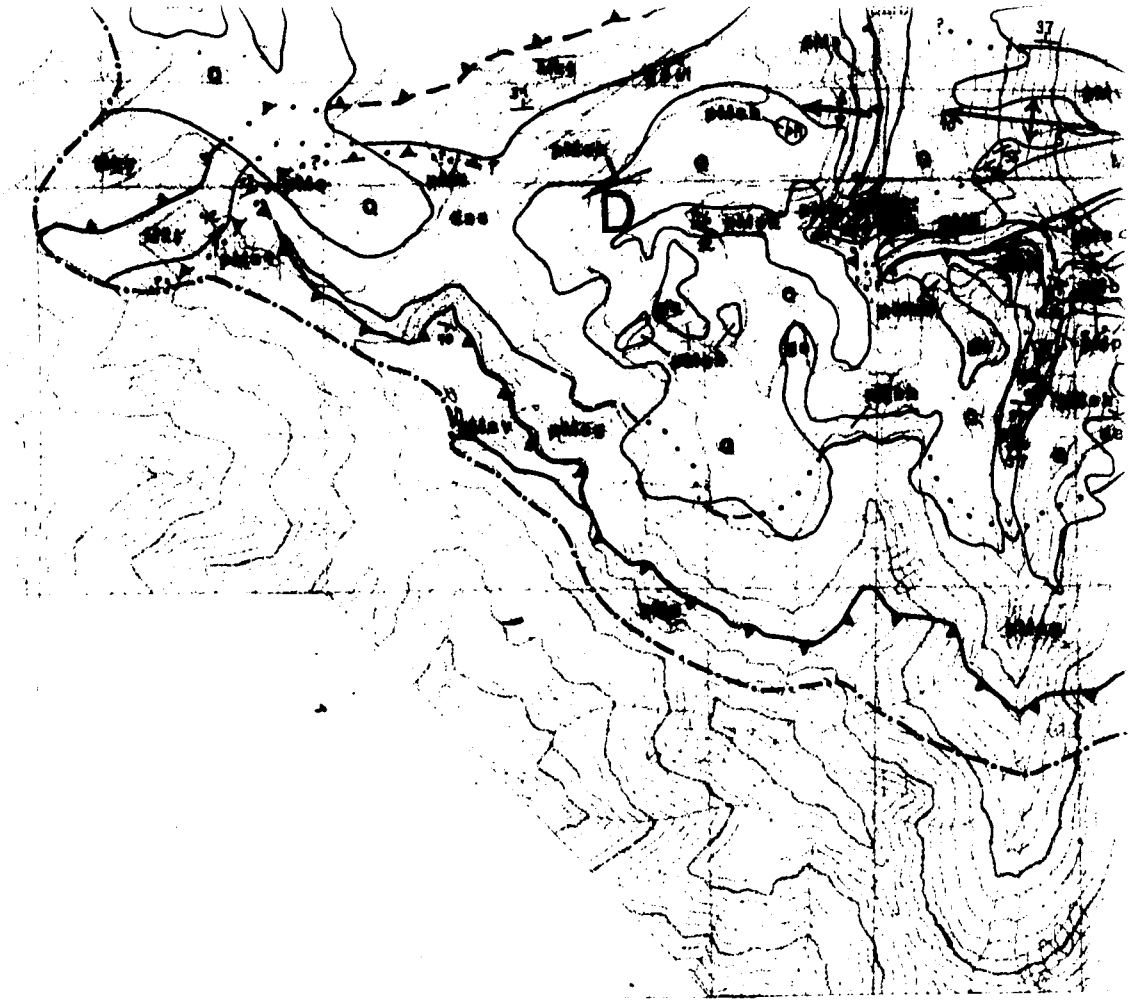

BY J.A. ZIE

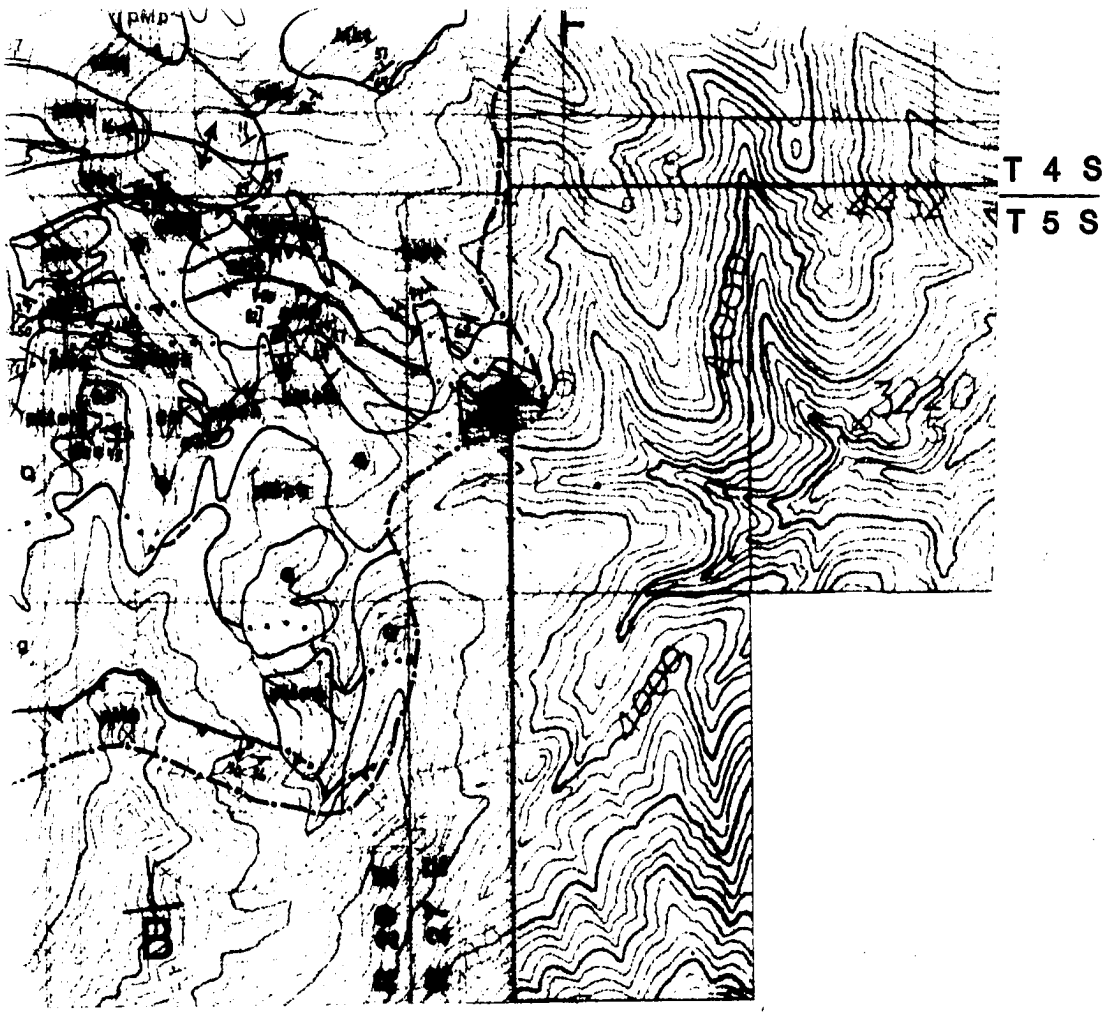

ZIEGLER 1989

T 4 S
T 5 S

lTriu	Lower
lTril	Lower T
Pe	Permian
Pw	Pennsyl
Mau	Mississip
Mal	Mississip
Mky	Mississip
Mkt	Mississip
pMsv	Pre-Miss
pMp	Pre-Miss
pMc	Pre-Miss
pMcg	Pre-Miss
pMsh	Pre-Miss
dss	Dol
gs	Gre
ch	Che
pMb	Pre-Miss
pMv	Pre-Miss

ITrid	Lower Triassic upper Ivishak Formation
ITril	Lower Triassic lower Ivishak Formation
Pe	Permian Echooka Formation
Pw	Pennsylvanian Wahoo Limestone
Mau	Mississippian upper Alapah Limestone
Mal	Mississippian lower Alapah Limestone
Mky	Mississippian Kayak Shale
Mkt	Mississippian Kekiktuk Conglomerate
pMsv	Pre-Mississippian Slate-Volcanic Unit
pMp	Pre-Mississippian Phyllite Unit
pMc	Pre-Mississippian Chloritic Phyllite Unit
pMcg	Pre-Mississippian Chert-Greenstone Unit
pMsh	Pre-Mississippian Shale Unit
	dss Dolostone/Sandstone
	gs Greenstone
	ch Chert
pMb	Pre-Mississippian Brecciated Unit
pMv	Pre-Mississippian Volcanic Unit

BASE ENLARGED FROM U

MT. MICHELSON QUADF

PROVISIONAL

0

SCALE

CONTOUR INT

) FROM U. S. GEOLOGICAL SURVEY

)N QUADRANGLE (A-3 AND A-4),

)VISIONAL EDITION 1983

1 2 MILES

SCALE 1 : 25,000

UR INTERVAL 100 FEET

EY

APPROXIM

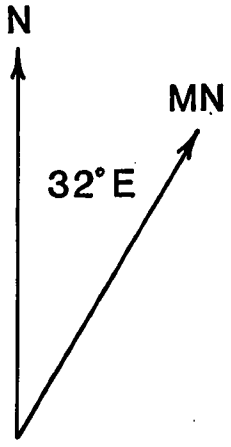

PROXIMATE DECLINATION, 1983

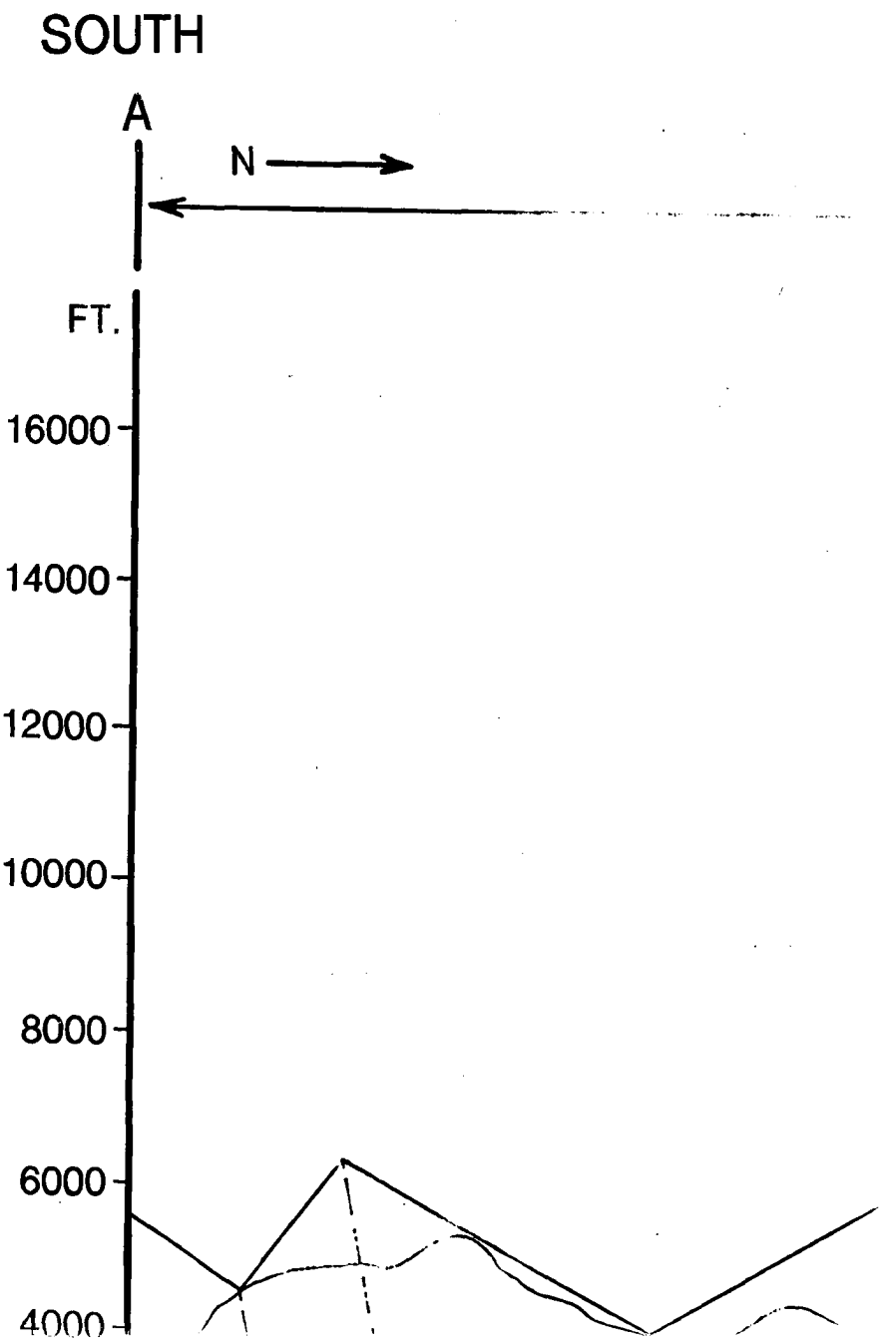

F

8.6 mi.
13.9 km

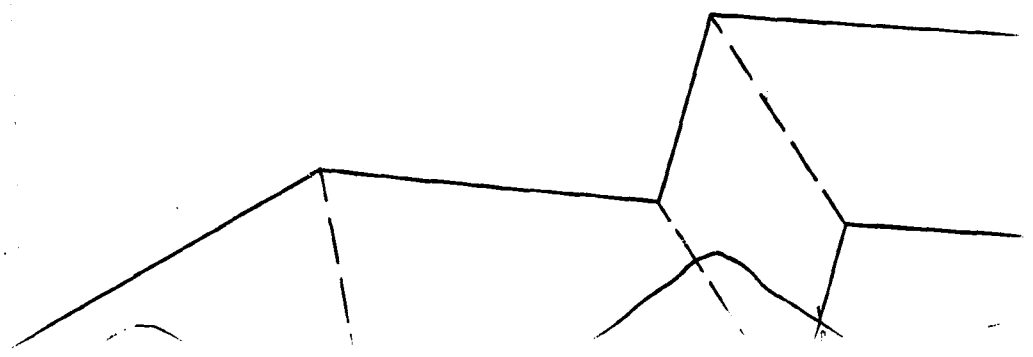

PLATE 2 PRIMARY BALAN(

8.6 mi.
13.9 km.

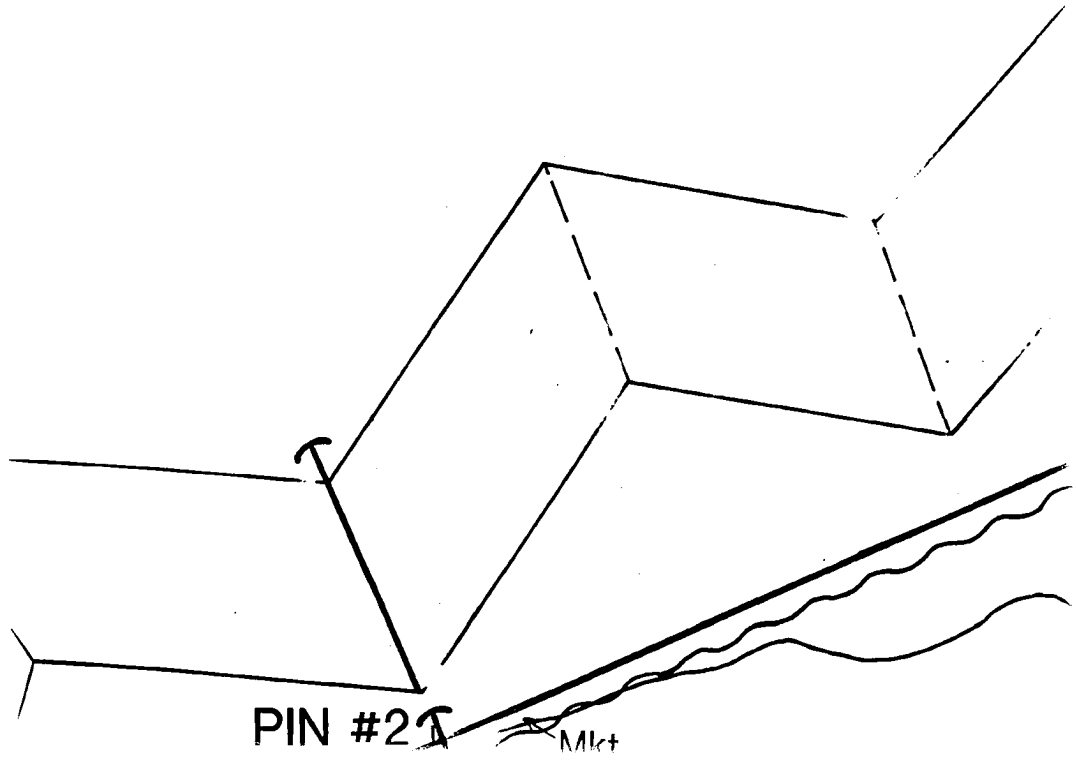

?Y BALANCED CROSS-SECTION ACI

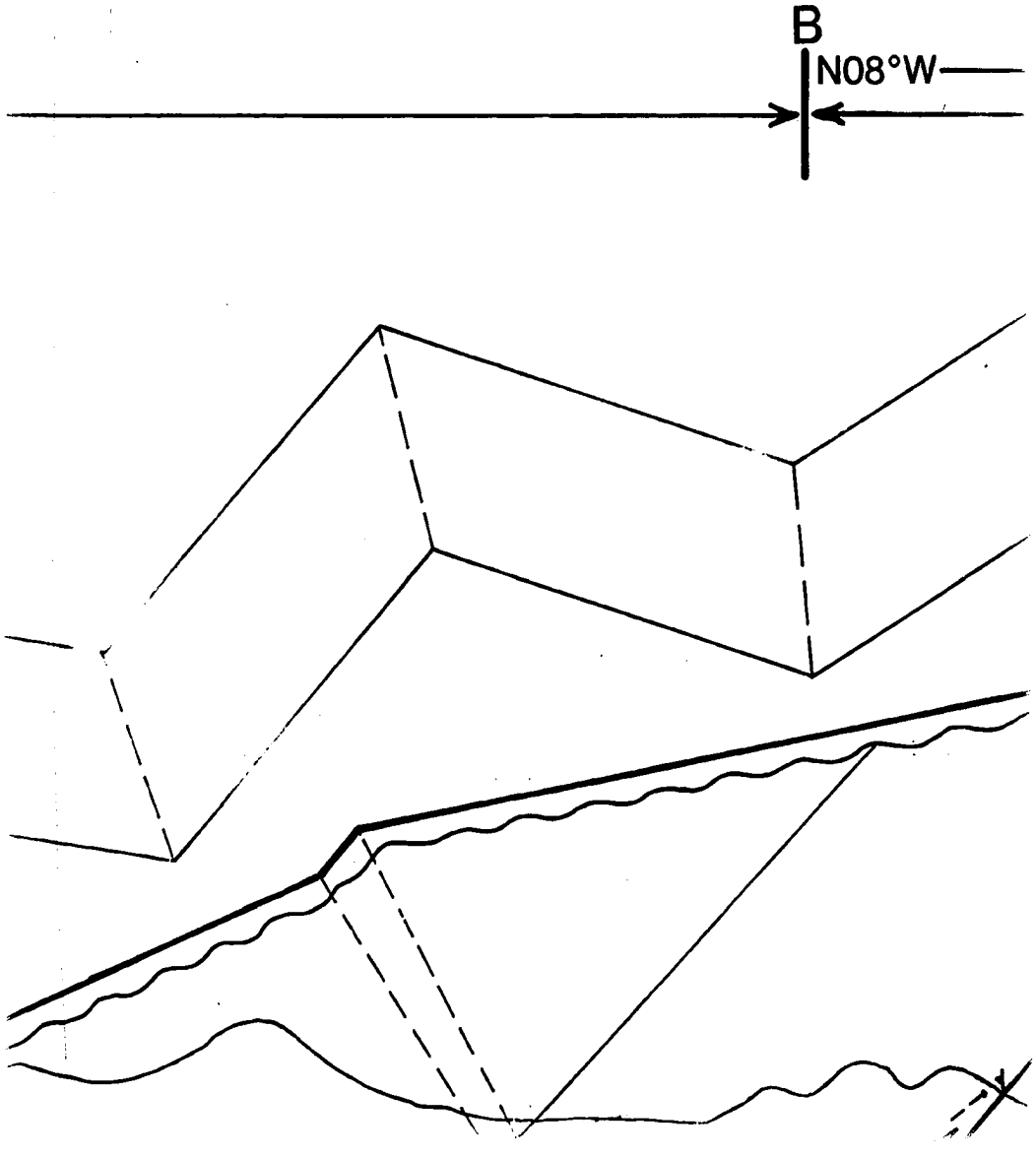

ON ACROSS THE FRANKLIN MOUNT

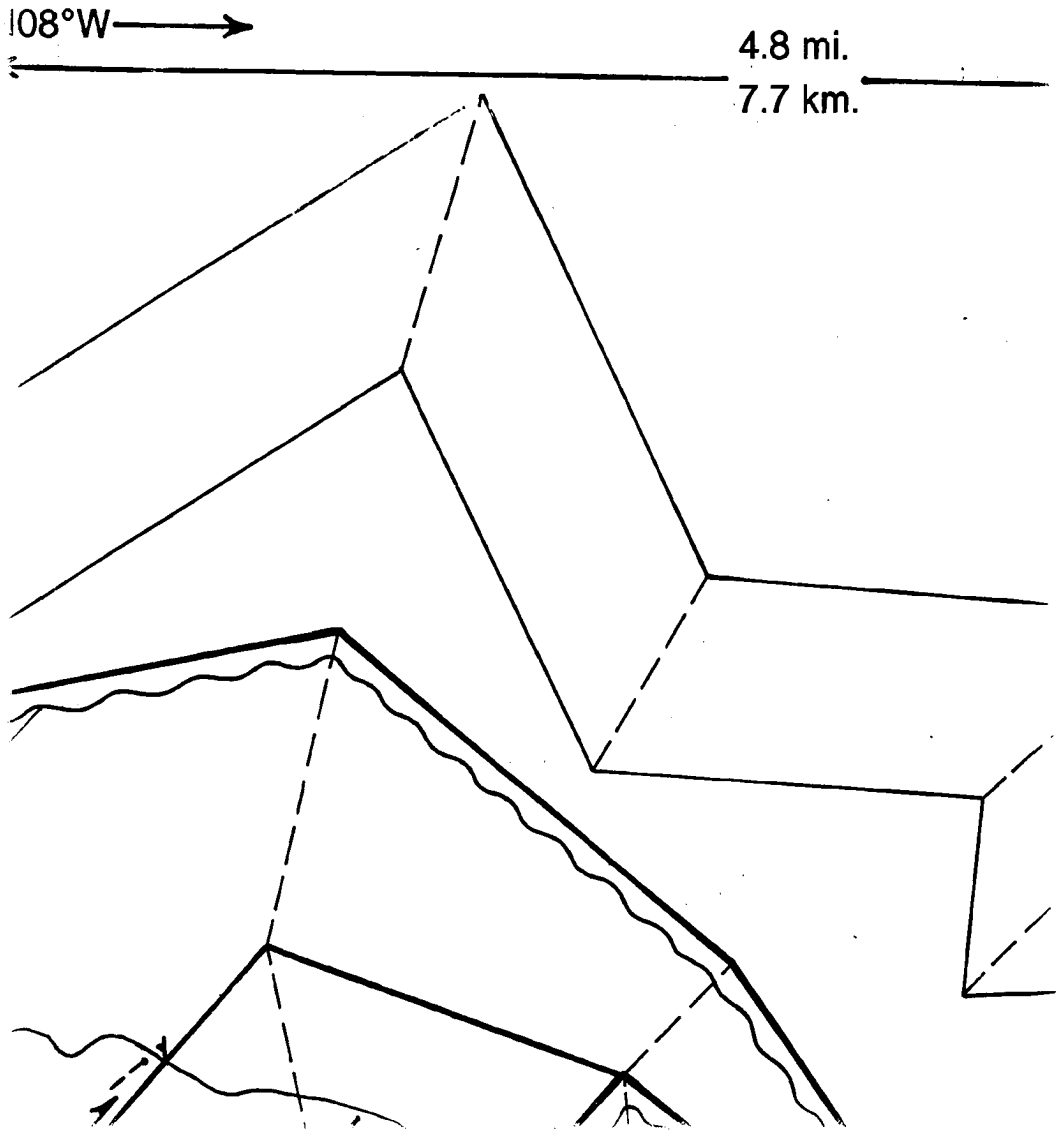

MOUNTAINS ANTICLINORIUM

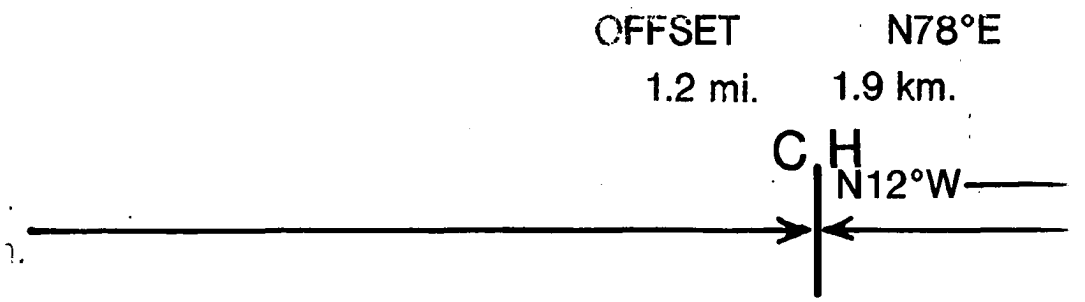

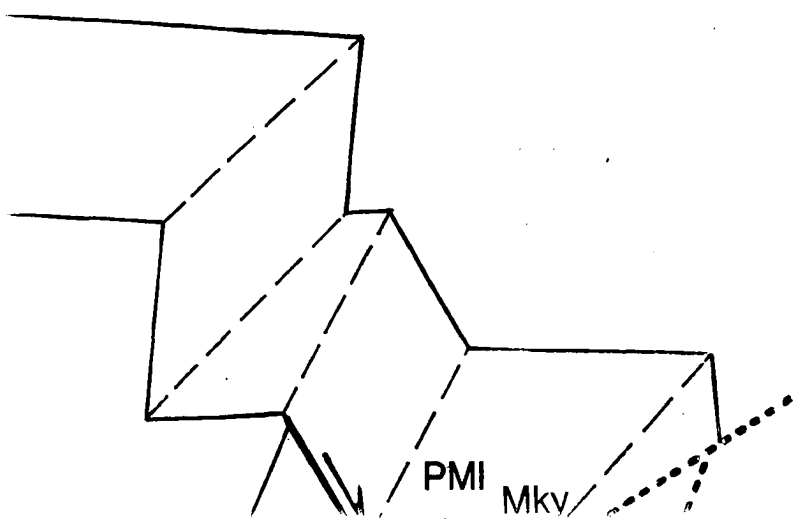

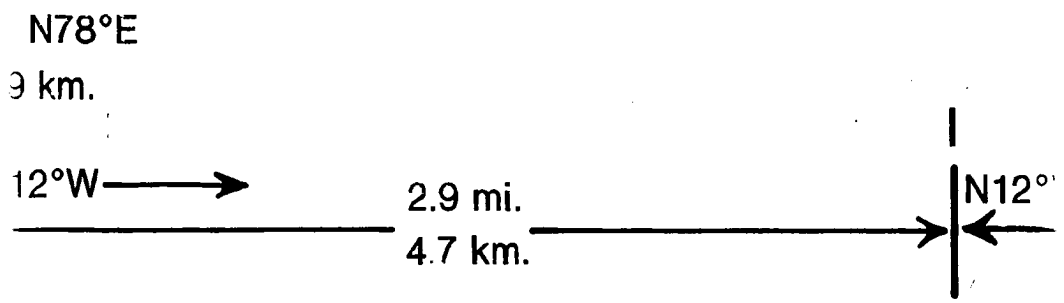

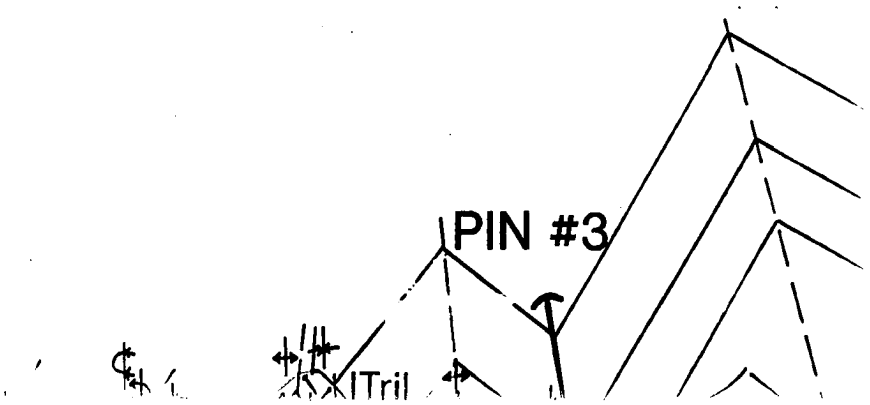

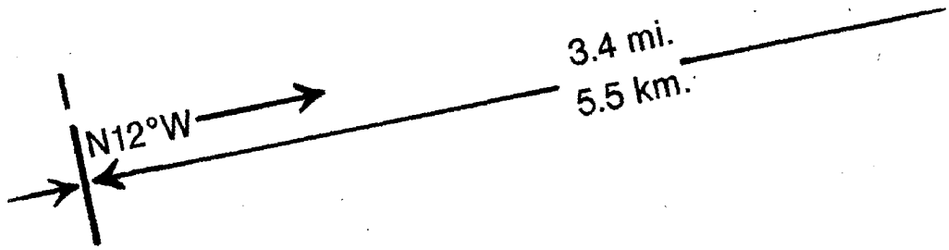

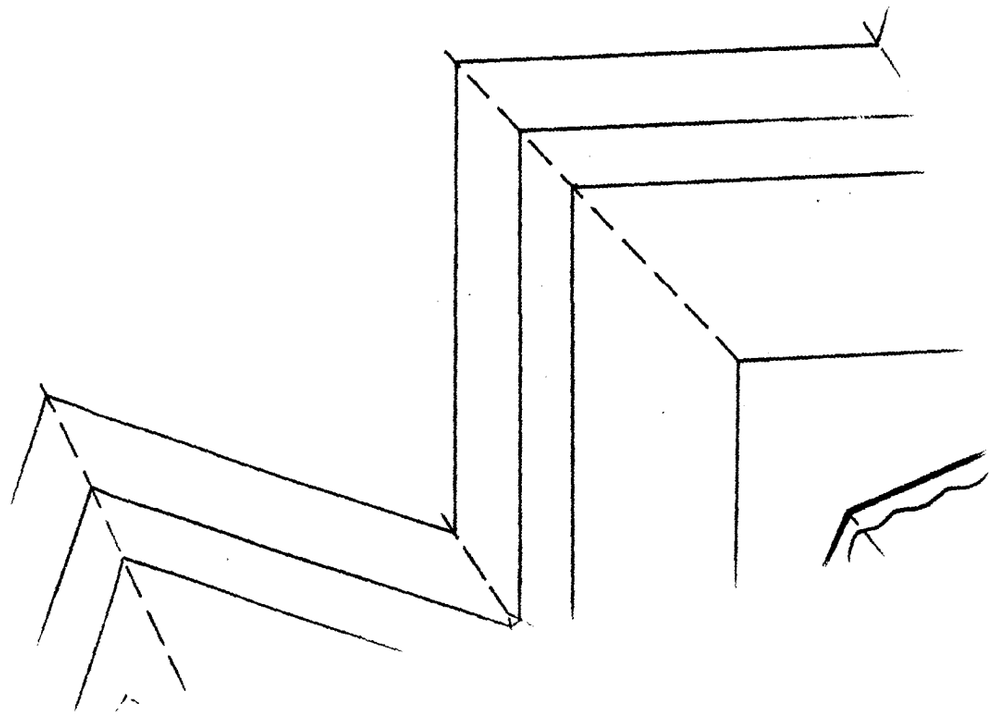

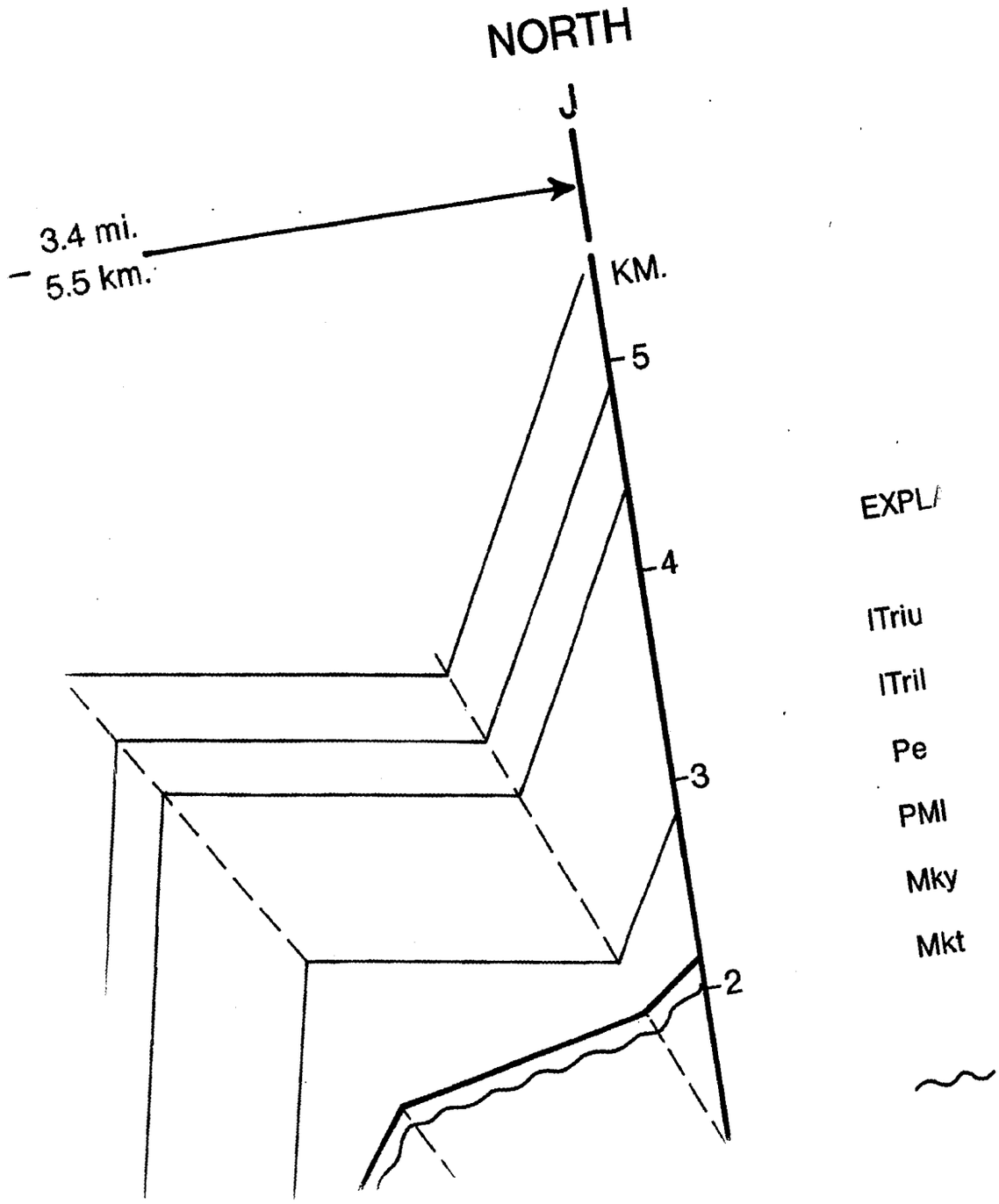

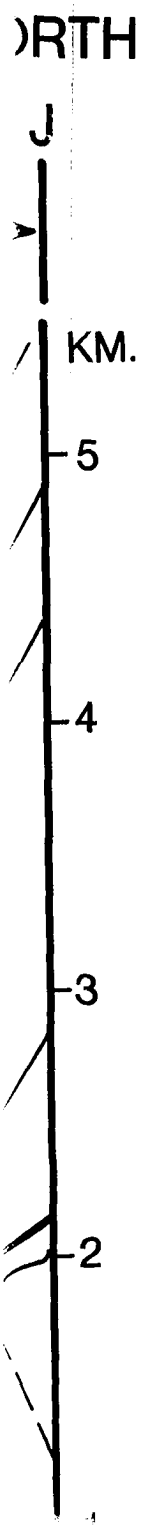

EXPLANATION OF SYMBOLS

lTriu	upper Ivishak Formation
lTril	lower Ivishak Formation
Pe	Echooka Formation
PMl	Lisburne Group
Mky	Kayak Shale
Mkt	Kekiktuk Conglomerate

~~~ sub-Mississippian unconformity

thrust fault or detachment
~~~

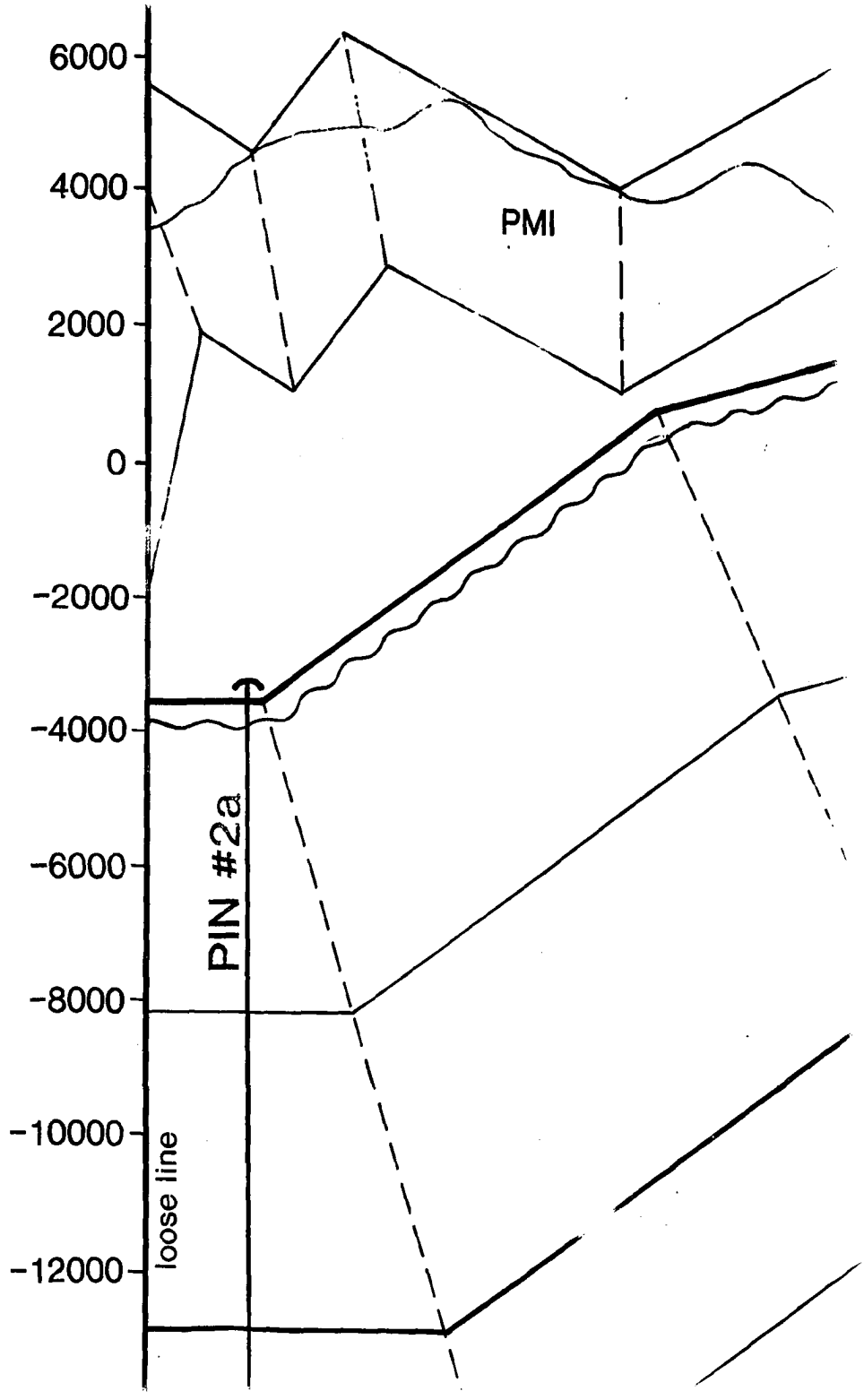

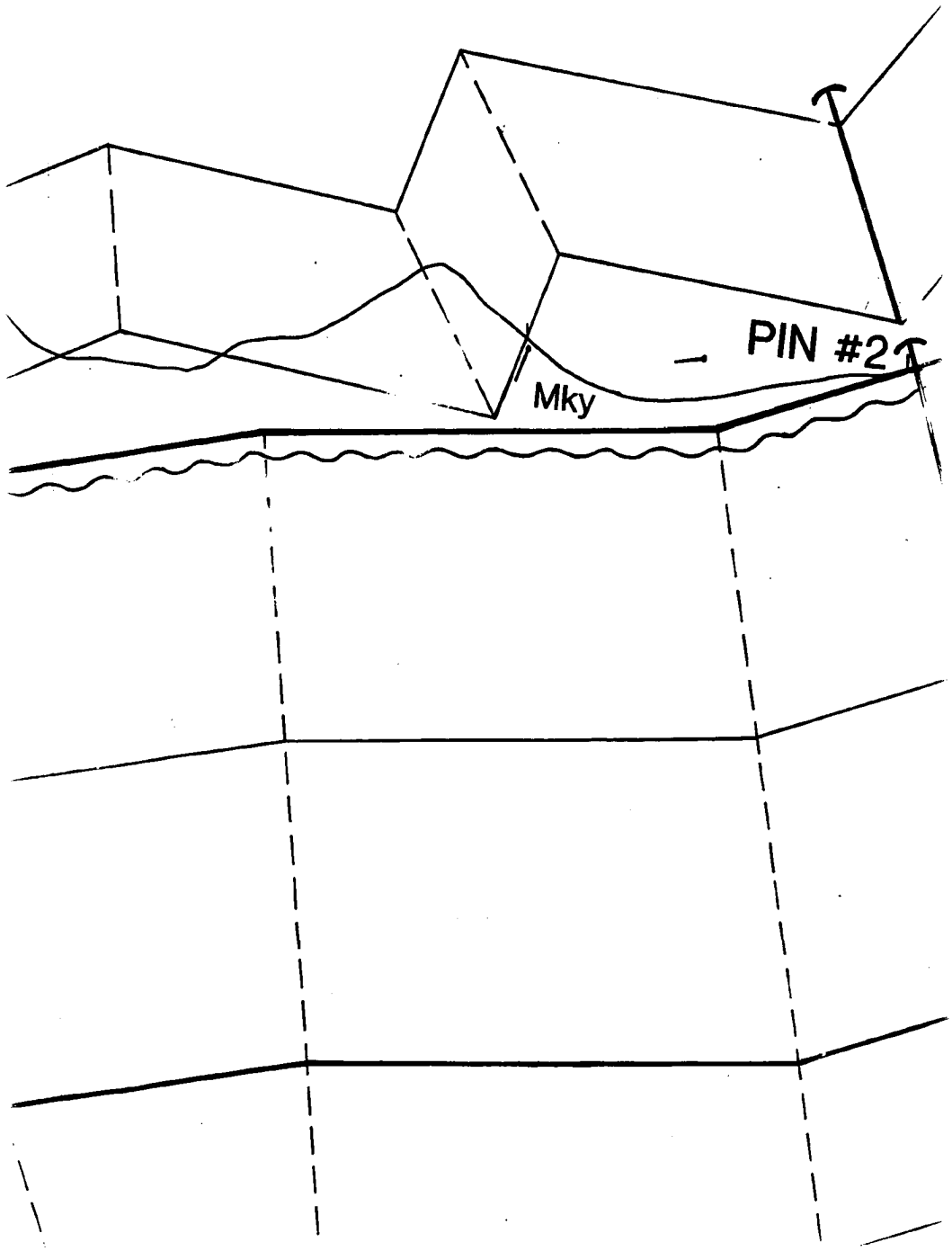

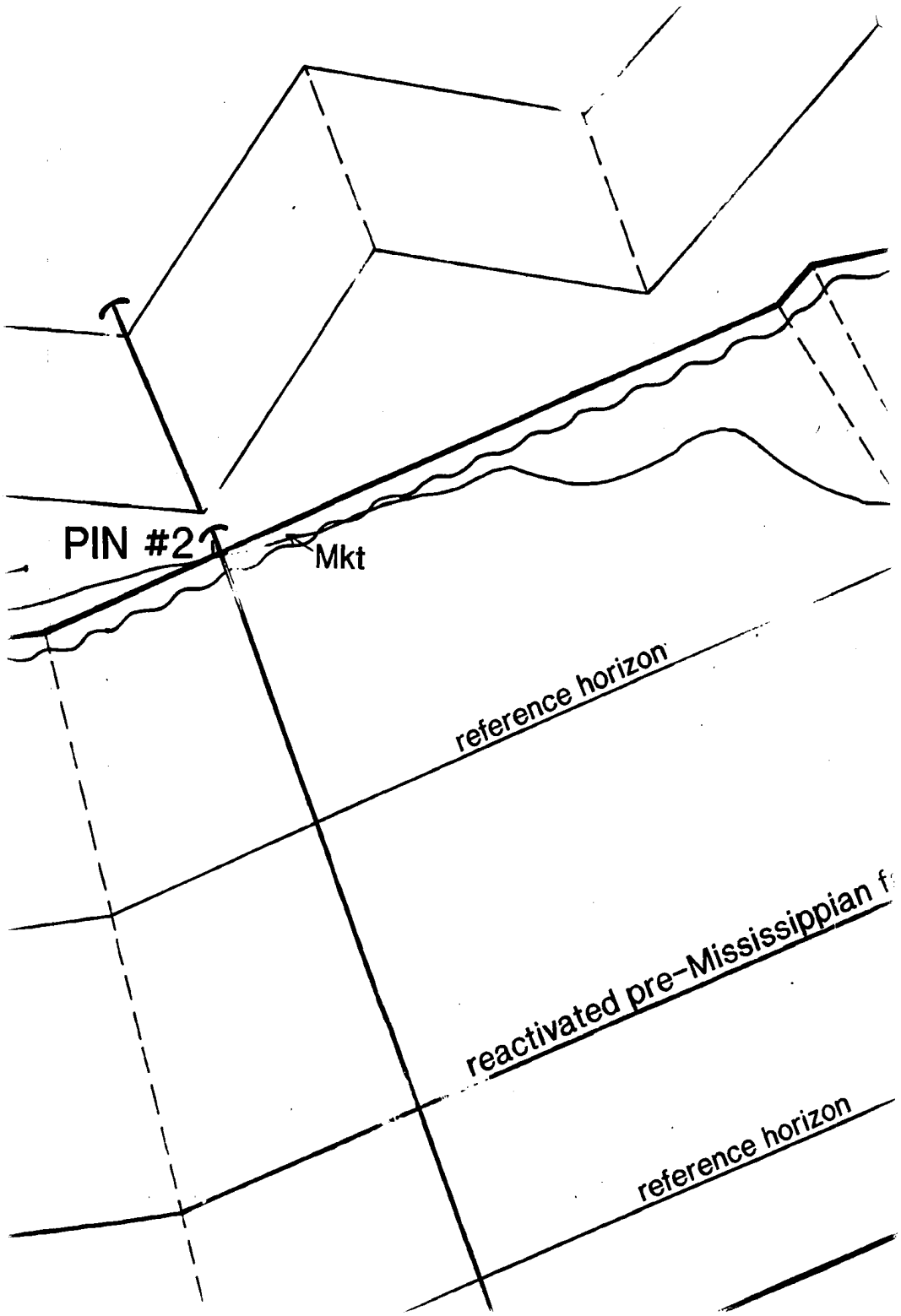

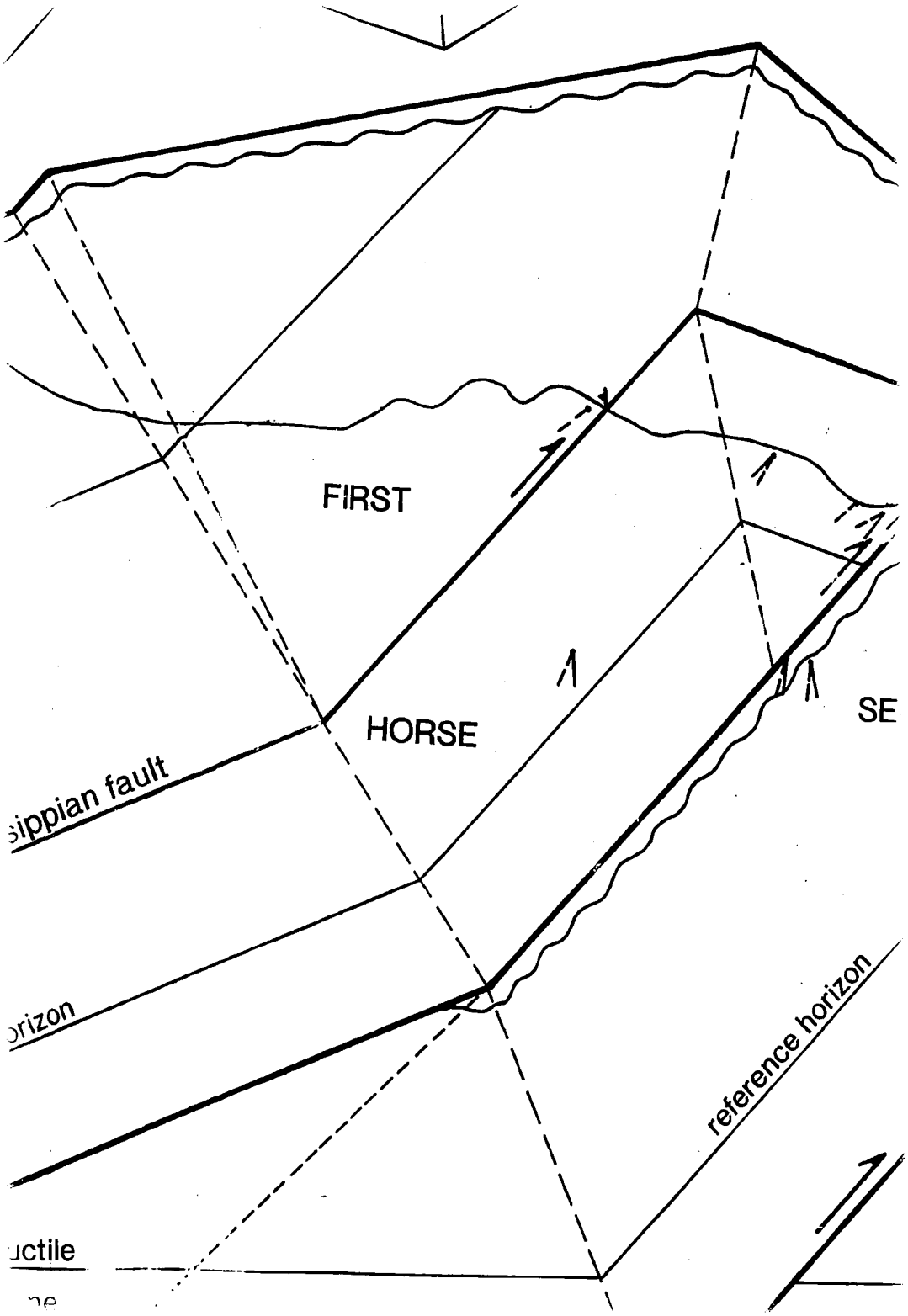

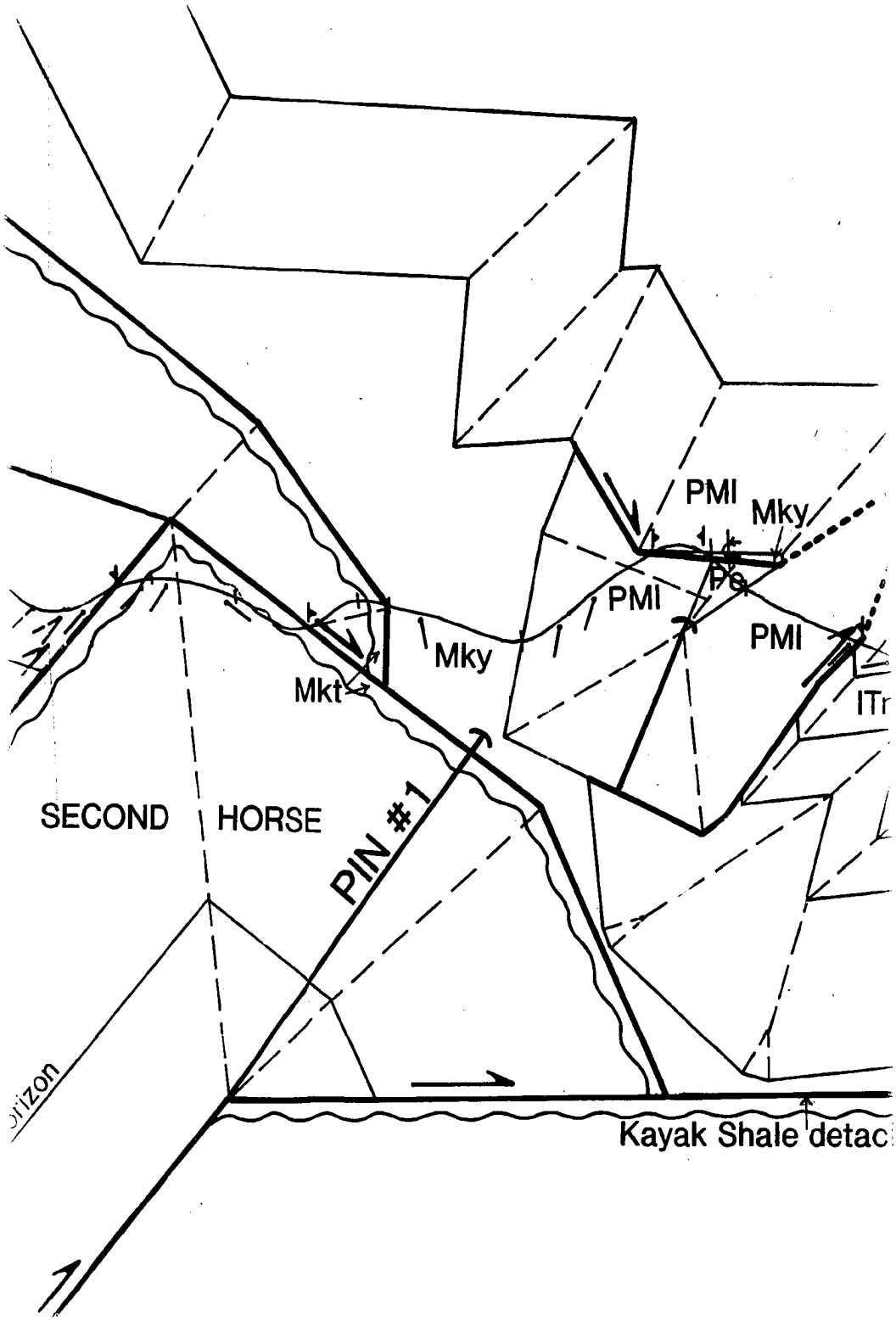

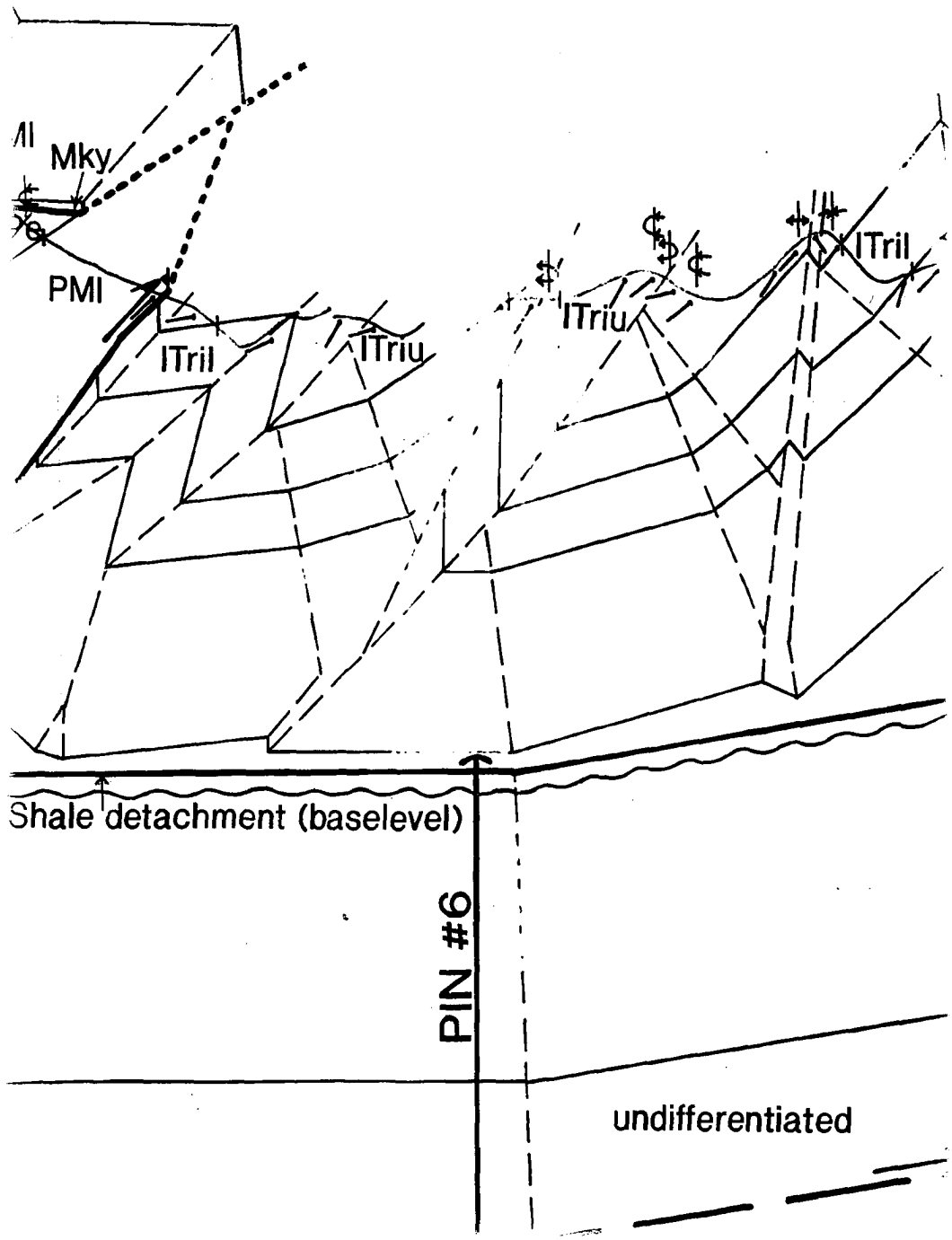

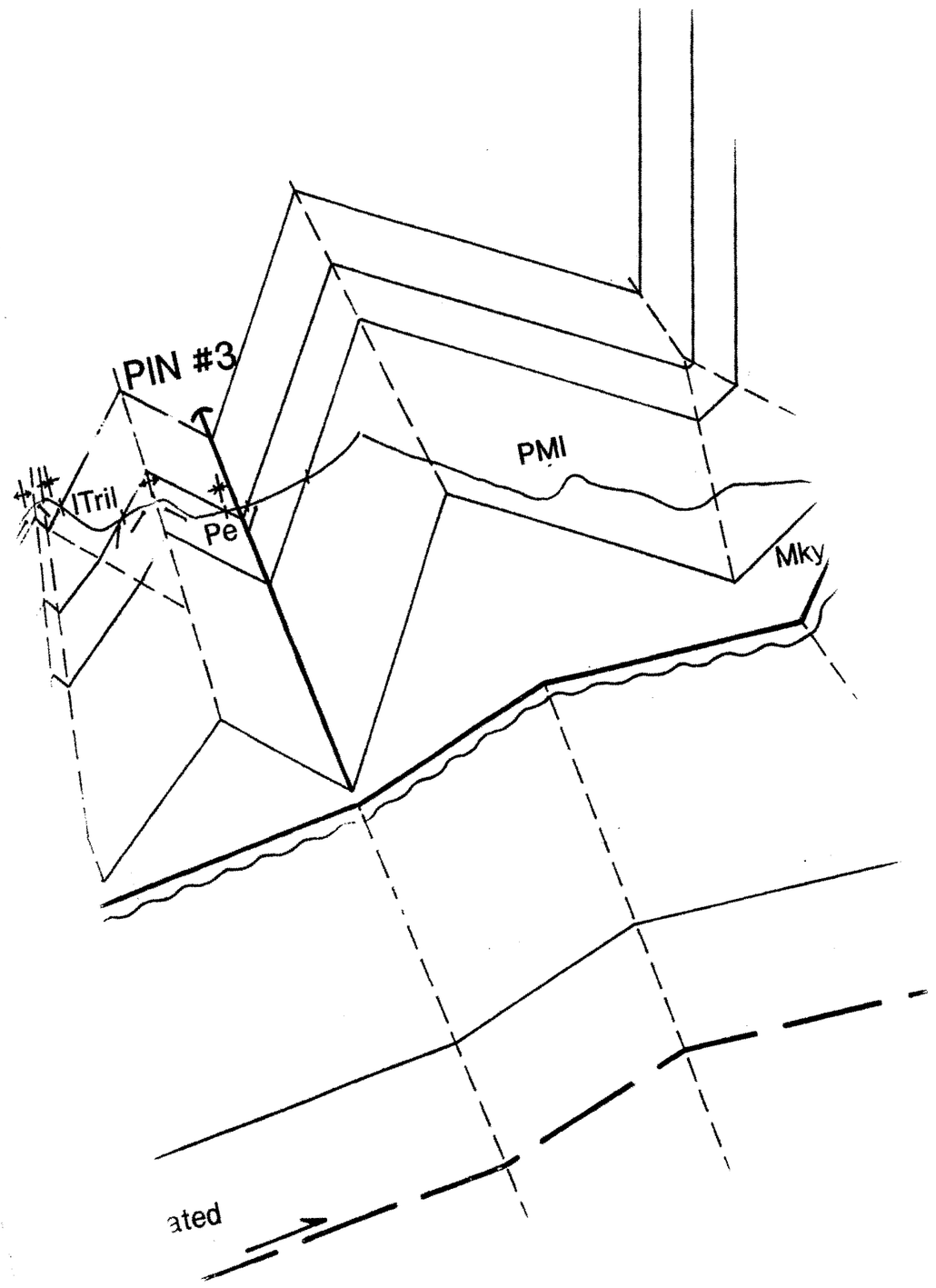

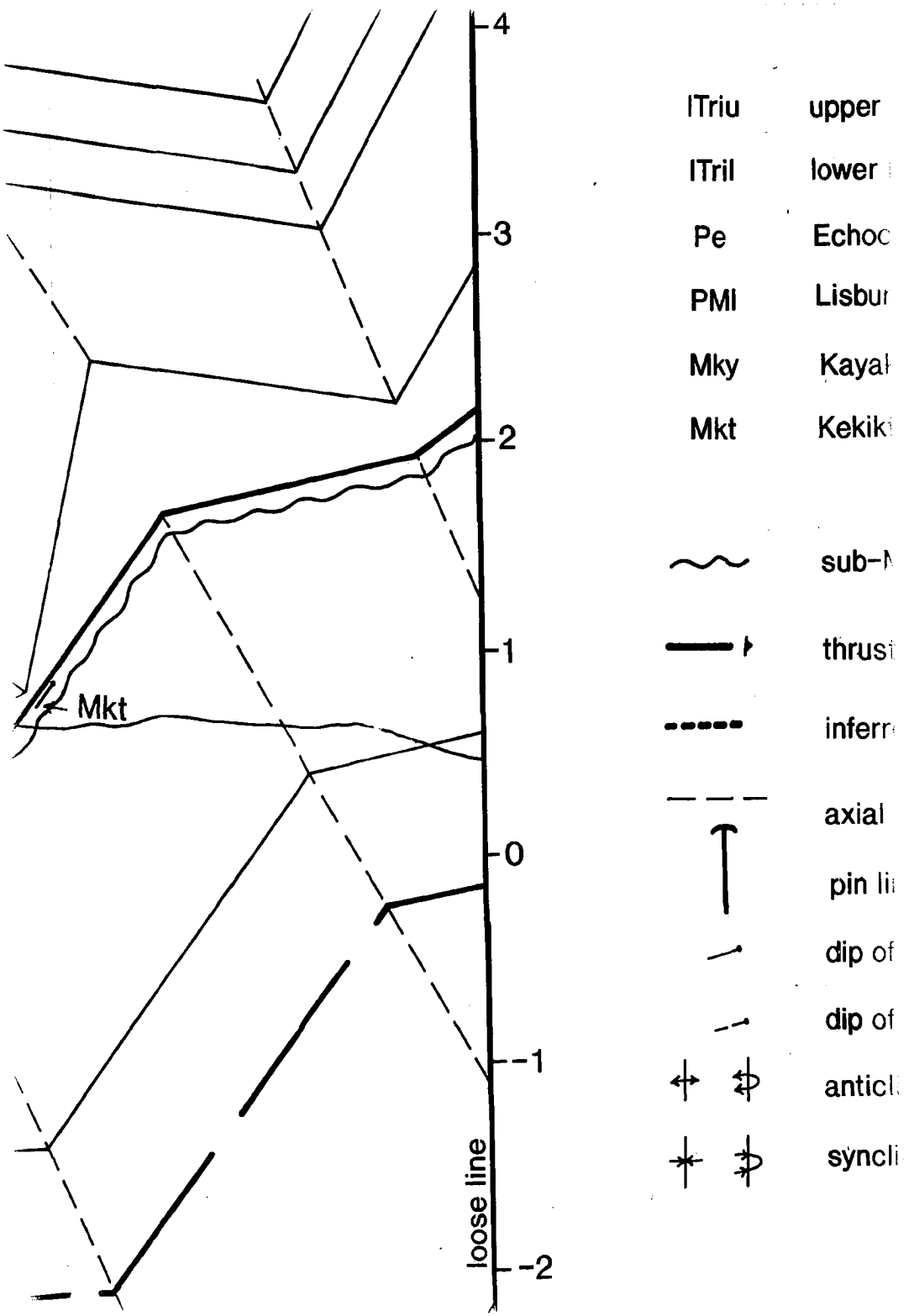

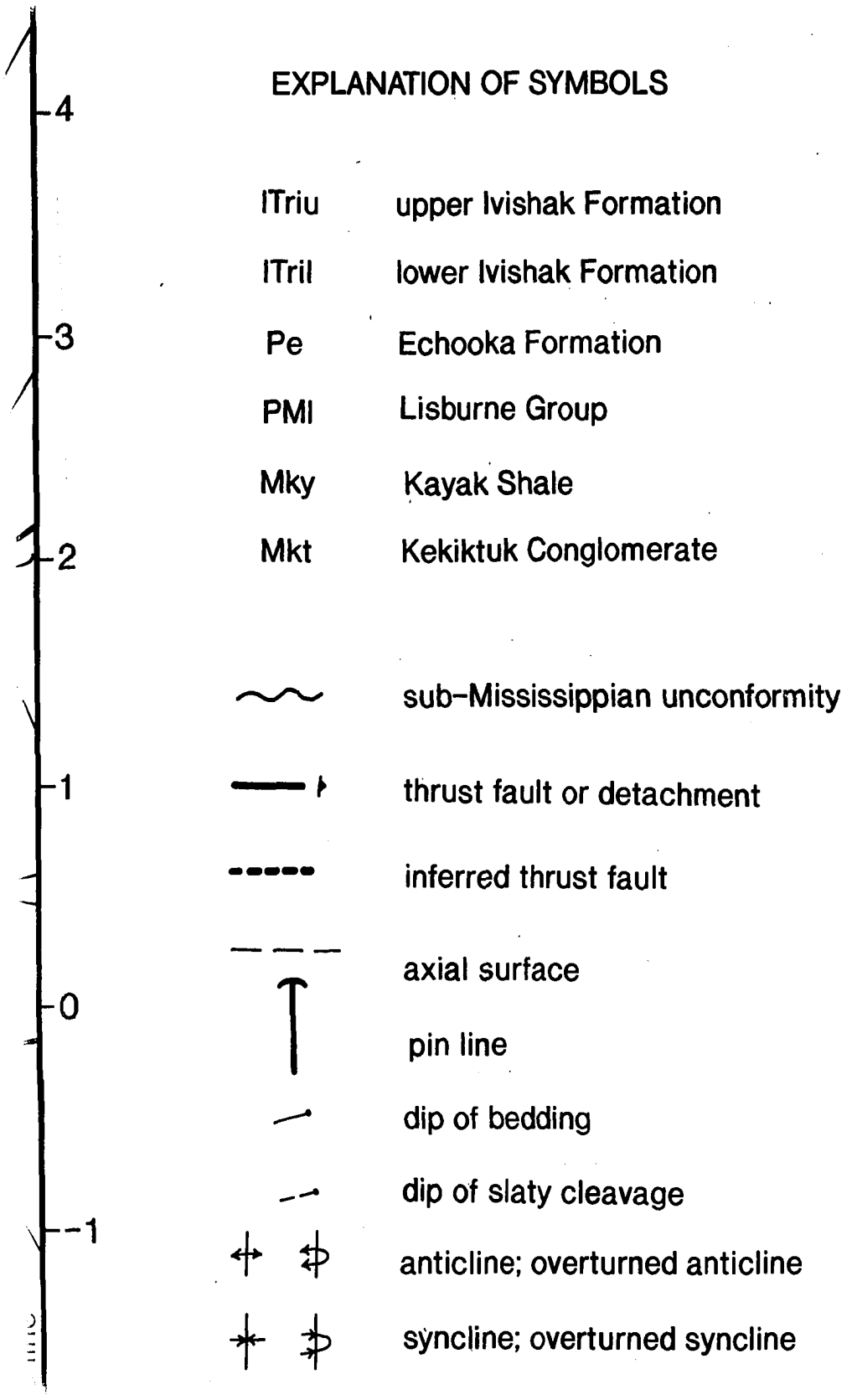

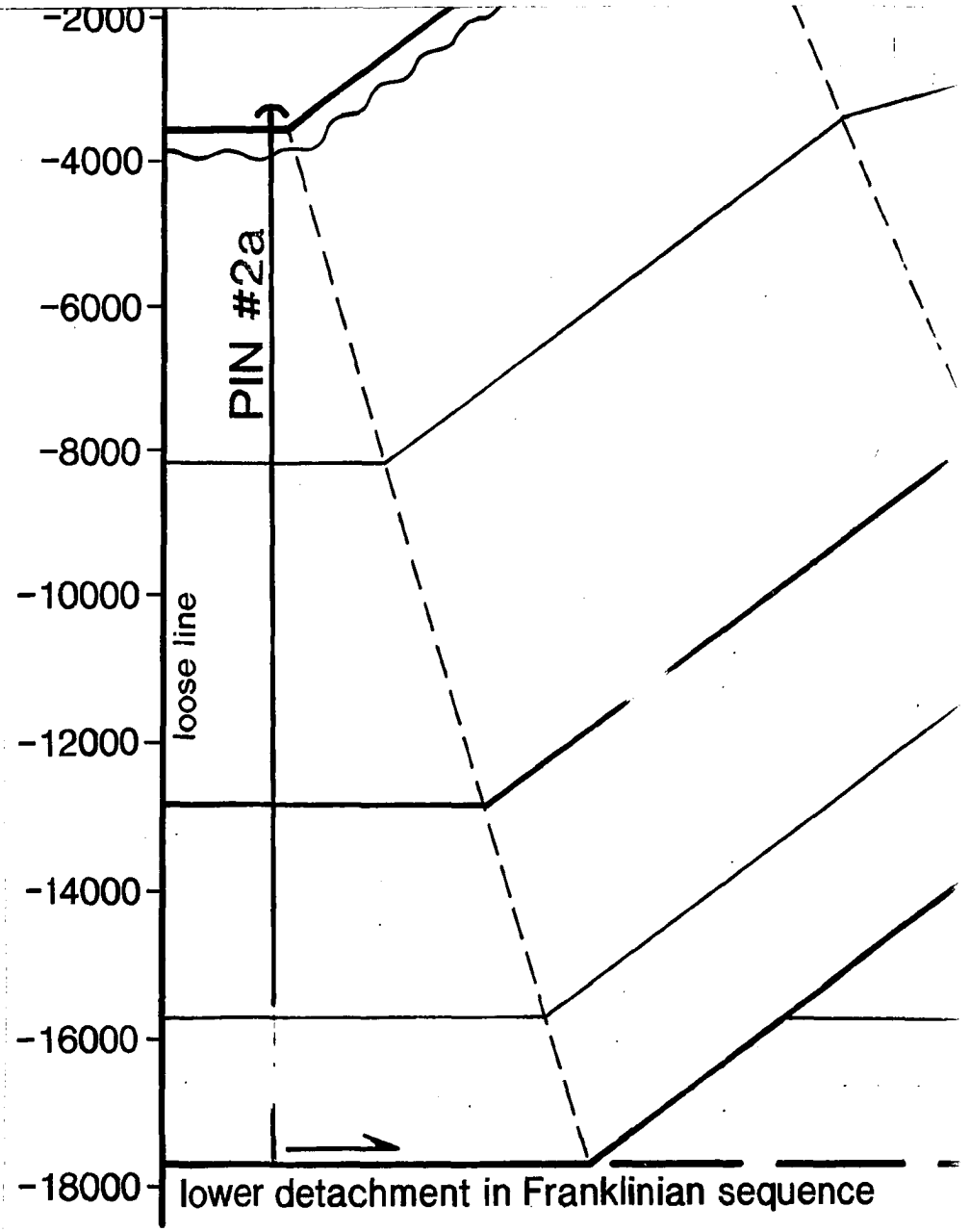

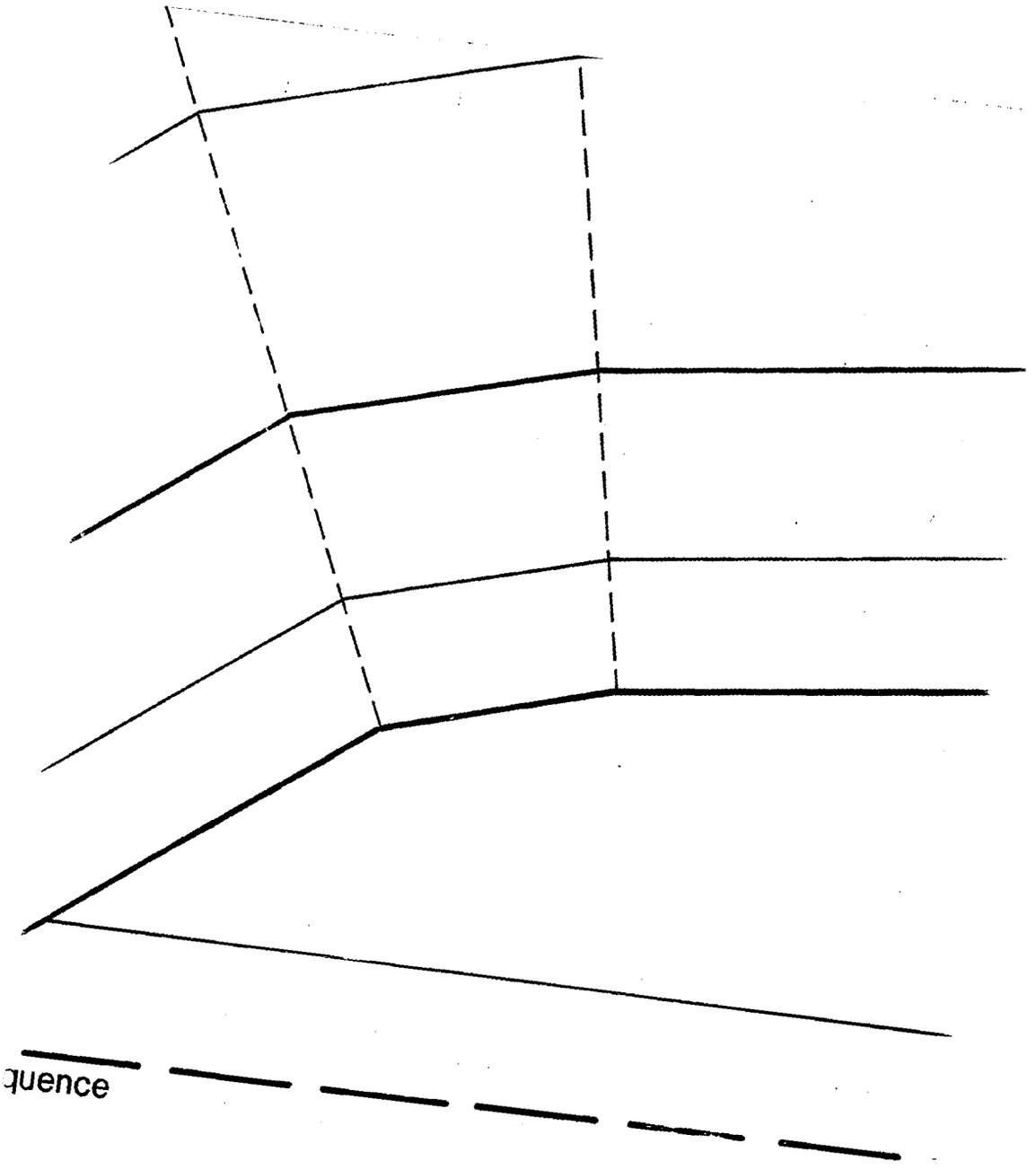

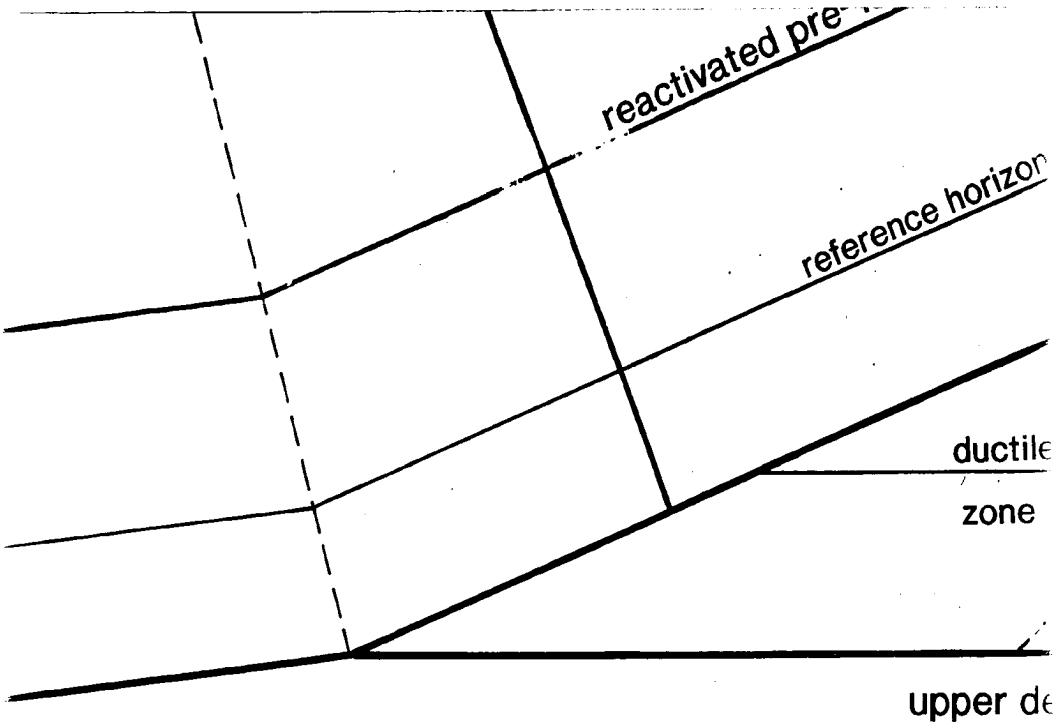

SCALE

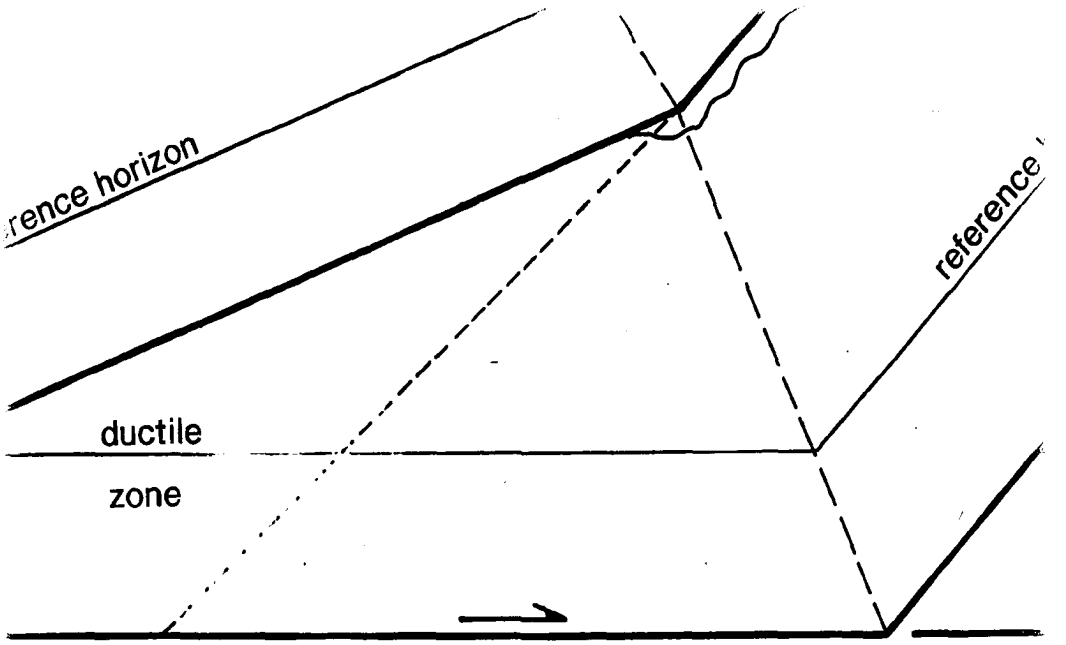

upper detachment in Franklinian sequence

SCALE 1:25,000 NC

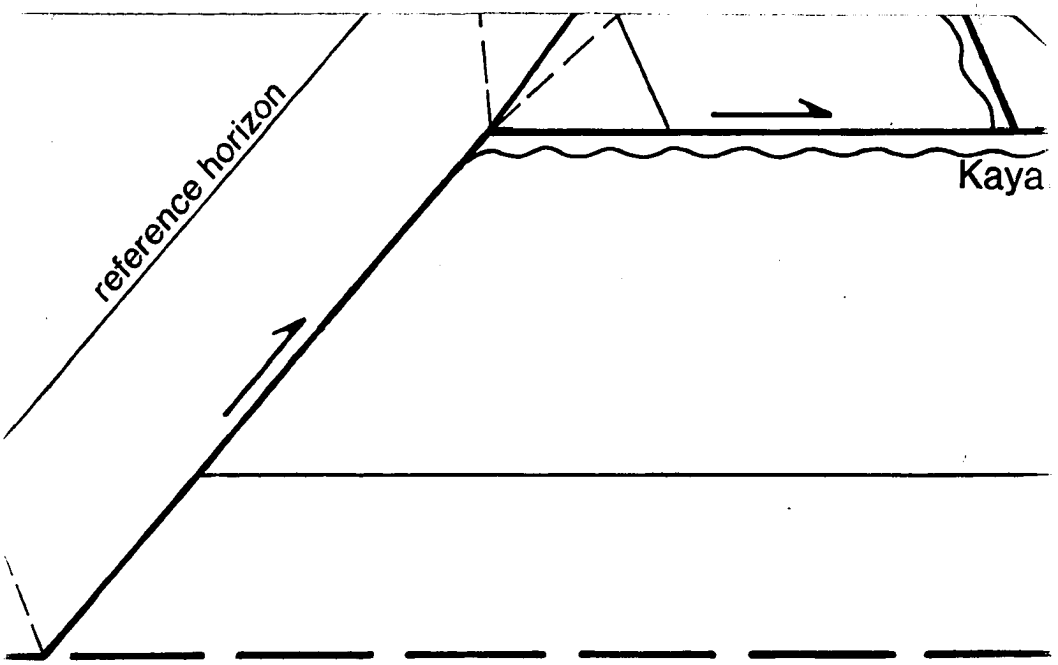

NO VERTICAL EXAGGERATION

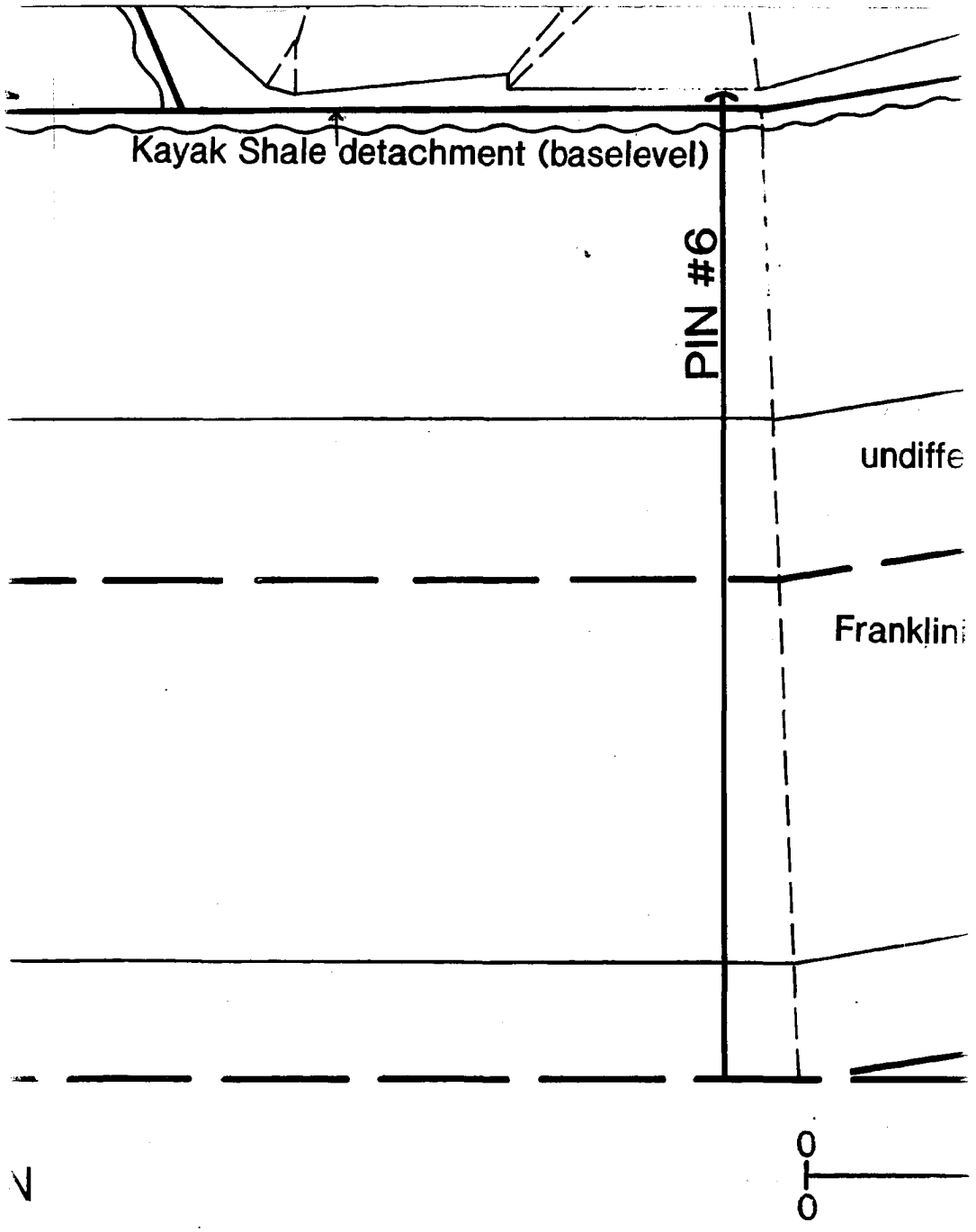

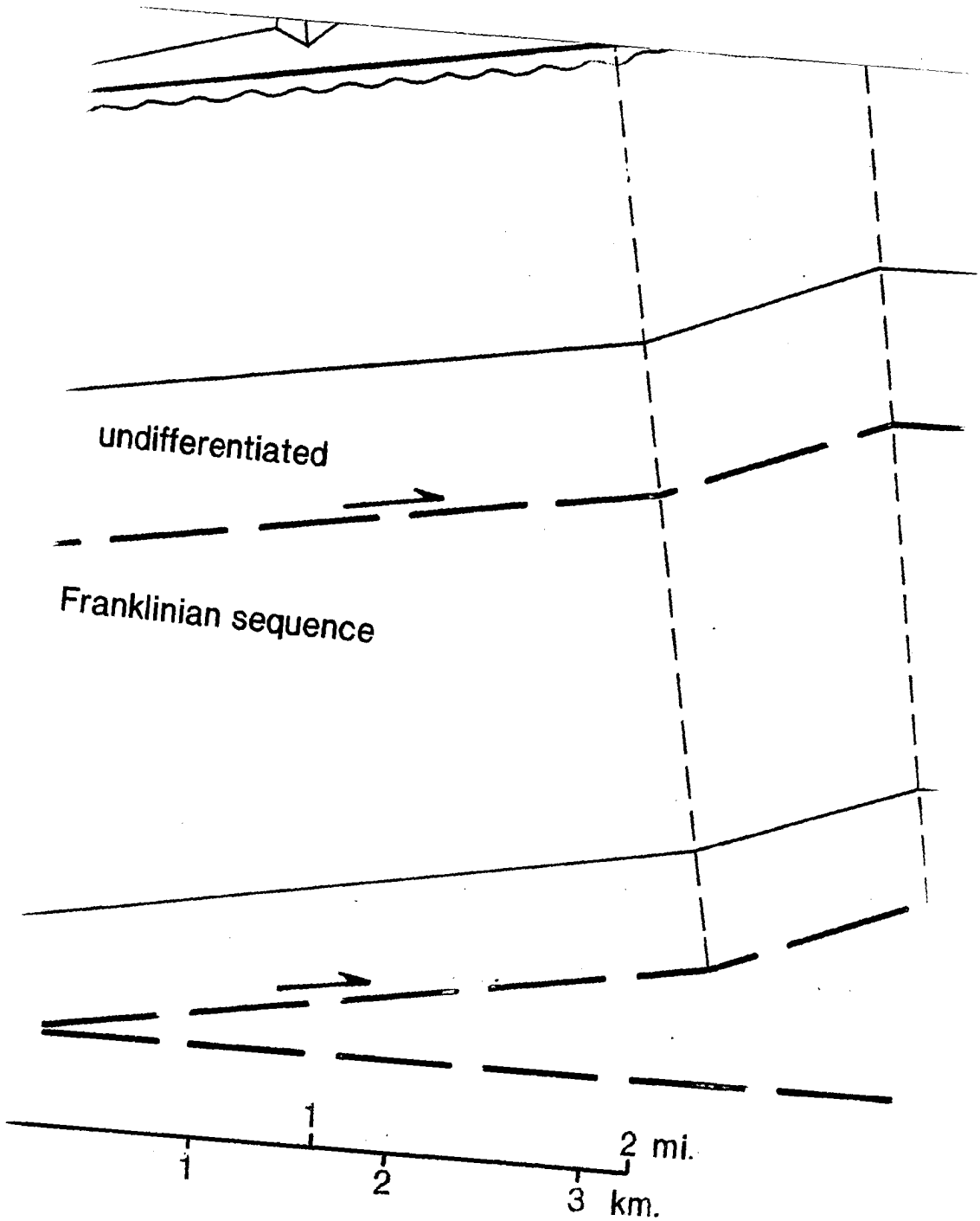

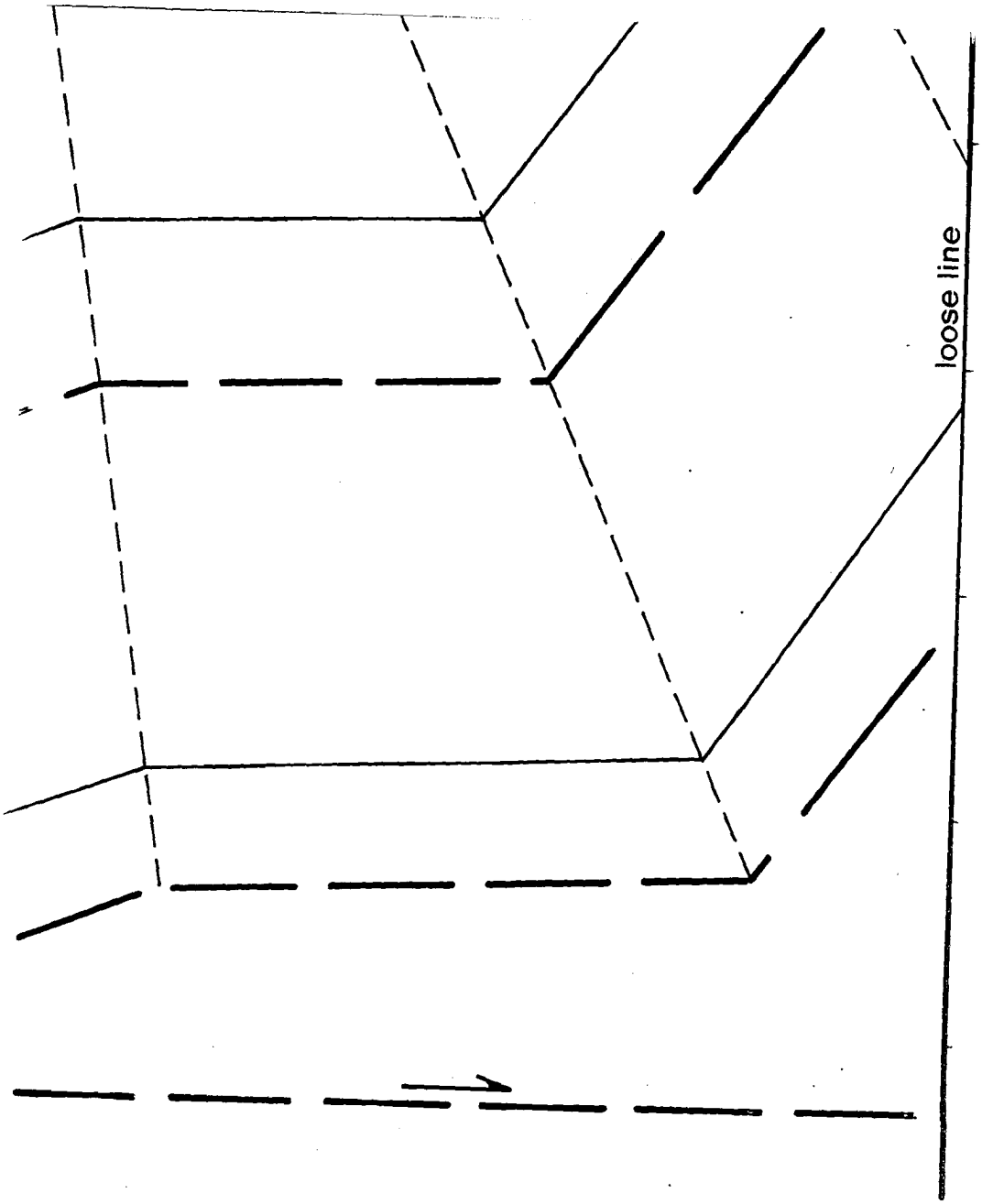

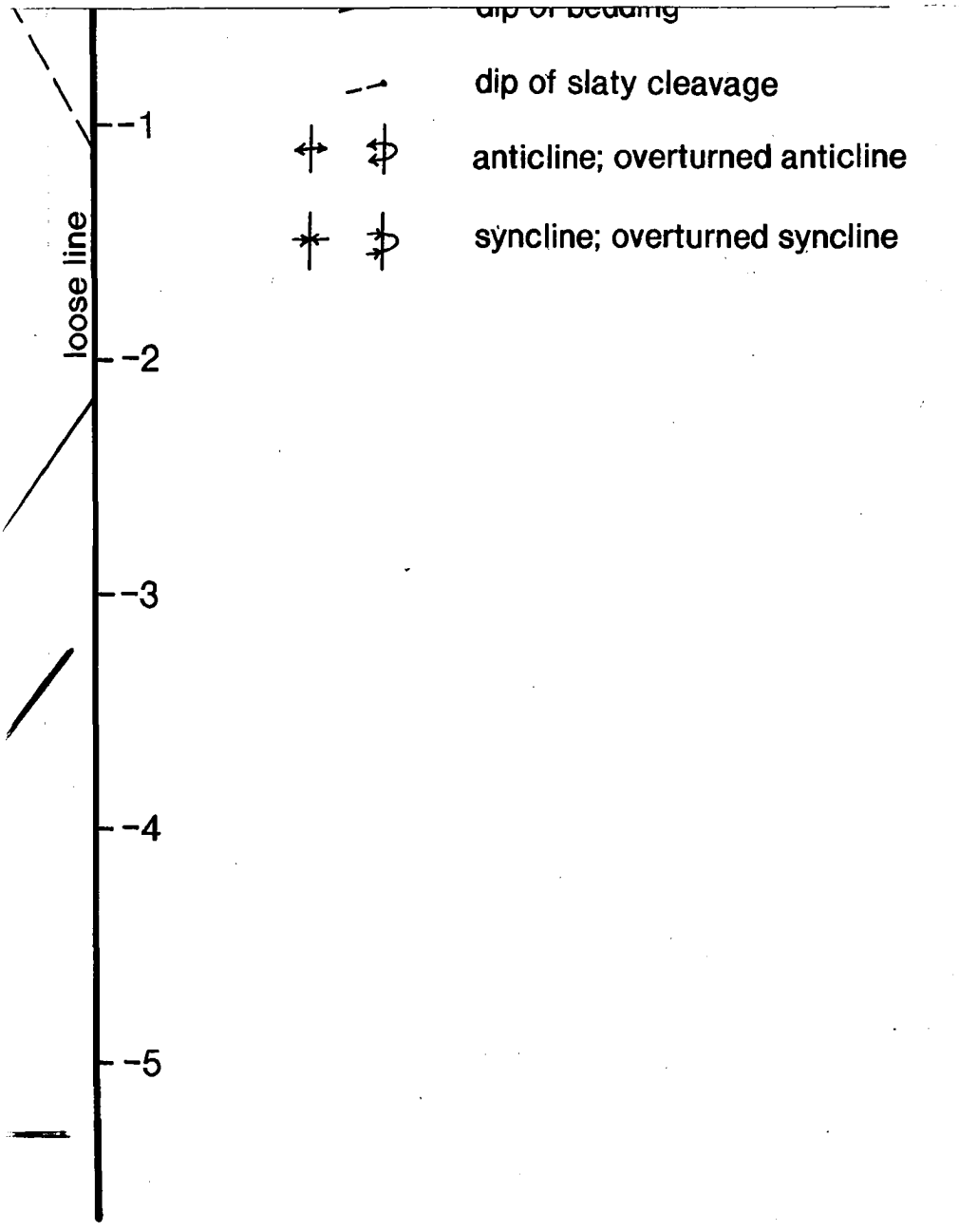

PLATE 3 PRIMARY BALA

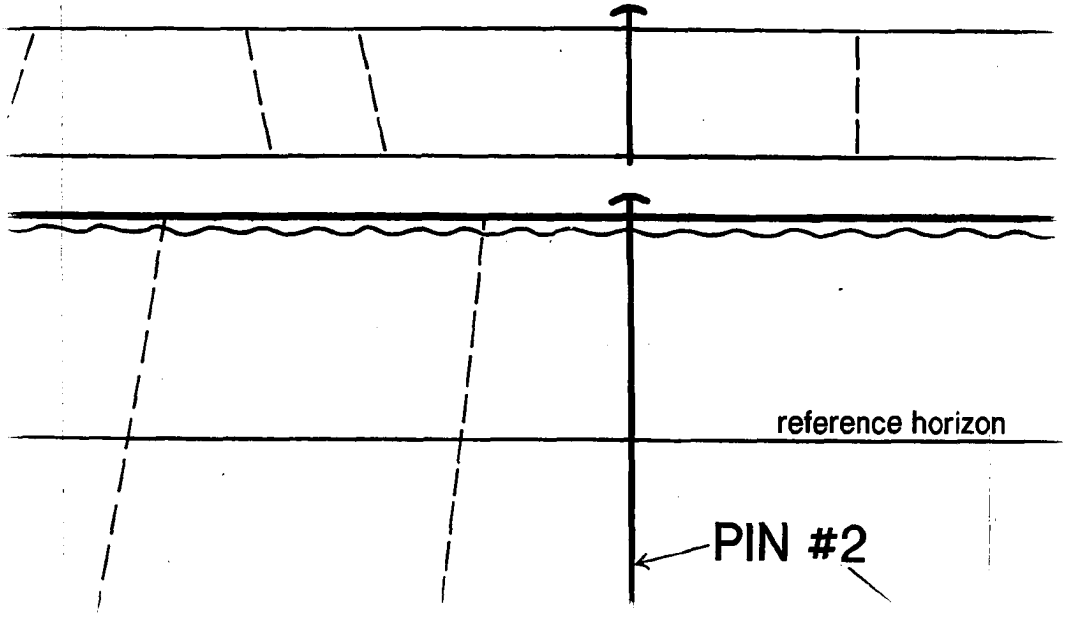

BALANCED CROSS-SECTION ACRO

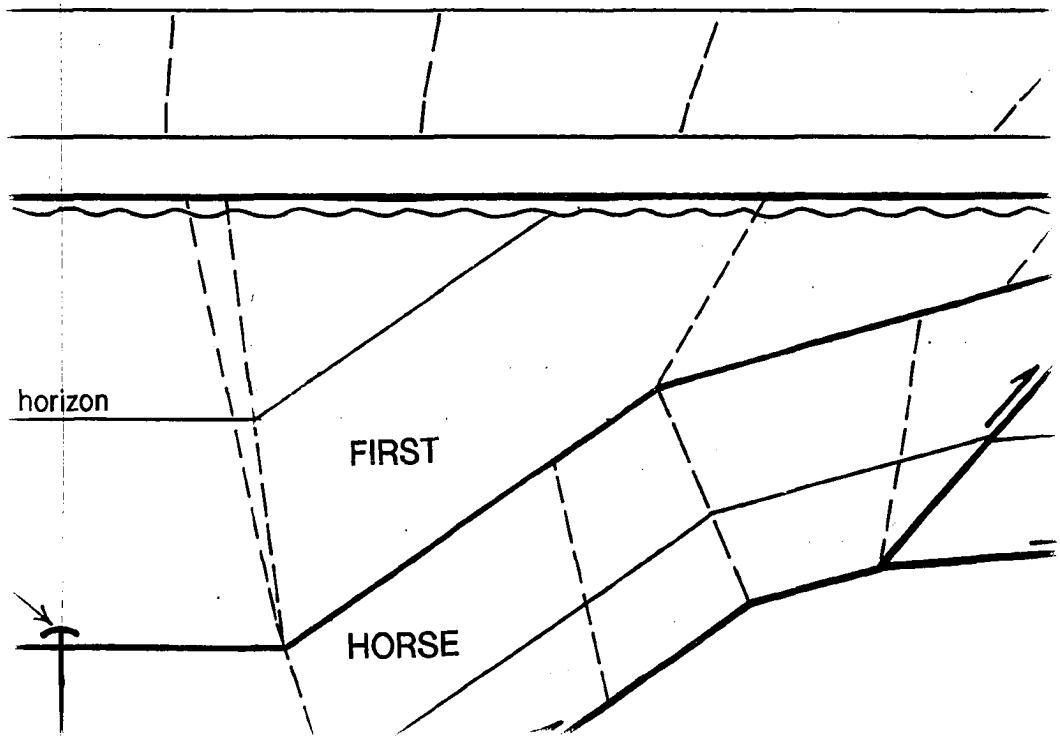

ACROSS THE FRANKLIN MOUNTAIN

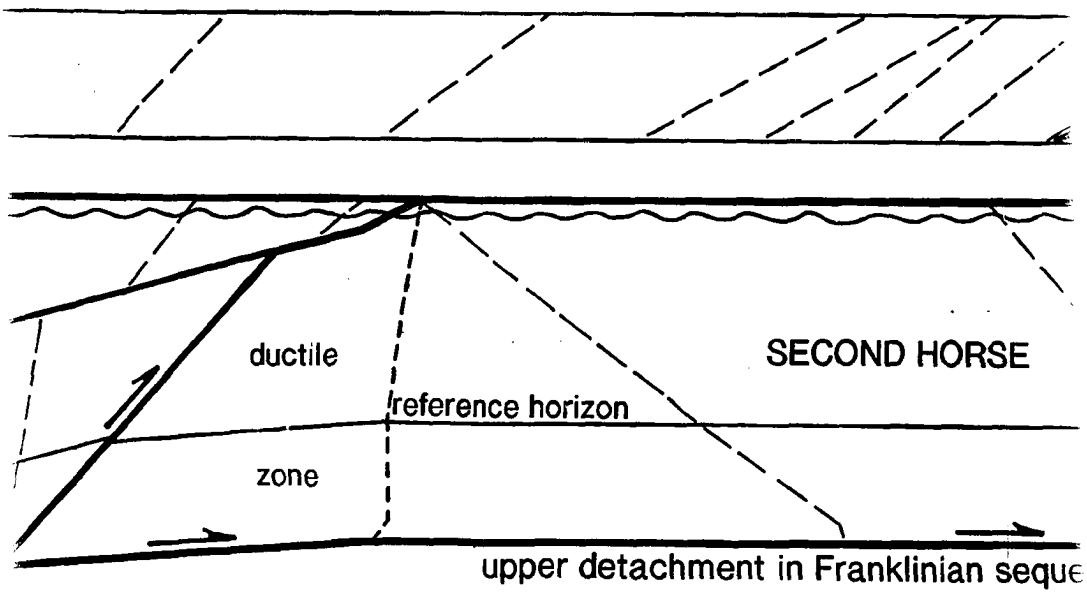

NTAINS ANTICLINORIUM, RECONSTI

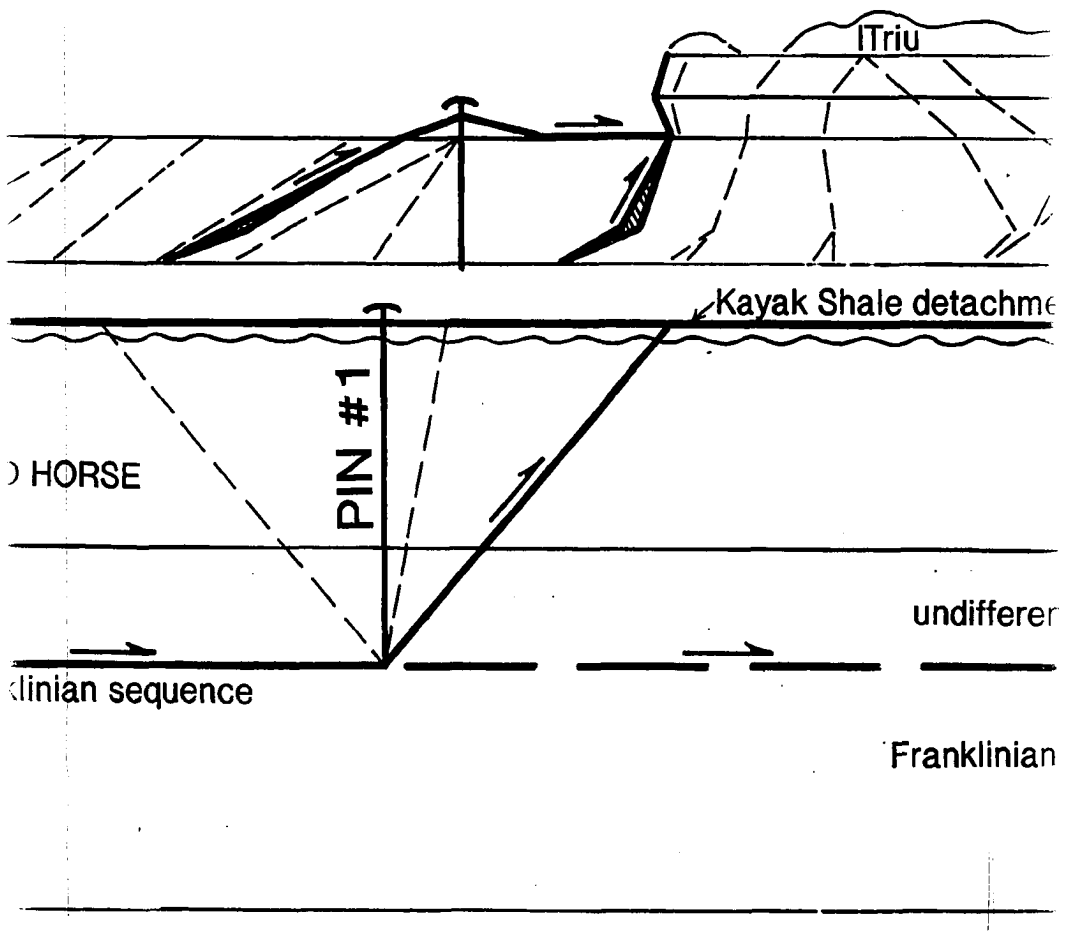

)NSTRUCTED TO PRE-CENOZOIC TI

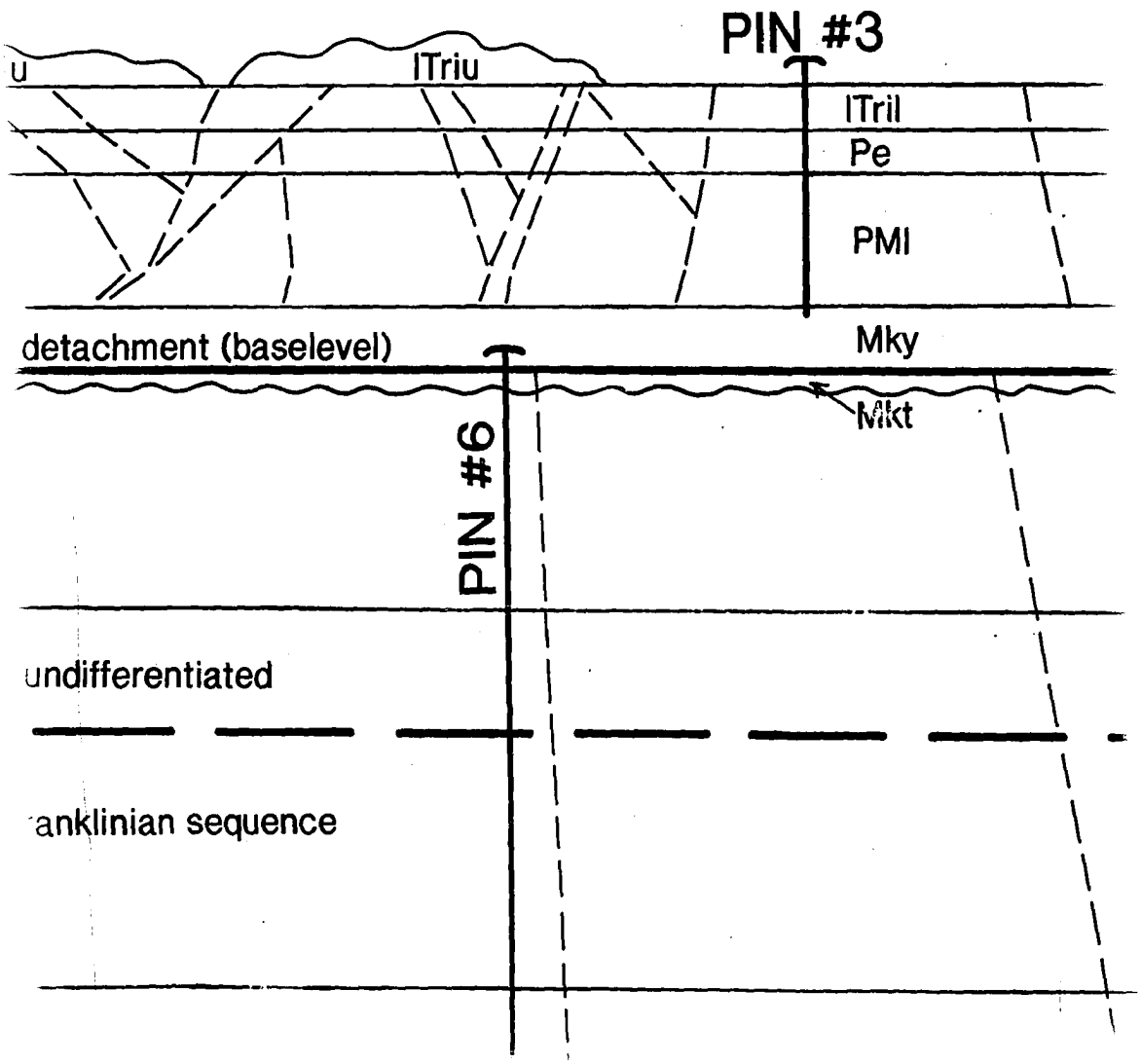

ɔIC TIME

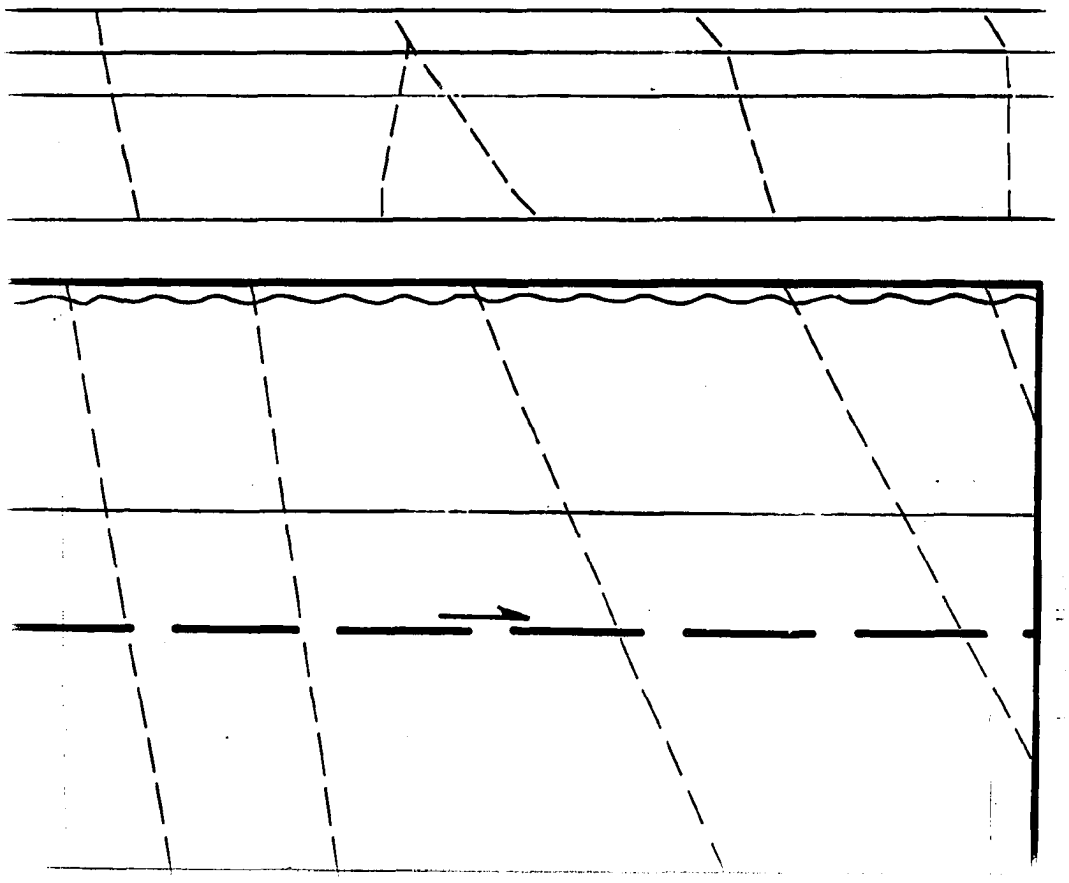

EXPLANATION OF SYMBOLS

lTriu	upper Ivishak Formation
lTril	lower Ivishak Formation
Pe	Echooka Formation
PMl	Lisburne Group
Mky	Kayak Shale
Mkt	Kekiktuk Conglomerate


sub-Mississippian unconformity

thrust fault or detachment

Cenozoic axial surface


pin line


area missing upon reconstruction

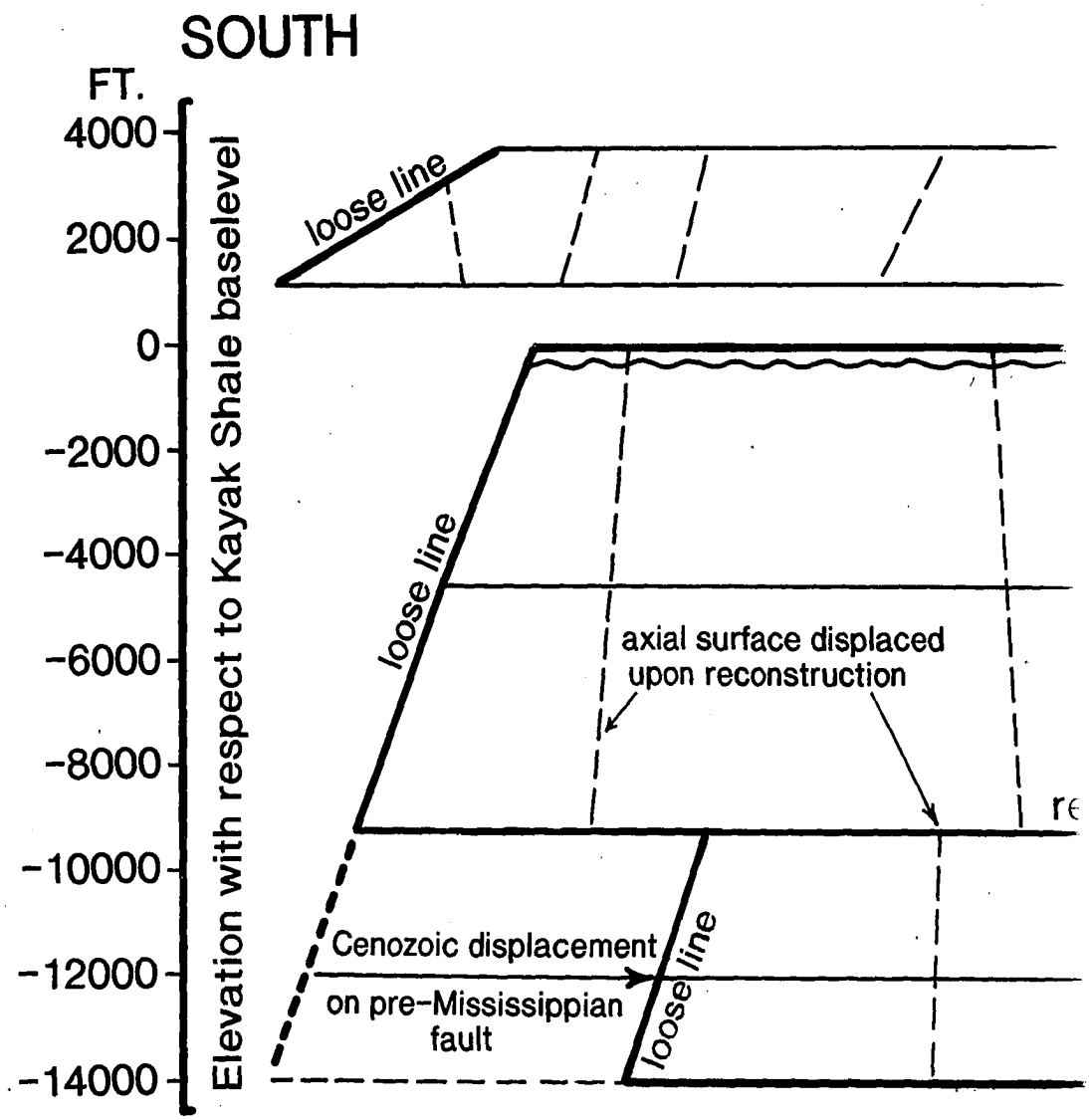

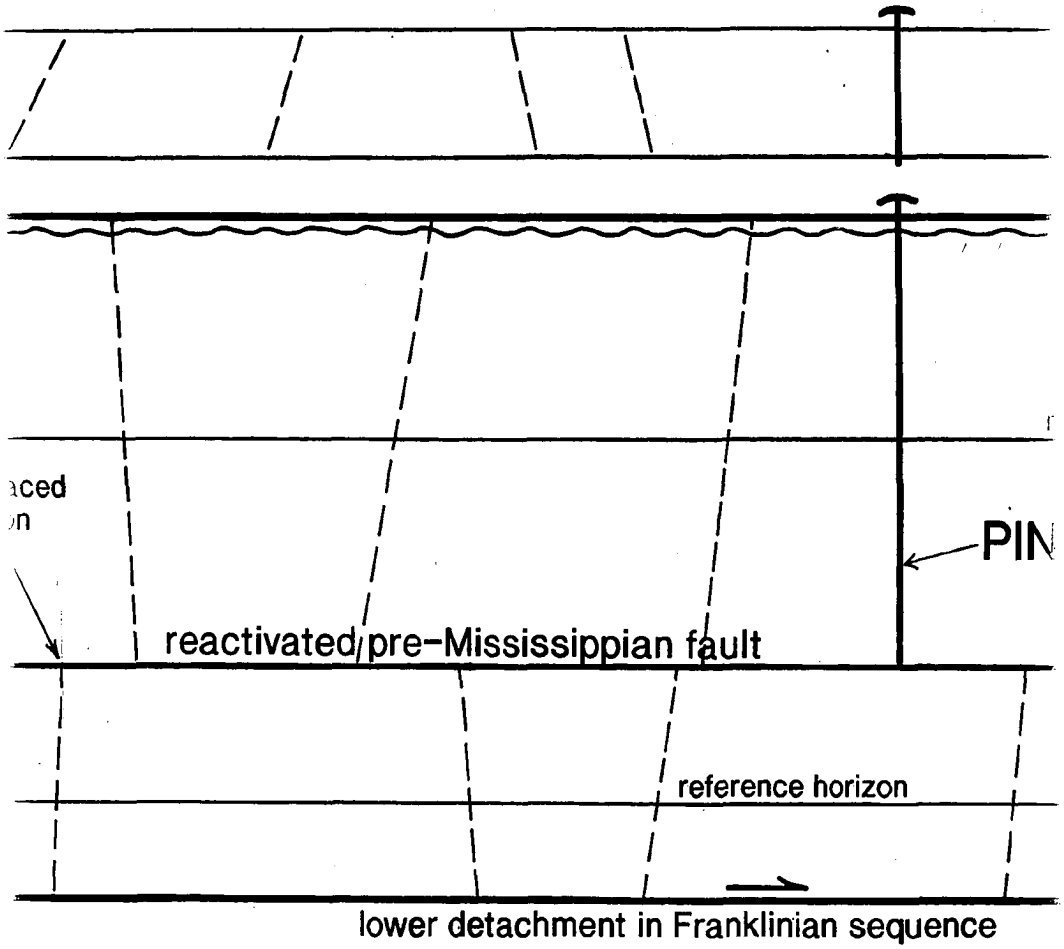

THIS RECONSTRUCTION OF

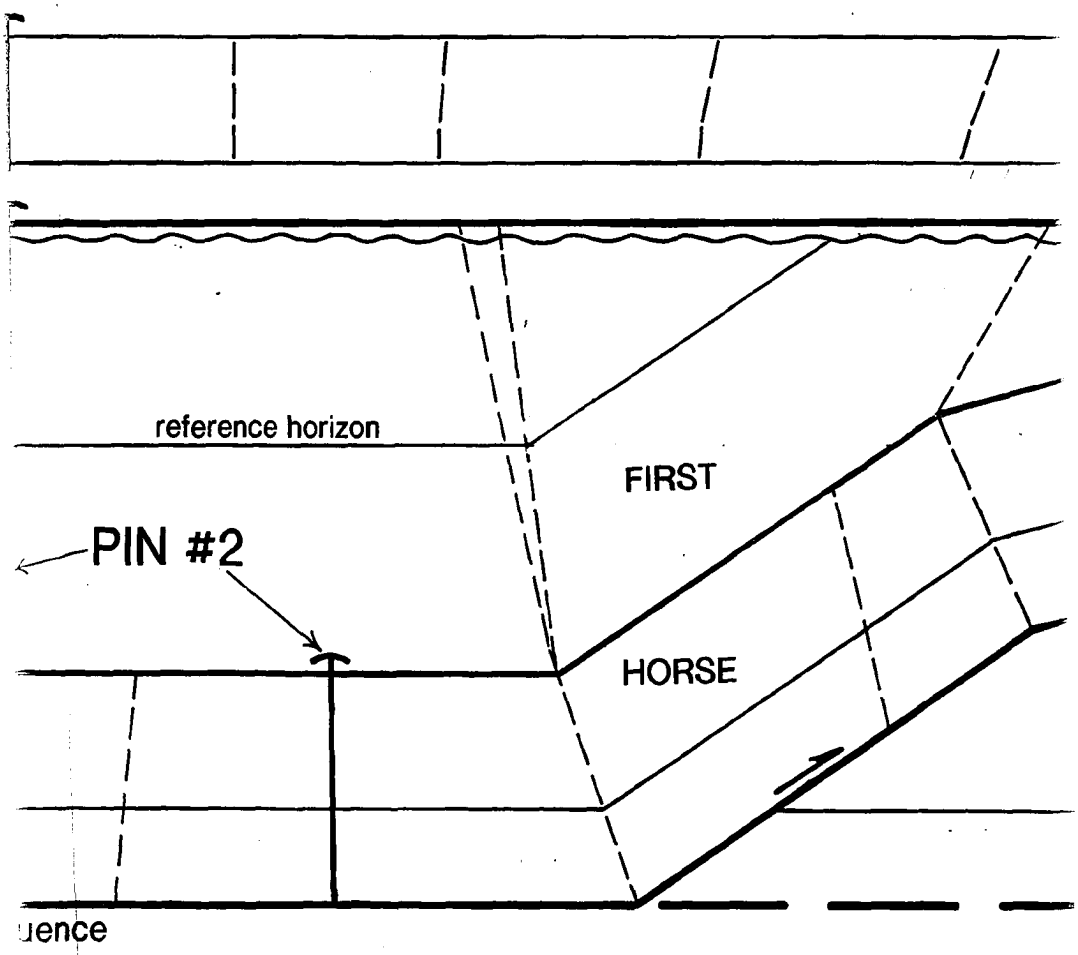

N OF DEFORMED CROSS-SECTION (PLATE 2

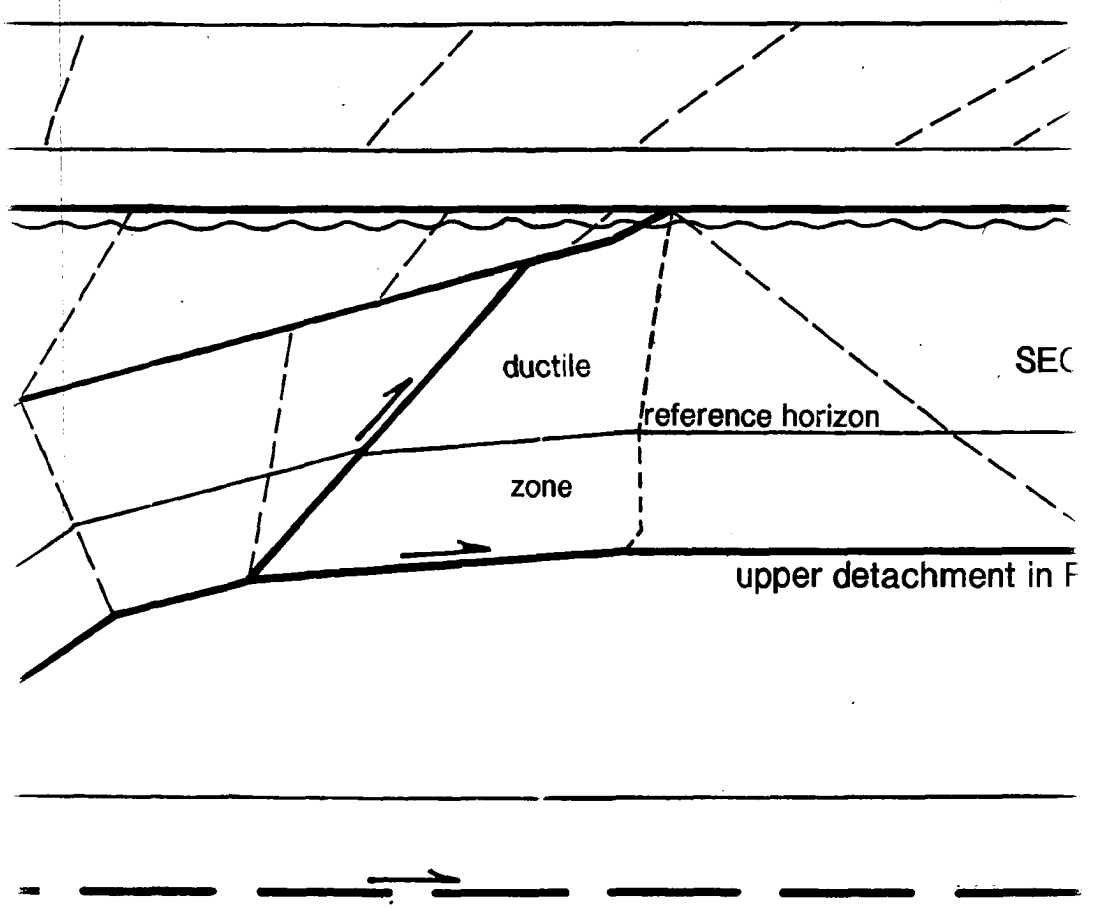

_ATE 2) IS REPRODUCED AT 64%

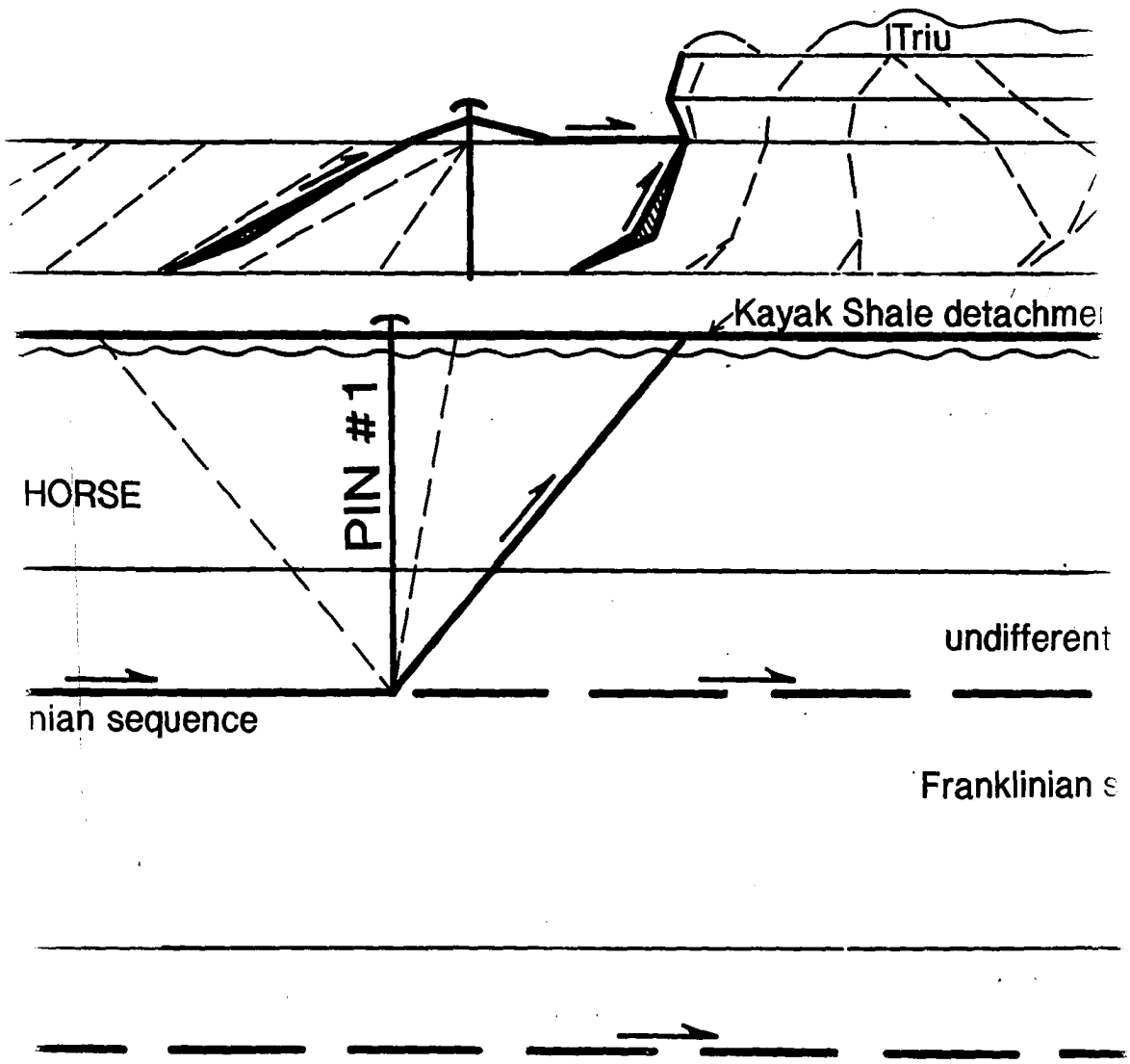

NO VERTICAL EXAGGERATION

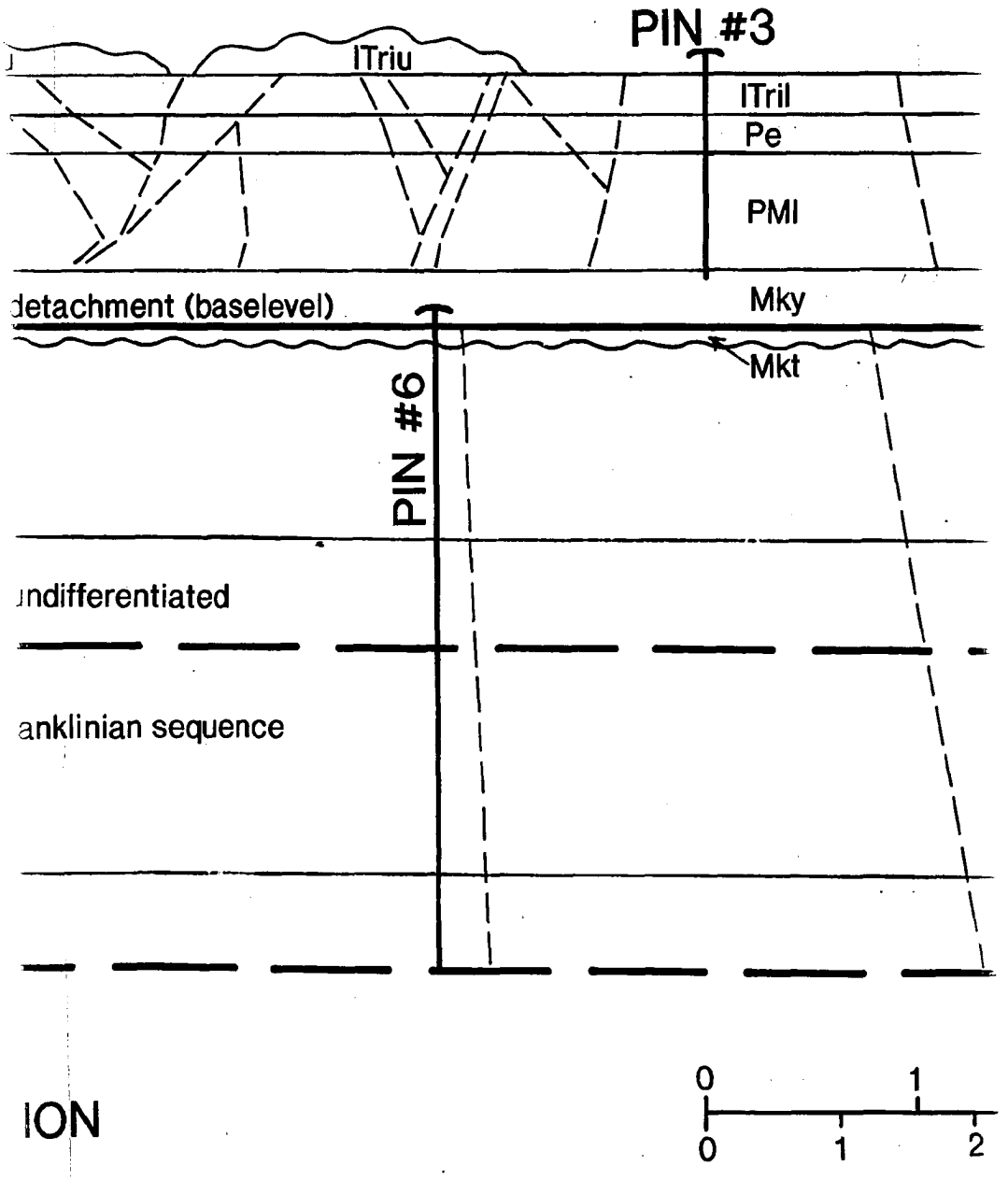

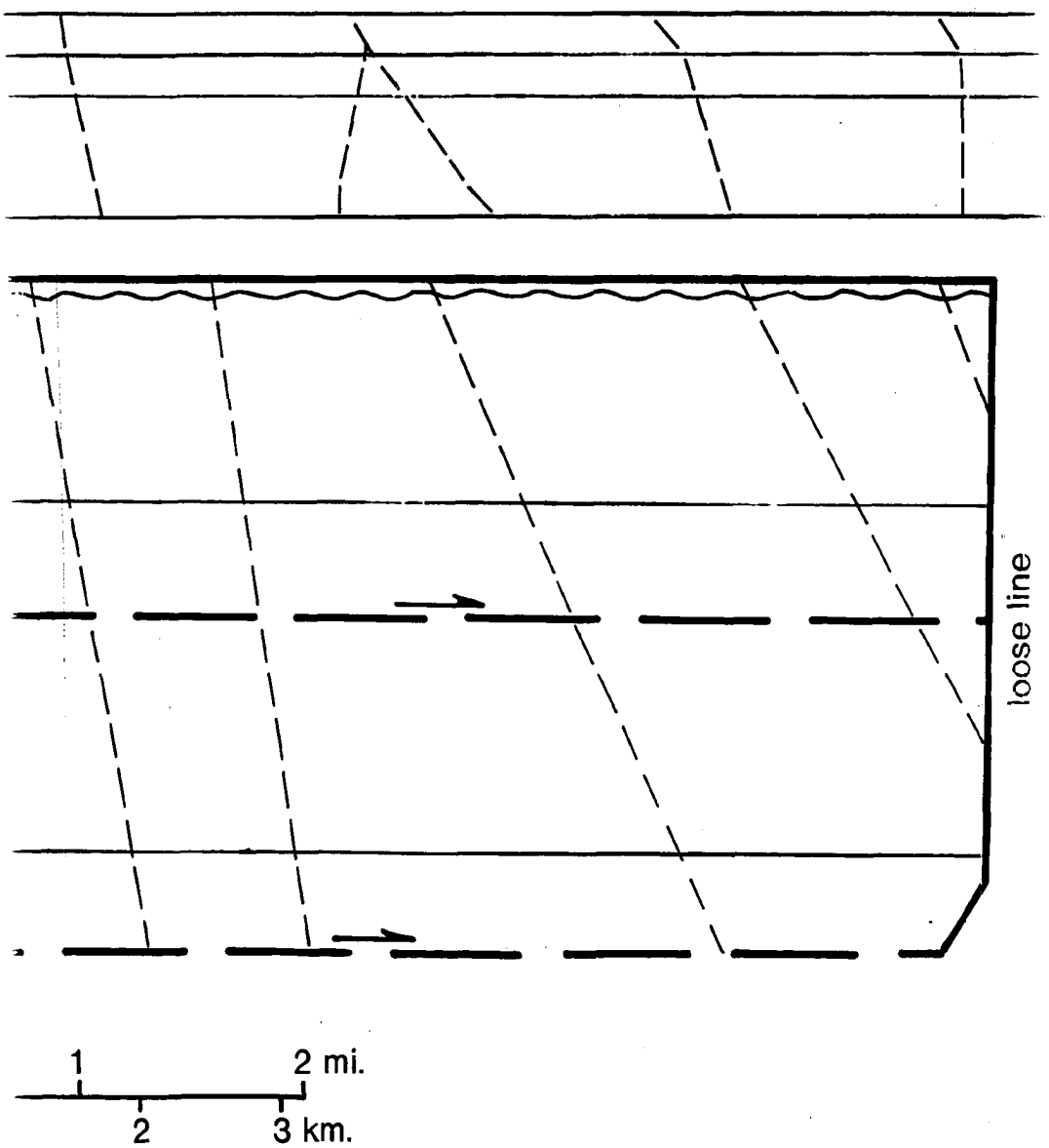

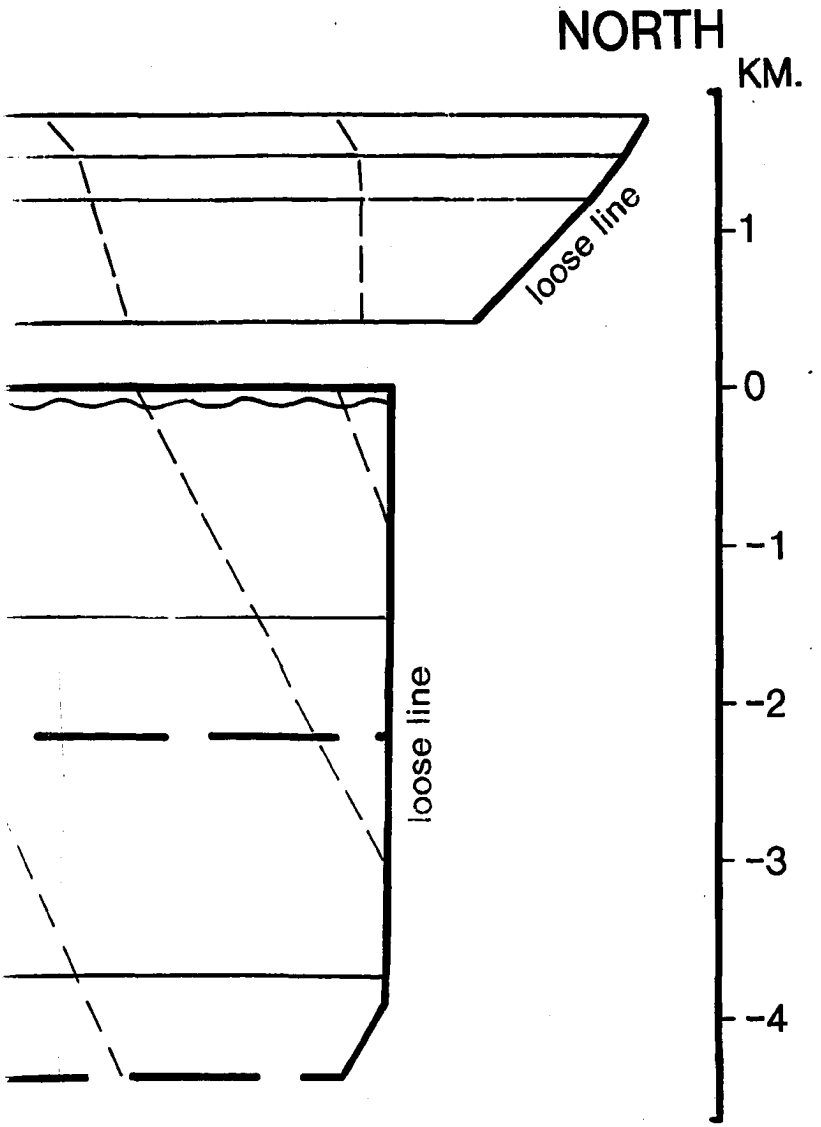

PLATE 4

RECONSTRUC

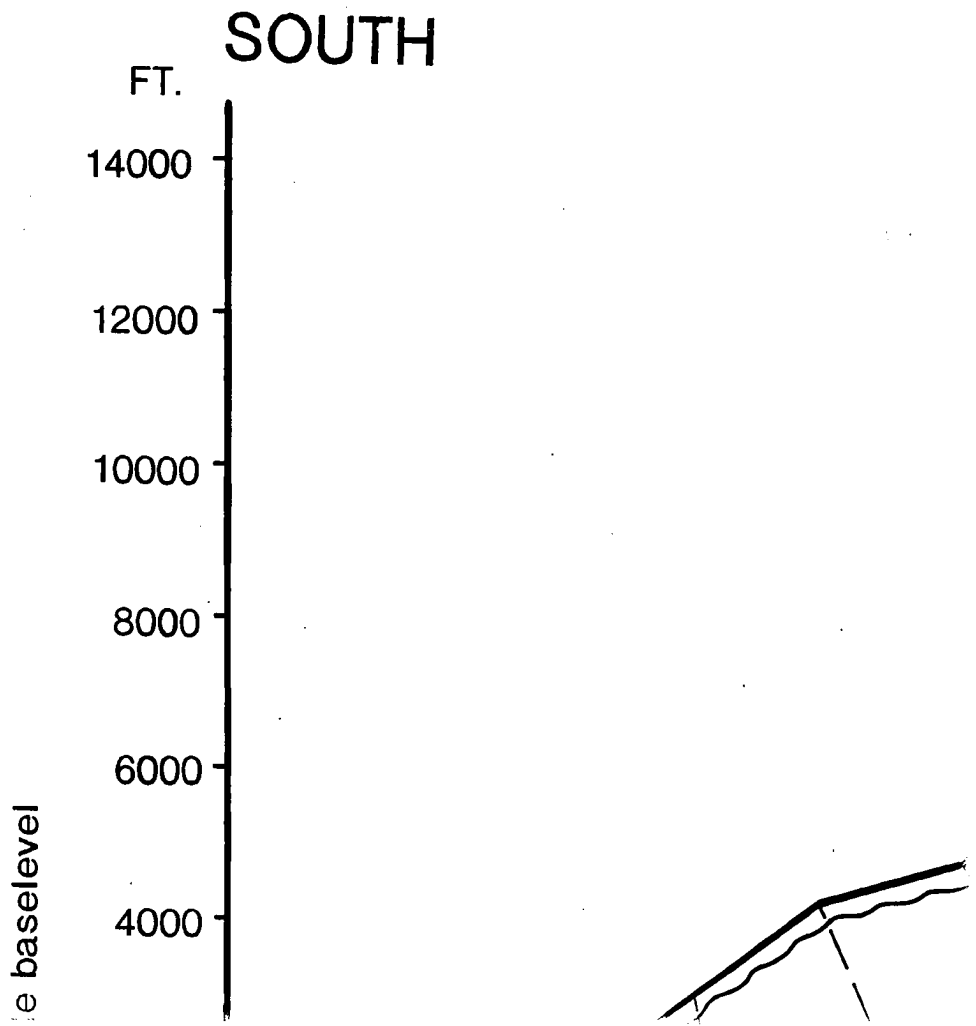

PRIMARY BALANCED CROSS-

TRUCTED TO CENOZOIC TIME FOLL

)SS-SECTION ACROSS THE FRANk

FOLLOWING THE EMPLACEMENT C

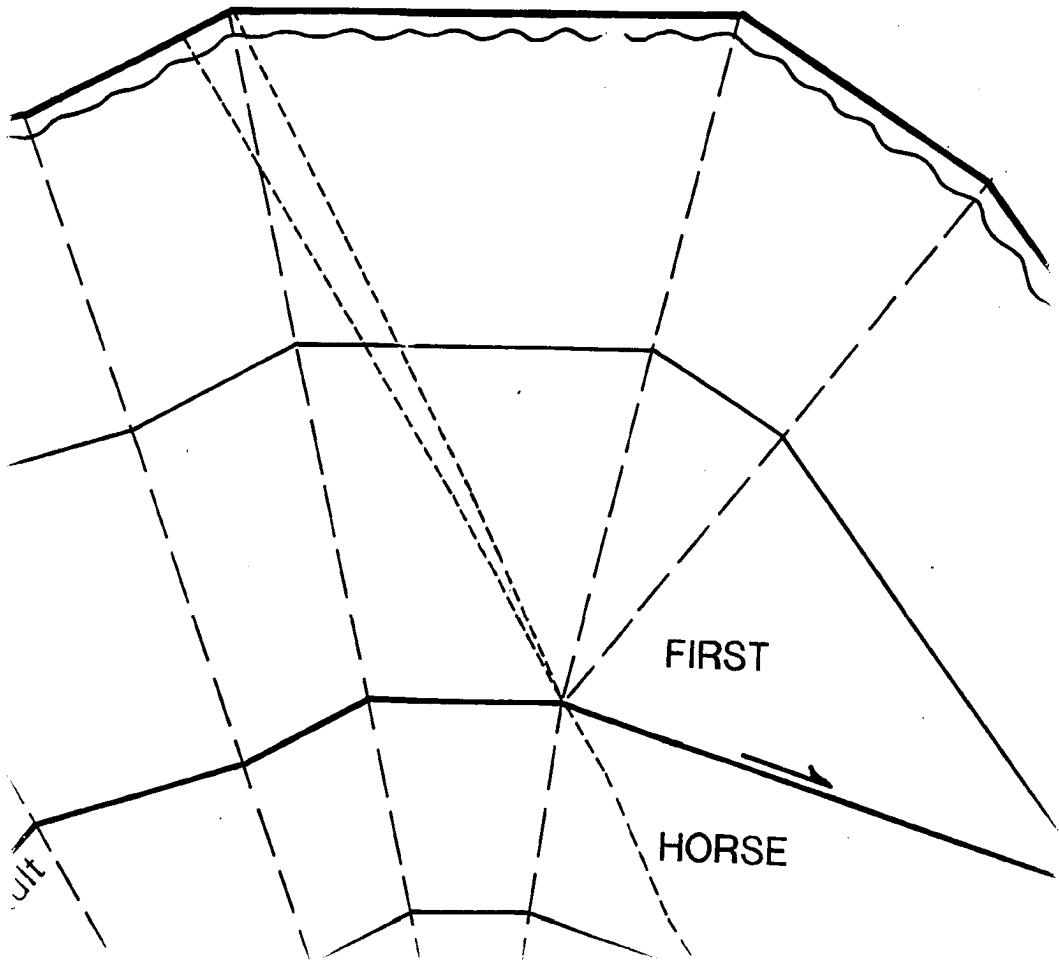

RANKLIN MOUNTAINS ANTICLINORI

:NT OF THE FIRST HORSE OF THE

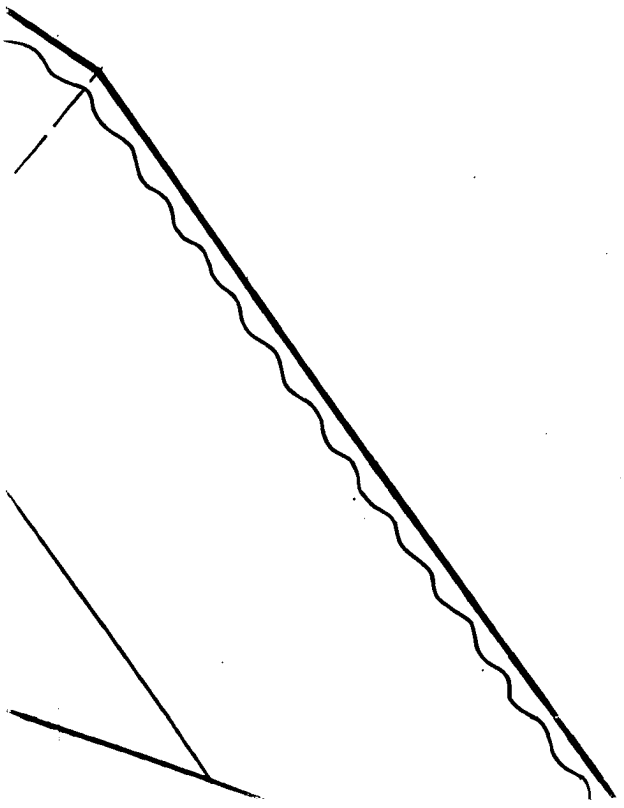

NORIUM,

THE ANTICLINORIUM

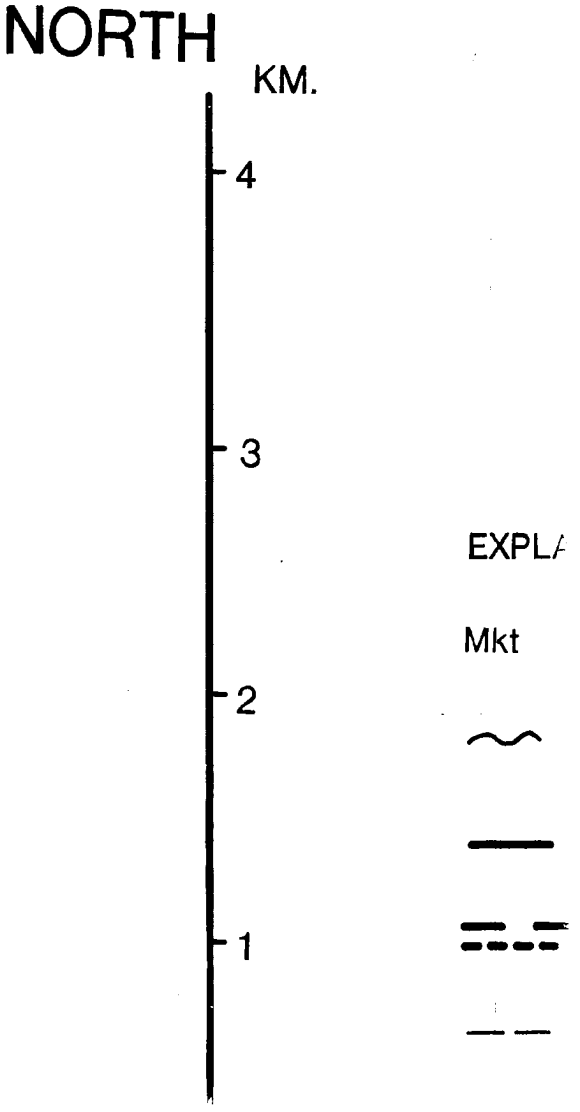

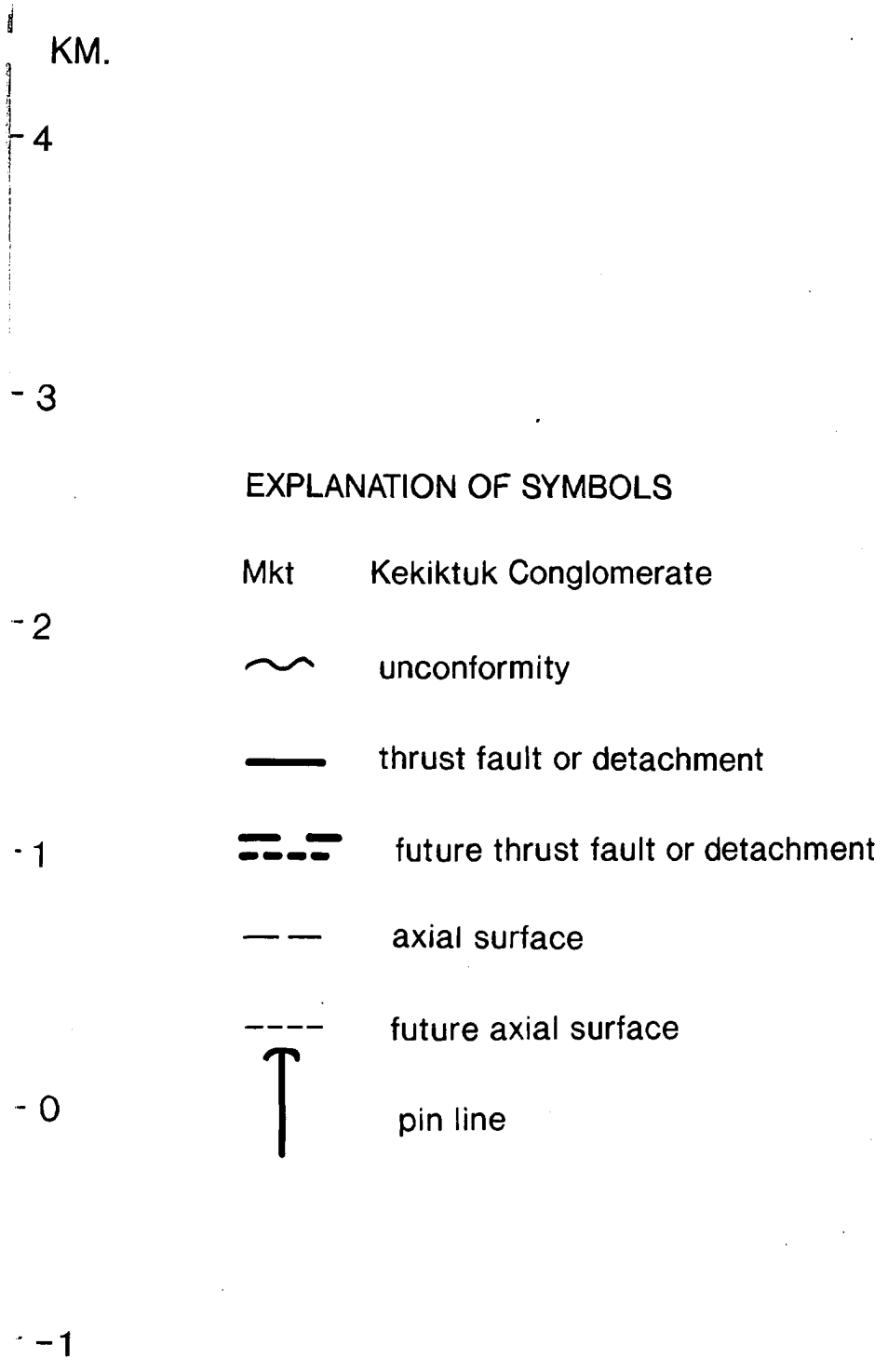

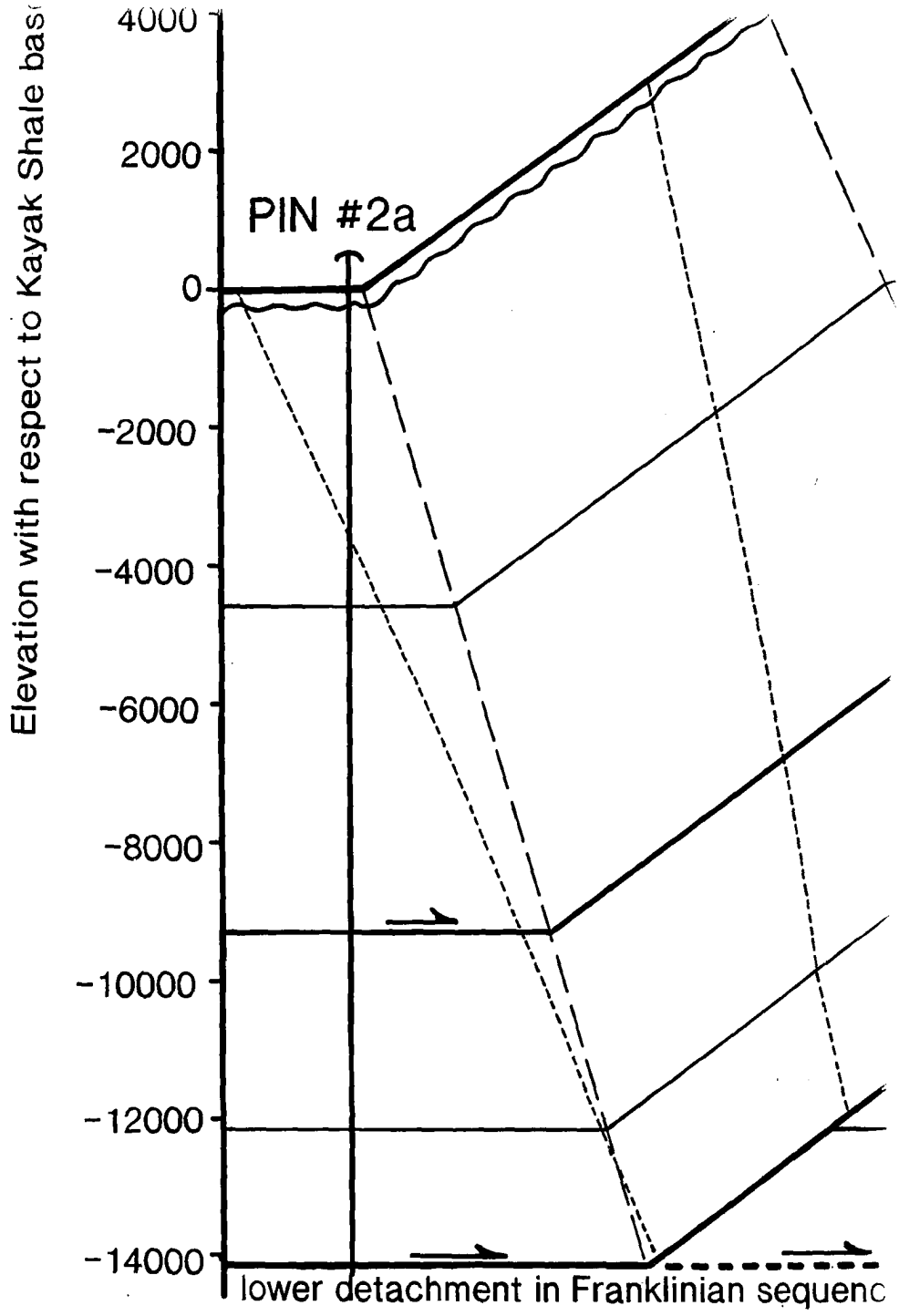

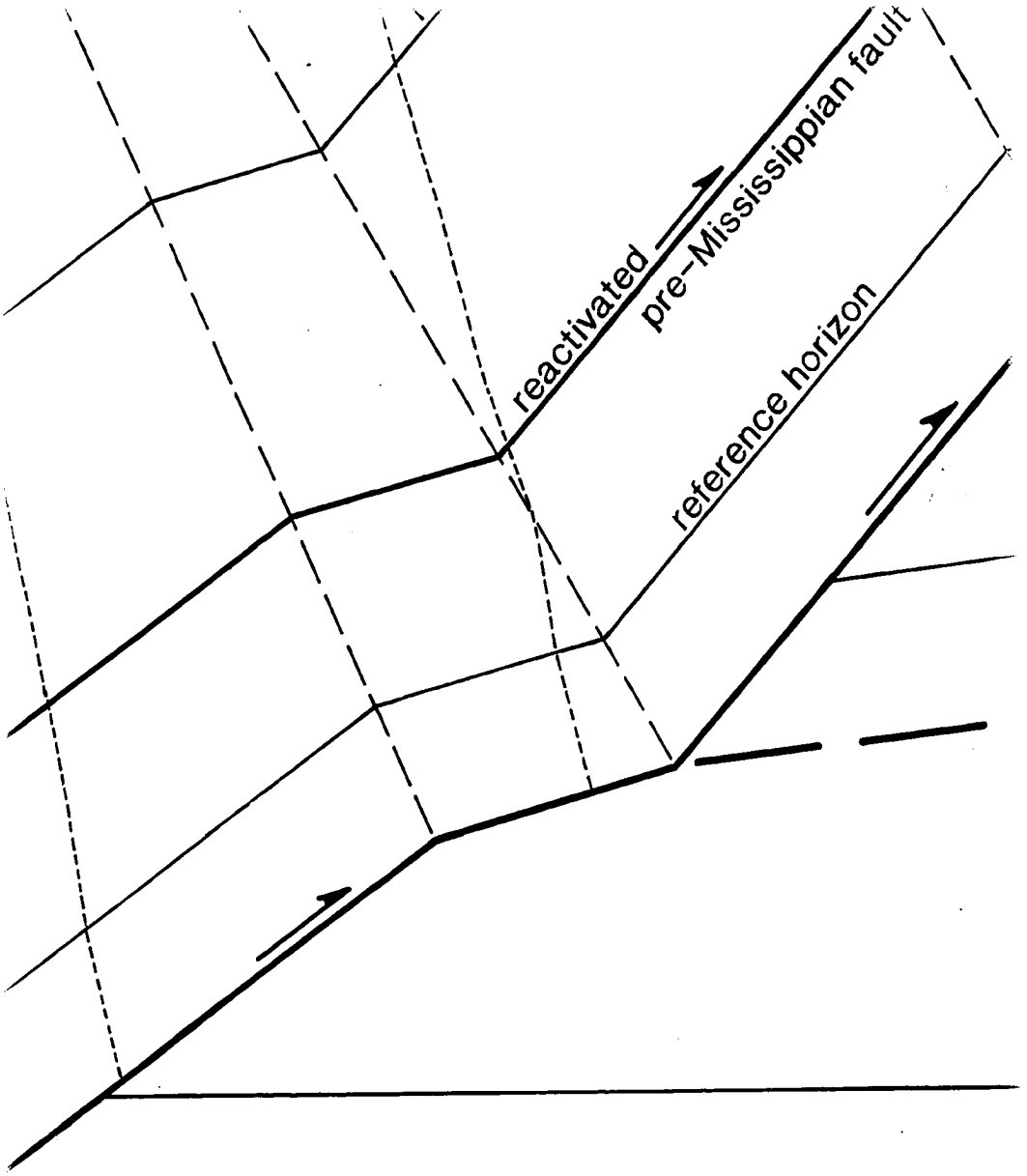

SCALE 1:25,000

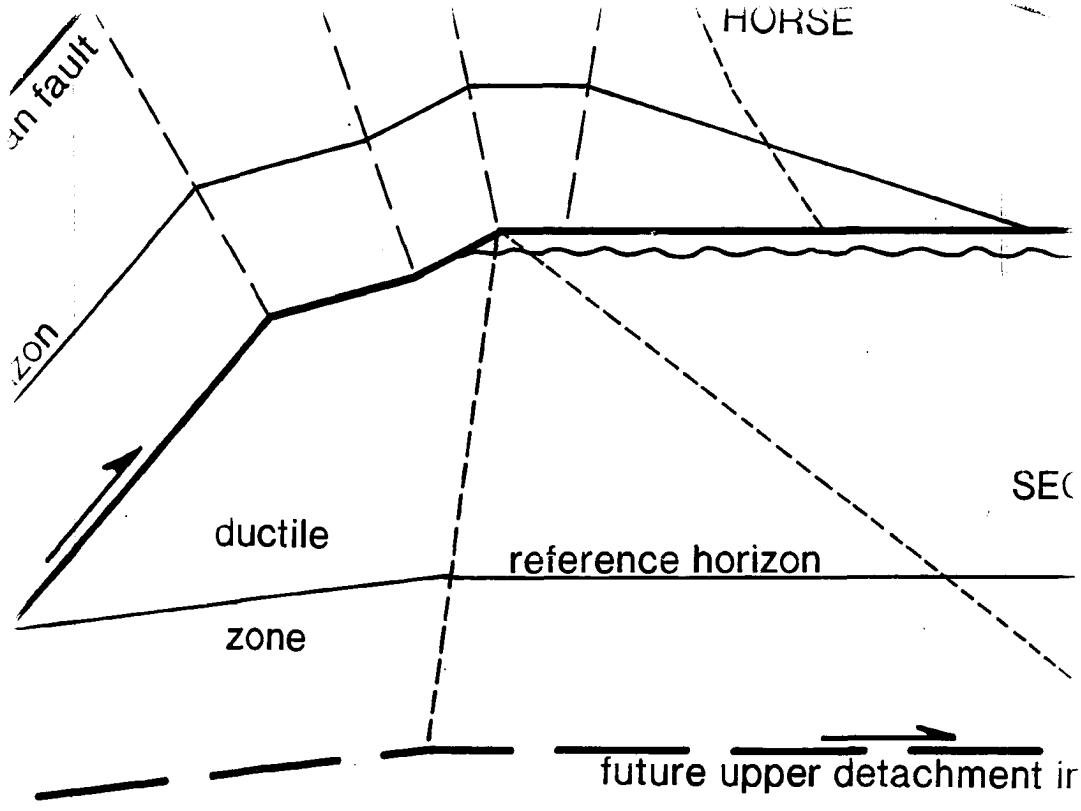

NO VERTICAL EXAGGERAT

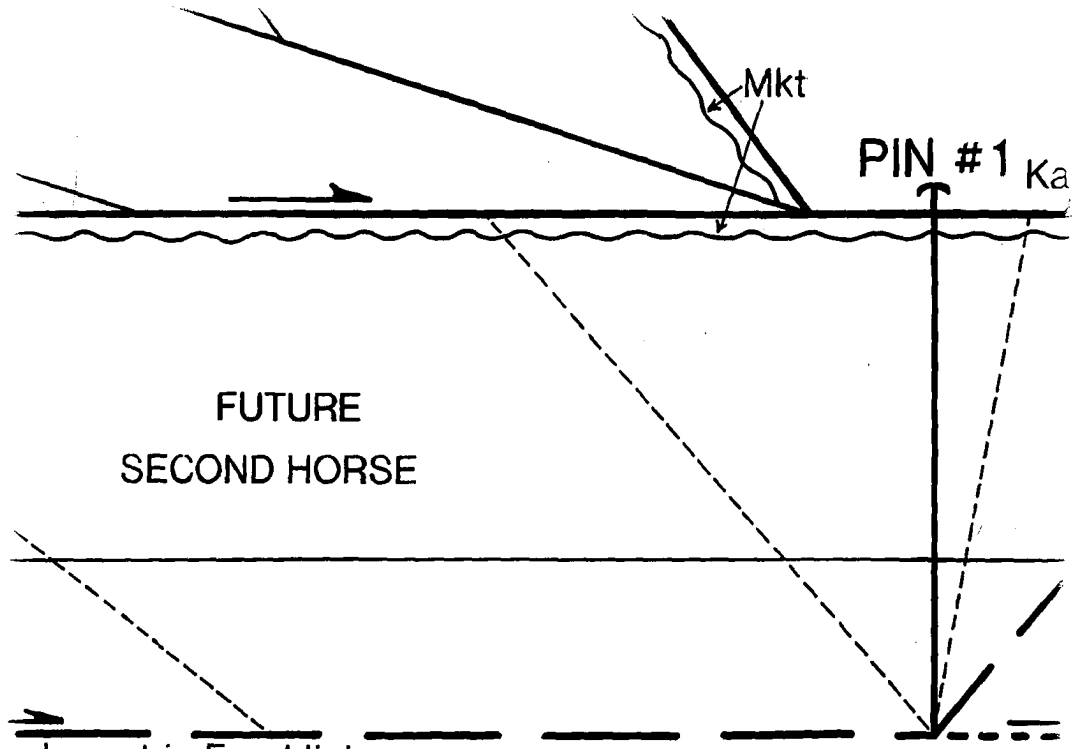

achment in Franklinian sequence

undifferentiat

Franklinian seq

GERATION

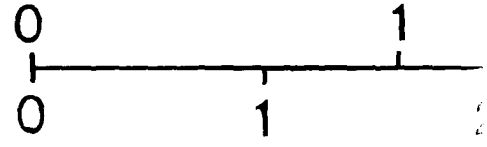

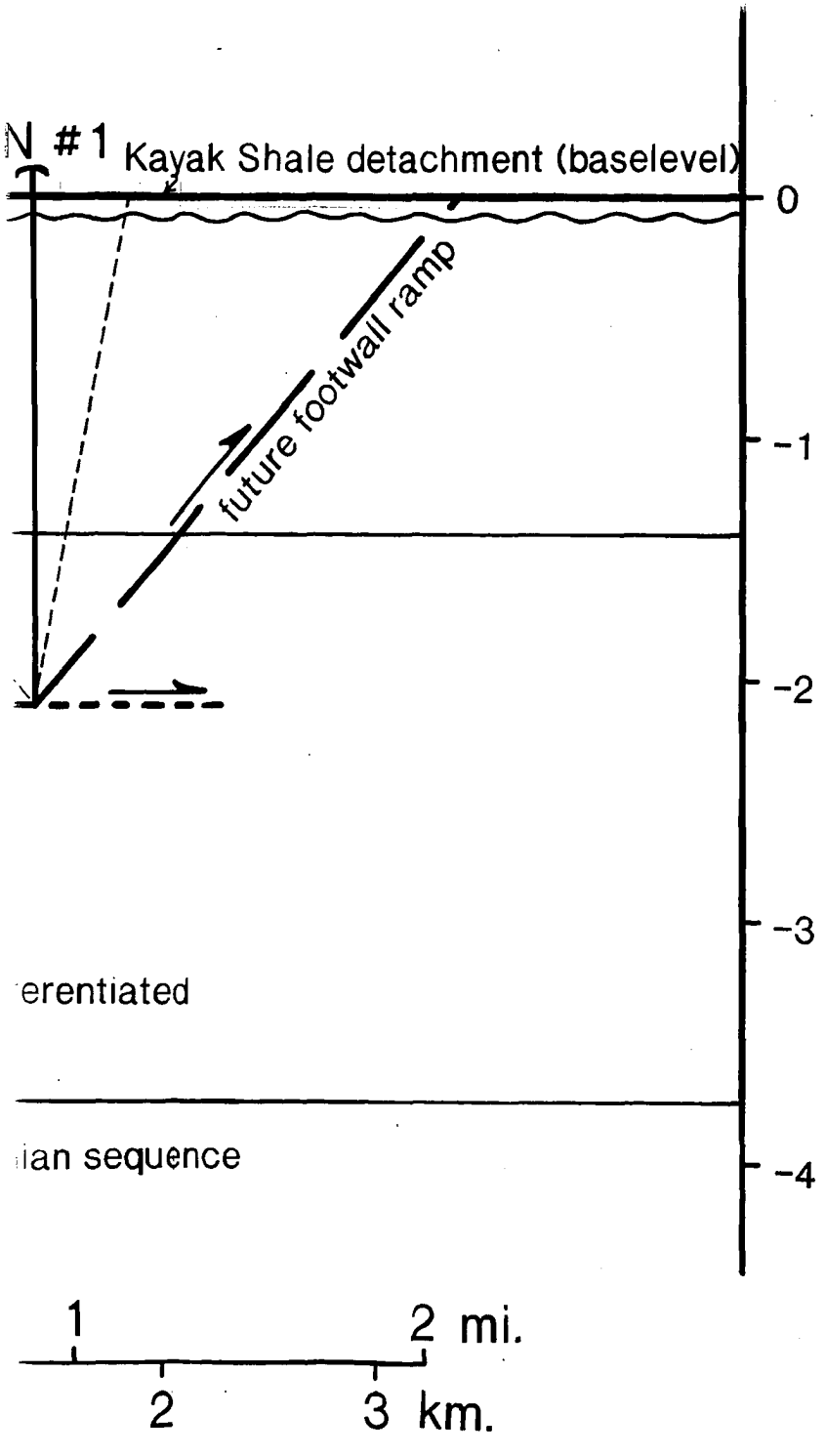

PLATE 5 BALANCED CROSS-
OF THE FRANKLIN M
TO THE WEST AND E

V

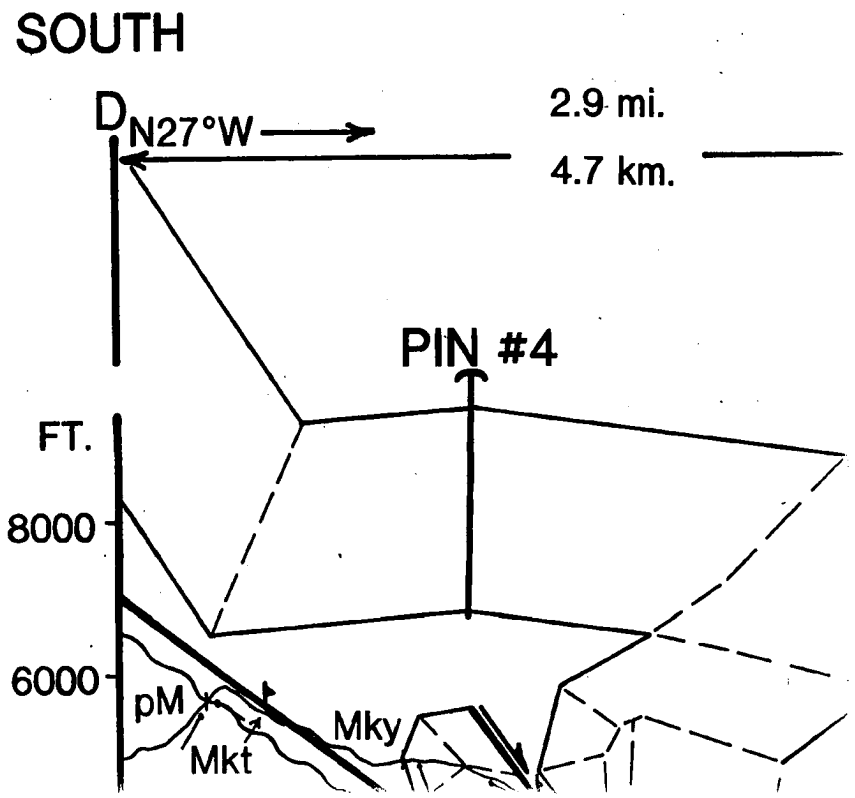

CROSS-SECTIONS CONSTRUCTED
NKLIN MOUNTAINS ANTICLINORIUM
ST AND EAST OF THE PRIMARY CRO

WESTERN CROSS-SECTION

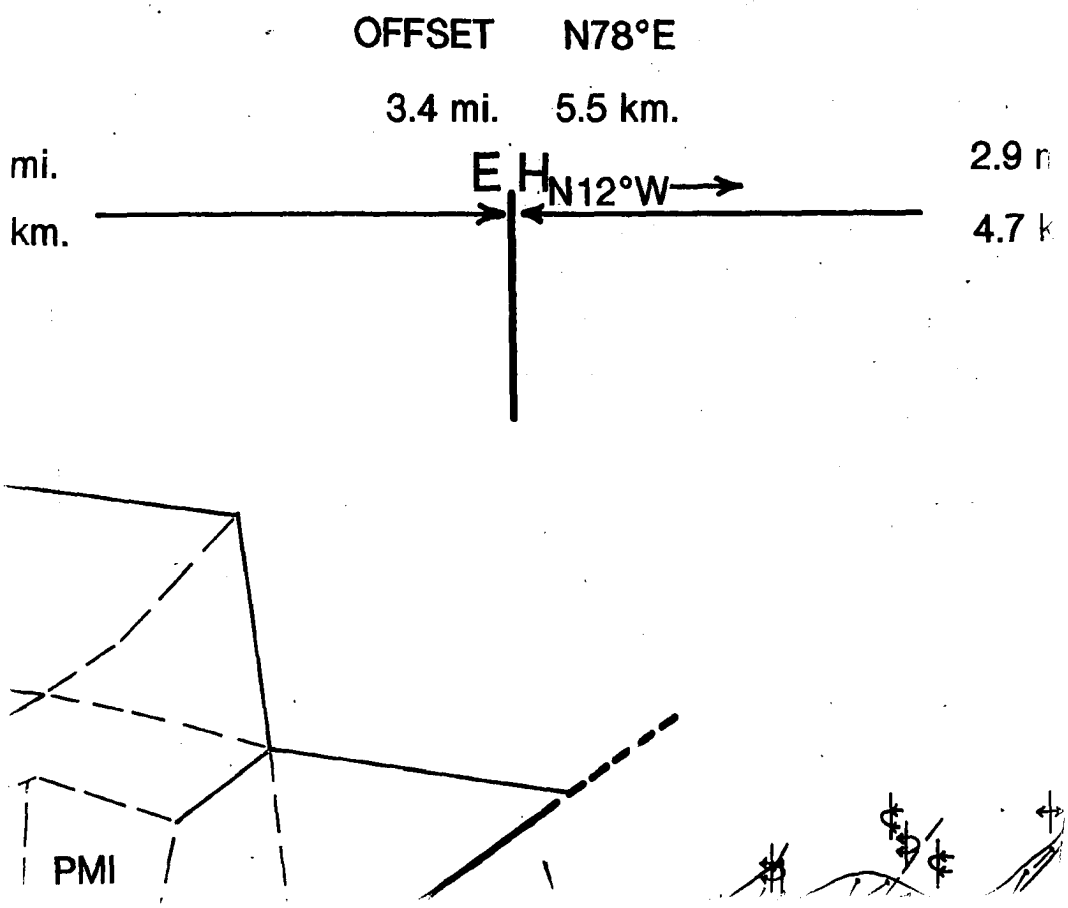

CTED ACROSS THE NORTHERN LIM
ORIUM
Y CROSS-SECTION

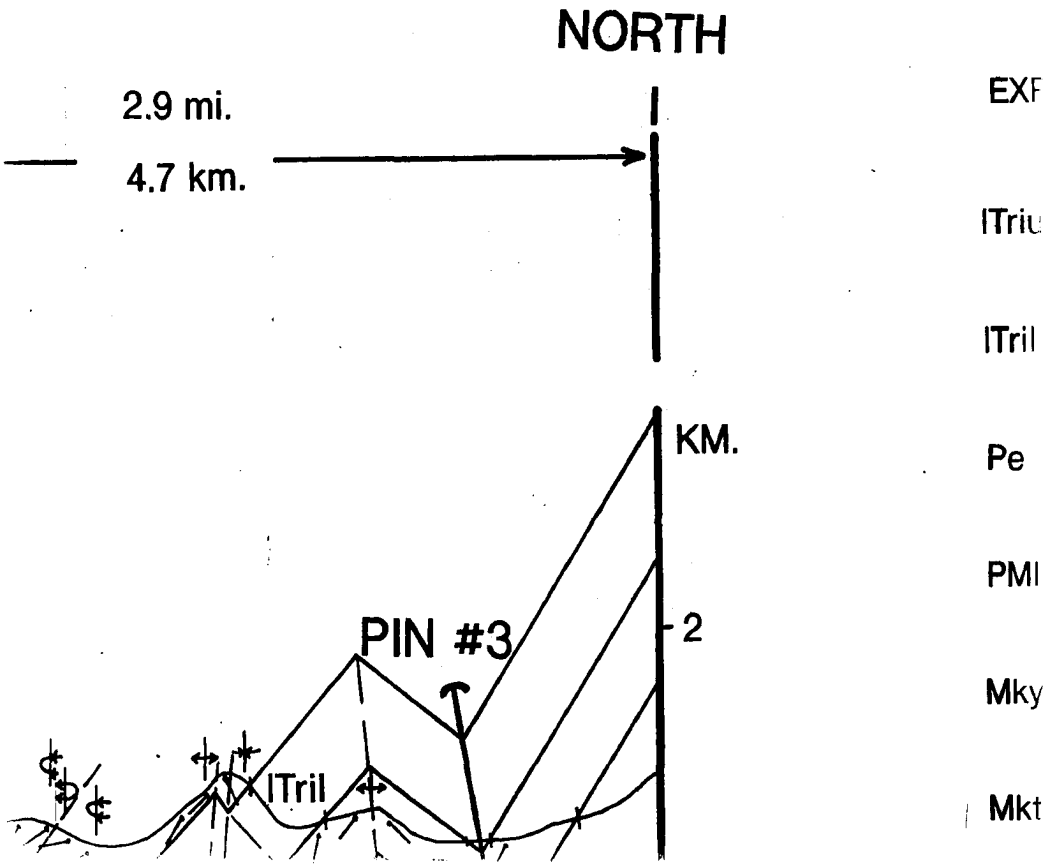

ORTHERN LIMB

RTH

EXPLANATION OF SYMBOLS

lTriu	upper Ivishak Formation
lTril	lower Ivishak Formation
Pe	Echooka Formation
PMl	Lisburne Group
Mky	Kayak Shale
Mkt	Kekiktuk Conglomerate

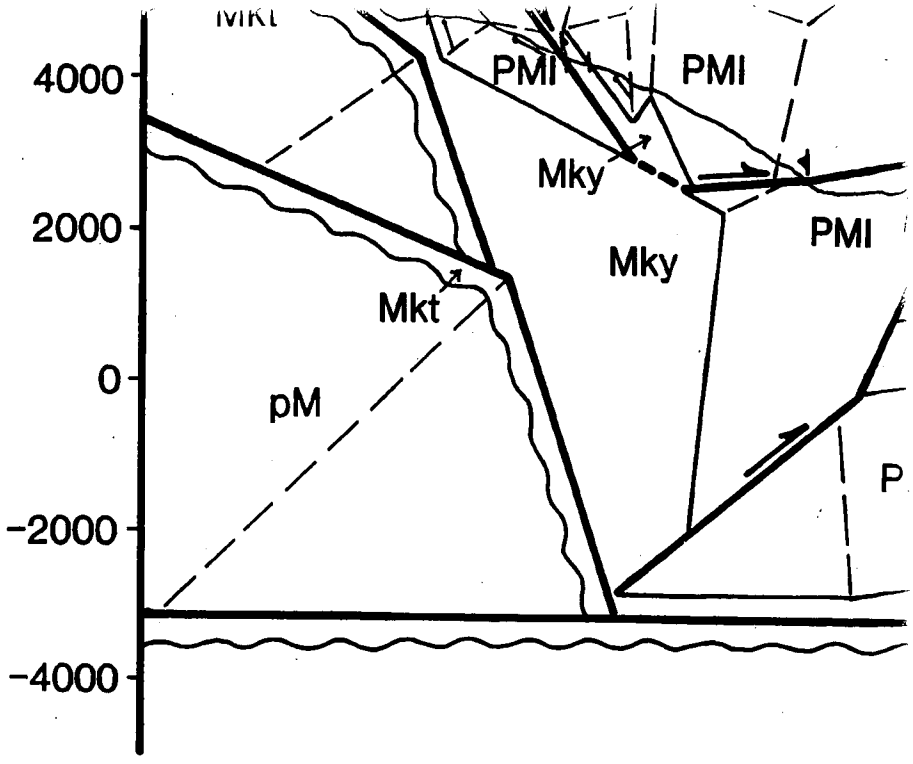

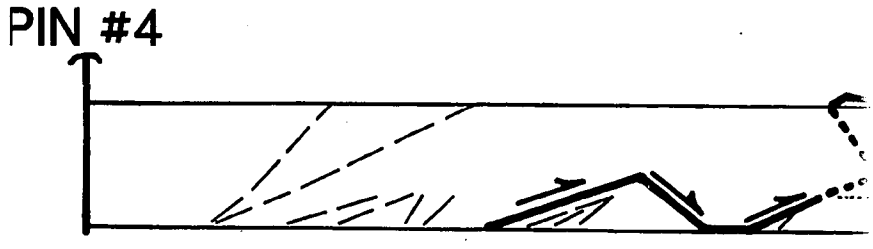

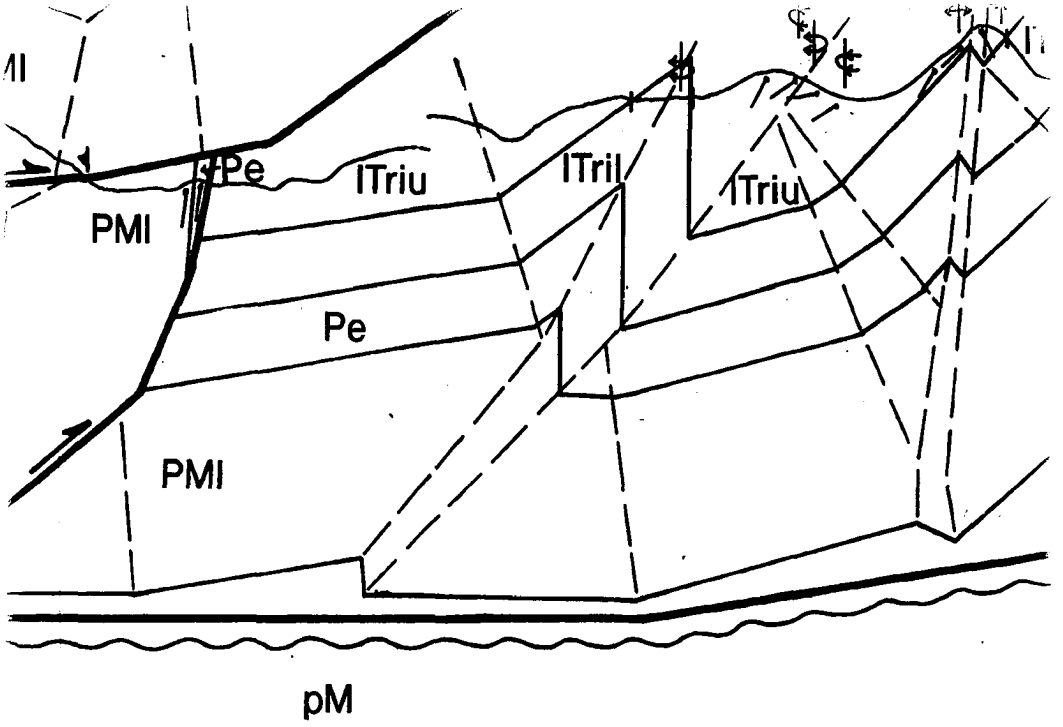

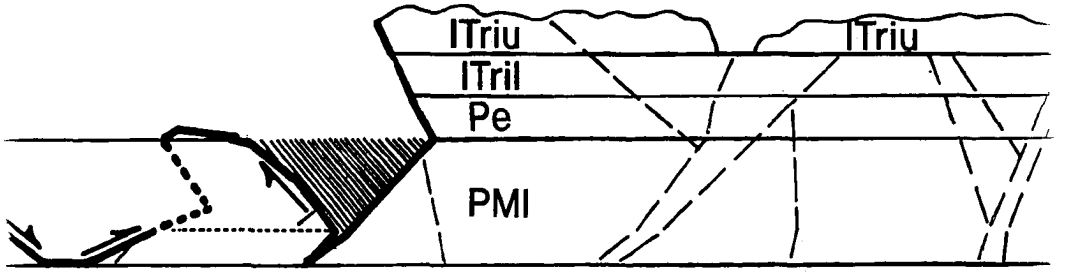

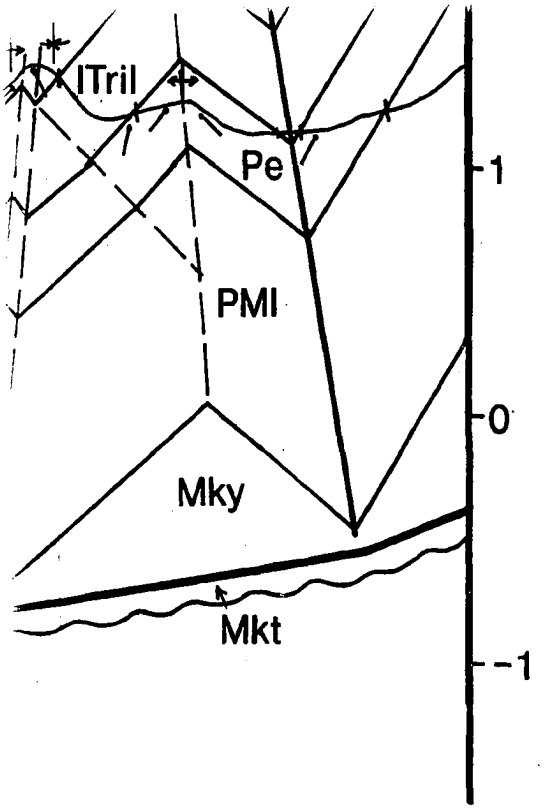

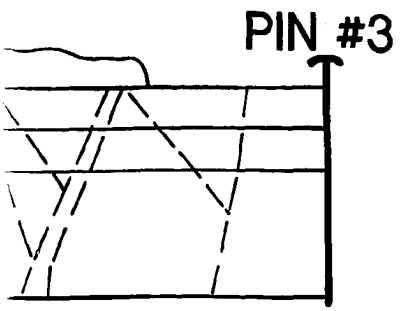

Mkt Kekikt

pM pre-Mi

unconf

thrust f

axial s

pin line

dip of b

anticlin

syncline

area mi

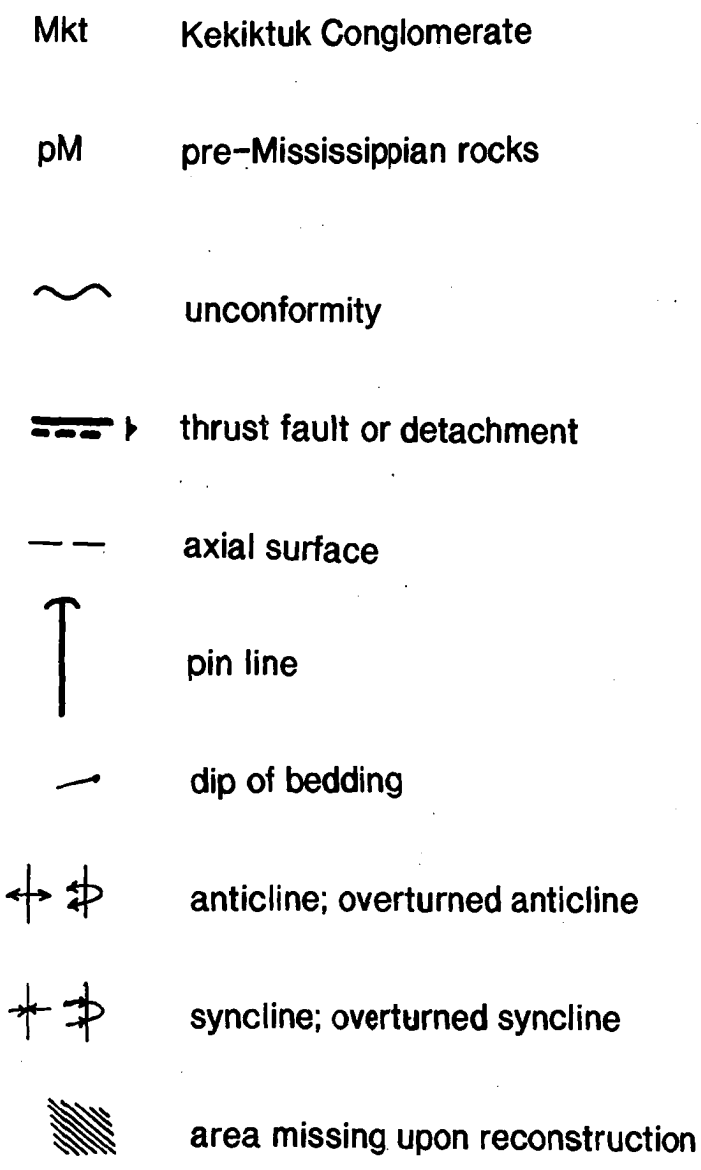

EASTE

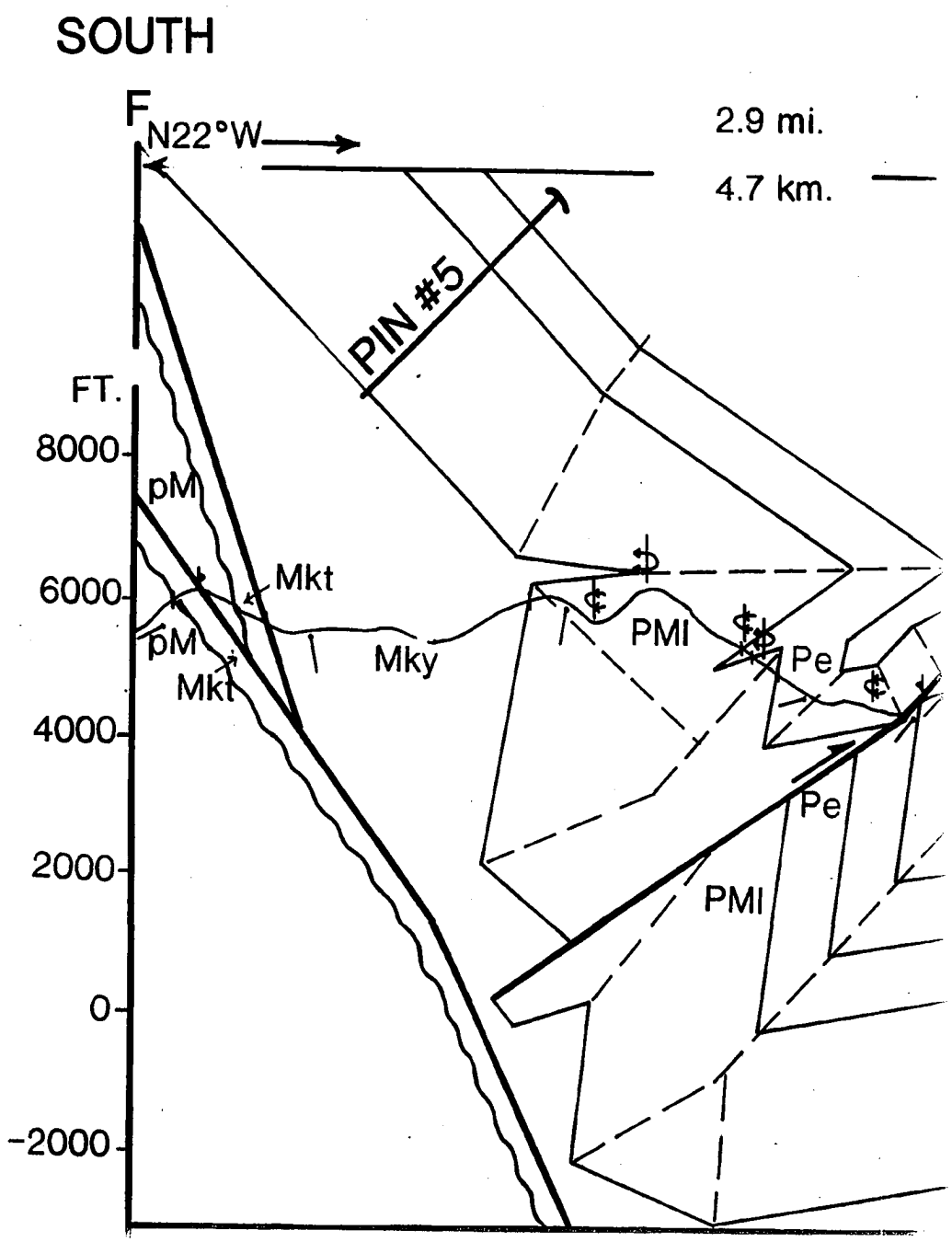

EASTERN CROSS-SECTION

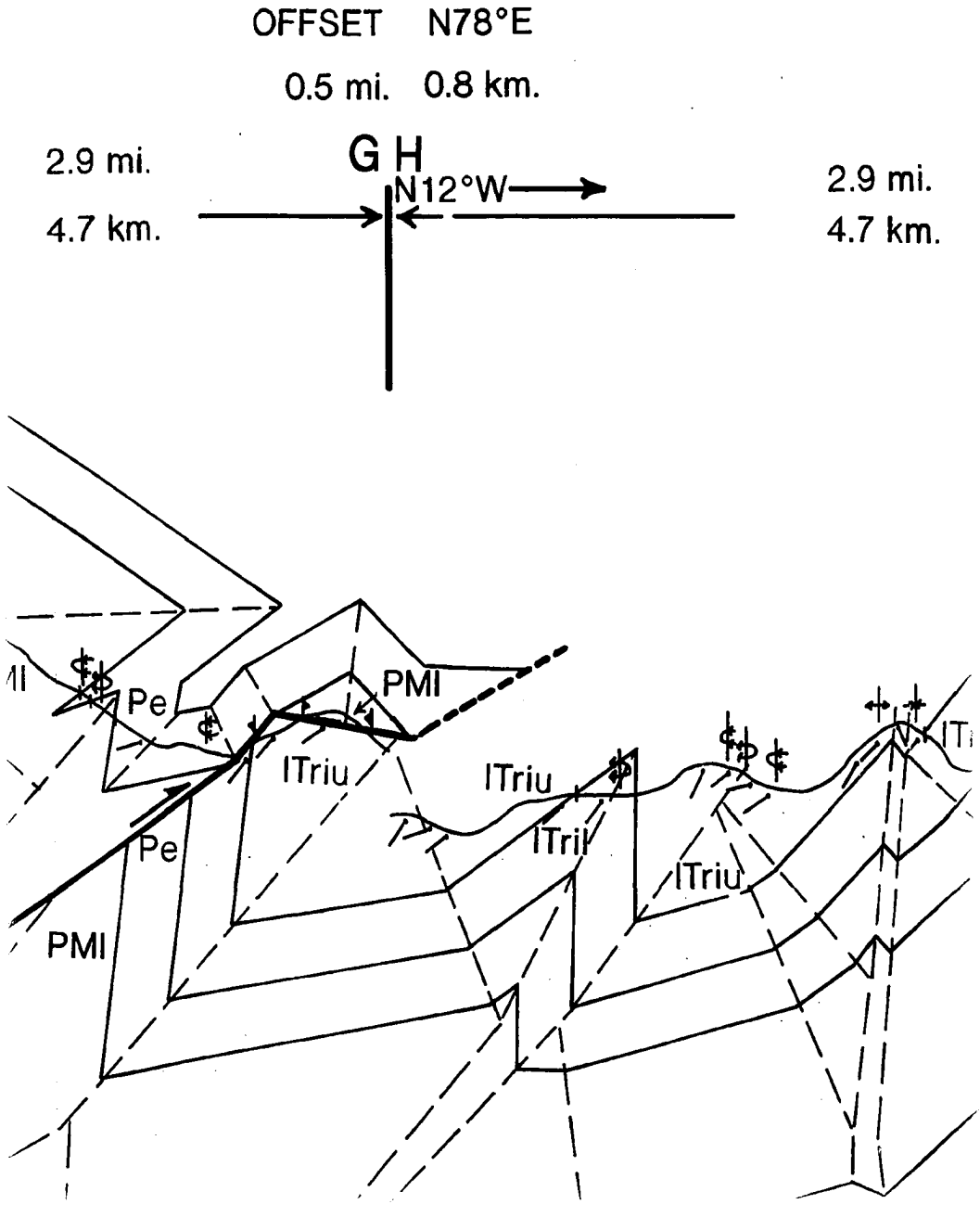

SCALE

NO V

RECO

OF DE

REPRO

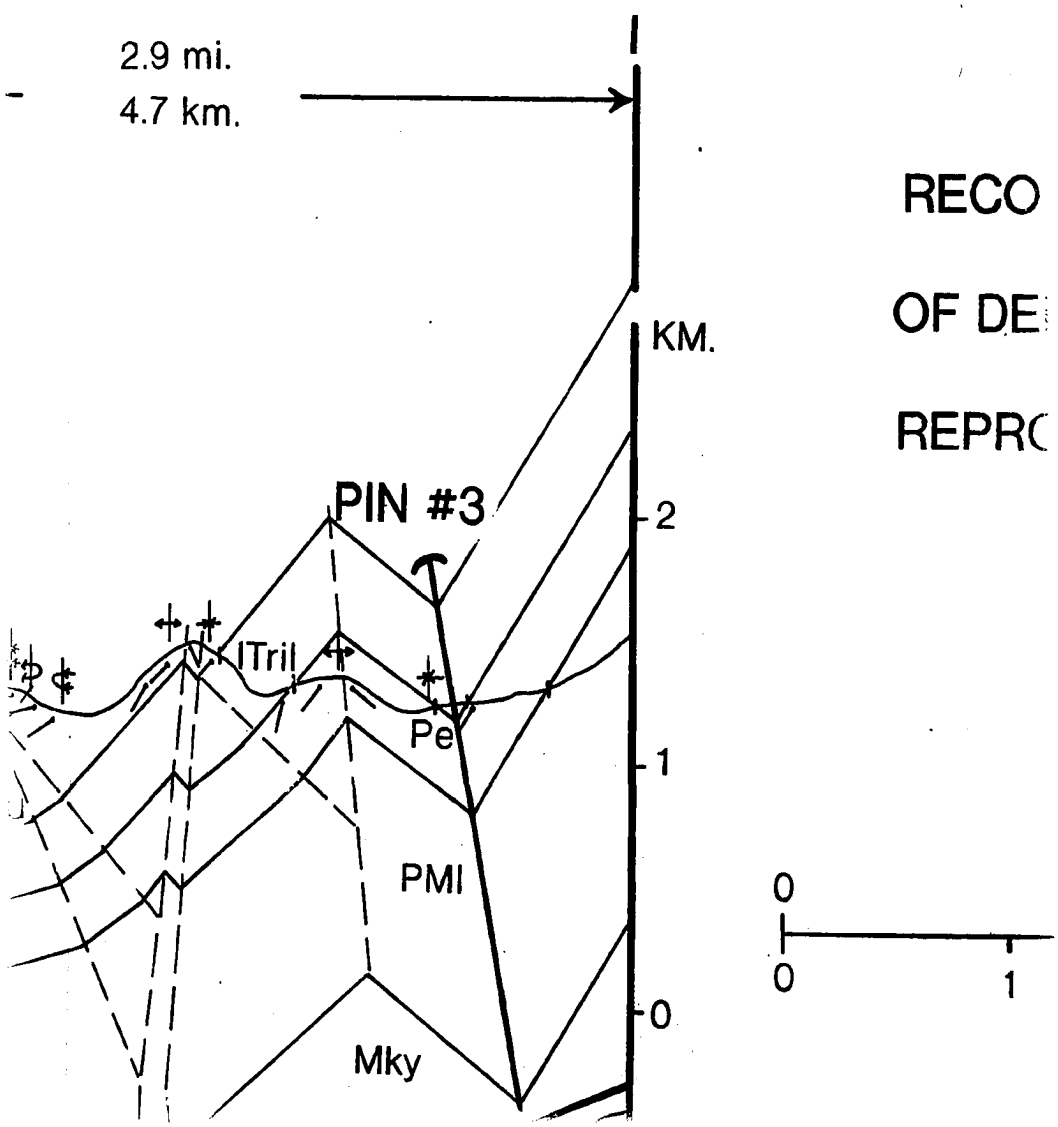

SCALE 1:25,000

NO VERTICAL EXAGGERATION

RECONSTRUCTIONS

OF DEFORMED CROSS-SECTIONS

REPRODUCED AT 64%

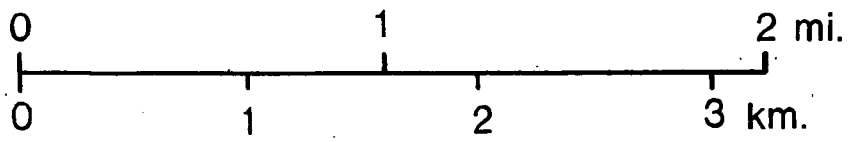

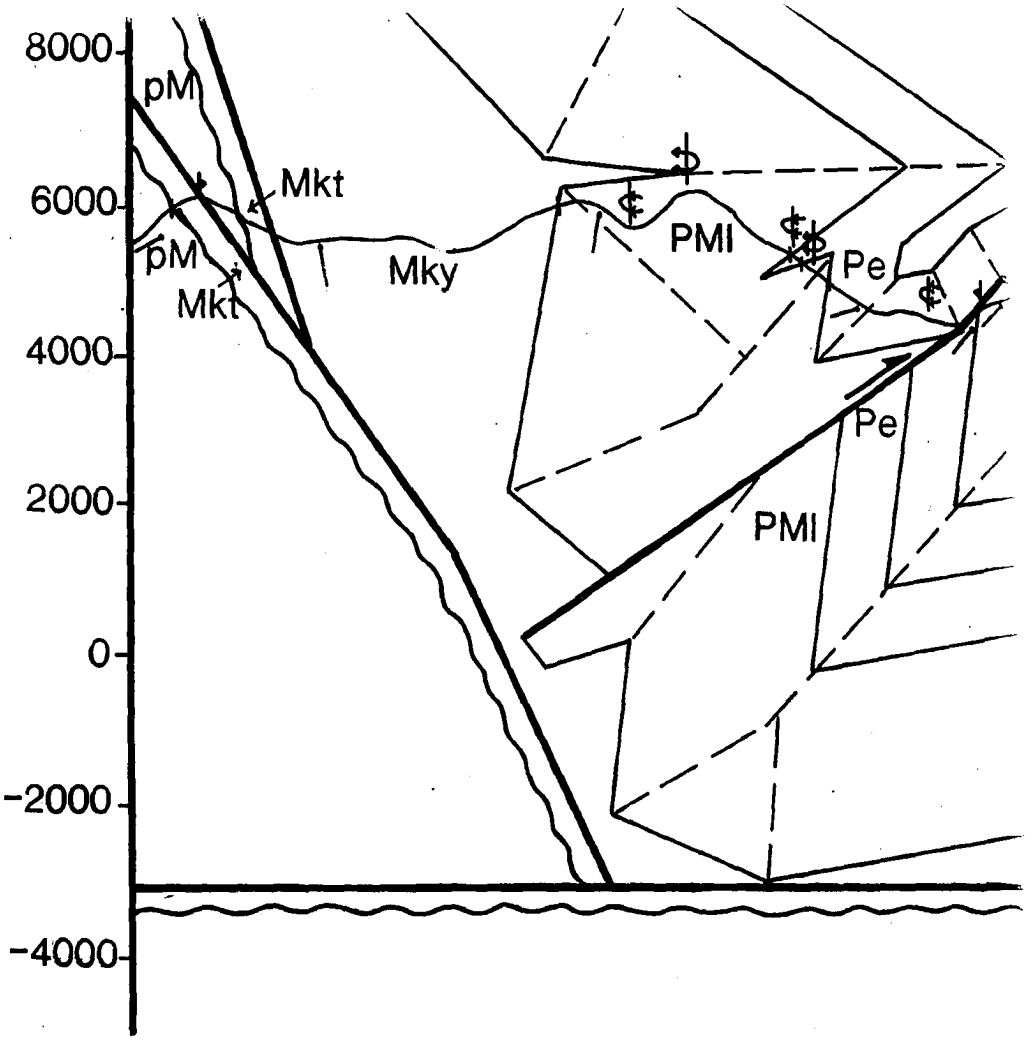

PIN #5

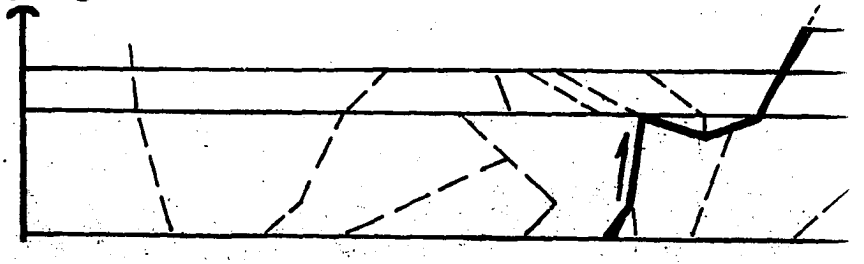

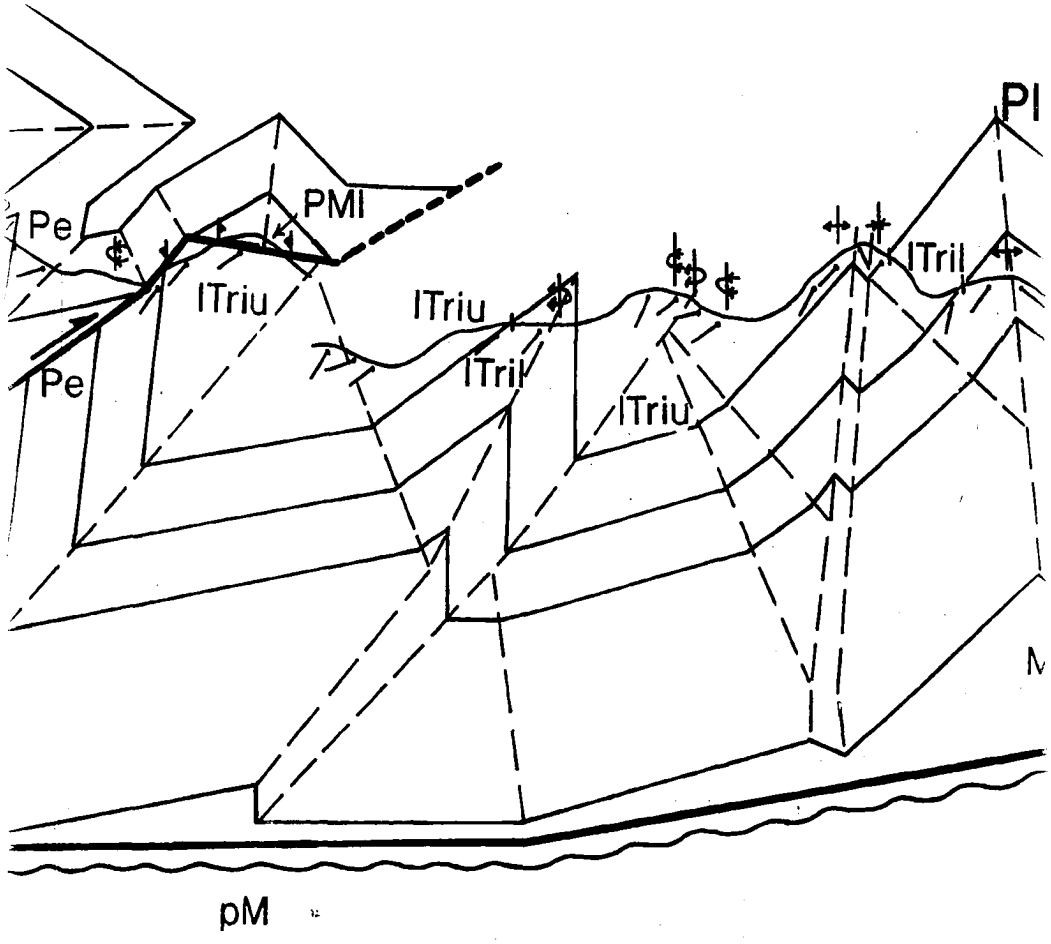

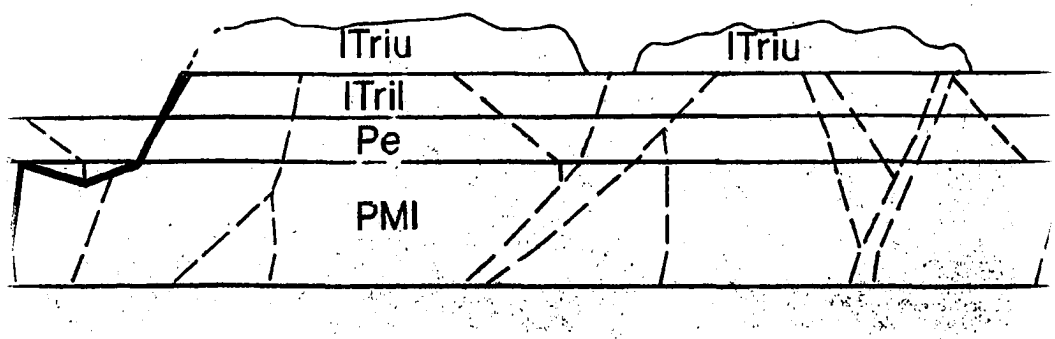

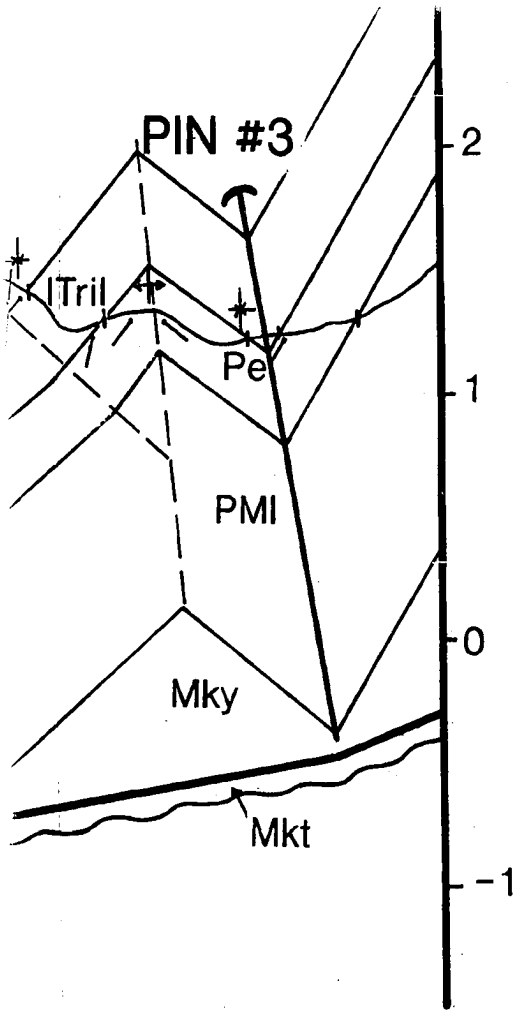

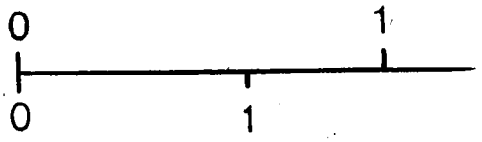

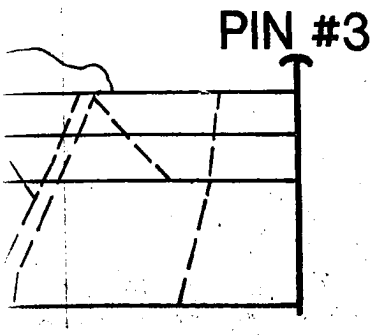

REPRODUCED AT 64%

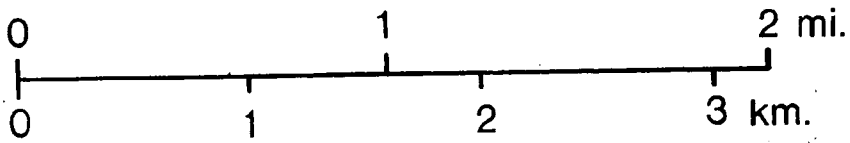

PLATE 1 GEOLOGIC MAP OF STUDY AREA BETWEEN FORKS C
NORTHEASTERN BROOKS RANGE, ALASKA

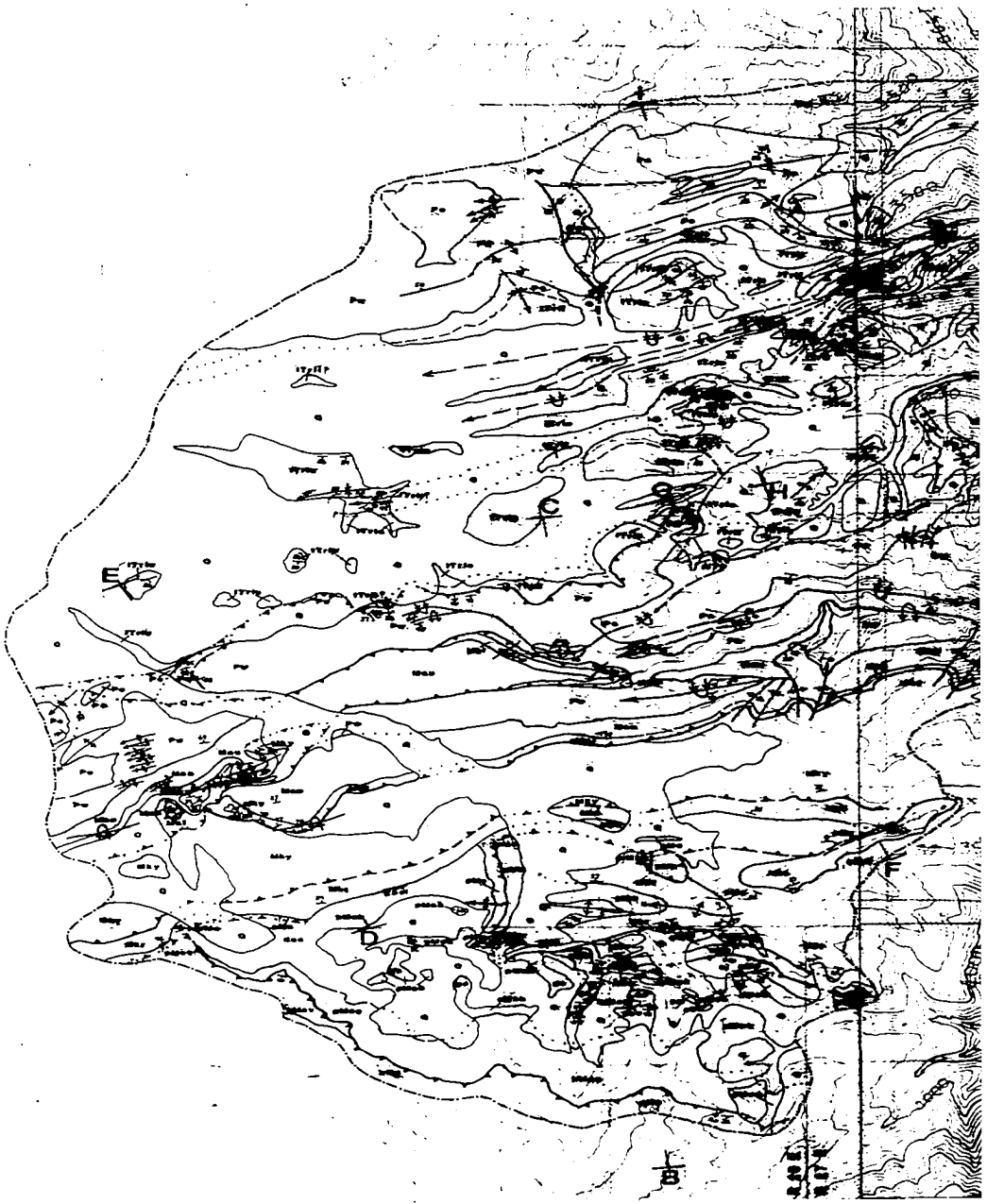

69°02'48"
146°00'

BY J.A. ZIEGLER 1989

0 1 2 MILES

SCALE 1 : 25,000
CONTOUR INTERVAL 100 FEET

BASE ENLARGED FROM U. S. GEOLOGICAL SURVEY
MT. MICHELSON QUADRANGLE (A-3 AND A-4),
PROVISIONAL EDITION 1983

APP

KS OF CANNING RIVER, FRANKLIN MOUNTAINS,

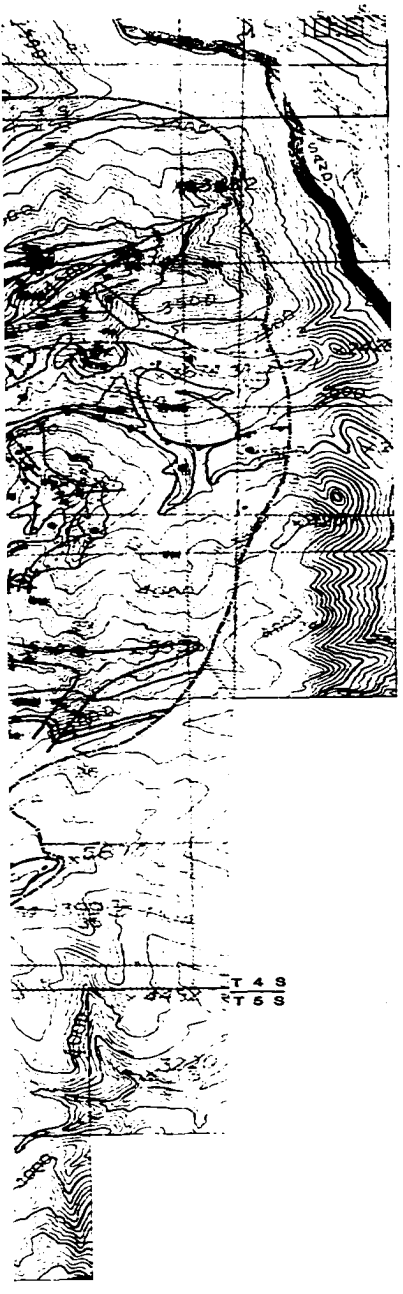

EXPLANATION OF MAP SYMBOLS

- Strike and dip of beds
- Strike and dip of bedding: uncertain
- Strike of vertical bedding
- Strike and dip of cleavage: foliation
- Anticline (top) and syncline, showing trace and dip of axial surface and plunge of axis; dashed where approximately located
- Overturned anticline (top) and overturned syncline, showing trace of axial surface and plunge of axis; dashed where approximately located
- Contact: solid where known, dashed where approximately located, dotted where inferred
- Thrust fault: solid where known, dashed where approximately located, dotted where inferred, sawteeth on upper plate (Also used to delineate a map unit which acts as a detachment or is brecciated.)
- Fault (D,downthrown side; U, upthrown side)

(Refer to Appendix B for description of map units.)

lTriu	Lower Triassic upper Ivishak Formation
lTril	Lower Triassic lower Ivishak Formation
Pe	Permian Echooka Formation
Pw	Pennsylvanian Wahoo Limestone
Mau	Mississippian upper Alapah Limestone
Mal	Mississippian lower Alapah Limestone
Mky	Mississippian Kayak Shale
Mkt	Mississippian Kekiktuk Conglomerate
pMsv	Pre-Mississippian Slate-Volcanic Unit
pMp	Pre-Mississippian Phyllite Unit
pMc	Pre-Mississippian Chloritic Phyllite Unit
pMcg	Pre-Mississippian Chert-Greenstone Unit
pMsh	Pre-Mississippian Shale Unit
	dss Dolostone/Sandstone
	gs Greenstone
	ch Chert
pMb	Pre-Mississippian Brecciated Unit
pMv	Pre-Mississippian Volcanic Unit

S

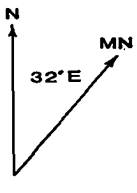

APPROXIMATE DECLINATION, 1983

PLATE 5 BALANCED CROSS-SECTIONS CONSTRUCTED ACROSS
OF THE FRANKLIN MOUNTAINS ANTICLINORIUM
TO THE WEST AND EAST OF THE PRIMARY CROSS-SECT

WESTERN CROSS-SECTION

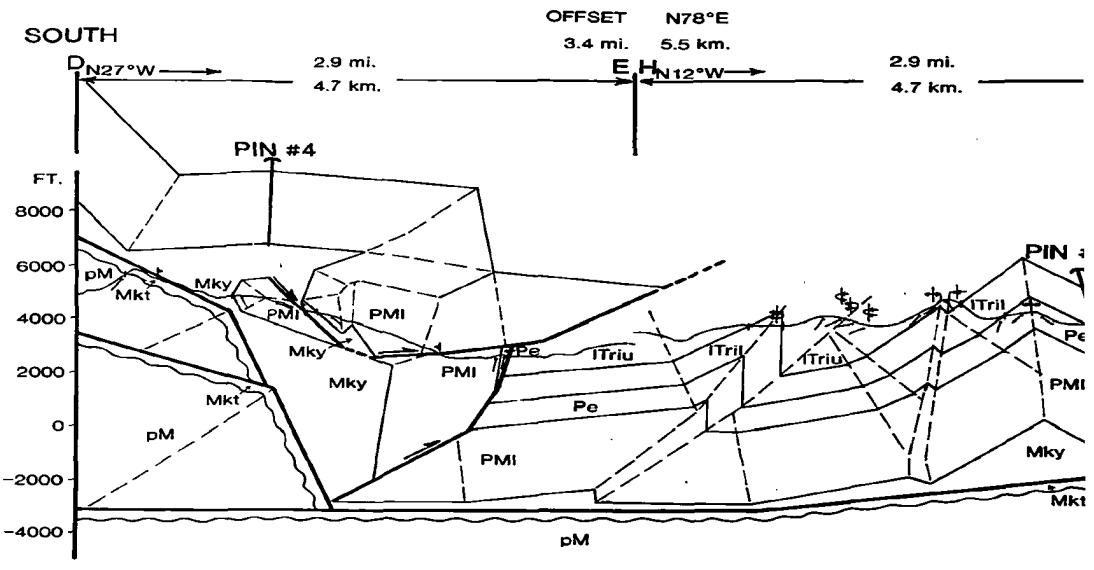

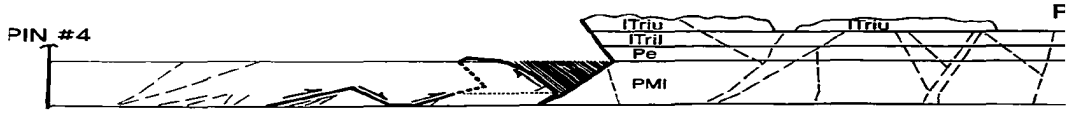

EASTERN CROSS-SECTION

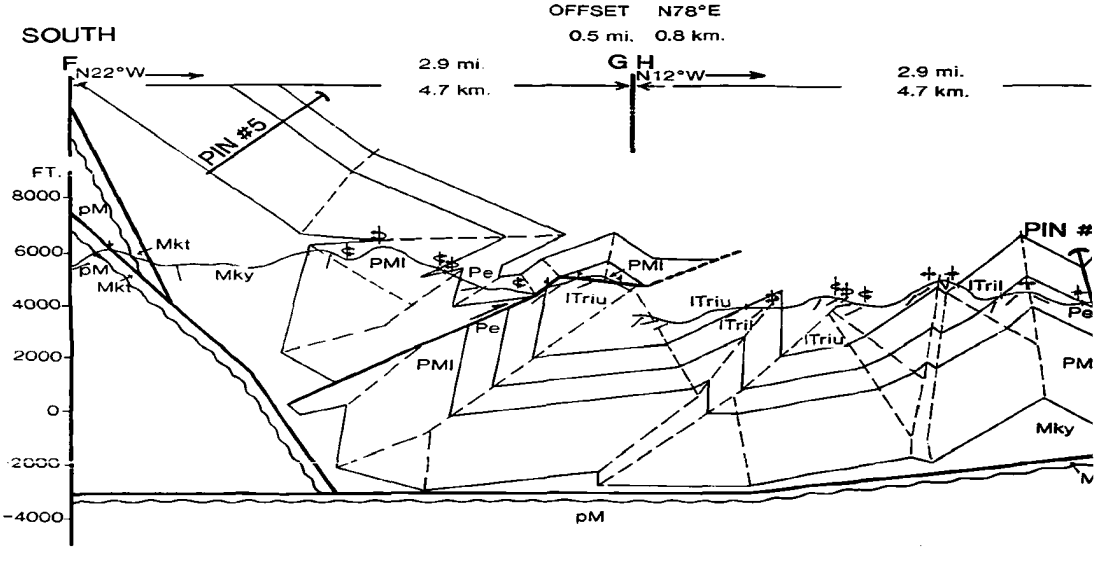

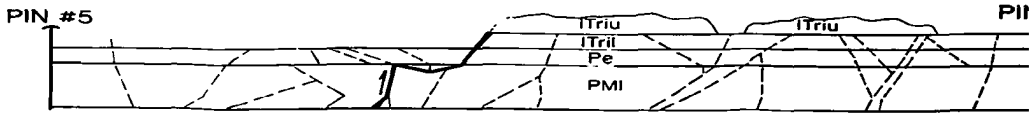

OSS THE NORTHERN LIMB

SECTION

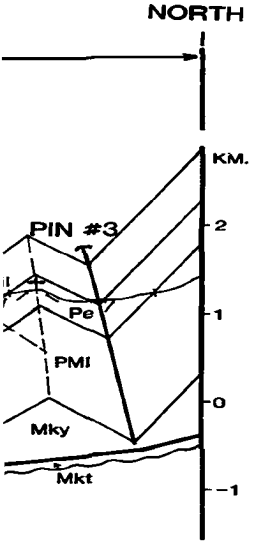

EXPLANATION OF SYMBOLS

lTriu	upper Ivishak Formation
lTril	lower Ivishak Formation
Pe	Echooka Formation
PMl	Lisburne Group
Mky	Kayak Shale
Mkt	Kekiktuk Conglomerate
pM	pre-Mississippian rocks

unconformity

thrust fault or detachment

axial surface

pin line

dip of bedding

anticline; overturned anticline

syncline; overturned syncline

area missing upon reconstruction

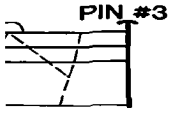

SCALE 1:25.000

NO VERTICAL EXAGGERATION

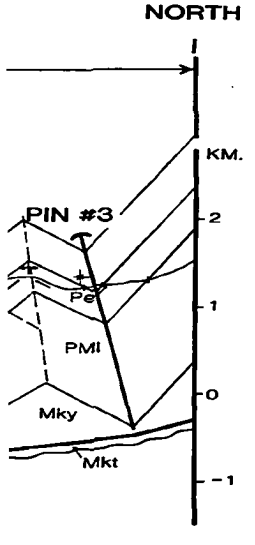

RECONSTRUCTIONS

OF DEFORMED CROSS-SECTIONS

REPRODUCED AT 64%

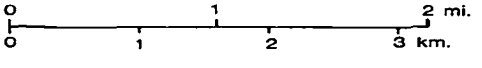

ZIEGLER, JENNIFER A.

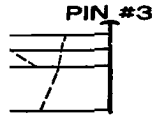

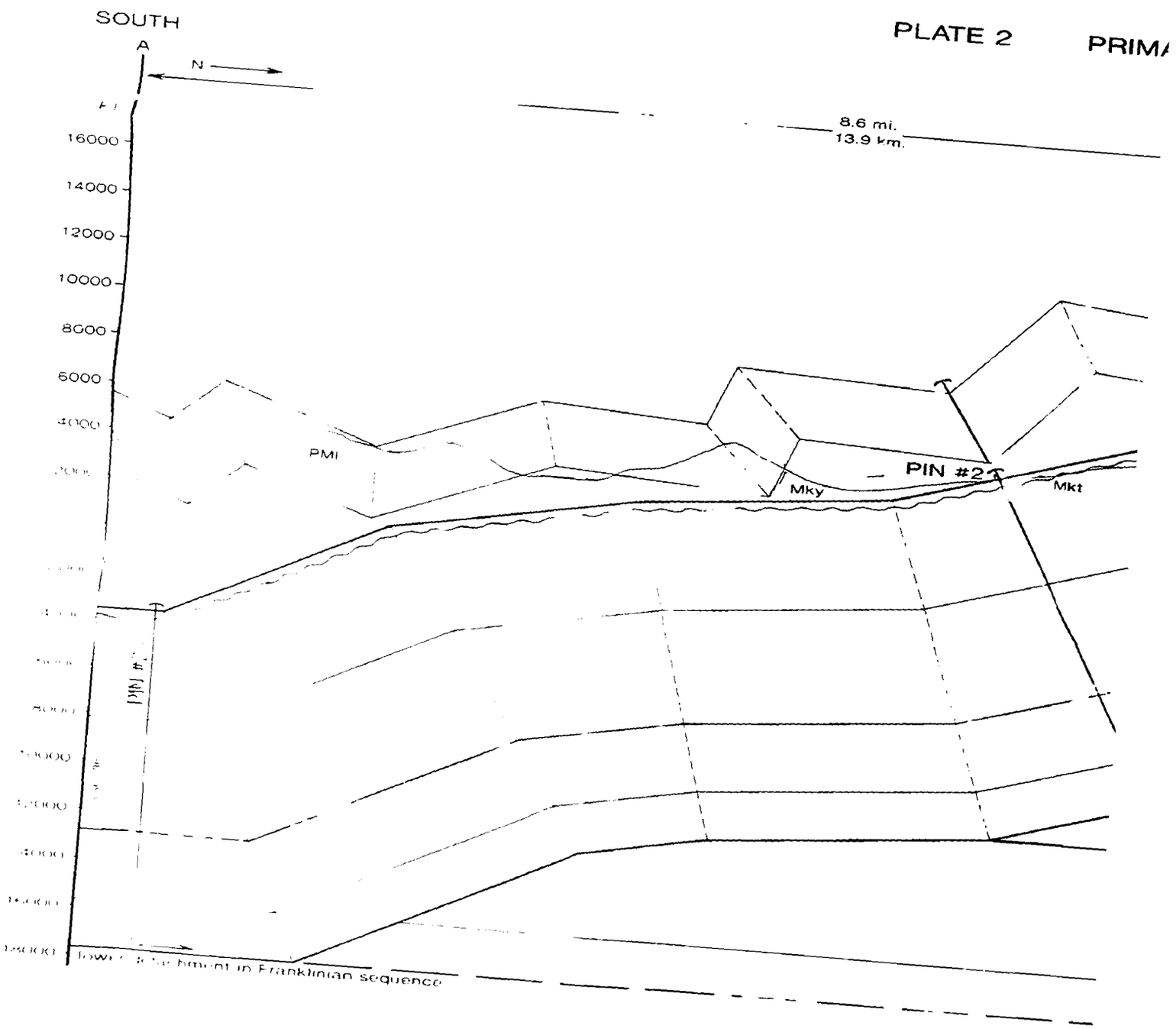

MARY BALANCED CROSS-SECTION ACROSS THE FRANKLIN MOUNTAINS A

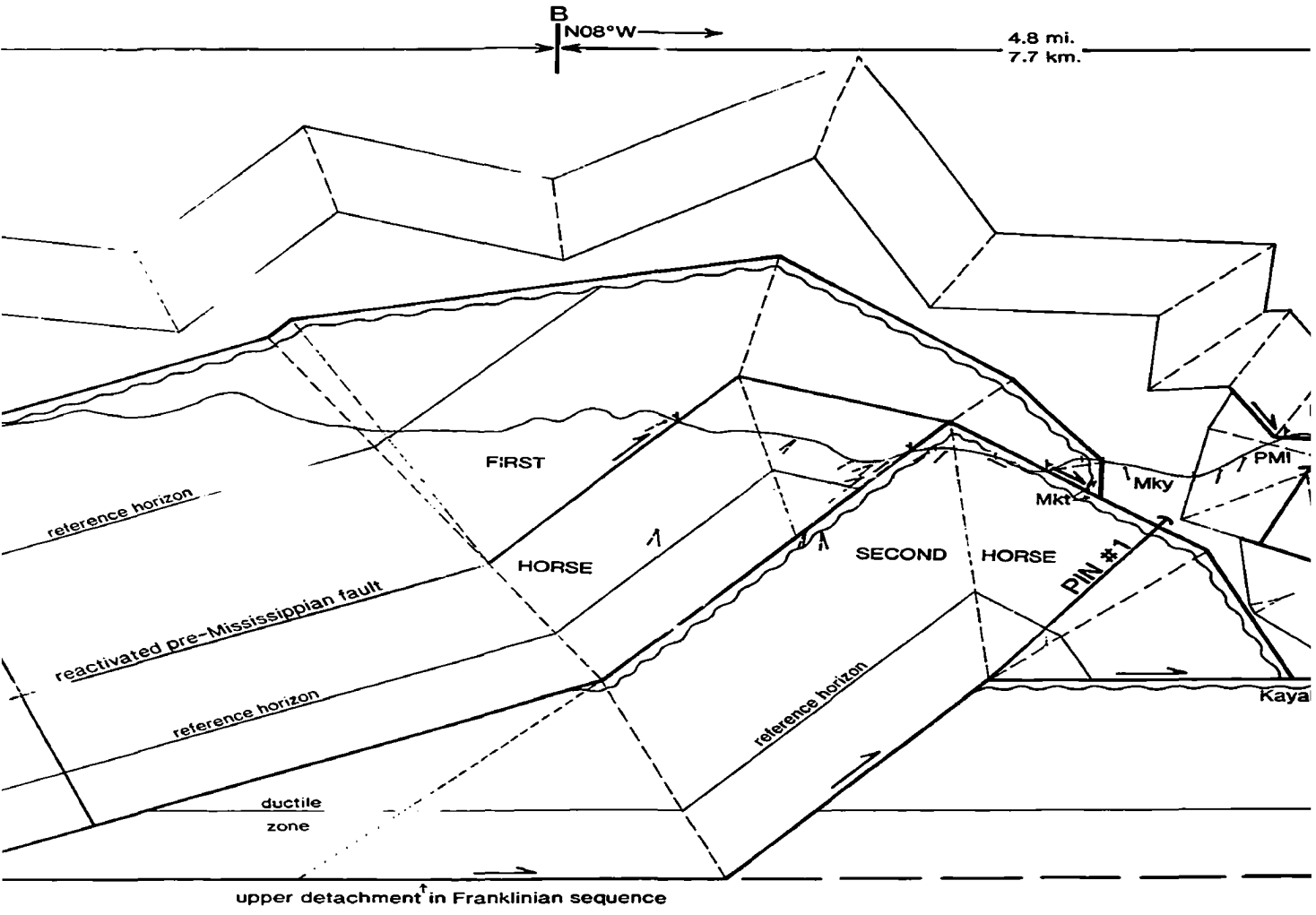

SCALE 1:25,000

NO VERTICAL EXAGGERATION

AINS ANTICLINORIUM

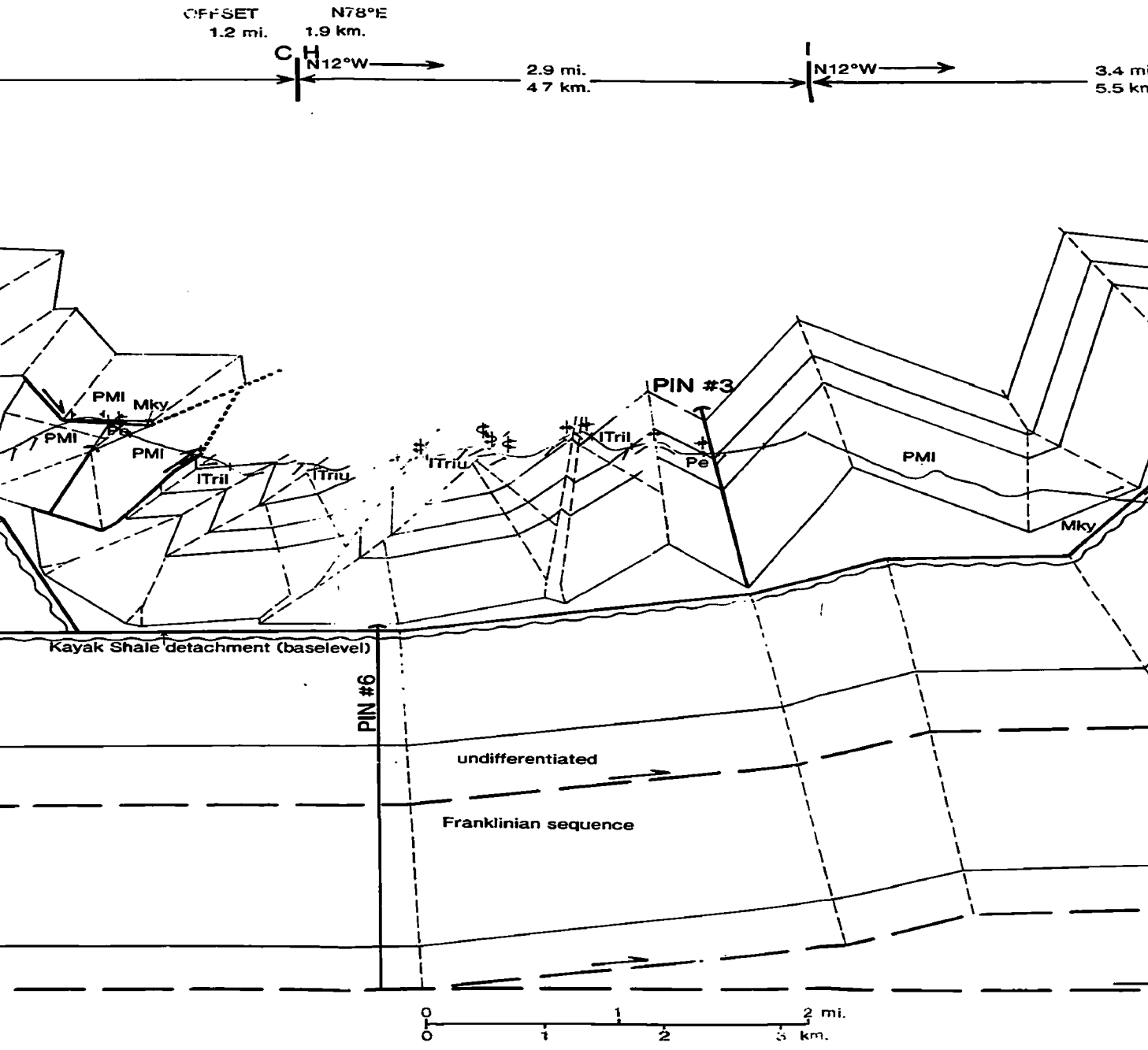

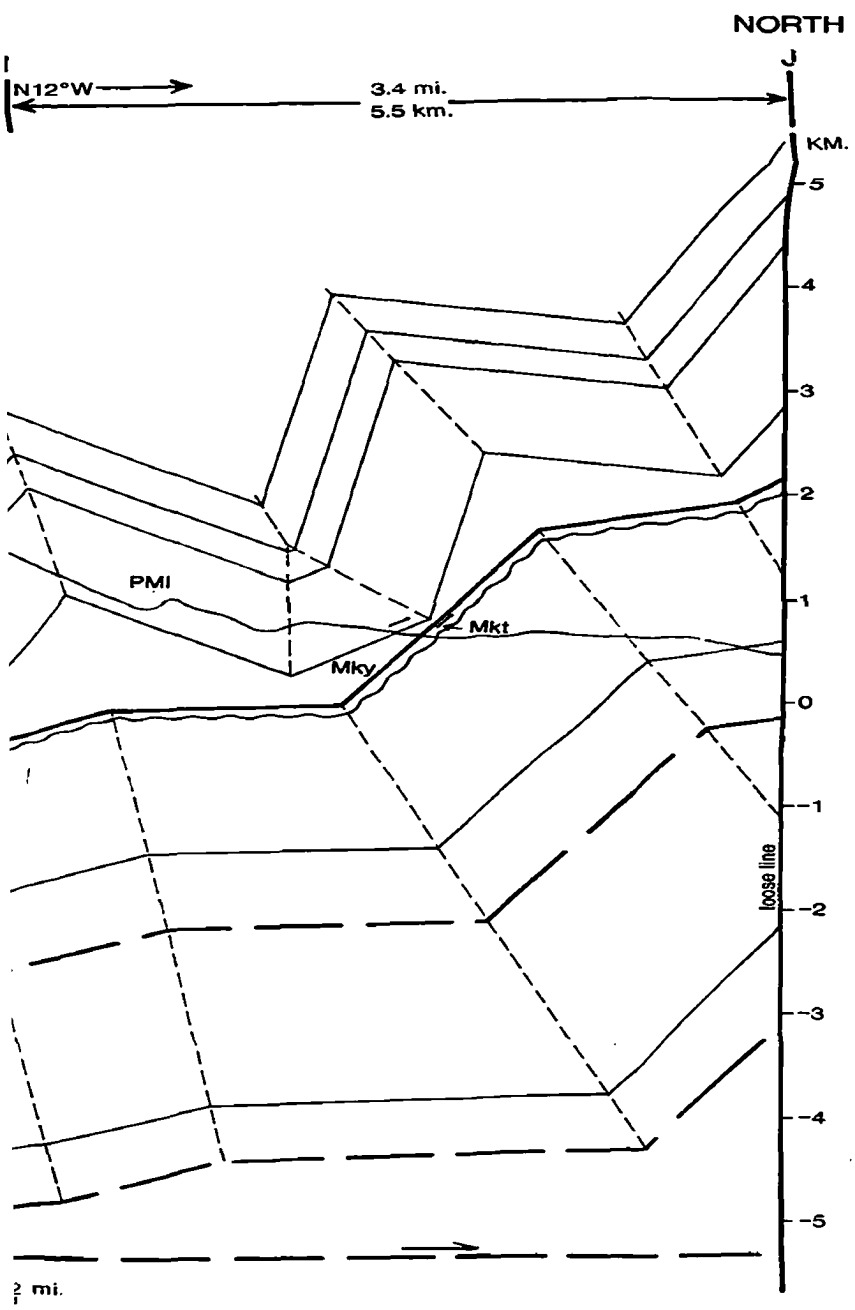

EXPLANATION OF SYMBOLS

lTriu	upper Ivishak Formation
lTril	lower Ivishak Formation
Pe	Echooka Formation
PMl	Lisburne Group
Mky	Kayak Shale
Mkt	Kekiktuk Conglomerate

sub–Mississippian unconformity

thrust fault or detachment

inferred thrust fault

axial surface

pin line

dip of bedding

dip of slaty cleavage

anticline; overturned anticline

syncline; overturned syncline

PLATE 3 PRIMARY BALANCED

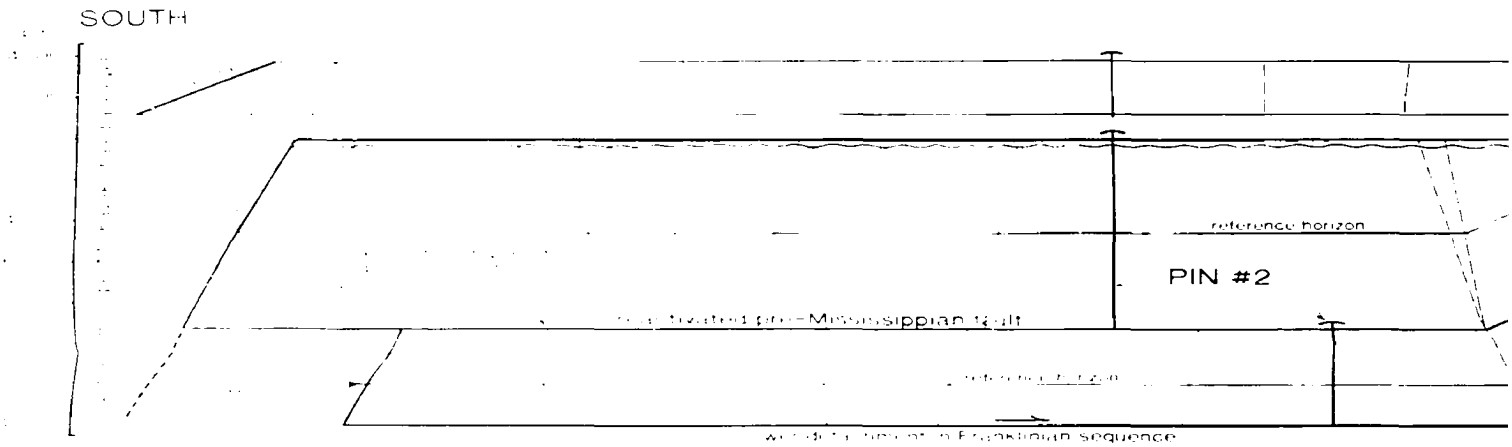

THIS RECONSTRUCTION OF DEFORMED CROS

ED CROSS-SECTION ACROSS THE FRANKLIN MOUNTAINS ANTICLINORIUM, RE

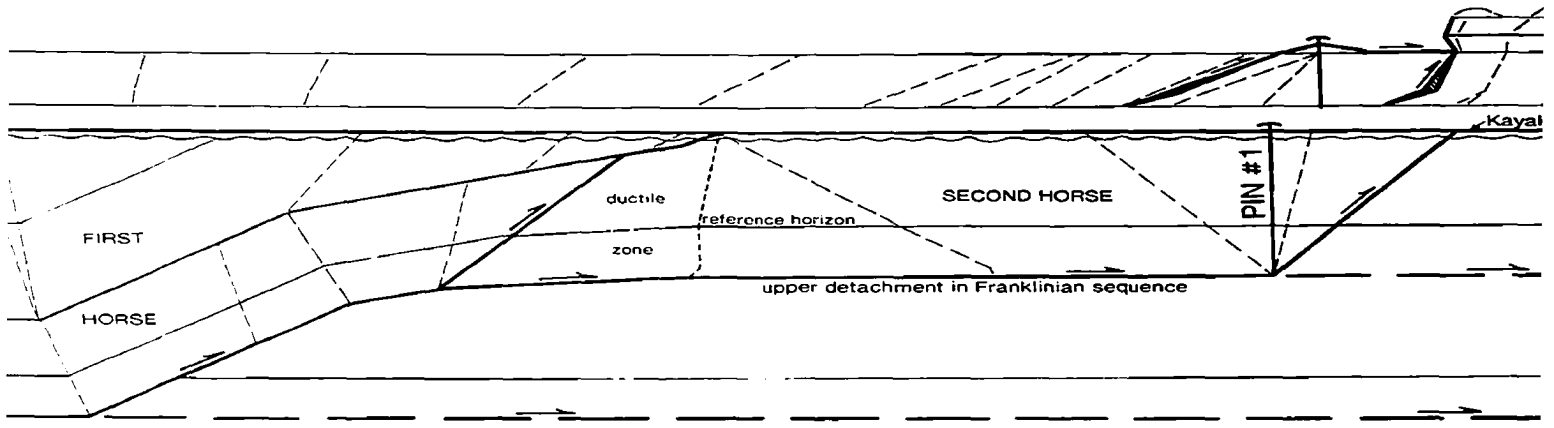

OSS-SECTION (PLATE 2) IS REPRODUCED AT 64%

NO VERTICAL EXAG

RIUM, RECONSTRUCTED TO PRE-CENOZOIC TIME

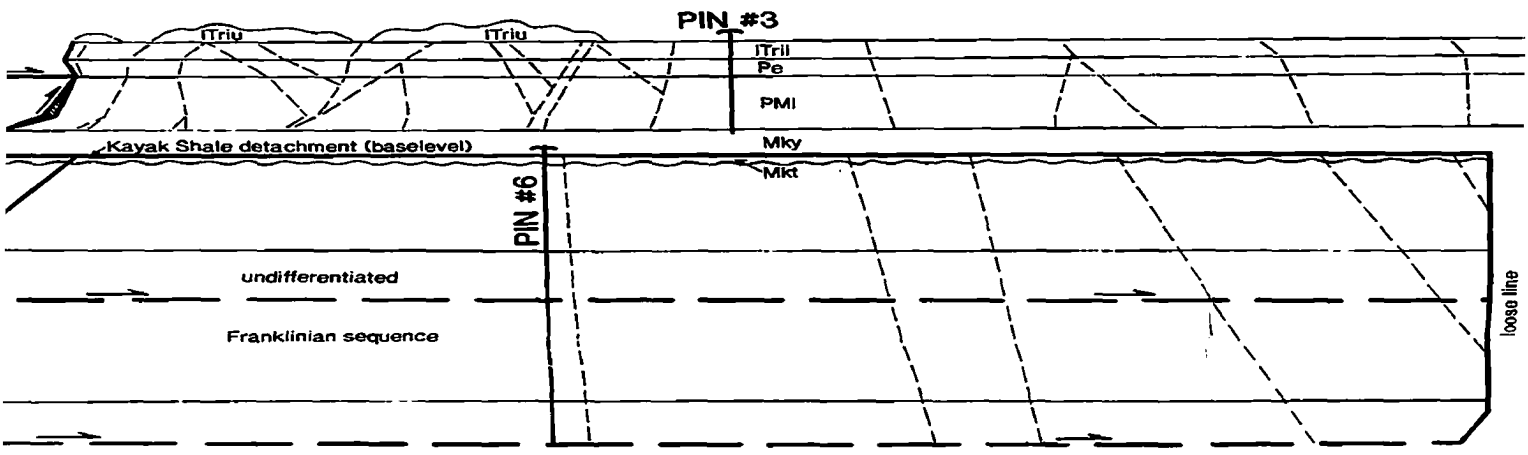

CAL EXAGGERATION

0 1 2 mi.
0 1 2 3 km.

ZIEGLER, JE
1339287

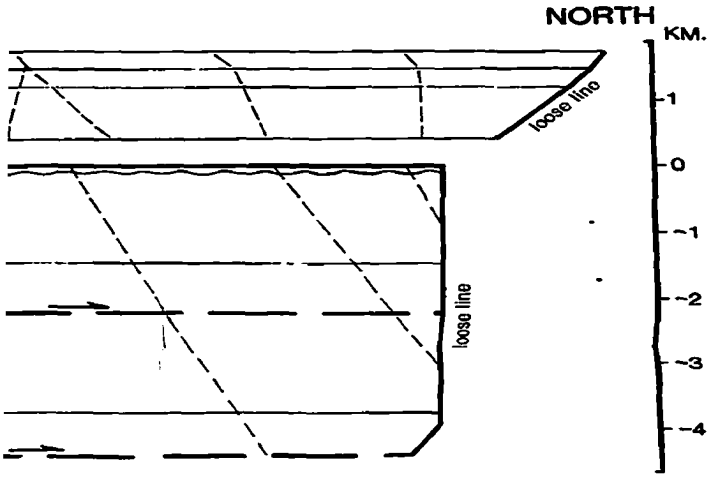

mi.
m.

EXPLANATION OF SYMBOLS

lTriu	upper Ivishak Formation
lTril	lower Ivishak Formation
Pe	Echooka Formation
PMl	Lisburne Group
Mky	Kayak Shale
Mkt	Kekiktuk Conglomerate
	sub–Mississippian unconformity
	thrust fault or detachment
	Cenozoic axial surface
	pin line
	area missing upon reconstruction

PLATE 4 PI

RECONSTRUCTE

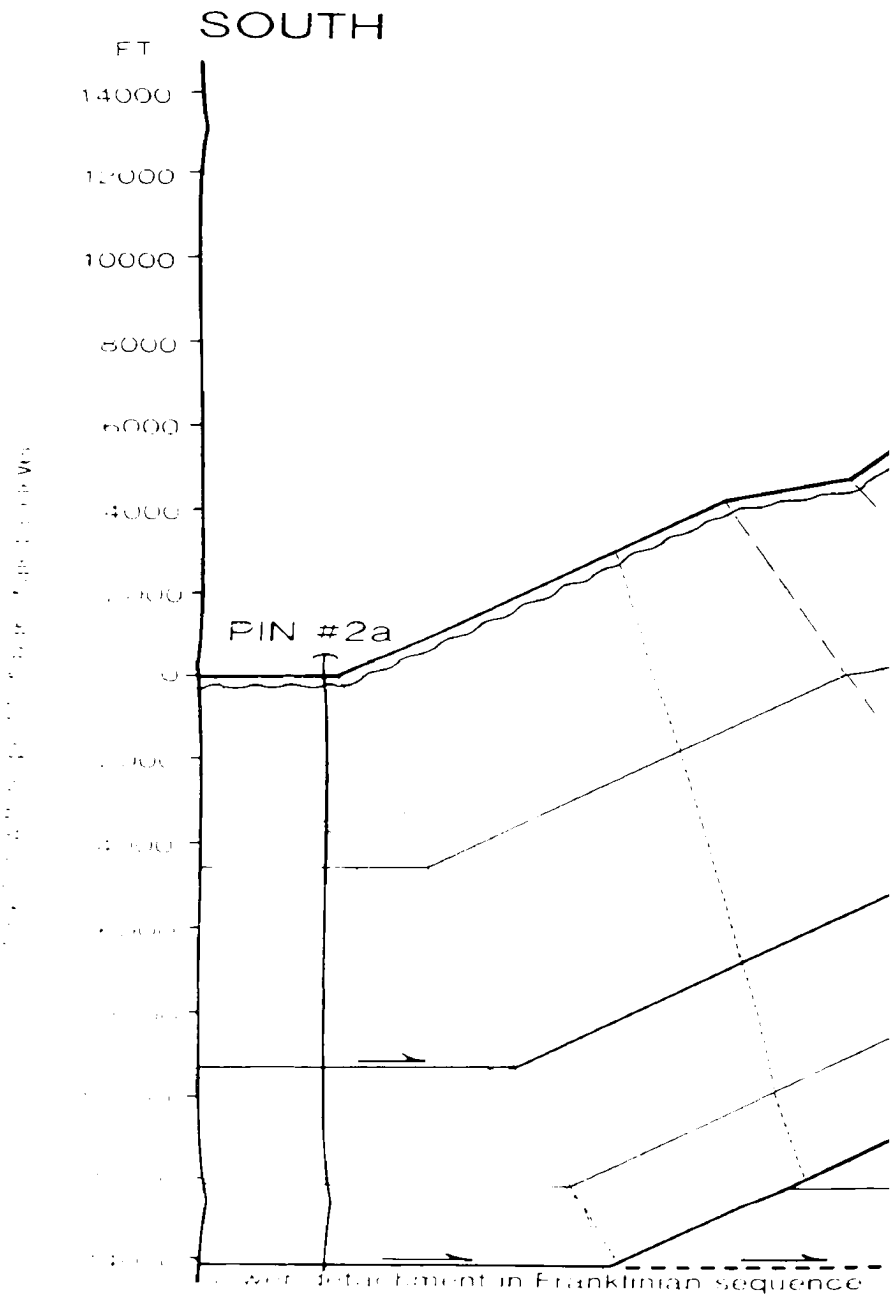

PRIMARY BALANCED CROSS-SECTION ACROSS THE FRA

CTED TO CENOZOIC TIME FOLLOWING THE EMPLACEMENT

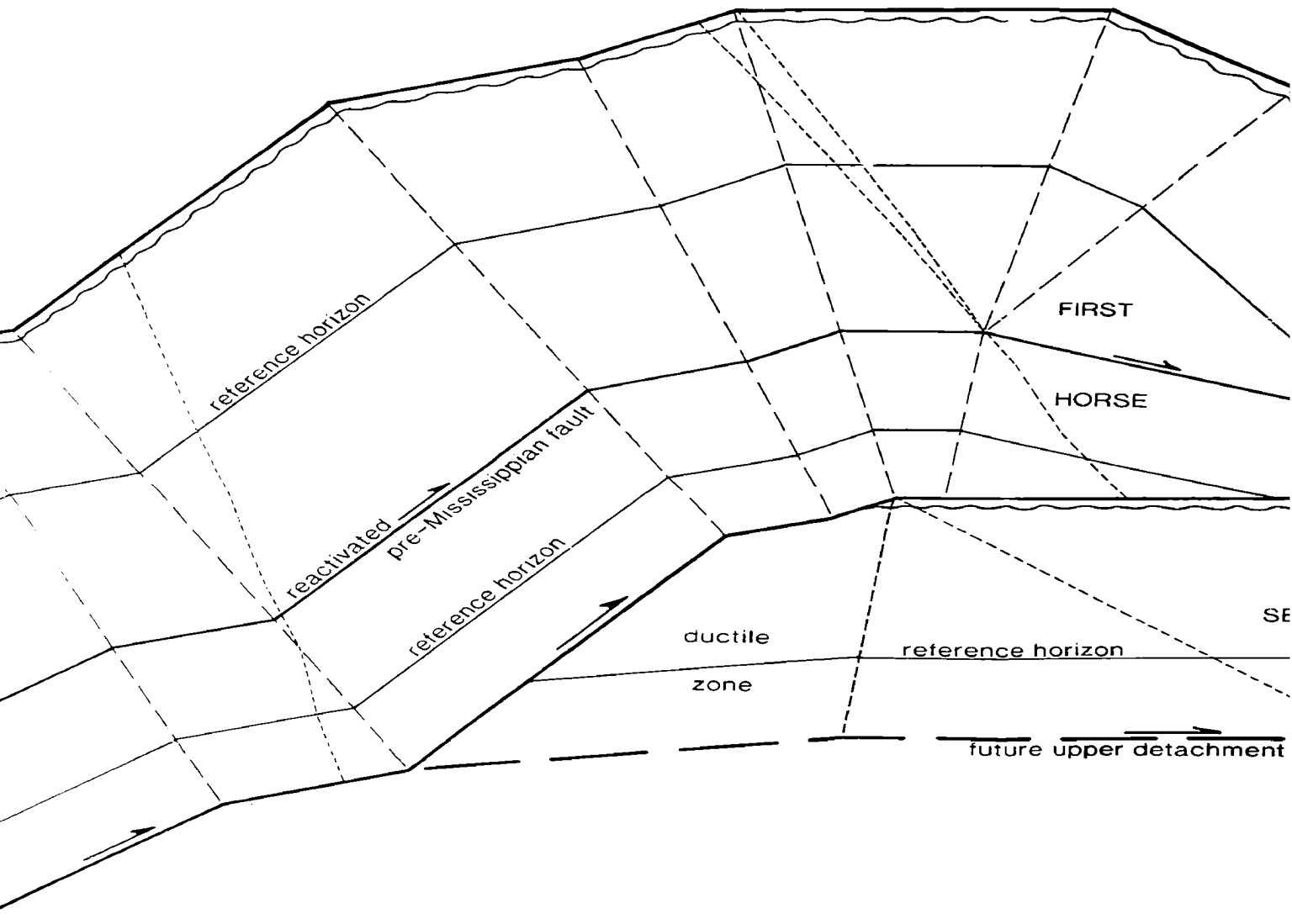

SCALE 1:25,000

NO VERTICAL EXAGGERA

E FRANKLIN MOUNTAINS ANTICLINORIUM,

EMENT OF THE FIRST HORSE OF THE ANTICLINORIUM

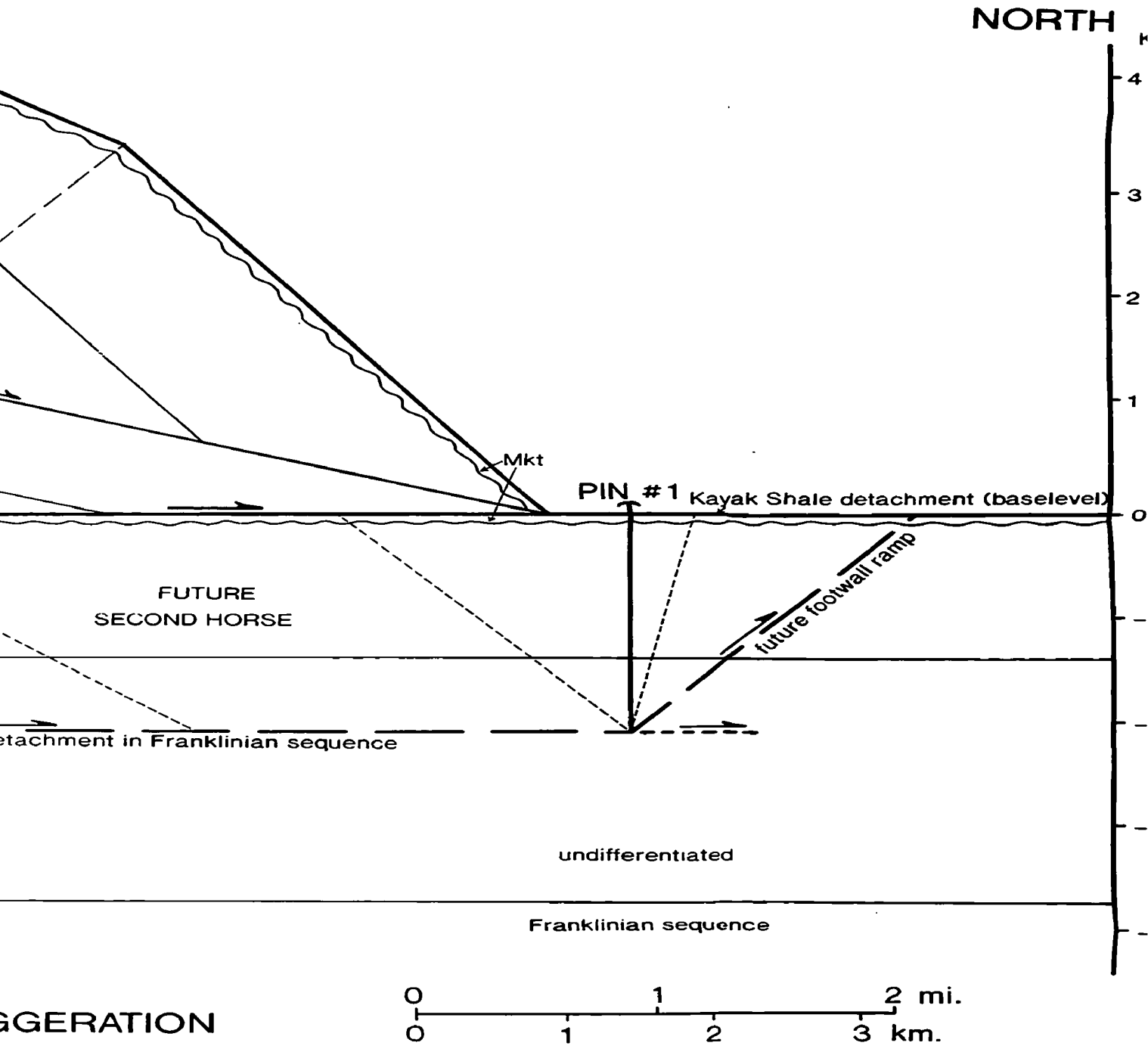

GGERATION

0 1 2 mi.

0 1 2 3 km.

M,

ITICLINORIUM